UNIVERSITÉ DE STRASBOURG

ÉCOLE DOCTORALE DES SCIENCES CHIMIQUES

Thèse de doctorat présentée par

Par

Quentin DHERBASSY

En vue de l'obtention du grade de

Docteur en chimie de l'Université de Strasbourg

« Contrôle de la chiralité axiale par activation de liaisons C-H: Accès à des molécules naturelles et ligands inédits »

Thèse dirigée par **Prof. Françoise Colobert et Dr Joanna Wencel-Delord**
(co-encadrant)

Soutenue le 30 novembre 2017 devant la commission d'examen composée de:

Professeur Olivier Baudoin, Université de Bâle, Rapporteur
Professeur Frédéric Patureau, Université de Kaiserslautern, Rapporteur
Dr Joseph Moran, Université de Strasbourg/ISIS, Examinateur
Professeur André Charette, Université de Montréal, Examinateur

I. Table des matières

A. Remerciements :

Merci au ministère de l'Éducation Nationale et de la Recherche, et à L'École doctorale des Sciences Chimiques à l'Université de Strasbourg et à l'Université de Haute Alsace pour cette bourse doctorale.

Merci au Prof. Françoise Colobert d'avoir initié ce projet et de m'avoir donné l'opportunité de travailler sur ce sujet porteur, ainsi que pour ses conseils

Merci au Dr. Joanna Wencel-Delord pour ses idées, son accompagnement de tous les jours, sa disponibilité son ouverture d'esprit et surtout pour les discussions stimulantes que nous avons ainsi pu avoir.

Et merci aux autres membres des laboratoires SynCat (Dr. Sabine Choppin, Dr Gilles Hanquet) et CoHa (Dr. F Leroux, Dr Armen Pannossian).

Merci également au Prof. Jean Pierre-Djukic pour ses calculs DFT et ses connaissances en chimie-physique organique.

Merci à l'équipe administrative, technique et analytique pour nous permettre de travailler dans de bonnes conditions.

Enfin merci à ceux qui, à la paillasse, ont ouvert la voie de l'utilisation des sulfoxyde en activation de liaisons C-H asymétrique et sans qui nous n'en serions pas là.

B. Liste des abréviations

* = denotes chirality

2,6-DMBQ = 2,6- dimethylbenzoquinone

Ac = acetyl

AMLA = Ambiphilic metal-ligand activation

BINAP = (2,2'-bis(diphenylphosphino)-1,1'-binaphthyl)

Bn = benzyl

Boc = *tert*-butyloxy carbonyl

Bpin = pinacol borane

bpy = bipyridine

BQ = benzoquinone

Bz = benzoyl

CG-50 = acidic resin

CMD = concerted metallation deprotonation

cod = cyclooctadiene

Cp = cyclopentadienyl

Cp* = pentamethylcyclopentadienyl

Cy = C_6H_{11}

D = dédoublement

d.r. = diastereomeric ratio

DC = dédoublement cinétique

DCD = dédoublement cinétique dynamique

DCE = 1,2-dichloroethane

DCM = dichloromethane

DET = diethyltartrate

DFT = density functional theory

DG = directing group

DIBAL-H = di-*iso*butyl aluminium hydride

DKR = dynamic kinetic resolution

DMAc = dimethylacetamide

DMAP N,N'-dimethylamino pyridine

DME = dimethoxyethane

DMF = dimethylformamide

DMSO = dimethylsulfoxide

Dpen = 1,2-Diphenyl-1,2-ethylenediamine

dppf = 1,1'-bis(diphenylphosphine)ferrocene

DYKAT = dynamic asymmetric transformation

e.r. = enantiomeric ratio

eq = equivalent

equiv =equivalent

GD = groupe directeur

HFIP = 1,1,1,3,3,3-hexafluoroisopropanol

IES = internal electrophilic substitution

IUAPC = union for pure and applied chemistry

KIE = kinetic isotope effect

KR = kinetic resolution

M = metal

$M_{cat=}$ metal in sub-stoichiometric quantity

ML = metal-ligand

MT = métaux de transition

NBS = *N*-bromo succinimide

NIS = *N*-iodo succinimide

Ns = nosyl

o =*ortho*

m = *meta*

p = *para*

Phth = phthaloyl

Piv =trimethylacetyl

*p*Tol = *para*-tolyl

R = resolution

r.d. = ratio diastéréomérique

r.e. = ratio énantiomérique

Segphos = 4,4'-Bi-1,3-benzodioxole-5,5'-diylbis(diphenylphosphane)

Sphos = 2-Dicyclohexylphosphino-2',6'-dimethoxybiphenyl

TBAB = *tert*-butyl ammonium bromide

TBDMS = *tert*-butyldimethylsilyl

TBHP = *tert*-butylhdroperoxyde

TEMPO = 2,2,6,6-Tetramethylpiperidinyloxyl

TES = triethylsilyl

Tf = triflate

THF = tetrahydrofuran

TMEDA = *N*,*N*,*N*',*N*'-tetramethylethylenediamine

TMS = trimethylsilyl

TMSO = tetramethylene sulfoxide

Introduction

II. Introduction

Une nouvelle stratégie vers l'obtention de biaryles à chiralité axiale atropoenrichis a été explorée lors de cette thèse. L'atropisomérie est un type particulier de chiralité axiale résultant d'une barrière de rotation élevée autour d'une liaison simple permettant l'existence de stéréoisomérie. L'atropisomérie caractérise certains composés naturels, des composés à activités biologiques (naturels ou synthétiques), des matériaux avancés et des ligands utilisés en catalyse grâce à leur excellent pouvoir d'induction asymétrique. Ainsi le contrôle de l'atropisomérie et le développement de nouvelles méthodes synthétiques permettant la synthèse de composés à chiralité axiale optiquement purs attire l'attention de la communauté scientifique.

Inspiré par le travail pionnier de Murai en 2000, de nouvelles méthodes d'obtention de biaryles atropoenrichis, impliquant l'activation de liaisons C-H, ont été développées. Le concept est basé sur l'observation que la fonctionnalisation de la liaison C-H en *ortho* de l'axe biarylique, augmente significativement la barrière de rotation autour de cet axe, permettant ainsi d'accéder à des biaryles atropisomériques à partir de biaryles non-atropisomériques.

De plus, une approche par activation de liaisons C-H ouvre la possibilité de réaliser les promesses souvent citées de la C-H : une économie d'étapes et de moyens dans un contexte de plus en plus tourné vers une chimie plus efficace et plus respectueuse de l'environnement. De plus cette stratégie permet d'accéder à des architectures moléculaires inédites.

Cependant, afin d'atteindre cet objectif, deux obstacles inhérents aux réactions d'activation de liaisons C-H doivent être surmontés : l'omniprésence des liaisons C-H et leur manque de réactivité ; omniprésence qui pose le problème de la régiosélectivité, le manque de réactivité appelant l'utilisation de conditions réactionelles dures qui peuvent compromettre la stabilité des produits atropenrichis

La solution générale pour pallier au problème de la régiosélectivité consiste en l'utilisation d'un groupement directeur. Dans le cadre de cette thèse nous proposons une nouvelle stratégie diastéréosélective où le groupement directeur (GD) joue le rôle d'inducteur de chiralité : cette approche par activation C-H diastéréosélective inédite a été rendue possible par l'utilisation d'un sulfoxyde énantiopur en tant que GD et auxiliaire de chiralité. Si les réactions diastéréosélectives semblent à première vue contraire aux principes d'économies d'activation de liaisons C-H, l'utilisation d'un sulfoxyde permet de surmonter cet écueil : en effet, en étant à la fois GD et inducteur de chiralité il assure deux fonctions. Ainsi, à partir d'un substrat non-atropisomérique, le sulfoxyde doit diriger le métal vers une liaison C-H *ortho'* : l'insertion du métal formant ainsi des métallacycles atropodiastéréomériques qui peuvent s'équilibrer (Figure II-1). A ce stade, la chiralité du sulfoxyde doit favoriser un des atropodiastéréomères qui, après fonctionnalisation, deviendra atropisomèrique et atropoenrichi par ce mécanisme de dédoublement cinétique dynamique (DCD).

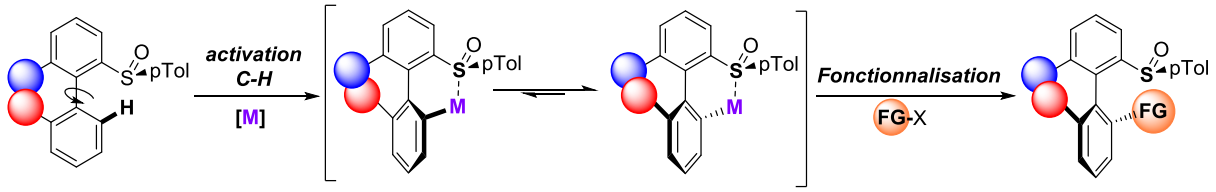

Figure II-1 : fonctionnalisation diastéréosélective de biaryles par métallo-catalyse

Enfin le sulfoxyde remplit une troisième essentielle : en effet la réaction d'échange sulfoxyde/lithium permet de diversifier les produits obtenus vers une large gamme : il est donc un groupe directeur sans traces. Ainsi, ce sulfoxyde « groupe fonctionnel trois-en-un », doit permettre l'obtention d'un panel important et inédit de biaryles atropisomériques.

Nous commencerons par une partie générale sur l'activation de liaisons C-H d'un point de vue historique et théorique ainsi qu'une partie traitant de la littérature sur l'activation de liaison C(sp^2)-H asymétrique non-atroposélective. Puis, après une définition du phénomène atropisomérique, ainsi que des facteurs influencant son existence, nous passerons en revues les méthodes de constructions atroposélectives de biaryles, et nous verrons l'importance que le contrôle de la chiralité axiale revêt dans le domaine des composés bioactifs, de la catalyse asymétrique et dans l'élaboration de matériaux moléculaires.

A partir de ce moment, le reste de ce manuscrit sera rédigé en anglais, et les parties suivantes seront extraites du travail publié dans les journaux scientifiques auquel sera joint une bibliographie dans les domaines cités à savoir la réaction de Fujiwara Moritani (chapitre IV), de C-H acétoxylation (chapitre V-B), C-H iodation (chapitre V-C) et C-H arylation (chapitre VII-C) de notre substrat biaryle-sulfoxyde. De plus l'application des méthodologies développées à la synthèse formelle de la steganone (chapire VI), ainsi qu'à la synthèse de ligands originaux sera présentée (chapitre VII-D).

Enfin, une dernière partie expérimantale générale (chapitre VIII) décrira les procédures permettant d'obtenir les biaryles (et leurs précurseurs) énantiopurs à l'atome de soufre, qui ont été utilisées dans chacun des chapitres de ce manuscrit.

Partie Générale

III. Partie générale

A. Activation de liaisons C-H

1. Historique, objet d'étude, définitions

La fonctionnalisation des liaisons C-H constitue un objectif important en chimie de synthèse : en effet le fait de ne pas faire apparaître les liaisons C-H dans la représentation formelle de la chimie organique est significatif d'une part de leur grand nombre mais aussi de leur manque de réactivité. L'activation et la subséquente fonctionnalisation directe de liaison C-H doit ainsi permettre d'ouvrir un nouveau pan de l'espace chimique, en faisant réagir des liaisons autrefois considérées comme inertes et ainsi changer notre façon d'appréhender la synthèse en rendant possible de nouvelles disconnections et aussi la construction d'architectures moléculaires jusqu'à lors inaccessibles. De plus, dans un contexte de plus en plus dirigé vers une chimie plus propre et respectueuse de l'environnement, l'application de ces pratiques au niveau industriel semble promettre une économie de moyens, d'étapes et de déchets.

Mais commençons tout d'abord par définir les termes et l'objet de ce chapitre : en effet le terme C-H activation peut recouvrir de nombreux types, et donc de nombreux mécanismes différents. Premièrement, et c'est une évidence, il faut noter que toute réaction aboutissant au remplacement d'une liaison C-H par une liaison C-C, C-X, ne peut être qualifiée de C-H activation : ainsi la formation d'un énolate, suivit d'une condensation avec un électrophile ne rentre pas dans le cadre de la C-H activation, de même que les substitutions électrophiles (ou nucléophiles) aromatiques. Une deuxième distinction que l'on donne aux réactions de C-H activation est qu'elles impliquent un métal : mais là aussi ce n'est pas suffisant ; ainsi l'oxy-mercuration d'alcènes ou la réaction de Reformatsky ne sont pas des réactions de C-H activation au sens entendu aujourd'hui.

Un troisième élément réside dans le type de métal utilisé : un des jalons souvent cité de la C-H activation est l'insertion d'oléfines dans la liaison C-H en *ortho* de cétones aromatiques par Murai[1] en 1993 (Figure III-1a) : à première vue, cette réaction semble avoir beaucoup de similitude avec les réactions d'*ortho*-métallations dirigées[2,3] (Figure III-1b) : une réaction en *ortho* d'un groupe coordinant, impliquant un métal et permettant de fonctionnaliser une liaison C-H forte et considérée comme peu réactive.

Ainsi dans les deux exemples Figure III-1, l'intermédiaire réactionnel proposé est similaire : un métal ligandé, formant une liaison C(sp^2)-M à la place d'une liaison C-H, stabilisé par la coordination d'un groupement coordinant en *ortho*.

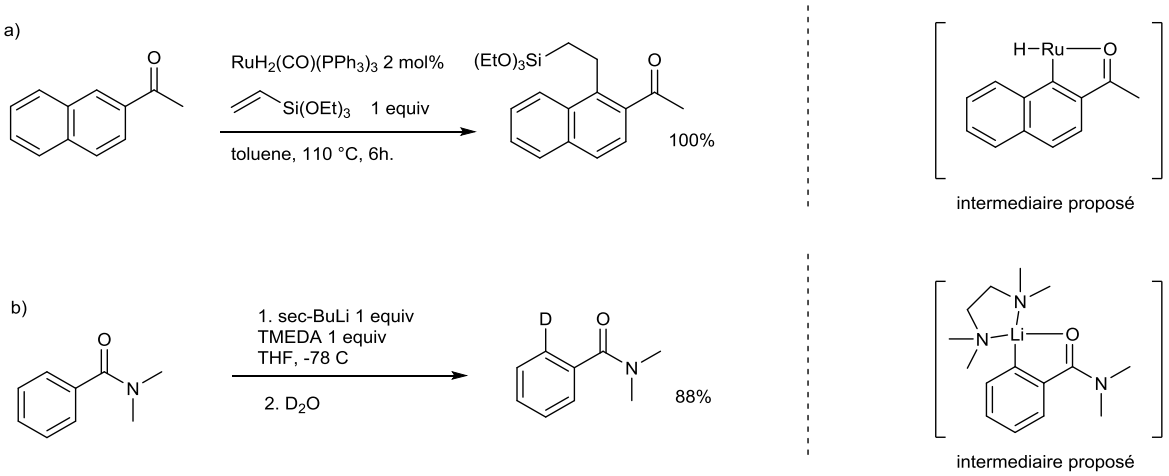

Figure III-1 activation C-H et métallation dirigée en *ortho*

Seulement le fait qu'elle implique dans un cas un métal alcalin, et dans l'autre un métal de transition rend le mécanisme, la portée et le type de fonctionnalisation possible complétement différent (au-delà de la constatation évidente que les réactions d'*ortho*-métallation dirigée ne sont pas catalytiques, alors que les réactions impliquant des métaux de transition peuvent l'être. C'est donc l'utilisation de métaux de transition qui constitue un élément important de définition (on pourra argumenter que la réactivité d'un alkyllithium réside dans la basicité/nucléophilie du ligand du métal, ici le carbanion, qui peut être modulé par la nature du métal utilisé (et dans une moindre mesure par des ligands, d'où l'utilisation de tétramethylethylènediamine TMEDA). D'autre part, dans le cas des métaux de transition la réactivité est centrée sur le métal en lui-même, ses degrés d'oxydation, et que ici se sont les ligands du métal qui permettent de moduler cette réactivité. Ainsi, nous adopterons comme définition du terme C-H activation la formation d'une liaison carbone-métal de transition par la rupture d'une liaison carbone hydrogène, comme l'avait précisé Labinger et Bercaw en 2002[4]. Remarquons que cette première définition divise en deux grands groupes les réactions conduisant à la fonctionnalisation de liaisons C-H et impliquant des métaux de transition selon que le mécanisme implique la première sphère de coordination du métal ou se fasse en dehors de cette sphère de coordination[5].

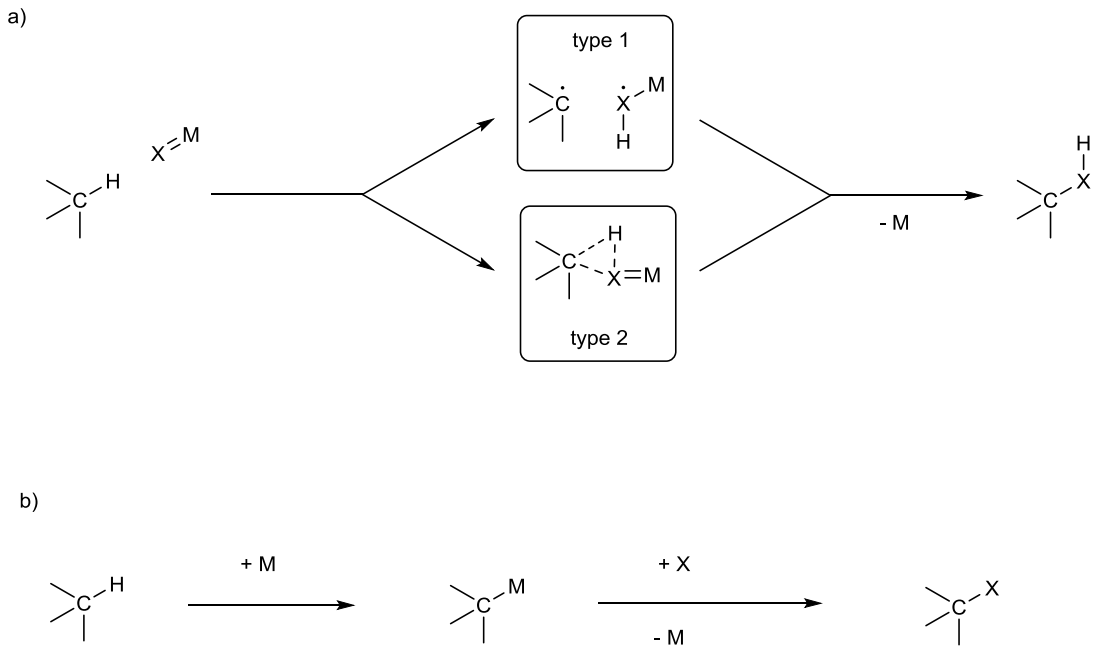

Figure III-2 : mécanismes par sphère interne et externe

Ainsi la Figure III-2a montre deux grands types de réaction par sphère externe : le type 1 illustre les mécanismes d'hydroxylation tel qu'ils se passent dans le cytochrome P450[6] ; le type 2, les réactions d'insertion de carbènes dans les liaisons C-H[7]. Une représentation schématique des mécanismes par sphère interne est proposée Figure III-2b, caractérisé par un intermédiaire où une liaison C-H est remplacée par une liaison C-M. Reste maintenant à ajouter un élément de définition ; en effet l'activation de liaison C-H pour former une liaison C-Métal de transition (C-MT) n'est pas en général le but ultime du chimiste organicien. En effet il cherche à fonctionnaliser la liaison C-H pour former de nouvelles liaisons. Ainsi la deuxième étape, qui concerne le remplacement de la liaison C-MT cette fois par une liaison C-C par exemple, est communément appelée fonctionnalisation de liaison C-H. Ainsi la libération du métal après la fonctionnalisation permet d'envisager un cycle catalytique où le métal est utilisé dans des proportions sub-stœchiométrique (par abus de langage on parle souvent de quantités catalytiques). C'est notre dernier élément de définition, c'est-à-dire que nous parlerons de réactions catalytiques.

Pour récapituler nous nous occupons de réactions catalytiques impliquant des métaux de transitions où l'activation de liaison C-H conduit au remplacement de cette liaison par une liaison C-M par un mécanisme de sphère interne, suivie de la fonctionnalisation vers des produits divers. Notons enfin qu'en-dehors des cas d'études mécanistiques, le terme « activation C-H » pourra être utilisé pour décrire le processus d'activation/fonctionnalisation dans sa totalité.

En suivant ces lignes directrices un des premiers exemples d'activation C-H, au sens où nous l'entendons, pouvant être cité est représenté Figure III-3a1 : Chatt et Davidson[8] ont ainsi isolé en 1965 le complexe 2-naphtylhydrure issu de l'insertion d'un ruthenium riche en électron dans la liaison C-H du naphtalène ; un autre exemple (de

Bennett et Milner[9] en 1967) impliquant un métal de transition tardif riche en électrons est présenté Figure III-3a2, et cette fois la C-H activation résulte en une cyclométallation intramoléculaire. Remarquons que dans ce dernier exemple le degré d'oxydation formel du métal augmente de +I à + III. Un autre type d'exemple précoce concerne les systèmes dit « électrophiles » dont le premier exemple date de 1972 par Shilov[10] et qui reste encore aujourd'hui d'actualité malgré l'utilisation de platine IV stœchiométrique comme étant l'un des rares permattant la fonctionnalisation sélective d'alcanes (Figure III-3b1). Ainsi si les exemples de la Figure III-3a sont plutôt classés comme activation nucléophile à cause de la richesse électronique du métal, les systèmes type Shilov de la Figure III-3b sont eux plutôt considérés comme activation électrophile[11]. Enfin, un dernier type d'activation concerne les complexes alkyles ou hydrures de métaux de transitions avec une configuration d^0 (scandium, lanthanides, actinides)[12] Figure III-3c1.

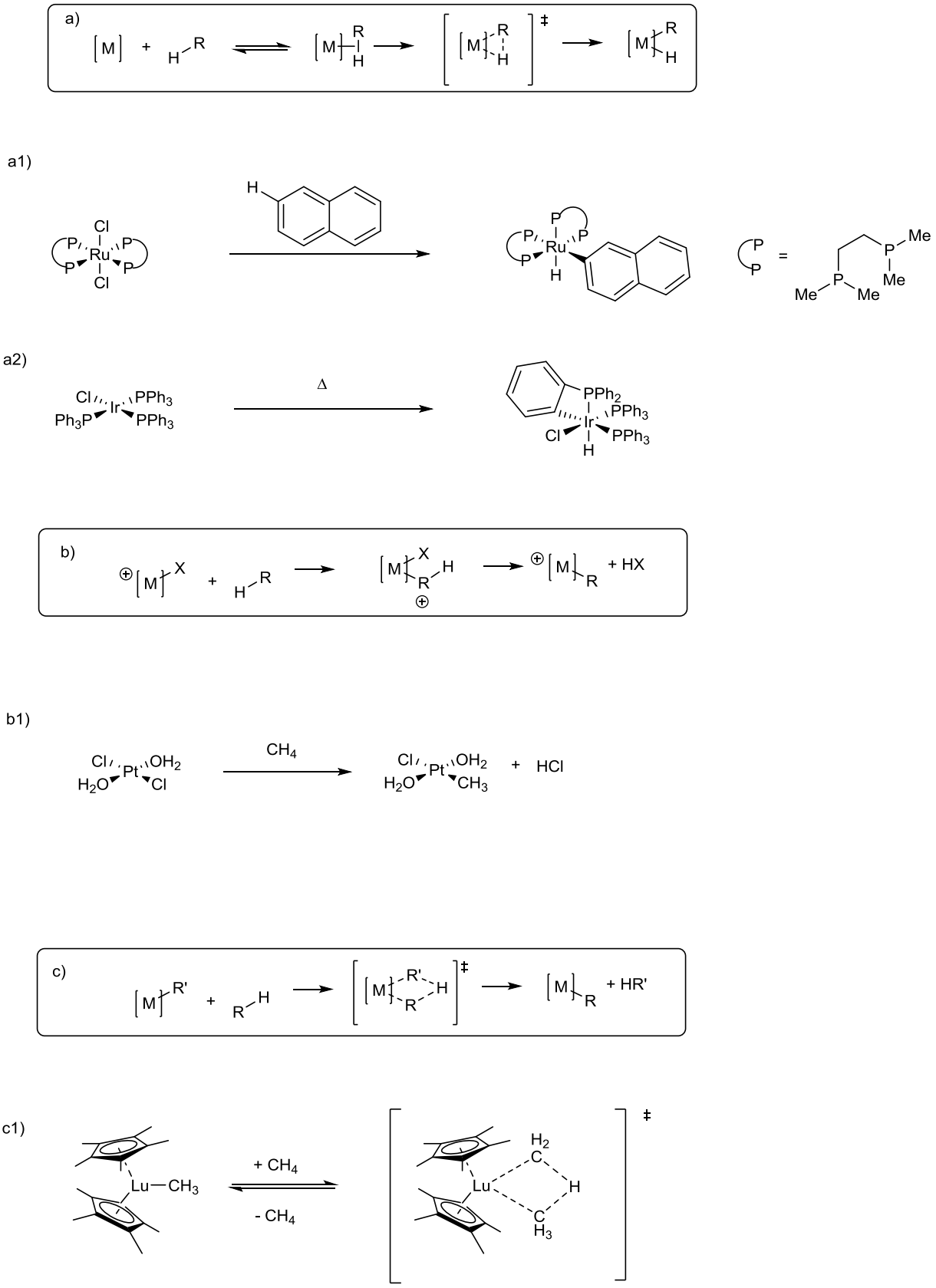

Figure III-3 : premiers mécanismes d'activation de liaisons C-H

Ainsi on a représenté ici les trois grands types historiques de mécanisme d'activation C-H[4] :

1- Addition oxydante Figure III-3a

2- Activation électrophile Figure III-3b

3- Métathèse de liaison σ Figure III-3c

Cependant cette classification historique des modes d'activations C-H est aujourd'hui progressivement complétée par un mode qui réunit les modes d'activation nucléophiles et électrophiles le long d'un continuum commun[13]. Ainsi la vision classique de l'addition oxydante d'un métal dans une liaison C-H implique comme interaction de frontière principale, le transfert de charge d'une orbitale occupée d_π basée sur le métal vers l'orbitale σ^* d'une liaison C-H coordinée : ainsi le métal est formellement oxydé de +II. Cependant, il faut également prendre en compte l'autre interaction frontière possible : celle de l'orbitale occupée σ C-H vers une orbitale d_σ inoccupée du métal. Ainsi la contribution des deux interactions à la stabilisation de l'état de transition de l'insertion C-H peut être très différente selon la combinaison métal-ligand étudiée : dans cette vue, les complexes où l'interaction stabilisante principale de l'état de transition provient de l'orbitale occupée σ C-H vers l'orbitale d_σ inoccupée seront qualifiés d'électrophiles.

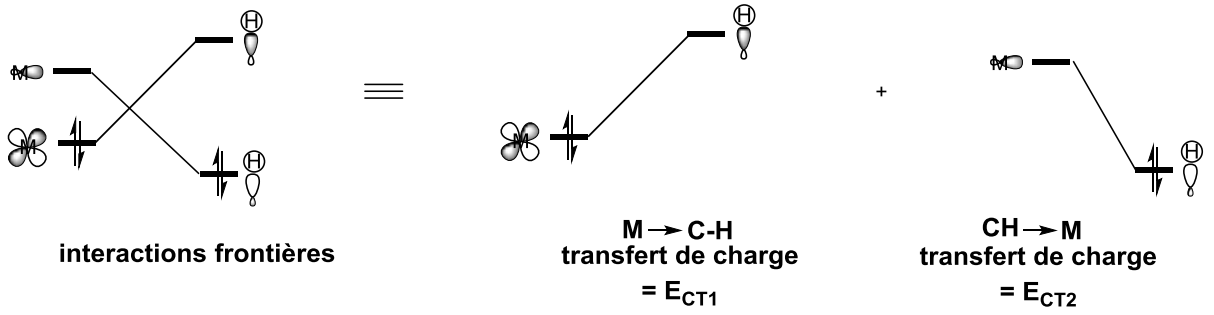

Figure III-4 : interactions frontières

Ainsi le calcul du mode dominant de stabilisation (M vers C-H ou C-H vers M) dans l'activation du méthane par des complexes à travers 20 états de transitions de 13 métaux différents montrera un continuum entre des métaux ayant un caractère électrophile, nucléophile et donc aussi ambiphile[13] (calculs DFT B3LYP) : la Table III-1 présente cette classification ; les métaux ayant un ratio E_{CT2}/E_{CT1} bien supérieur à 1 sont considérés électrophiles, et donc ceux inférieurs à 1 nucléophile. Ainsi Pt^{II}, Pd^{II}, Rh^{III} seront qualifiés d'électrophiles, les ambiphiles représenté par Ru^{II} et Ir^{III}, et les nucléophiles par Ir^{I}, Rh^{I} et Sc^{III}.

Table III-1 : rapport du transfert de charge C-H →M sur M→ C-H dans l'état de transition

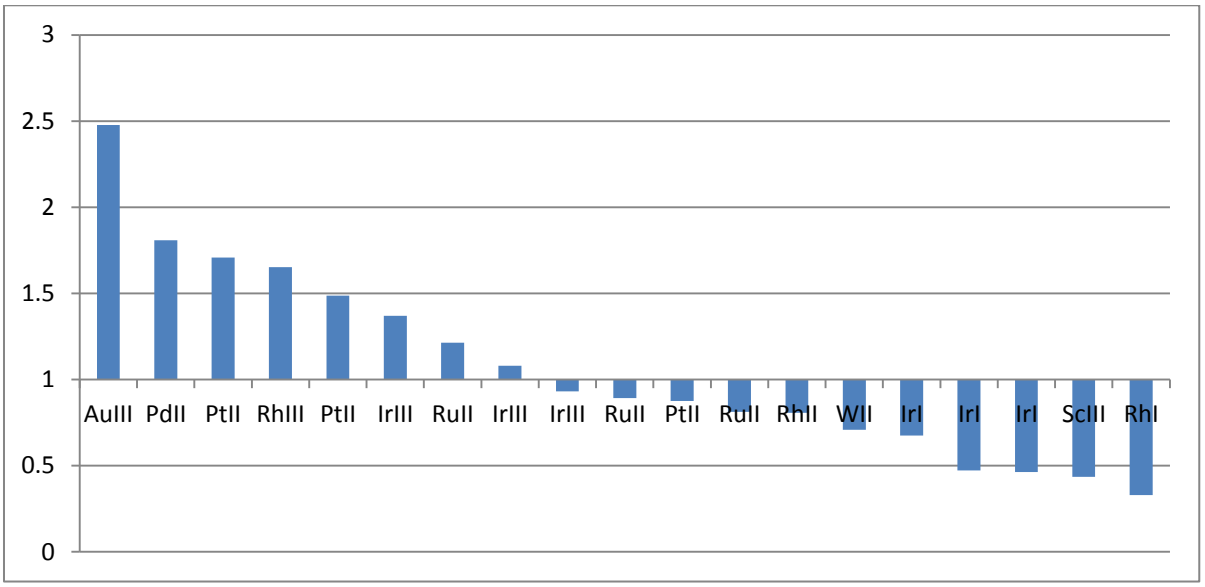

D'un point de vue pratique, on peut donc s'attendre, pour les métaux électrophiles par exemple, que la diminution de l'énergie des orbitales inoccupées d_σ du métal (par des ligands électroattracteurs), ainsi que l'augmentation de l'énergie de l'orbitale σ C-H (substrats riches en électrons) renforcera l'interaction frontière contribuant le plus à la stabilisation de l'état de transition, et ainsi facilitera l'insertion du métal dans la liaison C-H. Cette vision d'un continuum permet de définir un nouveau type de mécanisme caractérisé non plus par une dichotomie électrophile/nucléophile, mais par la participation d'un ligand bi-fonctionnel, possédant un site basique disponible, à l'insertion du métal dans une liaison C-H ; et ce type de mécanisme a connu plusieurs dénominations :

-CMD : Concerted Metallation Deprotonation[14]
-IES : Internal Electrophilic Substitution[15]
-AMLA : Ambiphilic Metal Ligand Activation [16]

Dans ces mécanismes l'insertion du métal dans la liaison C-H se fait de façon concertée avec la déprotonation assistée par un ligand, le plus souvent de type carboxylate, mais aussi carbonate ou phosphate, et ainsi le degré d'oxydation formel du métal ne change pas.

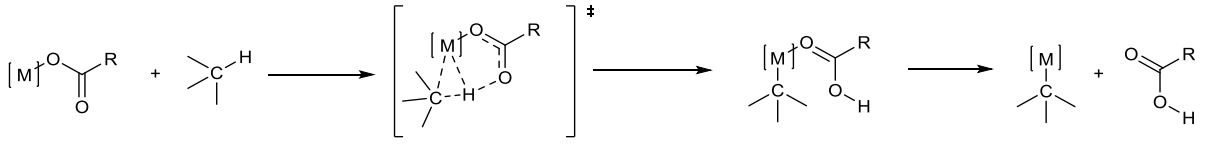

Figure III-5 : mécanisme CMD/AMLA

De plus, ce type de mécanisme a très tôt été associé aux réactions de C-H activation dirigées, c'est-à-dire où le substrat contient un groupe basique capable de coordiner le métal et ainsi l'amener à proximité de la liaison C-H à rompre : en effet les complexes cyclométallés ainsi créés sont alors assez stables pour être isolés, caractérisés et étudiés. Cependant, si les premières réactions de cyclopalladation/platination stoechiometriques ont été conduites à partir de différents complexes de chlorure de palladium/platinium (Cope et Sieckman[17] en 1965 Figure III-6a, puis Cope et Friedrich[18] en 1968 Figure III-6b) il fut montré dès 1974 par le groupe de Shaw[19] que la présence d'ions acétates facilitent les métallations intramoléculaires (Figure III-6c).

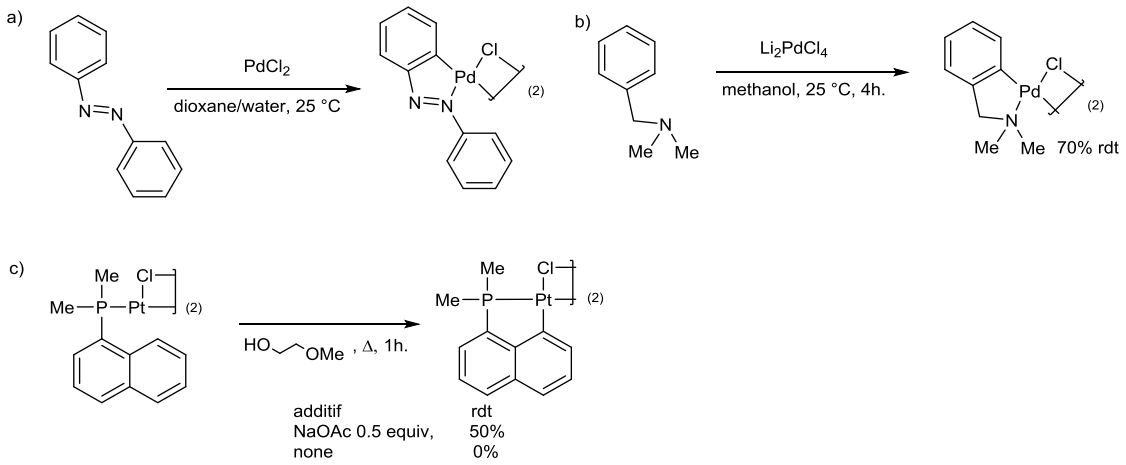

Figure III-6 : premières réactions de cyclométallation du groupe d10

Puis le même phénomène fut observé par Gaunt et Shaw[20] en 1975 lors de la palladation du *N*,*N*'-dimethylaminomethylferrocène, ce qui inspirera Sokolov la première utilisation de sels d'acides aminés énantiopurs afin de promouvoir des métallations énantiosélectives : on peut considérer, à notre connaissance, que c'est ici la première apparition d'un mécanisme CMD/AMLA. En effet Sokolov réfute la formation d'un intermédiaire de Wheland en comparant la métallation du *N*,*N*'-dimethylaminomethylferrocène (Figure III-7a) avec celle de la *N*,*N*'-dimethylbenzylamine (Figure III-6b) : en effet dans des conditions comparables (c'est-à-dire sans ajout d'acétate de sodium), seul la *N*,*N*'-dimethylbenzylamine produit un métallacycle, alors que dans l'hypothèse d'un mécanisme de substitution électrophile le cycle cyclopentanediènyle devrait être plus susceptible aux attaques électrophiles qu'un cycle phényle. De plus la participation de la base carboxylate à l'état de transition (ou à un intermédiaire) menant au produit cyclométallé fut présumée sur le fait que l'addition d'autres types de bases ne produisait pas le produit attendu, donnant ainsi un rôle plus important à l'acétate que de simplement piéger l'équivalent d'HCl libéré par la palladation (les auteurs précisent que seules des conditions alcalines aqueuses leur ont permis de former en partie le produit recherché, cependant dans un mélange avec d'autres composés, sans toutefois préciser si ils ont réussi à l'isoler). Enfin, se basant sur l'hypothèse de la participation des carboxylates à l'état de transition de la métallation, les auteurs utiliseront des sels carboxylates d'acides aminés N-acyles protégés pour induire une cyclopalladation asymé-

trique sur le même substrat (Figure III-7b) : la réussite de leur entreprise renforçant ainsi l'hypothèse de la participation du carboxylate à l'étape de cyclométallation, et ainsi ils proposeront l'état de transition présenté Figure III-7c.

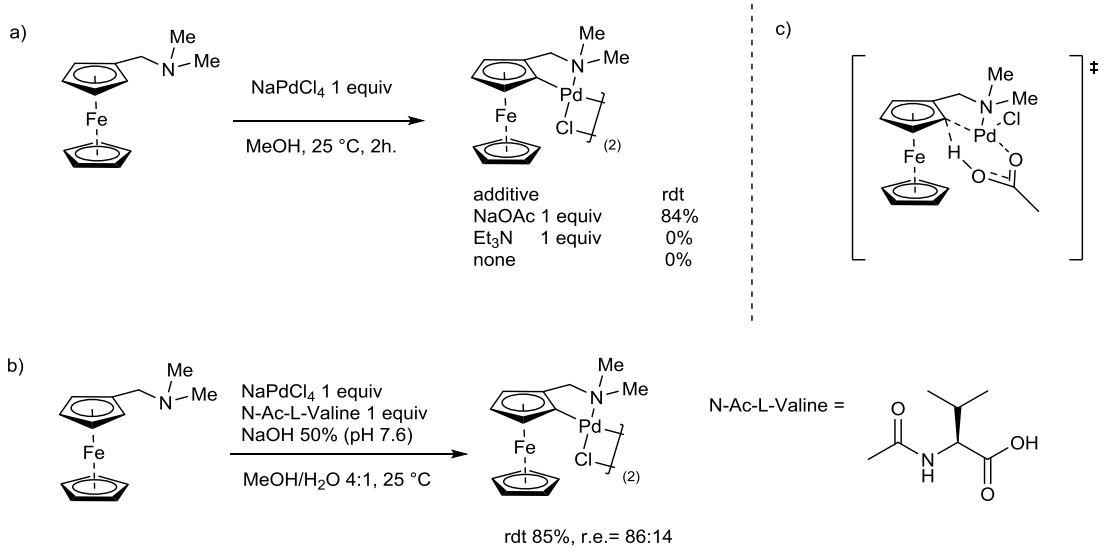

Figure III-7 : cyclopalladation du N,N'-dimethylaminomethylferrocène

En effet jusqu'alors les mécanismes proposés se rapprochaient plus d'une substitution électrophile aromatique avec un intermédiaire de Wheland, assisté par la base carboxylate intramoléculaire. Ainsi, Ryabov en étudiant en détail le mécanisme de la palladation de la *N*,*N*'-dimethylbenzylamine assistée par des ions acétates trouvera que : la rupture de la liaison C-H est bien l'étape limitante (KIE 2.2), avec une pente de la droite de Hammet de ρ = - 1.6, indiquant par là une nature électrophile. De plus, l'entropie d'activation de -250 kJ/mol indique un état de transition très ordonné : ces données pousseront Ryabov à proposer l'état de transition suivant, où, bien qu'il ne le cite pas explicitement dans le texte, on voit apparaître un intermédiaire de Wheland concomittant avec la déprotonation assistée par la base carboxylate. Aujourd'hui, la classification du palladium^{II} comme métal électrophile dans les réactions de C-H activation permet d'éclairer sous un nouveau jour les données de la courbe de Hammet. Cette même réaction a fait l'objet d'un traitement plus récent de la part de Davies, Donald et Macgregor[21] en 2005, et permet de jeter quelques bases mécanistiques : en partant du complexe plan carré $Pd(OAc)_2$-*N*,*N*'-dimethylbenzylamine, avec un acétate κ^1 et l'autre κ^2 (Figure III-8): le déplacement κ^2-κ^1 de l'acétate κ^2 permet la formation d'une liaison agostique avec la future liaison C-H à rompre, mais aussi la formation d'une liaison hydrogène avec l'acétate déplacé. Ces deux effets ont pour conséquence de polariser et d'allonger la liaison C-H (augmentation de la charge atomique naturelle de +0.09 pour l'hydrogène, augmentation de la longueur de liaison de 1.10 à 1.15 Å) et de placer idéalement l'acétate pour la déprotonation dans un état de transition à 6 membres avec une barrière minimale. L'étape limitante est donc la formation de l'intermédiaire réactionnel complexe agostique plutôt que le complexe de Wheland. Pour disqualifier ce dernier, les

auteurs soulignent que : l'augmentation maximum de la charge positive des carbones du cycle aromatique n'est que de +0.05 et la diminution de la charge positive du palladium n'est que de -0.03 ; de plus la valeur de la pente de la courbe de Hammet négative (ρ = -1.6) et le KIE de 2.2 peuvent être rationalisés en considérant que l'étape limitante (la formation du complexe agostique) implique l'élongation de la liaison C-H, élongation facilitée par la présence de substituants donneurs d'électrons (le KIE modélisé est de 1.2 et les auteurs signalent qu'ils reproduisent de façon qualitative la courbe de Hammet). On peut également remarquer que le profil réactionnel est assez plat, et donc l'intermédiaire agostique a généralement une durée de vie très courte. Ainsi le processus en deux étapes peut être difficile à étudier expérimentalement : savoir si c'est le premier état de transition ou bien le deuxième qui est plus haut en énergie peut s'interpréter dans la pratique par des états de transition respectivement tôt et tardif.

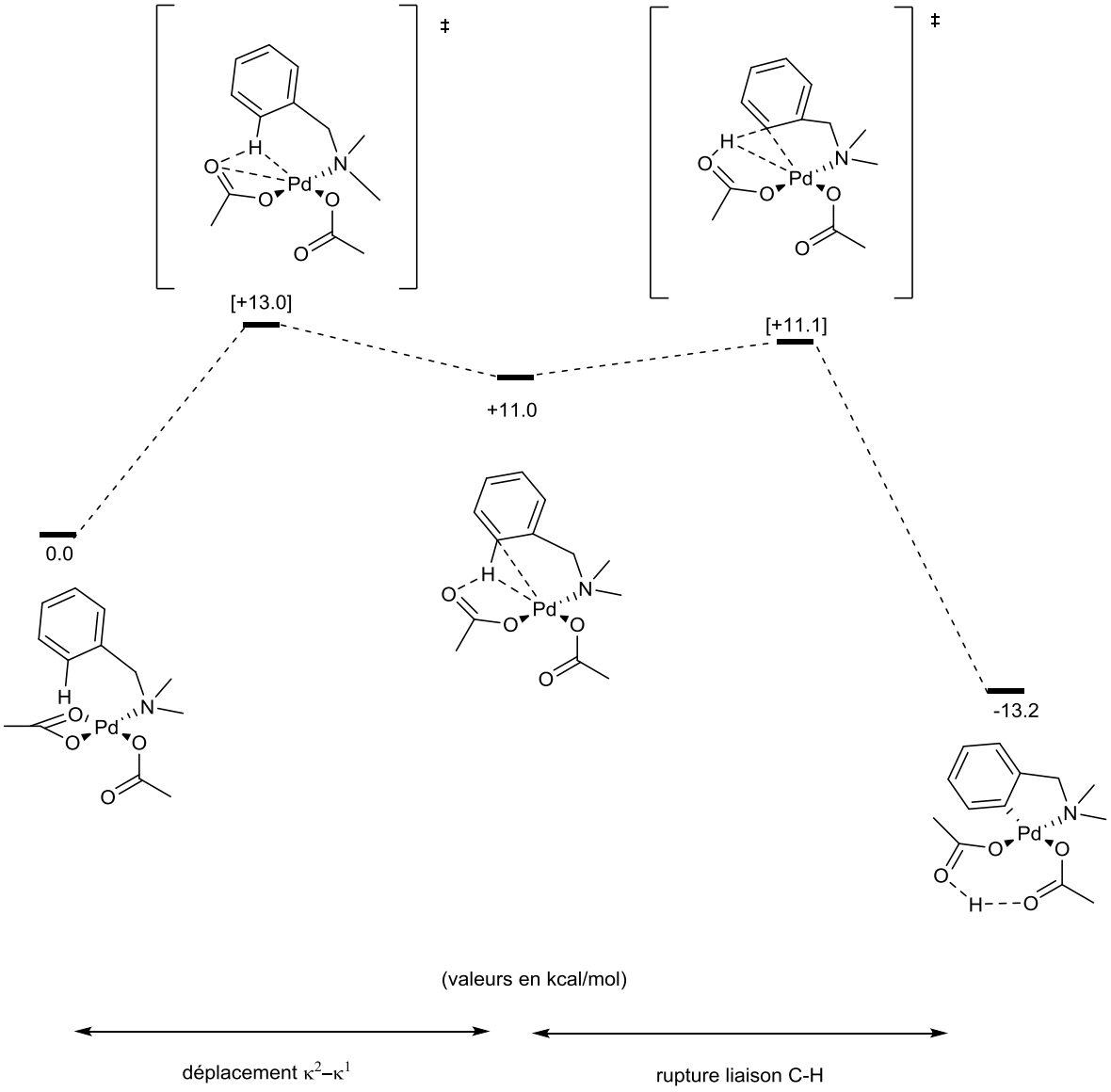

Figure III-8 : mecanisme de la cyclopalladation de la *N,N'*-dimethylbenzylamine

Depuis, de nombreuses études ont permis d'élargir et d'effectuer une comparaison modélisation/expérience, et ainsi nous survolerons les références suivantes pour dégager d'autre grandes caractéristiques en nous concentrant sur les réactions dirigées au palladium : Davies et Macgregor[16], Lapointe et Fagnou[14], Davies et Macgregor[22].

Ainsi D. L. Davies, S. A. Macgregor et C. L. McMullin soulignent que les dénominateurs communs aux réactions d'activation C-H de ce type est la combinaison d'un métal pauvre en électrons et d'un ligand bidendate jouant le rôle de base, rôle facilité par une liaison agostique entre le métal et la liaison C-H à rompre qui augmente la polarisation (et donc l'acidité) de la liaison C-H. L'activation de liaisons C-H est donc ici un processus en deux étapes : en effet, la formation de cette liaison agostique implique qu'un site de coordination soit vacant ; ainsi le premier état de transition concerne le déplacement κ^2-κ^1 de l'acétate, et ce processus peut contribuer de façon significative (voir être le composant majeur) de la barrière de réaction. Le deuxième concerne la rupture de la liaison C-H à proprement parler. De façon générale, ils soulignent que l'intermédiaire agostique a généralement une durée de vie très faible et qu'ainsi on peut voir à l'image des états de transition tôt et tard que le premier état de transition ou respectivement le deuxième soit le plus haut en énergie.

Enfin les mécanismes de types AMLA/CMD, qui sont donc ambiphiliques par nature, permettent d'expliquer des constatations expérimentales qui montrent tantôt que les substrats pauvres en électrons réagissent préférentiellement, tantôt l'inverse (quand la rupture de la liaison C-H a été déterminée comme étape limitante par de effets cinétiques isotopiques) : ainsi, lorsque les substrats riches en électrons réagissent préférentiellement on peut interpréter que l'état de transition est tôt (formation de la liaison agostique), et inversement les substrats pauvres en électrons correspondrait à un état de transition tardif (rupture de la liaison C-H). En effet, les substrats pauvres en électrons augmentent l'acidité des liaisons C-H, et ainsi la base carboxylate aura moins de difficulté à effectuer la déprotonation (Fagnou[23] Figure III-9a). D'un autre côté, les substrats riches en électrons sont capables, comme nous l'avons vu, de former des liaisons agostiques plus fortes ceci, couplé au caractère électrophile du palladium^{II}, explique que les substrats plus riches en électrons réagissent préférentiellement dans certains cas (Fagnou[24]). De plus l'accélération des mécanismes d'activation C-H par l'addition d'acides de Lewis a été démontrée par Tischler et Novàk[25,26] dans deux études successives portant sur l'acylation d'acétanilide. Après avoir montré que l'étape d'activation C-H est bien l'étape limitante, des calculs DFT indiqueront que la coordination de l'acide de Lewis à un des acétates ligandés au palladium permet d'augmenter l'électrophilie de ce dernier et ainsi de faciliter tout le processus d'activation C-H.

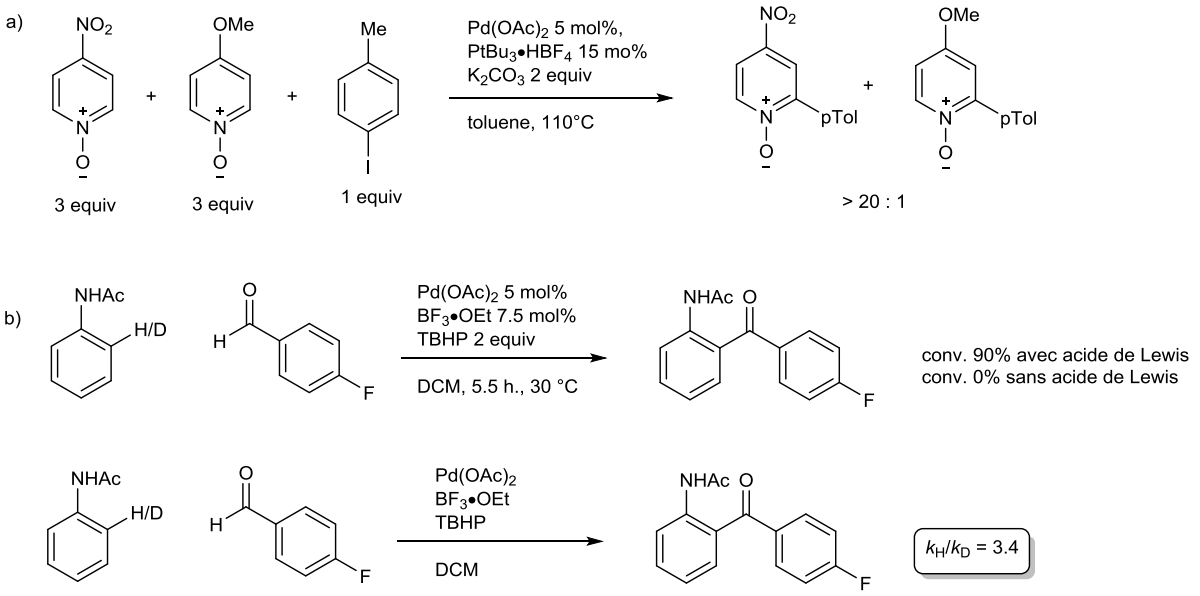

Figure III-9 : accélération des mécanismes d'activation de liaisons C-H

Ainsi, les études par modélisation des réactions d'activation C-H ont montré que les mécanismes de types AMLA/CMD sont très répandus montrant ainsi le rôle essentiel des ligands basiques bidentates de types carboxylates[22]. Ces constatations, ainsi que le travail pionnier de Sokolov en 1979[27], ont certainement été un moteur dans l'adoption de ligands carboxylates énantiopurs permettant d'effectuer l'activation de liaisons C(sp^2)-H de façon asymétrique, sujet faisant l'objet de la prochaine partie.

2. Activation C(sp²)-H dirigée asymétrique

Ici, nous limiterons notre étude aux réactions de C-H activation dirigées où, en partant d'un substrat soit chiral, soit pro-chiral, l'insertion du métal dans la liaison C-H conduit à la formation de métallacycles diastéréomères et est ainsi l'étape stéréodiscriminante permettant la formation de produits optiquement actifs. De plus nous nous limiterons aux réactions catalysées par des complexes de type palladium carboxylate. Ainsi, par nature, les réactions étudiées seront soit des désymétrisations soit des dédoublements cinétiques (simples ou dynamiques). D'un point de vue plus pratique, trois cas distincts existent dans la littérature, et nous dirigeons le lecteur vers deux revues récentes pour un complément d'information[28,29].

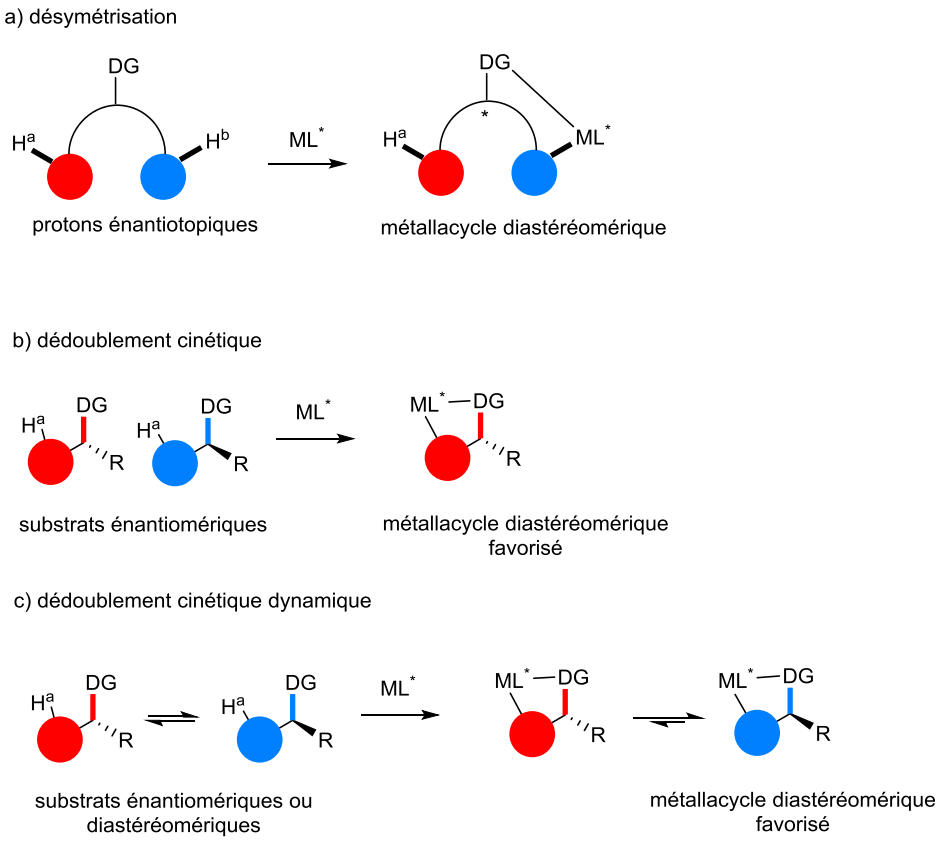

Figure III-10 : cyclométallation diastéréomérique

La première activation dirigée énantiosélective de liaisons C(sp²)-H par des complexes de type palladium carboxylate a été réalisée par le groupe de Yu en 2008[30]. L'alkylation de dérivés de 2-[di(phenyl)methyl]pyridine se fait après une insertion stéréodiscriminante du palladium permettant la désymétrisation de ces substrats (Figure III-11a). Le concept sera par la suite étendu à des substrats de type acide diphénylacétique[31] pour la formation de liaison C-C ou diphenylmethanamine pour la formation de liaisons C-C[32] et C-I[33]. Enfin l'acétoxylation intramoléculaire d'acide diphénylacétique permettra d'accéder à des benzofuranones chiraux[34] (Figure III-11b).

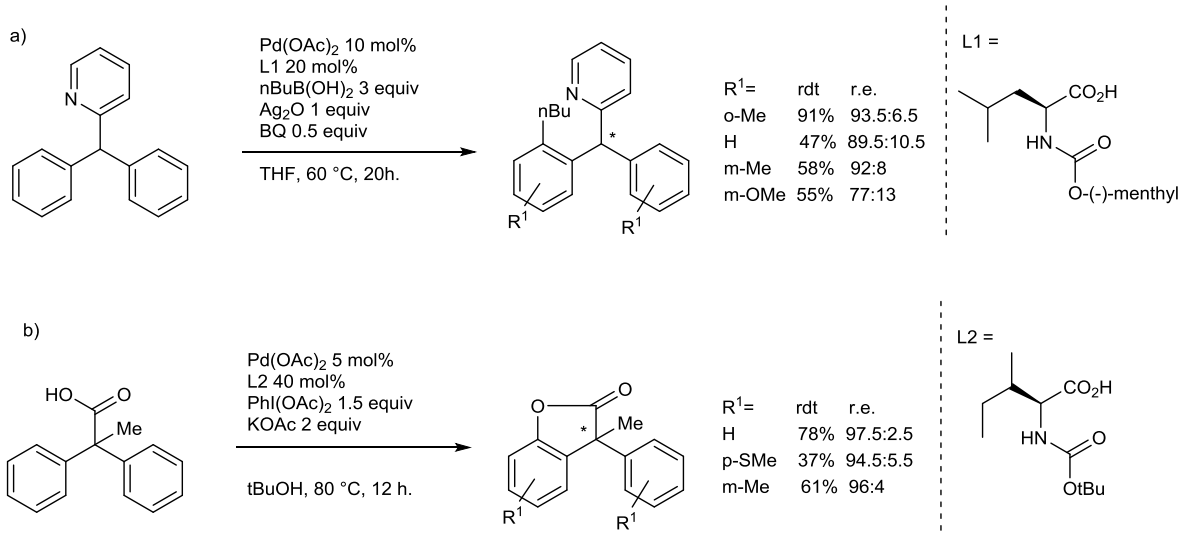

Figure III-11 : activation C-H énantiosélective par désymétrisation

Cette approche sera ensuite utilisée avec succès par Du et collaborateurs dans le groupe de Han[35] (Figure III-12) pour préparer des phosphinamides stéréogènes à l'atome de phosphore, les produits obtenus pouvant être dérivés vers des phosphines avec cependant une légère diminution du rapport énantiomérique.

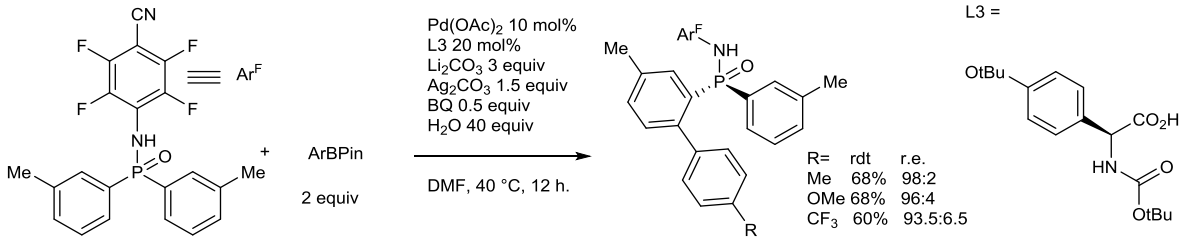

Figure III-12 : obtention de phosphinamides énantioenrichis par activation C-H

De façon surprenante, il faudra attendre 2014 pour voir apparaître le premier dédoublement cinétique catalysé au palladium par activation de liaison C(sp^2)-H dans le groupe de Yu[36]. L'iodation de substrats type benzylamines (Figure III-13a), β-aminoesters (Figure III-13b) (mais aussi alcools) se fera avec d'excellentes sélectivités en utilisant une nouvelle fois des acides aminés mono-protégés.

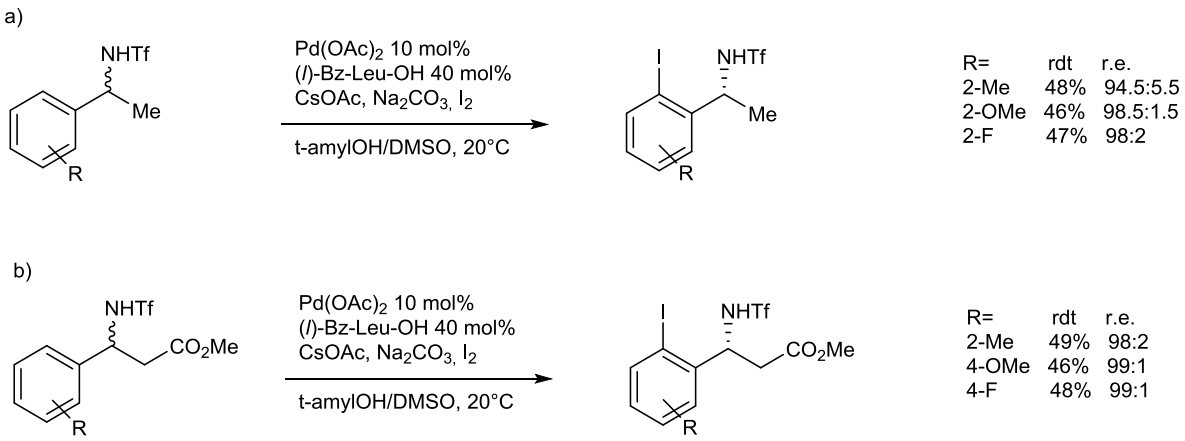

Figure III-13 : déboublement cinétique par C-H activation

Le concept sera ensuite étendu en 2016 vers l'olefination[37] (Figure III-14a) et l'arylation[38] (Figure III-14b) de substrats similaires. Notons que dans chaque cas le groupe protecteur de l'amine de départ, le ligand chiral, ses groupement protecteurs et sa charge catalytique ont dut être optimisés.

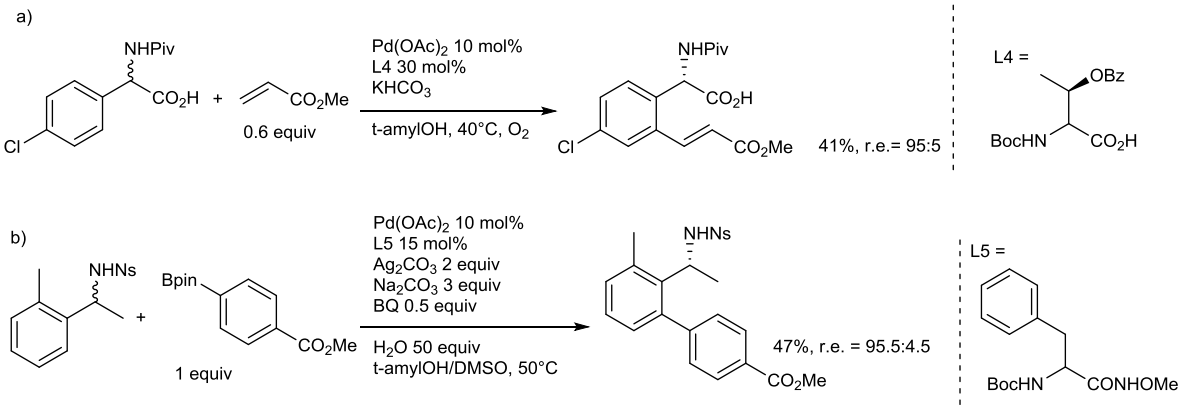

Figure III-14 : déboublement cinétique par C-H activation

Enfin la dernière catégorie concerne l'activation de liaison C(sp^2)-H par dédoublement cinétique dynamique. Dans la pratique cette approche a trouvé des applications dans la synthèse de biaryles ou hétérobiaryles atropisomériques à partir de substrats (ou intermédiaires) non-atropisomériques, et cette thématique sera présentée dans la partie III.B.2.c)(1) de ce manuscrit.

B. Chiralité axiale

1. Historique, généralités

a) Définitions

La chiralité axiale, par la définition de l'IUPAC, est un type de stéréoisomérie résultant de l'arrangement non-planaire de 4 groupes autour d'un axe de chiralité : la molécule ainsi obtenue ne possède pas d'axe de rotation impropre (centre de symétrie ou axe de symétrie), elle n'est donc pas superposable à son image miroir. La première reconnaissance de ce phénomène dans la littérature date de 1922, quand Christie et Kenner[39] réussirent à dédoubler le 2,2'-dinitro-6,6'-dicarboxylate-1,1'-biphenyl.

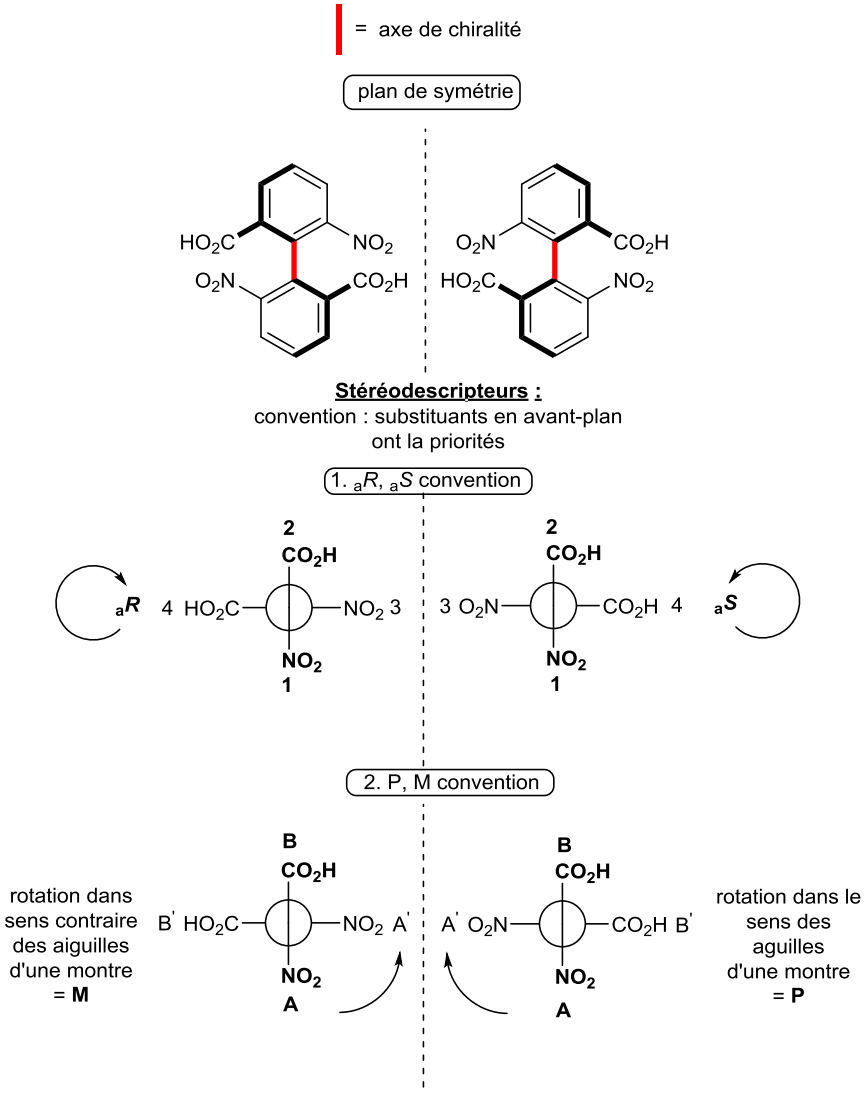

Figure III-15 : convention de chiralité axiale

Il existe deux types de convention pour décrire la configuration absolue des molécules à chiralité axiale (Figure III-15): les stéréodescripteurs $_aR$ (*axially rectus*) et $_aS$ *(axially sinister)* ainsi que *P (Plus)* et *M (Minus)*. Cependant, comme on peut le constater (Figure III-15), $_aR$ ne correspond pas à *P* (sens de rotation des aiguilles d'une montre) pour une molécule donnée (mais à *M*). Ainsi nous utiliserons uniquement les stéréodescripteurs $_aR$ et $_aS$ dans cette thèse. Remarquons que l'exemple de la Figure III-15 représente un type de chiralité axiale qui sera nommé atropisomérisme en 1933 par Khun[40] : l'atropisomérie se définit comme un type de stéréoisomérie où une barrière de rotation suffisamment haute autour d'une liaison simple donne naissance à deux conformères, qui deviennent ainsi des énantiomères ou des diastéréomères, et qui peuvent être séparés à une température donnée. Il est important de noter que la notion d'atropisomérie n'est donc pas absolue : en effet, la même molécule peut, suivant les conditions (température, solvant…), devenir ou cesser d'être atropisomèrique. De plus, la définition qui stipule que la seule *possibilité* d'isoler des atropisomères à une température donnée (définition qui sera précisée par Oki en 1983[41]) et qu'ils aient une demi-vie de racémisation d'au moins 1000 secondes à une température donnée ; 22 kcal/mol à 27 °C est incommode pour le chimiste à la paillasse : en effet l'axe de chiralité des atropisomères ainsi isolés peut ne pas être stable à température ambiante, rendant ainsi nulle la séparation des stéréoisomères sur une échelle de temps raisonnable (heures, jours).

Dans cette thèse nous utiliserons donc notre propre définition de l'atropisomérie : une barrière de rotation autour d'une liaison simple donnant naissance à des stéréoisomères stables, c'est-à-dire où l'épimérisation de l'axe de chiralité est, à l'échelle du temps de cette thèse, négligeable. Comme valeur repère, nous pouvons citer une barrière de rotation de 30 kcal/mol à 25 °C ce qui correspond donc à des conformères qui ont une demi-vie de 35 ans à 25 °C.

De plus pour marquer la différence entre chiralité axiale et atropisomérie, nous utiliserons la convention suivante (Figure III-16) :

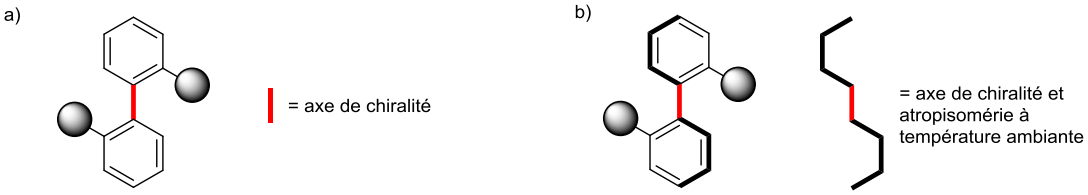

Figure III-16 : formalisme graphique concernant l'atropisomérie

b) Conformation et atropisomérisation

(1) Substituants en position ortho

Comme modèle, nous nous intéresserons aux biphenyles substitués (la plupart des études de la littérature traitent de ce cas), étant entendu qu'il est possible d'extrapoler ces données en première approximation à d'autres types de molécules. L'énergie relative d'un biphenyle suivant l'angle dièdre (Figure III-17 représenté par l'angle formé entre les deux plans contenant les atomes colorés en noir) permet de rationaliser conformation et stabilité des biaryles.

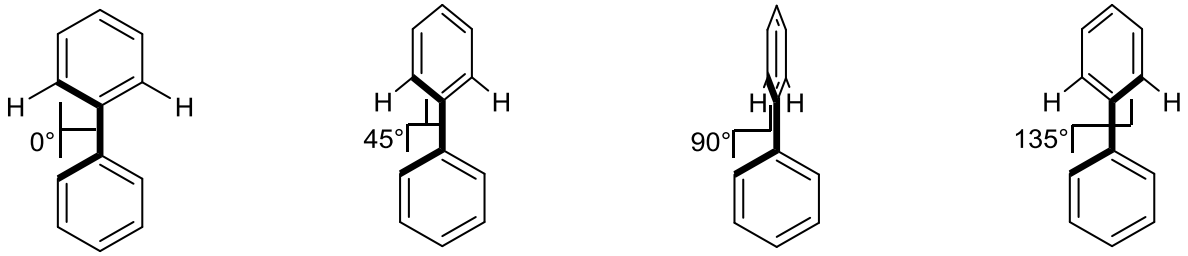

Figure III-17 : angle dièdre du biphényle

Il est intéressant de remarquer que dans le cas le plus simple (le biphényle) la conformation de plus basse énergie n'est ni celle où les deux aryles sont coplanaires (délocalisation maximum possible des électrons π), ni celle où l'angle dièdre est de 90° (répulsion stérique minimum entre les substituants *ortho*Table III-2). Ainsi l'angle optimal (calcul DFT au niveau B3LYP/6-311+G*) se trouve être proche de 45°[42], indiquant une balance entre les effets de délocalisation d'électrons et les effets stériques. Le même effet se retrouve sur les biphényles substitués en 2- ou 2,2'- par les substituants les plus petits, mais, logiquement, l'angle dièdre optimal devient rapidement proche de 90° lorsque l'encombrement stérique des substituants en *ortho* augmente.

Table III-2 : énergie relative (kcal/mol) en fonction de l'angle dièdre optimal

		Angle dièdre					
entrée	Substituants en 2,2'-	0°	45°	90°	135°	180°	Angle dièdre optimal
1	H,H	2.17	0.02	1.79	/	/	42.50°
2	H,F	3.04	0.00	1.20	/	/	45.13°
3	F,F	10.82	0.79	0.72	0.19	4.79	57.87°
4	Cl,Cl	30.11	7.54	0.01	3.38	17.61	84.86°
5	Me,Me	168.77	5.37	0	2.82	16.72	90.69°

On peut donc voir que les effets électroniques ont une influence relativement faible par rapport aux effets stériques sur la conformation des biphényles : cette constata-

tion permet d'estimer aisément la barrière de rotation relative d'un biphényle substitué lorsque l'on change un substituant, *et un seul*. En effet la contribution d'un substituant (*et un seul)* à la barrière de rotation a été déterminée expérimentalement et compilée dans une table. Une telle table, dénommé « B-Values » et rappelant ainsi les « A-values » pour les cyclohexanes substitués, a été proposée pour la première fois en 2009 par Ruzziconi et al.[43] : affinée au fil des ans elle contient aujourd'hui plus de trente substituants[44] (une sélection est proposée Table III-3) . Rappelons cependant qu'elle n'est pas une table d'additivité, c'est-à-dire que la barrière de rotation d'un biphényle tri-substitués ne peut être estimée en additionnant les B-Values de chacun des trois substituants. Elle permet néanmoins d'estimer de façon qualitative quel biphényle aura la barrière de rotation la plus haute en comparant ses substituants un à un. Pour les biphenyls 2,2'-disubtitués, on peut citer le travail de Bott et collaborateurs dans le groupe de Sternhell[45] : ici les enthalpies et entropies d'atropisomérisation ont été mesurées expérimentalement, et on remarquera que les deux paramètres contribuent à la barrière de rotation, l'entropie négative résultant de la réduction de la liberté conformationnelle des substituants *ortho* dans l'état de transition encombré.

Table III-3 : $\Delta G_{rot}^{\ddagger}$ (kcal/mol) expérimentale de biphenyles substitués en *ortho* relative au biphényle

ortho	$\Delta G_{rot}^{\ddagger}$	*ortho*	$\Delta G_{rot}^{\ddagger}$	*ortho*	$\Delta G_{rot}^{\ddagger}$	*ortho*	$\Delta G_{rot}^{\ddagger}$	*ortho*	$\Delta G_{rot}^{\ddagger}$
Me	7.4	OH	5.4	F	4.4	SMe	8.6	$Si(Me)_3$	10.4
Et	8.7	OMe	5.6	Cl	7.7	SPh	8.3	$Sn(Me)_3$	9.1
i-Pr	11.1	OCF_3	5.5	Br	8.7	SOPh	8.6	PPh_2	9.4
t-Bu	15.4	OCH_2OCH_3	5.7	I	10.0	SO_2Ph	12.8	$POPh_2$	10.2
Ph	7.7	CO_2H	7.7	COMe	8.0	SePh	9.1	PCy_2	11.8
CHO	10.2	CO_2Me	7.7	$CHCH_2$	8.2	TePh	9.9	CCH	6.0
NH_2	8.1	NO_2	7.6	NMe_2	6.9	$^{+}NMe_3$	18.1	CN	5.9

On peut dégager quelques tendances en regardant cette table : si on rationalise régulièrement la stabilité conformationelle des biaryles en regardant le rayon de Van der Walls du substituant en *ortho* (F<Cl<Br<I), c'est en fait parfois la nature même de l'atome en *ortho* qui joue le rôle le plus important ; ainsi dans la Table III-3, remarquons les différences d'effets sur la barrière de rotation entre les groupes $C(Me)_3$, $Si(Me)_3$ et $Sn(Me)_3$ (15.4,10.4 et 9.1 kcal/mol) ainsi que par contraste l'absence de différence sur la barrière de rotation des groupes OH, OMe, OCF_3 et OMOM (5.4, 5.6, 5.5 et 5.7 kcal/mol). Ces valeurs peuvent s'expliquer si l'on examine l'état de transition pour passer d'un atropisomére à l'autre (Figure III-18): dans le cas de biaryles 2,2'-di-substitués, il existe deux possibilités (Figure III-18.A). Soit les hydrogènes vont chacun croiser un des substituants R, état de transition trans-coplanaire $\mathbf{A_1}$, soit ils vont se croiser et donc les substituants R se rencontreront, état de transition cis-coplanaire $\mathbf{A_2}$; l'état de transition le plus favorable est ainsi $\mathbf{A_1}$ et rares sont les cas où on observe l'atropisomérisme à température ambiante. Pour les biaryles tri-substitués (Figure III-18.B), les substituants R sont obligés de se croiser, donnant lieux à des barrières de rotation plus élevées, et ainsi les biaryles tri-substitués sont

généralement atropisomériques à température ambiante. Cependant il faut remarquer que cet état de transition n'est pas strictement coplanaire, pour diminuer la répulsion stérique entre les substituants *ortho*, les cycles aromatiques sont légèrement courbés en-dehors du plan, comme l'ont montrés des calculs DFT sur l'atropisomérisation des binaphthyles et dérivés[46].

De même, la propension des substituants *ortho* à adopter une conformation qui minimise les répulsions stériques dans l'état de transition est importante : ainsi la contribution décroissante à la barrière de rotation des groupes $C(Me)_3$, $Si(Me)_3$ et $Sn(Me)_3$ (Table III-3), qui va à l'encontre des rayons de Van der Walls, peut s'expliquer par les longueurs de liaisons croissantes C-C, C-Si et C-Se (respectivement 1.54, 1.89, et 2.15 Å, valeurs moyennes[47]) qui permettent de diminuer la répulsion stérique dans l'état de transition en éloignant les groupes *tert*-butyles du substituant qu'ils doivent croiser. L'absence significative de différence sur la barrière de rotation des groupes OH, OMe, OCF_3 s'expliquant par la possibilité des substituants de l'oxygène d'adopter une conformation où ils pointent à l'opposé du substituant *ortho* qu'ils croisent dans l'état de transition.

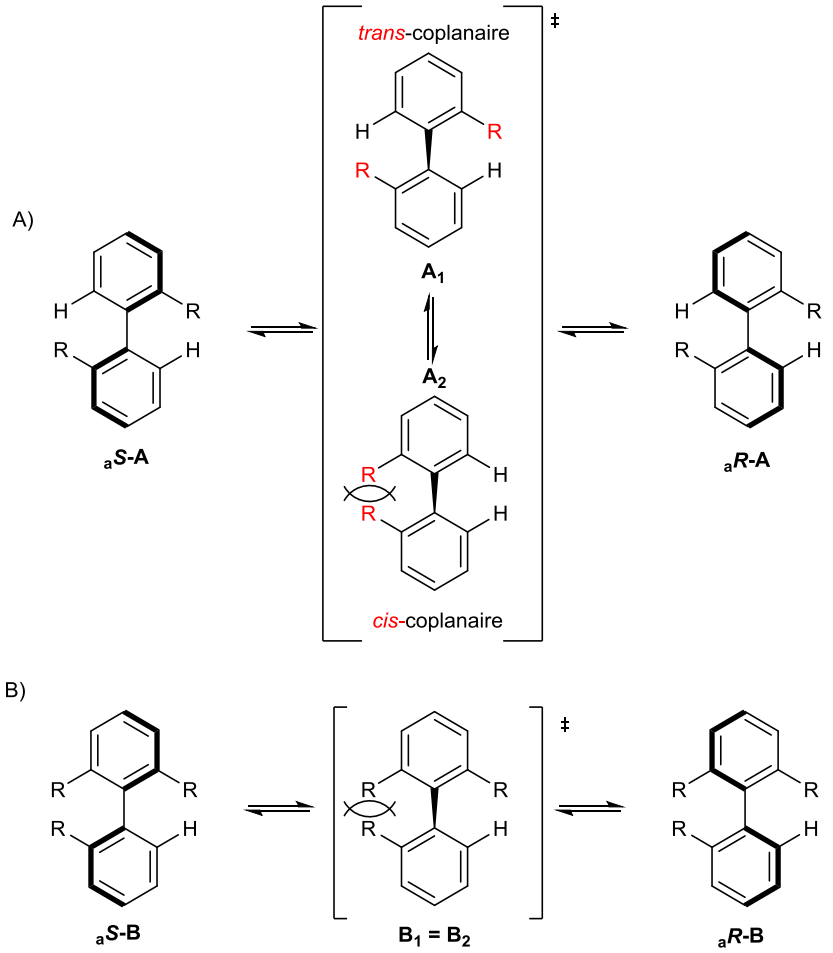

Figure III-18 : mécanisme d'atropisomérisation

(2) Substituants en position *meta*

La possibilité d'adopter une conformation qui minimise l'encombrement stérique explique en grande partie l'influence des substituants *meta* sur la barrière de rotation. Ces derniers, par un effet dit de contrefort, vont en effet diminuer les conformations accessibles par un substituant *ortho* adjacent[48] (Figure III-19a), et/ou diminuer la possibilité de ces substituants de se courber à l'opposé du substituant lui faisant face pour diminuer l'énergie de l'état de transition[49] (Figure III-19b), et ainsi vont contribuer à augmenter la barrière de rotation.

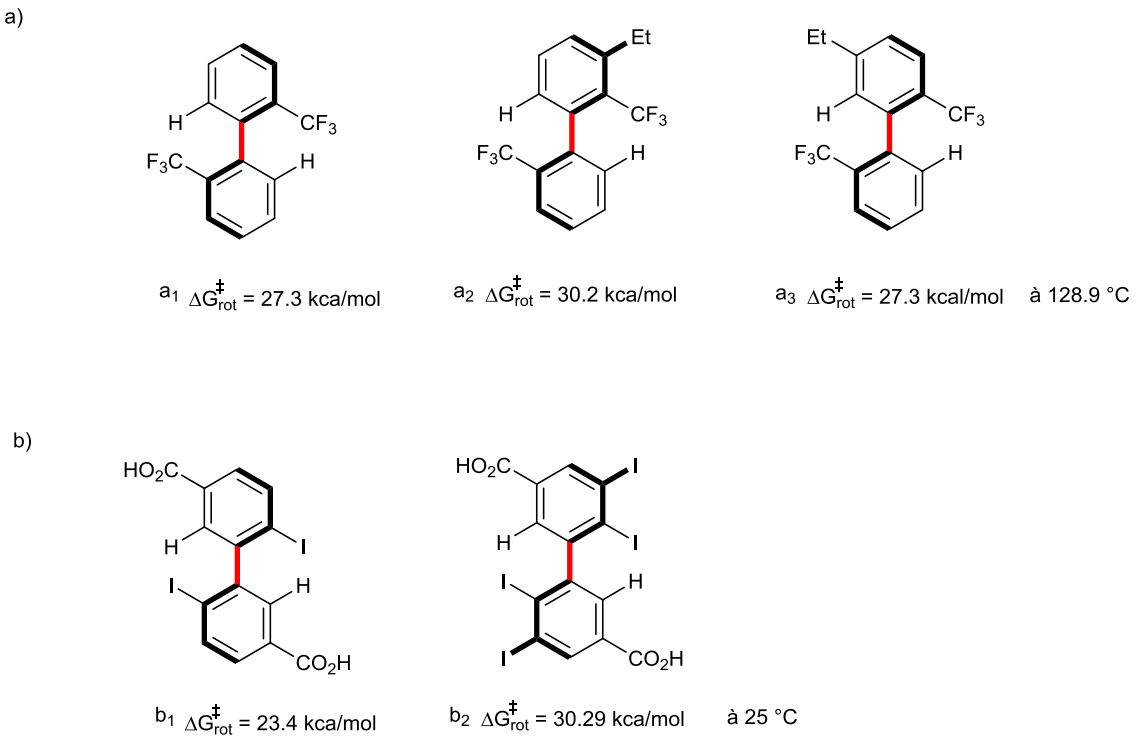

Figure III-19 : influence des substituants *meta*

(3) Substituants en position para

L'influence des substituants en position *para,* basée sur des effets électroniques est, comme nous l'avons vu plus faible. Une étude systématique sur des 2,2'ditrifluoromethylbiphenyls réalisé par Wolf et collaborateurs[50] (Figure III-20) montre que les substituants donneurs d'électrons par effet mésomère diminuent la barrière, alors que des accepteurs l'augmentent. Ceci étant dû à l'augmentation de la population des orbitales π* qui diminue le caractère sp^2 et ainsi facilite la courbure en dehors du plan des cycles aromatiques dans l'état de transition pour les groupes donneurs d'électrons. Pour les groupes accepteurs, on observe le phénomène inverse avec augmentation du caractère sp^2 et augmentation de la barrière de rotation.

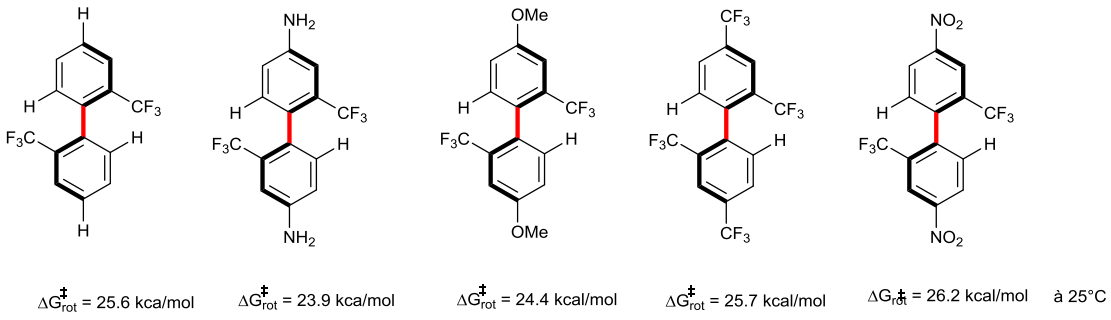

Figure III-20 : influence des substituants *para*

(4) Substituants pontants

La formation d'un pont peut avoir une grande influence sur l'atropostabilité des biaryles : la formation d'un pont à cinq membres fait significativement baisser la barrière de rotation (Figure III-21). Ainsi la barrière de rotation du binaphthyl a été mesuré à 24.1 kcal/mol[51], tandis chez que son homologue comprenant un substituant *ortho* pontant elle a été mesurée à 13.4 kcal/mol[52]. On pourra argumenter que le pont tendu diminue la liberté conformationelle et force les deux aromatiques à adopter une conformation où leur angle dièdre est proche de celui requis dans l'état de transition coplanaire. Le même effet peut être trouvé dans le formation d'un pont à 6- ou 7-membres comme le montre l'étude de Bringmann sur la formation d'un pont lactone à 6 chainons[53], ou celle de Seki sur un pont anhydride d'acide à 7 chainons[54].

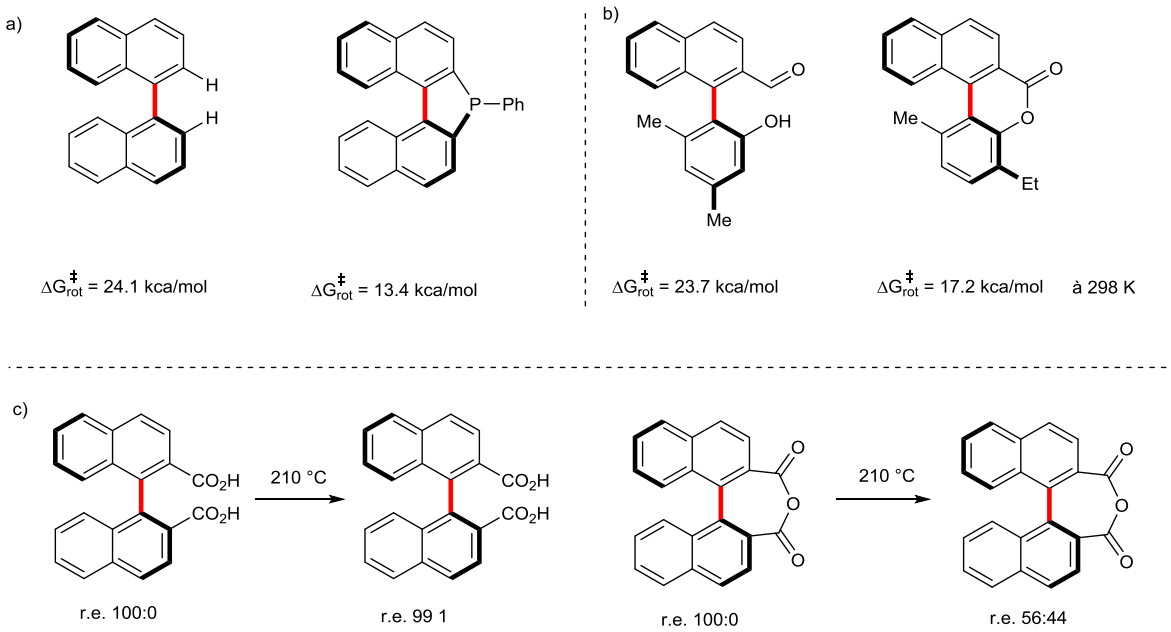

Figure III-21 : influence de substituants pontants

Cependant on peut se demander quel rôle joue la nature même du pont. En effet dans les exemples présentés Figure III-21 b et c, la possible conjugaison des substi-

tuants pontants avec le cycle est attendue d'apporter une stabilisation supplémentaire dans l'état de transition coplanaire.

Enfin notons que la présence d'éléments stéréogènes dans le pont, en créant des atropodiastéréomères, peut influencer fortement la conformation du biaryle ; il est alors difficile de savoir avec certitude, quand on est en présence d'un seul diastéréomère, s'il est effectivement atropisomèrique (effet cinétique résultant d'une barrière de rotation élevée), ou si l'équilibre entre les deux diastéréomères est complétement déplacé dans un sens (effet thermodynamique). Deux exemples illustrent la complexité de ce problème : dans l'exemple Figure III-22a les auteurs ont mesuré la barrière de rotation des deux atropodiastéréomères, et le $\Delta G°_{298K}$ correspond bien à la constante d'équilibre trouvé par ^{1}H RMN[55]. Dans le cas présenté Figure III-22b, les rapports diastéréomériques mesurés sont bien différents pour les deux composés. Cependant les barrières de rotation sont équivalentes ce qui implique que les barrières de rotation dans le sens inverse sont, elles différentes, et qu'ainsi la présence d'un substituant stéréogène supplémentaire modifie l'équilibre[56]. Notons aussi le cas présenté Figure III-22c, où, bien qu'il n'y ait aucun substituant *ortho* le tripeptide biphenomycin A n'a été observé que sous cette forme atropisomérique.

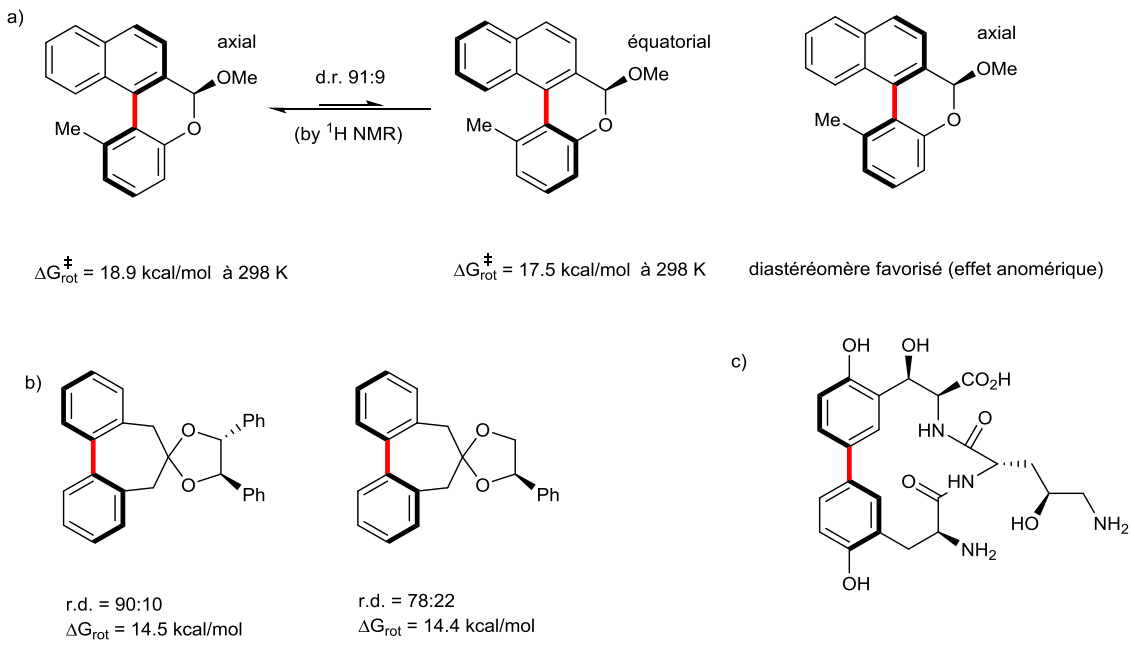

Figure III-22 : influence des substituants pontants stéréogènes

2. Méthodes synthétiques

Les méthodes de constructions atroposélectives d'un biaryle peuvent être arbitrairement regroupées en trois grandes catégories utiles, suivant l'état d'avancement de construction de la liaison qui constitue le futur axe de chiralité (Figure III-23): chaque catégorie sera ensuite examinée en regroupant les réactions similaires dans des sous-catégories pertinentes. De plus les exemples du même type que le travail réalisé dans cette thèse seront décrits de façon exhaustive, c'est-à-dire les réactions d'activation C-H, soit par arylation directe (catégorie A, partie III.B.2.a)(2)), soit par activation C-H sur un biaryle existant (catégorie C, partie III.B.2.c)(1)).

a) catégorie A : la liaison Ar-Ar n'existe pas encore : on assiste ici au couplage de deux aromatiques.
b) catégorie B : La liaison existe, mais elle n'est pas une liaison Ar-Ar : on va donc construire un, ou des, cycles aromatiques autour du futur axe de chiralité.
c) catégorie C : La liaison Ar-Ar existe déjà : ici nous avons affaire à des biaryles qui sont soit chiraux mais non-atropisomériques, soit à des biaryles prochiraux.

Nous dirigeons le lecteur vers des revues plus complètes[57–59] pour un supplément d'information.

a) catégorie A : couplage de deux aryles, ex : couplage oxydant, couplage par métaux de transitions

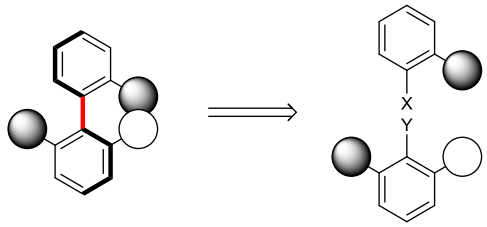

b) catégorie B : construction de cycle(s) aromatique(s), ex: cycloadditions, transfert de chiralité

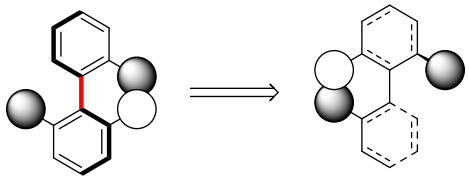

c) catégorie C : modification dun biaryle existant, ex: désymétrisation ($R^1=R^2$), dédoublement ($R^1 \neq R^2$)

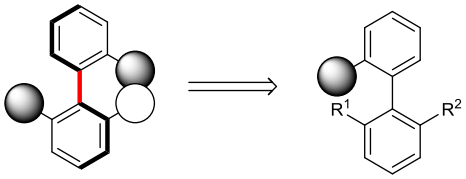

Figure III-23 : méthodes de synthèse atroposélectives

a) Couplage Aryle-Aryle

Ici, nous pouvons séparer la synthèse des biaryles suivant le degré de fonctionnalisation des unités aryliques couplées (Figure III-24): aucune (1: coupage C-H/C-H), une (2: coupage C-Y(Z)/C-H), ou les deux (3: coupage C-Y/C-Z) positions des unités aryliques couplées peuvent être fonctionnalisées.

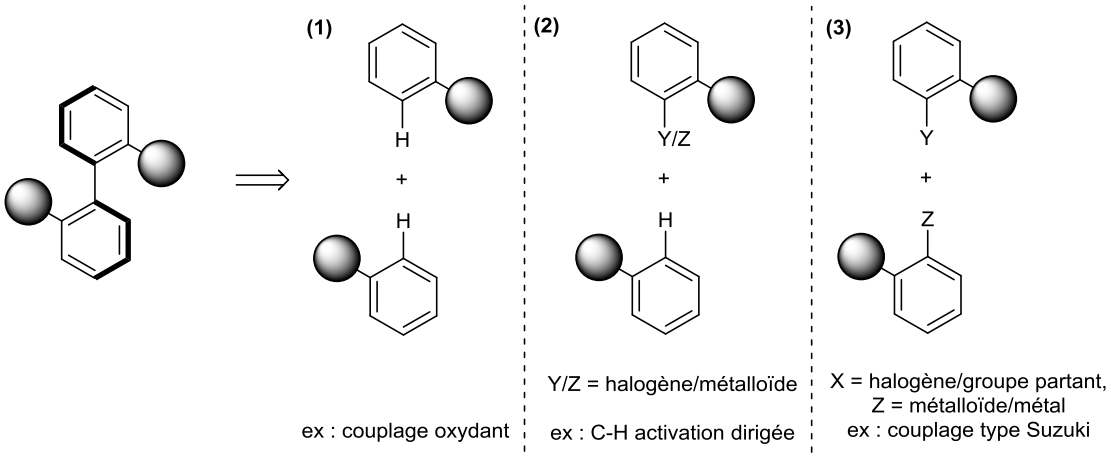

Figure III-24 : types de couplages Ar-Ar

(1) Couplage à partir de deux partenaires non-préfonctionnalisés

Ce type de couplage, par sa nature, est plus aisé à réaliser dans les cas d'homocouplage, de polymérisation, et de couplage intramoléculaire (pas de différenciation entre les deux partenaires de couplage). Sa nature oxydante le rend plus adaptés aux aryles comportant des substituants donneurs en électrons (-OH,-OMe,-NH_2), placés à des positions où ils pourront exercer leurs effet mésomère donneur (donc *ortho* et *para* de l'axe biarylique à former). Il mérite d'être mentionné pour les raisons suivantes:

1) les produits naturels pouvant être construits par cette stratégie : ainsi le couplage oxydant du naphthol iodé (Figure III-25a) en présence de cuivre permet d'accéder à des dérivés de BINOLs constituant une plateforme commune vers les produits naturels de la famille perylenequinone[60], phototoxines responsable de maladie chez de nombreuses espèces de plantes cultivées. Un autre exemple important est l'obtention du fragment biarylique de l'antibiotique vancomycine, en utilisant cette fois comme oxydant stoichiométrique un complexe de vanadium[61] (Figure III-25b).

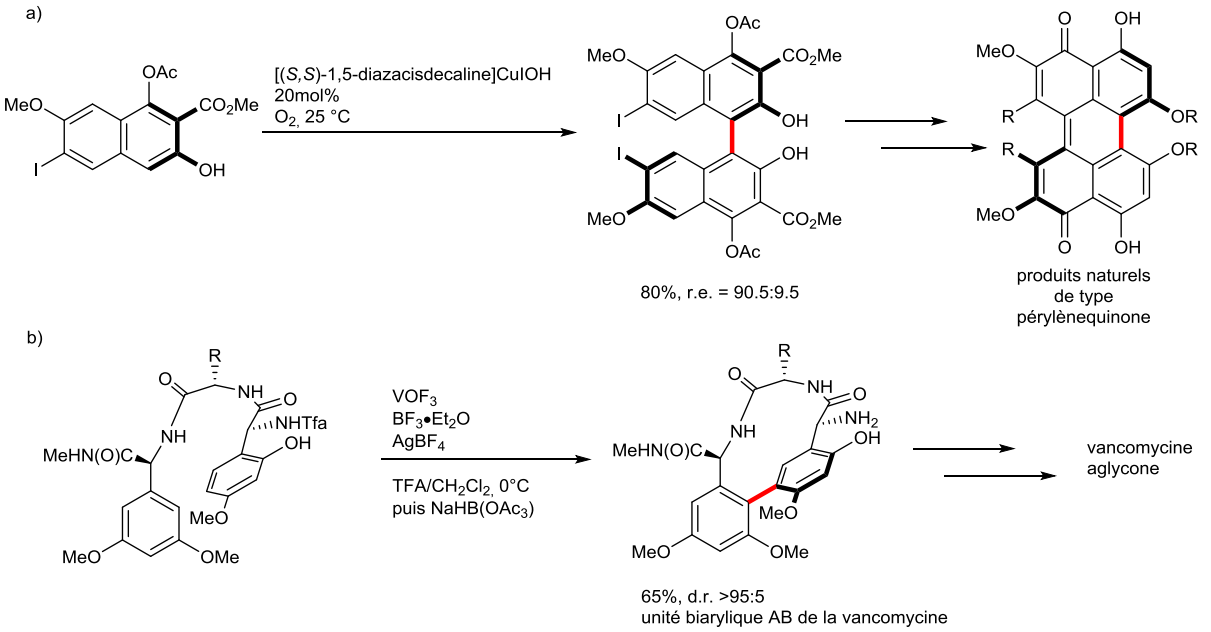

Figure III-25 : produits naturels obtenus par couplage oxydant

2) l'accès aux squelettes de type BINOLs, plateformes vers de nombreux ligands à chiralité axiale importants[62] (acides phosphoriques, phosphoramides, BINAP), cette fois par utilisation catalytique d'un complexe bimétallique atropisomérique de vanadium, l'oxygène de l'air pouvant être utilisé comme oxydant terminal (Figure III-26).

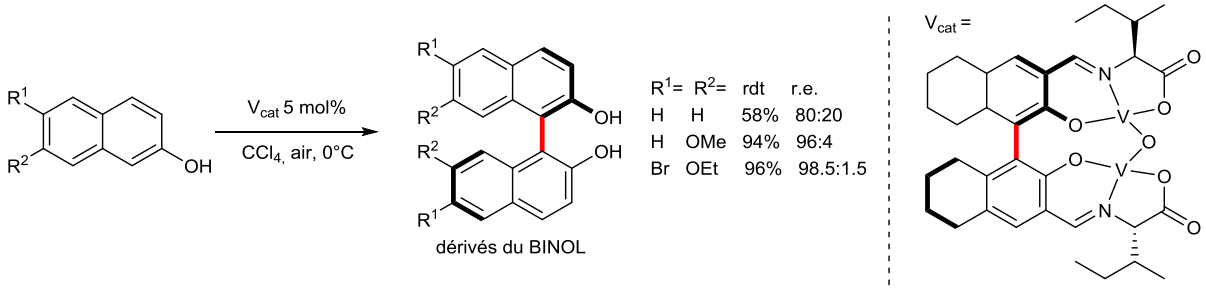

Figure III-26 : couplage oxydant utilisant l'air comme oxydant terminal

Plus récemment des couplages de type organocatalysés se sont montrés très efficaces pour obtenir des squelettes atropisomériques. En effet ils exhibent généralement une économie d'atomes impressionnante car ils n'utilisent pas de réactifs, seulement un catalyseur et les substrats. Ils ont tout d'abord été limités au départ à des couplages intramoléculaires et à des squelettes symétriques (Kürti, Ess, Devonas et collaborateurs[63] puis List et collaborateurs[64] en 2013 Figure III-27).

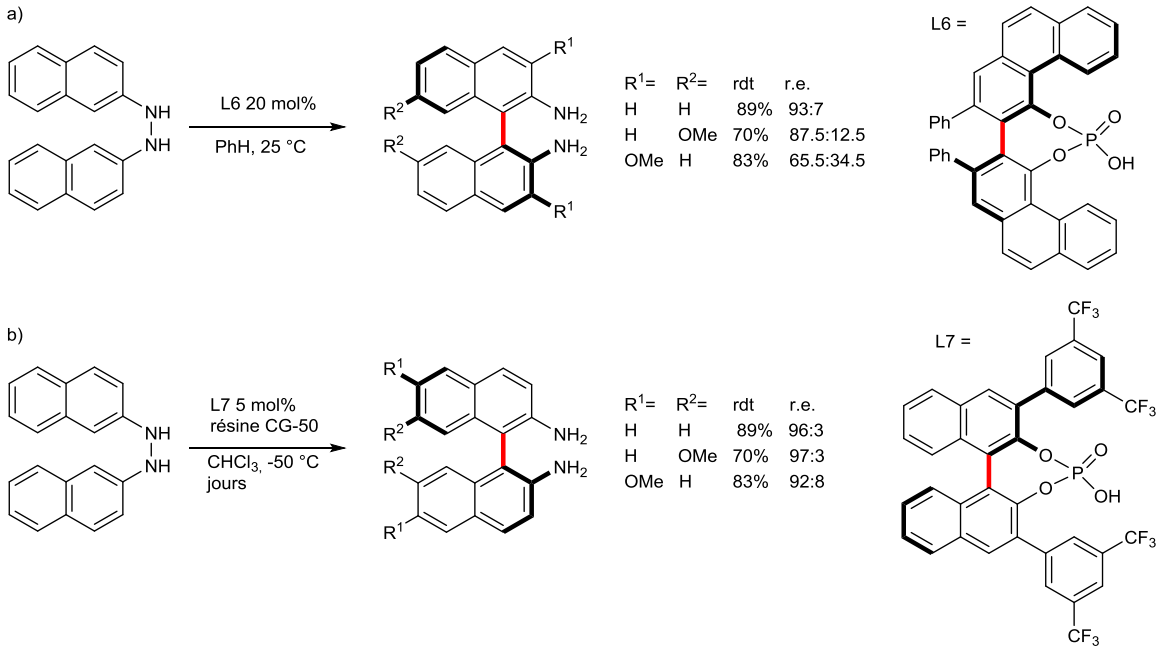

Figure III-27 : couplage oxydant intramoléculaire organocatalysé

Puis des auteurs ont su utiliser la dichotomie électrophile/nucléophile des substrats pour s'affranchir de ces limitations. Ainsi Zhang, Li Shi et collaborateurs[65] mettent au point un couplage entre des naphtols (nucléophile) et des indoles substitués en position 2 par un motif *gem*-diphenylethanol. La formation d'un carbocation tertiaire aromatique à cette position permet à l'indole de jouer le rôle d'électrophile, obtenant ainsi les produits de couplage avec d'excellents rendements et sélectivités sélectivi-

tés (Figure III-28a). Puis en 2017, Qi, Mao et Tan reportent une arylation atropoénantiosélective d'indoles permettant, suivant la substitution de la position 2 de l'indole d'accéder à deux types de produits atropisomériques différents (Figure III-28b et c), avec cette fois l'indole dans le rôle du nucléophile et un azonaphthalène N-substitué par un groupement électroattracteur dans le rôle de l'électrophile. Les indoles substitués par un groupement *tert*-butyle conduisent à des biaryles de type aminonaphthyle-indoles avec des rendements et énantiosélectivités excellent (Figure III-28b). Puis en utilisant des indoles substitués par un groupement moins encombrant en position 2, on obtient des produits originaux représentés Figure III-28c. Si les rendements sont cette fois corrects à très bons, les énantiosélectivités sont presque parfaites (le mécanisme de formation de ces produits est présenté Figure III-29). Soulignons que toutes ces approches organocatalytiques se basent sur un transfert de chiralité centrale à axiale dans un processus de réaromatisation. D'autres approches organocatalytiques où le transfert de chiralité centrale à axiale se fait dans une étape séparée, sont présentés plus loin dans ce manuscrit.

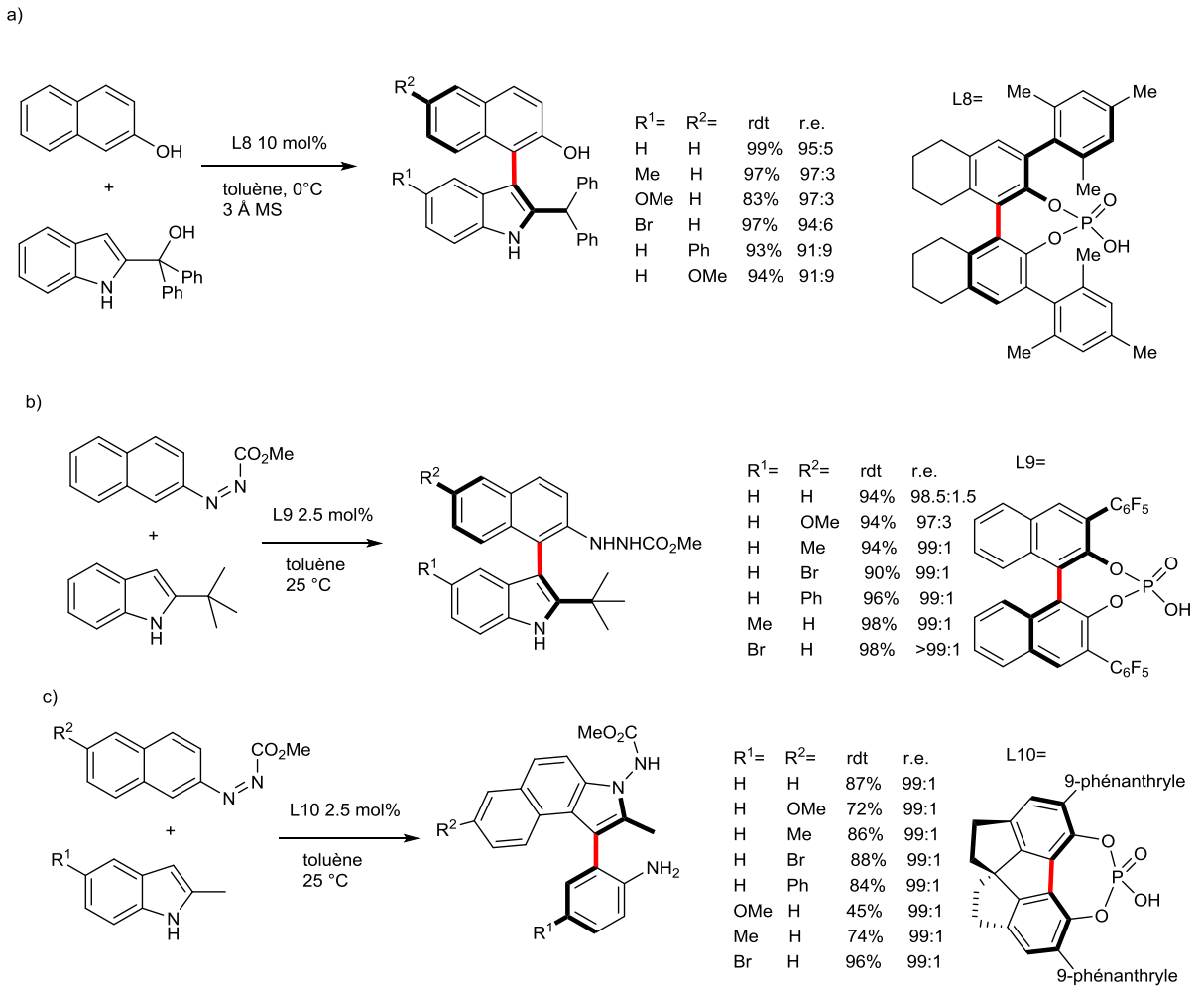

Figure III-28 : arylation organocatalytique utilisant des indoles

Le mécanisme de formation des produits Figure III-28c est original et intéressant à examiner : A) après attaque nucléophile de l'azoaryle par l'indole, deux centres asy-

métriques sont créés. B) la réaromatisation de l'azodérivé créé une première atropisomérie C(sp^2)-C(sp^3) et un premier transfert de chiralité central vers axiale, puis l'attaque de la position 2 de l'indole, si le groupe R n'est pas trop encombrant, interromps le processus de réaromatisation de l'indole pour former un bicycle fusionné (C) avec un transfert de chiralité axiale vers centrale qui s'opère. Enfin (D) la fragmentation de l'intermédiaire reconduit à un biaryle atropisomérique avec un nouveau transfert de chiralité centrale vers axiale, pour former le produit.

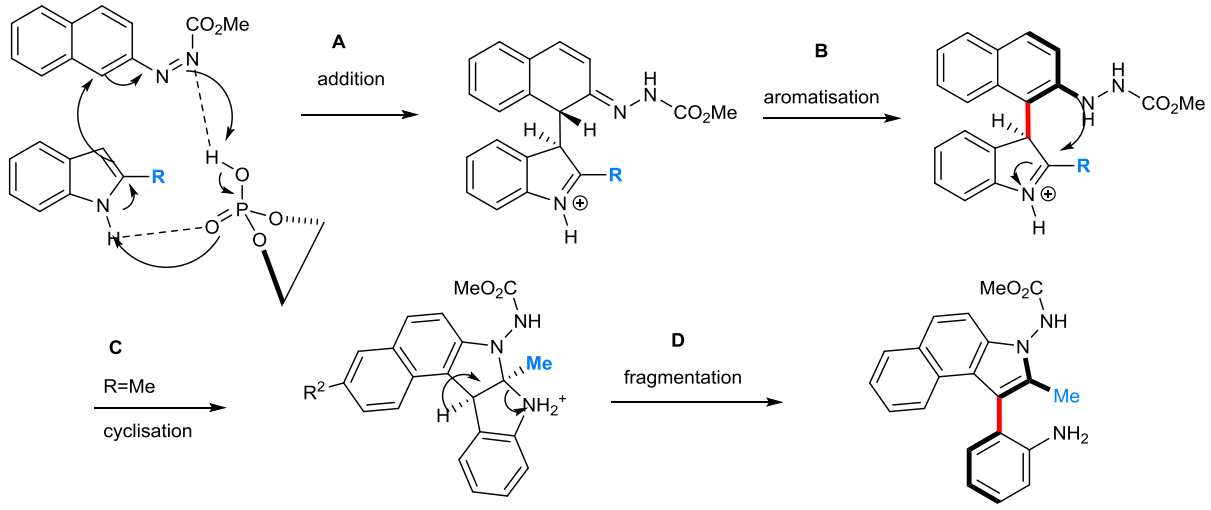

Figure III-29 : mécanisme de formation des produits Figure III-28c

(2) Couplage avec un des deux partenaires préfonctionnalisé

Contrairement à l'importance prise par les réactions de C-H fonctionnalisation pour la construction non-atroposélective de biaryles (arylation directe, nous renvoyons le lecteur à une revue utile pour se familiariser avec l'état des connaissances[66]), il n'existe, à notre connaissance, qu'un seul véritable exemple d'arylation directe atroposélective intermoléculaire[67,68] (Figure III-30 par le groupe d'Itami). La réaction fut tout d'abord développée dans une version non-énantiosélective, impliquant le couplage de thiophènes avec des acides boroniques, catalysé au palladium avec un ligand bis-oxazoline symétrique C_2 et avec le 2,2,6,6-tetramethylpiperidine1-oxyl (TEMPO) comme oxydant stœchiométrique dans le diméthyleformamide. Puis, l'ajout d'acide trifluoroacétique permettra une excellente régiosélectivité en faveur de la position β des thiophènes. Enfin, pour obtenir une atroposélectivité modérée, un remaniement des conditions réactionnelles fut nécessaire, pour finalement conduire la réaction dans le 1-propanol avec le ligand présenté Figure III-30a. L'induction asymétrique se fait ici au dépend de la réactivité car les produits R = Me, *i*-Pr avaient pu être obtenus avec respectivement 63% et 37% de rendement et des ratios énantiomériques de 70.5 :29.5 et 86 :14. Les auteurs revisiteront ensuite leur réaction pour permettre l'utilisation de l'oxygène de l'air comme oxydant terminal (Figure III-30b): ayant remarqué l'effet bénéfique du DMSO d'abord comme solvant, puis comme additif sub-stoechiométrique, les auteurs développeront le ligand sulfoxyde-

oxazoline présenté Figure III-30b. Notons que pour obtenir une meilleure induction asymétrique, ils préformeront le complexe (L12) avant la réaction de couplage.

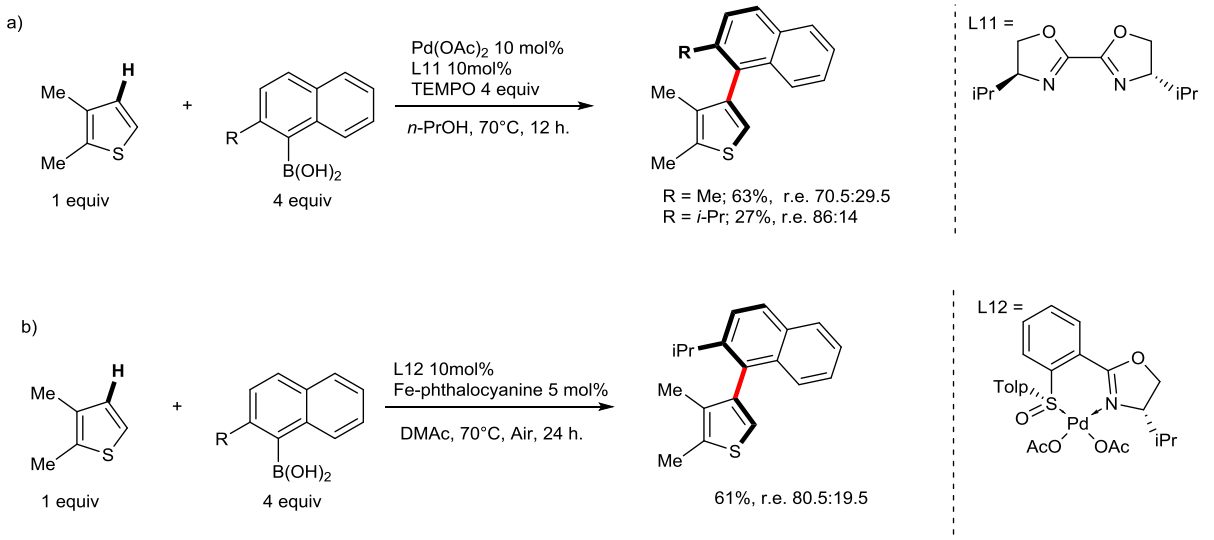

Figure III-30 : arylation directe atroposélective

Le deuxième exemple d'arylation directe dirigée atroposélective intermoléculaire a été reporté en 2017 par Jia, Antonchick, Waldmann et collaborateurs[69] (Figure III-31), ce n'est pas à strictement parler un couplage Ar-Ar : en effet le complexe rhodium^{I} cyclopentadiényle énantiopur s'insère en *ortho* d'une *N*-méthoxybenzamide (où l'une des positions *ortho* est bloquée pour permettre l'insertion du métal dans la position la plus encombrée). L'originalité venant du fait que le partenaire de couplage n'est pas un aryle mais un diazonaphthalèn-2(1H)-one : ce dernier, après aromatisation, conduit donc à des biaryles de type phényle-naphtyles avec généralement de bons rendements et de bonnes atroposélectivités. Si trois des positions *ortho* ne sont donc pas modulables (*N*-méthoxyamide, hydroxyle, naphthyle) durant le couplage, l'obtention de biaryles tetra-substitués par couplage intermoléculaire est remarquable. De plus, la réaction tolère des aryles substitués par de l'iode ou du brome, ce qui permet de diversifier les produits obtenus. Enfin remarquons que pour l'instant seul le ligand présenté Figure III-31 a été obtenu directement sous forme énantiopur, les autres dérivés synthétisés nécessitant une séparation par HPLC chirale préparatoire.

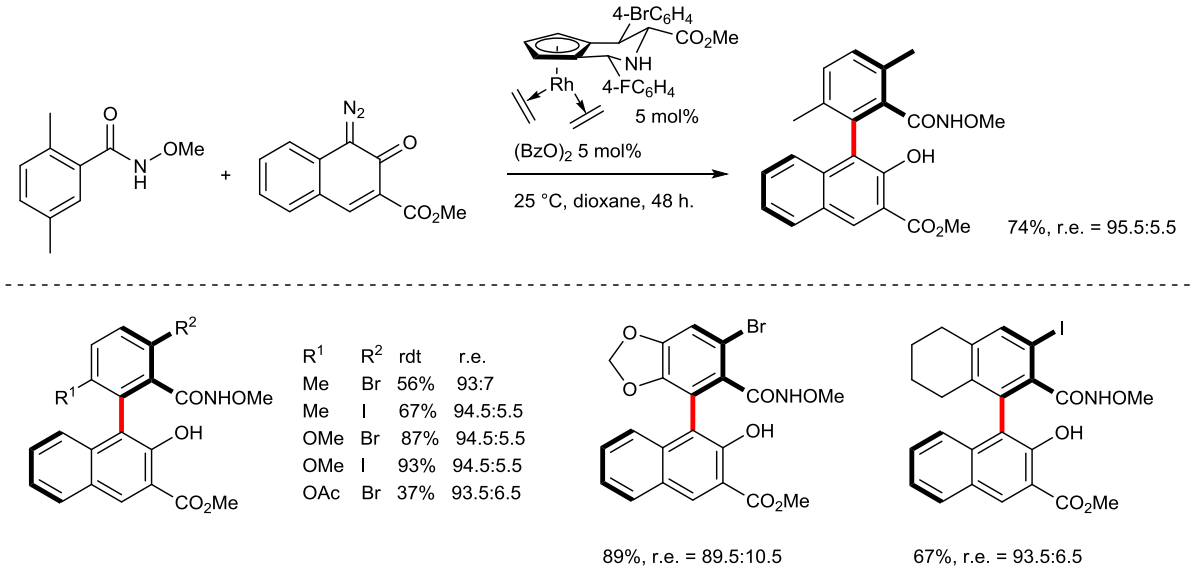

Figure III-31 : couplage intermoléculaire atroposélectif

Ce nombre d'exemples limités illustre bien l'antagonisme existant dans les réactions d'arylation directe atroposélective : l'efficacité du couplage diminue rapidement avec l'augmentation de l'encombrement stérique autour du futur axe de chiralité, l'encombrement stérique étant par ailleurs une condition nécessaire pour l'existence de l'atropisomérie. D'un point de vue plus pratique on pourrait également dire que l'augmentation de la température de réaction nécessaire au couplage de partenaires encombrés diminue le champ des produits atropisomériquement stables accessible dans les conditions réactionnelles. Enfin, remarquons que le problème de régiosélectivité inhérent à la C-H activation se trouve exacerbé dans le cas de couplage atroposélectif. Prenant comme exemple le cas le plus simple, un biaryle tri-substitué où l'un des substituants joue le rôle de groupe directeur : il existe donc deux possibilités de réaliser un tel couplage, Figure III-32a ou Figure III-32b. Dans le cas a) la liaison C-**H**$^{\mathbf{a}}$ se trouve de fait à la position la plus encombrée ; ainsi l'insertion du métal se fera certainement dans la liaison C-**H**$^{\mathbf{b}}$. De plus, dans le cas b), c'est cette fois le partenaire de couplage qui comporte deux substituants *ortho.* Pour que le produit soit atropisomérique, les deux substituants doivent être relativement volumineux et ainsi la sélectivité vers le produit a*R* ou a*S* lors de la formation de la liaison Ar-Ar sera difficile. Par ailleurs, la synthèse d'un panel relativement large de tels iodoarenes *ortho,ortho'*-disubstitués dissymétriques présente, en soi, un défi synthétique.

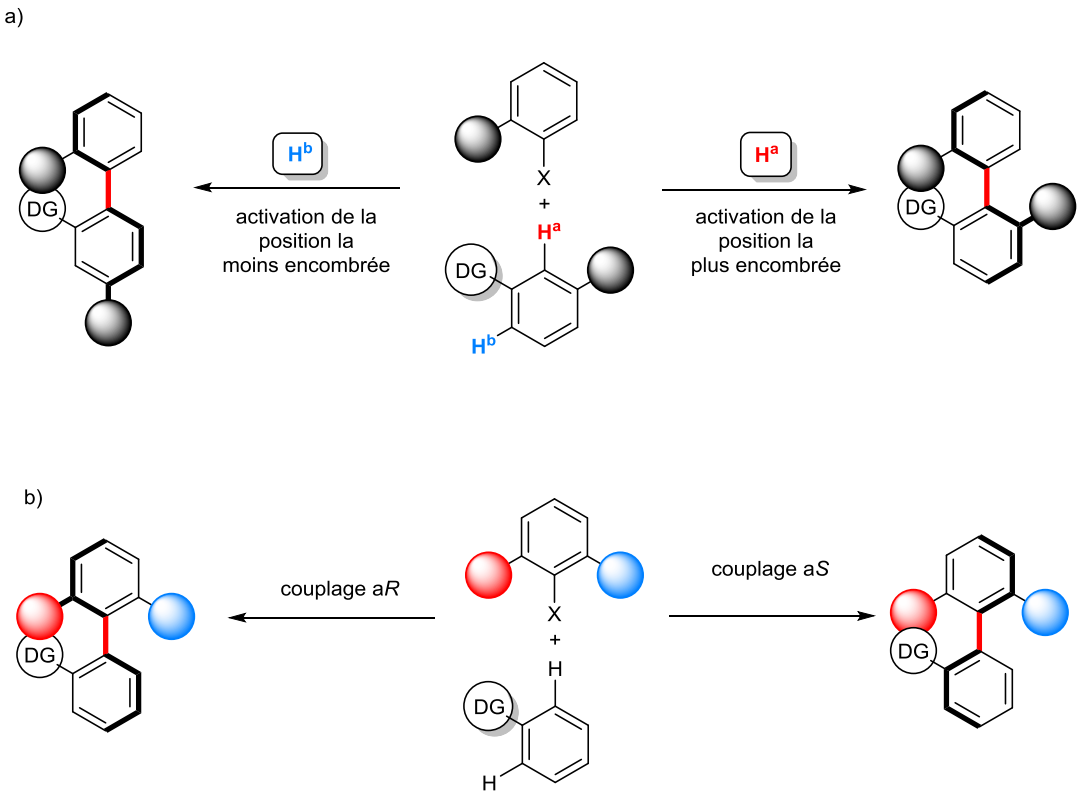

Figure III-32 : défis spécifiques du couplage Ar-Ar atroposélectif

(3) Couplage à partir de deux partenaires préfonctionnalisés

Nous entrons ici dans la partie la plus féconde de la construction atroposélective par couplage Ar-Ar : en effet, il s'agit de l'application atroposélective de réactions faisant partie des classiques de la chimie (couplage de Suzuki-Miyaura, couplage d'Ullmann, S_NAr). Dans ce manuscrit, nous présenterons seulement des exemples représentatifs de ces différentes approches.

(a) Couplage de Suzuki-Miyaura

Concernant le couplage de Suzuki-Miyaura, des approches diastéréosélectives ont rencontré un certain succès dans la construction du cycle A-B de la vancomycine : ainsi Leermann et collaborateurs dans le groupe Colobert ont utilisés un β-hydroxysulfoxyde comme auxiliaire de chiralité dans la construction de l'unité biarylique AB de la vancomycin[70] avec une excellente diastéréosélectivité (Figure III-33a). Une extension plus générale en rapprochant l'auxiliaire de chiralité du futur axe de chiralité a par la suite été explorée[71] (Figure III-33b), qui illustre bien l'antagonisme existant généralement entre encombrement stérique et efficacité du couplage en passant d'un auxiliaire *para*-tolylsulfoxyde à *tert*-butylsulfoxyde.

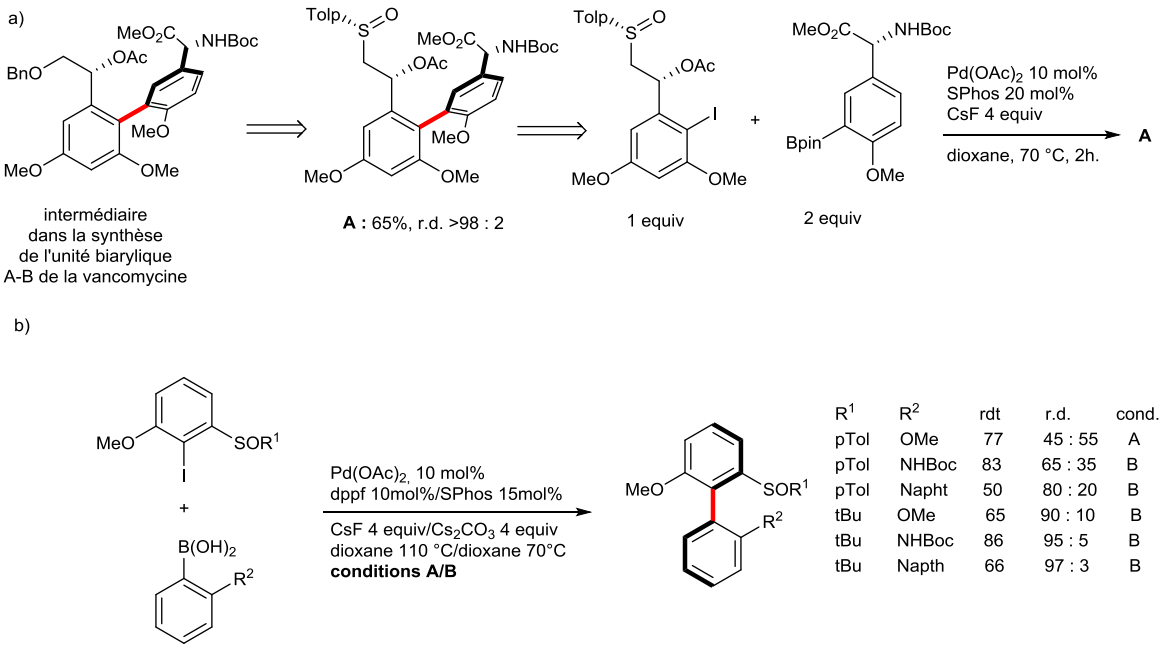

Figure III-33 : couplage atropodiastéréosélectif utilisant un sulfoxyde énantiopur

L'approche diastéréosélective développée par Uemura et collaborateurs, s'appuie sur un transfert de chiralité planaire à axiale grâce à la formation dans un premier temps d'un complexe η^6 entre un métal de transition ($Cr(CO)_3$) et un halogénure d'aryle pour réaliser un couplage atropodiastéréosélectif avec un acide boronique[72](Figure III-34.a). Cette stratégie sera par ailleurs appliquée avec succès à la synthèse de deux produits naturels bioactifs (Figure III-34.b), la (-)-steganone (à laquelle nous aurons occasion de nous intéresser plus en détail plus tard) et les deux énantiomères de la *O,O'*-dimethylkorupensamine A.

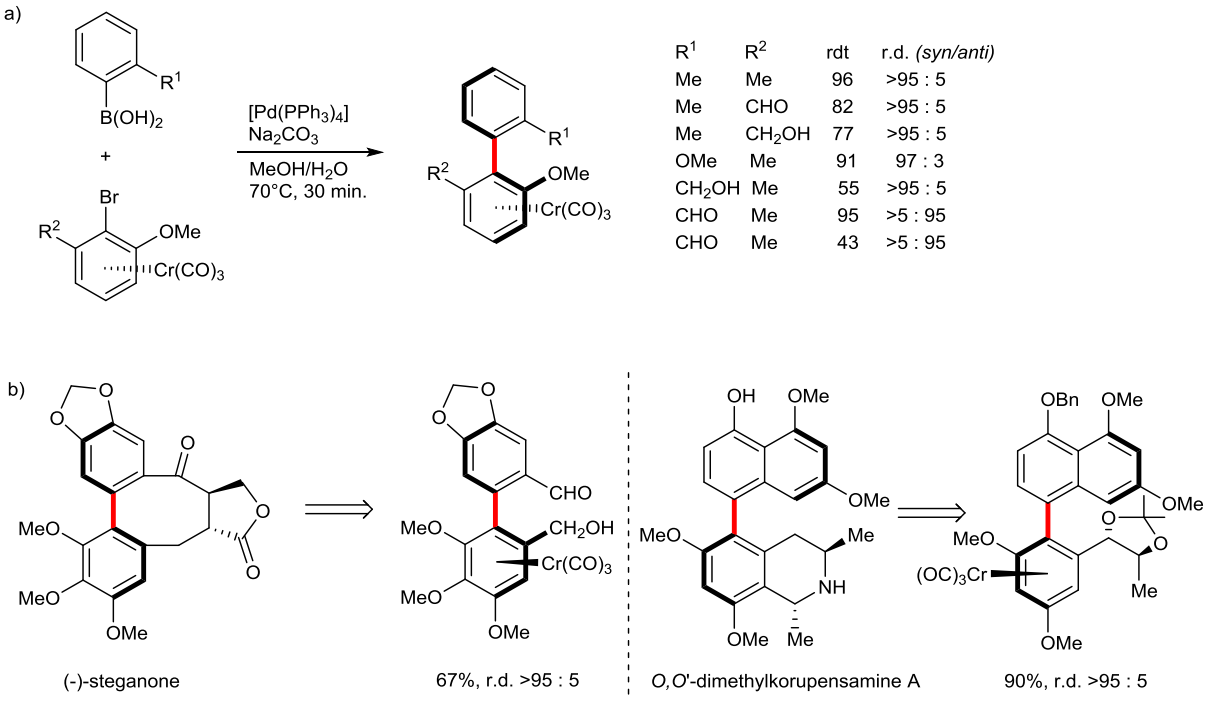

Figure III-34 : couplage atropodiastéréosélectif

Bien entendu, les recherches intenses sur cette réaction classique ont donné naissance à des versions énantiosélectives, et nous renvoyons le lecteur vers des revues[73,74] sur ce sujet. Les premiers couplages énantiosélectifs ont été rapportés de façon indépendante par les groupes de Cammidge[75] (Figure III-35a) et Buchwald[76] (Figure III-35b) en 2000, et il est intéressant de remarquer que les deux groupes ont obtenu leurs meilleurs résultats en utilisant des ligands mixtes de types PR_2–NMe_2. Il sera ensuite déterminé, en 2010 par le groupe de Buchwald[77], grâce à des expériences stœchiométriques et des structures aux rayons-X des complexes intermédiaires obtenus après l'addition oxydante du substrat, que le ligand est à ce stade monodentate et qu'un des sites de coordination est occupé par l'oxygène de l'oxyde de phosphine. Cette constatation ouvrira la voie à l'utilisation de ligand monodentate en combinaison avec des substrats possédant un groupe coordinant en position *ortho* du futur axe de chiralité.

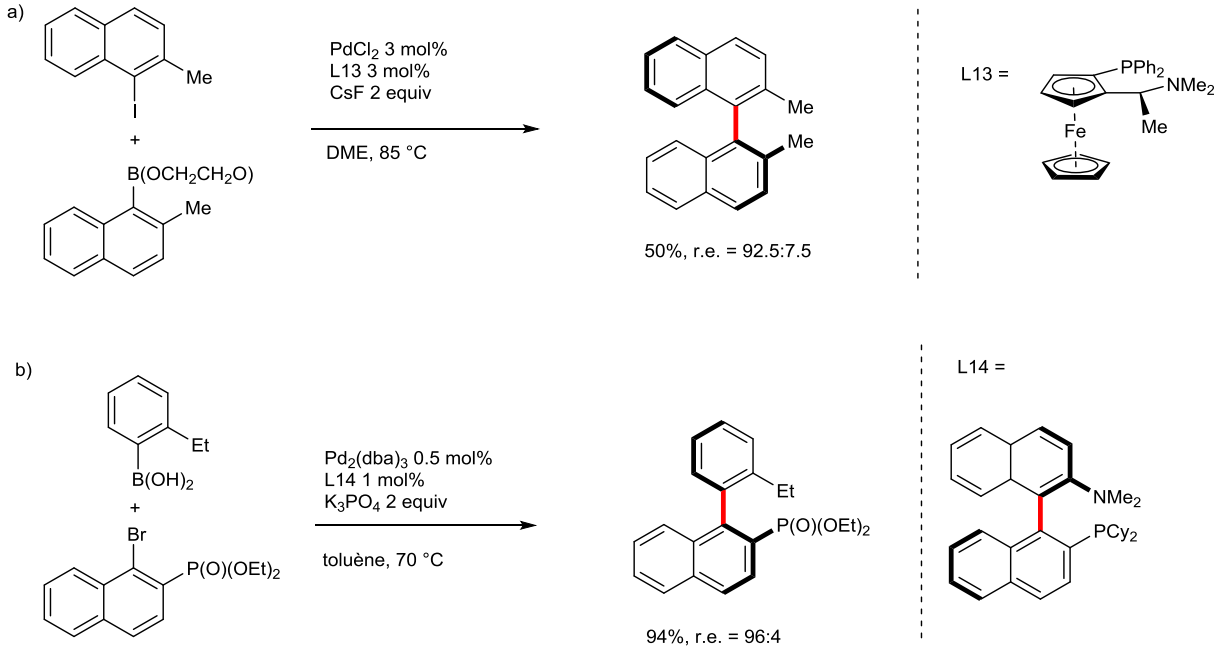

Figure III-35 : couplages atropoénantiosélectifs avec des ligands N-P

Ainsi Tang et collaborateurs[78] (Figure III-36) utiliseront une monophosphine biarylique, l'induction asymétrique provient ainsi d'un atome de phosphore chiral. Là aussi, l'halogénure doit posséder en *ortho* un groupement coordinant. De très bons rendements et énantiosélectivités ont pu être obtenus pour certains motifs de substitutions.

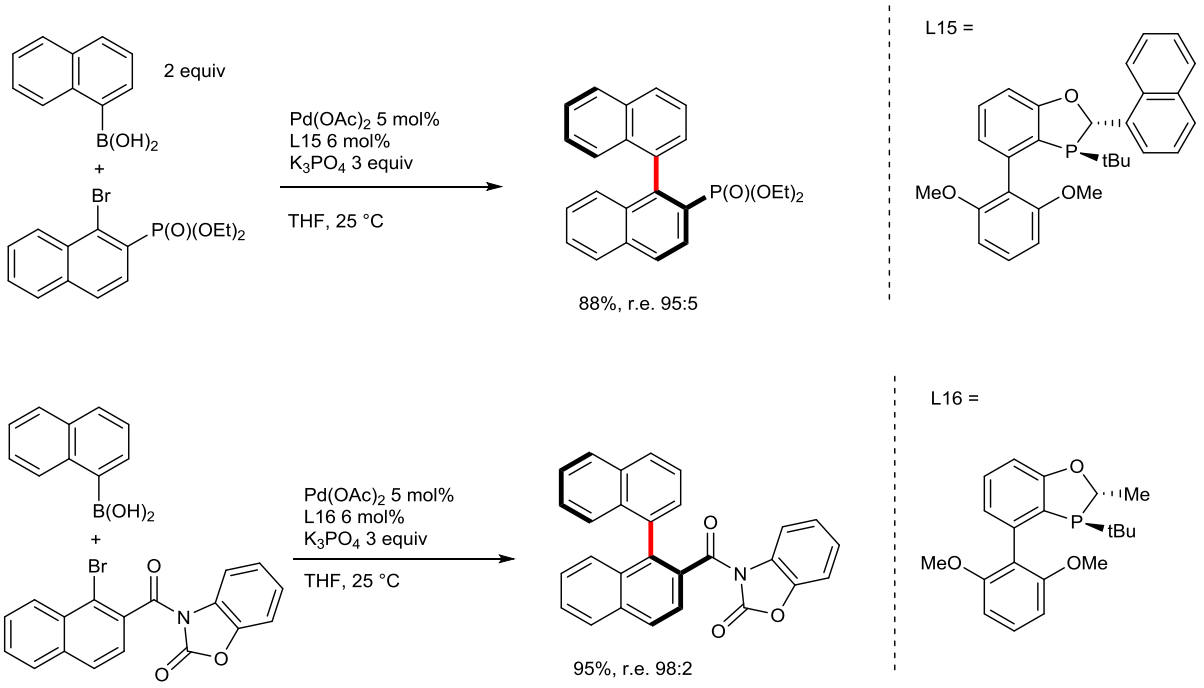

Figure III-36 : couplage atropoénantiosélectif avec des ligands monodentates

Signalons ensuite l'approche de Lassaletta[79] avec l'utilisation d'un nouveau ligand de type bis-hydrazone permettant de s'affranchir de la présence d'un groupe coordinant en *ortho* de l'halogènure. Si des r.e. >99:1 ont pu être obtenus, sur des produits tri-substitués de types naphthyl-phenyls ou binaphthyls, on notera que les auteurs utilisent des complexes pré-formés ainsi que l'importance de conditions précises sur la stéréosélectivité pour chaque substrat.

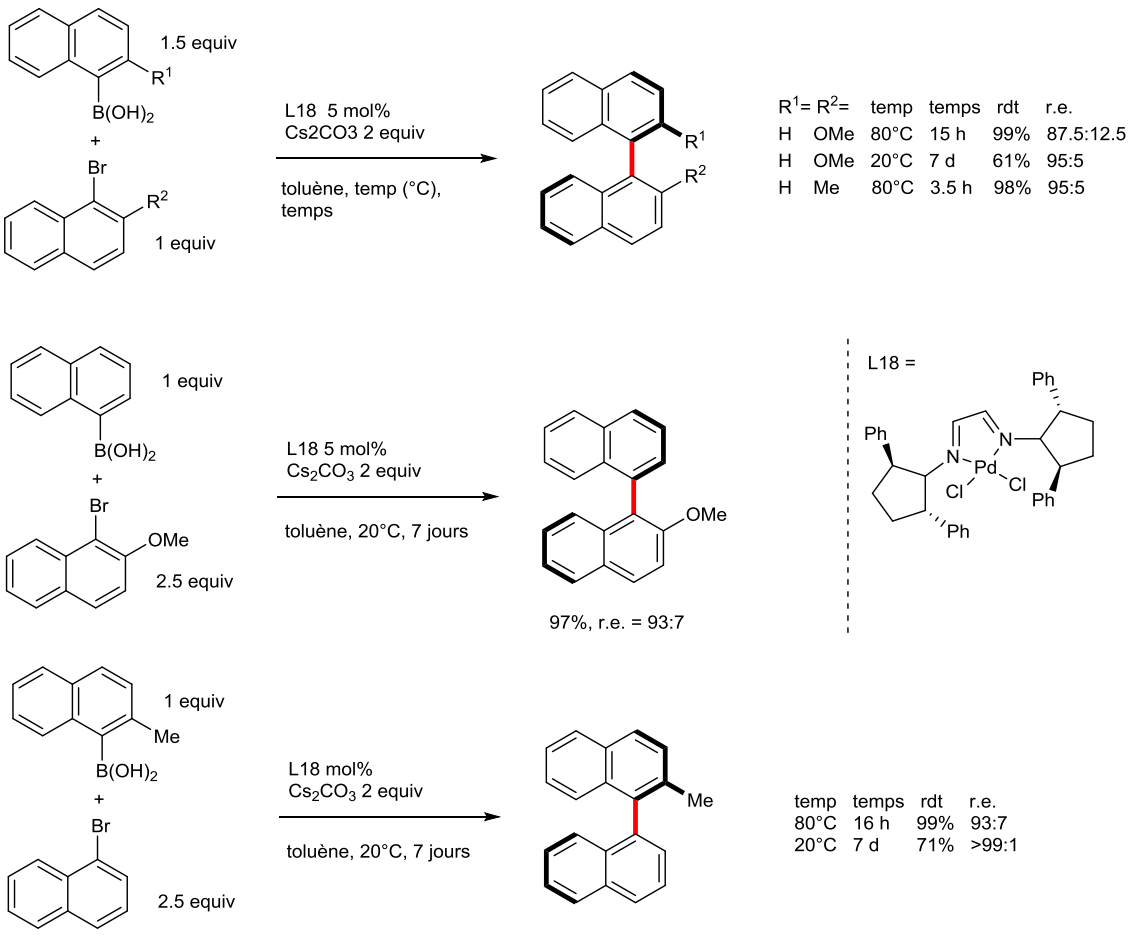

Figure III-37 : couplage à l'aide d'une bis-hydrazone

Une autre stratégie qui a son importance d'un point de vue historique, est le couplage S_NAr : l'addition atropodiastéréosélective d'un Grignard sur un aryle porteur d'un goupe partant et d'un groupe électro-attracteur en *ortho* (pour permettre un contrôle par chélation) permet d'accéder à des biaryles ou binaphtyles. L'auxiliaire de chiralité peut soit être le groupe partant, soit le groupe électro-attracteur positionné en *ortho*. Un exemple de ces concepts développés concerne l'utilisation d'un ether méthylique comme groupe partant et d'une oxazoline énantiopure et cette méthodologie a été appliquée à la synthèse de la (-)-steganone[80] (Figure III-38, a). Par ailleurs l'utilisation d'un sulfinyl énantiopur comme groupe partant avec un ester en position *ortho* par Sargent dans la synthèse d'un binaphthyl[81] (Figure III-38, b) permet également d'obtenir d'excellentes diastéréselectivités.

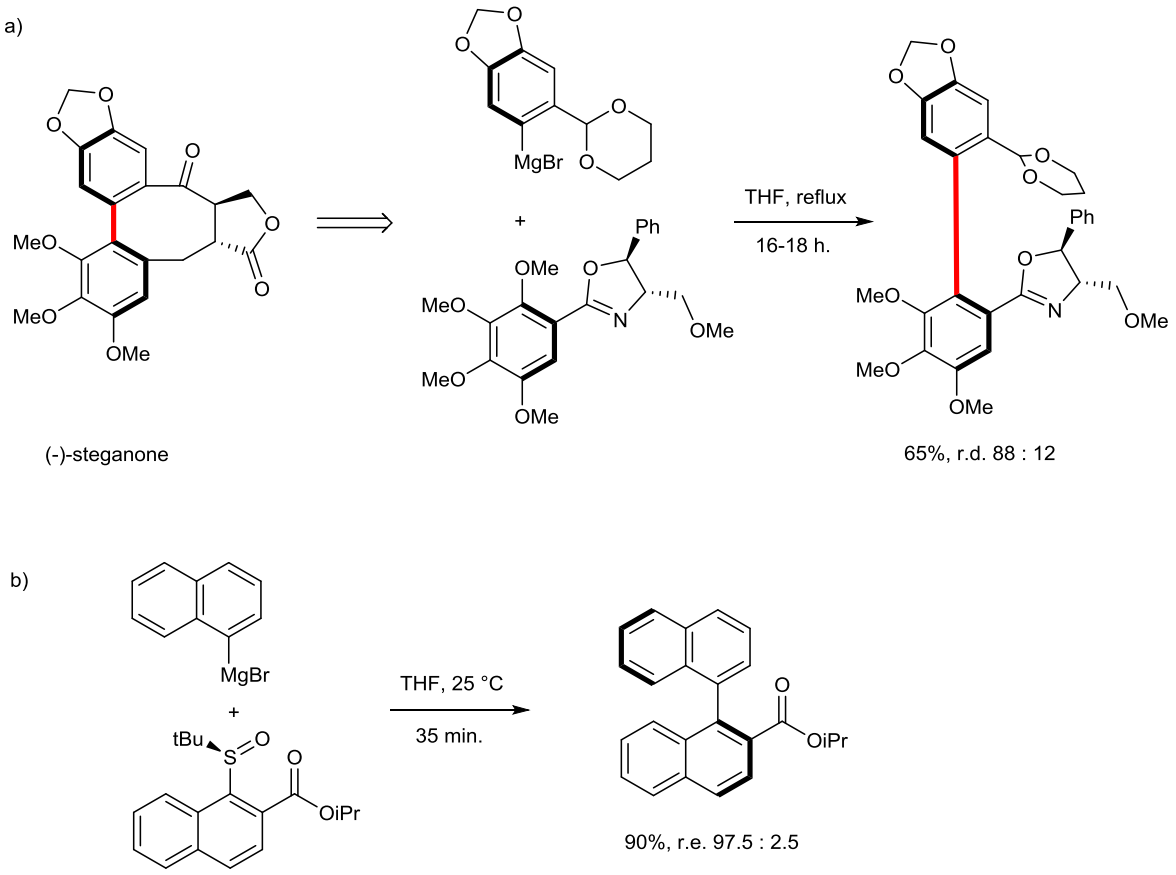

Figure III-38 : couplage par S_NAr

Enfin, nous finirons cette partie par les couplages de type Ullmann, avec deux stratégies représentatives : soit le futur biaryle est relié par un pont chiral avant le couplage, soit il comporte deux substituants chiraux en position *ortho,ortho'*. Plus adapté aux réactions d'homocouplage, il reste néanmoins possible d'accéder à des biaryles non C_2 symétrique (Figure III-39a), ainsi que d'échapper aux températures élevés caractéristiques d'un couplage dUllmann « classique » (Figure III-39. b). Ces deux stratégies (a/b et c) ont été appliquées à la synthèse de plusieurs produits naturels avec succès. Soulignons tout de même un travail synthétique important pour arriver à installer puis à enlever le pont chiral dans les exemples a) et b), et l'utilisation de deux équivalents de l'auxiliaire de chiralité dans le cas c).

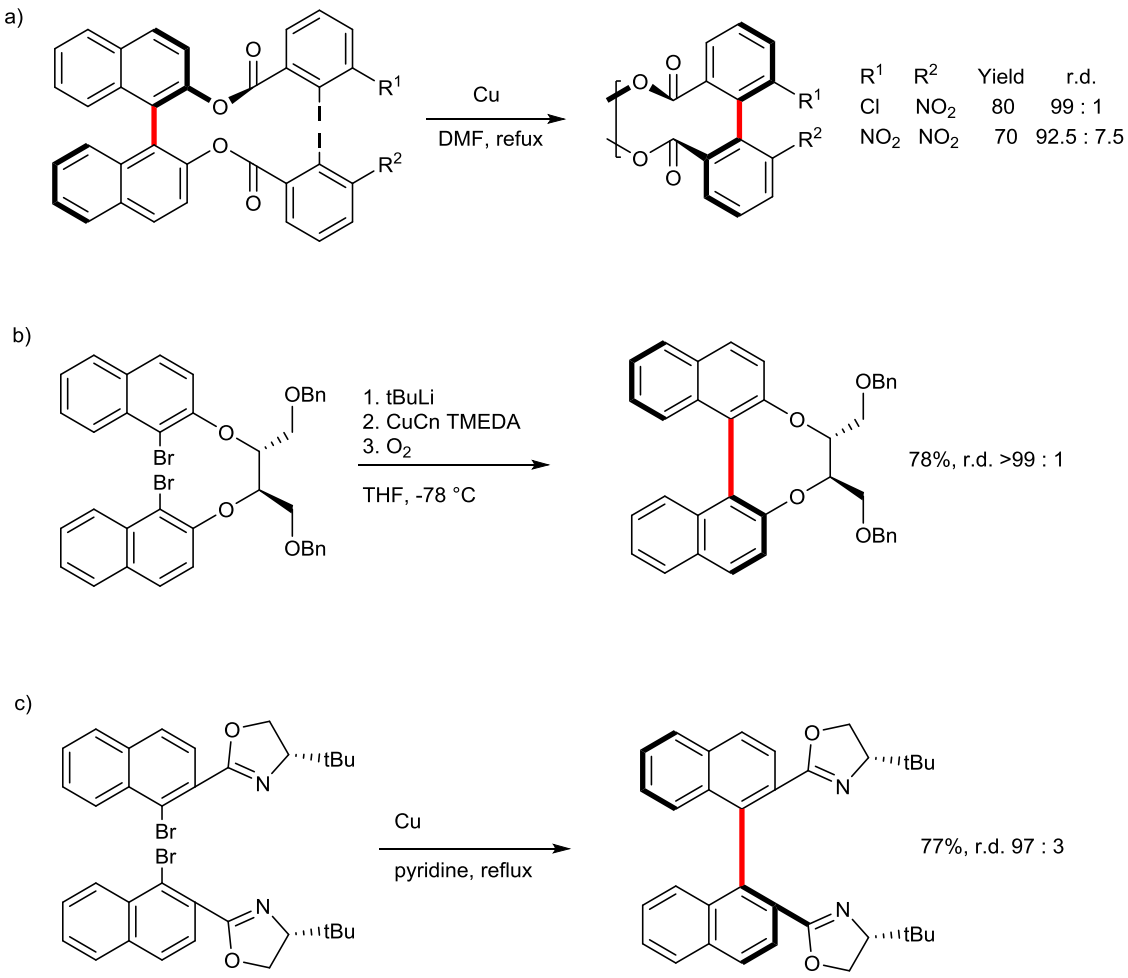

Figure III-39 : couplage de type Ullman

b) Construction d'un (des) cycle(s) aromatique(s)

Nous pouvons séparer les travaux sur la construction d'un cycle aromatique en deux grands groupes : soit la construction du cycle se fait par une réaction type cycloaddition [2+2+2] (donc création de plusieurs liaisons σ), soit par aromatisation d'un cycle existant (transfert de chiralité centrale vers axiale).

(1) Cycloadditions

Généralement basé sur des cycloadditions [2+2+2] d'alcynes catalysées par des complexes phosphines-rhodium ou iridium (mais aussi cobalt), ces réactions permettent d'accéder à des produits originaux. Un schéma représentatif de la cycloaddition d'un diyne relié par un pont avec un alcyne est représenté à la Figure III-40a. Une autre possibilité est représentée à la Figure III-40b, et chacune des deux stratégies conduit à des motifs de substitutions différents, permettant ainsi d'optimiser la préparation des substrats suivant le type de biaryle voulu.

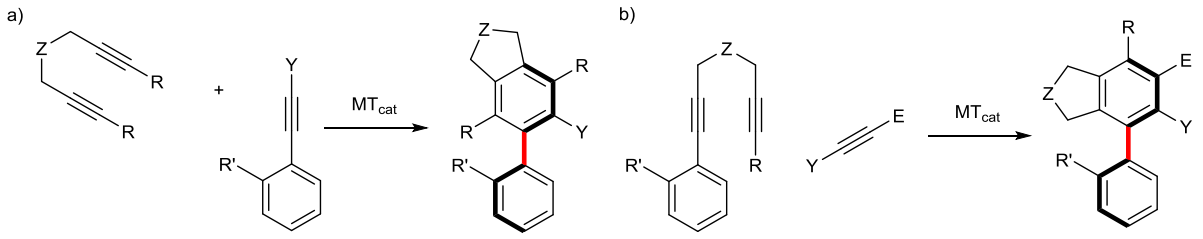

Figure III-40 : schéma général de cycloaddition

Faisant l'objet de deux revues récentes[82,83], nous nous contenterons de remarquer que les atroposélectivités généralement élevés, l'économie d'atomes et de moyen (réactions catalytiques et énantiosélectives) les rendent attirantes, mais la préparation très spécifique des substrats pour une réaction et les restrictions sur le motif de substitution des biaryles formés (problème de régiosélectivités inhérent à ce type de réaction) restreignent leur champ d'application. Cependant une grande force de ces réactions est de pouvoir obtenir des produits tétra-substitués dans des conditions douces (Figure III-41a), ainsi que des produits hétéroaromatiques, travail rapporté par Tanaka et collaborateurs[84] [85] (Figure III-41b).

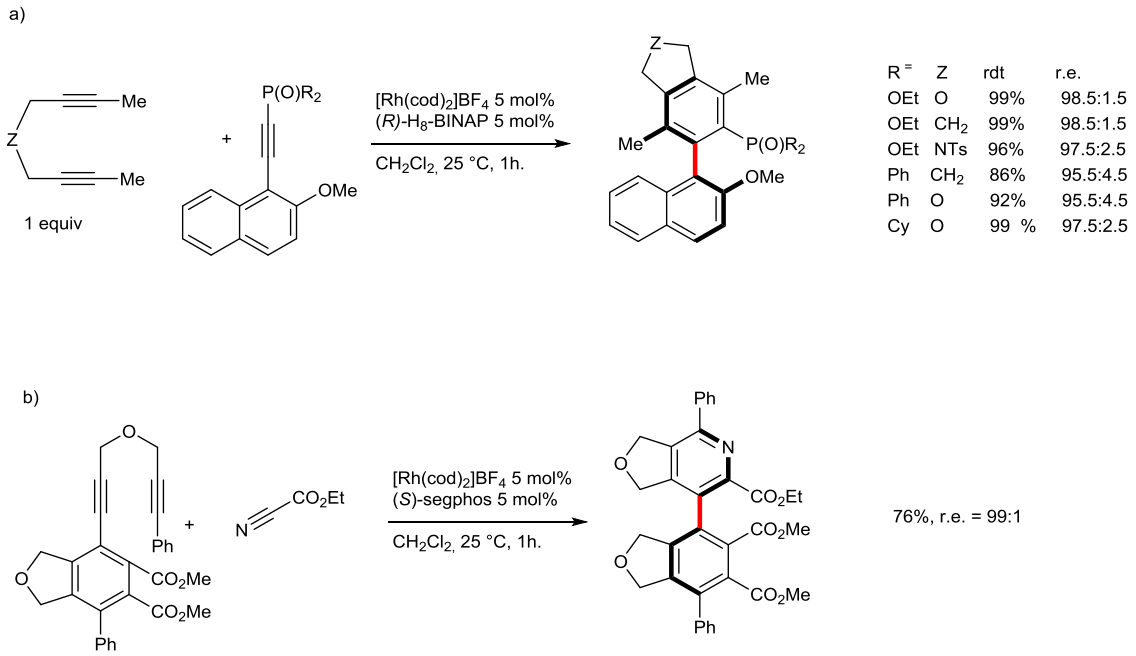

Figure III-41 : exemple de cycloadditions atropoénantiosélectives

Les cycloadditions qui aboutissent à des produits présentant plusieurs axes de chiralité seront vus de façon exhaustive dans la partie traitant de la réaction d'arylation directe dévelopée au cours de cette thèse (chapitre VII).

Enfin notons l'approche de Link et Sparr[86] qui utilisent une approche organocatalytique pour construire de façon atroposélective des cycles naphthalenes par des condensations aldoliques en présence d'un catalyseur bi-fonctionel (Figure III-42). Cette stratégie permettra de construire un teraryle avec deux axes de chiralité (Lotter,

Sparr et collaborateurs Figure III-42b). C'est le deuxième exemple connu de construction d'*ortho*-teraryles hautement atroposélective.

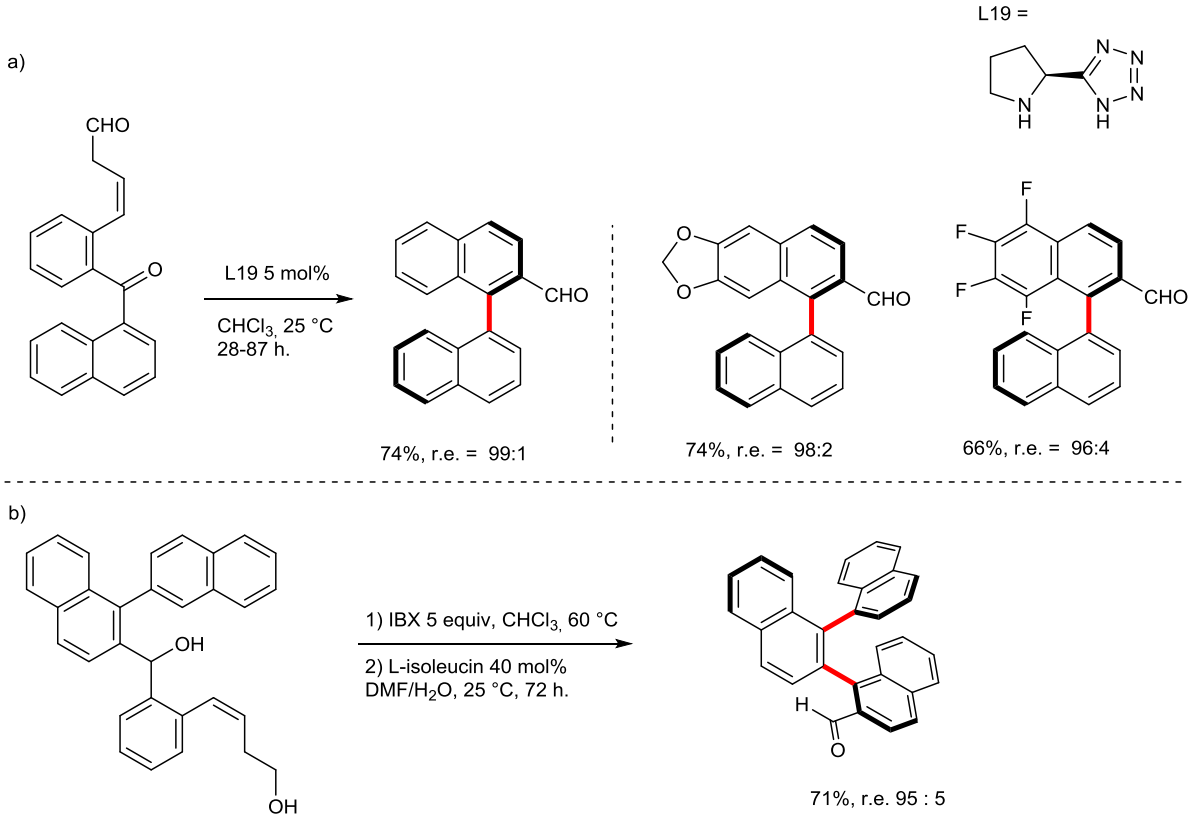

Figure III-42 : condensations aldoliques atroposélectives organocatalytiques

(2) Construction de cycle aromatique par aromatisation

Le concept consiste ici au contrôle de la chiralité centrale des carbones d'un bicycle au plus près du futur axe de chiralité ; l'introduction d'insaturations jusqu'à la formation du biaryle permet de transférer cette chiralité centrale en chiralité axiale, généralement avec d'excellentes énantiosélectivités. Citons le travail (2011) de Guo, Thomson et collaborateurs[87] vers des phénols tétra-substitués et des énantiosélectivités presque totales (Figure III-43a). L'ajout d'un acide de Lewis dans des conditions anhydres permet la déprotection sélective de l'acétal, puis l'aromatisation. Remarquons le travail récent (2017) de Rault, Bonne, Rodriguez et collaborateurs vers les premiers aryles-furans C-C atropisomériques[88] (Figure III-43b). L'addition 1,4 énantiosélective de l'énolate de la dione sur le dérivé nitro α,β-insaturé permet une O-alkylation diastéréosélective produisant un dihydrofurane tetrasubstitué avec une sélectivité presque parfaite. L'ajout d'un oxydant permet l'aromatisation avec une légère perte d'énantiosélectivité conduisant à des produits originaux.

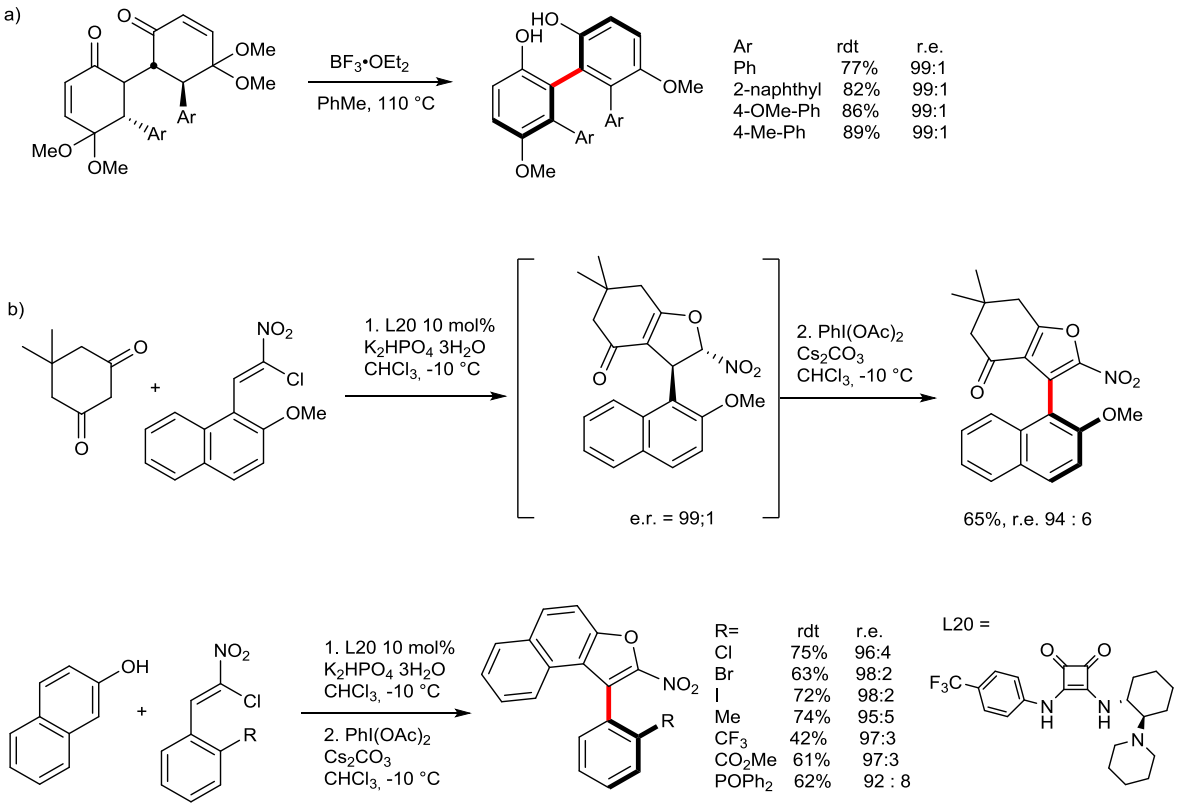

Figure III-43 : transfert de chiralité centrale à axiale.

Enfin remarquons le travail de Jolliffe, Smith et collaborateur en 2017[89] qui est une combinaison de la stratégie d'aromatisation avec celle de dédoublement (Figure III-44) : en effet, en partant d'un dérivé de cyclohexanone substitué en alpha par un 2-méthoxynaphthalène, composé à chiralité centrale mais racémique (a) , l'action d'une base conduit à la formation d'un énolate où la chiralité centrale est convertie en chiralité axiale (b) : le composé obtenu est donc chiral, racémique mais il n'est pas atropisomérique, ce qui permet d'utiliser une quantité sub-stoichiométrique d'un dérivé de quinine quaternaire qui va former un complexe supramoléculaire atropo-diastéreomérique (c) et ensuite permettre d'augmenter la barrière de rotation par une O-alkylation atroposélective (d) ; l'intermédiaire de l'étape (b) n'étant pas atopisomérique on assiste ici à un dédoublement cinétique dynamique, permettant d'accéder, après aromatisation par oxydation au DDQ (e), à des biaryles de type BINOL-*O*,*O*'-alkyles, avec des rendements bien supérieurs à 50% en partant pourtant d'un substrat racémique.

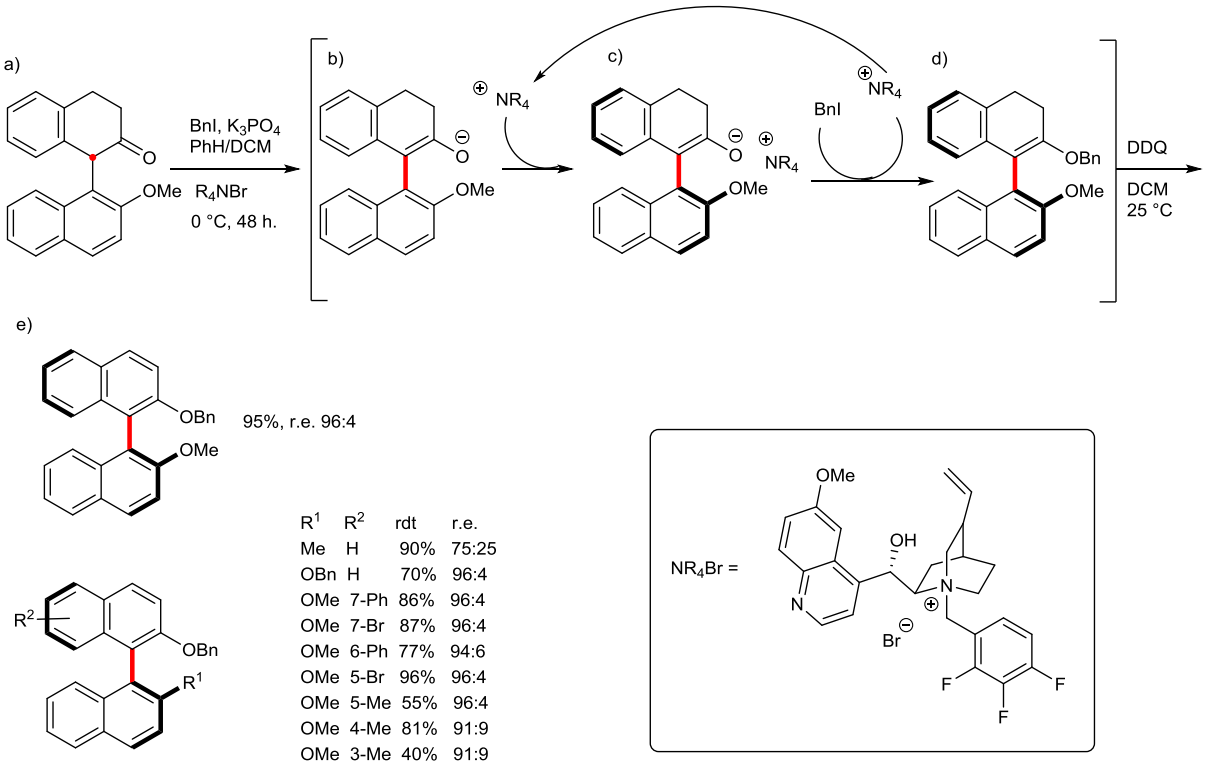

Figure III-44 : O-alkylation atroposélective

c) Dédoublement cinétique et désymétrisation

Ce dernier exemple nous permet une transition vers le dernier grand type de synthèse atroposélective de biaryles : en partant d'un biaryle déjà existant, la fonctionnalisation atropodiastéréo- ou atropénantiosélective, soit par l'introduction d'un nouveau substituant, soit par une modification de substituant existant, permettant d'accéder à des produits atropopurs. Remarquons que cette fonctionnalisation se produit forcément soit sur un biaryle déjà chiral (dédoublement cinétique) ou sur un biaryle prochiral (désymétrisation).

La stratégie de fonctionnalisation d'un biaryle existant est spécialement efficace lorsqu'elle permet d'augmenter significativement la barrière de rotation autour de l'axe de chiralité : en effet il est alors possible de partir d'un biaryle chiral mais non atropisomérique qui s'équilibre relativement rapidement, la fonctionnalisation préférentielle d'un des conformères donnant ici lieu à un processus de dédoublement cinétique dynamique permettant de dépasser les ~50% de rendement habituel d'un dédoublement simple.

Il est important de noter que le dédoublement cinétique dynamique semble particulièrement bien adapté à une co-stratégie de C-H activation, c'est-à-dire la fonctionnalisation d'une liaison C-H en *ortho* de l'axe biarylique : en effet pour que l'augmentation de la barrière de rotation soit suffisante pour passer d'un substrat non-atropisomérique à un produit atropisomérique, la différence d'encombrement stérique doit être maximale.

Dernier point, la stratégie d'insertion d'un nouveau substituant par C-H (et donc métallocatalysée) est potentiellement la plus versatile car le complexe formé après insertion dans la liaison C-H est un intermédiaire commun ouvrant la porte à de nombreux types de fonctionnalisation (ainsi la Figure III-45b représente les couplagesles plus connus accessibles par un intermédiaire palladium^{II} [90]). C'est cette stratégie (dédoublement cinétique dynamique par C-H activation au palladium) qui a été suivie tout au long de cette thèse ; nous verrons donc dans une première partie exhaustive les différents exemples d'introduction de substituant atroposélectif par C-H activation (dédoublement cinétique/dédoublement cinétique dynamique et désymétrisation). La deuxième partie sera consacrée aux modifications atroposélectives de substituants déjà existants, mais en mettant l'accent sur la modification d'un substituant *ortho* catalysée par des métaux de transition ; en effet cette approche est, mécanistiquement parlant, un proche parent de la stratégie par C-H activation. En effet, après insertion du métal dans une liaison C-H ou C-X, l'intermédiaire réactionnel est identique (Figure III-45). Dans la dernière partie seront présentées les autres méthodes de synthèse par modifications de substituants d'un biaryle.

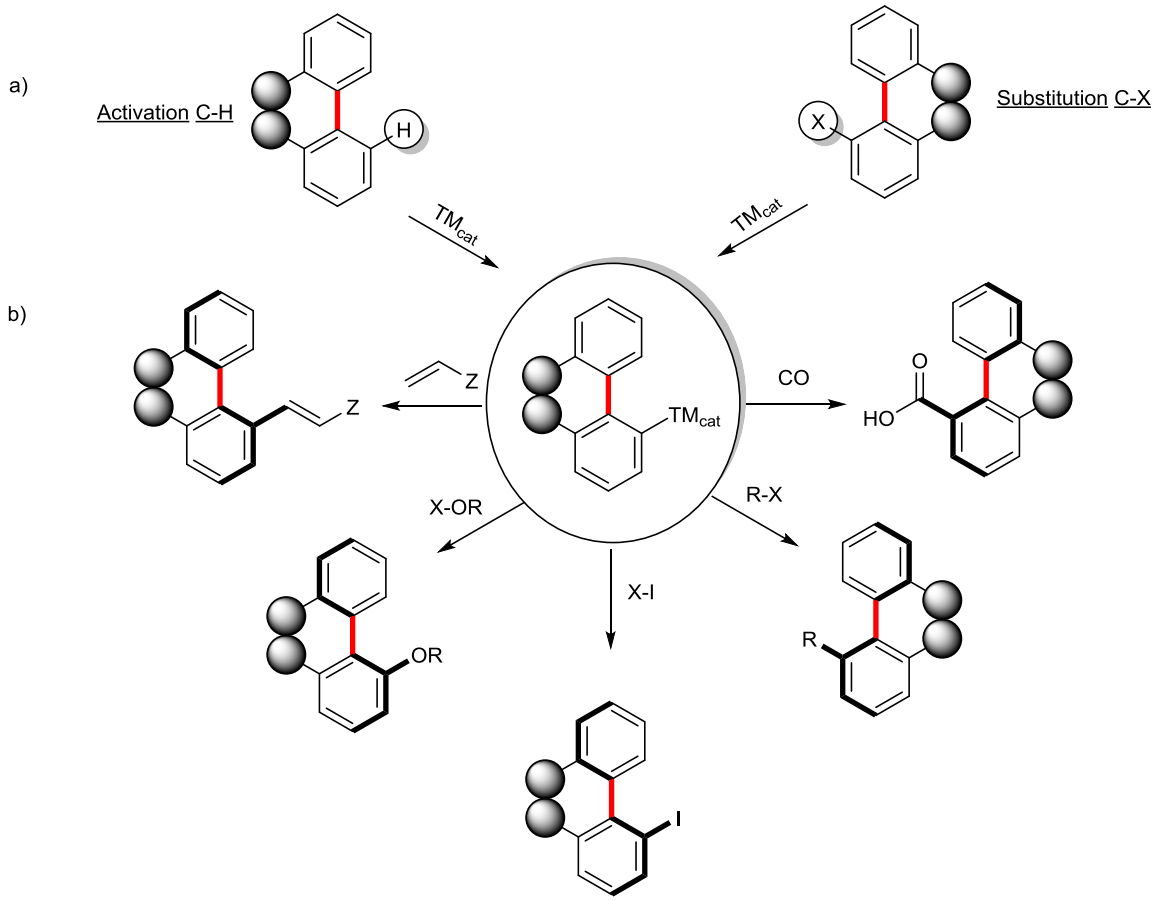

Figure III-45 : possibilités d'insertion d'un nouveau substituant offertes par les métaux de transition

Rappelons maintenant la différence entre dédoublement, dédoublement cinétique, dédoublement cinétique dynamique, et le dédoublement cinétique dynamique par transformation asymétrique (Figure III-46).

a) R= Dédoublement : une modification chimique réversible utilisant un auxiliaire énantiopur, transforme des énantioméres en diastéréoméres, ces derniers sont séparés et la modification inverse permet d'obtenir le substrat énantiopur. Le rendement maximum est donc de 50% et on a besoin d'un équivalent de l'auxiliaire chiral.

b) KR= Dédoublement cinétique : une modification chimique transforme un des deux énantioméres plus rapidement que l'autre. Le rendement maximum est de 50%, et l'auxiliaire peut être utilisé en quantité catalytique. Remarquons que si le produit et le substrat n'ayant pas réagi peuvent être obtenus énantiopurs, il est plus facile d'obtenir le substrat énantiopur.

c) DKR= Dédoublement cinétique dynamique : une modification chimique transforme un des deux énantioméres plus rapidement que l'autre, pendant que, dans le même temps, les deux énantiomères du substrat s'interconvertissent. Le rendement maximum est de 100%, et l'auxiliaire peut être utilisé en quantité catalytique.

d) DYKAT= dédoublement cinétique dynamique par transformation asymétrique : une modification chimique transforme les deux énantioméres dans un premier intermédiaire, qui, peut s'interconvertir ; cet intermédiaire réagit ensuite avec des vitesses différentes pour donner un produit optiquement enrichi. Le rendement maximum est de 100%, et l'auxiliaire peut être utilisé comme en quantité catalytique.
Si en théorie la différence entre DKR et DYKAT est claire, en pratique il peut être difficile de déterminer quel mécanisme est à l'œuvre, voir même si les deux mécanismes ne sont pas en œuvre simultanément.

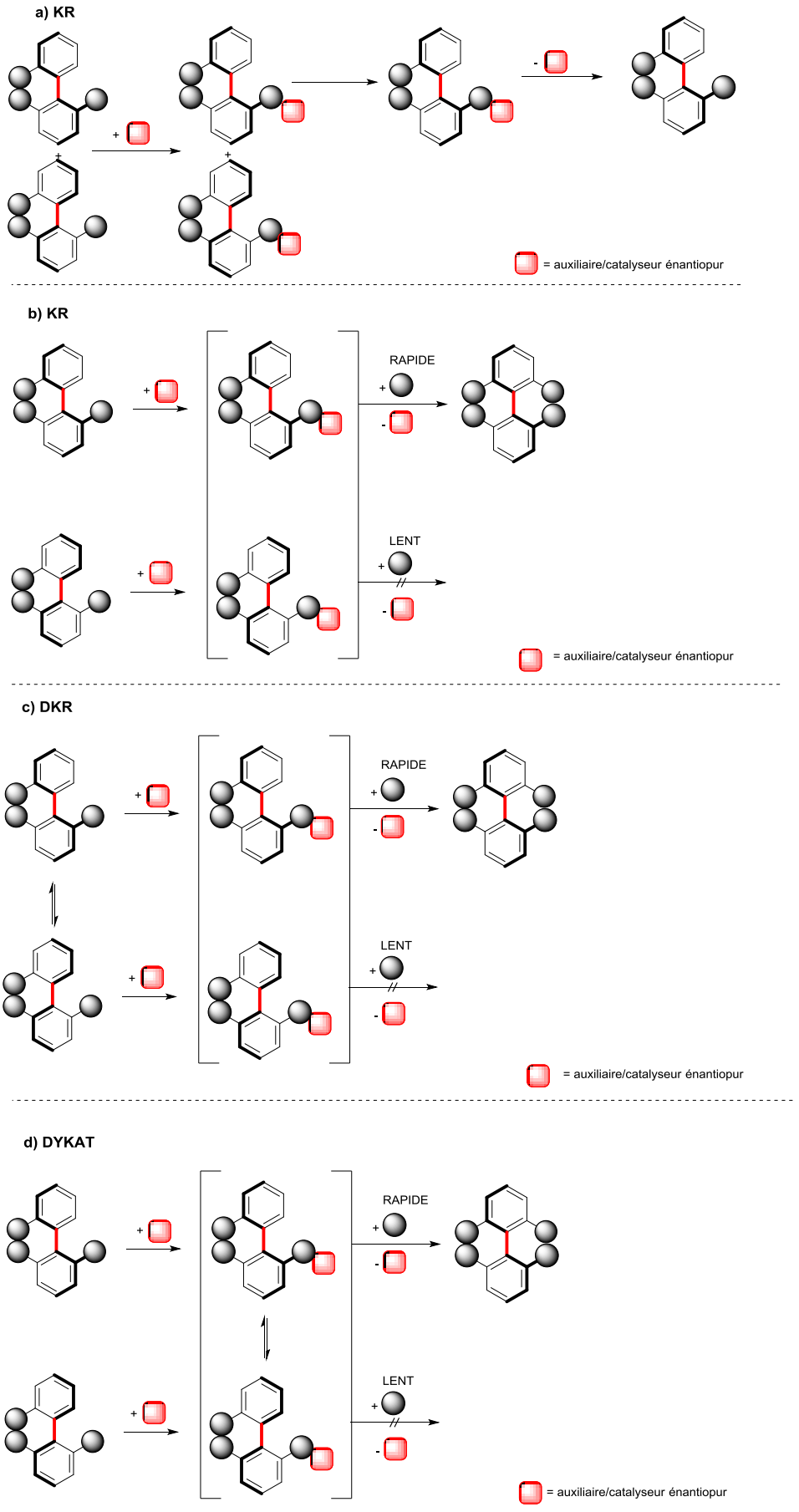

Figure III-46 : classification des dédoublements

Nous finirons cette introduction par un exemple important qui a montré le potentiel de l'introduction atroposélective de substituants : en 2010 Gustafson, Miller et collaborateurs[91], ont réalisé la tri-bromation énantiosélective d'un *ortho*-CO_2H-*meta'*-OH biphényle, catalysé par un peptide (Figure III-47). Remarquons que le mécanisme par S_EAr (et donc ne peut être classé comme C-H activation) introduit deux substituants identiques en position *ortho*' ; c'est donc la présence du substituant en position *méta'*-OH qui est à l'origine de la chiralité. Remarquons aussi qu'après l'introduction du premier brome en position *ortho'* le produit intermédiaire est chiral et probablement non-atropisomérique à 25°C, et que nous avons donc à partir de ce moment un dédoublement cinétique dynamique à l'œuvre.

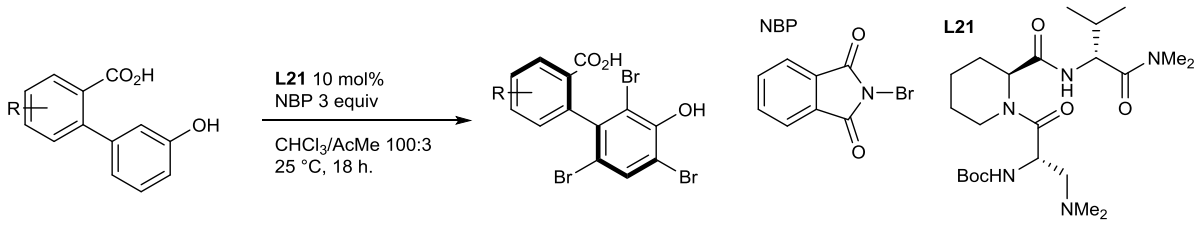

R=	rdt	r.e.
H	80%	97:3
4-NO_2	85%	97:3
5-NO_2	75%	96.5:3.5
5-OMe	70%	96:4
4-OMe	80%	94:6
5-F	70%	97:3
4-F	65%	96.5:3.5
3-Me	85 %	97:13

Figure III-47 : bromation atropoénantiosélective

(1) Introduction atroposélective de substituant par C-H activation.

Si, comme nous l'avons dit, la stratégie d'activation C-H semble être la plus directe et versatile pour la synthèse atroposélective d'un biaryle pré-existant, il existe de fait deux écueils inhérents à surmonter : la température élevée souvent nécessaire aux réactions de C-H activation et le problème de régiosélectivité. Le défi représenté par cette stratégie est bien illustré par les treize ans qu'il aura fallu attendre entre la première mention de cette stratégie dans la littérature (2000) et sa réapparition en 2013 par notre groupe ; c'est quelques mois après cette avancée que débute cette thèse. Une année supplémentaire (2014) sera finalement nécessaire pour affiner cette approche et permettre un accès à un panel respectable de biaryles avec de très bons rendements et atroposélectivités.

En effet, en 2000 donc, le travail pionner de Kakiuchi et collaborateurs dans le groupe de Murai[92] sur des hétérobiaryles types naphthylpyridine et naphthylisoquinoline aboutira à des rendements et énantiosélectivités très modestes, puisque le meilleur est un rendement de 37% avec un r.e. de 74:26.

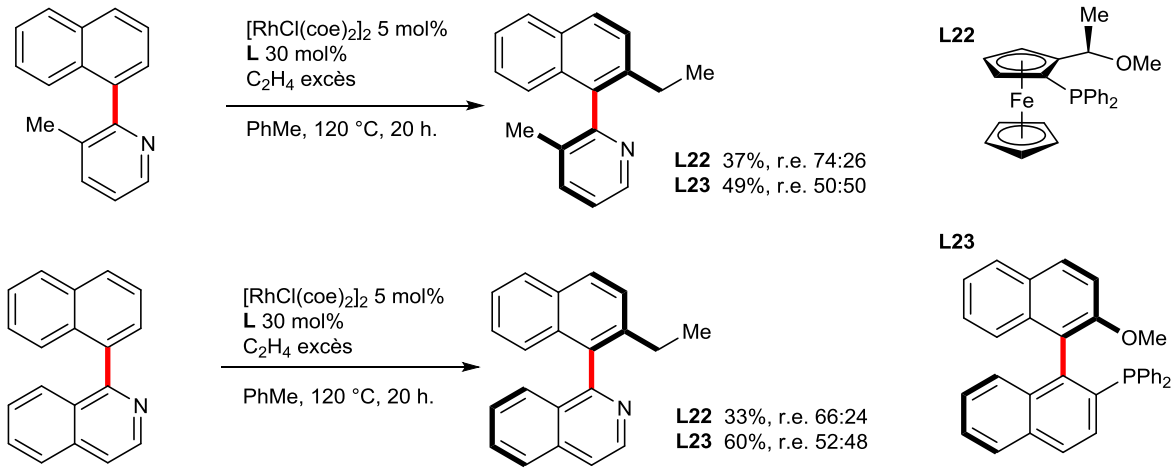

Figure III-48 : premier exemple de fonctionnalisation de liaison C-H atroposélective

Remarquons que l'on pourrait qualifier les ligands utilisés d'hémi-labile en comparant le pouvoir coordinant de l'azote hérérocyclique avec celui d'un méthoxy : il s'agit ici d'un moyen de contrôler la régiosélectivité de l'insertion du métal, puisque l'azote coordinant du substrat va diriger le métal vers la position *ortho* la plus proche.

Un an plus tard, Gao et collaborateurs dans le groupe de You[93], publient un premier article décrivant l'iodation de napthylisoquinolines N-oxides avec des rendements modestes mais de bonnes énantiosélectivités ; la préparation du catalyseur *in-situ* à partir de $Pd(OAc)_2$ et d'acides aminés N-protégé rend le protocole facilement modulable et simple à mettre en œuvre. Remarquons que le mécanisme opérant est une KR simple et non pas une DKR.

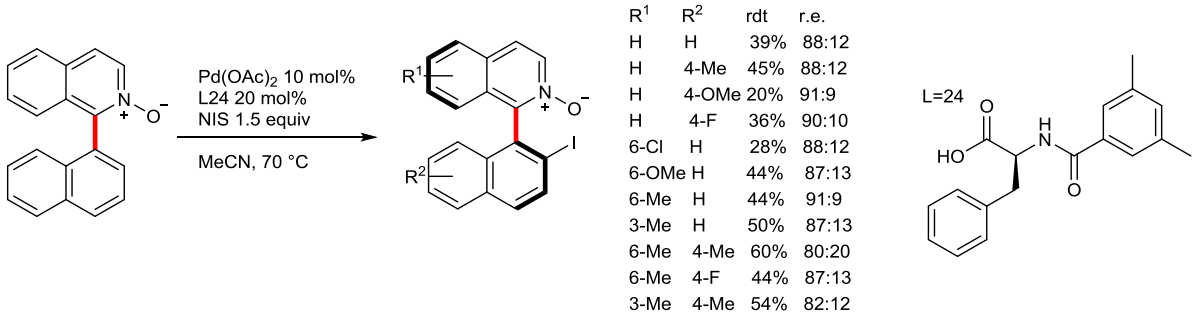

R^1	R^2	rdt	r.e.
H	H	39%	88:12
H	4-Me	45%	88:12
H	4-OMe	20%	91:9
H	4-F	36%	90:10
6-Cl	H	28%	88:12
6-OMe	H	44%	87:13
6-Me	H	44%	91:9
3-Me	H	50%	87:13
6-Me	4-Me	60%	80:20
6-Me	4-F	44%	87:13
3-Me	4-Me	54%	82:12

Figure III-49 : iodation atroposélective par KR

Quelques mois plus tard une réaction de Fujiwara-Moritani est rapportée par Zhen et You[94] sur des biaryles type naphthylbenzoisoquinoline (Figure III-50) où la partie benzoisoquinoline est utilisée comme groupement directeur. Cependant le catalyseur utilisé est cette fois plus compliqué à mettre en œuvre et à préparer (coût élevé du rhodium, ligand non-commercial).

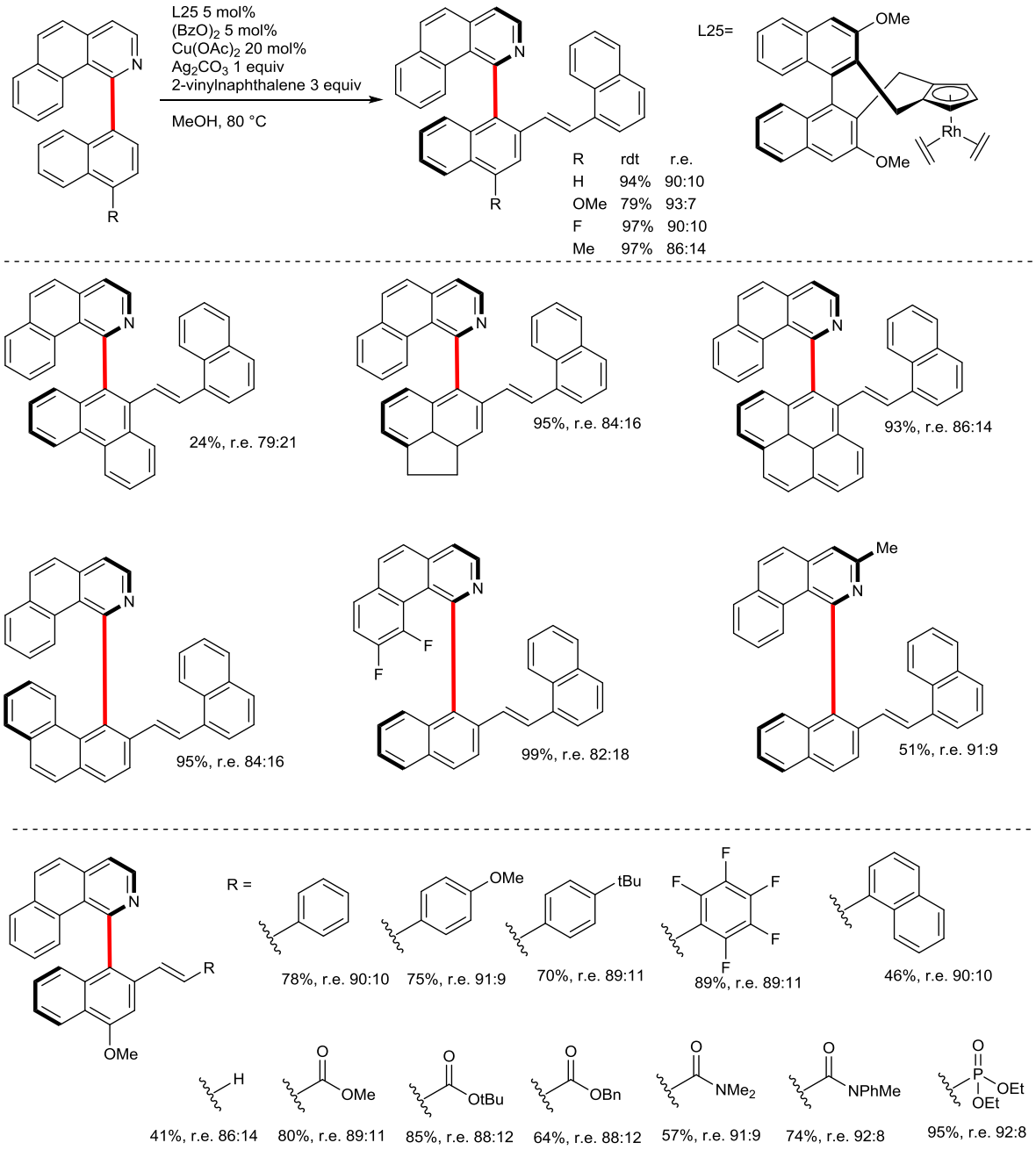

Figure III-50 : oléfination aropoénantiosélective

Concomitamment, notre laboratoire a développé une stratégie d'activation de liaisons C-H hautement atropodiastéréosélective. Ce travail constitue l'essentiel de cette thèse et ainsi sera présenté en détail dans les chapitres suivants de ce manuscrit. En 2015, Ma et collaborateurs dans le groupe de Yang[95] (Figure III-51) proposent une adaptation de notre stratégie diastéréosélective en utilisant un phosphinate énantiopur comme groupe directeur, principalement par une réaction de Fujiwara-Moritani (Figure III-51a) mais aussi acétoxylation et iodation (Figure III-51b) avec des diastéréosélectivités excellentes mais des rendements modestes.

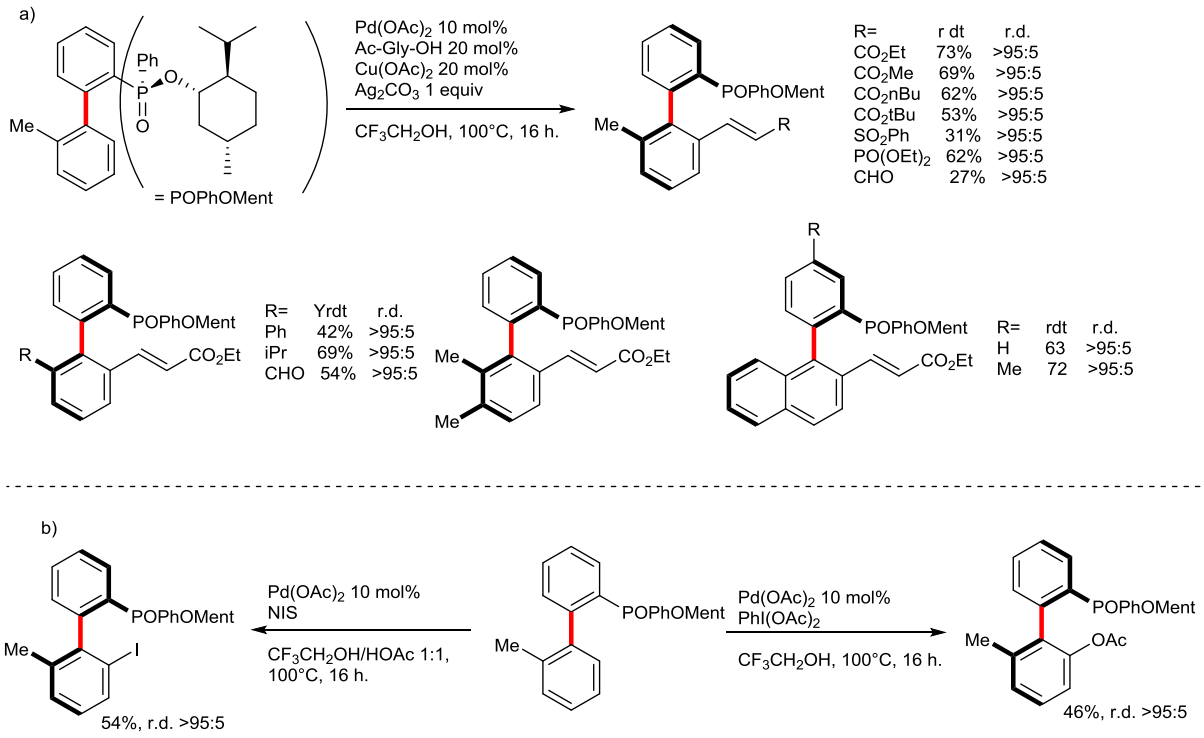

Figure III-51 : fonctionnalisation atropodiastéréosélective à l'aide d'un phosphinate énantiopur

Peu après, Zheng et collaborateurs dans le groupe de You[96] (Figure III-52) améliore leur réaction de Fujiwara-Moritani en développant un nouveau ligand 1,1'-spirobiinane extrêmement tendu (inspiré comme précédemment du travail de Cramer et Rovis) : la chiralité axiale est cependant contrôlée ici par la chiralité centrale du squelette carboné. Le système catalytique est ainsi nettement plus actif et plus sélectif, permettant de réaliser la transformation à température ambiante et avec des énantiosélectivités améliorées.

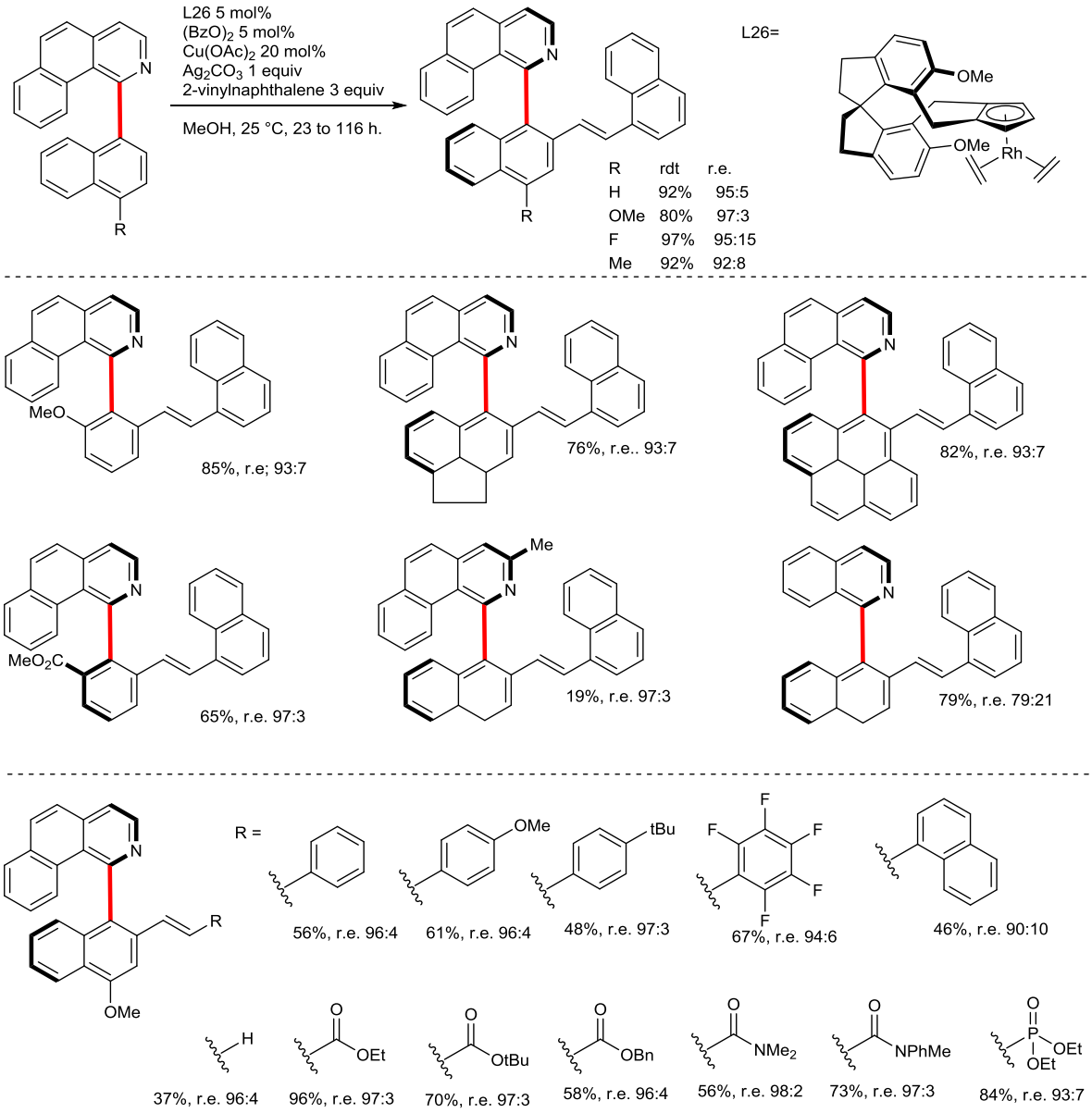

Figure III-52 : oléfination atropoénantiosélective

Enfin en 2017 deux élargissements de stratégies existantes permettent tout d'abord à Li et collaborateurs dans le groupe de Yang[97] de réaliser une réaction de Fujiwara-Moritani énantiosélective en utilisant une phosphine oxyde comme groupe directeur grâce à une combinaison catalytique palladium /acide aminé N-protégé (Figure III-53).

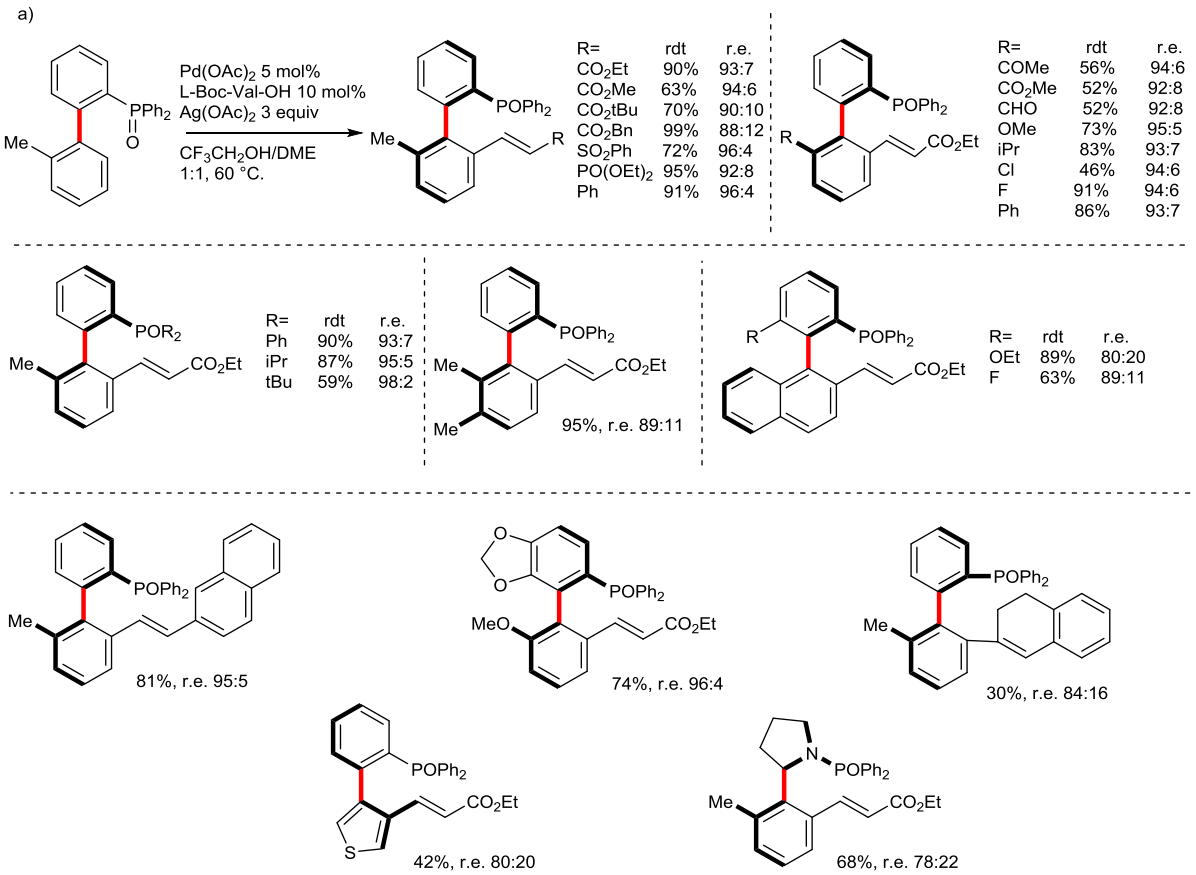

Figure III-53 : oléfination atropoénantiosélective avec un oxyde de phosphine comme DG

Enfin, en 2017 toujours, Yao et collaborateurs dans le groupe de Shi[98] réalisent une réaction de Fujiwara-Moritani énantiosélective avec un aldéhyde comme groupe directeur et grâce cette fois à un acide aminé N-protégé utilisé comme co-groupement directeur transitoire. De bons rendements et d'excellentes énantiosélectivités sont obtenus, Un protocole aisé, grâce à l'utilisation d'acides aminés comme ligands énantiopurs et de l'utilisation d'oxygène de l'air comme oxydant terminal en combinaison avec 10 mol% de benzoquinone comme co-oxydant, font certainement de cette technique la référence pour l'oléfination par DKR d'*ortho*-carbaldehydebiaryles (Figure III-54). Il sera intéressant d'observer l'extension vers d'autres types de fonctionnalisation.

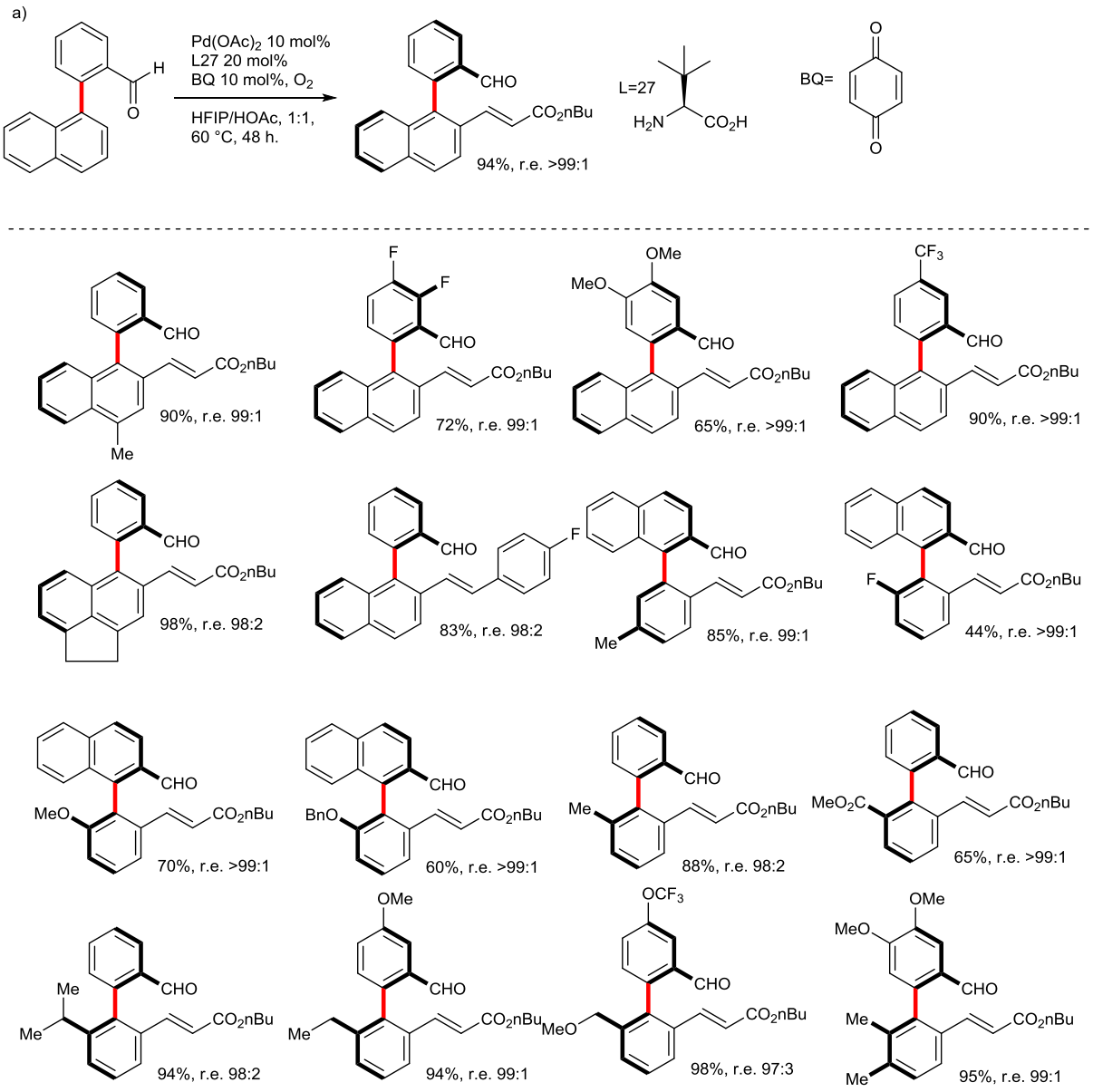

Figure III-54 : oléfination atropoénantiosélective par DKR grâce à un groupe directeur transitoire

Les biaryles tétra-substitués, comportant une barrière de rotation plus élevée, exception faite de ceux substitués par –OR ou F, réagissent suivant un mécanisme de KR, là aussi avec d'excellentes énantiosélectivités (Figure III-55).

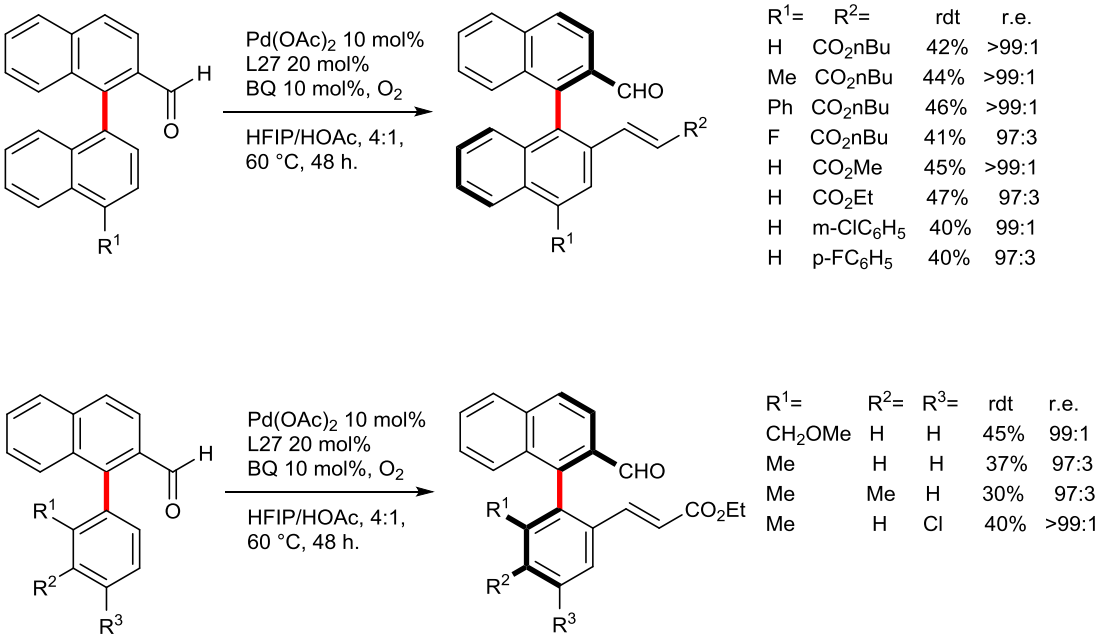

Figure III-55 : oléfination atropoénantiosélective par KR grâce à un groupe directeur transitoire

(2) Substitution atroposélective d'un substituant par des métaux de transition

Le premier exemple en 1995 par Hayashi et collaborateurs[99], par désymétrisation d'un *ortho*,*ortho*-ditriflate présente l'avantage de pouvoir fonctionnaliser de nouveau le produit de la réaction (Figure III-56).

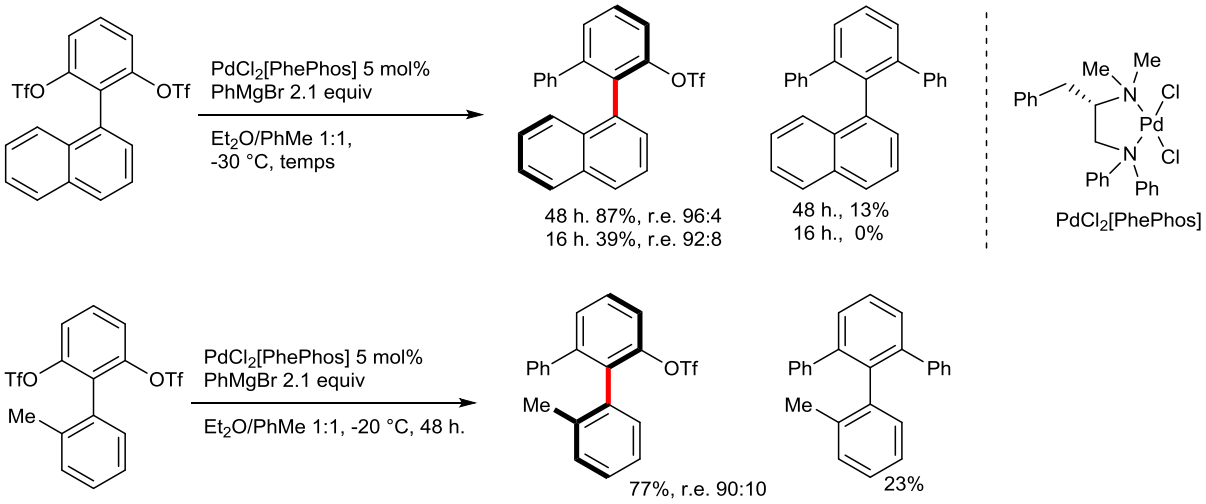

Figure III-56 : désymétrisation catalytique de di-triflates

En 2013, concomitamment Bhat et collaborateurs dans le groupe Stoltz et Virgil[100], et Ros et collaborateurs avec Fernandez et Lassaletta[101] développent une fonctionnalisation de dérivés bromés et/ou triflates de naphthylisoquinoline : les deux publications utilisant du palladium avec un cycle Pd^0/Pd^{II}; il est intéressant de comparer leurs études et hypothèses en opposition concernant le mécanisme rendant possible le dédoublement dynamique et de remarquer qu'ils y parviendront chacun en utilisant

un triflate comme groupe partant et en invoquant un complexe intermédiaire cationique.

Stoltz et Virgil parviendront à préparer le ligand QUINAP avec un très bon rendement et énantiosélectivité en utilisant une biphosphine et grâce à un protocole très précis : c'est en effet l'addition lente du partenaire de couplage sur 4 heures (au lieu d'une heure) qui permet d'augmenter le r.e. de 80:20 à 95:5 (Figure III-57a contre b). Une étude sur l'épimérisation thermique du substrat disqualifie un mécanisme par DKR simple (Figure III-57d). Les auteurs proposent ainsi un mécanisme par DYKAT, avec comme état de transition un complexe cationique, stabilisé par une liaison agostique par l'hydrogène en position C8 lorsque les deux cycles aromatiques se trouvent dans un arrangement *trans*-coplanaire (Figure III-57e). Ceci étant supporté par le fait que l'addition de TBAB fait tomber l'énantiosélectivité de 80:20 à 54:46 (contre-ion bromure coordinant contre triflate non-coordinant Figure III-57b contre c).

.

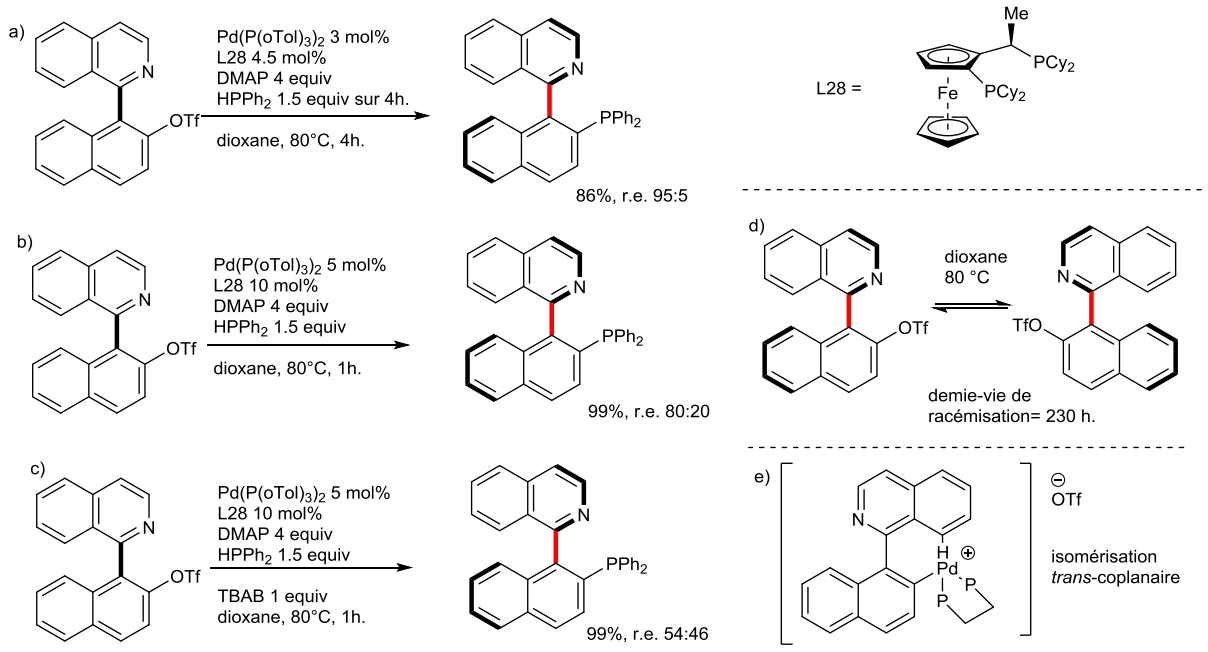

Figure III-57 : phosphination atropoénantiosélective par DKR

Fernandez et Lassaletta proposent quant à eux l'arylation de la même famille de substrats dans une réaction de Suzuki-Miyaura énantiosélective grâce cette fois à l'utilisation d'une phosphoramidite monodentate avec de très bons rendements et énantiosélectivités (Figure III-58a). Là aussi l'énantiosélectivité de la réaction est sujette à des conditions très précises : comme Stoltz et Virgil ils constatent l'importance d'un contre-ion non coordinant (bromure contre triflate Figure III-58c), ainsi que l'utilisation d'un partenaire de couplage moins réactif (boroxines contre acide boronique Figure III-58b) permet d'augmenter l'énantiosélectivité. On peut ainsi penser que l'épimérisation du substrat dans le complexe intermédiaire est relativement lente par rapport à l'élimination réductrice (typiquement étape cinétiquement limitante dans ces types de réactions), et qu'il faille laisser du temps au complexe diastéréomérique

intermédiaire pour s'équilibrer selon un mécanisme DYKAT. Cependant, ils invoquent un mécanisme DYKAT différent de Stoltz et Virgil : la formation du palladacycle à 5 membres avec l'azote hétérocyclique conduit à une augmentation des angles de liaisons autour de l'axe biarylique, et ainsi diminue la barrière de rotation dans un état de transition *cis*-coplanaire (Figure III-58e). Cette hypothèse étant supportée par la structure déterminée par rayons-X d'un palladacycle cationique montrant effectivement cette augmentation des angles de liaison (Figure III-58d), cependant avec un ligand très différent de celui utilisé dans leur réaction (une phosphine-hydrazone bidentate). Remarquons enfin que seules des boroxines riches en électrons ont pu être utilisées, et que la réaction a pu être étendue à d'autres hétérocycles (quelques exemples sont présentés Figure III-58f).

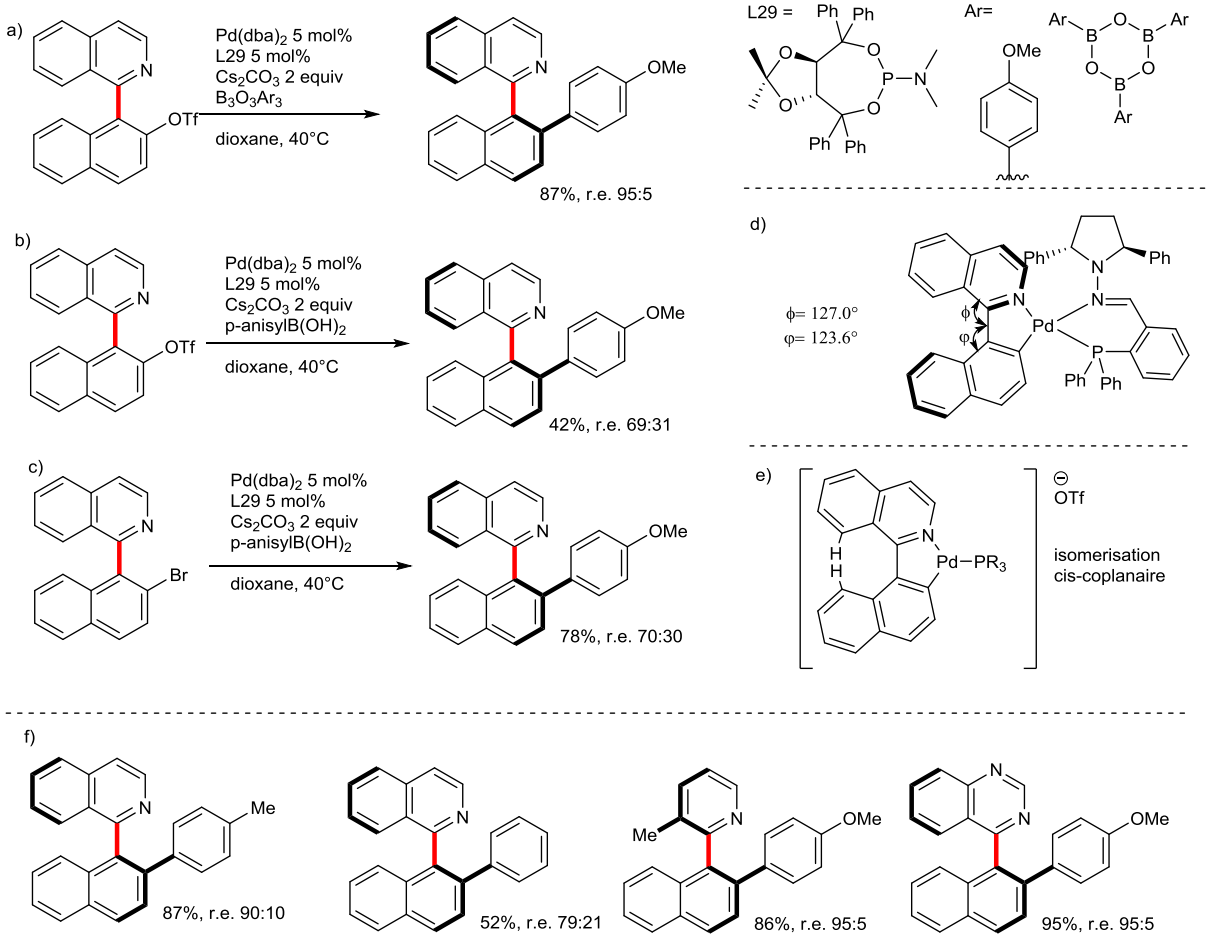

Figure III-58 : arylation atropoénantiosélective par DKR

En 2016 le groupe de Lassaletta[102] développe également une phosphination énantiosélective des mêmes substrats, en appuyant cette fois leurs hypothèses sur l'origine de la DYKAT sur des calculs DFT. Cette fois ils utilisent également une phosphine bidentate de type JOSIPHOS. L'emploi de trimethylsilyldiphenylphosphine permet de libérer progressivement le réactif de couplage (au lieu d'une addition lente chez Stoltz et Virgil). Notons que l'énantiosélectivité de la réaction reste très sensible aux conditions, comme l'atteste le besoin, pour obtenir des r.e. supérieurs à 90:10,

d'utiliser du THF distillé et dégazé le jour même, le besoin de préparer et de purifier les partenaires de couplages au laboratoire (même si ils sont par ailleurs disponibles commercialement), ainsi que l'utilisation de $Pd(dba)_2$ plutôt que $Pd_2(dba)_3$. Dans ces conditions, d'excellents rendements et énantiosélectivités ont pu être généralement obtenus, en notant que ces derniers semblent être plus dépendants de la phosphine utilisée que du substrat (quelques exemples sont présentés Figure III-59).

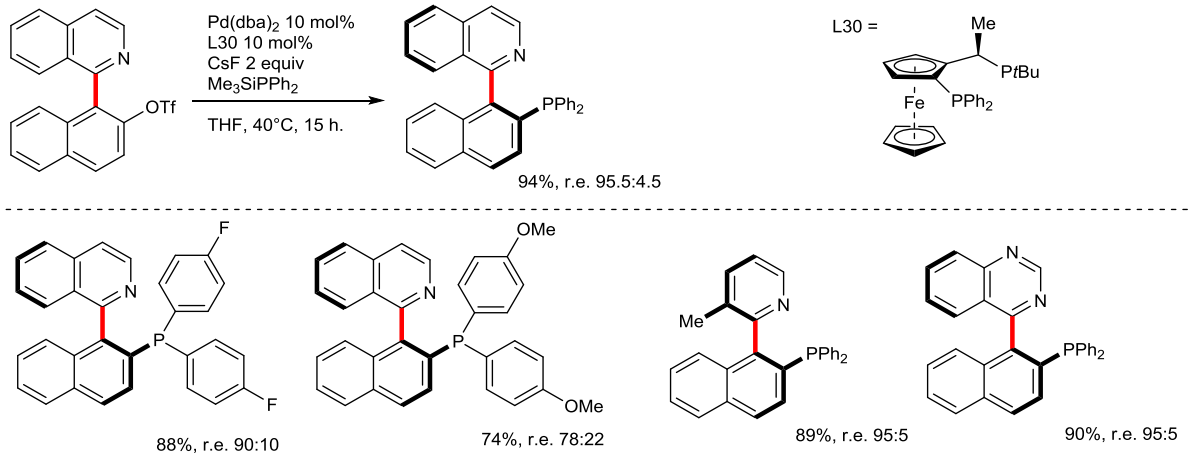

Figure III-59 : phosphination atropoénantiosélective par DKR dans le groupe Lassaletta

Puis en 2016 la méthode est étendue par le groupe de Lassaletta[103] vers une amination énantiosélective en utilisant cette fois comme ligand la QUINAP, avec à nouveau d'excellentes énantiosélectivités (une sélection de résultats est présenté Figure III-60), puis vers alkynylation énantiosélective[104].

.

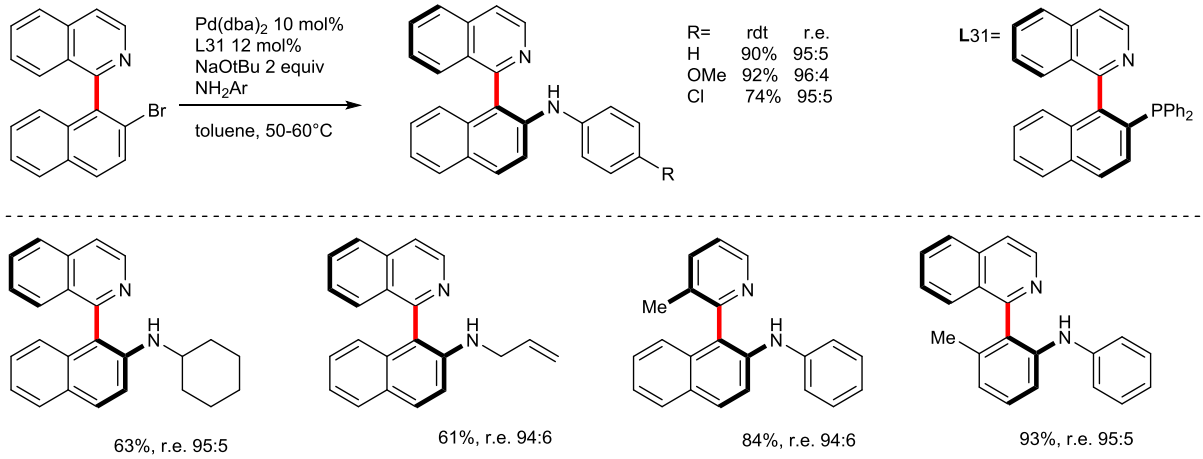

Figure III-60 : amination atropoénantiosélective

(3) Modification atroposélective de substituant existant

On peut recenser trois grandes méthodes dans cette catégorie :

a) les réactions par désymétrisation d'un biaryle à la barrière de rotation assez élevée pour être configurationellement stable avant et après la modification,

b) les réactions par DKR consistant en la coupure d'un pont (grâce à un réactif énantiopur) sur un biaryle chiral mais non atropisomérique,

c) les réactions par DKR consistant en la formation d'un pont (énantiopur) sur un biaryle chiral mais non atropisomérique.

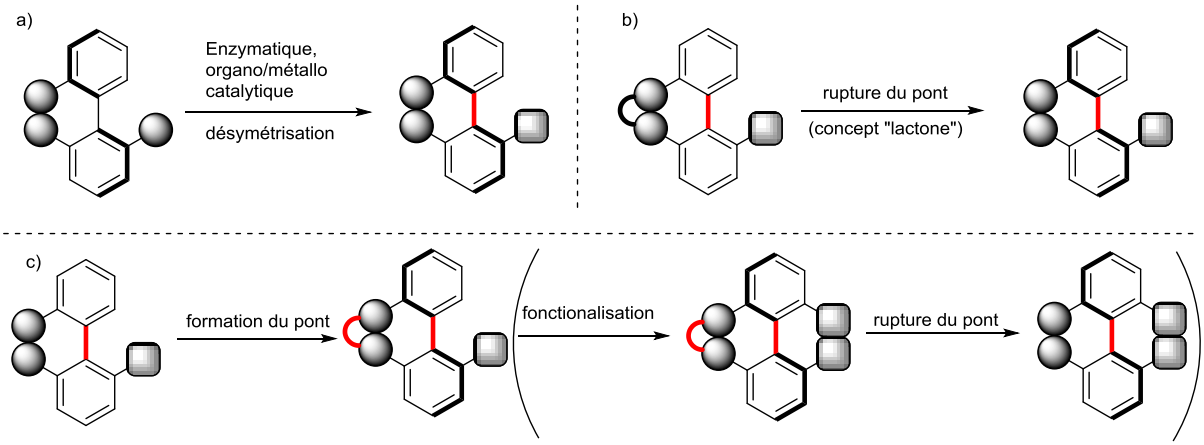

Figure III-61 : stratégies atroposélectives par modification de substituants existants

(a) Désymétrisation

Signalons, dans les réactions enzymatiques, l'hydrolyse énantiosélective de diacetoxybiaryles, avec d'excellentes énantiosélectivités mais des rendements modestes[105] (Figure III-62a), ainsi que l'oxydation énantiosélective de dihydroxymethylbiaryles[106] (Figure III-62b). Cependant, comme souvent dans le cas réactions enzymatiques, une grande spécificité de substrats et des conditions réactionnelles peu pratiques (très faible concentration, milieu aqueux, long temps de réaction) rendent le procédé encore rare.

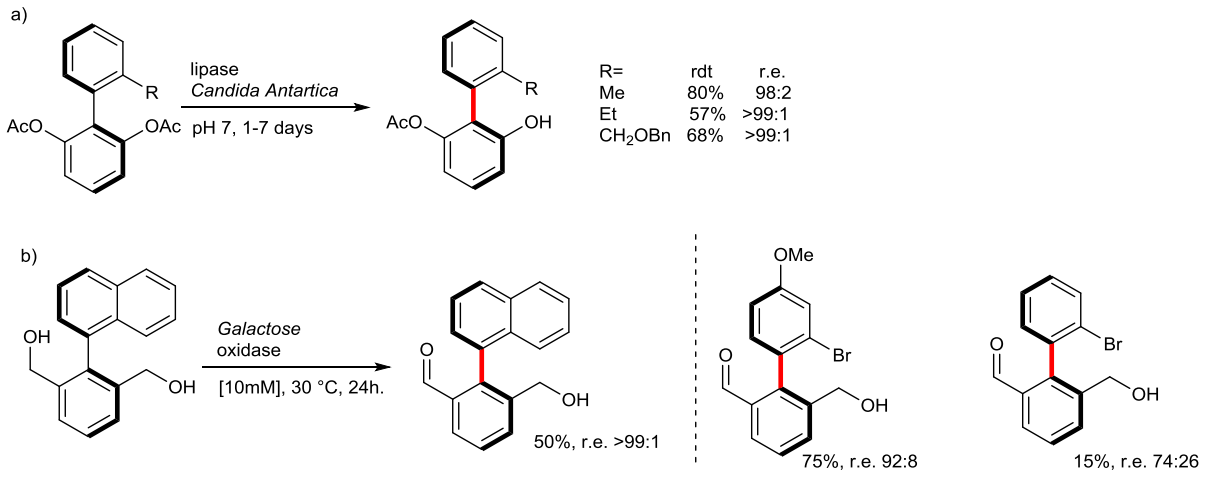

Figure III-62 : exemples de réactions enzymatiques énantiosélectives

Remarquons aussi une désymétrisation originale par lithiation d'une position benzylique grâce à un ligand énantiopur : l'utilisation de (-)-sparteine offrant une énantiosélectivité modeste[107] (Figure III-63a). Plus récemment, l'approche similaire par échange halogène/lithium en présence d'un diéther catalytique énantiopur donnera de bon rendement et énantiosélectivité[108] (Figure III-63b). Cette stratégie permet d'acéder à un large panel de composés grâce à la compatibilité de cette stratégie avec des électrophiles variés, et la possibilité de fonctionnaliser plus avant les produits.

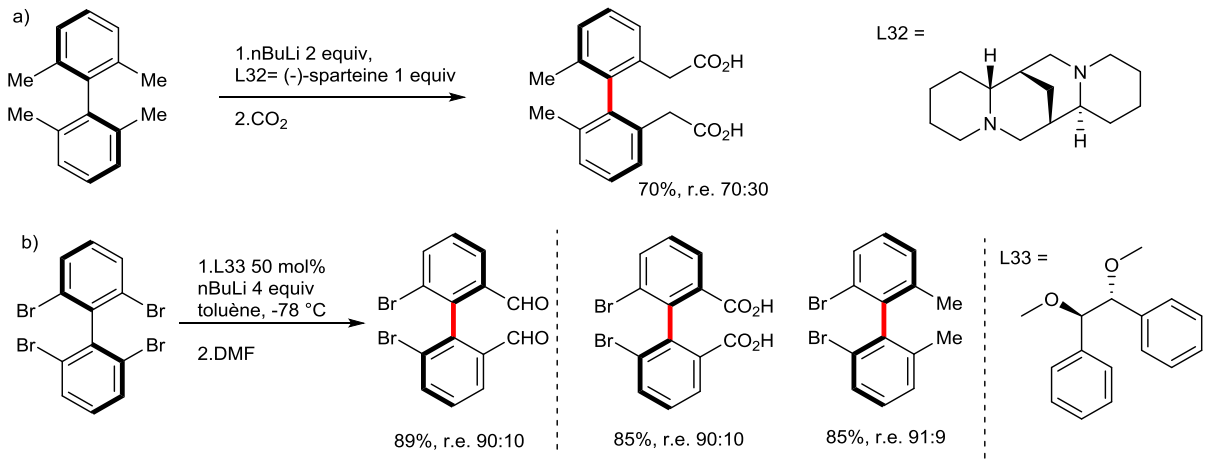

Figure III-63 : désymétrisation atroposélective par des bases lithiées

(b) Coupure atroposélective d'un pont

C'est certainement, par l'intermédiaire de la « méthode lactone » l'approche la plus répandue dans cette partie I.A.1.a)(1). Le concept a été développé par Bringmann et collaborateurs en 1992 et consiste en la formation non-atroposélective d'un biaryle où deux substituants *ortho,ortho'*- forment un pont sous la forme d'une lactone. La formation du pont à 6-membres ainsi que la tendance de la lactone (conjuguée au biaryle) à être planaire diminue la barrière de rotation du biaryle chiral jusqu'à qu'il ne soit plus atropisomérique. Ainsi l''utilisation d'un nucléophile chiral, qui va s'additionner à la lactone de façon atroposélective selon un mécanisme de DKR, puis l'ouverture de cette lactone permet au biaryle de retrouver l'atropisomérie (Figure III-64).

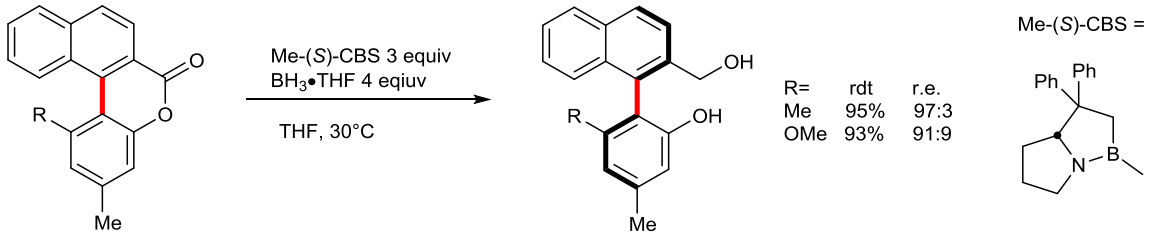

Figure III-64 : concept « de la lactone »

Le concept a pu être été étendu à différents nucléophiles chiraux, et deux exemples sont présentés Figure III-65. Si La principale limitation de la méthode est bien entendu l'obligation posée sur deux des substituants *ortho* pour pouvoir former la lactone, la méthode a néanmoins pu être appliquée à la préparation de nombreux produits naturels[109,110].

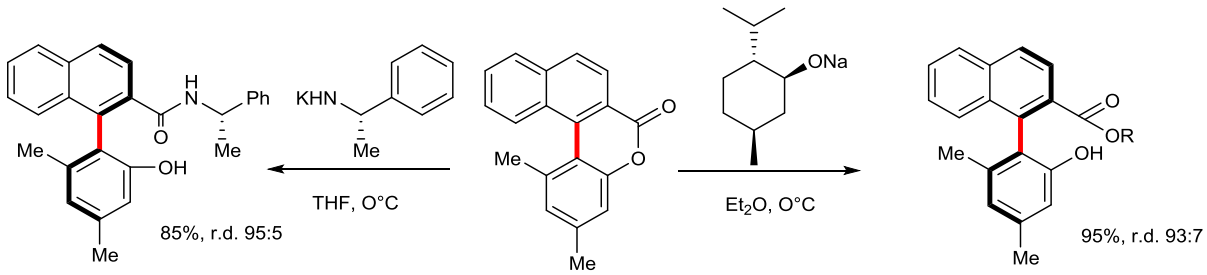

Figure III-65 : extension du concept de la lactone à l'addition de divers nucléophiles chiraux

(c) Formation atroposélective d'un pont

Si, comme nous l'avons vu, les ponts à 5-6 membres sans substituants chiraux conduisent à diminuer la barrière de rotation de l'axe, la formation de pont plus grand et/ou énantiopur, peut constituer un biais conformationnel et ainsi être atroposélective.

L'approche peut soit être diastéréosélective : la formation d'un pont lactame à 7 membres à partir d'une oxazoline énantiopure permettant, grâce à un mécanisme DKR, d'obtenir de bons rendements et d'excellentes atroposélectivités[111] (Figure

III-66a).
Où elle peut être énantiosélective si la fonctionnalisation de l'intermédiaire ponté, en augmentant la barrière de rotation, permet d'enlever le pont : ainsi l'estérification d'un chlorure d'acide atropisomériquement pur permet d'induire l'atropisomérie d'une 2,2'-bipyridine substituée par deux alcools benzyliques en positions *ortho* et *ortho*'[112]. L'oxydation suivie d'hydrolyse conduit à la formation de bipyridines-*N,N'*-dioxides avec des rendements corrects et de bonnes sélectivités (Figure III-66b).

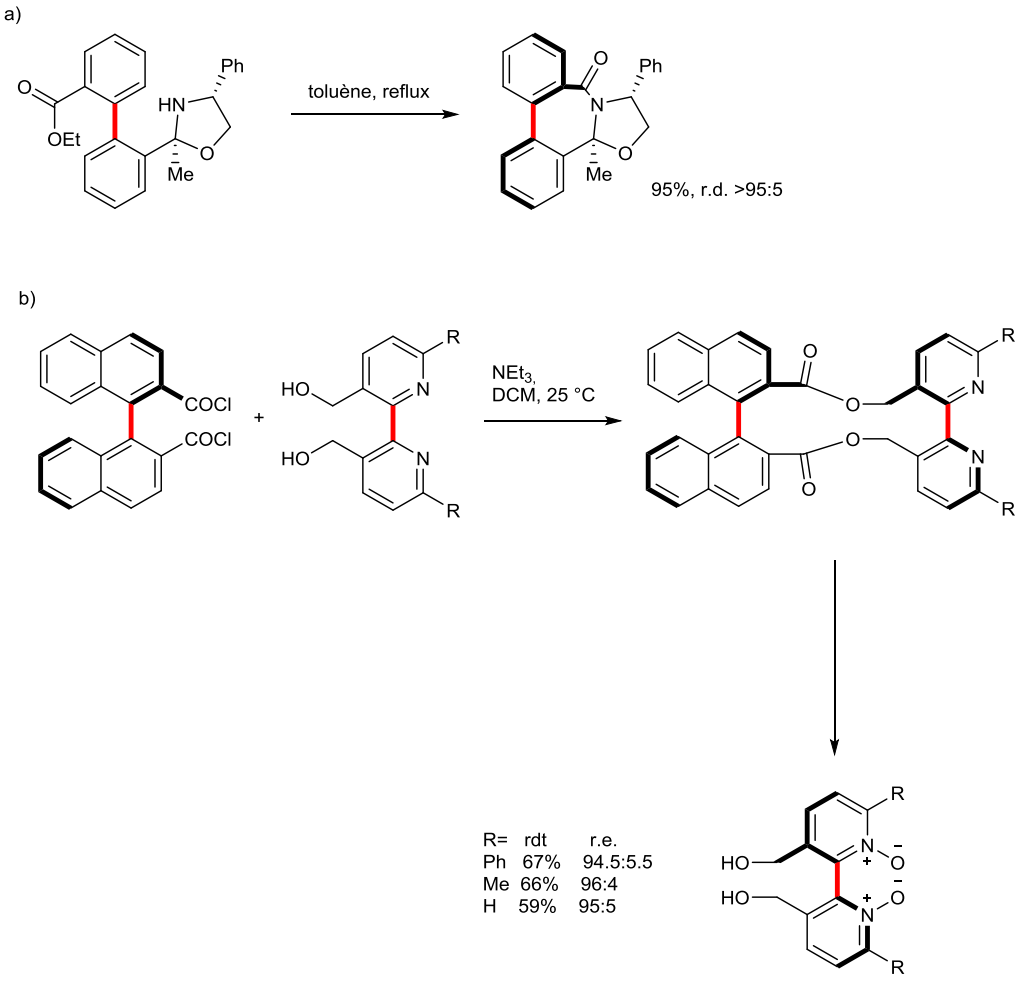

Figure III-66 : formation atroposélective d'un pont

Une approche apparentée originale à mentionner est le concept de ligand *tropos* : dans un premier temps, la coordination d'un biaryle chiral mais non atropisomérique chélatant un métal forme un complexe racémique. L'adjonction d'un inducteur de chiralité permet d'induire un biais conformationnel et ainsi d'obtenir un complexe diastéréopur, donc un complexe *atropos* (Figure III-67a[113]). Soulignons qu'il est parfois possible d'enlever l'inducteur de chiralité et de conserver la chiralité axiale du biaryle (Figure III-67b[113]) : en effet, lorsqu'il est coordiné, les deux substituants du biaryle sont forcés dans un état de transition *cis*-coplanaire pour l'épimérisation, qui ne peut alors se faire à température ambiante. Bien sûr, d'autres facteurs sont à prendre en compte, comme la nature de la liaison de coordination (la liaison P-Pd plus forte que la liaison P-Rh permet aux complexes du premier métal de conserver

leur chiralité axiale sans l'inducteur de chiralité dans certaines conditions), le solvant, et bien sur la température (voir différences dans les conditions permettant l'isomérisation entre Figure III-67a et c[114]). Il est également possible d'accéder à des formes originales d'atropisomérisme (Figure III-67d[115]), et nous renvoyons le lecteur vers une revue récente et complète sur l'obtention, les propriétés et les utilisations de ce type de ligand[116].

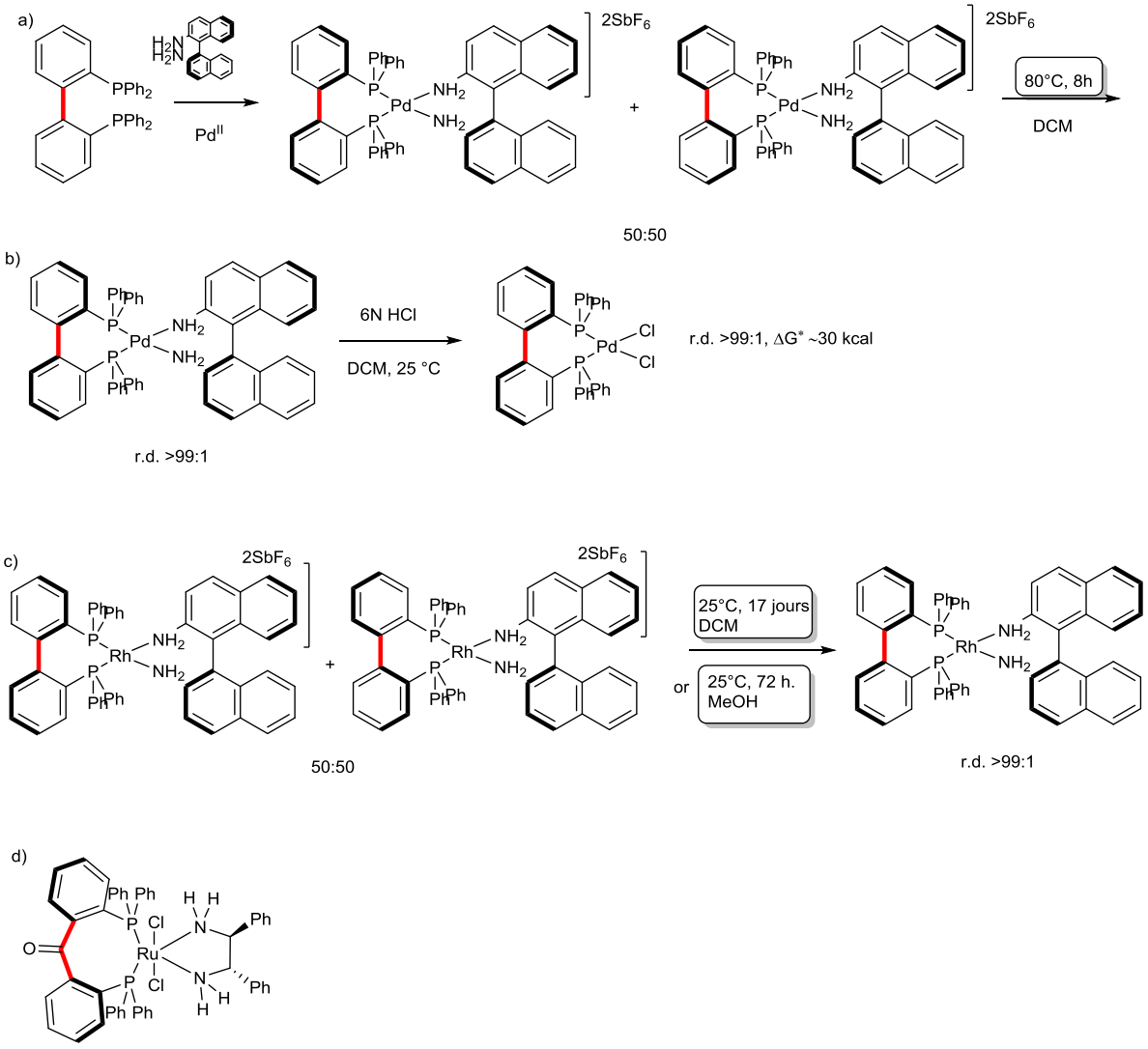

Figure III-67 : concept de ligands *tropos* et *atropos*

3. Occurrence et application

a) Composés biologiquement actifs

La chiralité et son contrôle occupe une place prépondérante dans l'industrie pharmaceutique actuelle. En effet il est bien établi que les énantiomères peuvent posséder des propriétés biologiques bien différentes[117] (activité, pharmacocinétique, toxicité). Ainsi, 65% des nouveaux médicaments mis sur le marché entre 2004 et 2006 l'ont été sous forme énantiopure et il existe de nombreux exemples où un énantiomère a montré un effet thérapeutique supérieur à l'autre[118]. Cependant l'atropisomèrisme présente des défis bien spécifiques dans le développement des molécules bioactives. Le premier étant de prédire la présence d'axes atropisomèriques : en effet, comme nous l'avons vu, la définition de l'atropisomèrie n'est pas absolu[119]. Le deuxième, découlant du premier, est de connaître aussi précisément que possible la valeur de la barrière de rotation dans les conditions métaboliques. Dans la pratique, il n'existe pas de règles formelles pour le développement d'atropisomères[120] (au 16/10/2017), et des auteurs[119] ont proposés la valeur limite haute de $\Delta G^{\ddagger}_{rot}$ = 29.4 kcal/mol : elle correspond à une demi-vie de 4609 jours dans le plasma humain (en appliquant un facteur correctif multiplicatif de 33 pour la valeur dans le plasma humain par rapport à la valeur dans l'eau[121]), et ainsi à une pureté atropisomérique >99.5% sur un passage de 24 heures dans le corps humain.

Il est intéressant de remarquer que, pour les composés ayant une barrière inférieure à cette limite haute, la réponse de l'industrie pharmaceutique dans le développement de nouveau médicament a souvent été de supprimer l'axe atropisomérique, soit en diminuant la barrière de rotation, soit en symétrisant la molécule. Cette situation est illustrée en considérant l'antagoniste du canal de transport monocarboxylate (MTC1) **A1** (Figure III-68a) : ce composé a été redessiné en son dérivé **A2** qui ne présente pas de propriétés atropisomèriques[122,123]. Dans une autre stratégie, l'antagoniste CCR5 du virus HIV **B1** (Figure III-68b) a été symétrisé en son dérivé **B2** pour éliminer ses propriétés atropisomériques[124,125].

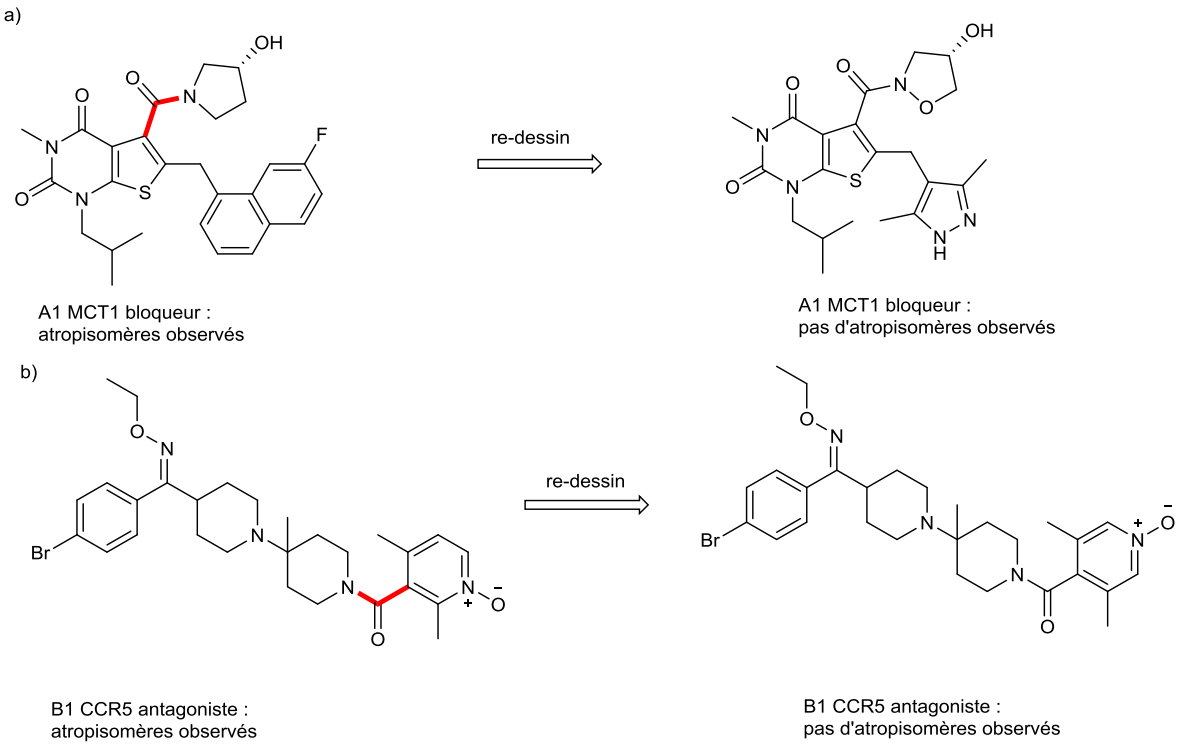

Figure III-68 : stratégie de contournement de l'atropisomérie

Si l'atropisomérisme de ces composés ne relève pas d'une atropisomérie aryle-aryle, ils illustrent néanmoins en quoi la multiplication des possibilités de contrôle de l'atropisomérie peut être bénéfique dans le développement de nouveaux médicaments : en effet la reformulation des composés précédents dans des versions non-atropisomériques n'a pas été motivé par l'amélioration de leurs effets thérapeutiques, mais par la difficulté apportée par le contrôle de ces éléments d'atropisoméries. Ainsi, on peut se demander dans quelle mesure la stratégie inverse (c'est-à-dire l'élévation de la barrière de rotation couplée à un contrôle des éléments atropisomériques) aurait permis d'améliorer l'effet thérapeutique de ces composés.

En effet il est bien connu que la modification de la configuration de l'axe de chiralité peut modifier significativement les propriétés d'une substance bioactive : ainsi le gossypol, composé naturel, était (en 2008) évalué en phase I et II de tests cliniques pour ses propriétés cytotoxiques, et il a été démontré que l'atropisomère ($_aR$) est l'isomère actif[126]. Cependant il n'existe aucune plante produisant exclusivement cet isomère, ni, à ce jour, de voies de synthèses atroposélectives viables[127].

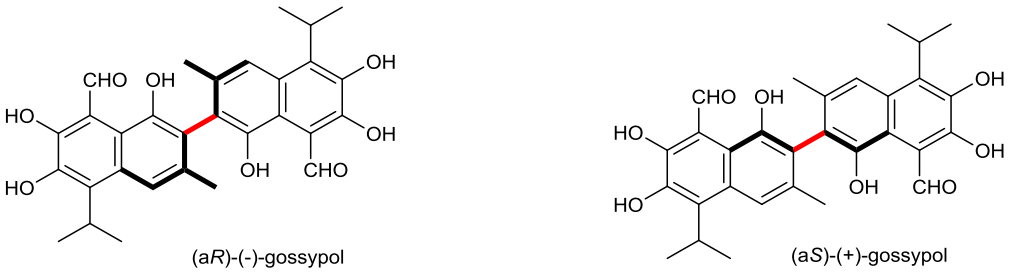

Figure III-69 : exemple de composé ayant des propriétés biologiques atropo-dépendantes

L'exemple de la vancomycine illustre un autre défi : cet antibiotique d'origine naturelle a en effet un rôle capital, étant l'un des rares largement actifs contre les bactéries résistant à la pénicilline et ce depuis des décennies[128]. Si ici il existe une source naturelle produisant un composé atropisomériquement pur, la possibilité de voir une multiplication des bactéries développant une résistance appelle au développement de dérivés, et ainsi exige des moyens de contrôler les éléments d'atropisomérie : cette constatation a ainsi été à l'origine d'intenses recherches dans ce domaine[129] , et pour le moment les modifications ont surtout concerné la chaine glycane[130] (Figure III-70).

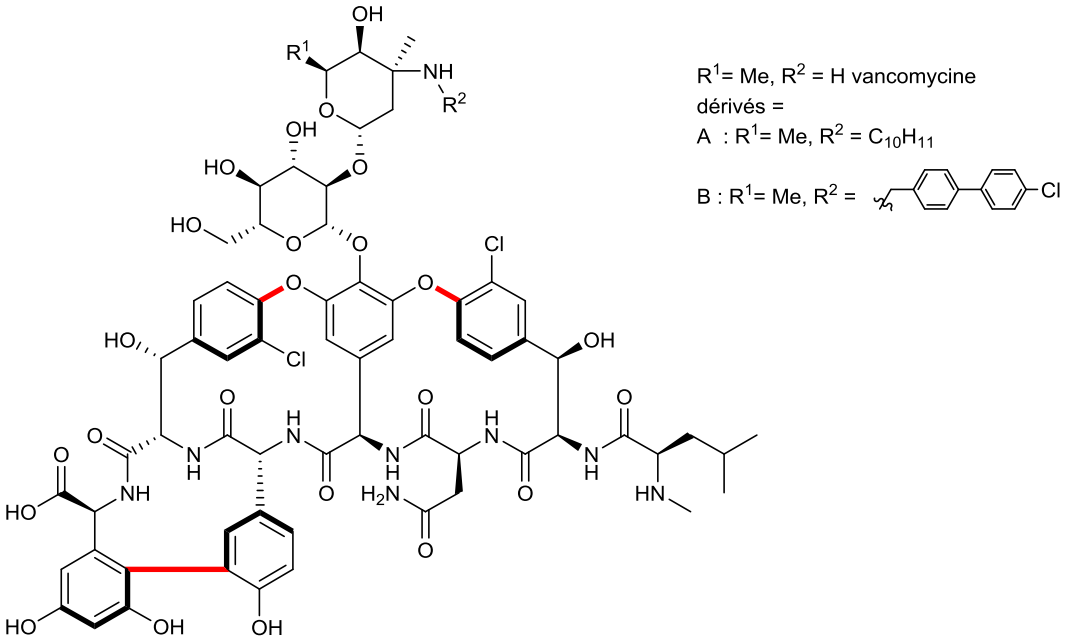

Figure III-70 : vancomycine et dérivés

Ensuite, dans un exemple plus récent, on peut voir comment la prise en compte de l'atropisomérie (et de dérivés autour de cette atropisomérie) dans l'évaluation d'un nouveau composé peut être intéressante : ainsi si les flavomannins A,B,C et D ont tous montré une activité contre le cytotoxique sur *B. subtilis,* seul les isomères B et D ont montré un effet sur le promoteur *yorB* de la protéine RecA[131,132] (indication d'une interaction directe avec la structure ADN). Ainsi la possibilité d'une modification du mode d'action basée uniquement sur le contrôle de l'axe atropisomérique, pourrait permettre la préparation aisée de dérivés.

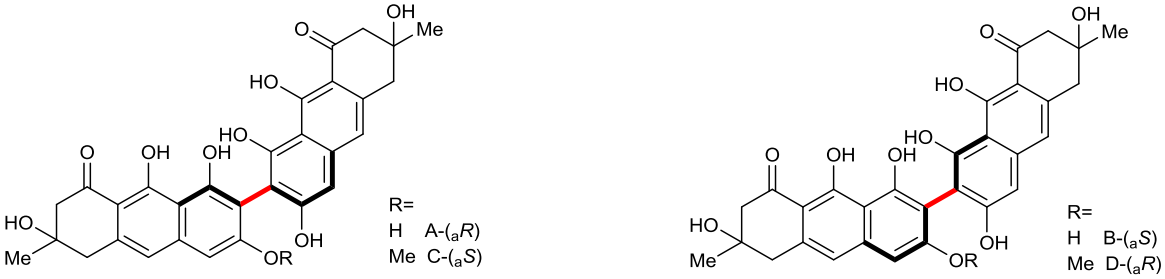

Figure III-71 : isomères des flavomannins A, B, C et D

Enfin, un dernier exemple nous permet d'apprécier ce que le dévoloppement de nouvelles méthodologies peut apporter à l'ndustrie pharmaceutique. La viriditoxine (Figure III-72a) a été découverte en 1971[133] et seul l'atropisomère a*S* est produit naturellement, en trop faible quantité. Bien qu'ayant montré un effet sur les protèines FtsZ des bactéries (les FtsZ sont l'équivalent chez les bactéries de la tubiline chez les humains : ces protèines sont indispensables pour accomplir la division cellulaire. Ainsi, en ciblant les FtsZ ont peut espérer une cytotoxicité importante chez les bactéries pathogènes tout en limitant la toxicité chez le patient[134]), il faudra attendre 2011 pour voir la première synthèse totale. En effet Shaw et collaborateurs[135] utiliseront un catalyseur bimétallique de vanadium, développé en 2007 (décrit dans le chapitre sur les couplages oxydants de ce manuscrit), pour réaliser l'étape clefs atroposélective de leur synthèse. Le catalyseur au vanadium (Figure III-72b) permet de réaliser un couplage avec un très bon rendement et une excellente atroposélectivité (Figure III-72c, synthèse de deuxième génération[136])

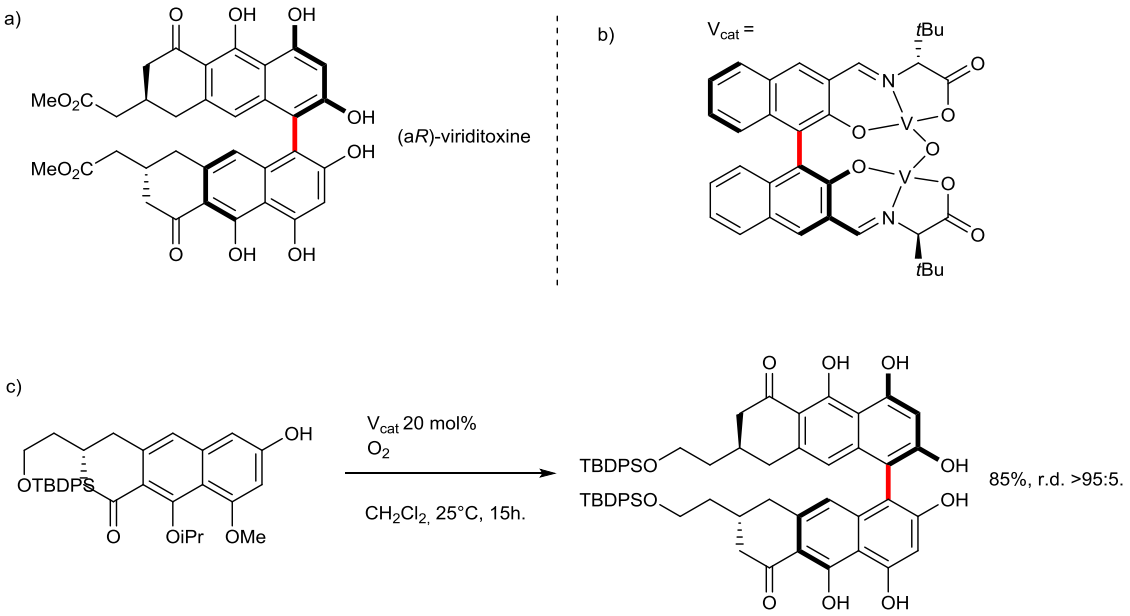

Figure III-72 : contruction atroposélective de l'unité biarylique de la viriditoxine

En conclusion, on peut penser que l'atropisomérie et son contrôle occuperont une place de plus en plus importante à l'avenir dans l'industrie pharmaceutique, comme en témoigne les revues récentes[119,127,130,137,138], ainsi que la multiplication des méthodes décrivant la synthèse de produits naturels atropisomériques bioactifs[110,139]

b) *Application comme inducteur de chiralité*

Historiquement, la catalyse homogène asymétrique à l'aide de métaux de transition doit son développement à grande échelle à deux découvertes : la découverte d'un catalyseur homogène extrêmement actif par Wilkinson en 1966[140], [$RhCl(PPh_3)_3$], suivie de la possibilité de préparer des phosphines stéréogènes à l'atome de phosphore par Horner en 1964 et Mislow en 1968[141,142]. La possibilité de coupler de basses charges catalytiques avec des transformations asymétriques a conduit à en d'intenses recherches (académique et industrielle) dans ce domaine. Si les premiers ligands développés étaient stéréogènes à l'atome de phosphore (Knowles[143] Figure III-73a ; et Horner[144] Figure III-73b en 1968), il fut rapidement démontré, avec l'utilisation de la bis-phosphine chélatante DIOP (Figure III-73c) en 1971 par Kagan[145], qu'un squelette carboné chiral avec une phospine non-stéréogène à l'atome de phosphore pouvait induire l'asymétrie. Enfin, la première application industrielle des réactions d'hydrogénation asymétrique consiste en l'utilisation de la bi-phosphine stéréogène à l'atome de phosphore DiPAMP en 1974[146] (Figure III-73d- synthèse de la L-dopa).

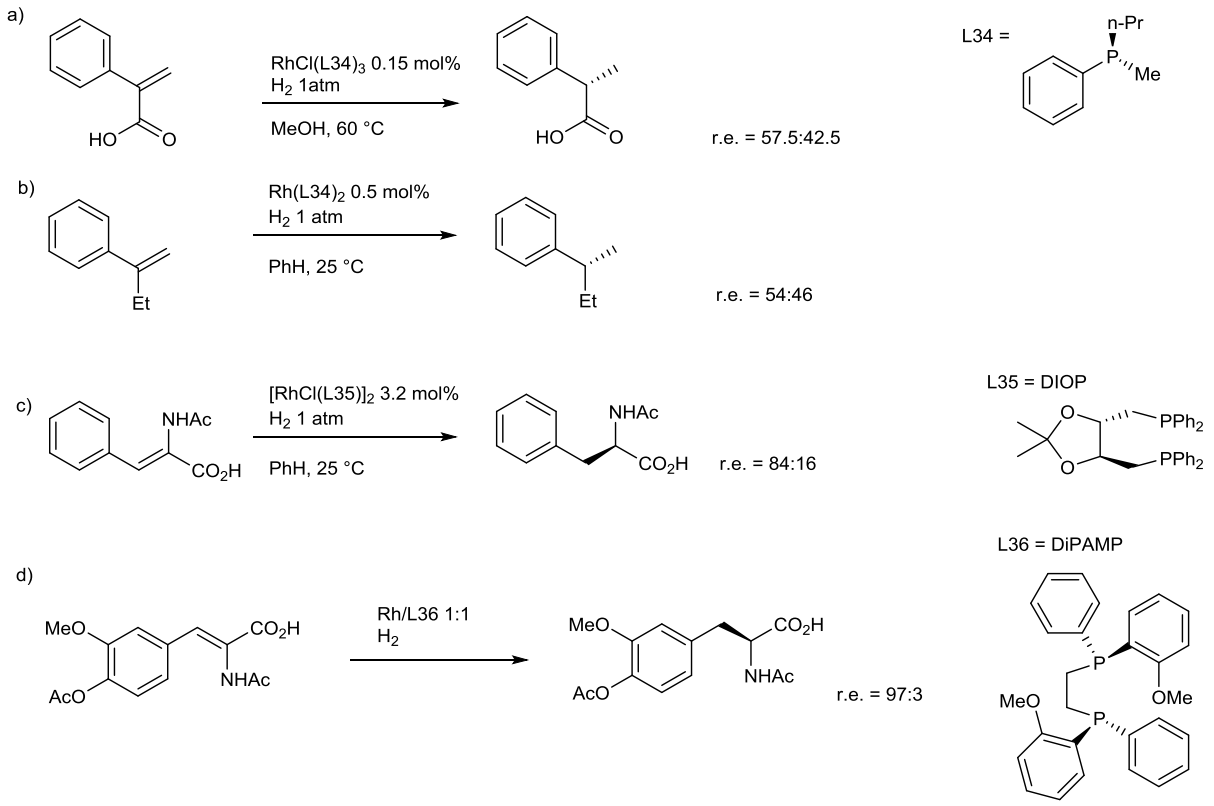

Figure III-73 : exemples précoces de catalyse homogène asymétrique avec des phosphines

Ainsi, la possibilité d'utiliser un squelette chiral en combinaison avec des phosphines achirales fut mise à profit pour explorer un nouveau type de squelette stéréogène atropisomèrique, celui du binaphtyle. Les premières mentions de phoshines atropisomèriques dans la littérature datent de 1977 quand Grubbs[147] et Kumada[148] repor-

tent respectivement de façon indépendante les ligands phosphinite et phosphite (Figure III-74a et b). Cependant, tous deux démontrent une activité relativement faible et des r.e. très dépendant des conditions.

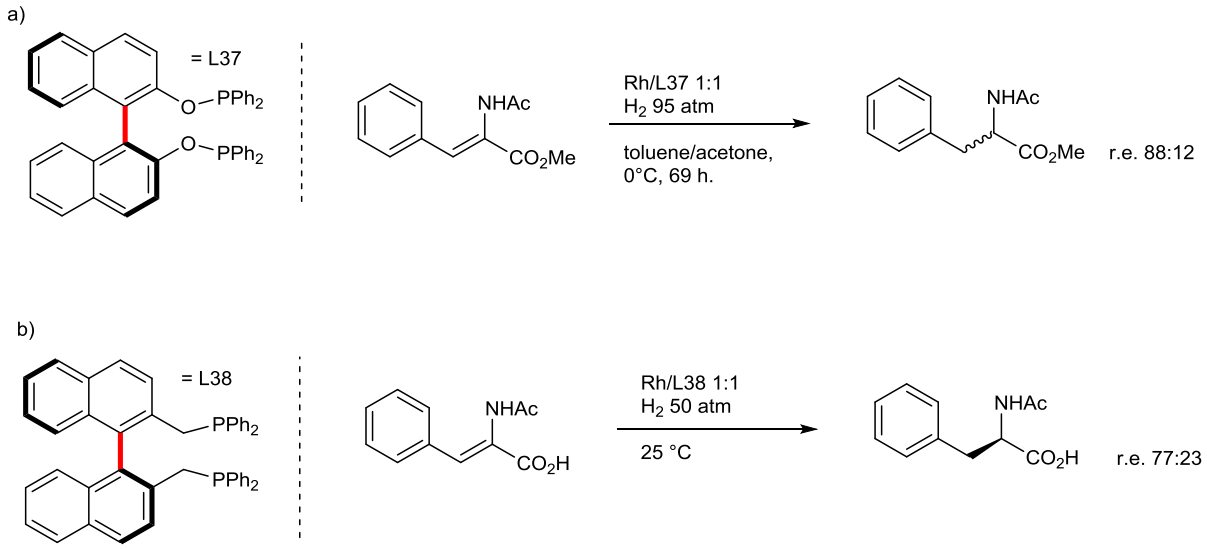

Figure III-74 : premières phosphines atropisomèriques

Le développement majeur interviendra quelques années plus tard lorsqu'en 1980 Noyori et collaborateurs[149] parviendront à dédoubler la BINAP de façon fiable. Ce ligand montrera d'excellentes activités et sélectivités pour l'hydrogénation asymétrique de précurseur d'acides aminés. Cependant, des conditions spécifiques (faible concentration et basse pression d'hydrogène) sont indispensables pour obtenir les meilleurs r.e., et ainsi la première application industrielle du système BINAP/Rh concernera l'isomérisation d'amines allyliques[150] en 1984 (Figure III-75b). Cette transformation permettra de développer une synthèse du (-)-menthol à l'échelle industrielle avec des r.e. >99 :1[151].

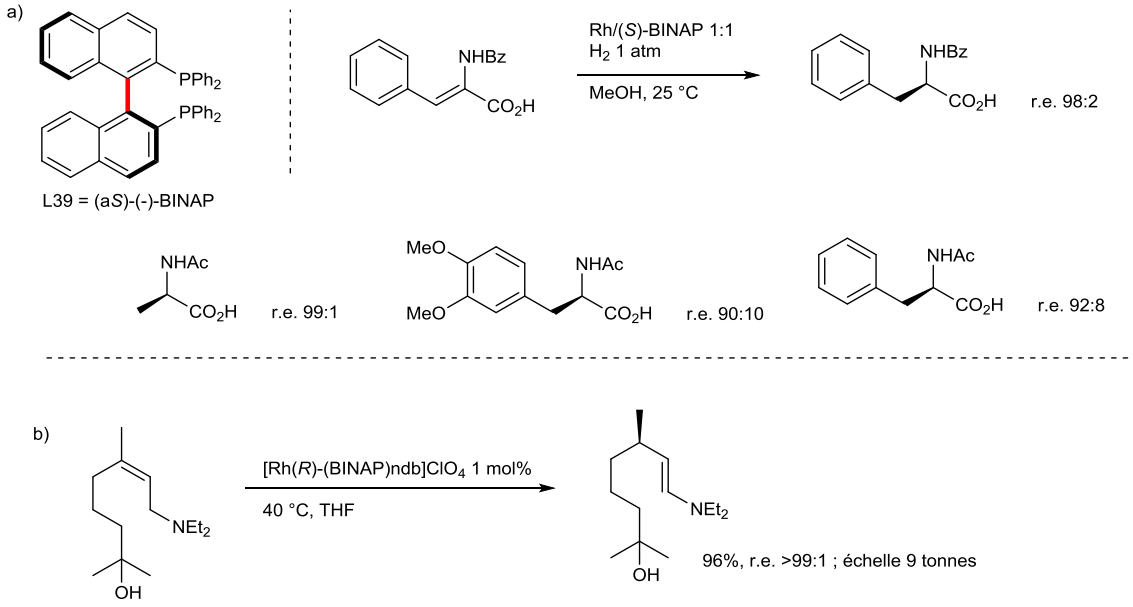

Figure III-75 : première utilisation académique et industrielle de la BINAP

Le prochain développement majeur consistera en la découverte de la performance des complexes BINAP/Ru dans les réactions d'hydrogénation d'oléfines en 1986[152]. En effet ces derniers montreront d'excellentes performances dans l'hydrogénation asymétrique sur une variété de substrats importants, et surtout une stéréosélectivité moins dépendante des conditions réactionnelles. Ainsi des rapports molaires substrat/catalyseur impressionnants ont pu être atteints en augmentant la pression d'hydrogène, la concentration ou la température de réaction. Ainsi les liaisons C=C activées et comportant un groupe coordinant seront hydrogénées par des complexes BINAP/Ru diacetate (Figure III-76a). Puis en 1988[153], ce seront les liaisons C=O de cétones avec un groupe coordinant en alpha ou beta qui seront hydrogénées par des complexes BINAP/Ru dichloride (Figure III-76b). Enfin en 1995, les cétones aromatiques non-fonctionnalisées seront hydrogénées par des complexes BINAP/Ru dichloride diamine (Figure III-76c). L'importance prise par ces transformations sera illustrée par quelques exemples des nombreuses applications industrielles des complexes BINAP/Ru (Figure III-76) (naproxen[154] : anti-inflamatoire – citronellol[155] ; parfumerie – levofloxacin[153] : antibiotique à large spectre – fosmomycin[156], antibiotique à large spectre – fluoxetine, anti-depresseur – BMS 181 100, anti-psychotique).

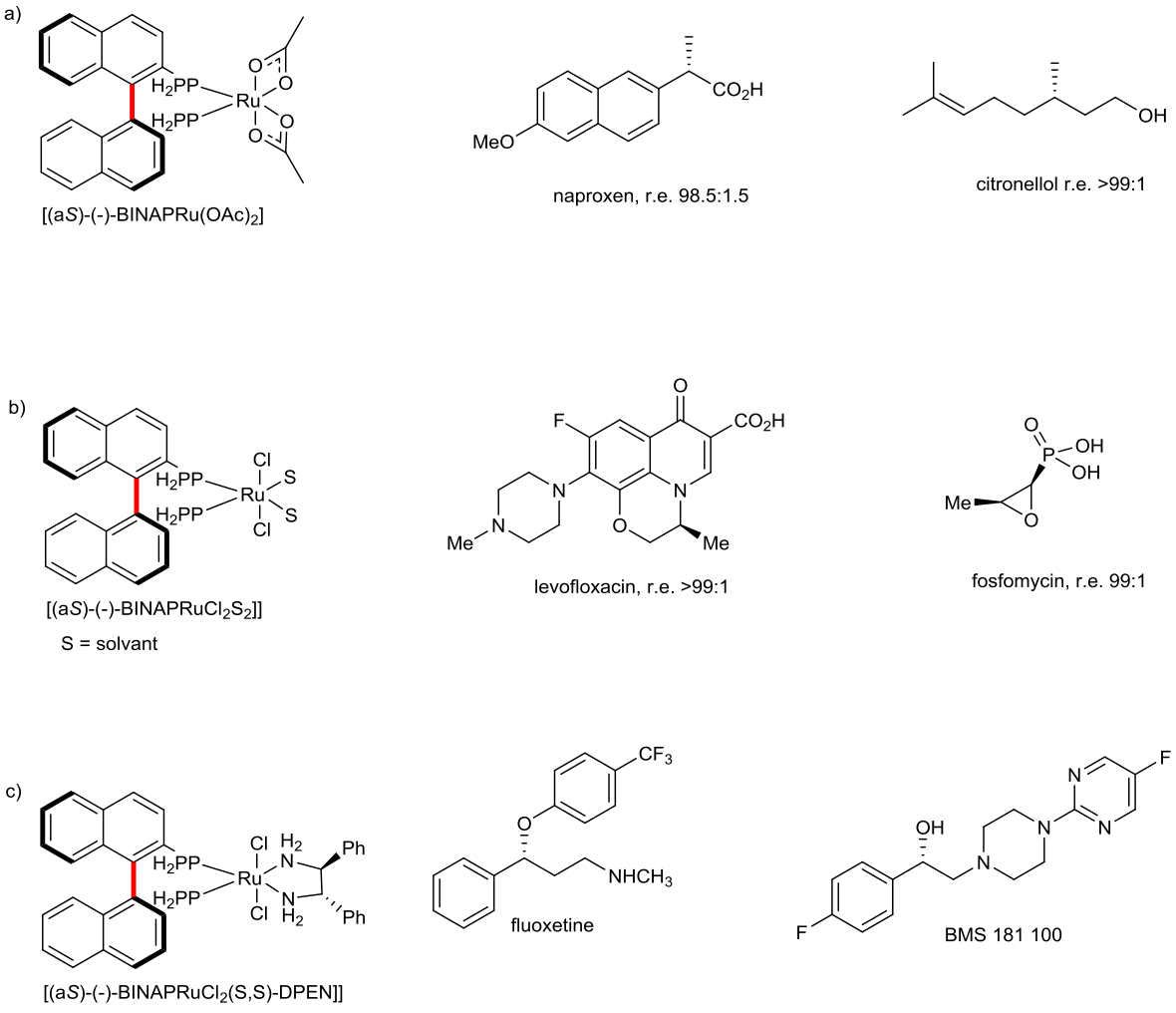

Figure III-76 : complexes BINAP/ruthenium et exemples d'applications industrielles

Le succès majeur rencontré par la BINAP dans les réactions d'hydrogénation encouragera le développement de nouveaux inducteurs de chiralité basés sur ce squelette et conduira ainsi à la création d'un véritable « famille » issue de la BINAP. En effet, par rapport aux ligands présentés Figure III-73, où la chiralité réside soit sur le squelette carboné, soit sur l'atome de phosphore, la chiralité axiale de la BINAP facilite le développement de dérivés : la modification du squelette autour de l'axe de chiralité permet un fin ajustement des propriétés stériques et électroniques sans transformer complétement l'environnement stéréogénique ce qui a fait le succès de la BINAP (Figure III-77 : H_8-BINAP[157], 3,3'-OR-BINAP[158]). Comparativement, il est beaucoup plus difficile de modifier le squelette à chiralité centrale d'un ligand comme le DIOP sans modifier de manière imprévisible son pouvoir d'induction asymétrique.

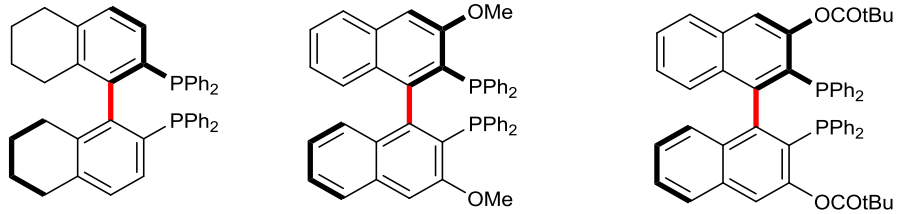

L40
H_8-BINAP : 1991

L41
3,3'-OMe-BINAP : 2005

L42
3,3'-OCOtBu-BINAP : 2005

Figure III-77 : modification du squelette de la BINAP

Ensuite, comparé aux ligands où la chiralité réside sur l'atome de phosphore, il est possible d'envisager d'utiliser d'autres hétéroatomes pour accommoder d'autres métaux, et donc d'élargir le champ d'application du squelette atropisomérique. Ainsi les phosphoramidites[159] montreront, par exemple, d'excellents résultats dans les additions conjuguées au cuivre. D'autre part les acides phosphoriques basés sur le même squelette atropisomérique sont reconnues pour leur potentiel en organocatalyse asymétrique[160]. Notons que la présence de substituants encombrants en position 3,3'- est indispensable pour obtenir une bonne induction asymétrique, soulignant encore une fois l'importance de la préparation aisée et modulable de dérivés optiquement purs.

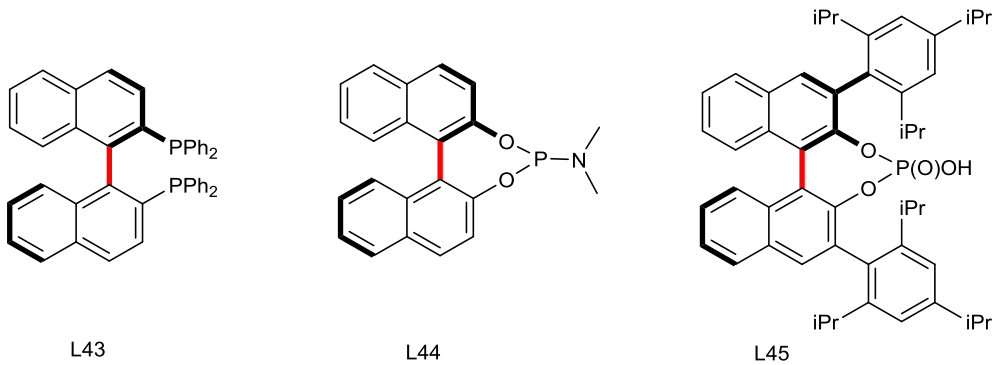

L43
(R)-BINAP : 1980

L44
(R)-MonoPhos : 1996

L45
(R)-TRIP : 2004

Figure III-78 : famille de ligands dérivés de la BINAP

Aujourd'hui, plus de 45 ans après la découverte de la BINAP, son squelette est encore utilisé pour développer de nouveaux concepts de ligands énantiopurs dans des domaines de pointe. Comme nous l'avons vu dans la partie III.B.2.c)(1) le squelette atropisomérique servira à synthétiser un nouveau type de ligand cyclopentadiènyle chiral dont les complexes de rhodium ont montré un fort potentiel en activation de liaison C-H asymétrique.

Cependant il faut garder à l'esprit que malgré l'immense succès rencontré par la BINAP et ses dérivés, il n'existe pas de ligand universel. En effet (en nous focalisant de nouveau sur les ligands utilisés en hydrogénation asymétrique) l'industrie pharmaceutique est toujours à la recherche du ligand idoine pour un substrat bien particulier. Comme le font remarquer Lennon et Pilkington[161], (Chirotech, Dow Chemical Company), cette recherche peut se faire en deux temps : tout d'abord identifier, parmi une collection de ligands, le type de squelette qui donne les meilleurs résultats ; puis, si possible, passer au crible les variations structurelles disponibles pour une optimisation finale. Ainsi, la modularité structurelle et/ou électronique aisée de nouveaux ligands est absolument essentielle pour développer des applications multiples et variées. Ce constat est clairement illustré à travers une étude visant de déterminer la structure privilégiée d'un ligand stéréogénique dans le domaine de l'hydrogénation asymétrique.

En effet en 1991 Burk et collaborateurs[162] présentent une nouvelle classe de phophines, basés sur des phospholanes chiraux où le centre stéréogène se trouve en position α de l'atome de phosphore (Figure III-79a). Les excellents premiers résultats sur l'hydrogénation de précurseur d'acides aminés (Figure III-79b) ainsi que la possibilité de préparer aisément des dérivés à partir de diols énantiopurs (ironiquement préparés par hydrogénation asymétrique de céto-esters grâce à un complexe BINAP/Ru) suscite un vif intérêt de la part de la communauté scientifique et des industriels[161,163]. Douze ans plus tard, Hoge[164] répertorie l'agrandissement spectaculaire de cette famille de ligands qui témoigne de son succès (Figure III-79c).

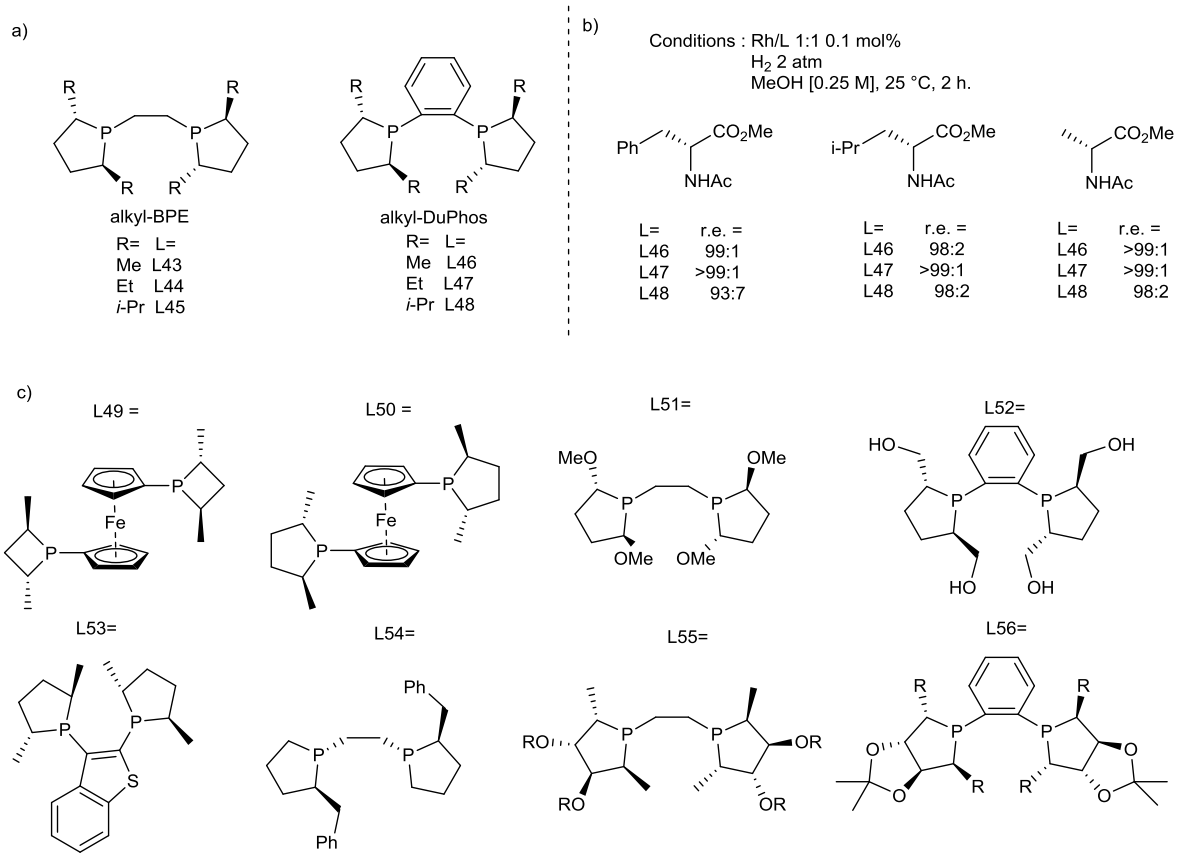

Figure III-79 : première apparition et famille de ligands de type « DuPhos »

Par contraste, prenons l'exemple d'un autre ligand disponible commercialement qui, après pourtant des premiers résultats en catalyse très prometteurs et donnant naissance à une nouvelle classe de ligand à chiralité planaire, ne donnera pas naissance à une « famille » de ligands. En effet en 1997 Pye, Kossen et collaborateurs[165] dédoublent le [2.2]paracyclophane substitué en position pseudo-*ortho* par des oxides de phosphines, pour ensuite obtenir la diphospine énantiopure **phanephos** (Figure III-80a). Cette dernière montrera une excellente activité et sélectivité dans l'hydrogénation de précurseurs d'acides aminés (Figure III-80b). Cependant, aujourd'hui, peu de dérivés existent : les modifications du squelette restent difficiles et limitées : une recherche dans Scifinder® révèle que seuls deux types de modulation du squelette de la diphosphine sont connus : les dérivés de l'acide et de l'alcool présentés Figure III-80c. De plus, les modifications des sites de coordinations demandent, pour chaque hétéroatome différent, une nouvelle procédure de dédoublement car il n'est pas possible d'accéder au pseudo-*ortho* dibromo[2.2]cyclophane énantiopur[166].

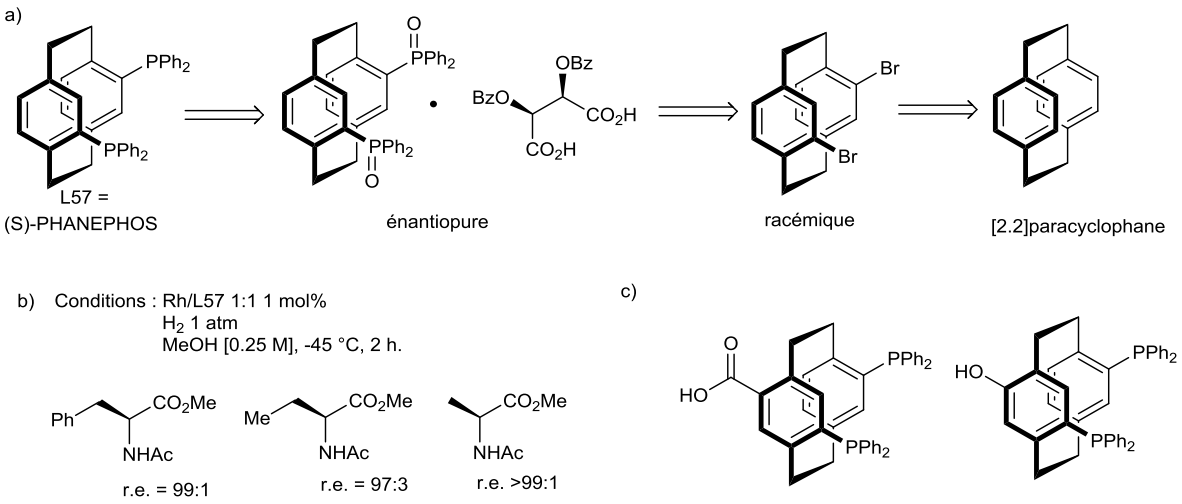

Figure III-80 : phosphines énantiopures basées sur le squelette du [2.2]*para*cyclophane

c) Machines moléculaires

Les machines moléculaires représentent un des domaines de recherche fondamentale le plus important en chimie, comme en témoigne le prix nobel attribué en 2016 à Ben Feringa, Jean-Pierre Sauvage, et Fraser Stoddar. En effet de nombreux processus cellulaires, et donc la vie elle-même, dépendent du fonctionnement de machines moléculaires et ainsi les chimistes se sont inspirés la nature pour initier de nouveaux axes de recherche.

Ainsi la machine moléculaire cellulaire fondamentale est L'ATP synthase, qui est basée sur une architecture supramoléculaire permettant un mouvement circulaire, le mouvement étant régulé par un gradient de pH entre l'intérieur et l'extérieur de la cellule. Ce type de mouvement et son contrôle, n'est pas sans rappeler la définition de l'atropisomérie (barrière de *rotation autour* d'une liaison simple) et ainsi il n'est pas surprenant que deux des premières machines moléculaires basées sur un mouvement circulaire utilisent le contrôle de l'atropisomérie pour créer une rotation unidirectionnelle.

En 1999 Kelly et collaborateurs[167] puis Feringa et collaborateurs reportent indépendamment les premiers moteurs rotatifs. Kelly utilisera une atropisomérie $C(sp^2)$-$C(sp^3)$ entre un hydroxy-hélicène et un amino-tryptycène. La jonction des deux éléments crée deux éléments de chiralité axiale : la chiralité hélicoïdale de l'hélicène stéréogène et l'atropisomérie entre l'hélicène et l'amino-tryptycène. A partir du stade initial 0, la formation d'un pont carbamide entre l'amine (entre-temps transformée en isocyanate) et l'alcool (stade 1), modifie et abaisse les barrières de rotation des deux atropodiastéréomères permettant l'équilibration vers le stade 2. La coupure du pont permet ensuite de recommencer le cycle, créant un mouvement unidirectionel contrôlé, et qui utilise donc un carburant chimique. Le moteur de Feringa est quant à lui basé sur l'isomérisation cis-trans d'un alcène contrôlé par deux éléments de chiralité

axiale hélicoïdale ainsi que deux centres asymétriques C(sp^3) et utilise comme carburant la lumière, il ne sera donc par revu ici.

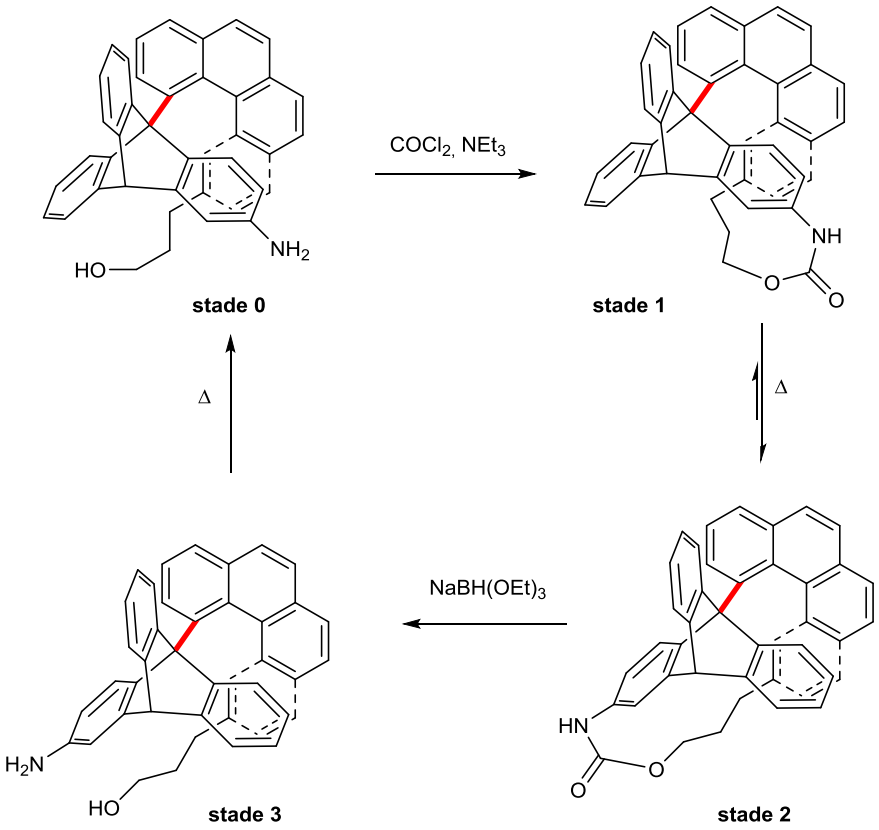

Figure III-81 : premier moteur moléculaire atropisomérique

Cependant, Feringa et collaborateurs utiliseront en 2005[168] une atropisomérie Ar-Ar C(sp^2)-C(sp^2) comme squelette de son moteur énantiosélectif basé sur le concept « lactone » développé par Bringmann. A partir du stade 1 l'ouverture réductrice de la lactone par Me-(S)-CBS, suivie de la protection du phénol par un groupement allyle et la ré-oxydation de l'alcool benzylique en acide permet d'accéder au biaryle atropisomérique (stade 2), avec un r.e. = 96.8 :3.2. La déprotection du groupe PMB et la formation d'une nouvelle lactone abaisse l'énergie de transition permettant ainsi l'atropisomérisation à température ambiante (stade 3). Une nouvelle ouverture réductrice de la lactone, toujours avec Me-(S)-CBS, suivie de nouveau de la protection de l'alcool avec un groupement PMB cette fois, et la ré-oxydation en acide, permet l'obtention d'un nouvel atropisomère avec un e.r. = 90.3 :9.7 (stade 4). Enfin une nouvelle déprotection sélective et formation de la lactone complète le cycle.

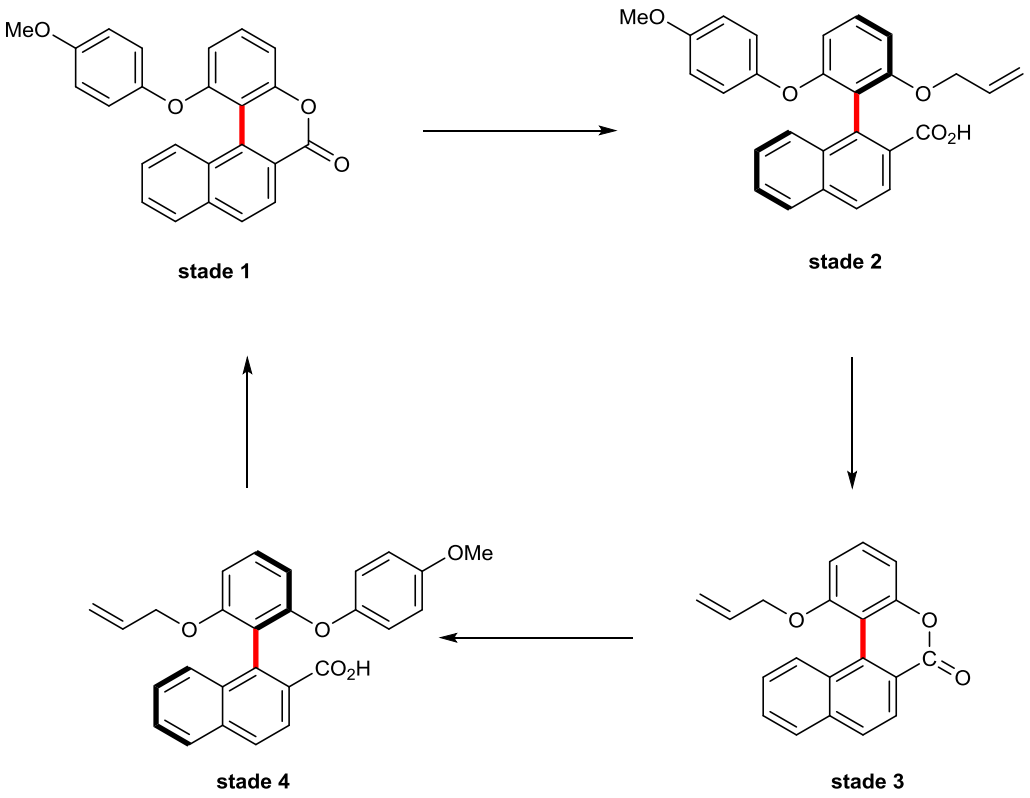

Figure III-82 : premier moteur moléculaire atropisomérique biarylique

Puis en 2016, Feringa et collaborateurs[169] utilisent l'approche développé par Colobert et collaborateurs (et présentée dans cette thèse) pour un moteur atropisomérique diastéréosélectif. Ici, à partir du biaryle suloxyde tri-substitué du stade 1, l'utilisation de palladium(II) permet la formation d'un pont par activation de liaison C-H, abaisse la barrière de rotation et permet ainsi l'équilibration vers le stade 2. Ainsi une première rotation de 180 °C a été effectuée. Après une déhydro-palladation reductrice (stade 2), l'utilisation de palladium(0) conduit à l'insertion dans la liaison C-Br, la formation d'un pont et l'équilibration vers le stade 3. Enfin, coupure du pont par NBS permet de compléter le cycle, et ainsi de réaliser le premier moteur moléculaire se basant sur un cycle red/ox d'un métal de transition, ouvrant ainsi des perspectives importantes considérant la richesse et la variété de cette chimie. Effectivement, les innombrables associations ligand-métaux possibles décuplent les possibilités offertes par la chimie organique.

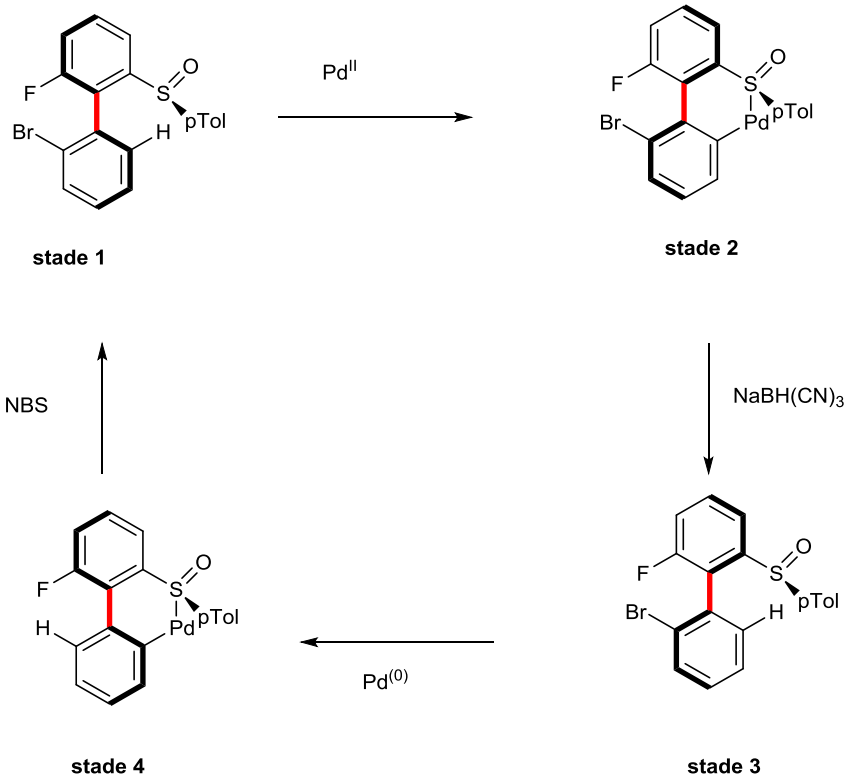

Figure III-83 premier moteur moléculaire fonctionnant sur le cycle red/ox d'un métal de transition

C. Sulfoxyde et catalyse asymétrique

Les recherches décrites dans ce manuscrit se basant sur l'utilisation de sulfoxydes en métallo-catalyse asymétrique, nous allons maintenant passer en revue les applications connues des sulfoxydes en tant que ligand de métaux de transition, puis plus particulièrement comme groupe directeur en activation de liaisons C-H. Leurs propriétés générales en tant que groupe coordinant seront également vues, ainsi que les moyens d'obtention de sulfoxydes énantiopurs, pour finir sur les mécanismes réactionnels stéréochimiques de ce groupe fonctionnel.

1. Champ d'application

Les sulfoxydes énantiopurs peuvent être utilisés dans deux grandes catégories de réactions : induction diastéréosélective[170,171], ou énantiosélective en tant que ligand d'un métal ou comme organocatalyseur[172].

Remarquons en préambule que la comparaison est souvent réalisée entre les sulfoxydes et les phosphines à cause de leur proximité sur le tableau périodique, leur capacité à la chiralité centrale et la possibilité de préparer les mêmes ligands à partir des mêmes substrats. Cependant ils n'ont pas encore rencontré le succès de leur voisin le phosphore, et ce malgré la meilleure stabilité à l'oxydation des sulfoxydes. Remarquons que les phosphines utilisées en catalyse sont le plus souvent achirales à l'atome de phosphore alors que la chiralité centrale des sulfoxydes est largement exploitée : si cet élément de chiralité supplémentaire semble être plus pour faire un réglage fin des propriétés d'induction asymétrique du ligand, il multiplie cependant les états de transitions possibles, compliquant la conception du ligand. Nous survolerons ici l'utilisation des sulfoxydes comme ligand des métaux de transition, pour finir sur une partie plus exhaustive de leur utilisation en tant que groupe directeur en C-H activation.

a) Ligand de métaux de transitions

Commençons par citer plusieurs revues récentes : l'une sur l'utilisation de composés porteurs d'un atome de soufre stéréogène en catalyse asymétrique[173], les autres sur les sulfoxydes en tant que ligands de métaux de transitions[174] : toute deux font remonter la première utilisation de sulfoxydes en catalyse asymétrique à 1976 par James[175] (Figure III-84) pour l'hydrogénation d'oléfines activées. Dans ce cas le sulfoxyde est cependant racémique, l'induction asymétrique provenant d'un carbone asymétrique ;

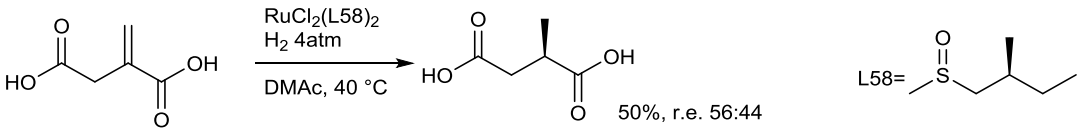

Figure III-84 : première réaction énantiosélective utilisant un ligand sulfoxyde

Par la suite des structures, dérivées de ligands classiques comme la DIOP ou plus originales, ont été testées, soit pour l'hydrogénation de liaisons C=O soit C=C, avec cependant peu de succès : un des exemples les plus réussis est présenté Figure III-85[176].

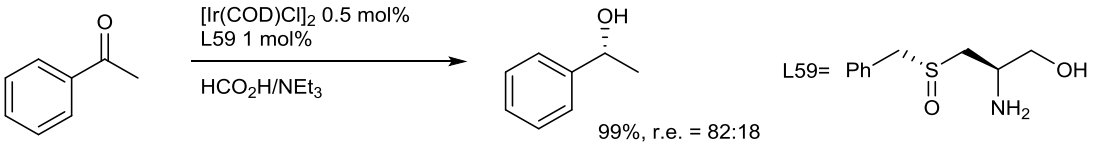

Figure III-85 : exemple de réaction utilisant un ligand sulfoxyde énantiopur

Très probablement les deux domaines où les sulfoxydes ont rencontrés le plus de succès sont dans les additions asymétriques 1,4-catalysées soit par des ligands bis-sulfoxydes, soit par des ligands sulfoxydes-alcènes, et dans les réactions de substitutions allyliques, soit de type Tsuji-Trost soit par un mécanisme de C-H activation. C'est d'ailleurs dans une réaction de substitution allylique asymétrique qu'apparaîtra le premier ligand bis-sulfoxyde énantiopur : en 1995 Tokunoh et collaborateurs dans le groupe de Shibasaki[177] publie la structure cristalline d'un complexe bis-sulfoxyde palladium qui confirme la coordination du ligand par le souffre (Figure III-86b); le ligand sera ensuite utilisé dans une réaction de type Tsuji-Trost avec un succès modéré (Figure III-86a).

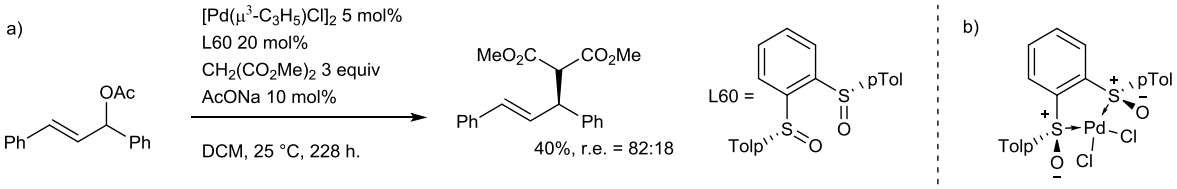

Figure III-86 : ligand bis-sulfoxyde énantiopur dans une réaction de Tsuli-Trost

Les ligands les plus couronnés de succès dans cette réaction de Tsuji-Trost, avec un sulfoxyde chiral, seront des ligands mixtes types S-N et surtout S-P. Des exemples de ligands sont présentés Figure III-87 : références : L61[178], L62[179], L63[180], L64[181], L65[182], L66[183]

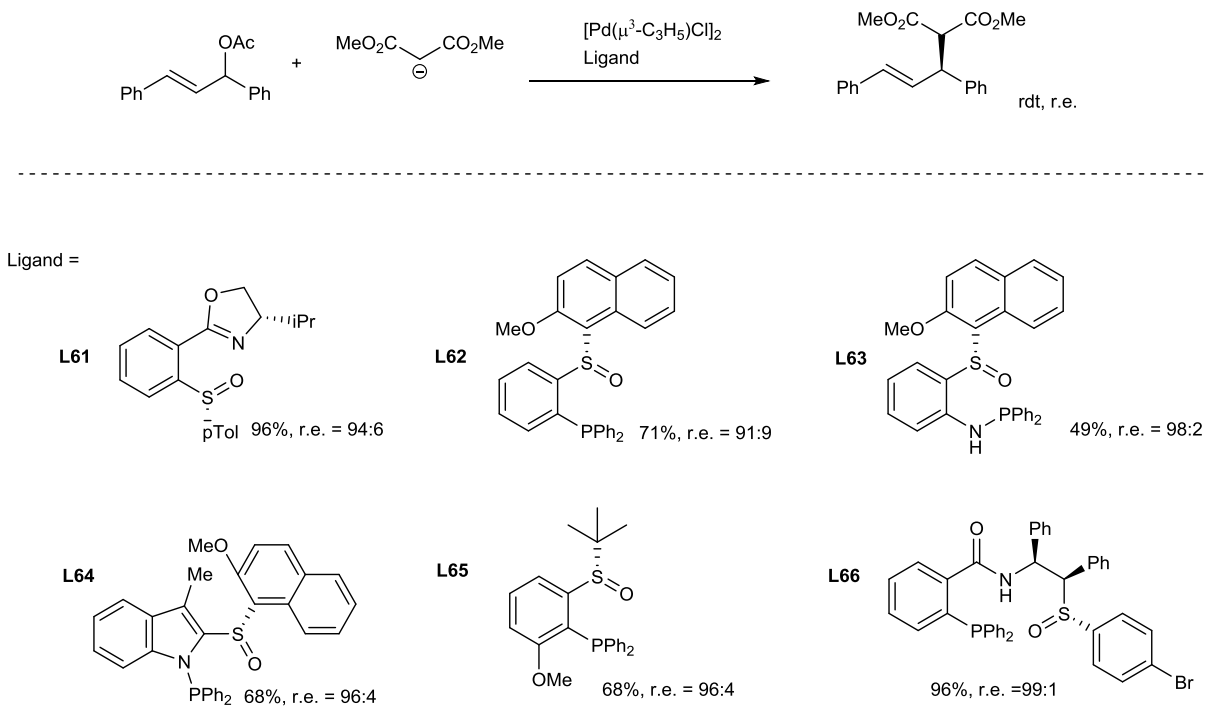

Figure III-87 : exemples de ligands efficaces comportant un sulfoxyde énantiopur

Une autre approche où les ligands sulfoxydes ont rencontré beaucoup de succès est la fonctionnalisation oxydante de positions allyliques catalysée au palladium : si l'effet bénéfique du DMSO comme adduit est connu depuis longtemps[184], c'est la découverte du ligand bis-sulfoxyde (Figure III-88a) qui donnera un nouvel élan à cette réaction. Chen et collaborateurs dans le groupe de White[185,186] montreront que le ligand permet un renversement de sélectivité en faveur du produit ramifié ; Puis un nouveau ligand, plus stable (Figure III-88b), a ensuite été utilisé dans de nombreuses réactions de C-H activation. Si le développement d'une version énantiosélective efficace reste encore à réaliser avec le ligand bis-sulfoxyde[187] (Figure III-88c), l'application d'un ligand mixte sulfoxyde/oxazoline permattra de réaliser une activation C-H allylique d'oléfines suivit d'un couplage C-O intramoléculaire avec de très bonnes énantiosélectivités (Figure III-88d).

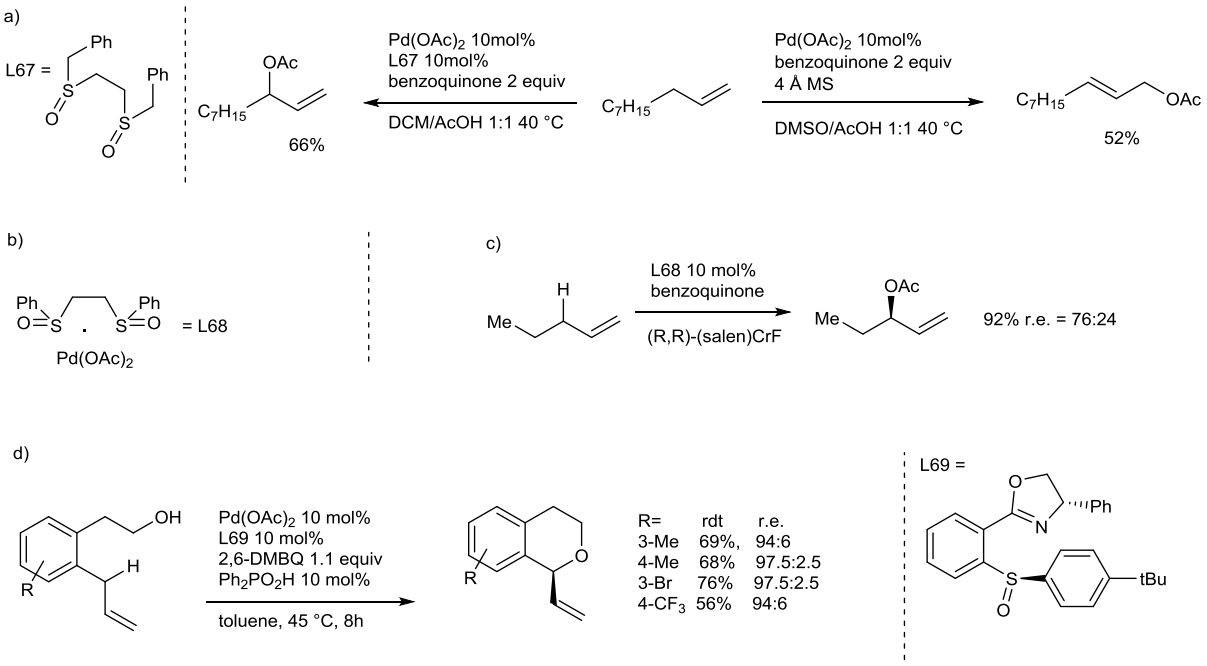

Figure III-88 : activation de liaisons C-H en présence de sulfoxydes

Enfin, l'autre domaine où les ligands sulfoxydes excellent est celui des additions 1,4 d'acides boroniques sur les ènones : c'est Mariz et collaborateurs dans le groupe de Dorta qui appliqueront un complexe de rhodium d'un ligand bis-sulfoxyde analogue à la BINAP à cette réaction avec d'excellents résultats[94] (Figure III-89a). Par la suite d'autres ligands bis-sulfoxydes sans chiralité axiale furent développés et montreront leurs efficacités, un exemple, par Chen et collaborateurs dans le groupe de Liao est présenté Figure III-89b[95]. Une avancée majeure sera la découverte par Thaler et collaborateurs dans le groupe de Knochel[190] (Figure III-89c) de l'activité et efficacité des ligands mixtes sulfoxyde-alcènes : il est intéressant de remarquer que l'induction asymétrique dépend de l'asymétrie venant de l'isomérie géométrique de l'alcène et non de la chiralité centrale du sulfoxyde. D'autres ligands de ce type suivront, avec des variations structurelles originales (Jin et collaborateurs, groupe de Xu [191], Figure III-89d).

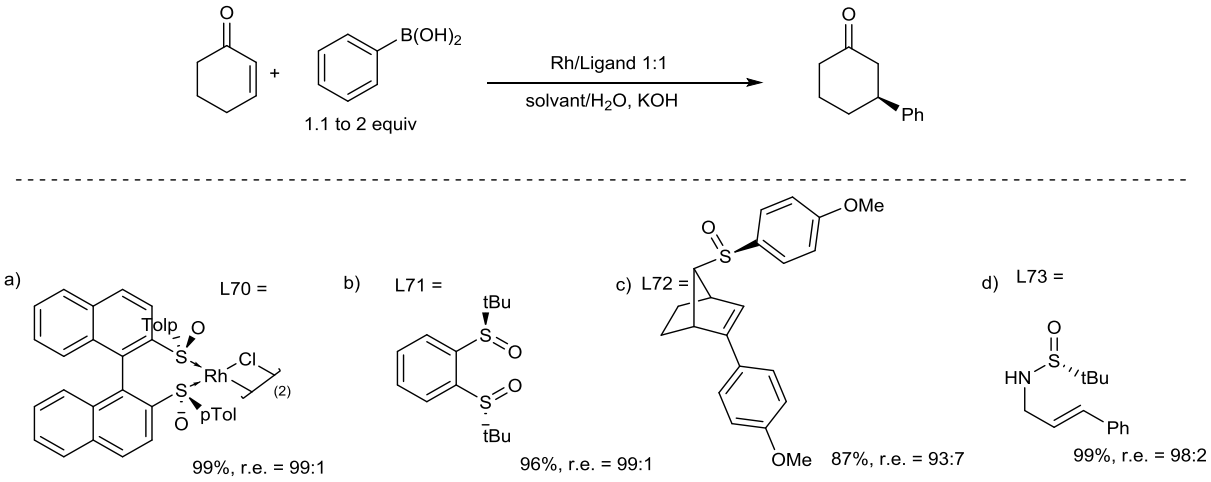

Figure III-89 : additions 1,4- asymétriques par des complexes de rhodium-sulfoxydes

b) Groupe directeur en C-H activation

Nous nous intéressons ici à des substrats contenant un sulfoxyde en tant que ligand dans la sphère de coordination interne du métal et qui va diriger l'insertion du métal dans une liaison C-H. Cette utilisation des sulfoxydes est relativement récente, et pour une vision plus générale des autres modes d'activation utilisant les sulfoxydes, nous dirigeons le lecteur vers une revue[192] récente. Les premiers exemples concernent l'utilisation du sulfoxyde comme groupe directeur en version racémique.

Un des premiers exemples concerne le travail de Coulter et collaborateurs dans le groupe de Dong[193] (Figure III-90) où un sulfoxyde permet d'opérer une hydroacylation catalysée au rhodium. L'utilisation d'un sulfoxyde permet de s'affranchir da s'affranchir d'utiliser un ligand énantiopur en rendant la réaction diastéréosélective. Un seul exemple utilisant un sulfoxyde est présenté.

Figure III-90 : hydroacylation diastéréosélective

Samanta et Antonchick[194] (Figure III-91) en 2011 proposent un travail original où un benzylarylsulfoxyde, en présence de palladium^{II} et d'un iodure d'aryle qui joue ici le rôle d'oxydant, conduit à la formation de dibenzothiophene-1-carbaldehyde par une cascade de réactions comprenant trois activations de liaisons C-H, la formation d'une liaison C-C et d'une liaison C-S ainsi qu'un réarrangement de Pummerer.

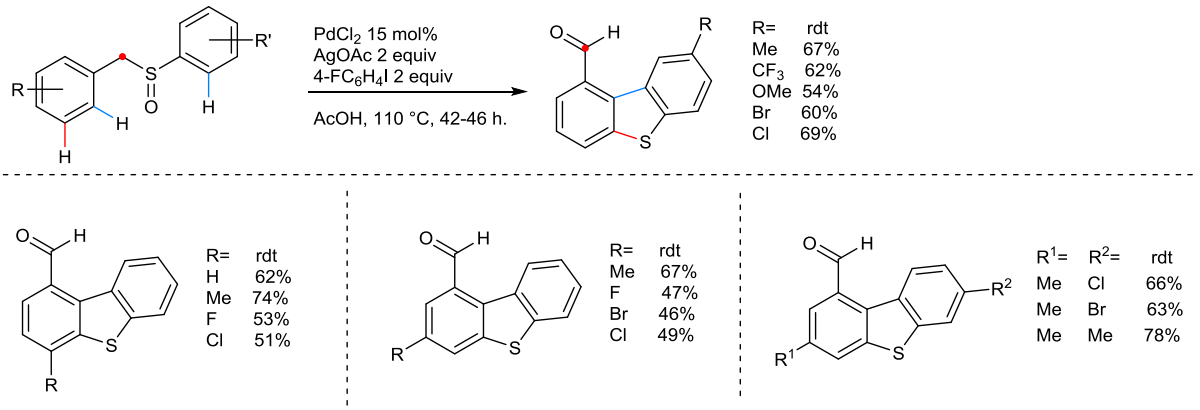

Figure III-91 : réactions en cascades utilisant un sulfoxyde

Wang et collaborateurs en 2014 dans le groupe de Zhang[195] s'inspireront de ce travail pour produire, en évitant l'étape Pummerer, des hétérocycles contenant un sulfoxyde pontant. Plus de 30 hétérocycles seront ainsi synthétisés avec des rendements modérés à bons, et quelques exemples sont présentés à la Figure III-92.

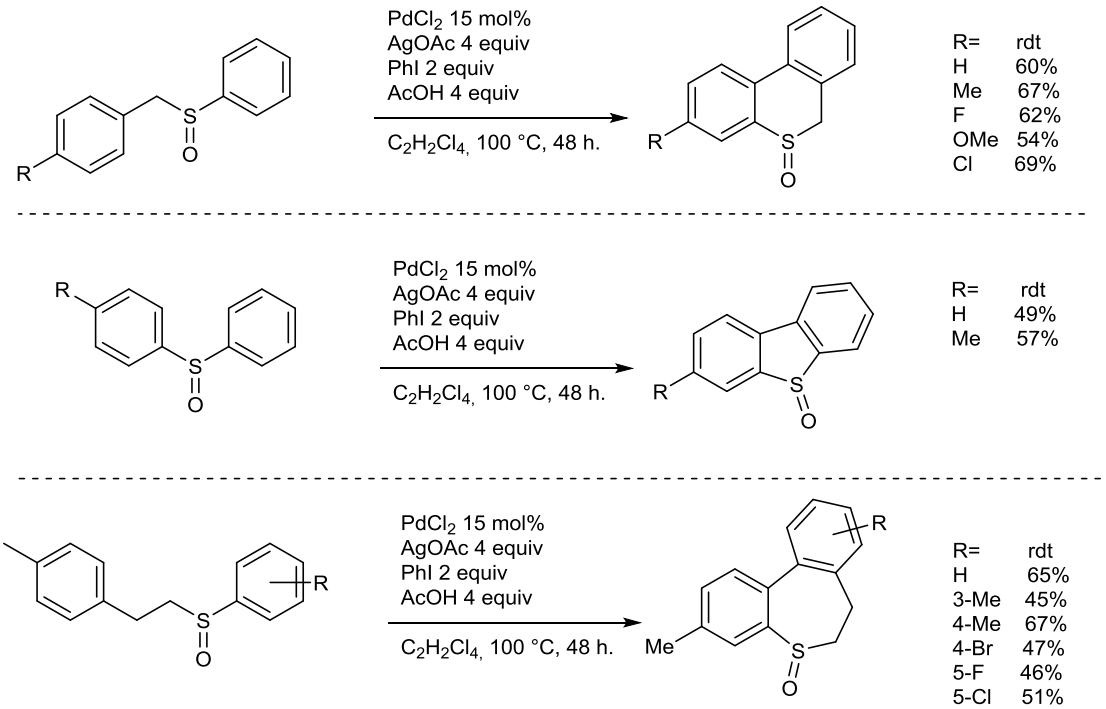

Figure III-92 : double activation de liaison C-H avec un sulfoxyde comme DG

Puis, toujours en 2014, Wang et collaborateurs dans le groupe de Zhang[196] (Figure III-93) décriront une oléfination oxydante par des acrylates sur des benzyl-, phenylethyl-, et phenylpropylsulfoxyde à l'aide de $Pd(OAc)_2$ en utilisant comme oxydant le selectfluor, ceci sur plus de 35 exemples. Notons l'utilisation d'HFIP comme solvant pour les fonctionnalisations les plus difficiles ; ainsi que l'isolation de palladacycles à 5- et 6-membres. L'effet cinétique isotopique bien supérieur à 1 mesuré (KIE = 2.57), suggère que la rupture de la liaison C-H est probablement l'étape limitante (seul un effet intermoléculaire intra-réactionnel a été mesuré).

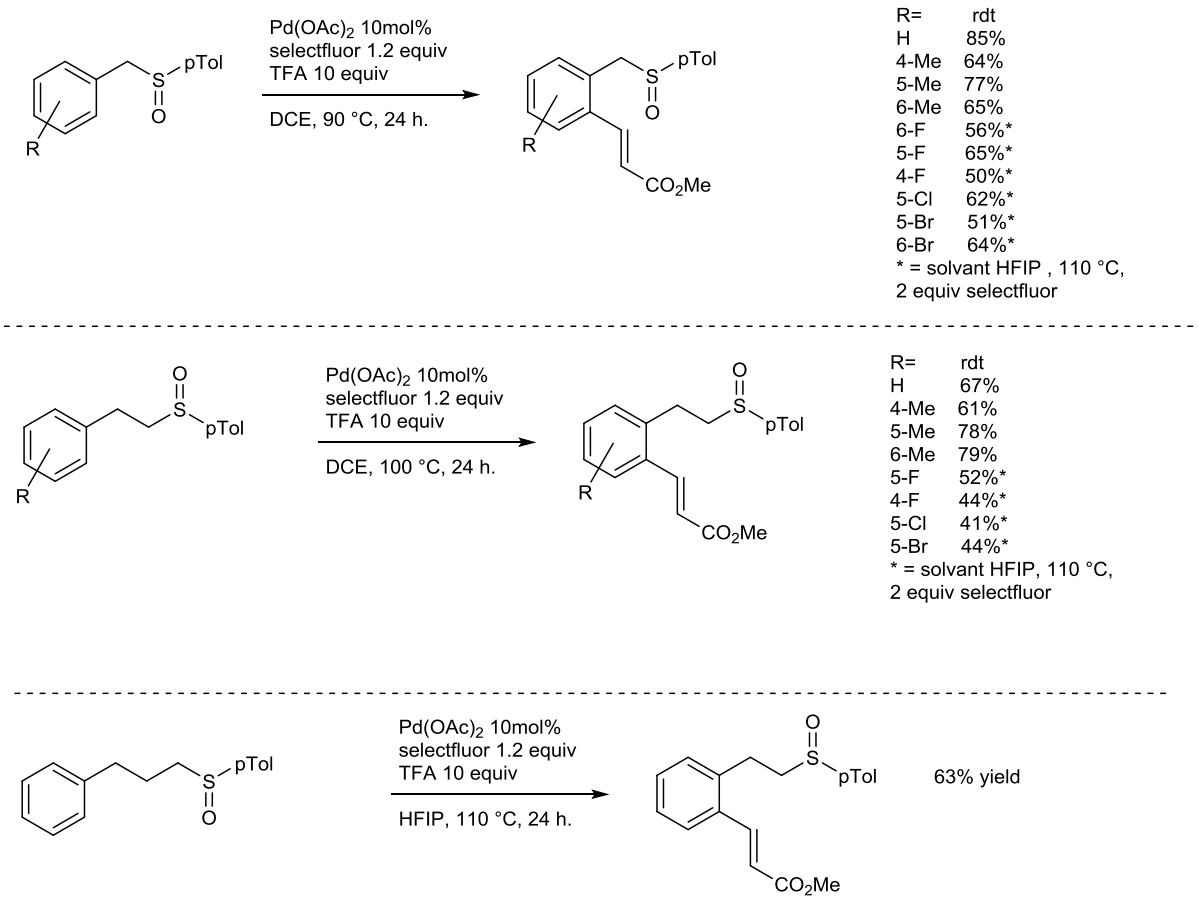

Figure III-93 : réaction de Fujiwara-Moritani dirigé par un sulfoxyde

Remarquons ensuite deux travaux proches pour réaliser l'oléfination d'arylsulfoxydes: cette fois, l'utilisation de complexes cationiques de rhodium et de ruthenium permet d'effectuer une coordination efficace par l'oxygène (et ainsi éviter la formation d'un métallacycle à 4-membres très défavorable). Le premier par Nobushige et collaborateurs dans le groupe de Miura[197] propose une oléfination soit oxydante soit par alcénylation par un complexe de rhodium cationique : l'oléfination (Figure III-94a) concernent exclusivement des acrylates alors que l'alcénylation (Figure III-94b) permet d'accéder à des oléfines tri-substituées aryle-aryle ou alryle-alkyle. Notons toutefois que le sulfoxyde est ici en excès et que les rendements sont calculés sur les acrylates ou sur l'alcyne ; remarquons aussi un effet cinétique isotopique de 5.7 pour l'oléfination oxydante.

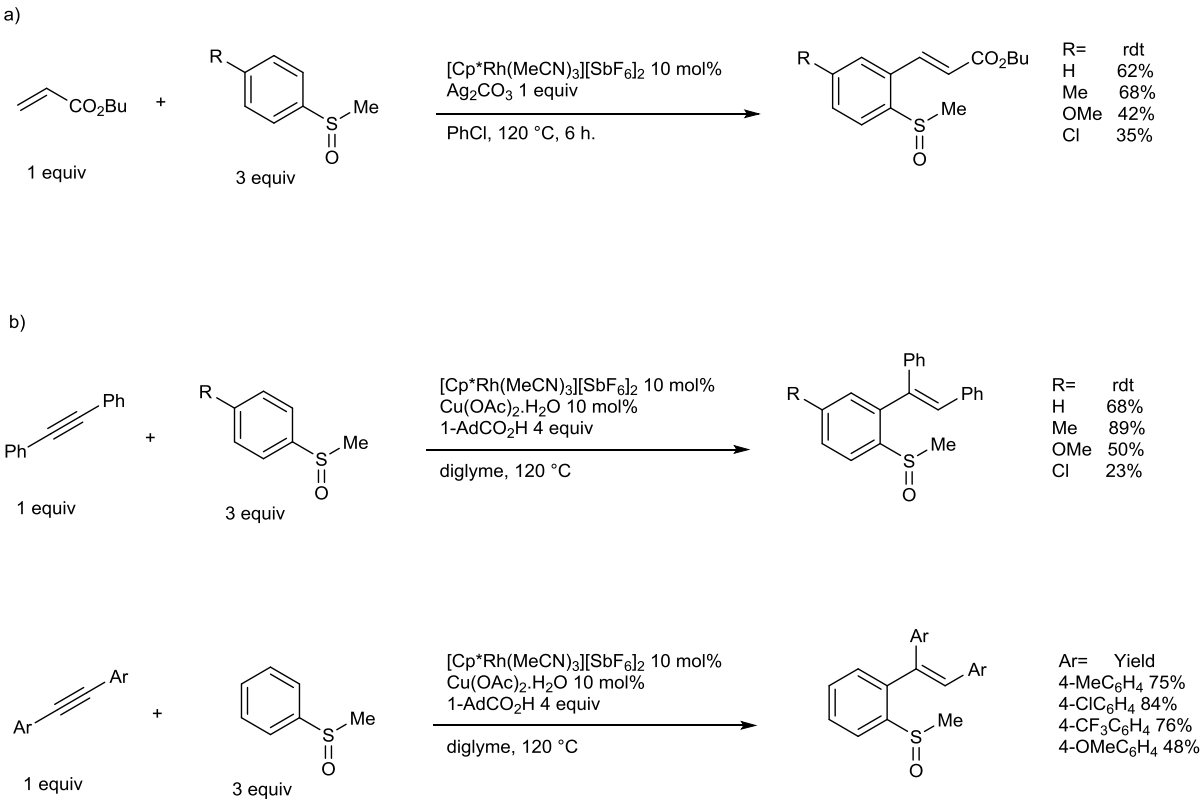

Figure III-94 : oléfination catalysée au rhodium

Le second système catalytique est décrit par Padala et Jeganmohan[198] (Figure III-95). Ils réalisent là aussi une alcénylation d'alkylarylsulfoxydes catalysée par un complexe de ruthénium cationique avec des rendements modérés à bons ; remarquons la meilleure efficacité de la réaction (le sulfoxyde est cette fois le réactif limitant), et une compatibilité avec une plus large diversité d'alkylarylalcynes.

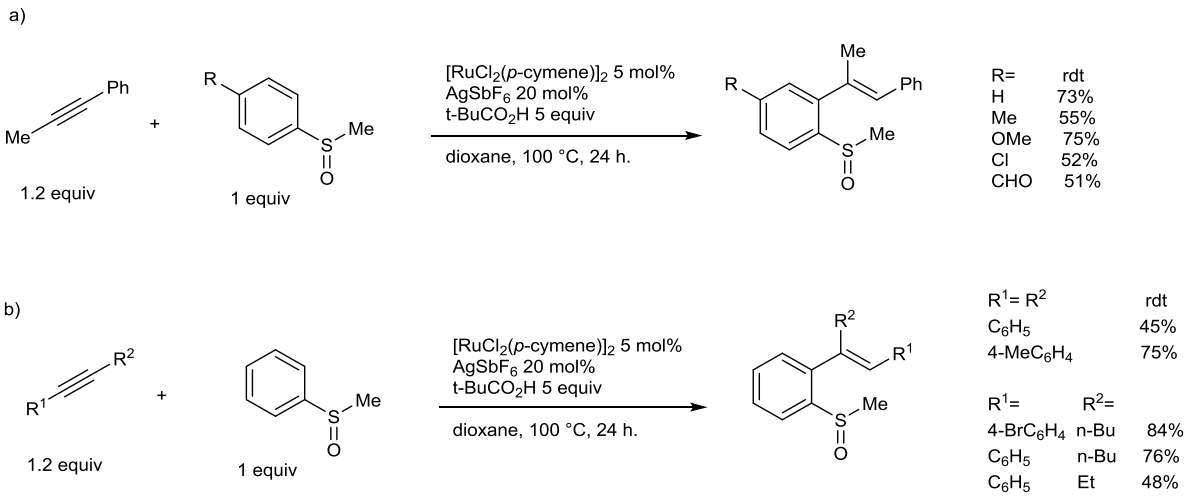

Figure III-95 : oléfination catalysée au ruthenium

Par ailleurs, notre groupe a pour la première fois utilisé le sulfoxyde chiral pour réaliser des réactions d'activation de liaisons C-H asymétrique. Il s'agit en tout premier lieu du travail qui sera dans ce manuscrit.

Puis en 2016 Jerhaoui et collaborateurs dans le groupe de Colobert[199] (Figure III-96) propose la première activation diastéréosélective de liaisons C(sp^3)-H dirigée par un sulfoxyde. L'arylation directe de motifs cyclopropanes est réalisée par un complexe $Pd(OAc)_2$ en présence d'iodures aromatiques. Si les diastéréosélectivités sont modestes (Figure III-96a), la possibilité de séparer facilement les produits obtenus, la bonne conversion et surtout la possibilité d'obtenir des cyclopropanes tri-substitués énantiopurs (Figure III-96b) rendent à cette réaction un intérêt synthétique. Remarquons qu'ici l'étape de C-H activation est réversible et qu'un effet cinétique isotopique de 1.28 a été mesuré. Ce KIE peut correspondre soit à effet isotopique d'équilibre, soit signifier que l'étape limitant le turnover intervient après la rupture de la liaison C-H, c'est-à-dire soit l'étape d'addition oxydante soit l'élimination réductrice (cependant la plus forte réactivité des iodures pauvres en électrons fait pencher en faveur de l'addition oxydante).

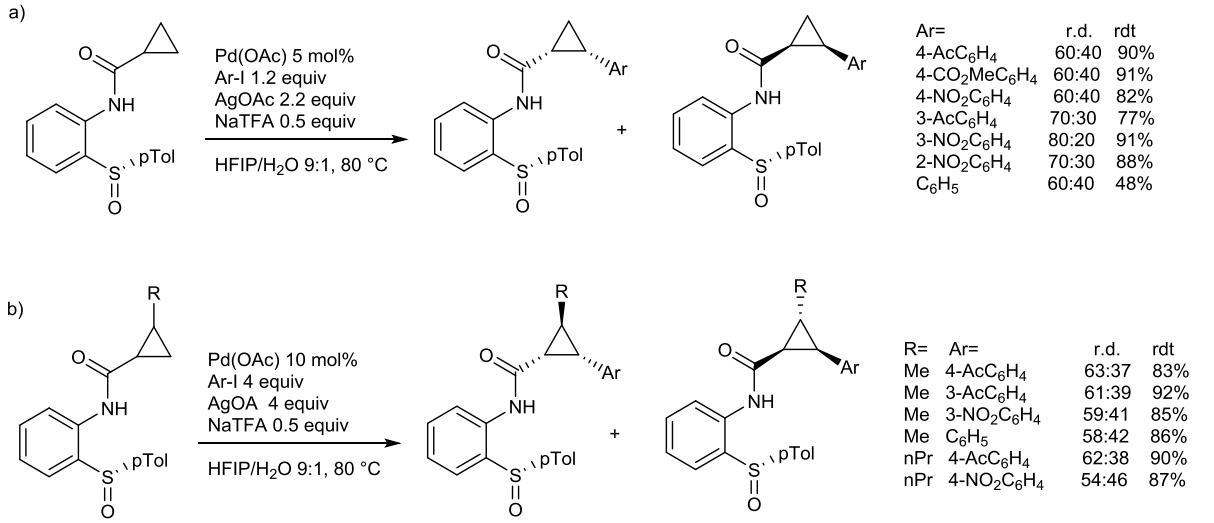

Figure III-96 : arylation diastéréosélective de cyclopropanes

Reprenant le même auxiliaire, Mu et collaborateurs dans le groupe de He[200] (Figure III-97) réaliseront en 2017 l'activation de liaison C(sp^3) dans la même position béta mais cette fois sur des chaines alkyles linéaires. Si les diastéréosélectivités sont là aussi modestes, on note une bonne régioséléctivité entre les positions béta et gamma (Figure III-97b). Deux types d'auxiliaires, methyl- et *para*-tolylsulfoxyde aniline, (seuls les résultats du *para*-tolyl sont présentés ici) ont été testés avec une meilleur réactivité et sélectivité du *para*-tolylsulfoxyde. Un effet cinétique isotopique, réalisé par compétition intermoléculaire, de 1.2 a été mesuré ; cependant il n'est pas fait mention d'étude sur la réversibilité de l'étape d'activation C-H. Notons enfin que les auteurs ont réalisé leur travail sur un sulfoxyde racémique : un seul exemple utilisant un sulfoxyde énantiopur a été décrit, sans cependant aucune mesure de l'énantiosélectivité.

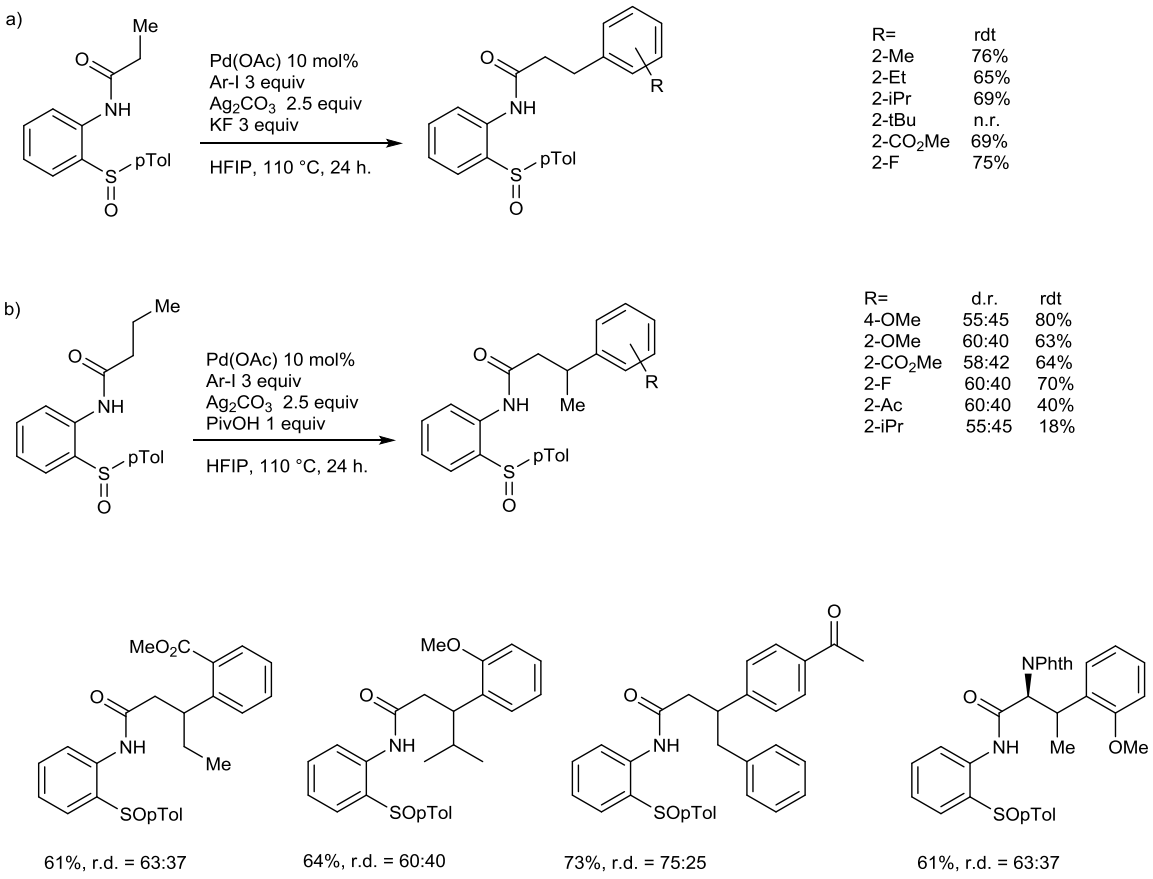

Figure III-97 : arylation diastéréosélective d'amides

Concomitamment Jerhaoui, Wencel-Delord et Colobert[201] reportent leur application de l'auxiliaire aminosulfoxyde pour l'activation de liaisons C(sp^3)-H en position béta d'un carbonyle (Figure III-98). Si les conditions et les résultats sont voisins, notons tout de même que la charge catalytique a pu être abaissée à 5 mol%. De plus, les auteurs ont axé leur étude exclusivement vers des réactions asymétriques et de très bonnes diastéréosélectivités ont parfois pu être obtenues, spécialement dans la fonctionnalisation de positions benzyliques (réactions à 80 °C, Figure III-98c). Notons qu'il est difficile de faire une corrélation entre les propriétés électroniques du partenaire de couplage et les diastéréosélectivités observées. Enfin, l'auxiliaire chiral énantiopur peut être recyclé après hydrolyse basique et un simple traitement acide/base, sans perte d'activité optique.

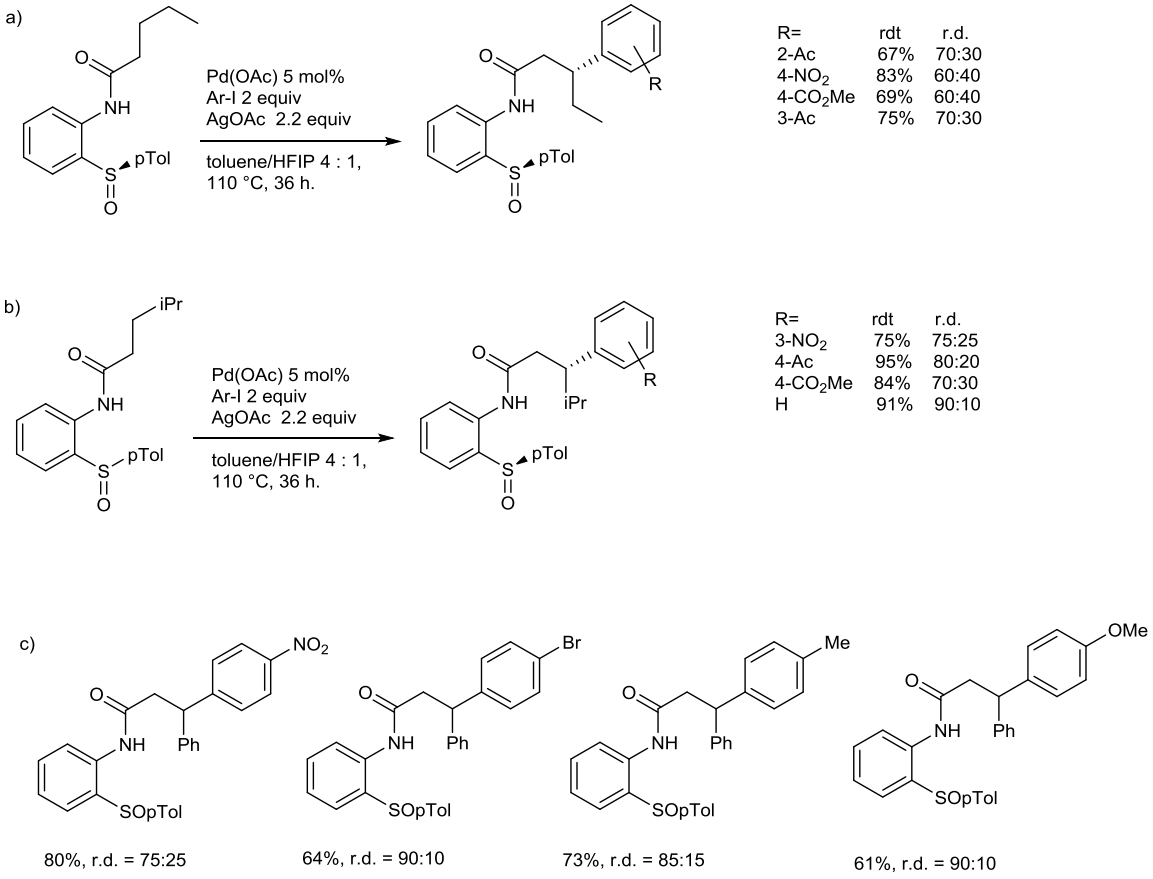

Figure III-98 : arylation diastéréosélective d'amides par le groupe Colobert

2. Préparation de sulfoxyde énantiopur

Certaines caractéristiques sont désirables pour l'utilisation d'un auxiliaire de chiralité : la première c'est évidemment une haute pureté optique, ensuite il doit être facilement accessible (nombres d'étapes limité pour sa préparation, réactifs facilement disponibles et faciles à mettre en œuvre), la synthèse à grande échelle doit être aisée (purification par cristallisation plutôt que par chromatographie), les deux configurations doivent être accessibles et enfin il doit être peu cher. Ainsi deux méthodes se sont imposées pour la préparation de sulfoxydes énantiopurs[202] : a) l'obtention, grâce à l'addition d'un auxiliaire de chiralité énantiopur, d'un précurseur, contenant un groupe sulfinyl, diastéréomériquement pur où l'auxiliaire de chiralité joue ensuite le rôle de groupe partant ; b) l'oxydation énantio- ou diastéréosélective d'un thioéther.

a) Substitution sur un précurseur énantiopur au soufre

C'est, historiquement et encore aujourd'hui, l'approche la plus efficace pour préparer de façon fiable des sulfoxydes énantiopurs, grâce à deux méthodes similaires. Elles reposent toutes deux sur la préparation d'un sulfinate énantiopur dans un premier temps, puis sur l'addition nucléophile d'un organométallique permettant ainsi d'accéder au sulfoxyde, la substitution se faisant suivant un mécanisme proche de la S_N2 avec inversion de configuration et non selon un mécanisme d'addition-élimination[203] (Figure III-99). Remarquons cependant la principale limitation: il faut dans un premier temps pouvoir accéder au précurseur avec un groupement sulfinyl énantiopur, et ainsi les groupements R accessibles sont limités. De fait, il existe principalement deux méthodes qui différent dans la façon d'accéder au précurseur sulfinate, ainsi que dans les groupements R accessibles.

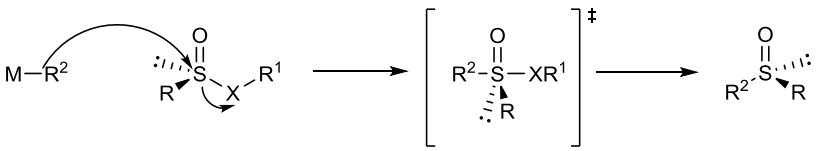

Figure III-99 : mécanisme d'inversion de configuration

Dans la méthode d'Andersen[204] le groupement R est principalement un *para*-tolyl et le précurseur est un sulfinate de menthyl obtenu diastéréomériquement pur par cristallisation. C'est cette étape de cristallisation qui limite les groupements R accessibles, de nombreux sulfinates n'étant pas cristallins et la séparation chromatographique n'est pas toujours possible (à notre connaissance, aucun alkyle sulfinate n'est cristallin). Ainsi, l'addition de (-)- ou (+)-menthol sur le chlorure de l'acide *para*-toluène sulfinique (Figure III-100-1), donne un mélange de deux diastéréoméres qui est facilement purifiable par cristallisation en faveur du diastéréomére.(-)-(*S*s) à partir du (-)-menthol (Figure III-100-2) ; (+)-(*R*s) à partir du (+)-menthol. D'autres sulfinates de menthyl sont accessibles par cette méthode[205], mais le *para*-tolyl reste largement

le plus utilisé. De plus, une amélioration apportée par Solladié[206] permet d'épimériser au soufre la liqueur mère après chaque cristallisation (Figure III-100-3), opérant ainsi un dédoublement dynamique thermodynamique permettant d'obtenir des rendements supérieurs à 50%. L'addition d'un organométallique permet ensuite d'obtenir l'alkyl- ou aryl-*para*tolylsulfoxyde (Figure III-100-4).

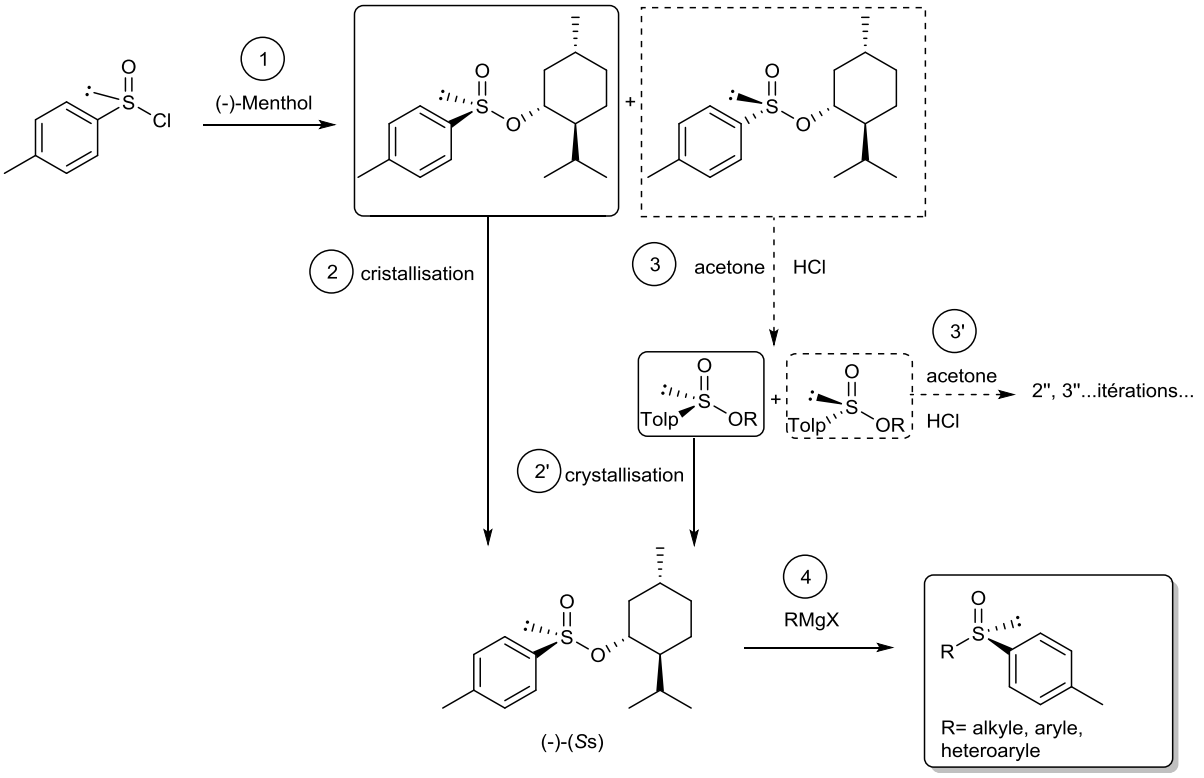

Figure III-100 : schéma générale de la méthode d'Andersen

La méthode d'Ellman[207,208] quant à elle repose sur l'oxydation énantiosélective d'un di*tert*butyldisulfide en un *tert*butyl*tert*butanethiosulfinate grâce à un catalyseur de vanadium et un ligand dérivé des (-)-cis- ou (+)-*cis*-aminoindanol, tous deux disponibles commercialement (Figure III-101a). Là aussi une étape de cristallisation est indispensable pour obtenir le thiosulfinate sous forme énantiopur après l'oxydation (Figure III-101b), ce qui limite son application à ce substrat spécifique, mais qui permet la préparation de *tert*butylaryl- ou alkylsulfoxydes, ce qui n'est pas possible avec la méthode d'Andersen.

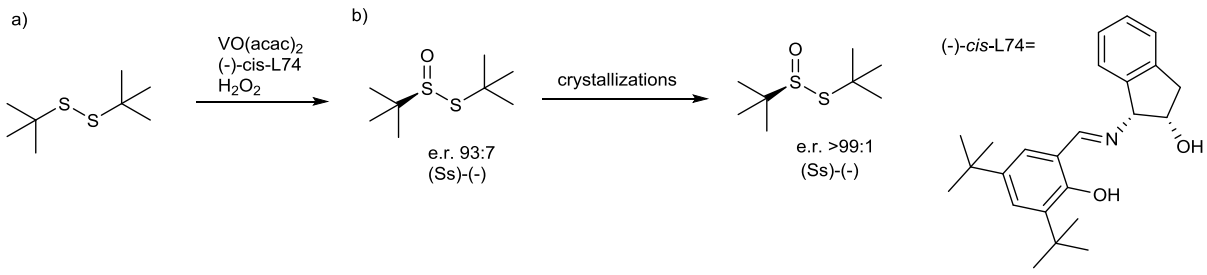

Figure III-101 : méthode d'Ellman

Les deux méthodes sont ainsi relativement complémentaires et offre un accès facile à deux groupements sulfinyls aux propriétés bien différentes : stériquement, électroniquement, ainsi qu'au niveau de la chimiosélectivité, le groupement *para*toluenesulfinyle n'étant pas stable en présence d'alkyl- et d'aryllithium (voir III.C.5), contrairement au groupement tertbutanesulfinyl. Ainsi livrons-nous à une rapide comparaison (du point de vue pratique du chimiste à la paillasse) des deux méthodes (Méthode d'Andersen MdA ; Méthode d'Ellmann MdE) :

Table III-4 : comparaison des méthode Andersen/Ellman

	MdA	**MdE**
Facilité de mise en oeuvre	++	+ (pompe à seringue recommandé)
Coût	++	++
Purification optique par crystallisation	++ (diastéréomères)	- (énantiomères, point de fusion proche de 25 °C)
Synthèse à grande échelle	- (dégagement SO_2, déchets stoechiométriques)	++ (réaction catalytique, bas point moléculaire)
Réactivité	++	+ (*t*-Bu)
Stabilité optique en présence d'organométallique	+ (racémisation possible en présence de lithiens)	++
Stabilité optique au stockage	+ (conservation à -18 °C plusieurs mois)	+ (conservation à -18 °C plusieurs mois)

b) Oxydation catalytique d'un thioéther

C'est, idéalement, la méthode la plus directe et la plus économique, surtout lorsqu'on connait la facilité avec laquelle les thioéthers sont oxydés en sulfoxyde. Cependant, comme souvent en catalyse énantiosélective, le résultat, très dépendant du substrat utilisé, demande une optimisation systématique de la réaction pour chaque composé et ainsi peu de méthodes générales existent. De plus signalons la réaction secondaire d'oxydation du sulfoxyde en sulfone qui peut compliquer la purification.

Ainsi les seules méthodes que l'on pourrait qualifier de générales sont celles dérivées de la procédure de Kagan[209] (Figure III-102a) dérivé de l'époxydation asymétrique de Sharpless, où l'utilisation d'un complexe de titane/diester de l'acide tartrique en présence d'un hydropéroxyde permet d'obtenir de bons résultats vers des alkylarylsulfoxydes. La procédure de Kagan, qui utilise à l'origine une quantité stoechiométrique de titane, sera optimisée à de nombreuses reprises (procédure de Modena[210]) en variant la stoechiométrie métal/ligand, l'hydropéroxyde, les solvants pour obtenir d'excellents résultats sur des substrats spécifiques, montrant ainsi dans le même temps sa puissance mais aussi ses limites dans un contexte académique. Soulignons quand même qu'elle a été utilisée dans la synthèse à l'échelle industrielle de

certains médicaments parmi les plus prescrits encore aujourd'hui (ésoméprazole[211] Figure III-102b).

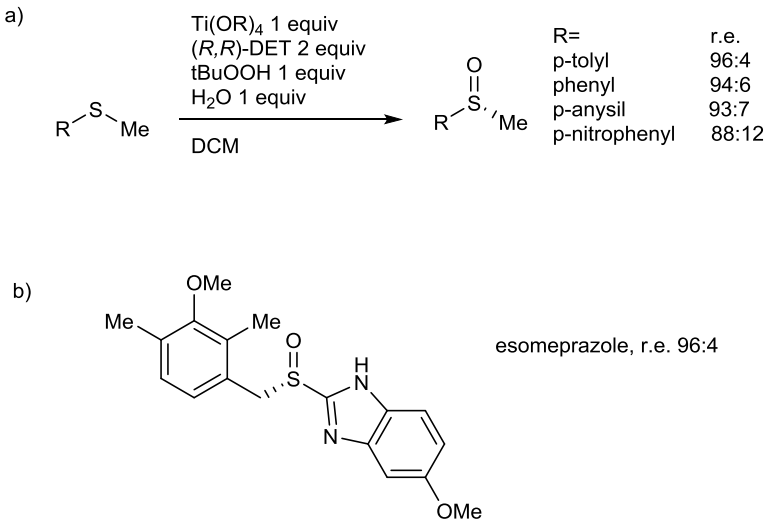

Figure III-102 : méthode de Kagan

3. Stabilité optique et mécanisme d'épimérisation

Les sulfoxydes possèdent une barrière d'activation élevée à la racémisation par inversion pyramidale[212] (Figure III-103a). Ainsi ils montrent des valeurs sensiblement plus élevées que les phosphines[213]. On retrouve également les mêmes tendances entre les deux éléments : l'introduction d'aryles diminue la barrière d'inversion, ainsi que l'introduction de substituants électro-attracteurs sur ces aryls[214]. Les valeurs constatées pour les sulfoxydes indiquent que la racémisation thermique intervient à partir de 200 °C[215] (valeurs expérimentales Figure III-103b) par un mécanisme d'inversion pyramidale, avec deux exceptions notables : les benzylsulfoxydes par un mécanisme de scisson homolytique (Figure III-103c), et les allylsulfoxydes, par réarrangement sigmatropique (Figure III-103d).

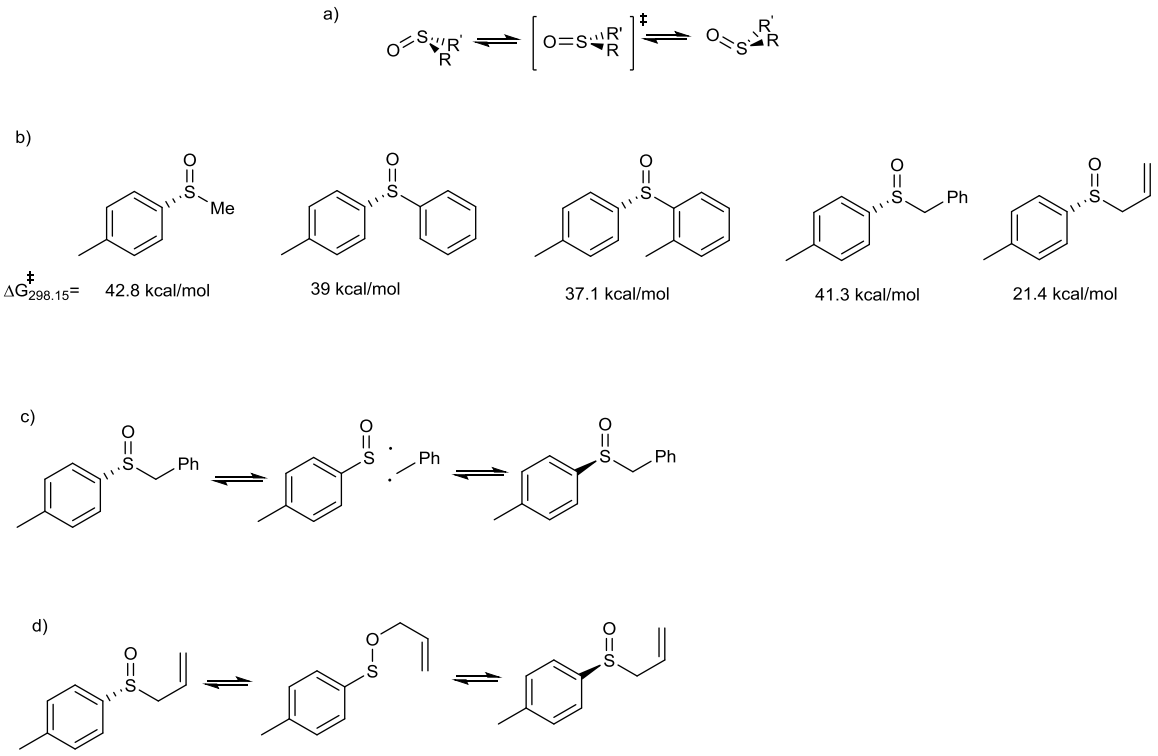

Figure III-103 : inversion pyramidale, barrières d'inversions et autres mécanismes d'épimérisation

D'autres mécanismes existent :

-par départ réversible de l'oxygène du sulfoxyde dans des conditions fortement acides en présence d'un contre-ion nucléophile[216] : L'oxygène, transformé en groupe partant par l'addition électrophile de deux protons, est substitué par un nucléophile. Ensuite deux possibilités: Figure III-104-1 un deuxième nucléophile attaque le nucléophile précédemment additionné au sulfonium, aboutissant à la réduction du sulfoxyde en thioéther ; ou, Figure III-104-2, l'attaque du soufre du sulfonium conduit à un sulfurane achiral. Dans les deux cas, l'équilibre étant généralement déplacé vers la gauche, on constate la réduction du sulfoxyde. Une exception notable est lorsque le nucléophile est un relativement bon réducteur, comme les ions io-

dures : l'équilibre est alors déplacé vers la droite par la formation d'iode[216]. Cette réaction est d'ailleurs mise à profit pour effectuer la réduction des sulfoxydes en thioéthers.

Notons que dans des conditions acides anhydres (HCl dans le dioxane[217]) la racémisation est largement accélérée, probablement en favorisant la protonation de l'oxygène du sulfoxyde (pas d'effet nivelant de l'eau) et départ d'H_2O. Enfin, notons le comportement particulier des *tert*- et *sec*-alkyles sulfoxydes qui, dans des conditions acides comparables[218] à celles citées auparavant, subissent une racémisation ainsi qu'une fragmentation.

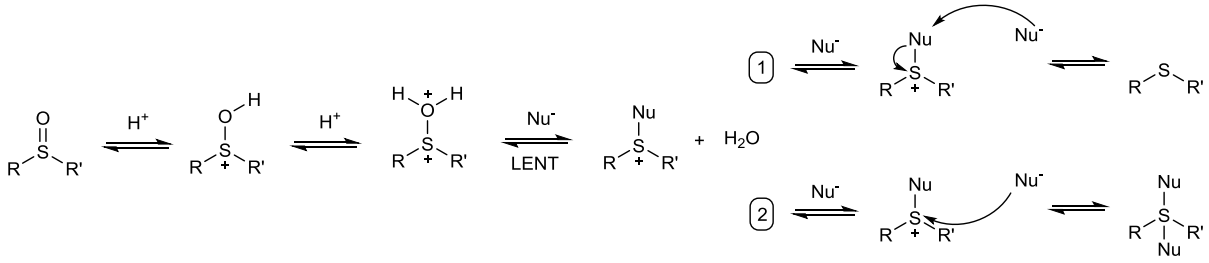

Figure III-104 : racémisation dans des conditions fortements acides

-par racémisation photochimique par l'intermédiaire de sulfoxydes radicaux cations[219] (Figure III-105).

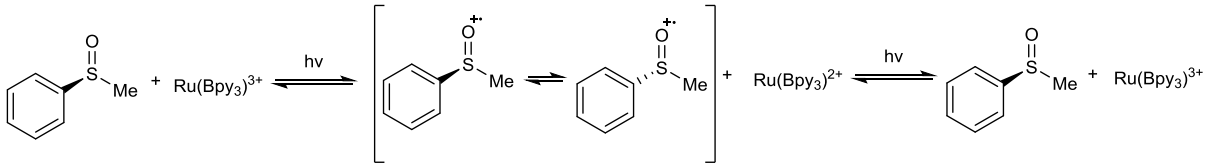

Figure III-105 : racémisation photochimique

Cependant les sulfoxydes sont très stables en conditions basiques : ainsi Oae et collaborateurs ont montré que le *tert*-butoxide de potassium ne racémise pas un alkylsulfoxyde entre 100 et 135 °C[220] (Figure III-106).

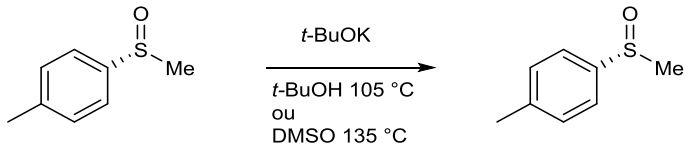

Figure III-106 : stabilité dans des conditions basiques

Concernant les mécanismes réactionnels au souffre tri-coordiné, nous nous contenterons de mentionner, considérant la grande variété de réactions existantes dans ce domaine, les principales réactions ayant été utilisées dans ce travail, à savoir : la substitution nucléophile par inversion de configuration sur les sulfinates, la racémisation des sulfinates, et le comportement des sulfoxydes en présence d'organométalliques.

Ainsi, dans son travail séminal sur la synthèse stéréosélective de sulfoxydes [205], Andersen et collaborateurs montreront des indications solides de la substitution nucléophile par inversion de configuration grâce à la comparaison de spectres de dispersion optique rotatoire, puis ce mécanisme par inversion de configuration sera prouvé par Mislow et collaborateurs qui relieront plusieurs sulfinates/sulfoxydes de configuration connue (par diffraction des rayons-X ou corrélation chimique) par une série d'étapes de substitutions utilisant des réactifs Grignard[221] (Figure III-107).

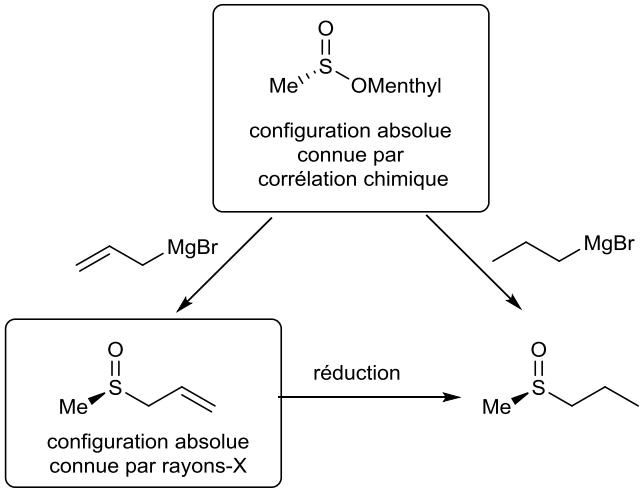

Figure III-107 : détermination des configurations absolues des sulfinates/sulfoxydes

Enfin Andersen et collaborateurs obtiendront un indice sur le mécanisme d'inversion au souffre tri-coordiné invoquant un sulfurane.[222]
Le mécanisme de racémisation des sulfinates dans les solvants organiques en présence d'acide aqueux avec un contre-ion est semblable à celui des sulfoxydes, tout en étant beaucoup plus facile. Il intervient par rupture de liaison S-O du meilleur groupe partant suivit d'un échange rapide du nucléophile à travers un état de transition symétrique[223] (Figure III-108).

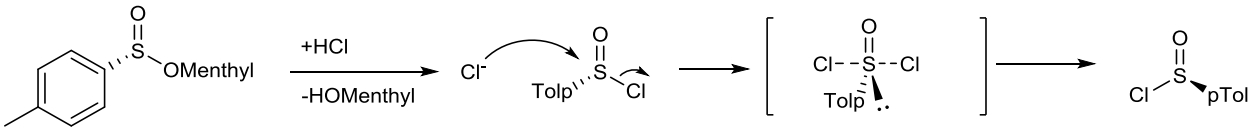

Figure III-108 : racémisation des sulfinates

Enfin la réaction prépondérante des sulfoxydes avec les organométalliques est l'échange de ligand : cette réaction, comme avec les sulfinates, intervient avec inversion de configuration par un intermédiaire type sulfurane, et favorise l'organométallique le plus stable.

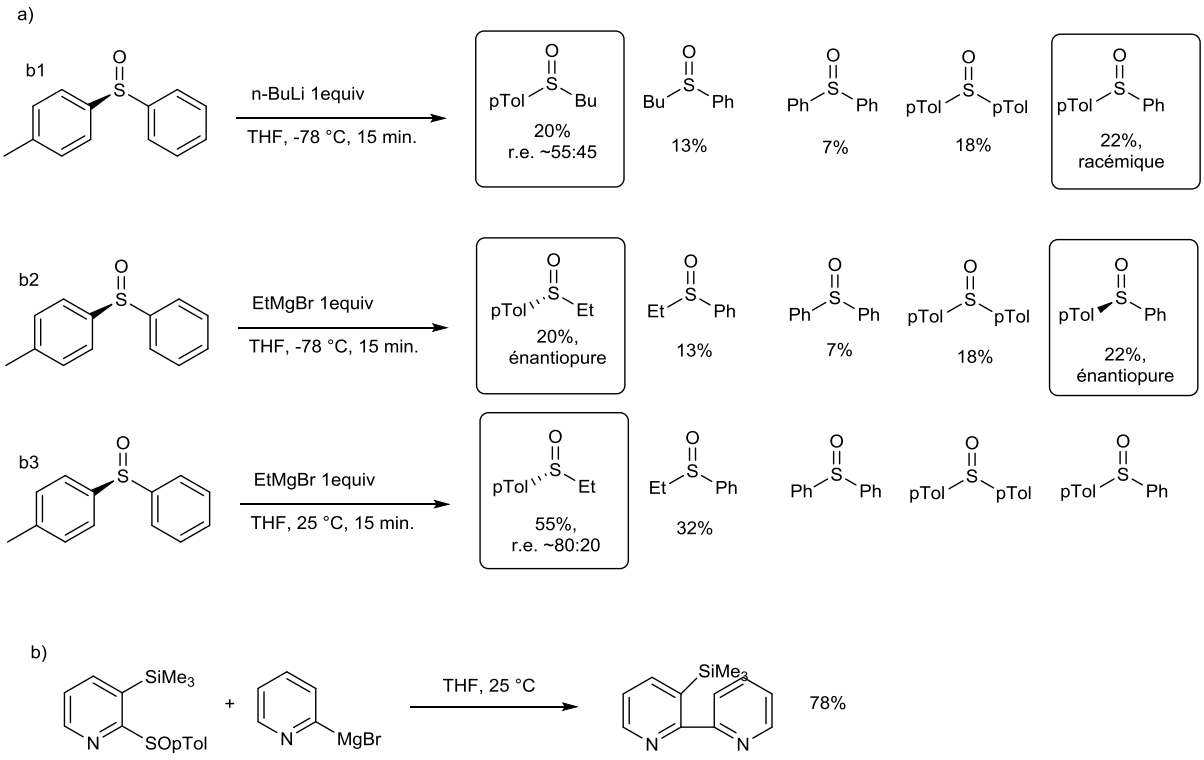

Figure III-109 : comportement des sulfoxydes en présence d'organométalliques

Cependant cette réaction est de peu d'intérêt synthétique : en effet l'organométallique formé lors de l'échange peu de nouveau s'additionner au nouveau sulfoxyde et faire un nouvel échange de ligand. En se répétant ainsi de façon itérative le processus peut conduire à la formation d'un mélange de produit et également à la racémisation des sulfoxydes (nous verrons par quel mécanisme dans la partie III.C.5 : Post-fonctionnalisation). L'étendue et la vitesse de ces échanges dépend principalement de l'organométallique utilisé et de la température. Ainsi, 1 équivalent de *n*-BuLi à -78 °C pendant 15 min sur le (R)-phenyl-*p*-tolylsulfoxyde conduit à un mélange de produits proche du statistique, ainsi qu'à une racémisation complète des produits analysés (Figure III-109a1). Par comparaison, 1 équivalent d'EtMgBr dans les mêmes conditions conduit au même mélange, mais en préservant cette fois la pureté optique des produits (Figure III-109a2), signe que l'échange de ligand ne s'est produit qu'une seule fois. Enfin à 25 °C, Le réactif de Grignard forme exclusivement des alkyles sulfoxydes avec cette fois une érosion de la pureté optique. Ainsi il est difficile de prévoir de façon fiable le comportement des sulfoxydes dans cette réaction d'échange de ligands, au-delà de la constatation pratique que la stabilité des sulfoxydes énantiopurs est compromise en présence d'organolithiens réactifs, même à basse température, alors que les réactifs de Grignard sont généralement compatibles.

Enfin, dans certains cas, il est possible d'assister à un couplage de ligands : cette réaction est surtout importante pour les ligands très électroattracteurs, ainsi il est possible de préparer avec un bon rendement des bipyridines à partir de 2-pyridylphenylsulfoxyde et de 2-pyridylGrignard[224] (Figure III-109b). Notons tout de

même que les lithiens moins réactifs (par exemple ceux issus d'une ortho-lithiation dirigée par un sulfoxyde[225] où le lithien est stabilisé par l'oxygène du sulfoxyde) sont compatibles avec les sulfoxydes énantiopurs : cependant il n'existe pas de règle pour prédire la stabilité optique des sulfoxydes dans ce type de conditions, et ainsi il faut apporter une attention particulière à la pureté optique des sulfoxydes dans ce contexte. Remarquons enfin que cet échange de ligand peut s'avérer très utile pour fonctionnaliser une molécule si on ne désire pas garder le sulfoxyde, car, après l'échange sulfoxyde/lithium, le lithien formé peut bien sûr être piégé par tous les électrophiles classiques, et nous verrons ces réactions plus en détails dans la partie post fonctionalisation. Pour conclure, on notera que de nombreuses réactions de substitution au soufre tri-coordiné se passent avec inversion de configuration, et on renverra le lecteur vers une revue[226] utile pour plus d'informations.

4. Complexes formés avec les métaux de transition

L'objet de cette partie est principalement de traiter du mode de coordination des sulfoxydes. En effet, grâce aux doublets libres au souffre et de l'oxygène, le sulfoxyde est un ligand ambidentate et il est donc important de connaître les facteurs influençant les modes de coordinations (toutes les données de cette partie sont tirées de trois revues[227–229]).

La coordination par le soufre est noté η^1-S (en prenant comme exemple le DMSO, on notera DMSO-S), par l'oxygène η^1-O (DMSO-O), par le soufre et l'oxygène comme ligand pontant μ-S,O (DMSO-S,O). Le facteur le plus important est la théorie HSAB : la coordination par l'oxygène est préférée pour les métaux durs, alors que la coordination par le soufre est préférée pour les métaux mous. La coordination par le soufre est π-accepteur, pas par l'oxygène. La coordination par le soufre conduit à un encombrement stérique plus important. Un bon indicateur du mode de coordination est la fréquence d'élongation de la liaison S=O : pour le DMSO libre, cette valeur est de 1055 cm^{-1} ; lors de la coordination η^1-O elle diminue (862-997 cm^{-1}, de pair avec un allongement de la liaison S=O) ; lors de la coordination η^1-S elle augmente (1080-1154, de pair avec une contraction de la liaison S=O)

Ceci étant dit, on remarquera que la coordination par l'oxygène est préférée pour la majorité des métaux ; on peut poser comme cas limite arbitraire « durs/mous » le ruthénium. En effet de nombreux complexes de ce métal avec le DMSO sont connus, et, si le DMSO préfère la coordination par le souffre pour des raisons électroniques, il est possible d'observer une isomérisation sur des complexes Ru^{II} -S vers Ru^{II}– O lorsqu'on :

1- ajoute des ligands π-accepteurs *trans* au sulfoxyde pour éviter une compétition dans la rétro-donation π.
2- sur le complexe cis-fac- $RuCl_2(DMSO\text{-}S)_3(DMSO\text{-}O)_1$ il est admis que le quatrième DMSO se coordine par l'oxygène pour des raisons stériques, en effet seuls les complexes trans- $RuCl_2(DMSO\text{-}S)_4$ ainsi que les complexes tetraméthylènesulfoxyde

(TMSO) cis-fac- $RuCl_2(TMSO\text{-}S)_4$ et trans-$RuCl_2(TMSO\text{-}S)_4$ sont connus (Figure III-110).
3- enfin les complexes cationiques (plus « durs ») favorisent la coordination par l'oxygène (ainsi cis-fac-$[RuCl_2(DMSO\text{-}O)_3(NO)]^+$).

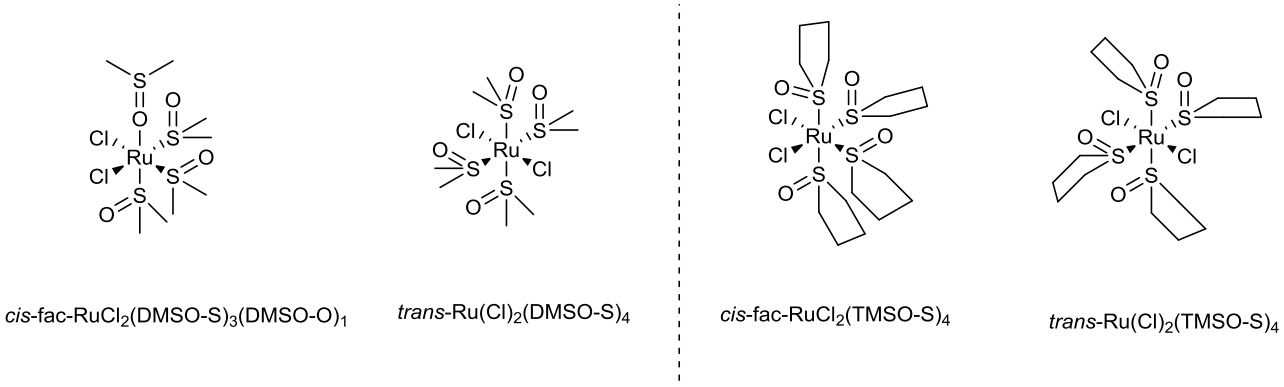

Figure III-110 : complexes ruthenium-sulfoxydes amdidentes

Remarquons enfin que les complexes de Cu^I, Ag^I se coordinent par l'oxygène, la rétro-donation π n'étant pas possible ici.

En conclusion, on considérera en première approximation que les complexes d'osmium, rhodium, iridium et dans une plus forte mesure, palladium et platine sont, sauf exceptions, coordinés par le souffre ; le ruthénium préfère la coordination par le souffre mais peut facilement être coordiné par l'oxygène lorsque des ligands à fort encombrement stérique et/ou qui rendent le métal plus dur sont présents ; les autres métaux sont coordinés par l'oxygène.

5. Post-fonctionnalisation des produits porteurs d'un sulfoxyde

En tant qu'auxiliaires de chiralité, les sulfoxydes se sont largement imposés. En effet si, nous l'avons dit, les groupements sulfinyls énantiopurs facilement accessibles restent limités, ils restent aisés à synthétiser à grande échelle et sont peu chers. Ensuite, le sulfoxyde peut être considéré comme un auxiliaire qui ne laisse pas de trace grâce à la relativement facile désulfinylation, en utilisant par exemple le nickel de Raney.

Cependant, un avantage majeur des sulfoxydes est leur réactivité vis à vis des bases lithiées. Ainsi, en présence des organolithiens l'échange sulfoxyde/lithium a lieu. Via cette stratégie, le groupement sulfoxyde peut être substitué par un large panel d'électrophiles[230]. Ainsi le sulfoxyde peut remplir deux rôles successifs: d'auxiliaire de chiralité il devient un groupe fonctionnel interchangeable[231]. Etant donné qu'il est relativement rare que le sulfoxyde soit requis dans le produit final, cette réaction prend une importance capitale pour élargir le champ d'application de l'utilisation des arylesulfoxydes. Nous parlons d'arylesulfoxydes car cet échange sulfoxyde/lithium (SO/Li) comporte tout de même certaines limitations par rapport à l'échange traditionnel halogène/lithium. L'examen de la littérature sur ce sujet est d'ailleurs révéla-

teur [232–234] et on peut dégager des observations qualitatives communes et importantes.

1-cette réaction peut être vue comme un échange de ligand/disproportionation au souffre avec formation/rupture de liaison C-S, en équilibre rapide (5-15 min.) et contrôlé thermodynamiquement même à des températures aussi basses que -95 °C (une expérience de pensée, s'appuyant sur le travail de Furukawa[234] est présentée Figure III-111 pour illustrer ce mécanisme).

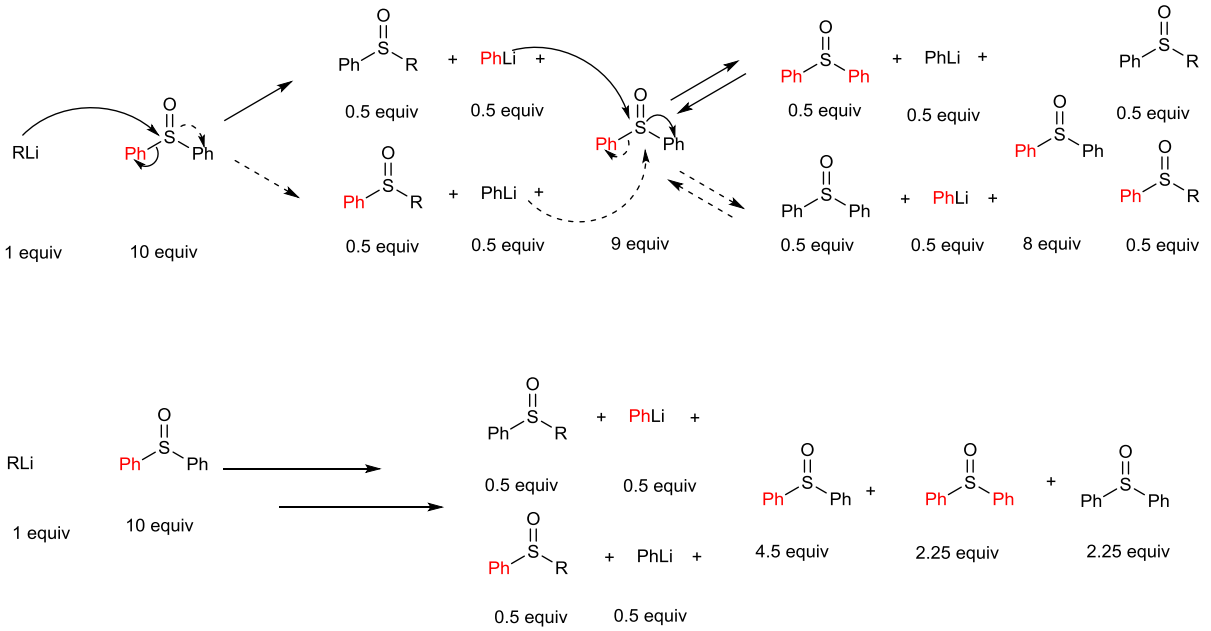

Figure III-111 : expérience dérivée du travail de Furukawa

2-la liaison S-O demeure intacte
3-les produits d'échange et la position des équilibres peuvent être rationalisés sur la base des pKas.
4-on peut considérer, en première approximation, que l'équilibre est complétement déplacé vers l'alkylsulfoxyde en cas d'échange alkyl/aryle, l'aryllithien étant beaucoup plus stable thermodynamiquement.
5-les réactions secondaires impliquant les arylsulfoxydes (*ortho*-lithiation) et les alkylsulfoxydes (α-déprotonation, élimination) ne sont pas favorisées cinétiquement mais sont favorisées thermodynamiquement (pas de retour en arrière) et doivent donc être prises en compte.
6-l'encombrement stérique au soufre à peu d'importance, excepté pour les *tert*-butyl sulfoxydes où l'addition d'un alkyl/aryllithium devient beaucoup plus difficile.
7-le procédé conduit à l'épimérisation au niveau de l'atome de soufre, même avec des quantités sub-stoichiométriques d'organolithium, sur une échelle de temps de dizaines de minutes même à -95 °C.

Ainsi certaines lignes directrices sont à suivre dans ce type de réaction :

1-le groupe à échanger et à fonctionnaliser doit être un aryle/hétéroaryle
2-les températures de -95 °C à -78 °C sont les plus adaptées
3-des temps de réactions rapide (entre <5 et 20 min.)
4-les solvants éthérés (Et_2O, THF, DME) sont bien adaptés, mais, contrairement à l'échange halogène lithium, les hydrocarbones peuvent être utilisés.
5-l'utilisation d'un excès de lithien (2 équivalent minimum) est recommandé
6-les aryllithiums, dans les cas favorables, sont supérieurs aux alkyllithiums[235,236]
7-la vitesse d'addition de l'électrophile à une influence sur l'issue de la réaction.

En suivant ces lignes directrices on obtient généralement un rendement de 50% minimum et plus souvent entre 65-75%. En cas de rendement décevant, le facteur le plus important à modifier semble être le solvant ; pour l'optimisation fine on se tournera plutôt vers sur la nature du lithien utilisé puis sur sa stœchiométrie. Enfin notons que les Grignards font des échanges plus propres par mécanisme proche de la S_N2, contrôlé cinétiquement et le soufre est donc très peu épimérisé[237] (Figure III-112). Cependant la température à laquelle s'effectue l'échange de façon efficace semble devoir être proche, généralement, de 0 °C, ce qui limite grandement leur utilisation. Les organométalliques avec une réactivité intermédiaire (RMgClLiCl) réagissent à des températures intermédiaires[238].

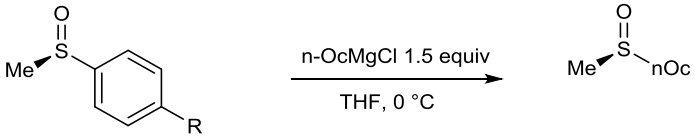

R=	r.e. (substrat)	r.e. (produit)	rdt
OMe	96:4	96:4	24%
Cl	94.5:5.5	94.5:5.5	73%
Br	>98	>98	84%

Figure III-112 : échange sulfoxyde/magnésium

D. References

[1] S. Murai, F. Kakiuchi, S. Sekine, Y. Tanaka, A. Kamatani, M. Sonoda, N. Chatani, *Nature* **1993**, *366*, 529–531.
[2] V. Snieckus, *Chem. Rev.* **1990**, *90*, 879–933.
[3] P. Beak, R. A. Brown, *J. Org. Chem.* **1977**, *42*, 1823–1824.
[4] J. A. Labinger, J. E. Bercaw, *Nature* **2002**, *417*, 507–514.
[5] R. Jazzar, J. Hitce, A. Renaudat, J. Sofack-Kreutzer, O. Baudoin, *Chem. – Eur. J.* **2010**, *16*, 2654–2672.
[6] J. Rittle, M. T. Green, *Science* **2010**, *330*, 933–937.
[7] H. M. L. Davies, R. E. J. Beckwith, *Chem. Rev.* **2003**, *103*, 2861–2904.
[8] J. Chatt, J. M. Davidson, *J. Chem. Soc. Resumed* **1965**, *0*, 843–855.
[9] M. A. Bennett, D. L. Milner, *Chem. Commun. Lond.* **1967**, *0*, 581–582.
[10] A. E. Shilov, N. F. Gold'dshleger, V. V. Es'kova, *Zhurnal Fizicheskoi Khimii* **1972**, *46*, 1353.
[11] A. S. Goldman, K. I. Goldberg, in *Act. Funct. C—H Bonds*, American Chemical Society, **2004**, pp. 1–43.
[12] P. L. Watson, *J. Am. Chem. Soc.* **1983**, *105*, 6491–6493.
[13] D. H. Ess, W. A. Goddard, R. A. Periana, *Organometallics* **2010**, *29*, 6459–6472.
[14] D. Lapointe, K. Fagnou, *Chem. Lett.* **2010**, *39*, 1118–1126.
[15] J. Oxgaard, W. J. Tenn, R. J. Nielsen, R. A. Periana, W. A. Goddard, *Organometallics* **2007**, *26*, 1565–1567.
[16] Y. Boutadla, D. L. Davies, S. A. Macgregor, A. I. Poblador-Bahamonde, *Dalton Trans.* **2009**, 5820–5831.
[17] A. C. Cope, R. W. Siekman, *J. Am. Chem. Soc.* **1965**, *87*, 3272–3273.
[18] A. C. Cope, E. C. Friedrich, *J. Am. Chem. Soc.* **1968**, *90*, 909–913.
[19] J. M. Duff, B. E. Mann, B. L. Shaw, B. Turtle, *J. Chem. Soc. Dalton Trans.* **1974**, *0*, 139–145.
[20] J. C. Gaunt, B. L. Shaw, *J. Organomet. Chem.* **1975**, *102*, 511–516.
[21] D. L. Davies, S. M. A. Donald, S. A. Macgregor, *J. Am. Chem. Soc.* **2005**, *127*, 13754–13755.
[22] D. L. Davies, S. A. Macgregor, C. L. McMullin, *Chem. Rev.* **2017**, DOI 10.1021/acs.chemrev.6b00839.
[23] L.-C. Campeau, S. Rousseaux, K. Fagnou, *J. Am. Chem. Soc.* **2005**, *127*, 18020–18021.
[24] S. I. Gorelsky, D. Lapointe, K. Fagnou, *J. Am. Chem. Soc.* **2008**, *130*, 10848–10849.
[25] O. Tischler, Z. Bokányi, Z. Novák, *Organometallics* **2016**, *35*, 741–746.
[26] O. Tischler, S. Kovács, G. Érsek, P. Králl, J. Daru, A. Stirling, Z. Novák, *J. Mol. Catal. Chem.* **2017**, *426*, *Part B*, 444–450.
[27] V. I. Sokolov, L. L. Troitskaya, O. A. Reutov, *J. Organomet. Chem.* **1979**, *182*, 537–546.
[28] J. Wencel-Delord, F. Colobert, *Chem. – Eur. J.* **2013**, *19*, 14010–14017.
[29] C. G. Newton, S.-G. Wang, C. C. Oliveira, N. Cramer, *Chem. Rev.* **2017**, *117*, 8908–8976.

[30] B.-F. Shi, N. Maugel, Y.-H. Zhang, J.-Q. Yu, *Angew. Chem. Int. Ed.* **2008**, *47*, 4882–4886.
[31] B.-F. Shi, Y.-H. Zhang, J. K. Lam, D.-H. Wang, J.-Q. Yu, *J. Am. Chem. Soc.* **2010**, *132*, 460–461.
[32] B. N. Laforteza, K. S. L. Chan, J.-Q. Yu, *Angew. Chem. Int. Ed.* **2015**, *54*, 11143–11146.
[33] L. Chu, X.-C. Wang, C. E. Moore, A. L. Rheingold, J.-Q. Yu, *J. Am. Chem. Soc.* **2013**, *135*, 16344–16347.
[34] X.-F. Cheng, Y. Li, Y.-M. Su, F. Yin, J.-Y. Wang, J. Sheng, H. U. Vora, X.-S. Wang, J.-Q. Yu, *J. Am. Chem. Soc.* **2013**, *135*, 1236–1239.
[35] Z.-J. Du, J. Guan, G.-J. Wu, P. Xu, L.-X. Gao, F.-S. Han, *J. Am. Chem. Soc.* **2015**, *137*, 632–635.
[36] L. Chu, K.-J. Xiao, J.-Q. Yu, *Science* **2014**, *346*, 451–455.
[37] K.-J. Xiao, L. Chu, J.-Q. Yu, *Angew. Chem. Int. Ed.* **2016**, *55*, 2856–2860.
[38] K.-J. Xiao, L. Chu, G. Chen, J.-Q. Yu, *J. Am. Chem. Soc.* **2016**, *138*, 7796–7800.
[39] G. H. Christie, J. Kenner, *J. Chem. Soc. Trans.* **1922**, *121*, 614–620.
[40] R. Khun, in *Mol. Asymmetrie*, Leipzig-Wien:Franz-Deutike, **1933**, pp. 803–824.
[41] M. Ōki, in *Top. Stereochem.* (Eds.: N.L. Allinger, E.L. Eliel, S.H. Wilen), John Wiley & Sons, Inc., **1983**, pp. 1–81.
[42] F. Grein, *J. Phys. Chem. A* **2002**, *106*, 3823–3827.
[43] R. Ruzziconi, S. Spizzichino, L. Lunazzi, A. Mazzanti, M. Schlosser, *Chem. – Eur. J.* **2009**, *15*, 2645–2652.
[44] L. Lunazzi, M. Mancinelli, A. Mazzanti, S. Lepri, R. Ruzziconi, M. Schlosser, *Org. Biomol. Chem.* **2012**, *10*, 1847–1855.
[45] G. Bott, L. D. Field, S. Sternhell, *J. Am. Chem. Soc.* **1980**, *102*, 5618–5626.
[46] L. Meca, D. Řeha, Z. Havlas, *J. Org. Chem.* **2003**, *68*, 5677–5680.
[47] F. H. Allen, O. Kennard, D. G. Watson, L. Brammer, A. G. Orpen, R. Taylor, *J. Chem. Soc. Perkin Trans. 2* **1987**, *0*, S1–S19.
[48] C. Wolf, *Dynamic Stereochemistry of Chiral Compounds: Principles and Applications*, Royal Society Of Chemistry, **2008**.
[49] M. Rieger, F. H. Westheimer, *J. Am. Chem. Soc.* **1950**, *72*, 19–28.
[50] C. Wolf, D. H. Hochmuth, W. A. König, C. Roussel, *Liebigs Ann.* **1996**, *1996*, 357–363.
[51] A. K. Colter, L. M. Clemens, *J. Phys. Chem.* **1964**, *68*, 651–654.
[52] A. A. Watson, A. C. Willis, S. B. Wild, *J. Organomet. Chem.* **1993**, *445*, 71–78.
[53] G. Bringmann, M. Heubes, M. Breuning, L. Göbel, M. Ochse, B. Schöner, O. Schupp, *J. Org. Chem.* **2000**, *65*, 722–728.
[54] M. Hatsuda, H. Hiramatsu, S. Yamada, T. Shimizu, M. Seki, *J. Org. Chem.* **2001**, *66*, 4437–4439.
[55] G. Bringmann, M. Heubes, M. Breuning, L. Göbel, M. Ochse, B. Schöner, O. Schupp, *J. Org. Chem.* **2000**, *65*, 722–728.
[56] S. Superchi, D. Casarini, A. Laurita, A. Bavoso, C. Rosini, *Angew. Chem. Int. Ed.* **2001**, *40*, 451–454.
[57] G. Bringmann, A. J. Price Mortimer, P. A. Keller, M. J. Gresser, J. Garner, M. Breuning, *Angew. Chem. Int. Ed.* **2005**, *44*, 5384–5427.
[58] T. W. Wallace, *Org. Biomol. Chem.* **2006**, *4*, 3197.
[59] J. Wencel-Delord, A. Panossian, F. R. Leroux, F. Colobert, *Chem. Soc. Rev.* **2015**, *44*, 3418–3430.

[60] B. J. Morgan, C. A. Mulrooney, M. C. Kozlowski, *J. Org. Chem.* **2010**, *75*, 44–56.
[61] D. A. Evans, M. R. Wood, B. W. Trotter, T. I. Richardson, J. C. Barrow, J. L. Katz, *Angew. Chem. Int. Ed.* **1998**, *37*, 2700–2704.
[62] Q.-X. Guo, Z.-J. Wu, Z.-B. Luo, Q.-Z. Liu, J.-L. Ye, S.-W. Luo, L.-F. Cun, L.-Z. Gong, *J. Am. Chem. Soc.* **2007**, *129*, 13927–13938.
[63] G.-Q. Li, H. Gao, C. Keene, M. Devonas, D. H. Ess, L. Kürti, *J. Am. Chem. Soc.* **2013**, *135*, 7414–7417.
[64] C. K. De, F. Pesciaioli, B. List, *Angew. Chem. Int. Ed.* **2013**, *52*, 9293–9295.
[65] H.-H. Zhang, C.-S. Wang, C. Li, G.-J. Mei, Y. Li, F. Shi, *Angew. Chem. Int. Ed.* **2017**, *56*, 116–121.
[66] L. Ackermann, R. Vicente, A. R. Kapdi, *Angew. Chem. Int. Ed.* **2009**, *48*, 9792–9826.
[67] K. Yamaguchi, J. Yamaguchi, A. Studer, K. Itami, *Chem. Sci.* **2012**, *3*, 2165–2169.
[68] K. Yamaguchi, H. Kondo, J. Yamaguchi, K. Itami, *Chem. Sci.* **2013**, *4*, 3753–3757.
[69] Z.-J. Jia, C. Merten, R. Gontla, C. G. Daniliuc, A. P. Antonchick, H. Waldmann, *Angew. Chem. Int. Ed.* **2017**, *56*, 2429–2434.
[70] T. Leermann, P.-E. Broutin, F. R. Leroux, F. Colobert, *Org. Biomol. Chem.* **2012**, *10*, 4095–4102.
[71] F. Colobert, V. Valdivia, S. Choppin, F. R. Leroux, I. Fernández, E. Álvarez, N. Khiar, *Org. Lett.* **2009**, *11*, 5130–5133.
[72] K. Kamikawa, M. Uemura, *Synlett* **2000**, *2000*, 0938–0949.
[73] O. Baudoin, *Eur. J. Org. Chem.* **2005**, *2005*, 4223–4229.
[74] D. Zhang, Q. Wang, *Coord. Chem. Rev.* **2015**, *286*, 1–16.
[75] A. N. Cammidge, K. V. L. Crépy, *Chem. Commun.* **2000**, *0*, 1723–1724.
[76] J. Yin, S. L. Buchwald, *J. Am. Chem. Soc.* **2000**, *122*, 12051–12052.
[77] X. Shen, G. O. Jones, D. A. Watson, B. Bhayana, S. L. Buchwald, *J. Am. Chem. Soc.* **2010**, *132*, 11278–11287.
[78] W. Tang, N. D. Patel, G. Xu, X. Xu, J. Savoie, S. Ma, M.-H. Hao, S. Keshipeddy, A. G. Capacci, X. Wei, et al., *Org. Lett.* **2012**, *14*, 2258–2261.
[79] A. Bermejo, A. Ros, R. Fernández, J. M. Lassaletta, *J. Am. Chem. Soc.* **2008**, *130*, 15798–15799.
[80] A. I. Meyers, J. R. Flisak, R. A. Aitken, *J. Am. Chem. Soc.* **1987**, *109*, 5446–5452.
[81] R. W. Baker, G. R. Pocock, M. V. Sargent, E. Twiss (née Stanojevic), *Tetrahedron Asymmetry* **1993**, *4*, 2423–2426.
[82] M. Amatore, C. Aubert, *Eur. J. Org. Chem.* **2015**, *2015*, 265–286.
[83] K. Tanaka, *Chem. – Asian J.* **2009**, *4*, 508–518.
[84] G. Nishida, K. Noguchi, M. Hirano, K. Tanaka, *Angew. Chem. Int. Ed.* **2007**, *46*, 3951–3954.
[85] G. Nishida, N. Suzuki, K. Noguchi, K. Tanaka, *Org. Lett.* **2006**, *8*, 3489–3492.
[86] A. Link, C. Sparr, *Angew. Chem. Int. Ed.* **2014**, *53*, 5458–5461.
[87] F. Guo, L. C. Konkol, R. J. Thomson, *J. Am. Chem. Soc.* **2011**, *133*, 18–20.
[88] V. S. Raut, M. Jean, N. Vanthuyne, C. Roussel, T. Constantieux, C. Bressy, X. Bugaut, D. Bonne, J. Rodriguez, *J. Am. Chem. Soc.* **2017**, *139*, 2140–2143.
[89] Jolliffe, J. D., Armstrong, R. J., Smith, M. D., *Nat. Chem.* **2017**, 558–562.
[90] K. M. Engle, T.-S. Mei, M. Wasa, J.-Q. Yu, *Acc. Chem. Res.* **2012**, *45*, 788–802.

[91] J. L. Gustafson, D. Lim, K. T. Barrett, S. J. Miller, *Angew. Chem. Int. Ed.* **2011**, *50*, 5125–5129.
[92] F. Kakiuchi, P. Le Gendre, A. Yamada, H. Ohtaki, S. Murai, *Tetrahedron Asymmetry* **2000**, *11*, 2647–2651.
[93] D.-W. Gao, Q. Gu, S.-L. You, *ACS Catal.* **2014**, *4*, 2741–2745.
[94] J. Zheng, S.-L. You, *Angew. Chem. Int. Ed.* **2014**, *53*, 13244–13247.
[95] Y.-N. Ma, H.-Y. Zhang, S.-D. Yang, *Org. Lett.* **2015**, *17*, 2034–2037.
[96] J. Zheng, W.-J. Cui, C. Zheng, S.-L. You, *J. Am. Chem. Soc.* **2016**, *138*, 5242–5245.
[97] S.-X. Li, Y.-N. Ma, S.-D. Yang, *Org. Lett.* **2017**, *19*, 1842–1845.
[98] Q.-J. Yao, S. Zhang, B.-B. Zhan, B.-F. Shi, *Angew. Chem. Int. Ed.* **2017**, *56*, 6617–6621.
[99] T. Hayashi, S. Niizuma, T. Kamikawa, N. Suzuki, Y. Uozumi, *J. Am. Chem. Soc.* **1995**, *117*, 9101–9102.
[100] V. Bhat, S. Wang, B. M. Stoltz, S. C. Virgil, *J. Am. Chem. Soc.* **2013**, *135*, 16829–16832.
[101] A. Ros, B. Estepa, P. Ramírez-López, E. Álvarez, R. Fernández, J. M. Lassaletta, *J. Am. Chem. Soc.* **2013**, *135*, 15730–15733.
[102] P. Ramírez-López, A. Ros, B. Estepa, R. Fernández, B. Fiser, E. Gómez-Bengoa, J. M. Lassaletta, *ACS Catal.* **2016**, *6*, 3955–3964.
[103] P. Ramírez-López, A. Ros, A. Romero-Arenas, J. Iglesias-Sigüenza, R. Fernández, J. M. Lassaletta, *J. Am. Chem. Soc.* **2016**, *138*, 12053–12056.
[104] V. Hornillos, A. Ros, P. Ramírez-López, J. Iglesias-Sigüenza, R. Fernández, J. M. Lassaletta, *Chem. Commun.* **2016**, *52*, 14121–14124.
[105] T. Matsumoto, T. Konegawa, T. Nakamura, K. Suzuki, *Synlett* **2002**, *2002*, 0122–0124.
[106] S. Staniland, B. Yuan, N. Giménez-Agulló, T. Marcelli, S. C. Willies, D. M. Grainger, N. J. Turner, J. Clayden, *Chem. – Eur. J.* **2014**, *20*, 13084–13088.
[107] L. M. Engelhardt, W.-P. Leung, C. L. Raston, G. Salem, P. Twiss, A. H. White, *J. Chem. Soc. Dalton Trans.* **1988**, *0*, 2403–2409.
[108] Q. Perron, A. Alexakis, *Adv. Synth. Catal.* **2010**, *352*, 2611–2620.
[109] G. Bringmann, D. Menche, *Acc. Chem. Res.* **2001**, *34*, 615–624.
[110] G. Bringmann, T. Gulder, T. A. M. Gulder, M. Breuning, *Chem. Rev.* **2011**, *111*, 563–639.
[111] M. Penhoat, V. Levacher, G. Dupas, *J. Org. Chem.* **2003**, *68*, 9517–9520.
[112] T. Shimada, A. Kina, T. Hayashi, *J. Org. Chem.* **2003**, *68*, 6329–6337.
[113] K. Mikami, K. Aikawa, Y. Yusa, M. Hatano, *Org. Lett.* **2002**, *4*, 91–94.
[114] K. Mikami, S. Kataoka, Y. Yusa, K. Aikawa, *Org. Lett.* **2004**, *6*, 3699–3701.
[115] K. Mikami, K. Wakabayashi, K. Aikawa, *Org. Lett.* **2006**, *8*, 1517–1519.
[116] K. Aikawa, K. Mikami, *Chem. Commun.* **2012**, *48*, 11050–11069.
[117] "Chirality and Biological Activity of Drugs," can be found under https://www.crcpress.com/Chirality-and-Biological-Activity-of-Drugs/Crossley/p/book/9780849391408, **1995**.
[118] A. M. Rouhi, *Chem. Eng. News* **2003**, *81*, 45–61.
[119] S. R. LaPlante, P. J. Edwards, L. D. Fader, A. Jakalian, O. Hucke, *ChemMedChem* **2011**, *6*, 505–513.
[120] C. for D. E. and Research, "Guidances (Drugs) - Development of New Stereoisomeric Drugs," can be found under https://www.fda.gov/drugs/guidancecomplianceregulatoryinformation/guidances/ucm122883.htm, **2017**.

[121] Y. S. Zhou, L. K. Tay, D. Hughes, S. Donahue, *J. Clin. Pharmacol.* **2004**, *44*, 680–688.
[122] S. D. Guile, J. R. Bantick, D. R. Cheshire, M. E. Cooper, A. M. Davis, D. K. Donald, R. Evans, C. Eyssade, D. D. Ferguson, S. Hill, et al., *Bioorg. Med. Chem. Lett.* **2006**, *16*, 2260–2265.
[123] S. D. Guile, J. R. Bantick, M. E. Cooper, D. K. Donald, C. Eyssade, A. H. Ingall, R. J. Lewis, B. P. Martin, R. T. Mohammed, T. J. Potter, et al., *J. Med. Chem.* **2007**, *50*, 254–263.
[124] A. Palani, S. Shapiro, J. W. Clader, W. J. Greenlee, D. Blythin, K. Cox, N. E. Wagner, J. Strizki, B. M. Baroudy, N. Dan, *Bioorg. Med. Chem. Lett.* **2003**, *13*, 705–708.
[125] A. Palani, S. Shapiro, J. W. Clader, W. J. Greenlee, S. Vice, S. McCombie, K. Cox, J. Strizki, B. M. Baroudy, *Bioorg. Med. Chem. Lett.* **2003**, *13*, 709–712.
[126] K. Dodou, *Expert Opin. Investig. Drugs* **2005**, *14*, 1419–1434.
[127] J. E. Smyth, N. M. Butler, P. A. Keller, *Nat. Prod. Rep.* **2015**, *32*, 1562–1583.
[128] D. H. Williams, B. Bardsley, *Angew. Chem. Int. Ed.* **1999**, *38*, 1172–1193.
[129] P. Lloyd-Williams, E. Giralt, *Chem. Soc. Rev.* **2001**, *30*, 145–157.
[130] M. Ge, Z. Chen, H. Russell, Onishi, J. Kohler, L. L. Silver, R. Kerns, S. Fukuzawa, C. Thompson, D. Kahne, *Science* **1999**, *284*, 507–511.
[131] N. Au, E. Kuester-Schoeck, V. Mandava, L. E. Bothwell, S. P. Canny, K. Chachu, S. A. Colavito, S. N. Fuller, E. S. Groban, L. A. Hensley, et al., *J. Bacteriol.* **2005**, *187*, 7655–7666.
[132] A. Urban, S. Eckermann, B. Fast, S. Metzger, M. Gehling, K. Ziegelbauer, H. Rübsamen-Waigmann, C. Freiberg, *Appl. Environ. Microbiol.* **2007**, *73*, 6436–6443.
[133] D. Weisleder, E. B. Lillehoj, *Tetrahedron Lett.* **1971**, *12*, 4705–4706.
[134] D. J. Haydon, N. R. Stokes, R. Ure, G. Galbraith, J. M. Bennett, D. R. Brown, P. J. Baker, V. V. Barynin, D. W. Rice, S. E. Sedelnikova, et al., *Science* **2008**, *321*, 1673–1675.
[135] Y. S. Park, C. I. Grove, M. González-López, S. Urgaonkar, J. C. Fettinger, J. T. Shaw, *Angew. Chem. Int. Ed.* **2011**, *50*, 3730–3733.
[136] C. I. Grove, J. C. Fettinger, J. T. Shaw, *Synthesis* **2012**, *44*, 362–371.
[137] J. Clayden, W. J. Moran, P. J. Edwards, S. R. LaPlante, *Angew. Chem. Int. Ed.* **2009**, *48*, 6398–6401.
[138] S. R. LaPlante, L. D. Fader, K. R. Fandrick, D. R. Fandrick, O. Hucke, R. Kemper, S. P. F. Miller, P. J. Edwards, *J. Med. Chem.* **2011**, *54*, 7005–7022.
[139] M. C. Kozlowski, B. J. Morgan, E. C. Linton, *Chem. Soc. Rev.* **2009**, *38*, 3193–3207.
[140] J. A. Osborn, G. Wilkinson, J. J. Mrowca, in *Inorg. Synth.* (Ed.: E.L. Muetterties), John Wiley & Sons, Inc., **1967**, pp. 67–71.
[141] O. Korpiun, R. A. Lewis, J. Chickos, K. Mislow, *J. Am. Chem. Soc.* **1968**, *90*, 4842–4846.
[142] L. Horner, *Pure Appl. Chem.* **1964**, *9*, 225–244.
[143] W. S. Knowles, M. J. Sabacky, *Chem. Commun. Lond.* **1968**, *0*, 1445–1446.
[144] L. Horner, H. Siegel, H. Büthe, *Angew. Chem. Int. Ed. Engl.* **1968**, *7*, 942–942.
[145] T. P. Dang, H. B. Kagan, *J. Chem. Soc. Chem. Commun.* **1971**, *0*, 481–481.
[146] W. S. Knowles, *Acc. Chem. Res.* **1983**, *16*, 106–112.
[147] R. H. Grubbs, R. A. DeVries, *Tetrahedron Lett.* **1977**, *18*, 1879–1880.
[148] K. Tamao, H. Yamamoto, H. Matsumoto, N. Miyake, T. Hayashi, M. Kumada, *Tetrahedron Lett.* **1977**, *18*, 1389–1392.

[149] A. Miyashita, A. Yasuda, H. Takaya, K. Toriumi, T. Ito, T. Souchi, R. Noyori, *J. Am. Chem. Soc.* **1980**, *102*, 7932–7934.
[150] K. Tani, T. Yamagata, S. Akutagawa, H. Kumobayashi, T. Taketomi, H. Takaya, A. Miyashita, R. Noyori, S. Otsuka, *J. Am. Chem. Soc.* **1984**, *106*, 5208–5217.
[151] *J. Chem. Educ.* **1993**, *70*, A146.
[152] R. Noyori, M. Ohta, Y. Hsiao, M. Kitamura, T. Ohta, H. Takaya, *J. Am. Chem. Soc.* **1986**, *108*, 7117–7119.
[153] M. Kitamura, T. Ohkuma, S. Inoue, N. Sayo, H. Kumobayashi, S. Akutagawa, T. Ohta, H. Takaya, R. Noyori, *J. Am. Chem. Soc.* **1988**, *110*, 629–631.
[154] T. Ohta, H. Takaya, M. Kitamura, K. Nagai, R. Noyori, *J. Org. Chem.* **1987**, *52*, 3174–3176.
[155] *Org. Synth.* **1995**, *72*, 74.
[156] M. Kitamura, M. Tokunaga, R. Noyori, *J. Am. Chem. Soc.* **1995**, *117*, 2931–2932.
[157] X. Zhang, K. Mashima, K. Koyano, N. Sayo, H. Kumobayashi, S. Akutagawa, H. Takaya, *Tetrahedron Lett.* **1991**, *32*, 7283–7286.
[158] J. M. Hopkins, S. A. Dalrymple, M. Parvez, B. A. Keay, *Org. Lett.* **2005**, *7*, 3765–3768.
[159] A. H. M. de Vries, A. Meetsma, B. L. Feringa, *Angew. Chem. Int. Ed. Engl.* **1996**, *35*, 2374–2376.
[160] T. Akiyama, J. Itoh, K. Yokota, K. Fuchibe, *Angew. Chem. Int. Ed.* **2004**, *43*, 1566–1568.
[161] I. C. Lennon, C. J. Pilkington, *Synthesis* **2003**, *2003*, 1639–1642.
[162] M. J. Burk, *J. Am. Chem. Soc.* **1991**, *113*, 8518–8519.
[163] M. J. Burk, J. E. Feaster, W. A. Nugent, R. L. Harlow, *J. Am. Chem. Soc.* **1993**, *115*, 10125–10138.
[164] G. Hoge, *J. Am. Chem. Soc.* **2003**, *125*, 10219–10227.
[165] P. J. Pye, K. Rossen, R. A. Reamer, N. N. Tsou, R. P. Volante, P. J. Reider, *J. Am. Chem. Soc.* **1997**, *119*, 6207–6208.
[166] S. E. Gibson, J. D. Knight, *Org. Biomol. Chem.* **2003**, *1*, 1256–1269.
[167] T. R. Kelly, H. De Silva, R. A. Silva, *Nature* **1999**, *401*, 150–152.
[168] S. P. Fletcher, F. Dumur, M. M. Pollard, B. L. Feringa, *Science* **2005**, *310*, 80–82.
[169] B. S. L. Collins, J. C. M. Kistemaker, E. Otten, B. L. Feringa, *Nat. Chem.* **2016**, *8*, 860–866.
[170] J. L. García Ruano, J. Alemán, M. B. Cid, M. Á. Fernández-Ibáñez, M. C. Maestro, M. R. Martín, A. M. Martín-Castro, in *Organosulfur Chem. Asymmetric Synth.* (Eds.: T. Toru, C. Bolm), Wiley-VCH Verlag GmbH & Co. KGaA, **2008**, pp. 55–159.
[171] A. Volonterio, M. Zanda, in *Organosulfur Chem. Asymmetric Synth.* (Eds.: T. Toru, C. Bolm), Wiley-VCH Verlag GmbH & Co. KGaA, **2008**, pp. 351–374.
[172] I. Fernández, N. Khiar, in *Organosulfur Chem. Asymmetric Synth.* (Eds.: T. Toru, C. Bolm), Wiley-VCH Verlag GmbH & Co. KGaA, **2008**, pp. 265–290.
[173] M. Mellah, A. Voituriez, E. Schulz, *Chem. Rev.* **2007**, *107*, 5133–5209.
[174] G. Sipos, E. E. Drinkel, R. Dorta, *Chem. Soc. Rev.* **2015**, *44*, 3834–3860.
[175] B. R. James, R. S. McMillan, K. J. Reimer, *J. Mol. Catal.* **1976**, *1*, 439–441.
[176] D. G. I. Petra, P. C. J. Kamer, A. L. Spek, H. E. Schoemaker, P. W. N. M. van Leeuwen, *J. Org. Chem.* **2000**, *65*, 3010–3017.
[177] R. Tokunoh, M. Sodeoka, K. Aoe, M. Shibasaki, *Tetrahedron Lett.* **1995**, *36*, 8035–8038.

[178] J. V. Allen, J. F. Bower, J. M. J. Williams, *Tetrahedron Asymmetry* **1994**, *5*, 1895–1898.
[179] K. Hiroi, Y. Suzuki, I. Abe, R. Kawagishi, *Tetrahedron* **2000**, *56*, 4701–4710.
[180] K. Hiroi, Y. Suzuki, *Tetrahedron Lett.* **1998**, *39*, 6499–6502.
[181] K. Hiroi, I. Izawa, T. Takizawa, K. Kawai, *Tetrahedron* **2004**, *60*, 2155–2162.
[182] J. Chen, F. Lang, D. Li, L. Cun, J. Zhu, J. Deng, J. Liao, *Tetrahedron Asymmetry* **2009**, *20*, 1953–1956.
[183] H.-G. Cheng, B. Feng, L.-Y. Chen, W. Guo, X.-Y. Yu, L.-Q. Lu, J.-R. Chen, W.-J. Xiao, *Chem. Commun.* **2014**, *50*, 2873–2875.
[184] H. Grennberg, A. Gogoll, J. E. Baeckvall, *J. Org. Chem.* **1991**, *56*, 5808–5811.
[185] M. S. Chen, M. C. White, *J. Am. Chem. Soc.* **2004**, *126*, 1346–1347.
[186] M. S. Chen, N. Prabagaran, N. A. Labenz, M. C. White, *J. Am. Chem. Soc.* **2005**, *127*, 6970–6971.
[187] D. J. Covell, M. C. White, *Angew. Chem. Int. Ed.* **2008**, *47*, 6448–6451.
[188] R. Mariz, X. Luan, M. Gatti, A. Linden, R. Dorta, *J. Am. Chem. Soc.* **2008**, *130*, 2172–2173.
[189] J. Chen, J. Chen, F. Lang, X. Zhang, L. Cun, J. Zhu, J. Deng, J. Liao, *J. Am. Chem. Soc.* **2010**, *132*, 4552–4553.
[190] T. Thaler, L.-N. Guo, A. K. Steib, M. Raducan, K. Karaghiosoff, P. Mayer, P. Knochel, *Org. Lett.* **2011**, *13*, 3182–3185.
[191] S.-S. Jin, H. Wang, T.-S. Zhu, M.-H. Xu, *Org. Biomol. Chem.* **2012**, *10*, 1764–1768.
[192] A. P. Pulis, D. J. Procter, *Angew. Chem. Int. Ed.* **2016**, *55*, 9842–9860.
[193] M. M. Coulter, P. K. Dornan, V. M. Dong, *J. Am. Chem. Soc.* **2009**, *131*, 6932–6933.
[194] R. Samanta, A. P. Antonchick, *Angew. Chem. Int. Ed.* **2011**, *50*, 5217–5220.
[195] B. Wang, Y. Liu, C. Lin, Y. Xu, Z. Liu, Y. Zhang, *Org. Lett.* **2014**, *16*, 4574–4577.
[196] B. Wang, C. Shen, J. Yao, H. Yin, Y. Zhang, *Org. Lett.* **2014**, *16*, 46–49.
[197] K. Nobushige, K. Hirano, T. Satoh, M. Miura, *Org. Lett.* **2014**, *16*, 1188–1191.
[198] K. Padala, M. Jeganmohan, *Chem. Commun.* **2014**, *50*, 14573–14576.
[199] S. Jerhaoui, F. Chahdoura, C. Rose, J.-P. Djukic, J. Wencel-Delord, F. Colobert, *Chem. – Eur. J.* **2016**, *22*, 17397–17406.
[200] D. Mu, F. Gao, G. Chen, G. He, *ACS Catal.* **2017**, *7*, 1880–1885.
[201] S. Jerhaoui, J.-P. Djukic, J. Wencel-Delord, F. Colobert, *Chem. – Eur. J.* **n.d.**, n/a-n/a.
[202] H. B. Kagan, in *Organosulfur Chem. Asymmetric Synth.* (Eds.: T. Toru, C. Bolm), Wiley-VCH Verlag GmbH & Co. KGaA, **2008**, pp. 1–29.
[203] K. Mislow, M. M. Green, P. Laur, J. T. Melillo, T. Simmons, A. L. Ternay, *J. Am. Chem. Soc.* **1965**, *87*, 1958–1976.
[204] K. K. Andersen, *Tetrahedron Lett.* **1962**, *3*, 93–95.
[205] K. K. Andersen, W. Gaffield, N. E. Papanikolaou, J. W. Foley, R. I. Perkins, *J. Am. Chem. Soc.* **1964**, *86*, 5637–5646.
[206] C. Mioskowski, G. Solladie, *Tetrahedron* **1980**, *36*, 227–236.
[207] G. Liu, D. A. Cogan, J. A. Ellman, *J. Am. Chem. Soc.* **1997**, *119*, 9913–9914.
[208] D. J. Weix, J. A. Ellman, *Org. Lett.* **2003**, *5*, 1317–1320.
[209] P. Pitchen, E. Dunach, M. N. Deshmukh, H. B. Kagan, *J. Am. Chem. Soc.* **1984**, *106*, 8188–8193.
[210] F. D. Furia, G. Modena, R. Seraglia, *Synthesis* **1984**, *1984*, 325–326.

[211] H. Cotton, T. Elebring, M. Larsson, L. Li, H. Sörensen, S. von Unge, *Tetrahedron Asymmetry* **2000**, *11*, 3819–3825.
[212] A. Rauk, L. C. Allen, K. Mislow, *Angew. Chem. Int. Ed. Engl.* **1970**, *9*, 400–414.
[213] K. Mislow, *Trans. N. Y. Acad. Sci.* **1973**, *35*, 227–242.
[214] H. Marom, P. U. Biedermann, I. Agranat, *Chirality* **2007**, *19*, 559–569.
[215] D. R. Rayner, A. J. Gordon, K. Mislow, *J. Am. Chem. Soc.* **1968**, *90*, 4854–4860.
[216] G. Modena, D. Landini, F. Montanari, G. Scorrano, *J. Am. Chem. Soc.* **1970**, *92*, 7168–7174.
[217] K. Mislow, T. Simmons, J. T. Melillo, A. L. Ternay, *J. Am. Chem. Soc.* **1964**, *86*, 1452–1453.
[218] G. Modena, U. Quintily, G. Scorrano, *J. Am. Chem. Soc.* **1972**, *94*, 202–208.
[219] C. Aurisicchio, E. Baciocchi, M. F. Gerini, O. Lanzalunga, *Org. Lett.* **2007**, *9*, 1939–1942.
[220] S. Oae, N. Furukawa, M. Kise, W. Tagaki, Y. H. Khim, *Bull. Chem. Soc. Japan* **1966**, *39*, 2556.
[221] M. Axelrod, P. Bickart, J. Jacobus, M. M. Green, K. Mislow, *J. Am. Chem. Soc.* **1968**, *90*, 4835–4842.
[222] B. K. Ackerman, K. K. Andersen, I. Karup-Nielsen, N. B. Peynircioglu, S. A. Yeager, *J. Org. Chem.* **1974**, *39*, 964–968.
[223] H. F. Herbrandson, R. T. Dickerson, *J. Am. Chem. Soc.* **1959**, *81*, 4102–4106.
[224] N. Furukawa, T. Shibutani, H. Fujihara, *Tetrahedron Lett.* **1989**, *30*, 7091–7094.
[225] F. Rebière, O. Riant, L. Ricard, H. B. Kagan, *Angew. Chem. Int. Ed. Engl.* **1993**, *32*, 568–570.
[226] J. G. Tillett, *Chem. Rev.* **1976**, *76*, 747–772.
[227] M. Calligaris, O. Carugo, *Coord. Chem. Rev.* **1996**, *153*, 83–154.
[228] M. Calligaris, *Coord. Chem. Rev.* **2004**, *248*, 351–375.
[229] E. Alessio, *Chem. Rev.* **2004**, *104*, 4203–4242.
[230] P. B. Hitchcock, G. J. Rowlands, R. Parmar, *Chem. Commun.* **2005**, *0*, 4219–4221.
[231] G. J. Rowlands, *Org. Biomol. Chem.* **2008**, *6*, 1527–1534.
[232] J. Jacobus, K. Mislow, *J. Am. Chem. Soc.* **1967**, *89*, 5228–5234.
[233] T. Durst, M. J. LeBelle, R. V. den Elzen, K.-C. Tin, *Can. J. Chem.* **1974**, *52*, 761–766.
[234] N. Furukawa, S. Ogawa, K. Matsumura, H. Fujihara, *J. Org. Chem.* **1991**, *56*, 6341–6348.
[235] S. Akai, N. Morita, K. Iio, Y. Nakamura, Y. Kita, *Org. Lett.* **2000**, *2*, 2279–2282.
[236] R. J. Kloetzing, P. Knochel, *Tetrahedron Asymmetry* **2006**, *17*, 116–123.
[237] M. A. M. Capozzi, C. Cardellicchio, F. Naso, P. Tortorella, *J. Org. Chem.* **2000**, *65*, 2843–2846.
[238] C. B. Rauhut, L. Melzig, P. Knochel, *Org. Lett.* **2008**, *10*, 3891–3894.

Foreword to the experimental work

From now on the general bibliographic introduction of this work will make room for the experimental work and the following sections, drafted in English, will be excerpt from pubished and peer-reviewed scientific work. Each section will be focused on a specific reaction enabeling the control of axial chirality by means of atropodiastereoselective C-H activation, and will be introduced by a short and specific bibliographic part on the relevant subject, namely: the Fujiwara-Moritani reaction (chapter IV), acetoxlation by means of C-H activation (chapter V-B), iodination by means of C-H activation (chapter V-C) and arylation by means of C-H activation (chapter VII-C). Furthermore, the implementation of the afromentioned Fujiwara-Moritany reaction to the asymmetric formal synthesis of steganone (chapter VI), along with implementation of the afromentioned arylation reaction to the synthesis of original ligands (chapter VII-D) will be described.

Finally, a general experimental part (chapter VIII) will described the procedures used to build-up the enantiopur, at the sulfur atom, biaryl substrates used throughout this manuscript.

Fujiwara-Moritani reaction

IV. Fujiwara-Moritani reaction

A. Introduction

Fujiwara-Mortani (F-M) reaction (sometimes called oxidative Heck reaction) refers to a coupling between a non-prefunctionnalized aromatic and an olefin. Interestingly the Fujiwara-Moritani reaction was the first catalytic C-H activation reaction (Pd^{II}-Pd^{0} cycle) and was developed a few years before the Mizuroki-Heck reaction (insertion into a C-X bond, Pd^{0}-Pd^{II} catalytic cycle Figure IV-1).

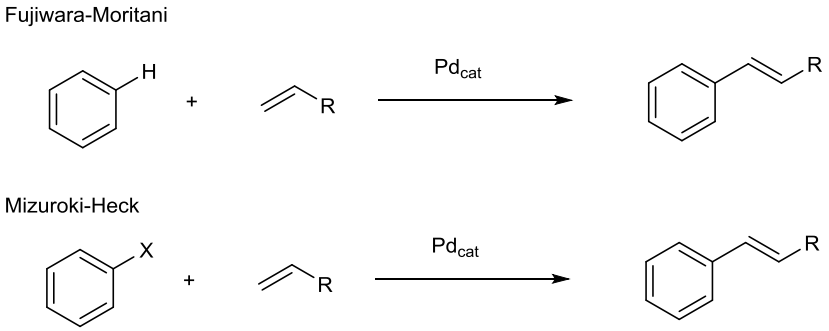

Figure IV-1 : Fujiwara-Moritani and Mizoriki-Heck reactions

However on should note that the Fujiwura-Moritani reaction was first developed with a stoichiometric amount of palladium. Indeed, when in 1967[239] the dimeric styrene palladium chloride was heated in benzene in presence of acetic acid, *trans*-stillbene was obtained in a yield of 26% (Figure IV-2a). Albeit low, it was a proof-of-concept example and in 1969[240] the catalytic transformation was achieved employing $Pd(OAc)_2$. It was also found that $Pd(OAc)_2$ could be used in catalytic amount as long as a terminal oxidant was present ($Cu(OAc)_2$ /oxygen system, Figure IV-2b).

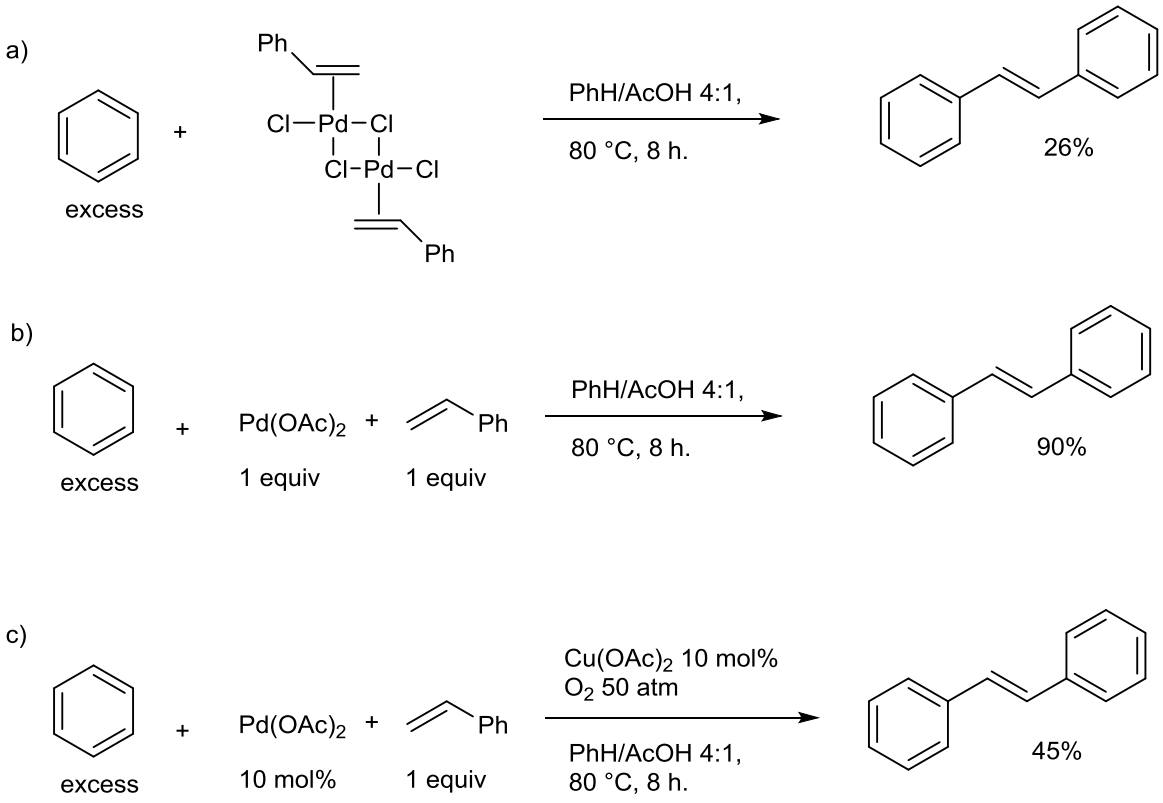

Figure IV-2 : original stoichiometric and catalytic Fujiwara-Moritani reaction

Several other oxidants have been evaluated[241] and have been found useful: a characteristic of the F-M reaction is the ease with which oxygen can be used as a terminal oxidant, as long as a catalytic capable co-oxidant ($Cu(OAc)_2$ or benzoquinone are popular co-oxidants) is present (Figure IV-3a). More recent examples have shown that the palladium re-oxidation can be mediated by a photoredox catalyst (Figure IV-3b).

Interestingly the electrophilic aromatic substitution mechanism is well evidenced by the reaction of substituted benzene substrates[242]: indeed electron-donating groups direct the functionalization *ortho* and predominantly *para*, whereas electron-withdrawing groups direct *meta*. Thus mixture of regioisomeric products are usually formed in the undirected Fujiwara-Moritani reaction with substituted benzenes (Figure IV-3c).

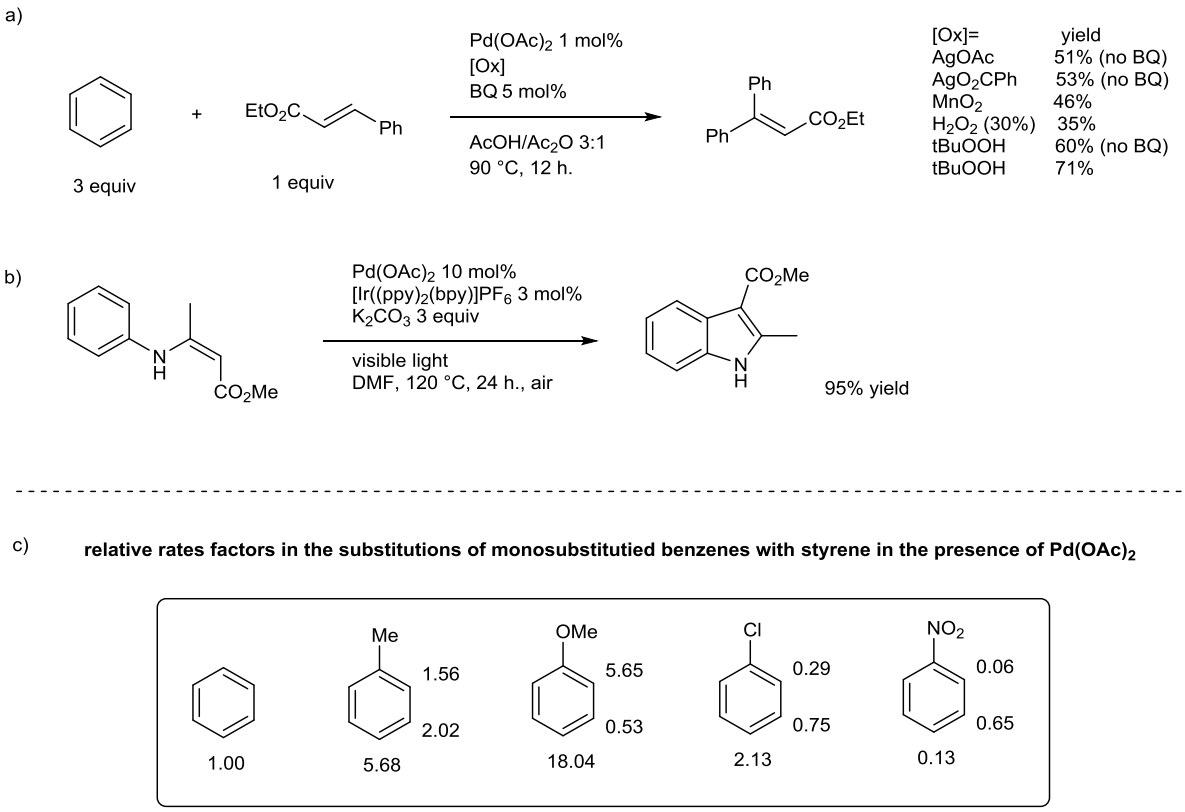

Figure IV-3 : scope of oxidants and regioselectivity of the Fujiwara-Moritani reaction

The scope of coupling partner is not restricted to hydrocarbons olefins, as alkenes substituted by polar group are also reactive. However alkenes substituted by electron-withdrawing groups react much more readily (when ethylene is reacted with benzene, *trans*-stillbene is formed as the major product[240] Figure IV-4a), and therefore acrylates established themselves as the more often used coupling partner (as it will be shown in the section concerning the directed Fujiwara-Moritani reaction), but acrylonitriles[243] and also vinylphosphonates[244] are popular. In addition, electron withdrawing alkenes deactivate the aromatic ring toward further functionalization, and the reaction usually stops cleanly at the mono-functionalization stage. Indeed one of the issues of the original Fujiwara-Moritani reaction is the need for a large excess of the aromatic coupling partner to avoid mixture of mono- and multiple addition products (Figure IV-2).

Mono-substituted olefins consistently yield *E*-alkene. Unsymmetrically di-substituted olefins often yield mixture of *E* and *Z* products, with the aryl adding to most electron-deficient carbon, whereas for tri-substituted olefins the aryl adds to the less-substituted carbon[245]. However the increase substitution of the olefin decreases its reactivity (Figure IV-4a and b).

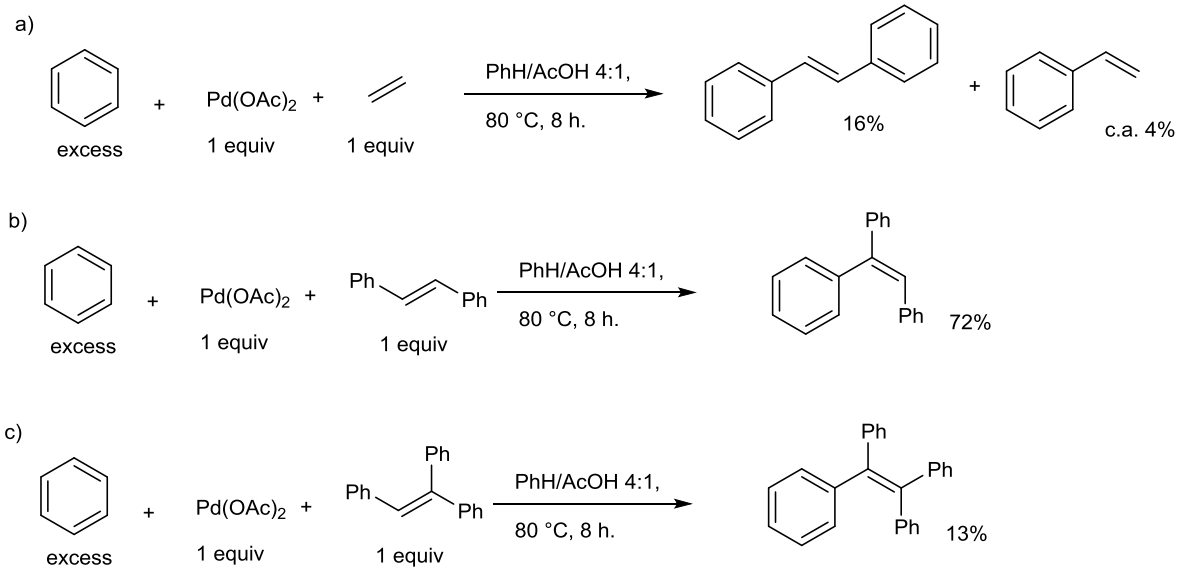

Figure IV-4 : scope of olefinics coupling partners

The accepted mechanism for the *undirected* reaction is as follow[246] : cationic Pd complex are though to react with aromatics by an electrophilic substitution mechanism to afford σ-arylpalladium complex (Figure IV-5a-A). Coordination of the olefin (Figure IV-5a-B) followed by 1,2-migratory insertion (Figure IV-5a-C), isomerization (Figure IV-5a-D) and β-H elimination (Figure IV-5a-E) afford the product along with palladium^0 which is then re-oxidized to start a new catalytic cycle (Figure IV-5a-F). Intermediate σ-arylpalladiam complex have been isolated with dialkylsulfides as stabilizing ligands[247] (Figure IV-5b).

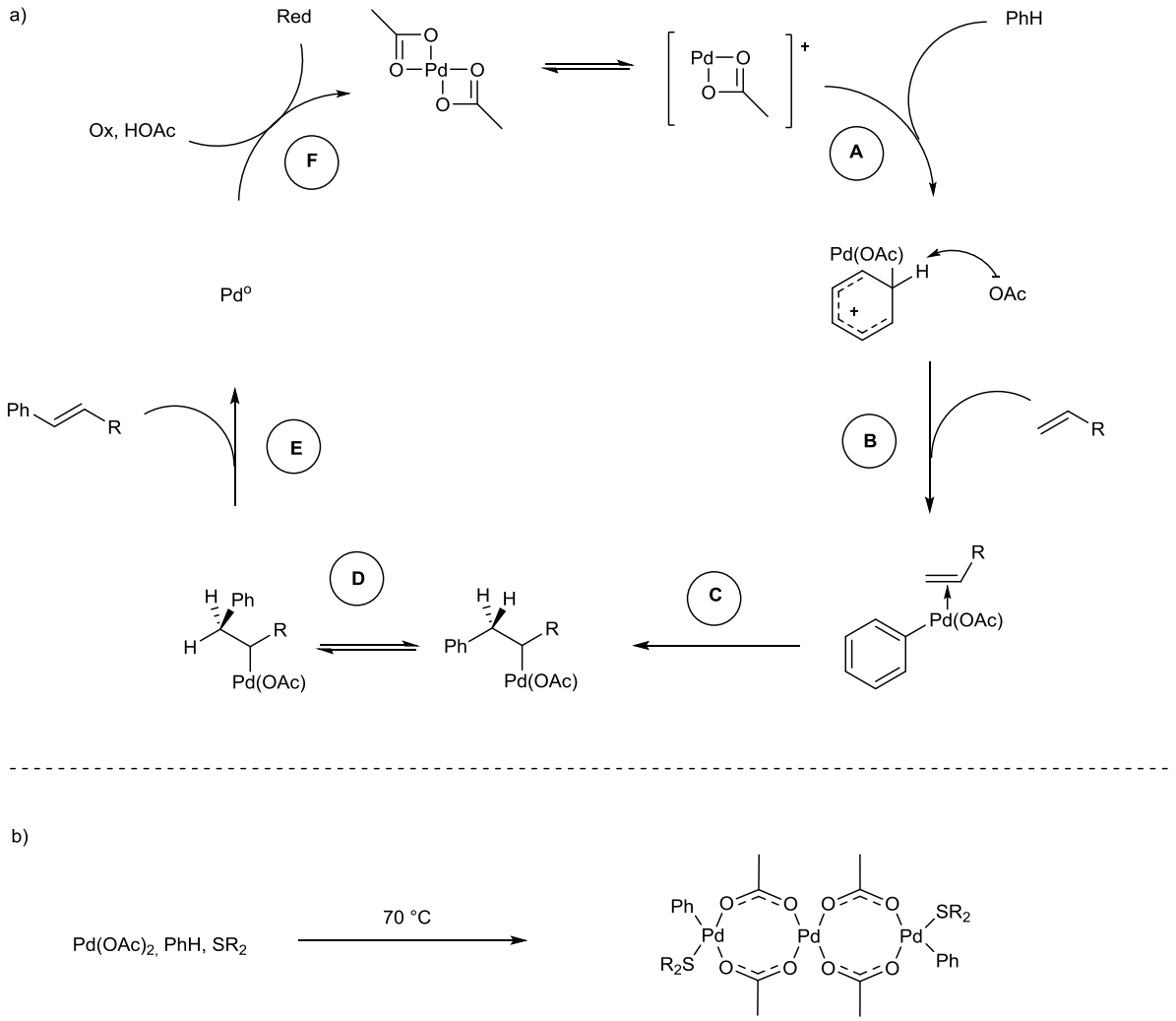

Figure IV-5 : mechanism of the Fuiiwara-Moritani reaction

This chemistry remained underdeveloped for few decades, as the regioselectivity issues hampered its synthetic utility towards the obtention of high value products. Thus, in 2002[248], the concept of directing (functional group carrying an heteroatom with a lone pair capable of pre-coordinating the palladium catalyst) was introduced as a way of controlling the regioselectivity (Figure IV-6a) : it was shown that acetanilide would cleanly be mono-functionalized *ortho* to the acetamide directing group (and to the least hindered position if a *meta* group is present) with good yields. Other examples of *directed* Fujiwara-Moritani reactions followed a few years later. Interestingly, because of the Pd^{II}-dominated catalytic cycle devoid of good σ-donor ligand, aryl bromide and even iodide are tolerated[249] (Figure IV-6b). Interestingly these first reports showed some characteristic data of directed Fujiwara-Moritani reactions : a rate determining C-H bond cleavage (as determined by kinetic isotope effect) and a higher reactivity for electron-rich substrates[248,249].

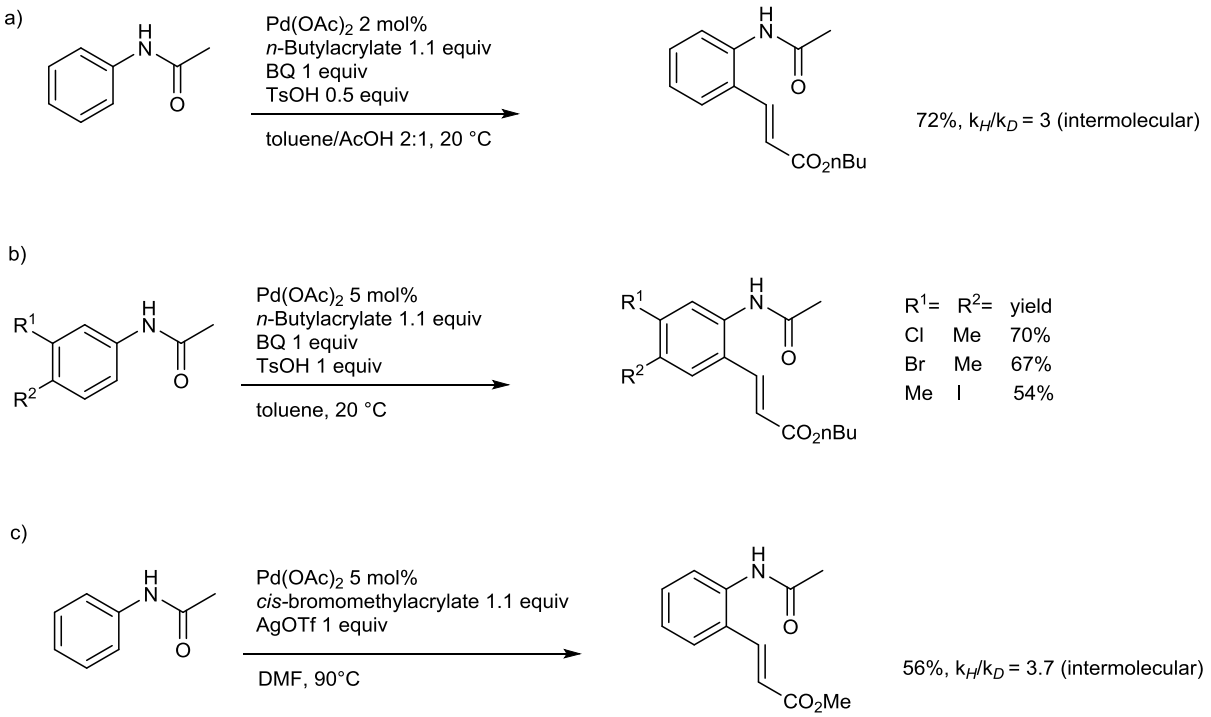

Figure IV-6 : example of directed Fujiwara-Moritani reaction

The following major advance probably resides in the use of σ-donor ligands (such as mono-protected amino acids MPAAs) on the palladium to enhance the rate and the regioselectivity of the rate-determining C-H activation step (Figure IV-7). The Yu group[250] first found out that MPAAs were able to significantly improve the regioselectivity of directed Fujiwara-Moritani olefination of 1,3,5-trisubstitued benzenes derivatives (Figure IV-7a). Furthermore, MPAAs enabled the use of then problematic electron deficient substrates[251] (and the use of molecular oxygen as a terminal oxidant Figure IV-7b). Mechanistic studies found out that the most efficient ligand was causing a switch in the rate-determining step (Figure IV-7c). Indeed without ligand a KIE of 6.1, indicating that C-H cleavage was the turnover-limiting step, was found. However when Ac-Ile-OH was used as a ligand, a KIE of 1.7 was measured. As this value was determined by intermolecular competition experiments (and not by rates comparison) the authors concluded that the C-H cleavage was not the turnover-limiting step, and that the turnover-limiting step should occur after the C-H activation event in the catalytic cycle[251] (Figure IV-7c).

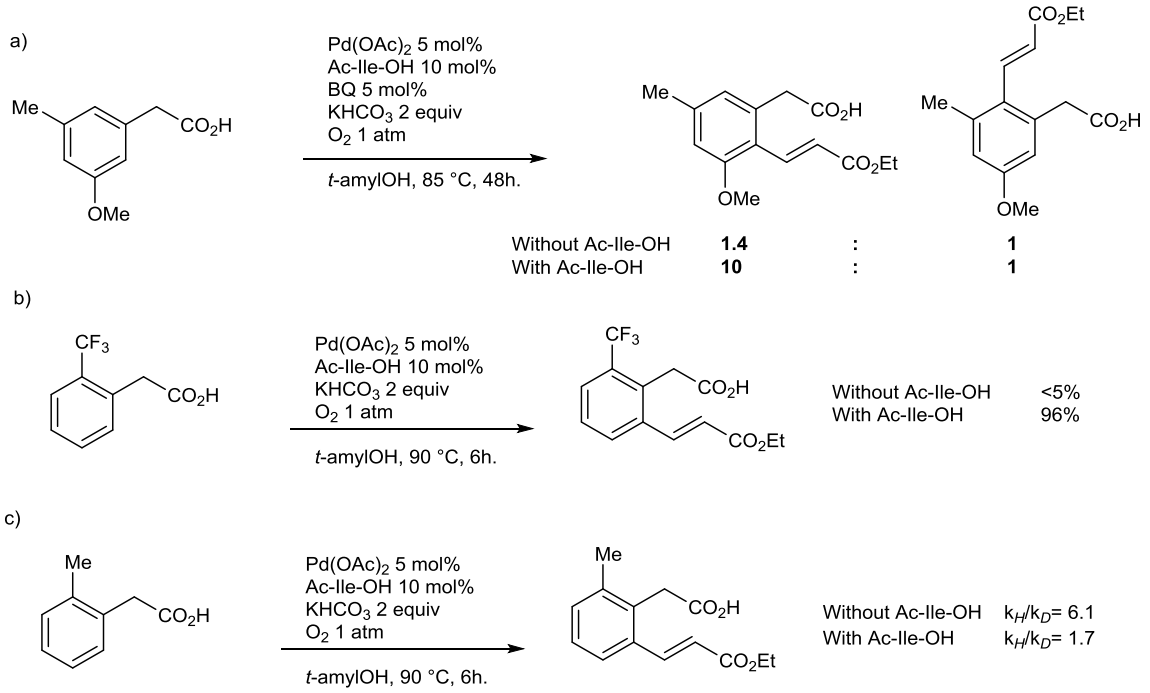

Figure IV-7 : use of MPAAs

Over the last decade hundreds of articles dealing with the F-M reaction were published. Not only different catalysts were used (Pd, Rh, Ru), but also a myriad of directing groups. Recently, the concept of directing groups has been extended to be able to functionalize not only C-H bonds *ortho* to the DG, but also *meta* to the DG : in this concept, the DG is used as an handle to support a template which carries another DG and allows *meta* selective functionnalization[252] (Figure IV-8c). Perhaps the culmination of this strategy resides in the remote supramolecular-directed *meta* C-H functionalization of 3-phenylpyridine substrate by the Yu group in 2017[253] (Figure IV-8b).

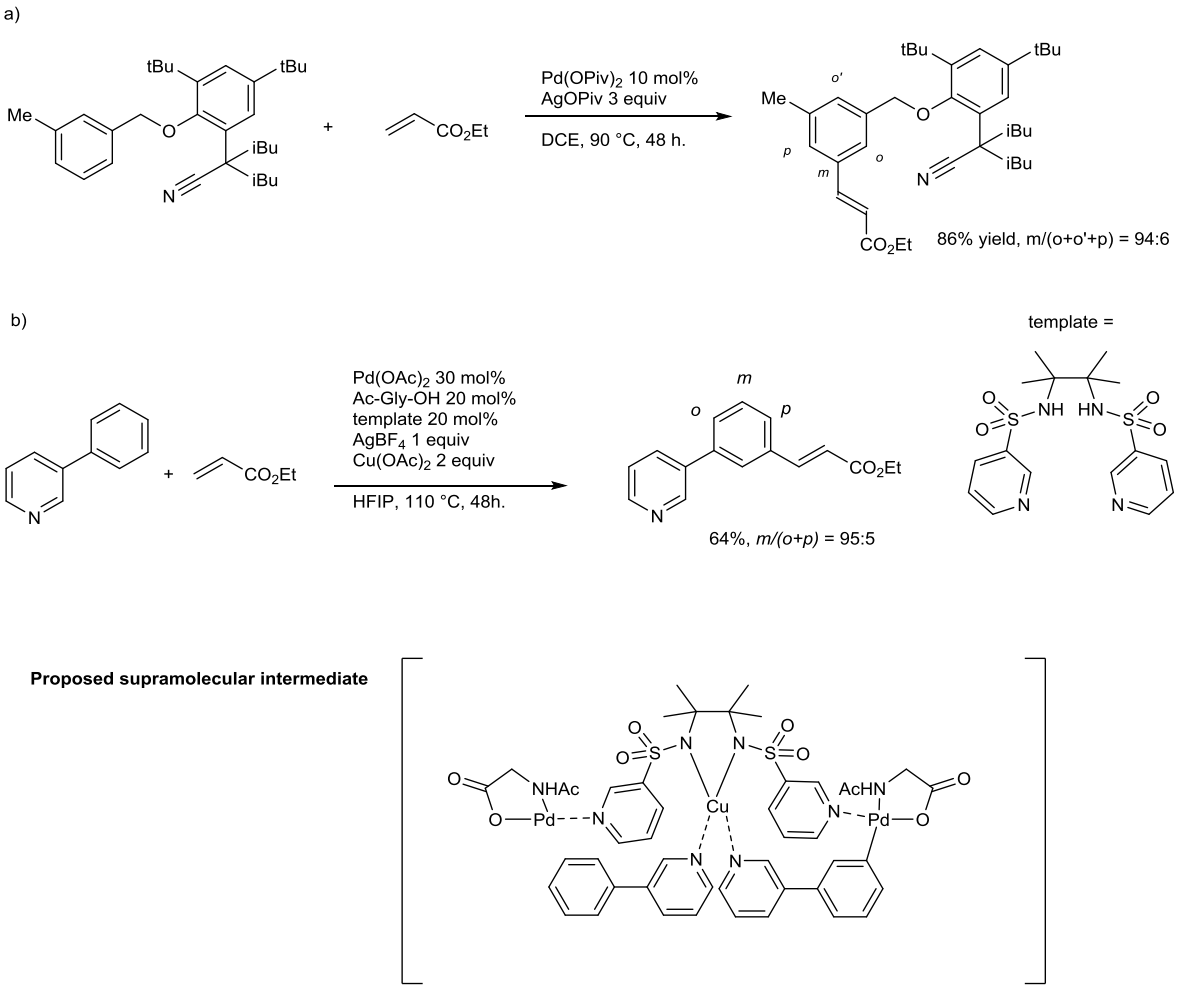

Figure IV-8 : *meta* selective F-M reactions

Concerning the research more closely related to the topic of this thesis, i.e. the control of axial chirality *via* atroposelective C-H activation of biaryls, the seminal work concerning the application of the Fujiwara-Moritani reaction came in 2013 by Wesch, Leroux in the Colobert group (a mere 13 years after the pioneer work of Murai[92]), and showcased a new strategy. Indeed biphenyls bearing a coordinating group *ortho* to the biaryl axis have been known to underwent Fujiwara-Moritani reaction cleanly at the *ortho*' position in two consecutive reports by the Miura group[254,255] (Figure IV-9).

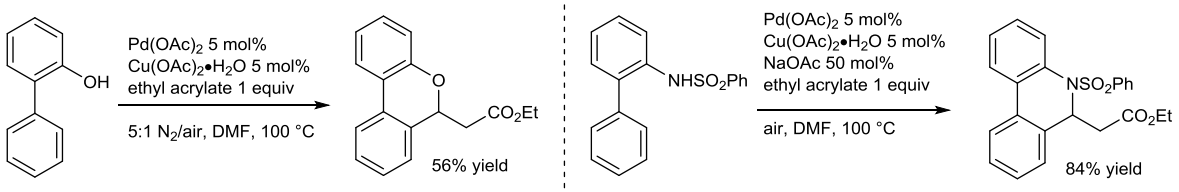

Figure IV-9 : F-M reactions on biaryls

Thus, this functionalization might be used to raise the rotational barrier of an existing non-atropisomeric biaryl by introducing a new substituent *ortho* to the chiral axis and thus to form an atropisomeric product. In this strategy, already chiral or prochiral biaryls could be resolved by kinetic resolution (KR) or dynamic kinetic resolution (DKR) into optically pure products, albeit with the proper source of chiral induction. Accordingly the major advance brought by the Colobert group[256] was to use an en-

antiopur sulfoxyde as the directing group (Figure IV-10). Indeed sulfoxydes, with their S-centered chirality *and* an available lone-pair on sulfur might be expected to play the role of both a directing group *and* a chirality inductor. The chirality element would thus be in close proximity to the catalyst, and high asymmetric induction (considering the difference of steric bulk of an oxygen compared to a *para*-tolyl substituent) would be expected.

However, if the expected functionalization did occur with very good to moderate yields (electron deficient substrates are clearly more challenging), the rather moderate diastereselectivites observed (Figure IV-10), the large excess of silver salt along with the relative high reaction temperature made the method less than ideal. Nevertheless, it was an important proof-of-concept example and a work to be built upon.(We refer the reader to the relevant part of the general introduction to familiarize himself with the state of asymmetric atroposelective C-H reactions as of 2016).

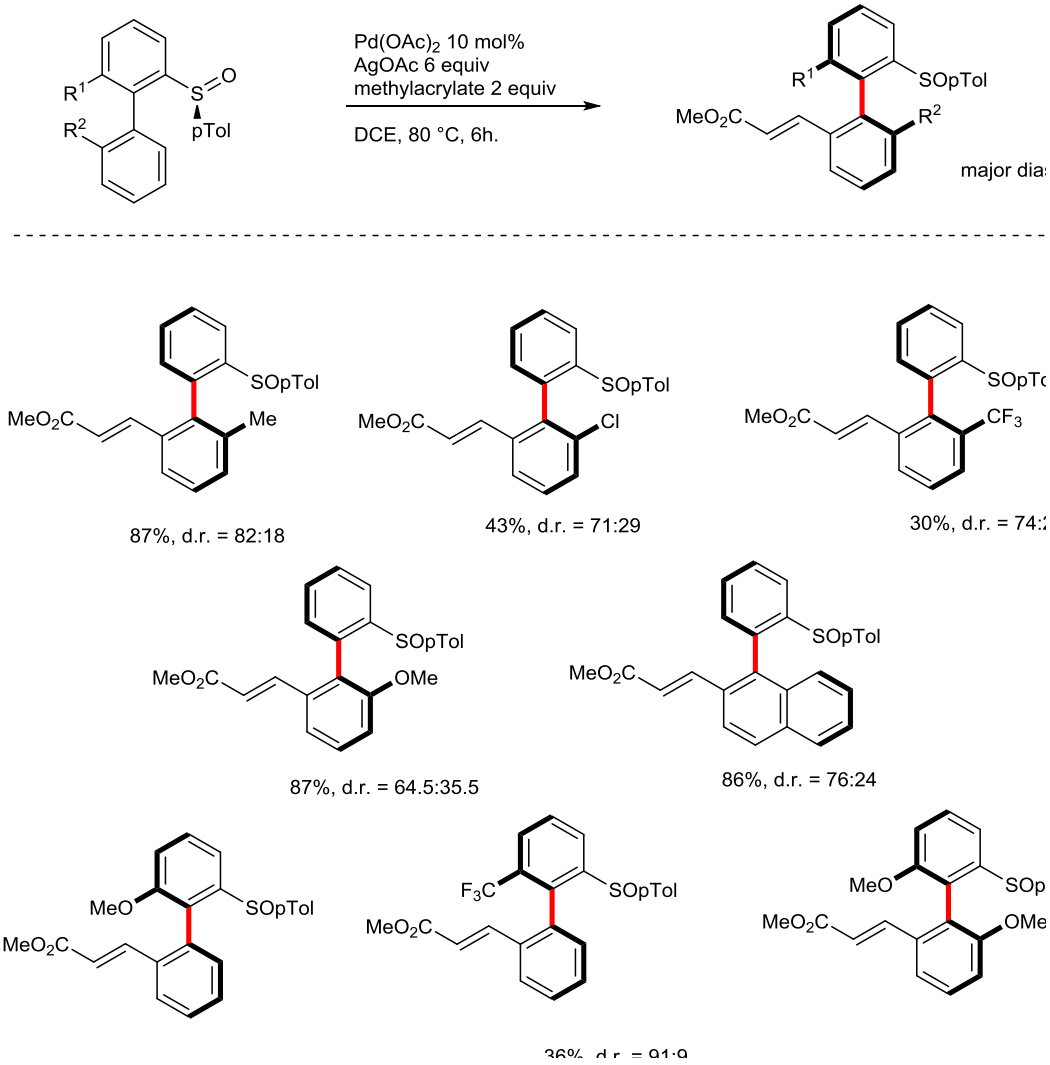

Figure IV-10 : seminal atroposelective F-M reaction

Consequently further research continued to ameliorate the catalytic system, and the major breakthrough was achieved by the dr. Geoffrey Schwertz in the Colobert group in 2014 by discovering the unique and intriguing role of 1,1,1,3,3,3-

hexafluoropropanol (HFIP) solvent in the atropodiastereoselective sulfoxyde directed C-C coupling. Notably, this polyfluorinated alcohol stood out recently as an optimal solvent for several challenging C-H activation reactions: its ready availability, affordable cost, easy removal have made it a staple amongst directed C-H activation reactions.

B. Results and Discussion

The following was realized in collaboration with the Dr. Geoffrey Schwertz

Indeed fluorinated alcohols have focused increasing attention of organic chemists as unusual medium to perform various transformations including both transition metal and organo-catalyzed reactions[257–259]. It has been observed that due to their unique properties such as high polarity (1.068 E_N^T) but moderate dielectric constant (ε_T = 17.8) and polarisibility (π = 0.65), high acidity (pKa = 9.3 (H_2O); 18.2 (DMSO)), extremely good hydrogen bond donor (α = 1.96) but conversely extremely weak hydrogen bond acceptor (β = 0) and low nucleophilicity (N = -4.23)[260,261], these solvents may exert an unexpected effect on the reaction outcome, modifying not only the reactivity of a catalytic system, but also its regio- and stereoselectivity. Thus, HFIP can be viewed as one of the few solvents that are at the same time an hydrogen bond donor but are not an hydrogen bond acceptor, conferring a high Lewis acidity to the reaction medium (being a non-coordinating solvent). This dual comportment toward hydrogen bond capability is expected to create an environment devoid of hydrogen bond network, in opposition to most hydroxyl-functional group containing solvents.

Accordingly, HFIP has been recently employed in several C-H activation reactions clearly outcompeting other organic solvents[252,253,262–264]. Intrigued by the unique features of HFIP, we performed our previously developed sulfoxyde-directed oxidative olefination in this polyfluorinated alcohol. Gratifyingly, the use of HFIP instead of DCE when keeping other reaction parameters constant, enabled smooth functionalization of our standard substrate 1a delivering 2a in 82% yield and, remarkably, as a sole atropisomer (Table IV-1, entry 2). Encouraged by this solvent-improved chiral induction we pursued the optimization. Surprisingly, reduction of the excess of the silver oxidant allowed further enhancement of the efficiency of this transformation, while conserving the total diastereoselectivity. The optimal 93% yield of 2a was obtained using only 2 equivalents of AgOAc (Table IV-1, entry 4) and merely a trace amount of 2a was generated in absence of this terminal oxidant (Table IV-1, entry 6). Besides, a lower catalyst loading (5 mol% of $Pd(OAc)_2$) resulted in a slightly decreased reaction yield (77%) (Table IV-1, entry 7). Importantly, these modified catalytic system turned out to be efficient under significantly milder reaction conditions; the coupling could be performed at room temperature but a longer reaction time was needed to complete this transformation. Finally, 2a was obtained in quantitative yield and with total atroposelection when using HFIP solvent and 10 mol% of $Pd(OAc)_2$ catalyst in combina-

tion with 2 equivalents of AgOAc, at room temperature and after 30 h of reaction (Table IV-1, entry 8).

Table IV-1 : Optimization of the oxidative olefination of 1a.

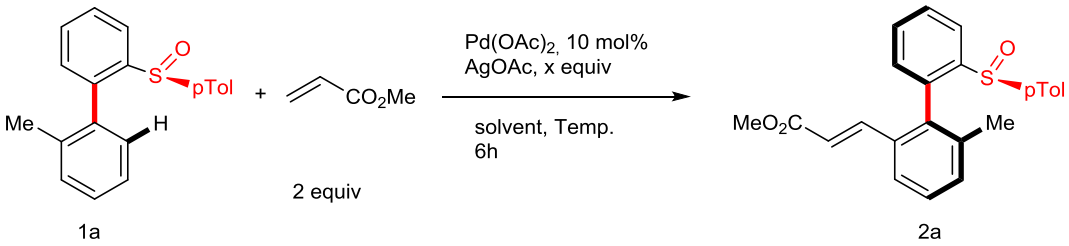

Entry	Solvent	AgOAc [x equiv]	Temp. [°C]	Yield [%][a]	dr [%][b]
1	DCE	6	80	87	82:18
2	HFIP	6	80	82	> 98:2
3	HFIP	4	80	88	> 98:2
4	HFIP	2	80	93	> 98:2
6	HFIP	-	80	8	> 98:2
7[c]	HFIP	2	80	77	> 98:2
8[d]	HFIP	2	RT	98	> 98:2

[a] Yield of isolated product; [b] dr of crude mixture analysed by ^{1}H NMR; [c] 5 mol% of $Pd(OAc)_2$; [d] 30 h.

With the re-optimized reaction conditions in hand, the scope of this transformation was explored (Figure IV-11). We were pleased to observe that the beneficial effect of HFIP in this stereoselective C-C coupling is general as now the reaction proceeded in quantitative yield and with excellent atropo-diastereoselectivity for an array of 2'-substituted biaryl sulfoxydes (Figure IV-11; Cond A: previously reported conditions, Cond B: the newly re-optimized catalytic system). Substrates bearing both electron donating (Figure IV-11, **1a-b**) and electron-withdrawing (Figure IV-11, **1d-g**) substituents could be functionalized smoothly delivering the desired atropopure scaffolds. Noteworthy, under the newly optimized reaction conditions, CF_3-substitued **1d** substrate could be efficiently functionalized delivering atropopure **2d** in 80% yield whereas the reaction conducted in DCE was extremely sluggish (30% yield and 74:26 d.r.). When **1g**, bearing two possible coordinating groups, i.e. a sulfoxyde and an ester, was submitted to the reaction conditions, the sulfoxyde-directed C-H activation occurred selectively at the anticipated 6'-position. Furthermore, the reaction outcome for a proaxially chiral 6-substituted biaryl was investigated; the expected **2h** product was obtained as sole atropisomer and in quantitative yield, showcasing that a double alkenylation is strongly disfavored. Finally, our attention turned towards *ortho*-trisubstituted substrates **1i-n**. **1i-j**, bearing not bulky substituents afforded **2i-j** in excellent yield and good diastereoselectivity. These results are of particular importance as the asymmetric synthesis of tetrasubstituted axially chiral scaffolds is a great synthetic challenge. Unfortunately, an increased steric demand around the biaryl linkage

has a detrimental effect on atroposelectivity; a modest diastereoselectivity was observed in the case of more hindered products **2k-n**. An increase of the reaction temperature to 80 °C generally does not enable to improve the chiral induction; **2l** and **2n** were obtained with the same diastereomeric ration. Only in the case of **2i** the stereocontrol could be slightly enhanced to reach 95:5 d.r. when performing the reaction under refluxing conditions.

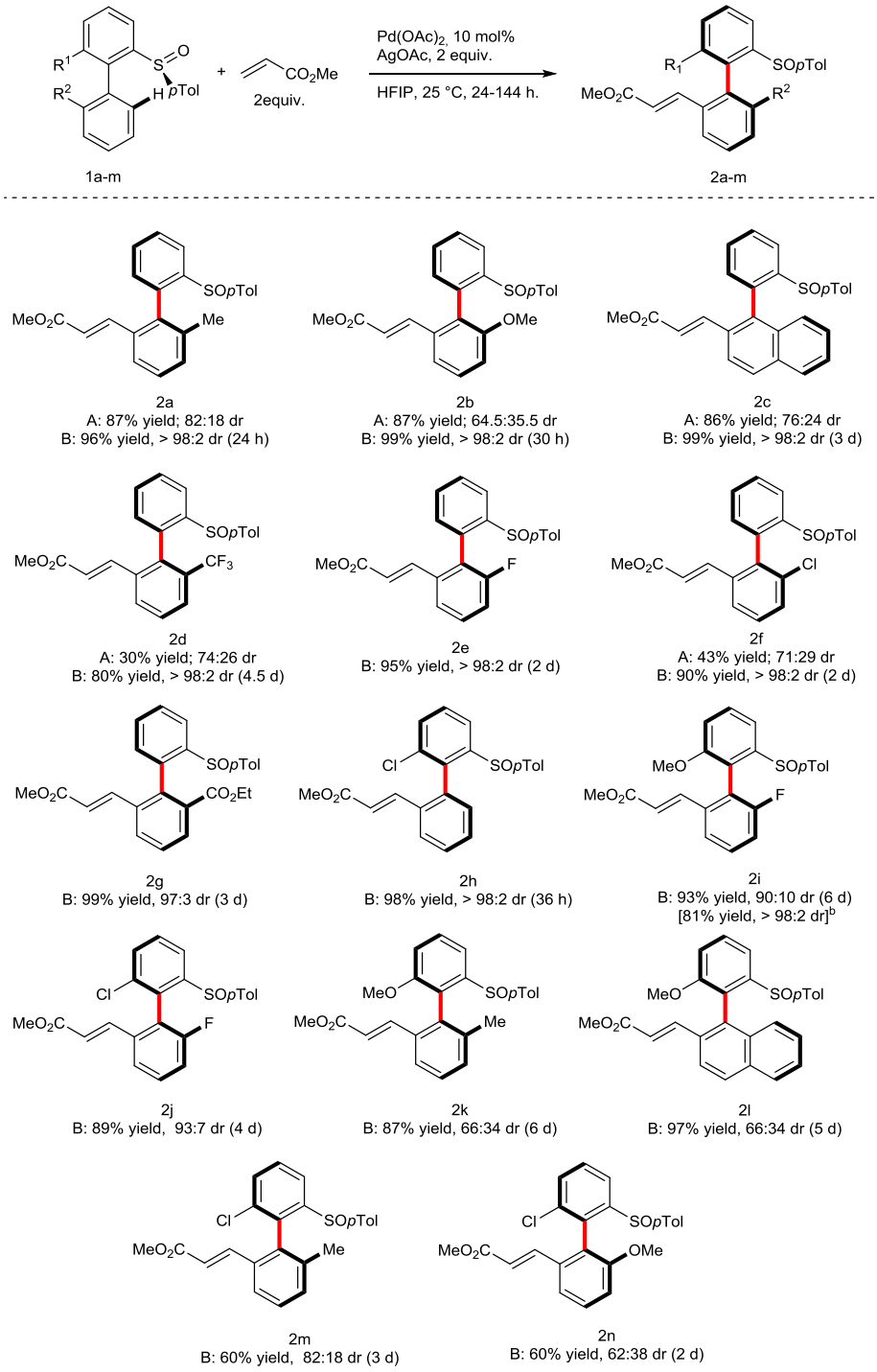

Figure IV-11 : scope of biphenylsulfoxyde partners with acrylate derivatives. [a] Isolated yield; dr determined by ^{1}H NMR; [b] After recristallization

The structure of **2c** was confirmed by X-ray diffraction analysis and the absolute (*SaR*) configuration was attributed (Figure IV-12 : X-Ray structure of **(*SaR*)-2c** and proposed favoured and unfavoured metallacyclic intermediates). This configuration of **2c** is coherent with the presumed favored palladacylic intermediate in which the steric hindrance generated by the *p*Tol-substituent of the sulfoxyde and the Pd-atom coordination sphere is minimized.

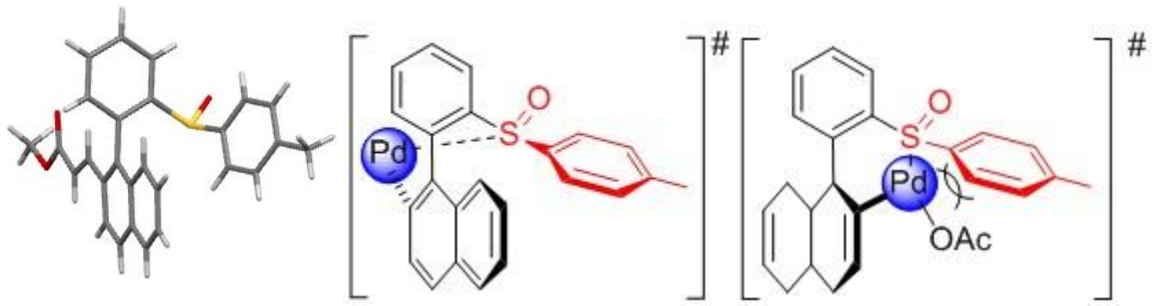

Figure IV-12 : X-Ray structure of (*SaR*)-2c and proposed favoured and unfavoured metallacyclic intermediates

Encouraged by the excellent results obtained with methyl acrylate, in term of both yield and atroposelectivity, we then focused on aplying other, less activated coupling partners (Figure IV-13). We were pleased to find that **1a**, when reacted with styrene at 80 °C, afforded desired **3a** as sole atropisomer but in significantly decreased yield (41%). The structure of **3a** was confirmed by X-Ray diffraction analysis and its SaR configuration was evidenced. Subsequently, the scope of this transformation with regard to the styrene coupling partner was examined. Introduction of an electron withdrawing substituent on the para position of the aromatic ring boosts the reactivity and the corresponding **3b-3e** were afforded in totally atroposelective manner. The best 80% yield and diastereomeric ratio superior to 98:2 were obtained while using 2,3,4,5,6-pentafluorostyrene. Unhopefuly, the reactivity was totally shut down when using the less reactive electron-rich styrene derivative such as 4-methoxystyrene. In addition, extensive polymerization side-reaction occurred with these electron-rich olefins in HFIP. Notably, this reaction tolerates well different substitution patterns of the biaryl substrate as **3f** and proaxially chiral **3g** were isolated in comparable yields and with excellent diastereoselectivity.

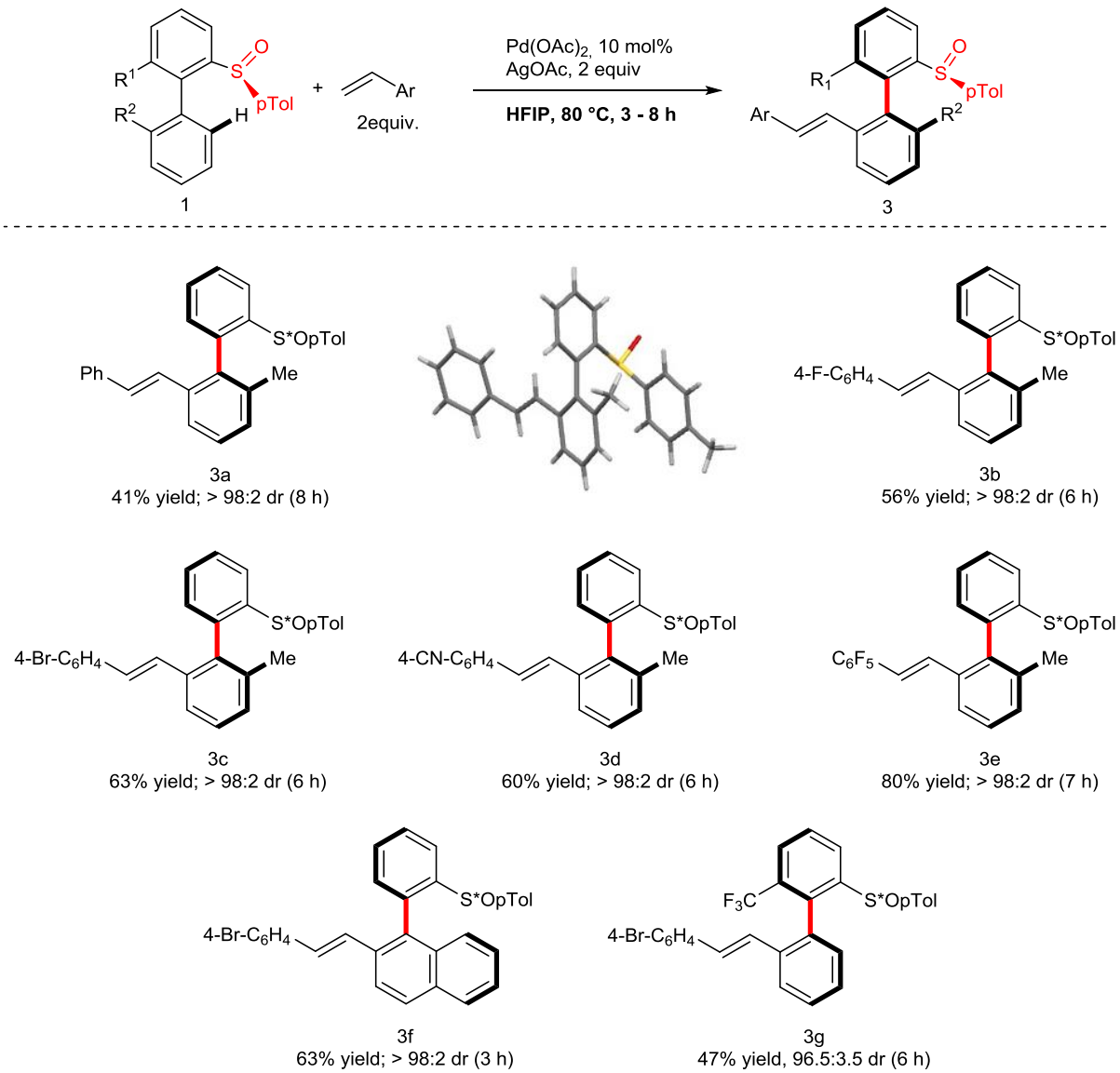

Figure IV-13 : scope of biphenylsulfoxyde partners with styrenes.[a] Isolated yield; dr determined by ^{1}H NMR.

Moreover, we were pleased to find that an atropopure biaryl product bearing a 1,1-disubstituted olefin moiety could also be synthesized Figure IV-14). Indeed, when diethyl 2-(ethoxymethyl)malonate was used as a precursor for diethyl 2-methylenemalonate, the reaction proceeded smoothly and the desired product 4 was generated in 89% yield and with an excellent chiral induction (dr = 97:3).

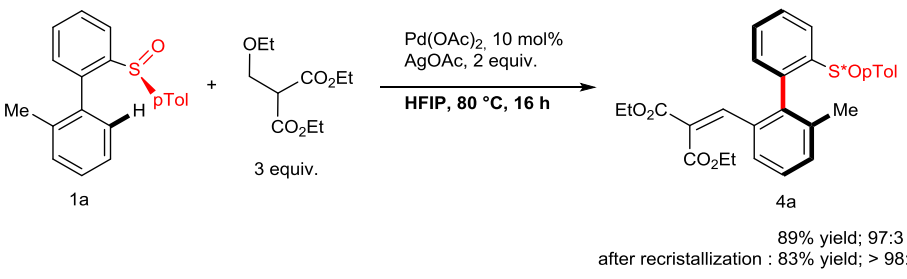

Figure IV-14 : synthesis of atropopure biaryl bearing a 1,1-disubstituted olefin moiety.

The results obtained for this oxidative Heck reaction clearly show the intriguing superiority of the catalytic system implying HFIP medium. Indeed, not only reactivity, but even more surprisingly, atroposelectivity could be drastically improved using this extremely polar, fluorinated solvent. We engaged therefore experimental efforts to shed some light on this particular feature of our catalytic system.

Firstly, in order to prove the unique reactivity of HFIP solvent, the standard olefination reaction of 1a with methyl acrylate was conducted in several other mediums (Table 2). Small scale solvent screening revealed that any coupling occurred when the non-fluorinated HFIP-congener, ie. *i*-PrOH was used as solvent, suggesting that higher polarity and/or stronger acidity induced by a presence of the fluorine atom in HFIP are crucial (Table 2, entry 1). Also AcOH, DCE and $CHCl_3$ were totally inefficient in this reaction (Table 2, entry 2-4). Then solvent mixtures were tested. No desired product was obtained when HFIP was added as co-solvent to *i*-PrOH (9:1 v/v mixture) or in DCE/AcOH co-solvents mixture (Table 2, entry 5, 7). Finally, reactivity could be restored in DCE/HFIP 9:1 mixture, although longer reaction time was required to complete this transformation (Table 2, entry 6). This spectacular effect prompted us to conduct a quantitative study of this "HFIP effect": thus different mixtures of DCE/HFIP were prepared (from 1 equivalent of HFIP relative to 1a to 20 equivalents, while keeping the concentration constant) and the conversion was monitored after 16 hours. Amazingly, it was shown that the addition of one equivalent of HFIP was enough to promote the previously inoperative transformation. Larger amount of HFIP resulted in an improve conversion but no linear correlation could be found. Finally, a comparable reactivity between DCE/HFIP co-solvents mixture and HFIP medium was observed when using at least 20 equivalents of HFIP compared to **1a**. This study clearly highlights the unique properties of HFIP solvent which cannot be attributed directly to its acidic character or its polarity. Moreover, the binary effect observed with one equivalent of HFIP *versus* none equivalent of HFIP (reaction *vs* no reaction) cannot be attributed to a mere solvent effect: at this low a concentration, this is more likely a catalytic effect, i.e. HFIP is certainly involved in the turnover-limiting step of the catalytic cycle.

Table IV-2 : Screening of the solvents for the oxidative olefination of 1a.

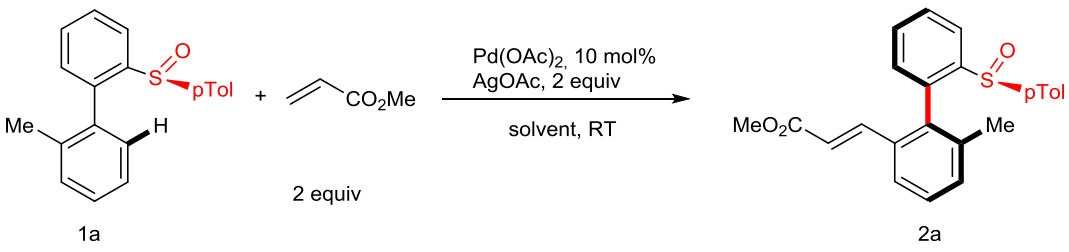

Entry	Solvent	E_N^T	α	pKa (H_2O)	Time	Conv. (%)[a]
1	*i*PrOH	0.546	0.76	16.5	3 d	0

2	AcOH	0.648	1.12	4.76	3 d	0
3	DCE	0.327	/	/	2 d	0
4	$CHCl_3$	0.259	0.2	/	3 d	< 5
5	*i*PrOH / HFIP (9:1 v/v)				3 d	0
6	DCE / HFIP (9:1 v/v)				5 d	98
7	DCE / AcOH (9:1 v/v)				2 d	0
8	DCE / HFIP (1 equiv) (47:1 v/v)				16 h	5
9	DCE / HFIP (5 equiv) (8.5:1 v/v)				16 h	10
10	DCE / HFIP (10 equiv) (3.2 :1 v/v)				16 h	30
11	DCE / HFIP (20 equiv) (1.4 :1 v/v)				16 h	46
12	HFIP	1.068	1.96	9.3	16 h	44

[a] conv. determined by ^{1}H NMR

Having demonstrated that HFIP is an exceptional solvent for our catalytic system, we have focused on the origin of the remarkable stereoselectivity improvement. Firstly, the influence of the temperature was studied. Indeed, as the olefination with acrylate occurs smoothly in HFIP at room temperature, this decrease of the reaction temperature, compared to 80°C in DCE, could account for the superior chiral induction. We have therefore performed coupling of biaryls **1a-d** with methyl acrylate in HFIP at 80°C (Figure IV-15). The corresponding products **2a-d** were isolated after only 6h. in respectively 93, 98, 85 and 96% yield. Importantly, this direct functionalization at 80°C occurred with no significant erosion of the atroposelection thus proving that the reaction temperature has only a minor impact on the chiral induction.

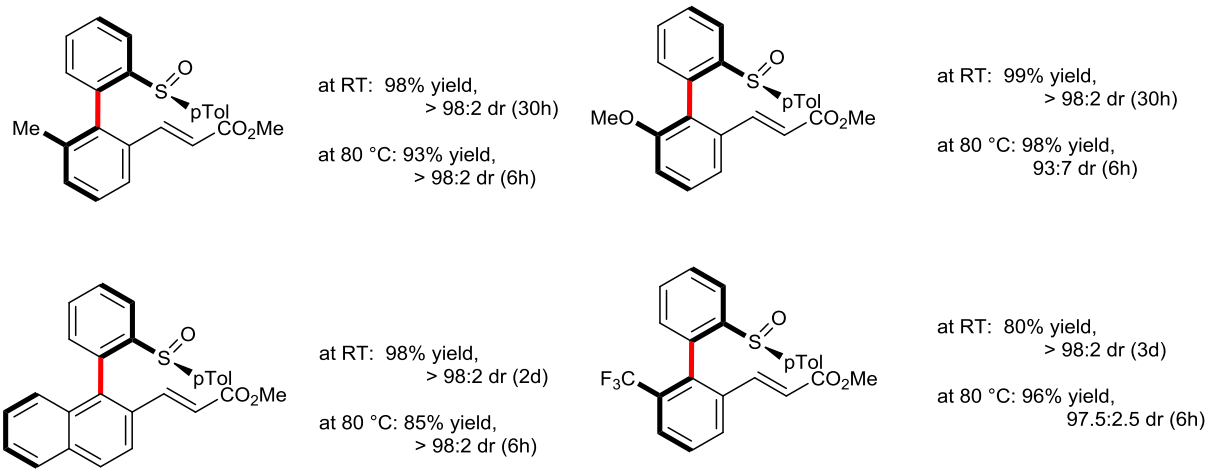

Figure IV-15 : Influence of the reaction temperature on the diastereoselectivity of the olefination reaction using HFIP as the solvent.

Subsequently, as HFIP is an excellent hydrogen bond donor[265–267], we surmised that this acidic fluorinated molecule might be involved in hydrogen bonding with the sulfoxyde moiety. Indeed, it is well known in the literature that sulfoxyde group is prompt to undergo hydrogen bonding with various solvents like alcohols, water, acetonitrile and carboxylic acids[268,269]. Such weak bonding results in lengthening the S=O bond and hence it can be reasonably expected that the coordinating properties of our directing group would be altered, directly impacting the reactivity of the substrate towards the C-H activation step. Consequently ^{1}H NMR studies have been undertaken (Figure IV-16). The titration of **1a** in $CDCl_3$ by HFIP shows a very strong downfield shift (from 2.810 ppm to 5.283 ppm; $\Delta\delta$ = 2.473 ppm) of the alcoholic proton of HFIP when present in a substoichiometric amount (0.4 equivalent) compared to pure HFIP in $CDCl_3$. In addition, the gradual upfield shift when the proportion of HFIP is increased is clearly indicative of an hydrogen bond involving the *H*-OCH$(CF_3)_2$[270]. Conversely, the *inverse* effect can be seen on the chemical shift of the proton *ortho* to the sulfoxyde, i.e. when the amount of HFIP relative to **1a** is increased, an upfield shift is observed (from 8.649 ppm to 8.487 ppm for the major atropisomer). In addition, when HFIP is present in large excess compare to **1a** (~36 equivalents), a significant upfield shift of the signal of the proton ortho to the sulfoxyde is evidenced 0.518 ppm for the major atropisomer), suggesting that the electron-withdrawing character of the sulfoxyde moiety decreases upon this hydrogen bonding.

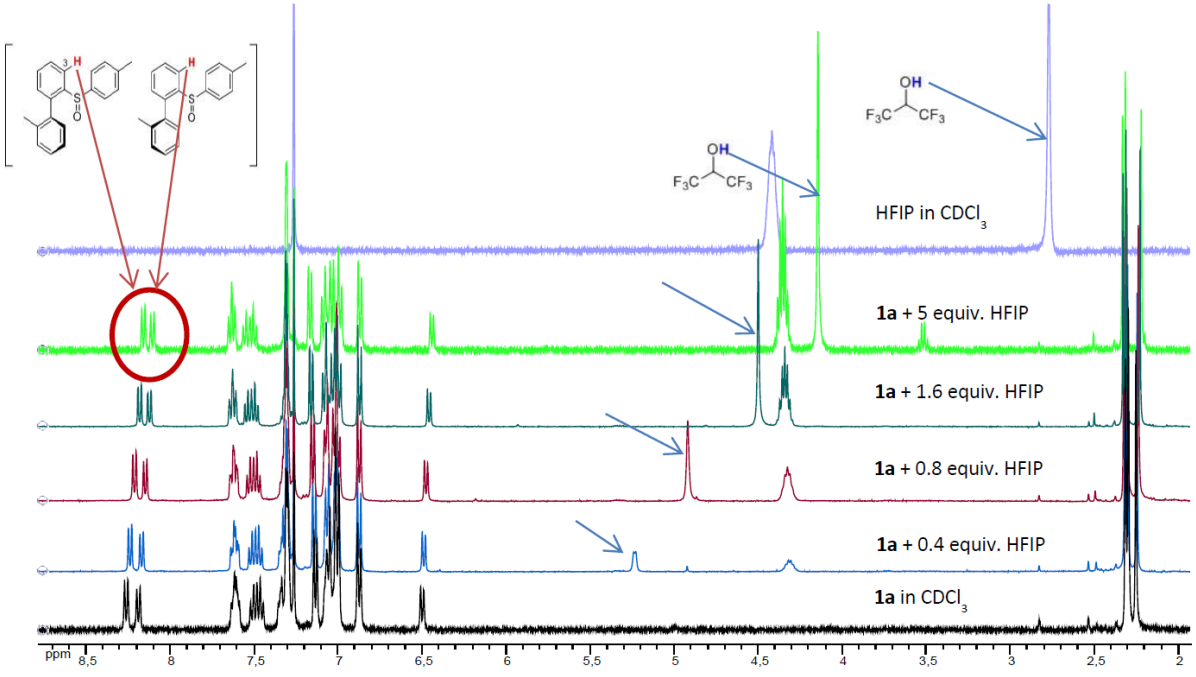

Figure IV-16 : ^{1}H NMR titration of 1a by HFIP in $CDCl_3$

Furthermore, the equilibrium constant for the formation of the H-bonded adduct between **1a** and HFIP was calculated by processing the NMR data[271,272]. Equilibrium constants K_{eq} of 18.5 ± 4.7 M^{-1} and 23.5 ± 9.8 M^{-1} for major and minor atropodiastereomer of **1a** have been determined clearly indicating a strong interaction between

H-bond donor HFIP and the H-bond acceptor sulfoxyde. These values are of the same order of magnitude as the ones reported in the related studies concerning H-bond complexes between various sulfoxydes and alcohols[273,274].

In addition, the expected complexation between HFIP and the sulfoxyde moiety was investigated by IR-analysis[275] (Figure IV-17). Initially, the stretching of the free O-H bond of HFIP absorbs infrared radiation sharply at a frequency of 3542.8 cm^{-1} while, upon an addition of **2c**, its absorption is shifted to lower frequencies and flattened to give a broad bond, characteristic for O-H bond involved in hydrogen bonding. Besides, the S=O moiety of **2c**, characterized by a stretching bond at 1038.6 cm^{-1}, when complexed with HFIP shows two absorption maximum at 1022.7 and 1011.1 cm^{-1}. The multiplicity of the S=O stretching frequency could be attributed either to the presence of two possible conformers (rotational isomerism about the S-C bond) or to Fermi resonance (an overtone of some other vibration which occurs near one-half of the S-O vibration frequency[276,277]).

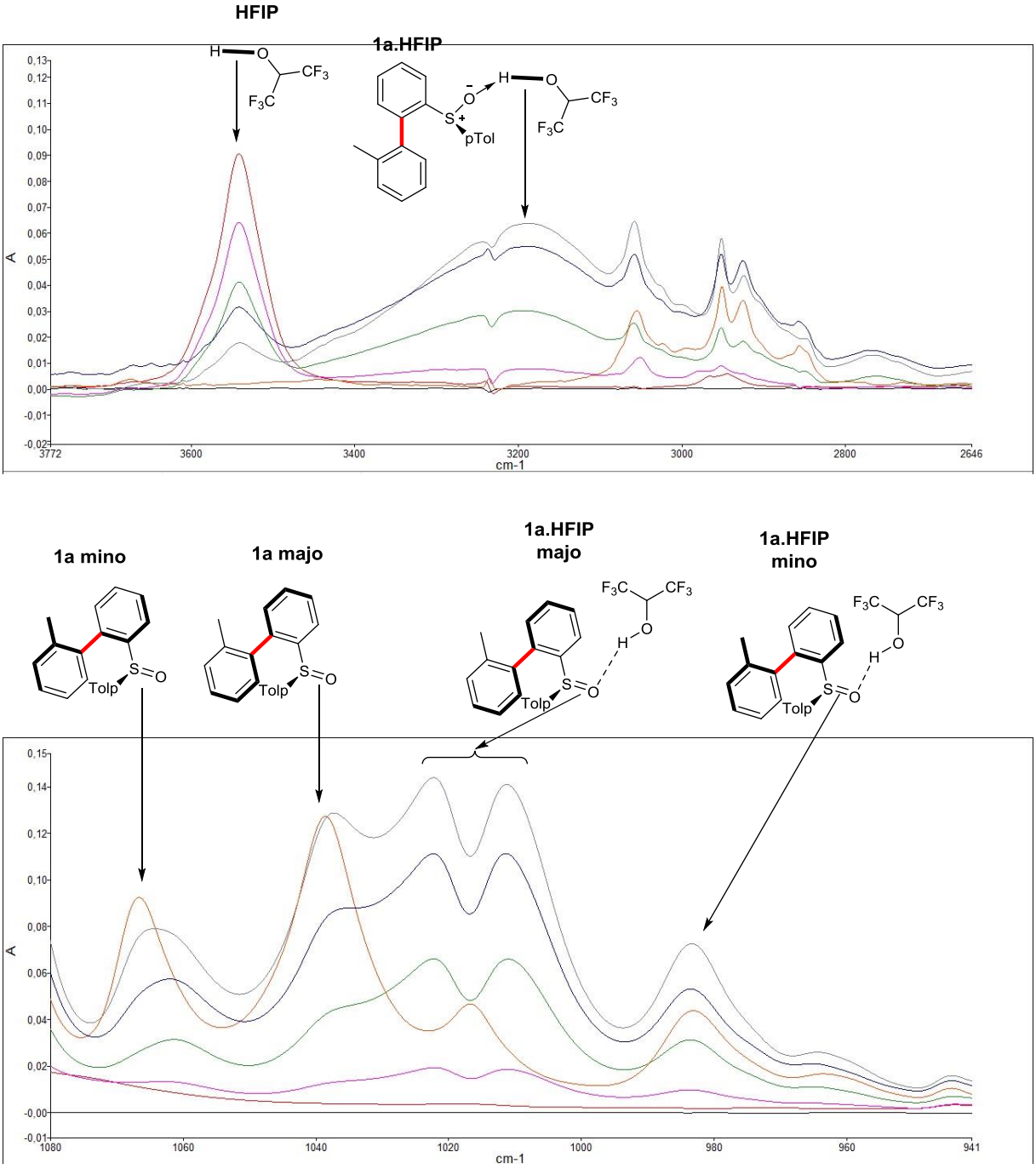

Figure IV-17 : IR study of hydrogen bond between 1a and HFIP (top : O-H bond; bottom S=O bond)

Accordingly, both ^{1}H NMR and IR studies corroborate the formation of the hydrogen bond between our chiral directing group and HFIP. It can hence be reasonably surmised that such substrate-solvent complexation has two major impacts on the outcome of the studied transformation. Firstly, as this hydrogen bond results in a weakening of the S=O bond, the electronic properties of this coordinating group are modified what can directly influence the rate of the C-H activation step. Moreover, if the metallation step is rate-determining, the kinetics of the overall transformation would therefore be altered. In pararel, the involvement of the sulfoxyde group in the hydrogen bond can reasonably influence the geometry of the pre-transition state and/or the key palladacyclic intermediate, hence enhancing an efficient stereoinduction.

In order to examine the influence of HFIP on the rate of this oxidative olefination, kinetic isotope effect studies were undertaken[278] (Figure IV-18). Two sets of experiments were conducted. In the first one, a KIE of 2.2 from the two parallel reactions using **1d** and **6'-1d** under the original reaction conditions (10 mol% of $Pd(OAc)_2$, 6 equiv. of AgOAc, DCE, 80 °C) was determined. In the second one, when using HFIP solvent, 2 equiv. of AgOAc and conducting the reaction at room temperature, much stronger KIE of 5.9 was mesured. These results indicate that in both cases the rate determining step involves the breaking of the C-H bond. If one must be cautious when interpreting the value of a KIE, the much stronger KIE in HFIP could suggest that distinct transition states in both cases could be expected: indeed lower KIE values suggest that the C-H bond is only slightly or nearly completely broken in the transition state, and thus that the transition is reactant or product like. A larger KIE value suggest that the transition is more symmetrical, that is that the degree of C-H bond-breaking and forming in the transition state is more equal[279]. This modified value of the KIE effect could also result from the geometry change of **1d** and the corresponding intermediates upon H-bonding by HFIP[280]. In addition, the reversibility of this oxidative Heck reaction was investigated (Figure IV-19). Under both reaction conditions no H/D scrambling was observed on **6'-1d** indicating the non-reversible character of the C-H cleavage and hence supporting its involvement in the turnover-limiting step.

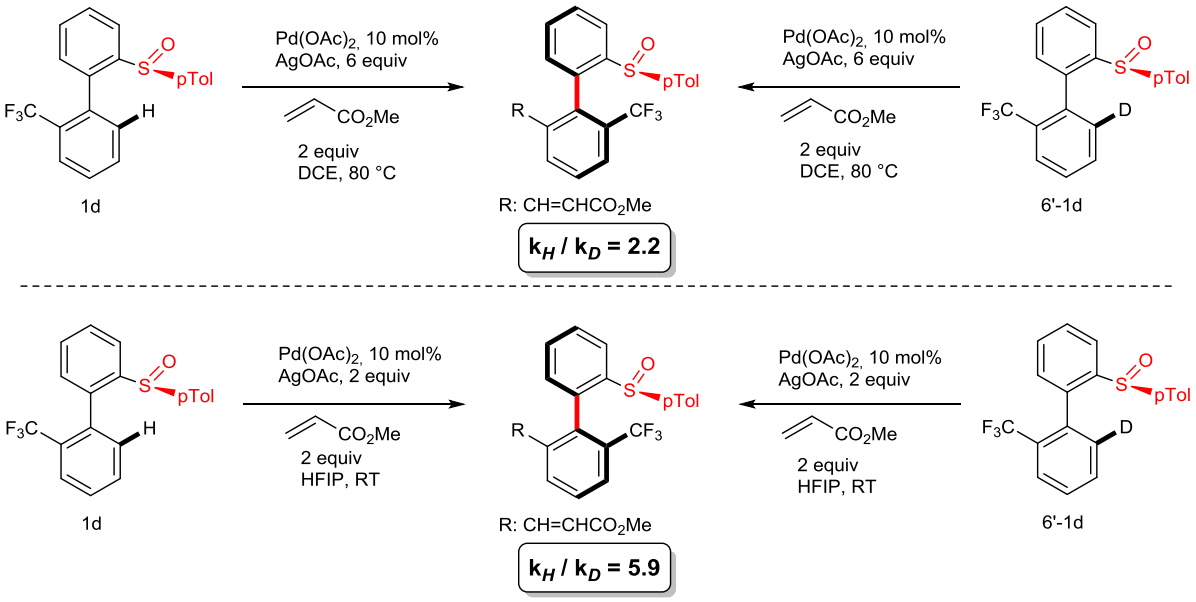

Figure IV-18 : KIEs study in DCE and in HFIP.

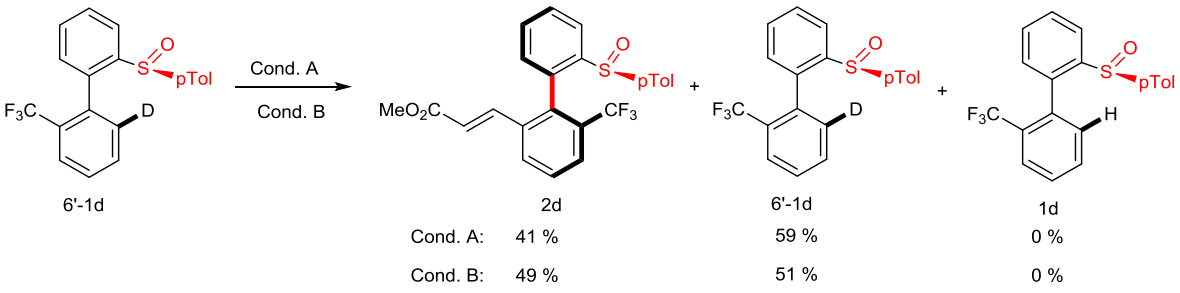

Figure IV-19 : reversibility study.

An alternative hypothesis to explain the enhancement of the turnover-limiting C-H cleavage step by HFIP will also involve the exceptional hydrogen-bonding ability of HFIP, this time not towards the sulfoxyde substrate but more so towards the palladium catalyst. Indeed it has been shown the addition of Lewis acids can enhanced C-H activation processes. Tischler, Novàk and coworkers[26] (Figure IV-20a) first demonstrated that the addition of various Lewis acids allowed a more efficient *ortho*-olefination of NH-aryl urea derivatives. DFT studies showed that the most favourable reaction pathway involved coordination of the Lewis acid to the κ^1 acetate ligand not involved in the C-H cleavage (*trans* to the future σ-aryl-Pd bond). This coordination is believed to enhance the electrophilic character of the Pd-catalyst. Accordingly the formation of H-Pd agnostic bond is slightly higher in energy than that without the Lewis acid (κ^2-κ^1 displacement; see the first part of this thesis) from 4.3 to 6.3 kcal. However he C-H cleavage, which is the major component of the overall barrier, is largely facilitated (from 18.8 to 12.9 kcal). In addition, the authors point out that this Lewis-acid accelerated C-H cleavage would be most efficient in C-H activation reactions that exhibit a higher reactivity on electron-rich substrates, as it is the case in our catalytic system. Furthermore this hypothesis of Lewis acid accelerated C-H activation by hydrogen-bonding is supported by the literature on related Pd^{II} complexes of HFIP and/or phenol. Indeed several Pd^{II} alkoxides complexes showing an intermolecular hydrogen bond between a phenolate and a phenol have been isolated, and their structures, as well as the hydrogen bond, confirmed by $^1H/^{13}C$ NMR (Figure IV-20b)[281] or $^1H/^{13}C$ NMR and X-ray analysis (Figure IV-20c)[282].

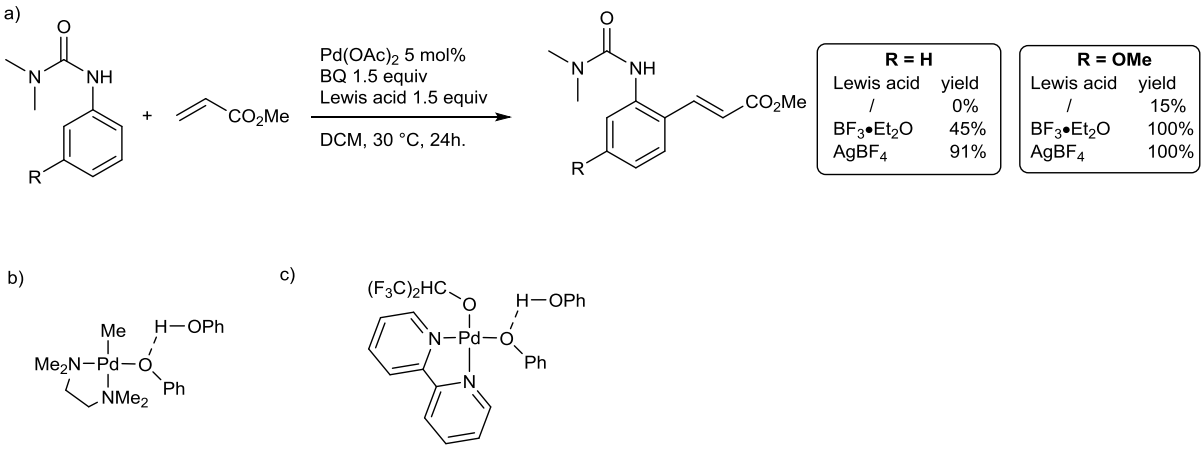

Figure IV-20 : lewis acid accelerated F-M reaction. Palladium complexes exhibiting H-bonding

An additional advantage of the reoptimized catalytic system involving HFIP solvent is that a decreased amount of silver salt oxidant, 2 equivalents versus 6 equivalents previously used, are sufficient to insure an optimal regeneration of the catalyst. The fluorinated solvents are prompt to reduce the oxidation potential of some organic species[283,284] and hence it could be possible that the reoxidation of the Pd(0) species in HFIP is facilitated[285]. Besides, the distinct solubility of AgOAc in both solvents could also impact this step.

On the basis of the above presented mechanistic studies and the literature data, a catalytic cycle presented in Figure IV-21 is proposed. Initially, a biarylsulfoxyde substrate interacts via H-bonding with HFIP to generate an “activated substrate”. This substrate-solvent intimate interaction is supposed to modify both the coordination properties and the steric features of the chiral directing group. Subsequently, precoordination of $Pd(OAc)_2$ followed by the irreversible, rate determining C-H bond cleavage occurs, affording the atropisomeric palladacyclic intermediates. The stereogenic environment of the sulfoxyde, further increased by the involvement of the O-atom of the sulfoxyde in H-bond with HFIP, results in the favourable generation of the intermediate Int A_{HFIP} with a decreased steric hindrance. Insertion of the olefin coupling partner into the C-Pd bond, followed by β–H elimination delivers the functionalized product **2** as a sole atropisomer. The catalytic cycle is completed by the reoxidation of Pd(0) into Pd(II) by the silver salt.

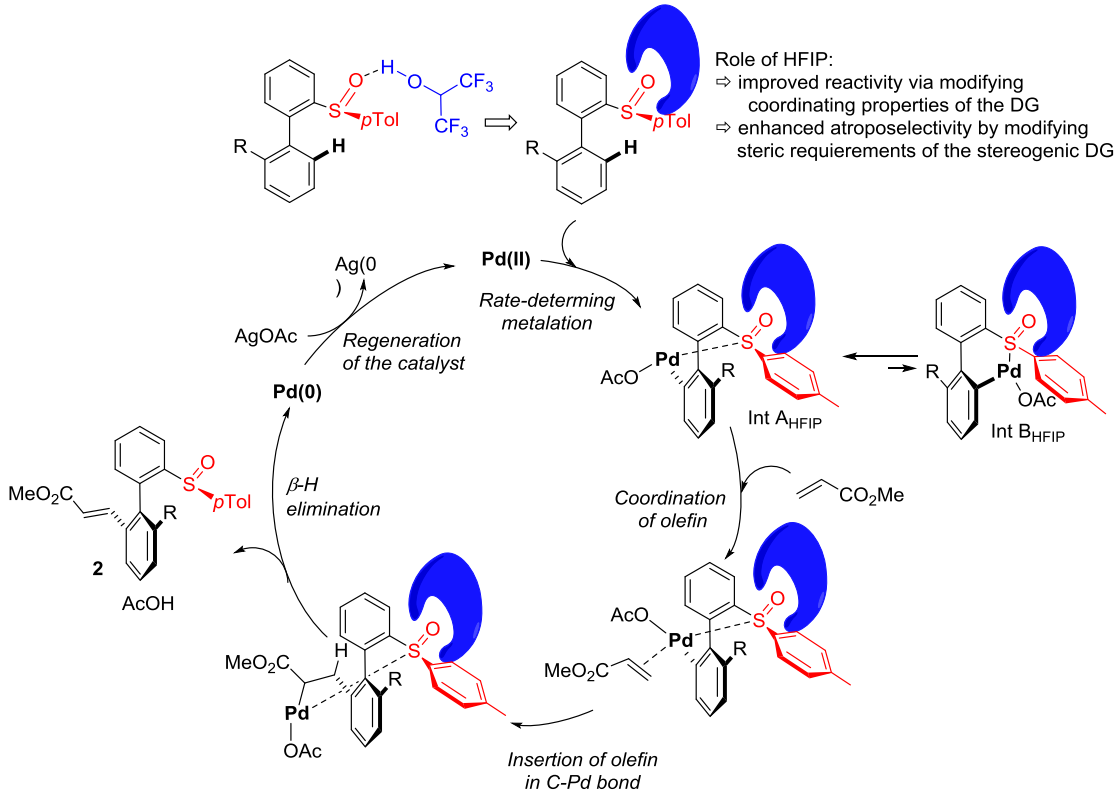

Figure IV-21 : Proposed catalytic cycle.

Finally, in order to illustrate the key advantage of the sulfoxyde directing group, i.e. its traceless character, post-modifications of **2a** have been undertaken (Figure IV-22). Rewardingly, the sulfoxyde DG could be efficiently transformed into several functionnal groups giving access to highly substituted atropopure biaryls.

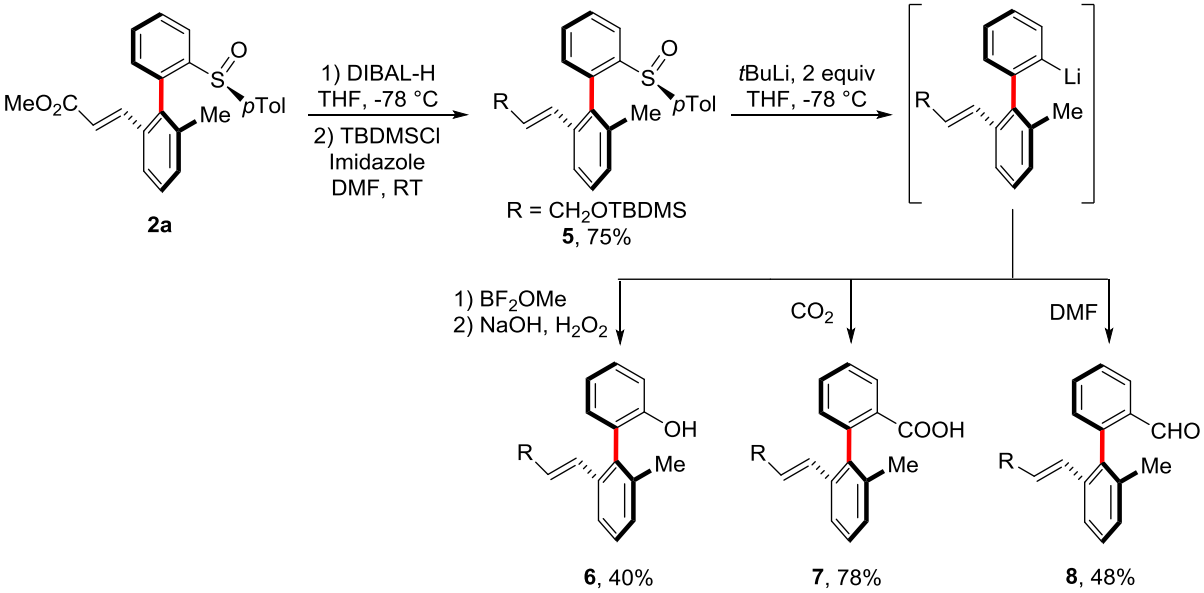

Figure IV-22 : Examples of transformation of sulfoxyde DG

As an example, optically pure atropisomeric **2a** (prepared in 98% yield and dr > 98:2) was firstly reduced with DIBAL-H followed by protection of the corresponding alcohol as a TBDMS silyl ether affording **5** in 75% yield (Figure IV-22). Subsequently exchange with tert-butyllithium at -78 °C in THF afforded the atropo-enantiopure biaryllithium species which was trapped with various electrophiles to afford the corresponding enantiopure biphenyl alcohol **6** in 40% yield, biphenyl carboxylic acid **7** (78% yield, e.r. >99:1, determined by chiral HPLC) and biphenyl aldehyde **8** (48% yield).

C. Conclusion

In summary, we have discovered that a very efficient atropo-diastereoselective oxidative olefination can now be performed by direct functionalization of biaryls bearing chiral sulfoxyde as the directing group. The reaction outcome in terms of both, efficiency and stereoselectivity is drastically improved using HFIP as reaction solvent, enabling accomplishment of this asymmetric C-H activation / C-C coupling at room temperature. Under these modified reaction conditions not only acrylates may be used as coupling partners, but also styrenes and 1,1-disubstituted activated olefin were applied efficiently. Mechanistic studies were undertaken to elucidate the particular role of HFIP in this reaction. The hydrogen bond between this solvent and the O-atom of the sulfoxyde directing group could be evidenced. The involvement of the sulfoxyde in H-bonding is expected to modify both the coordinating properties of this DG and its steric requirements hence allowing evidently superior transformation. Finally, the traceless character of this stereogenic DG was evidenced by performing

post-modifications of the atropopure scaffolds. Three parent axially chiral compounds could hence be obtained without loss of the optical purity. Furthermore, the importance of enantiopure atropisomeric scaffolds coupled to the spectacular effect of HFIP on the palladium catalysed, sulfoxyde-directed functionalization of biaryl, encouraged us to explore other mode of functionalization which will be seen in the next section of this manuscript.

This work has been published in Chemistry a European Journal 2016, 22, 1735-1743.

D. Experimental part

1. Atropo-diastereoselective reaction with acrylates

General procedure for the diastereoselective olefination with acrylate olefins : P2

The reaction was conducted under air. An oven-dried sealed tube (with a teflon-lined screw cap) was loaded with the substrate (1 equiv., 0.3 mmol), AgOAc (2 equiv., 0.6 mmol) and $Pd(OAc)_2$ (10 mol%, 0.03 mmol). HFIP (0.2 M) and methyl acrylate (2 equiv., 0.6 mmol) were then added by syringe. The reaction mixture was stirred at 25 °C and the progress of the reaction was monitored by TLC until total consumption of the starting material. The reaction mixture was then diluted with Et_2O and filtrated through a celite plug. The plug was washed with Et_2O and the solvent was removed under reduced pressure. The crude product was purified by flash chromatography.

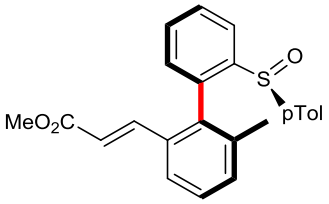

methyl (*E*)-3-((*R*)-6-methyl-2'-((*S*)-*p*-tolylsulfinyl)-[1,1'-biphenyl]-2-yl)acrylate
Chemical Formula: $C_{24}H_{22}O_3S$
Molecular Weight: 390,4970

2a: methyl (*E*)-3-((*R*)-6-methyl-2'-((*S*)-p-tolylsulfinyl)-[1,1'-biphenyl]-2-yl)acrylate
From (*S*)-2-methyl-2'-(p-tolylsulfinyl)-1,1'-biphenyl (1 equiv, 92 mg, 0.3 mmol), following the P2 for 24 hours yielded the title compound (112 mg, 0.287 mmol, 96 %); dr > 98 : 2.

^{1}**H-NMR** ($CDCl_3$, 400 MHz) : 8.32 (dd, J = 8.0, 1.2 Hz, 1H), 7.71 (dt, J = 7.7, 1.2 Hz, 1H), 7.58 (d, J = 7.3 Hz, 1H), 7.55 (dt, J = 7.5, 1.2 Hz, 1H), 7.34 (t, J = 7.7 Hz, 1H), 7.34 (d, J = 15.9 Hz, 1H), 7.10 (dd, J = 7.5, 1.2 Hz, 1H), 7.04 (d, J = 7.03 Hz, 1H), 7.02 (***AA'***BB'm, 2H), 6.88 (AA'***BB'***m, 2H), 6.32 (d, J = 15.9 Hz, 1H), 3.69 (s, 3H), 2.31 (s, 3H), 1.09 (s, 3H) ppm.
^{13}**C-NMR** ($CDCl_3$, 101 MHz): 166.9, 143.9, 142.4, 142.1, 140.7, 138.5, 137.0, 136.4, 133.7, 131.8, 130.9, 130.6, 129.6 (2 $C_{p\text{-}Tol}$), 129.2, 128.9, 126.8 (2 $C_{p\text{-}Tol}$), 124.3, 123.9, 120.3, 51.8, 21.5, 19.7 ppm.
$[\alpha]_D^{20}$ = -86.6 ° (c = 1.175, $CHCl_3$).
HRMS see[256]

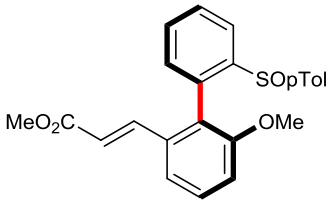

methyl (*E*)-3-((a*S*)-6-methoxy-2'-((*S*)-*p*-tolylsulfinyl)-[1,1'-biphenyl]-2-yl)acrylate
Chemical Formula: $C_{24}H_{22}O_4S$
Molecular Weight: 406,4960

2b: methyl (*E*)-3-((*aS*)-6-methoxy-2'-((*S*)-p-tolylsulfinyl)-[1,1'-biphenyl]-2-yl)acrylate. From (*S*)-2-methoxy-2'-(p-tolylsulfinyl)-1,1'-biphenyl (1 equiv., 97 mg, 0.30 mmol), following the P2 for 30 hours yielded the title compound (121 mg, 0.30 mmol, 99 %); dr > 98 : 2.

^{1}**H-NMR** ($CDCl_3$, 400 MHz) : 8.16 (dd, J = 7.9, 1.2 Hz, 1H), 7.65 (dt, J = 6.3, 1.3 Hz, 1H), 7.53 (dt, J = 6.1, 1.3 Hz, 1H), 7.39-7.31 (m, 3H), 7.14 (dd, J = 6.3, 1.2 Hz, 1H), 7.03 (***AA'BB'***m, 4H), 6.66 (d, J = 7.5 Hz, 1H), 6.33 (d, J = 16.0 Hz, 1H), 3.69 (s, 3H), 3.15 (s, 3H), 2.31 (s, 3H) ppm. ^{13}**C-NMR** ($CDCl_3$, 101 MHz): 166.9, 157.2, 144.1, 141.9, 141.7, 141.5, 135.0, 134.1, 131.5, 130.8, 130.0, 129.4 (2 C_{pTol}), 129.2, 126.9 (2 C_{pTol}), 126.7, 124.8, 120.8, 118.6, 111.5, 54.9, 51.8, 21.5 ppm. $[\alpha]_D^{20}$ = -100.0 ° (c = 1.725, $CHCl_3$). **HRMS** see [1]

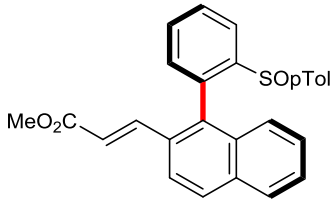

methyl (*E*)-3-(1-((a*S*)-2-((*S*)-*p*-tolylsulfinyl)phenyl)naphthalen-2-yl)acrylate
Chemical Formula: $C_{27}H_{22}O_3S$
Molecular Weight: 426,5300

2c: methyl (*E*)-3-(1-((*aS*)-2-((*S*)-p-tolylsulfinyl)phenyl)naphthalen-2-yl)acrylate. From (S)-1-(2-(p-tolylsulfinyl)phenyl)naphthalene (1 equiv, 103 mg, 0.30 mmol), following the P2 for 3 days yielded the title compound (127.3 mg, 0.30 mmol, 99 %); dr > 98 : 2.

^{1}**H-NMR** ($CDCl_3$, 400 MHz) : 8.37 (dd, J = 8.0, 1.3 Hz, 1H), 7.90 (d, J = 8.7 Hz, 1H), 7.82 (d, J = 8.0 Hz, 1H), 7.80 (dt, J = 7.8, 1.3 Hz, 1H), 7.72 (d, J = 8.2 Hz, 1H), 7.62, (dt, J = 6.1, 1.3 Hz, 1H), 7.53 (d, J = 16.0 Hz, 1H), 7.30 (ddd, J = 8.2, 6.9, 1.1 Hz, 1H), 7.22 (dd, J = 7.3, 1.3 Hz, 1H), 6.84 (ddd, J = 8.6, 6.9, 1.3 Hz, 1H), 6.54 (***AA'BB'***m, 4H), 6.52 (d, J = 16.0 Hz, 1H), 6.45 (d, J = 8.4 Hz, 1H), 3.73 (s, 3H), 2.04 (s, 3H).
^{13}**C-NMR** ($CDCl_3$, 101 MHz): 167.0, 145.3, 142.0, 141.6, 140.3, 135.9, 135.1, 133.8, 132.6, 131.6, 130.7, 130.6, 129.6, 129.5, 129.2 (2 C_{pTol}), 127.7, 126.5, 126.5, 126.4, 126.2 (2 C_{pTol}), 124.2, 122.9, 120.6, 51.9, 21.2 ppm.

$[\alpha]_D^{20}$ = -13.5 ° (c = 0.57, $CHCl_3$). **HRMS** see [256]

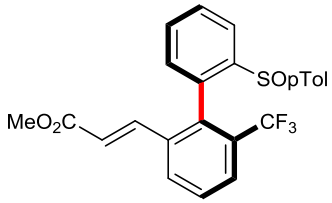

methyl (*E*)-3-((a*S*)-2'-((*S*)-*p*-tolylsulfinyl)-6-(trifluoromethyl)-[1,1'-biphenyl]-2-yl)acrylate
Chemical Formula: $C_{24}H_{19}F_3O_3S$
Molecular Weight: 444,4682

2d : methyl (*E*)-3-((*aR*)-2'-((*S*)-p-tolylsulfinyl)-6-(trifluoromethyl)-[1,1'-biphenyl]-2-yl)acrylate; From (*S*)-2-(p-tolylsulfinyl)-2'-(trifluoromethyl)-1,1'-biphenyl (1 equiv, 108 mg, 0.30 mmol), following the P2 for 4.5 days yielded the title compound (106 mg, 0.24 mmol, 80 %); dr > 98:2.

^{1}**H-NMR** ($CDCl_3$, 400 MHz) : 8.09 (d, J = 8.0 Hz, 1H), 7.92 (d, J = 7.6 Hz, 1 H), 7.70-7.58 (m, 3H), 7.54 (t, J = 7.5 Hz, 1H), 7.29 (d, J = 16.0 Hz, 1H), 7.22 (d, J = 7.5 Hz, 1H), 7.06 (***AA'***BB', 2H), 6.95 (AA'***BB'***, 2H), 6.39 (d, J = 16.0 Hz, 1H), 3.69 (s, 3H), 3.30 (s, 3H).
^{13}**C-NMR** ($CDCl_3$, 101 MHz): δ = 166.4, 144.3, 142.2, 140.8, 139.8, 136.2, 135.7 (q, J = 1.8 Hz), 134.4, 130.8, 130.6 (q, J = 29.6 Hz), 130.3 (q, J = 1.8 Hz), 130.2, 130.1, 129.6 (2 C_{pTol}), 129.2, 127.8 (q, J = 5.2 Hz), 126.1 (2 C_{pTol}), 124.7, 123.1 (q, J = 274.5 Hz), 122.2, 51.9, 21.5.
^{19}**F-NMR** ($CDCl_3$, 377 MHz): -58.1 ppm.
$[\alpha]_D^{20}$ = -196.3 ° (c = 1.25, $CHCl_3$).
HRMS see [256]

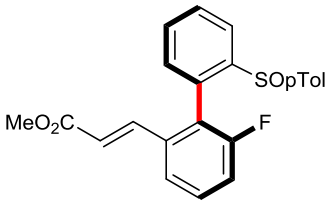

methyl (*E*)-3-((a*S*)-6-fluoro-2'-((*S*)-*p*-tolylsulfinyl)-[1,1'-biphenyl]-2-yl)acrylate
Chemical Formula: $C_{23}H_{19}FO_3S$
Molecular Weight: 394,4604

2e: methyl (*E*)-3-((*aS*)-6-fluoro-2'-((*S*)-p-tolylsulfinyl)-[1,1'-biphenyl]-2-yl)acrylate.
From (*S*)-2-fluoro-2'-(p-tolylsulfinyl)-1,1'-biphenyl (1 equiv., 61 mg, 0.20 mmol)), following the P2 for 48 hours yielded the title compound (73.4 mg, 0.19 mmol, 95 %); dr > 98 : 2.

^{1}**H-NMR** ($CDCl_3$, 400 MHz) : 8.17 (dd, J = 7.8, 1.1 Hz, 1H), 7.70 (dt, J = 7.6, 1.2 Hz, 1H), 7.57 (dt, J = 7.5, 1.2 Hz, 1H), 7.52 (d, J = 7.8 Hz, 1H), 7.40 (dt, J = 8.0, 5.5 Hz, 1H), 7.34 (d, J = 15.9 Hz, 1H) 7.20 (dd, J = 7.5, 0.8 Hz, 1H), 7.07 (***AA'***BB'm, 2H), 7.03 (AA'***BB'***m, 2H), 6.90 (dt, J = 8.3, 0.8 Hz, 1H), 6.35 (d, J = 15.9 Hz, 1H), 3.71

(s, 3H), 2.32 (s, 3H) ppm.
^{13}**C-NMR** ($CDCl_3$, 101 MHz): 166.6, 160.2 (d, J = 246.9 Hz), 144.7, 142.0, 141.1, 140.7 (d, J= 3.3 Hz), 135.8 (d, J= 2.9 Hz), 131.3 (d, J= 1.1 Hz), 131.1 (d, J = 1.1 Hz), 131.1, 130.4 (d, J= 8.8 Hz), 130.0, 129.8 (2 C_{pTol}), 126.9, 126.8, 126.2 (d, J = 0.7 Hz), 125.8 (d, J = 17.2 Hz), 125.1, 122.4 (d, J = 3.3 Hz), 121.7, 116.7 (d, J = 22.7 Hz), 51.9, 21.6 ppm.
^{19}**F-NMR** ($CDCl_3$, 377 MHz): -111.1 ppm.
$[\alpha]_D^{20}$ = -138.3 ° (c = 2.275, $CHCl_3$).
EA : *Calcd. for* $C_{23}H_{19}O_3FS$: 70.03 (C), 4.86 (H) ; *found* : 69.89 (C), 4.69 (H).

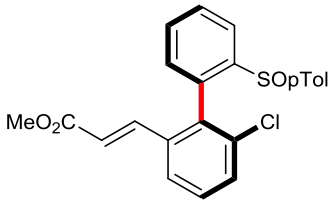

methyl (*E*)-3-((a*S*)-6-chloro-2'-((*S*)-*p*-tolylsulfinyl)-[1,1'-biphenyl]-2-yl)acrylate
Chemical Formula: $C_{23}H_{19}ClO_3S$
Molecular Weight: 410,9120

2f: methyl (*E*)-3-((*S*)-6-chloro-2'-((S)-p-tolylsulfinyl)-[1,1'-biphenyl]-2-yl)acrylate From (*S*)-2-chloro-2'-(p-tolylsulfinyl)-1,1'-biphenyl (1 equiv., 98 mg, 0.30 mmol), following the P2 for 2 d yielded the title compound (111 mg, 0.27 mmol, 90 %), dr > 98 : 2.

^{1}**H-NMR** ($CDCl_3$, 400 MHz) : 8.19 (dd, J = 8.0, 1.2 Hz, 1H), 7.70 (dt, J = 7.8, 1.2 Hz, 1H), 7.64 (dd, J = 7.8, 1.1 Hz, 1H), 7.57 (dt, J = 7.5, 1.4 Hz, 1H), 7.38 (t , J = 8.0 Hz, 1H), 7.31 (d, J = 15.9 Hz, 1H), 7.27 (d, J = 7.8 Hz, 1H), 7.18 (dd, J = 7.5, 1.2 Hz, 1H), 7.07 (***AA'***BB'm, 2H), 7.01 (AA'***BB'***m, 2H), 6.34 (d, J = 15.9 Hz, 1H), 3.70 (s, 3H), 2.32 (s, 3H) ppm.
^{13}**C-NMR** ($CDCl_3$, 101 MHz): 166.5, 144.0, 142.2, 141.3, 140.4, 136.2, 136.1, 136.0, 134.7, 131.0, 131.0, 130.7, 130.0, 129.9, 129.8 (2 $C_{p\text{-}Tol}$), 126.5 (2 $C_{p\text{-}Tol}$), 125.2, 124.6, 121.7, 51.9, 21.6 ppm.
$[\alpha]_D^{20}$ = -55.8 ° (c = 1.745, $CHCl_3$).
HRMS see[256]

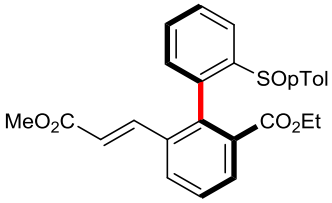

methyl (*E*)-3-((a*R*)-6-methyl-2'-((*S*)-*p*-tolylsulfinyl)-[1,1'-biphenyl]-2-yl)acrylate
Chemical Formula: $C_{24}H_{22}O_3S$
Molecular Weight: 390,4970

2g : ethyl (*aR*)-6-((*E*)-3-methoxy-3-oxoprop-1-en-1-yl)-2'-((*S*)-p-tolylsulfinyl)-[1,1'-biphenyl]-2-carboxylate. From ethyl (*S*)-2'-(p-tolylsulfinyl)-[1,1'-biphenyl]-2-

carboxylate (1 equiv., 109 mg, 0.30 mmol), following the P2 for 3 days yielded the title compound (134 mg, 0.30 mmol, 99 %); dr = 97 : 3.

^{1}**H-NMR** ($CDCl_3$, 400 MHz): 8.14 (dd, J = 8.0, 1.2 Hz, 1H), 7.99 (dd, J = 7.8,1.2 Hz, 1H), 7.88 (dd, J = 7.9, 1.2 Hz, 1H), 7.65 (dt, J = 7.7, 1.2 Hz, 1H), 7.55 (t, J = 7.9 Hz, 1H), 7.50 (dt, J = 7.5, 1.3 Hz, 1H), 7.31 (d, J = 16.0 Hz, 1H), 7.10 (dd, J = 7.5, 1.1 Hz, 1H), 7.02 (***AA'BB'***m, 4H), 6.36 (d, J = 16.0 Hz, 1H), 3.69 (s, 3H), 3.70 ; 3.56 (***AB***X_3m, J_{AB} = 10.9 Hz, $J_{AX} = J_{BX}$ = 7.2 Hz, 2H), 2.29 (s, 3H), 0.79 (AB***X_3***m, J = 7.2 Hz, 3H).
^{13}**C-NMR** ($CDCl_3$, 101 MHz): 166.6, 165.4, 143.1, 141.7, 141.4, 140.7, 138.3, 137.3, 135.4, 132.2, 131.8, 130.6, 130.4, 130.3, 129.5 (2 $C_{p\text{-}Tol}$), 129.3, 129.0, 126.3 (2 $C_{p\text{-}Tol}$), 124.5, 121.5, 60.7, 51.9, 21.5, 13.6 ppm.
$[\alpha]_D^{20}$ = -112.6 ° (c = 1.58, $CHCl_3$).
EA : *Calcd. for* $C_{26}H_{24}O_5S$: 69.62 (C), 5.39 (H) ; *found* : 69.52 (C), 5.38 (H).

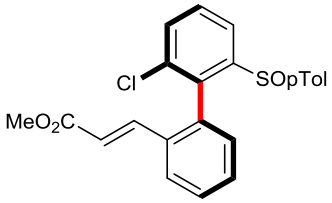

methyl (*E*)-3-((a*S*)-2'-chloro-6'-((*S*)-*p*-tolylsulfinyl)-[1,1'-biphenyl]-2-yl)acrylate
Chemical Formula: $C_{23}H_{19}ClO_3S$
Molecular Weight: 410,9120

2h: methyl (*E*)-3-((*aS*)-2'-chloro-6'-((*S*)-p-tolylsulfinyl)-[1,1'-biphenyl]-2-yl)acrylate

From (*S*)-6'-chloro-2'-(p-tolylsulfinyl)-1,1'-biphenyl (1 equiv., 98 mg, 0.30 mmol), following the P2 for 36 hours yielded the title compound (120 mg, 0.29 mmol, 98 %); dr > 98 : 2.

^{1}**H-NMR** ($CDCl_3$, 400 MHz) : 8.20 (dd, J = 6.4, 2.6 Hz, 1H), 7.75 (d, J = 7.8 Hz, 1H), 7.69-7.62 (m, 2H), 7.43 (t, J = 8.4 Hz, 1H), 7.33 (d, J = 15.9 Hz, 1H), 7.14 (t, J = 7.6 Hz, 1H), 7.06 (***AA'***BB'm, 2H), 6.96 (AA'***BB'***m, 2H), 6.37 (d, J = 8.4 Hz, 1H), 6.34 (d, J = 15.9 Hz, 1H), 3.71 (s, 3H), 2.33 (s, 3H) ppm.
^{13}**C-NMR** ($CDCl_3$, 101 MHz): 166.8, 146.4, 142.4, 141.2, 141.1, 135.9, 134.7, 134.6, 133.5, 132.1, 132.1, 130.3, 129.8 (2 $C_{p\text{-}Tol}$), 129.6 (2 $C_{p\text{-}Tol}$), 129.4, 127.0, 126.9, 122.9, 120.8, 51.9, 21.6 ppm.
$[\alpha]_D^{20}$ = -150.66 ° (c = 1.55, $CHCl_3$).
HRMS (ESI): *calc. for* $C_{23}H_{19}ClNaO_3S^+$ *433.0636* ; found 433.0629.

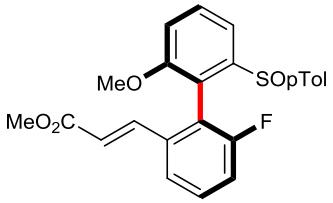

methyl (*E*)-3-((a*S*)-6-fluoro-2'-methoxy-6'-((*S*)-*p*-tolylsulfinyl)-[1,1'-biphenyl]-2-yl)acrylate
Chemical Formula: $C_{24}H_{21}FO_4S$
Molecular Weight: 424,4864

2i: methyl (*E*)-3-((*aS*)-6-fluoro-2'-methoxy-6'-((*S*)-p-tolylsulfinyl)-[1,1'-biphenyl]-2-yl)acrylate. From 2'-fluoro-2-methoxy-6-((*S*)-p-tolylsulfinyl)-1,1'-biphenyl (1 equiv., 102 mg, 0.30 mmol), following the P2 for 6 days yielded the title compound (118 mg, 0.28 mmol, 93 %); dr = 90 : 10. Recrystallization by liquid-liquid diffusion of *n*-hexane into DCM gave methyl (*E*)-3-((*aS*)-6-fluoro-2'-methoxy-6'-((*S*)-p-tolylsulfinyl)-[1,1'-biphenyl]-2-yl)acrylate (103 mg, 0.243 mmol, 81 %); dr > 98 : 2.

^{1}**H-NMR** ($CDCl_3$, 400 MHz) : 7.80 (d, J = 7.3 Hz, 1H), 7.67 (t, J = 8.1 Hz, 1H), 7.53 (d, J = 7.8 Hz, 1H), 7.38 (ddd, J = 8.1, 7.9, 6 Hz, 1H), 7.30 (d, J = 16.0 Hz, 1H), 7.11 (d, J = 8.1 Hz, 1H), 7.03 (**AA'BB'**m, 4H), 6.84 (t, J = 8.5 Hz, 1H), 6.36 (d, J = 16.0 Hz, 1H), 3.72 (s, 3H), 3.71 (s, 3H), 2.32 (s, 3H) ppm. ^{13}**C-NMR** ($CDCl_3$, 101 MHz): 166.8, 160.6 (d, J_{C-F} = 247 Hz), 157.4, 146.0, 142.0, 141.0 (d, J_{C-F} = 11.6 Hz), 140.9, 136.0 (d, J_{C-F} = 3.3 Hz), 131.1, 130.3 (d, J_{C-F} = 9.1 Hz), 129.7 (2 $C_{p\text{-}Tol}$), 126.3, 126.3, 122.4 (d, J_{C-F} = 3.3 Hz), 122.1 (d, J_{C-F} = 17.9 Hz), 121.3, 119.6, 116.6, 116.5 (d, J_{C-F} = 22.9 Hz), 113.5, 56.3, 51.9, 21.6 ppm. ^{19}**F-NMR** ($CDCl_3$, 377 MHz): -111.0 ppm. $[\alpha]_D^{20}$ = -161.5 ° (c = 0.745, $CHCl_3$). **HRMS (ESI) :** *calc. for $C_{24}H_{22}FO_4S^+$ 425.1217*; found 425.1181.

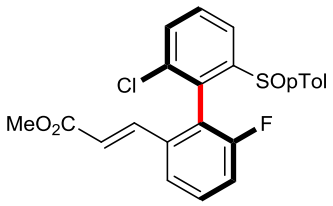

methyl (*E*)-3-((a*R*)-2'-chloro-6-fluoro-6'-((*S*)-*p*-tolylsulfinyl)-[1,1'-biphenyl]-2-yl)acrylate
Chemical Formula: $C_{23}H_{18}ClFO_3S$
Molecular Weight: 428,9024

2j: methyl (*E*)-3-((*aR*)-2'-chloro-6-fluoro-6'-((*S*)-p-tolylsulfinyl)-[1,1'-biphenyl]-2-yl)acrylate. From 2-chloro-2'-fluoro-6-((*S*)-p-tolylsulfinyl)-1,1'-biphenyl (1 equiv., 103 mg, 0.30 mmol), following the P2 for 4 days yielded the title compound (115 mg, 0.27 mmol, 89 %); dr = 93 : 7.

^{1}**H-NMR** ($CDCl_3$, 400 MHz, *mixture of atropodiastereomers 93 : 7, only the major diastereomer is reported)* : 8.16 (dd, J = 7.2, 2.0 Hz, 1H), 7.71-7.62 (m, 2H), 7.55 (d, J = 7.8 Hz, 1H), 7.44 (dt, J = 8.0, 5.5 Hz, 1H), 7.27 (d, J = 16.0 Hz, 1H), 7.07 (***AA'***BB'm, 2H), 6.99 (AA'***BB'***m, 2H), 6.83 (t, J = 8.3 Hz, 1H), 6.36 (d, J = 16.0 Hz,

1H), 3.72 (s, 3H), 2.33 (s, 3H) ppm. **^{13}C-NMR** ($CDCl_3$, 101 MHz, *mixture of atropodiastereomers 93 : 7, only the major diastereomer one is reported*) : 166.5, 160.2 (d, J = 248.3 Hz), 146.8, 142.6, 140.4, 140.0 (d, J = 3.3 Hz), 135.6 (d, J = 2.9 Hz), 135.6 (d, J = 1.1 Hz), 131.9, 131.1 (d, J = 8.8 Hz), 131.0, 129.9 (2 C_{pTol}), 129.8, 126.6, 126.6, 123.3, 122.7 (d, J = 3.3 Hz), 122.6 (d, J = 17.2 Hz), 122.1, 116.7 (d, J = 22.4 Hz), 52.0, 21.6 ppm**.** **^{19}F-NMR** ($CDCl_3$, 377 MHz): -110.6 ppm. **HRMS (ESI):** *calc. for $C_{23}H_{18}ClFO_3S^+$ 429.0722*; found 429.0703.

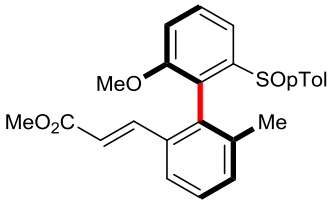

methyl (*E*)-3-((a*R*)-2'-methoxy-6-methyl-6'-((*S*)-*p*-tolylsulfinyl)-[1,1'-biphenyl]-2-yl)acrylate
Chemical Formula: $C_{25}H_{24}O_4S$
Molecular Weight: 420,5230

2k : methyl (*E*)-3-((*aR*)-2'-methoxy-6-methyl-6'-((*S*)-p-tolylsulfinyl)-[1,1'-biphenyl]-2-yl)acrylate. From 2-methoxy-2'-methyl-6-((*S*)-p-tolylsulfinyl)-1,1'-biphenyl, (1 equiv., 102 mg, 0.31 mmol) following the P2 for 6 days yielded the title compound (111.4 mg, 0.27 mmol, 87 %); dr = 66 : 34.

^{1}H-NMR ($CDCl_3$, 400 MHz, mixture of atropodiastereomers 66 : 34) : 7.92 (t, J = 7.8 Hz, 1H minor+ 1H major), 7.68 (t, J = 8.1 Hz, 1H minor), 7.68 (t, J = 8.1 Hz, 1H major), 7.59 (d, J = 7.8 Hz, 1H major), 7.37 (d, J = 15.8 Hz, 1H major), 7.38-7.28 (m, 1H major + 2H minor), 7.10 (t, J = 8.2 Hz, 1H minor+ 1H major), 7.02-7.00 (m, 3 H major), 6.98 (***AA'***BB'm, 2H minor), 6.93 (AA'***BB'***m, 2H minor), 6.87 (AA'***BB'***m, 2H major), 6.34 (d, J = 15.9 Hz, 1H major), 6.34 (d, J = 15.8 Hz, 1H minor), 5.72 (d, J = 15.8 Hz, 1H minor), 3.70 (s, 3H major), 3.69 (s, 3H major), 3.67 (s, 3H minor), 3.61 (s, 3H minor), 2.30 (s, 3H major), 2.23 (s, 3H minor), 2.12 (s, 3H minor), 1.05 (s, 3H major) ppm.
^{13}C-NMR ($CDCl_3$, 101 MHz) : major atropodiastereomer : 167.0, 156.7, 145.3, 142.6, 142.0, 140.8, 139.7, 133.9, 133.3, 131.3, 130.3, 129.4 (2 $C_{p\text{-}Tol}$), 128.8 (2 $C_{p\text{-}Tol}$), 126.8, 124.7, 124.3, 120.0, 115.7, 113.2, 56.0, 51.6, 21.4, 18.8 ppm ; minor atropodiastereomer : 166.7, 156.6, 145.1, 142.2, 142.0, 140.7, 137.6, 134.6, 133.9, 132.0, 130.3, 129.6 (2 $C_{p\text{-}Tol}$), 128.7, 127.0 (2 $C_{p\text{-}Tol}$), 125.2, 123.4, 117.6, 116.1, 113.5, 56.2, 51.3, 21.3, 20.4 ppm.
HRMS (ESI): *calc. for $C_{25}H_{25}O_4S^+$ 421.1468*; found 421.1474.

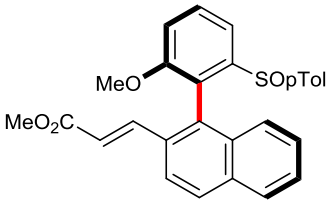

methyl (*E*)-3-(1-((a*S*)-2-methoxy-6-((*S*)-*p*-tolylsulfinyl)phenyl)naphthalen-2-yl)acrylate
Chemical Formula: $C_{28}H_{24}O_4S$
Molecular Weight: 456,5560

2l: methyl (E)-3-(1-((aS)-2-methoxy-6-((S)-p-tolylsulfinyl)phenyl)naphthalen-2-yl)acrylate. From (2-methoxy-6-((*S*)-p-tolylsulfinyl)phenyl)naphthalene (1 equiv., 112 mg, 0.30 mmol),) following the P2 for 5 days yielded the title compound (133 mg, 0.29 mmol, 97 %); dr = 66 : 34. The reaction was conducted at reflux and at 80 °C with the same yield and dr.

^{1}**H-NMR** ($CDCl_3$, 400 MHz, *mixture of atropodiastereomers 66 : 34)* : 8.02 (d, J =7.4 Hz, 1H minor), 7.98 (d, J = 7.5 Hz, 1H major), 7.90-7.86 (m, 2H minor + 1H major), 7.85 (d, J = 15.8 Hz, 1H minor), 7.82 (d, J = 8.9 Hz, 1 H minor), 7.78 (t, J = 7.5 Hz, 1H minor), 7.76 (t, J = 8.1 Hz, 1H major), 7.69 (d, J = 8.1 Hz, 1H major), 7.56 (d, J = 15.9 Hz, 1H major), 7.52 (t, J = 5.9 Hz, 1H minor), 7.52 (d, J = 4.4 Hz, 1H minor), 7.42-7.41 (m, 1H major), 7.27 (t, J = 7.8 Hz, 1H major), 7.18 (t, J = 7.6 Hz, 1H major), 7.17 (d, J = 8.6 Hz, 1H minor) 6.97 (***AA'***BB'm, 2H minor), 6.87 (AA'***BB'***m, 2H minor), 6.80 (t, J = 8.2 Hz, 1H major), 6.55 (t, J = 3.9 Hz, 1H minor), 6.53 (d, J = 15.9 Hz, 1H major), 6.52 (***AA'BB'***m, 4H major), 6.40 (d, J = 8.4 Hz, 1H major), 5.93 (d, J = 15.8 Hz, 1H minor), 3.72 (s, 3H major), 3.64 (s, 3H minor), 3.61 (s, 3H minor), 3.59 (s, 3H major), 2.22 (s, 3H minor), 2.04 (s, 3H major) ppm. ^{13}**C-NMR** ($CDCl_3$, 101 MHz); major atropodiastereomer : 167.1, 157.5, 146.5, 142.1, 141.5, 140.1, 133.7, 132.7, 132.4, 131.0, 130.7, 129.4, 129.1 (2 $C_{p\text{-}Tol}$), 127.7, 127.1, 126.3, 126.3, 126.2 (2 $C_{p\text{-}Tol}$), 123.4, 123.0, 120.3, 116.1, 113.3, 56.2, 51.8, 21.2 ppm ; minor atropodiastereomer: 166.7, 157.5, 146.1, 142.2, 141.7, 141.2, 140.1, 134.2, 132.6, 132.3, 131.9, 130.8, 129.6, 129.4 (2 $C_{p\text{-}Tol}$), 128.2, 127.6, 127.4, 126.1 (2 $C_{p\text{-}Tol}$), 123.7, 122.2, 118.0, 116.0, 113.6, 56.3, 51.4, 21.4 ppm. **HRMS (ESI):** *calc. for $C_{28}H_{24}NaO_4S^+$ 479.1288*; found 479.1278.

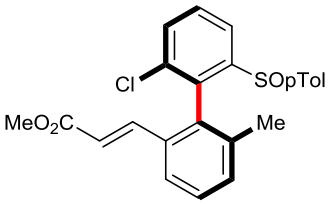

methyl (*E*)-3-((*S*)-2'-chloro-6-methyl-6'-((*S*)-*p*-tolylsulfinyl)-[1,1'-biphenyl]-2-yl)acrylate
Chemical Formula: $C_{24}H_{21}ClO_3S$
Molecular Weight: 424,9390

2m : methyl (*E*)-3-((a*S*)-2'-chloro-6-methyl-6'-((S)-p-tolylsulfinyl)-[1,1'-biphenyl]-2-yl)acrylate. From 2-chloro-2'-methyl-6-((*S*)-p-tolylsulfinyl)-1,1'-biphenyl (1 equiv.,

103 mg, 0.30 mmol), following the P2 for 3 days yielded the title compound (77 mg, 0.18 mmol, 60 %); dr = 82 : 18.

^{1}**H-NMR** ($CDCl_3$, 400 MHz, mixture of atropodiastereomers 82 : 18): 8.26 (d, J = 7.6 Hz, 1H major + 1H minor), 7.71-7.65 (m, 1H major + 2H minor), 7.64-7.60 (m, 2H major), 7.41-7.36 (m, 1H major + 2H minor), 7.33-7.30 (m, 1H minor), 7.26 (d, J = 15.8 Hz, 1H major), 7.05-7.03 (m, 3H major), 7.00-6.98 (***AA'***BB', 2H minor), 6.94-6.92 (AA'***BB'***, 2H minor), 6.90-6.88 (AA'***BB'***, 2H major), 6.34 (d, J = 15.8 Hz, 1H major), 6.20 (d, J = 15.8 Hz, 1H minor), 5.73 (d, J = 15.8 Hz, 1H minor), 3.70 (s, 3H major), 3.62 (s, 3H minor), 2.32 (s, 3H major), 2.24 (s, 3H minor), 2.11 (s, 3H minor), 1.04 (s, 3H major) ppm.
^{13}**C-NMR** ($CDCl_3$, 101 MHz); major atropodiastereomer: 166.8, 146.3, 142.6, 141.7, 140.1, 139.3, 134.9, 134.8, 133.8, 133.7, 131.8, 131.7, 130.3, 129.7 (2 $C_{p\text{-}Tol}$), 129.5, 127.0 (2 $C_{p\text{-}Tol}$), 124.6, 122.6, 120.8, 51.7, 21.5, 18.6 ppm; minor atropodiastereomer: 166.5, 146.1, 142.8, 140.7, 140.0, 137.3, 135.1, 134.7, 134.5, 134.3, 132.2, 131.9, 130.3, 129.8 (2 $C_{p\text{-}Tol}$), 129.5, 127.3 (2 $C_{p\text{-}Tol}$), 123.7, 122.8, 118.3, 51.4, 21.4, 20.3 ppm.
HRMS (ESI) : *calc. for $C_{24}H_{21}ClNaO_3S^+$ 447.0792* ; found 447.0793.

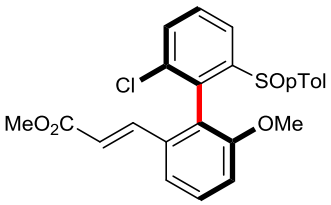

methyl (*E*)-3-((*R*)-2'-chloro-6-methoxy-6'-((*S*)-*p*-tolylsulfinyl)-[1,1'-biphenyl]-2-yl)acrylate
Chemical Formula: $C_{24}H_{21}ClO_4S$
Molecular Weight: 440,9380

2n: methyl (*E*)-3-((a*R*)-2'-chloro-6-methoxy-6'-((S)-p-tolylsulfinyl)-[1,1'-biphenyl]-2-yl)acrylate. From 2-chloro-2'-methoxy-6-((*S*)-p-tolylsulfinyl)-1,1'-biphenyl (1 equiv., 107 mg, 0.30 mmol), following the P2 for 2 days yielded the title compound (79 mg, 0.18 mmol, 60 %); dr = 62 : 38.

^{1}**H-NMR** ($CDCl_3$, 400 MHz, mixture of atropodiastereomers 62 : 38) : 8.23 (d, J = 7.6 Hz, 1H major), 8.15 (d, J = 7.9 Hz, 1H minor), 7.67-7.59 (m, 2H major + 2H minor), 7.47-7.39 (m, 1H major + 1H minor), 7.34 (d, J = 7.8 Hz, 1H minor), 7.26 (d, J = 15.9 Hz, 1H minor), 7.11-7.07 (m, 1H major + 1H minor), 7.05-7.03 (***AA'***BB', 2H minor), 6.98-6.96 (AA'***BB'***, 2H minor; ***AA'***BB', 2H major), 6.90-6.88 (AA'***BB'***, 2H major), 6.62 (d, J = 8.1 Hz, 1H minor), 6.35 (d, J = 15.9 Hz, 1H major), 6.22 (d, J = 15.9 Hz, 1H major), 5.78 (d, J = 15.9 Hz, 1H major), 3.80 (s, 3H major), 3.70 (s, 3H minor), 3.62 (s, 3H major), 3.10 (s, 3H minor), 2.32 (s, 3H minor), 2.22 (s, 3H major) ppm. ^{13}**C-NMR** ($CDCl_3$, 101 MHz) : (mixture of atropodiastereomers 62 : 38) 166.7, 166.3, 157.2, 156.7, 147.0, 146.3, 142.4, 141.9, 141.2, 141.1, 140.6, 140.4, 135.6, 135.6, 135.0, 134.7, 132.7, 132.2, 131.6, 131.5, 130.7, 130.6, 130.0, 130.0, 129.7 (2 $C_{p\text{-}Tol}$),

129.4 (2 $C_{p\text{-}Tol}$), 127.1 (2 $C_{p\text{-}Tol}$), 127.0 (2 $C_{p\text{-}Tol}$), 123.6, 123.4, 123.0, 122.1, 121.2, 119.0, 118.7, 118.3, 112.5, 111.4, 56.2, 54.8, 51.7, 51.4, 21.4, 21.3 ppm. **HRMS (ESI):** *calc. for* $C_{24}H_{21}ClO_4S^+$ *441.0922*; found 441.0921.

2. Atropo-diastereoselective reaction with styrenes

General procedure: P3

(the olefins were freshly distillated before their used)
In an oven-dried Schlenk (with a teflon-lined screw cap) were loaded, under air, the substrate (1 equiv., 0.16 mmol), followed by AgOAc (2 equiv., 0.32 mmol) and $Pd(OAc)_2$ (10 mol%, 0.016 mmol). HFIP (0.2 M) and methyl acrylate (2 equiv., 0.32 mmol) were then added by syringe and the reaction mixture was stirred at 80 °C for 3 – 8 h.
The reaction mixture was then diluted with dichloromethane and filtrated through a celite plug. The plug was washed with dichloromethane, and the solvent was removed under reduced pressure. The crude product was purified by automatic Biotage® flash chromatography.

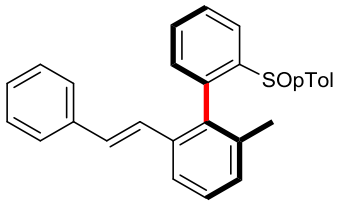

(a*R*)-2-methyl-6-((*E*)-styryl)-2'-((*S*)-*p*-tolylsulfinyl)-1,1'-biphenyl
Chemical Formula: $C_{28}H_{24}OS$
Molecular Weight: 408,5590

3a: (a*R*)-2-methyl-6-((*E*)-styryl)-2'-((*S*)-p-tolylsulfinyl)-1,1'-biphenyl; From (*S*)-2-methyl-2'-(p-tolylsulfinyl)-1,1'-biphenyl (1 equiv., 49 mg, 0.16 mmol), following the P3 for 8 h yielded the title compound (27 mg, 0.07 mmol, 41 %); dr > 98 : 2.

^{1}H NMR ($CDCl_3$, 400 MHz): δ = 8.33 (dd, J = 8.00, 1.10 Hz, 1H), 7.73-7.62 (m, 2H), 7.54 (dt, J = 7.50, 1.20 Hz, 1H), 7.33 (t, J = 7.9 Hz, 1H), 7.25-6.89 (m, 10H), 6.75 (d, J = 16.20 Hz, 1H), 2.31 (s, 3H), 1.10 (s, 3H).
^{13}C NMR ($CDCl_3$, 101 MHz): δ = 141.8, 137.8, 137.4, 137.2, 136.2, 135.5, 130.9, 130.7 (2 C_{Ar}), 129.4 (2 C_{Ar}), 129.2, 128.7, 128.6 128.6 (2 C_{Ar}), 127.7, 126.7 (2 C_{Ar}), 126.6 (2 C_{Ar}), 126.3, 123.5, 122.9, 21.4, 19.7 ppm + 2 C_{quat} overlapping. $[\alpha]_D^{20}$ =-153.0° (c = 0.5, $CHCl_3$);
HRMS (ESI): *calc. for* $C_{28}H_{25}OS^+$ *409.1621*; found 409.1643.

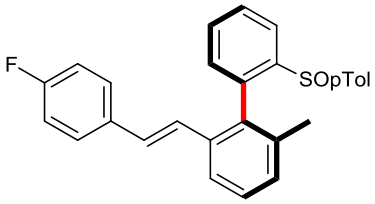

(a*R*)-2-((*E*)-4-fluorostyryl)-6-methyl-2'-((*S*)-*p*-tolylsulfinyl)-1,1'-biphenyl
Chemical Formula: $C_{28}H_{23}FOS$
Molecular Weight: 426,5494

3b: (a*R*)-2-((*E*)-4-fluorostyryl)-6-methyl-2'-((*S*)-p-tolylsulfinyl)-1,1'-biphenyl. From (*S*)-2-methyl-2'-(p-tolylsulfinyl)-1,1'-biphenyl (1 equiv., 50 mg, 0.16 mmol), following the P3 for 6 h yielded the title compound (39 mg, 0.0914 mmol, 56 %); dr > 98 : 2.

^{1}**H-NMR** ($CDCl_3$, 400 MHz) : 8.32 (d, J = 7.89 Hz, 1H), 7.69 (t, J = 7.70 Hz, 1H), 7.65 (d, J = 7.98 Hz, 1H), 7.55 (t, J = 7.43 Hz, 1H), 7.34 (t, J = 7.75 Hz, 1H), 7.24-7.20 (m, 2H), 7.13 (d, J = 7.52 Hz, 1H), 7.04 (d, J= 8.25 Hz, 2H), 6.99-6.92 (m, 6H), 6.66 (d, J = 16.14 Hz, 1H), 2.31 (s, 3H), 1.12 (s, 3H) ppm.

^{13}**C-NMR** ($CDCl_3$, 101 MHz): 162.5 ($^{1}J_{C\text{-}F}$ = 247.2 Hz), 144.2, 142.0, 141.0, 138.0, 137.5, 136.1, 135.6, 133.6 ($^{4}J_{C\text{-}F}$ = 3.3 Hz), 130.9 ($^{3}J_{C\text{-}F}$ = 6.1 Hz, 2 C_{Ar}), 129.8 ($^{6}J_{C\text{-}F}$ = 0.9 Hz), 129.6 (2 $C_{p\text{-}Tol}$), 129.4, 128.9, 128.8, 128.4, 128.3, 126.7 (2 $C_{p\text{-}Tol}$), 126.2 ($^{5}J_{C\text{-}F}$ = 2.4 Hz), 123.7, 122.9, 115.6 ($^{2}J_{C\text{-}F}$ = 21.6 Hz, 2 C_{Ar}), 21.6, 19.9 ppm.

^{19}**F-NMR** ($CDCl_3$, 377 MHz): -114.1 ppm.

$[\alpha]_D^{20}$ = -153.0° (c = 0.5, CHCl3).

HRMS (ESI): *calc. for $C_{28}H_{23}FOSNa^{+}$ 449.1346*; found 449.1335.

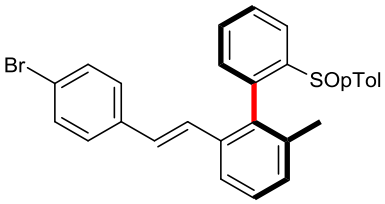

(*R*)-2-((*E*)-4-bromostyryl)-6-methyl-2'-((*S*)-*p*-tolylsulfinyl)-1,1'-biphenyl
Chemical Formula: $C_{28}H_{23}BrOS$
Molecular Weight: 487,4550

3c: (a*R*)-2-((*E*)-4-bromostyryl)-6-methyl-2'-((*S*)-p-tolylsulfinyl)-1,1'-biphenyl. From (*S*)-2-methyl-2'-(p-tolylsulfinyl)-1,1'-biphenyl (1 equiv., 50 mg, 0.16 mmol), following the P3 for 6 h yielded the title compound (50 mg, 0.10 mmol, 63 %); dr > 98 : 2.

^{1}**H-NMR** ($CDCl_3$, 400 MHz) : 8.31 (d, J = 8.07 Hz, 1H), 7.69, (t, J = 7.79 Hz, 1H), 7.64 (d, J = 7.89 Hz, 1H),, 7.55 (t, J = 7.29 Hz, 1H), 7.37-7.32 (m, 3H), 7.13-7.10 (m, 3H), 7.04 (d, J = 7.43 Hz, 2H), 6.99-6.93 (***AA'BB'***m, 4H), 6.73 (d, J = 16.51 Hz, 1H), 2.31 (s, 3H), 1.12 (s, 3H) ppm.

^{13}**C-NMR** ($CDCl_3$, 101 MHz): 144.0, 141.9, 140.8, 137.9, 137.2, 136.2, 135.9, 135.6, 131.7 (2 C_{Ar}), 130.8 130.7, 129.6, 129.5, 129.5 (2 C_{Ar}), 128.8, 128.7, 128.1 (2 C_{Ar}), 127.1, 126.6 (2 C_{Ar}), 123.6, 122.9, 121.5, 21.4, 19.7 ppm.

$[\alpha]_D^{20}$ = -147.1° (c = 0.51, $CHCl_3$).
HRMS (ESI): *calc. for $C_{28}H_{23}BrOSNa^+$ 509.0545*; found 509.0501.

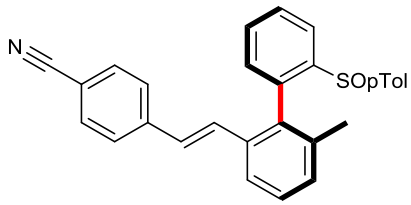

4-((*E*)-2-((a*R*)-6-methyl-2'-((*S*)-*p*-tolylsulfinyl)-[1,1'-biphenyl]-2-yl)vinyl)benzonitrile
Chemical Formula: $C_{29}H_{23}NOS$
Molecular Weight: 433,5690

3d: 4-((*E*)-2-((a*R*)-6-methyl-2'-((*S*)-p-tolylsulfinyl)-[1,1'-biphenyl]-2-yl)vinyl)benzonitrile. From (*S*)-2-methyl-2'-(p-tolylsulfinyl)-1,1'-biphenyl (1 equiv., 49 mg, 0.16 mmol), following the P3 for 6 h yielded the title compound (41 mg, 0.10 mmol, 60 %); dr > 98 : 2.
^{1}**H-NMR** ($CDCl_3$, 400 MHz) : 8.31 (d, J = 7.9 Hz, 1H), 7.71 (t, J = 7.7 Hz, 1H), 7.66 (d, J = 7.8 Hz, 1H), 7.56 (t, J = 7.7 Hz, 1H), 7.52 (d, J = 8.0 Hz, 2H), 7.37 (t, J = 7.7 Hz, 1H), 7.31 (d, J = 8.1 Hz, 2H), 7.14, (d, J = 7.3 Hz, 1H), 7.06-7.01 (***AA'BB'***m, 4H), 6.95 (d, J = 7.9 Hz, 2H), 6.85 (d, J = 16.1 Hz, 1H), 2.31 (s, 3H), 1.16 (s, 3H) ppm.
^{13}**C-NMR** ($CDCl_3$, 101 MHz): 144.3, 142.1, 141.8, 140.8, 138.2, 137.1, 136.1, 135.4, 132.5 (2 C_{Ar}), 131.0, 130.8, 130.3, 130.2, 129.6 (2 C_{Ar}), 129.1, 129.0, 128.9, 127.2 (2 C_{Ar}), 126.6 (2 C_{Ar}), 123.8, 123.2, 119.1, 110.8, 21.6, 19.9 ppm.
$[\alpha]_D^{20}$ = -163.1° (c = 0.26, $CHCl_3$).
HRMS (ESI): *calc. for $C_{29}H_{23}NOSNa^+$ 456.1393*; found 456.1382.

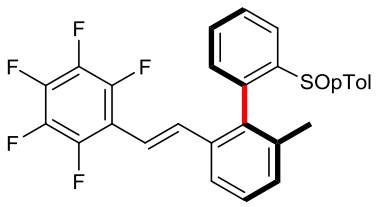

(a*R*)-2-methyl-6-((*E*)-2-(perfluorophenyl)vinyl)-2'-((*S*)-*p*-tolylsulfinyl)-1,1'-biphenyl
Chemical Formula: $C_{28}H_{19}F_5OS$
Molecular Weight: 498,5110

3e : (a*R*)-2-methyl-6-((*E*)-2-(perfluorophenyl)vinyl)-2'-((*S*)-p-tolylsulfinyl)-1,1'-biphenyl. From (*S*)-2-methyl-2'-(p-tolylsulfinyl)-1,1'-biphenyl (1 equiv., 50 mg, 0.163 mmol), following the P3 for 7 h yielded the title compound (65 mg, 0.13 mmol, 80 %); dr > 98 : 2.
^{1}**H-NMR** ($CDCl_3$, 400 MHz) : 8.31 (d, J = 7.6 Hz, 1H), 7.70 (td, J = 1.2 Hz, J = 7.6 Hz, 1H), 7.65 (d, J = 8.0 Hz, 1H), 7.55 (t, J = 7.4 Hz, 1H), 7.38 (t, J = 7. 8 Hz, 1H), 7.13 (dd, J = 1.2 Hz, J = 7.6 Hz, 1H), 7.08 (d, J = 16.8 Hz, 1H), 7.05-7.03 (m, 3H), 6.94-6.92 (m, 2H), 6.90 (d, J = 11.6 Hz, 1H), 2.31 (s, 3H), 1.14 (s, 3H) ppm.
^{13}**C-NMR** ($CDCl_3$, 101 MHz): 144.7 (d, J_{CF} = 257 Hz, 2 C_{Ar}), 144.1 (br s), 141.9, 140.8 (br s), 139.9 (d, J_{CF} = 247 Hz), 138.1, 137.7 (d, J_{CF} = 257 Hz, 2 C_{Ar}), 136.7, 136.1,

135.6, 135.0 (t, J_{CF} = 8Hz), 130.7, 130.5, 130.4, 129.5 (2 C_{Ar}), 129.0, 128.8, 126.6 (2 C_{Ar}), 123.6, 122.9, 114.6, 112.4 (td, J_{CF} = 13, Hz, J_{CF} = 4 Hz), 21.4, 19.6 ppm. ^{19}**F-NMR** ($CDCl_3$, 377 MHz): -142.6 (dd, J = 26.4, J = 11.3), -156.4 (t, J = 20.7), -162.9 (td, J = 7.1 Hz, J = 21.1 Hz) ppm. $[\alpha]_D^{20}$ = -97.0° (c = 1.01, $CHCl_3$); **HRMS (ESI):** *calc. for $C_{28}H_{19}F_5OSNa^+$ 521.0969*; found 521.0914

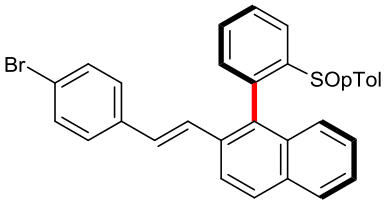

2-((*E*)-4-bromostyryl)-1-((a*S*)-2-((*S*)-*p*-tolylsulfinyl)phenyl)naphthalene
Chemical Formula: $C_{31}H_{23}BrOS$
Molecular Weight: 523,4880

3f : 2-((*E*)-4-bromostyryl)-1-((a*S*)-2-((*S*)-p-tolylsulfinyl)phenyl)naphthalene From(*S*)-1-(2-(p-tolylsulfinyl)phenyl)naphthalene (1 equiv., 50 mg, 0.15 mmol), following the P3 for 3 h yielded the title compound (48 mg, 0.09 mmol, 63 %); dr > 98 : 2.
^{1}**H-NMR** ($CDCl_3$, 400 MHz) : 8.37 (d, J = 7.89 Hz, 1H), 7.96-7.89 (m, 2H), 7.79 (t, J = 7.66 Hz, 1H), 7.73 (d, J = 7.98 Hz, 1H), 7.63 (t, J = 7.38 Hz, 1H), 7.40 (d, J = 7.43 Hz, 2H), 7.29-7.24 (m, 2H), 7.19-7.15 (m, 3H), 6.94 (d, J = 16.14 Hz, 1H), 6.85 (t, J = 7.52 Hz, 1H), 6.63-6.57 (m, 4H), 6.46 (d, J = 8.53 Hz, 1H), 2.07 (s, 3H) ppm. ^{13}**C-NMR** ($CDCl_3$, 101 MHz): 145.6, 141.5, 140.4, 136.3, 136.2, 133.1, 132.9, 132.9, 132.8, 131.9 (2 C_{Ar}), 131.9, 130.7, 130.1, 129.3, 129.2, 129.2 (2 C_{Ar}), 128.3 (2 C_{Ar}), 127.7, 127.0, 126.2, 126.1, 125.9 (2 C_{Ar}), 125.5, 124.1, 122.6, 121.8, 21.3 ppm. $[\alpha]_D^{20}$ = -116.8° (c = 0.34, $CHCl_3$). **HRMS (ESI):** *calc. for $C_{31}H_{23}BrOSNa^+$ 545.0545*; found 545.0510

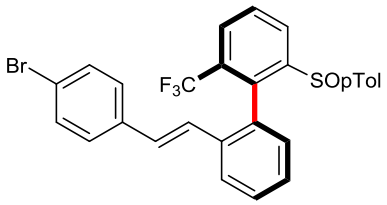

(a*R*)-2'-((*E*)-4-bromostyryl)-2-((*S*)-*p*-tolylsulfinyl)-6-(trifluoromethyl)-1,1'-biphenyl
Chemical Formula: $C_{28}H_{20}BrF_3OS$
Molecular Weight: 541,4262

3g : (a*R*)-2'-((*E*)-4-bromostyryl)-2-((*S*)-p-tolylsulfinyl)-6-(trifluoromethyl)-1,1'-biphenyl.From (S)-2-(p-tolylsulfinyl)-6-(trifluoromethyl)-1,1'-biphenyl (1 equiv., 46 mg, 0.13 mmol), following the P3 for 6h yielded the title compound (32 mg, 0.06 mmol, 47 %); dr = 96 : 4.
^{1}**H-NMR** ($CDCl_3$, 400 MHz) : 8.50, (d, J = 7.8 Hz, 1H), 7.94 (d, J = 7.7 Hz, 1H), 7.83 (t, J = 8.0 Hz, 1H), 7.79 (d, J = 7.8 Hz, 1H), 7.44 (t, J = 7.7 Hz, 1H), 7.38 (d, J = 8.3 Hz, 2H), 7.13 (d, J = 8.3, 2H), 7.08 (d, J = 8.0 Hz, 2H), 7.04-6.96 (m, 4H), 6.66 (d, J = 16.0 Hz, 1H), 6.38 (d, J = 7.5 Hz, 1H), 2.33 (s, 3H) ppm.

^{13}C-NMR ($CDCl_3$, 101 MHz): 147.1, 142.3, 140.9, 136.1, 135.9, 131.7 (4 C_{Ar}), 130.4 (1CH_{Ar} + 1C_{quat}), 129.7 (2 C_{Ar}), 129.3 (1CH_{Ar} + 1C_{quat}), 129.2 (1CH_{Ar} + 1C_{quat}), 128.7 (bs, CF_3), 128.2 (2 C_{Ar}), 127.5, 126.8, 126.6 (2 C_{Ar}), 126.0, 125.3, 121.7, 21.5 ppm. **^{19}F-NMR** ($CDCl_3$, 377 MHz): -58.2 ppm. $[\alpha]_D^{20}$=-201.1° (c = 1.24, $CHCl_3$). **HRMS (ESI):** *calc. for $C_{28}H_{20}BrF_3OSNa^+$ 563.0263*; found 563.0240.

3. Oxidative olefination with a 1,1-disubstituted olefin

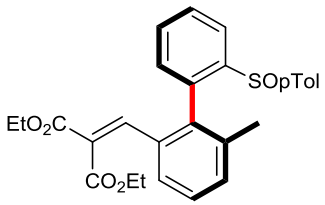

diethyl 2-(((a*R*)-6-methyl-2'-((*S*)-*p*-tolylsulfinyl)-[1,1'-biphenyl]-2-yl)methylene)malonate
Chemical Formula: $C_{28}H_{28}O_5S$
Molecular Weight: 476,5870

4: Diethyl 2-(((*aR*)-6-methyl-2'-((*S*)-p-tolylsulfinyl)-[1,1'-biphenyl]-2-yl)methylene)malonate.

In an oven dried screw-cap tube (7 mL, cap lined with Teflon) were loaded under air (*S*)-2-methyl-2'-(p-tolylsulfinyl)-1,1'-biphenyl (1 equiv., 71 mg, 0.23 mmol), AgOAc (2 equiv., 77.2 mg, 0.46 mmol) and $Pd(OAc)_2$ (10 mol%, 5.2 mg, 0.023 mmol). Then, diethyl ethoxymethylmalonate[286] (3 equiv., 150 mg, 100 µL, 0.69 mmol) and HFIP (1200 µL) were added by syringe and the reaction mixture was stirred at 80 °C for 16 hours. HFIP was then removed under reduced pressure; the crude residue was diluted with diethyl ether and filtrated through a silica/celite plug. Purification of the crude reaction mixture by flash chromatography yielded the title compound (98.3 mg, 0.21 mmol, 89%); dr = 97 : 3. Purification by flash column chromatography enable separation of two atropodiastereomers yet affording atropo-pure diethyl 2-(((*aR*)-6-methyl-2'-((*S*)-p-tolylsulfinyl)-[1,1'-biphenyl]-2-yl)methylene)malonate (91.9 mg, 0.19 mmol, 83 %).

^{1}H NMR ($CDCl_3$, 400 MHz): δ = 8.31 (d, J = 7.8 Hz, 1H), 7.68 (t, J = 7.6 Hz, 1H), 7.53 (t, J = 7.4 Hz, 1H), 7.42 (d, J = 7.7 Hz, 1H), 7.38 (s, 1H), 7.29 (t, J = 7.7 Hz, 1H), 7.08 (d, J = 7.4 Hz, 1H), 7.04 (d, J = 7.7 Hz, 2H), 7.02 (d, J = 8.2 Hz, 1H), 6.92 (d, J = 8.1 Hz, 2H), 4.31 (dq, J = 5.9, 1.2 Hz, 2H), 4.18 (dq, J = 4.9, 2.3 Hz, 2H), 2.31 (s, 3H), 1.27 (t, J = 7.1 Hz, 3H), 1.23 (t, J = 7.1 Hz, 3H), 1.09 (s, 3H) ppm. **^{13}C NMR** ($CDCl_3$, 101 MHz): δ = 166.4, 163.7, 144.2, 142.1, 140.9, 140.9, 138.4, 137.3, 136.2, 132.8, 131.8, 130.8, 130.4, 129.6 (2 $C_{p\text{-}Tol}$), 129.2, 128.6, 128.2, 126.8 (2 $C_{p\text{-}Tol}$), 125.8, 123.8, 61.6, 61.5, 21.5, 19.6, 14.1, 14.0 ppm. $[\alpha]_D^{20}$ = -37.34 ° (c = 1.02, $CHCl_3$). **HRMS (ESI) :** *calc. for $C_{28}H_{29}O_5S^+$ 477.1730* ; found 477.1748.

4. Post-functionalization of 2a

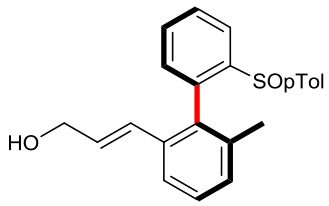

(*E*)-3-((a*R*)-6-methyl-2'-((*S*)-*p*-tolylsulfinyl)-[1,1'-biphenyl]-2-yl)prop-2-en-1-ol
Chemical Formula: $C_{23}H_{22}O_2S$
Molecular Weight: 362,4870

(*E*)-3-((*aR*)-6-methyl-2'-((*S*)-p-tolylsulfinyl)-[1,1'-biphenyl]-2-yl)prop-2-en-1-ol: To a solution of methyl (*E*)-3-((a*R*)-6-methyl-2'-((*S*)-p-tolylsulfinyl)-[1,1'-biphenyl]-2-yl)acrylate (1 equiv., 300 mg, 0.77 mmol) in THF (11 mL) at -78 °C was added DIBAL (4 equiv., 3.1 mL, 3.09 mmol, 1 M in THF) and the reaction mixture was stirred at -78 °C for 6 h. The mixture was quenched at -78 °C with a sat. solution of sodium tartrate and stirred at room temperature overnight. The crude mixture was extracted with EtOAc, washed with water, brine and dried over Na_2SO_4. Flash chromatography (DCM : EtOAc from 80/20 to 50/50) afforded (*E*)-3-((*aR*)-6-methyl-2'-((*S*)-p-tolylsulfinyl)-[1,1'-biphenyl]-2-yl)prop-2-en-1-ol (235 mg, 0.65 mmol, 85 %).

^{1}H NMR ($CDCl_3$, 400 MHz): δ = 8.10 (d, *J* = 7.4 Hz, 1H$_{Ar}$), 7.61 (t, *J* = 8.0 Hz, 1H$_{Ar}$), 7.52-7.47 (m, 2H$_{Ar}$), 7.32 (t, *J* = 7.6 Hz, 1H$_{Ar}$), 7.14 (d, J = 7.6, 1H$_{Ar}$); 7.10-7.09 (m, 3H$_{Ar}$), 7.04-7.02 (m, 2H$_{Ar}$), 6.34-6.23 (m, 2H$_{vinyl}$), 4.18-4.07 (m, 2H), 2.31 (s, 3H), 1.47 (s, 3H) ppm.
^{13}C NMR ($CDCl_3$, 101 MHz): δ = 144.8, 141.6, 140.9, 137.5, 137.1, 136.4, 135.4, 132.6, 130.9, 130.4, 130.0, 129.6 (2 C$_{p\text{-}Tol}$), 129.5, 129.1, 128.7, 125.5 (2 C$_{p\text{-}Tol}$), 124.5, 123.6, 63.8, 21.4, 20.1 ppm.
$[\alpha]_D^{20}$ = -85.4° (c = 0.50, $CHCl_3$).

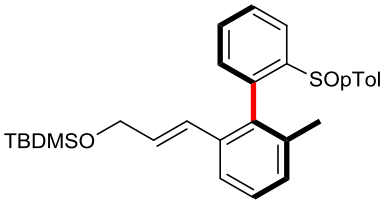

tert-butyldimethyl(((*E*)-3-((a*R*)-6-methyl-2'-((*S*)-*p*-tolylsulfinyl)-[1,1'-biphenyl]-2-yl)allyl)oxy)silane
Chemical Formula: $C_{29}H_{36}O_2SSi$
Molecular Weight: 476,7500

5 : di-tert-butyl(methyl)(((*E*)-3-((a*R*)-6-methyl-2'-((*S*)-p-tolylsulfinyl)-[1,1'-biphenyl]-2-yl)allyl)oxy)silane. To a solution of TBDMSCl (1.2 equiv., 111 mg, 0.13 mL, 0.74 mmol) in DMF (1.25 mL) at 0°C was added imidazole (2.5 equiv., 105 mg, 1.54 mmol). The reaction mixture was stirred at 0 °C for 5min. Then a solution of **(*E*)-**

3-((*aR*)-6-methyl-2'-((*S*)-p-tolylsulfinyl)-[1,1'-biphenyl]-2-yl)prop-2-en-1-ol (1 equiv., 224 mg, 0.62 mmol) in DMF (1.25 mL) was added and the reaction mixture was stirred at room temperature overnight. The reaction mixture was quenched with water and diluted with EtOAc. The aqueous layer was extracted twice with EtOAc. The combined organic layers were washed with brine, dried over Na_2SO_4, filtered and concentrated to afford the crude product which was purified by flash chromatography (cyclohexane/EtOAc from 95:5 to 85:15) to afford the titled compound **5** (258 mg, 0.54 mmol, 88%).

^{1}H NMR ($CDCl_3$, 400 MHz): δ = 8.29 (d, *J* = 7.9 Hz, 1H$_{Ar}$), 7.64 (td, *J* = 7.9, 1.2 Hz, 1H$_{Ar}$), 7.54-7.44 (m, 2H$_{Ar}$), 7.28 (t, *J* = 7.7 Hz, 1H$_{Ar}$), 7.11-6.83 (m, 6H$_{Ar}$), 6.32-6.17 (m, 2H$_{vinyl}$), 4.21 (qd, *J* = 15.1, 3.7 Hz, 2H), 2.30 (s, 3H), 1.06 (s, 3H), 0.80 (s, 9H), -0.03 (s, 3H), -0.04 (s, 3H) ppm.
^{13}C NMR ($CDCl_3$, 101 MHz): δ = 144.1, 141.9, 141.1, 137.8, 137.6, 136.2, 135.2, 131.7, 130.7, 130.7, 129.5 (2 C$_{p\text{-}Tol}$), 129.0, 128.7, 128.6, 127.0, 126.8 (2 C$_{p\text{-}Tol}$), 123.6, 123.3, 63.8, 26.1, 21.6, 19.8, 18.4, -5.1, -5.2 ppm.
$[\alpha]_D^{20}$ = -84.0° (c = 0.50, $CHCl_3$).
HRMS (ESI): *calc. for $C_{29}H_{36}O_2SSiNa^+$ 499.2097*; found 499.2086

Sulfoxyde-Metal Exchange and further functionnalization

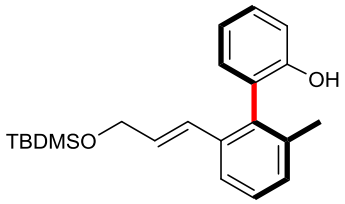

(a*R*,*E*)-2'-(3-((*tert*-butyldimethylsilyl)oxy)prop-1-en-1-yl)-6'-methyl-[1,1'-biphenyl]-2-ol
Chemical Formula: $C_{22}H_{30}O_2Si$
Molecular Weight: 354,5650

6: (a*R,E*)-2'-(3-((tert-butyl(dimethyl)silyl)oxy)prop-1-en-1-yl)-6'-methyl-[1,1'-biphenyl]-2-ol. To a solution of **5** (1 equiv., 50 mg, 0.11 mmol) in THF (1.20 mL) at -78 °C *n*-BuLi (2 equiv., 1.6 M, 0.13 mL, 0.21 mmol) was added. After 10 min of stirring at -78 °C a solution of trimethyl borate (10 equiv., 108 mg, 0.12 mL, 1.05 mmol) and ethoxyethane trifluoroborane (5 equiv., 74.4 mg, 66 µL, 0.52 mmol) in Ether (0.2 mL) was cannulated. The reaction mixture was allowed to warm up to 0 °C and stirred for 30 min. Then, NaOH 3M (5.72 equiv., 0.2 mL, 0.60 mmol) and H_2O_2 (5.6 equiv., 66.6 mg, 0.06 mL, 0.59 mmol) were quickly added and the reaction mixture was allowed to warm up to room temperature. The reaction mixture was worked-up with DCM and water, the phases were separated and the combined organic phases were dried over sodium sulfate. Evaporation of the solvent under reduced pressure yielded the crude product, which was purified by flash chromatography (cyclohexane / EtOAc 95:5) to afford (a*R,E*)-2'-(3-((tert-butyl(dimethyl)silyl)oxy)prop-1-en-1-yl)-6'-methyl-[1,1'-biphenyl]-2-ol (15 mg, 0.042 mmol, 40%).

^{1}H NMR ($CDCl_3$, 400 MHz): δ = 7.55 (d, J = 8.2 Hz, 1H), 7.35-7.18 (m, 3H), 7.07-6.96 (m, 3H), 6.32-6.16 (m, 2H), 4.53 (s, 1H), 4.18 (d, J = 8.1 Hz, 2H), 2.04 (s, 3H), 0.82 (s, 9H), -0.08 (s, 6H) ppm.
^{13}C NMR ($CDCl_3$, 101 MHz): δ = 152.5, 138.2, 137.1, 133.8, 130.8, 130.4, 129.3, 129.2, 128.5, 126.9, 125.5, 123.3, 120.7, 115.4, 63.6, 25.9 (3 $C_{t\text{-}Bu}$), 20.3, 18.3, -5.4 (2 C) ppm.
HRMS (ESI): *calc. for $C_{24}H_{36}O_2SiNa^+$ 377.1907* ; found 377.1926

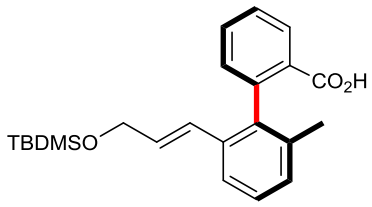

(a*R*,*E*)-2'-(3-((*tert*-butyldimethylsilyl)oxy)prop-1-en-1-yl)-6'-methyl-[1,1'-biphenyl]-2-carboxylic acid
Chemical Formula: $C_{23}H_{30}O_3Si$
Molecular Weight: 382,5750

7: (*aR,E*)-2'-(3-((di-tert-butyl(methyl)silyl)oxy)prop-1-en-1-yl)-6'-methyl-[1,1'-biphenyl]-2-carboxylic acid. To a solution of tert-butyl(dimethyl)(((*E*)-3-((a*R*)-6-methyl-2'-((*S*)-p-tolylsulfinyl)-[1,1'-biphenyl]-2-yl)allyl)oxy)silane (1 equiv., 30 mg, 0.063 mmol) in THF (1.20 mL) at -78 °C was added a solution of *t*-BuLi (2.1 equiv., 1.7 M, 78 µL, 0.13 mmol). The reaction mixture was stirred at -78 °C for 10 min then was poured into a solution of freshly crushed dry ice in THF (3.6 mL) and the reaction mixture was stirred at room temperature for 15min. The mixture was quenched with water, diluted with EtOAc and acidified with a 1M HCl solution to pH 1. The aqueous layer was extracted twice with EtOAc. The combined organic layers were washed with brine, dried over Na_2SO_4, filtered and concentrated under reduced pressure to afford the crude product. Flash chromatography (cyclohexane : EtOAc 90/10 to 80/20) yielded atropisomerically pure (*aR,E*)-2'-(3-((di-tert-butyl(methyl)silyl)oxy)prop-1-en-1-yl)-6'-methyl-[1,1'-biphenyl]-2-carboxylic acid **7** (19 mg, 0.05 mmol, 78 %).

^{1}H NMR ($CDCl_3$, 400 MHz): δ = 8.10 (dd, *J* =7.9, 1.1 Hz, 1H_{Ar}), 7.58 (td, *J* =7.6, 1.5 Hz, 1H_{Ar}), 7.48-7.38 (m, 2H_{Ar}), 7.22 (t, *J* = 7.6 Hz, 1H_{Ar}), 7.16-7.08 (m, 2H_{Ar}), 6.11-6.06 (m, 2H_{vinyl}), 4.14 (qd, *J* = 15.4, 6.1, 1.8 Hz, 2H), 1.94 (s, 3H), 0.77 (s, 9H), -0.08 (s, 3H), -0.09 (s, 3H) ppm.
^{13}C NMR ($CDCl_3$, 101 MHz): δ = 167.7, 137.2, 136.3, 135.4, 134.9, 134.4, 130.8, 128.9, 128.7, 127.5, 127.4, 123.9, 121.0, 104.4, 92.5, 64.3, 27.3, 26.8 (3 $C_{t\text{-}Bu}$), -1.3 (2 C) ppm.
$[\alpha]_D^{20}$ = -58.3 ° (c = 0.52, $CHCl_3$).
HRMS (ESI): *calc. for $C_{23}H_{30}O_3SSiNa^+$ 405.1846*; found 450.1842.

HPLC : colonne AD-H, hexane/*i*-PrOH 85:15, flow: 1mL/min; C = 1mg/mL; R_T = 3.88 min; R_T = 5.13 min

Racemic sample

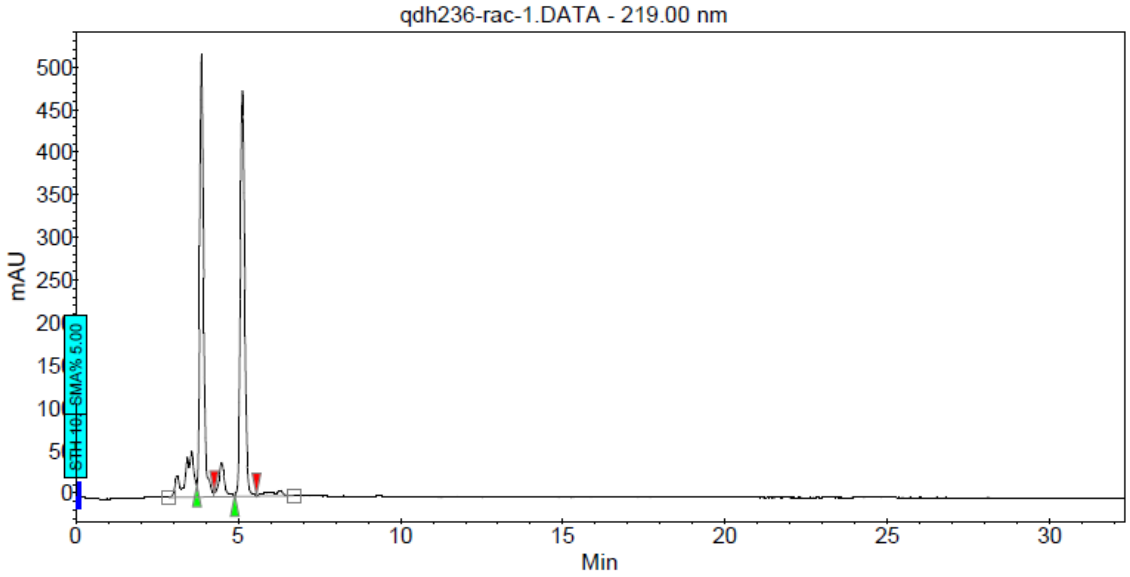

Peak results :

Index	Name	Time [Min]	Quantity [% Area]	Height [mAU]	Area [mAU.Min]	Area % [%]
1	UNKNOWN	3.88	48.89	520.0	72.1	48.888
2	UNKNOWN	5.13	51.11	476.2	75.3	51.112
Total			100.00	996.2	147.4	100.000

Atropo-enantiopur sample:

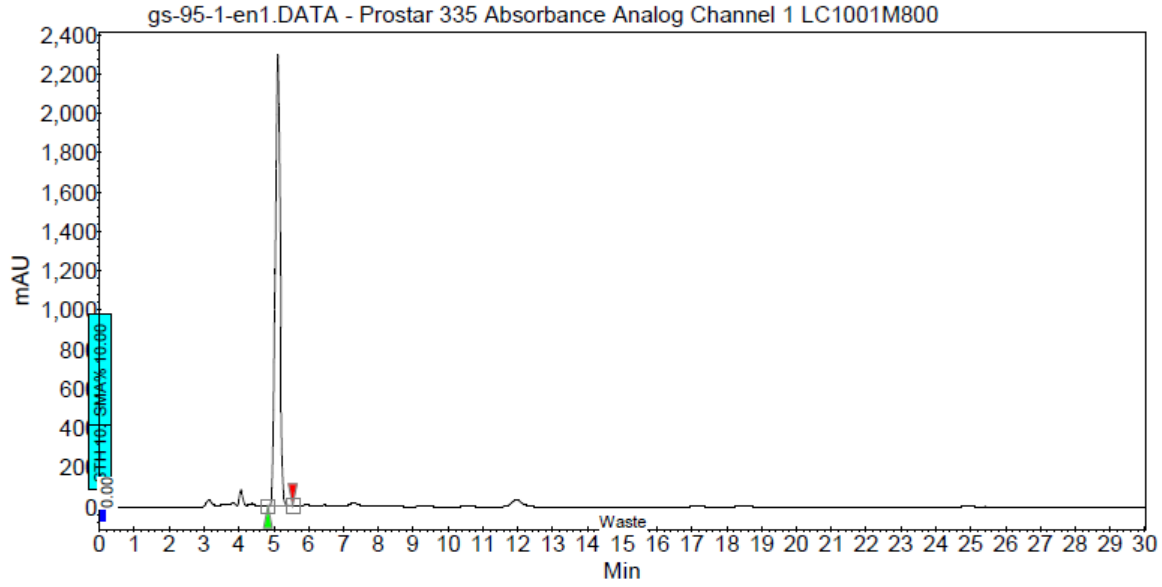

Peak results :

Index	Name	Time [Min]	Quantity [% Area]	Height [mAU]	Area [mAU.Min]	Area % [%]
1	UNKNOWN	5.12	100.00	2297.8	377.7	100.000
Total			100.00	2297.8	377.7	100.000

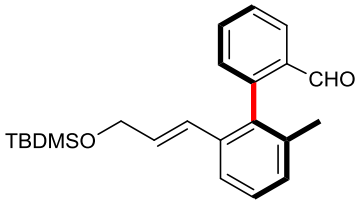

(*R*,*E*)-2'-(3-((*tert*-butyldimethylsilyl)oxy)prop-1-en-1-yl)-6'-methyl-[1,1'-biphenyl]-2-carbaldehyde
Chemical Formula: $C_{23}H_{30}O_2Si$
Molecular Weight: 366,5760

8 : (*aR,E*)-2'-(3-((di-tert-butyl(methyl)silyl)oxy)prop-1-en-1-yl)-6'-methyl-[1,1'-biphenyl]-2-carbaldehyde. To a solution of **5** (1 equiv., 50 mg, 0.105 mmol) in THF (1.20 mL) at -78 °C was added a solution of *t*-BuLi (2 equiv., 1.6 M, 0.13 mL, 0.21 mmol). The reaction mixture was stirred at -78 °C for 15 min. then neat DMF (6.16 equiv., 28.4 mg, 0.03 mL, 0.39 mmol) was added and the reaction mixture was stirred for 1 while being allowed to warm up. The reaction was quenched by a saturated aqueous solution of ammonium chloride and worked-up with ethyl acetate and water. The crude product was purified by flash chromatography, yielding (*aR,E*)-2'-(3-((di-tert-butyl(methyl)silyl)oxy)prop-1-en-1-yl)-6'-methyl-[1,1'-biphenyl]-2-carbaldehyde **8** (11 mg, 0.030 mmol, 48 %).

^{1}H NMR ($CDCl_3$, 400 MHz): δ = 8.59 (d, J = 0.6 Hz, 1H), 8.02 (dd, J = 7.8, 1.0 Hz, 1H), 7.65 (td, J = 7.5, 1.4 Hz, 1H), 7.51-7.46 (m, 2H), 7.29 (t, J = 7.7 Hz, 1H), 7.21 (d, J = 7.0, 1H), 7.17 (d, J = 7.5 Hz, 1H), 6.14 (brs, 2H), 4.14 (brs, 2H), 1.96 (s, 3H), 0.75 (s, 9H), 0.09 (s, 3H), -0.10 (s, 3H) ppm.
^{13}C NMR ($CDCl_3$, 101 MHz): δ = 192.1, 144.2, 136.7, 136.5, 135.9, 134.2, 134.1, 131.0, 130.9, 128.8, 128.2, 128.0, 127.3, 127.0, 122.9, 63.3, 25.8 3 ($C_{t\text{-}Bu}$), 20.9, 18.2, -5.4 (2 C) ppm.
HRMS (ESI) : *calc. for $C_{23}H_{30}O_2SSiNa^+$ 389.1907* ; found 389.1908

5. Mechanistic studies

Glassware and magnetic stirrers were washed with an *aqua regia* solution, dried in an oven, cooled down and kept in a silica gel dessicator containing a cobalt chloride indicator. HFIP and $CDCl_3$ were kept on 4 Å molecular sieves (activated by heating them at 180 °C under vacuum overnight).

For quantitative NMR the FT-FID was treated as follow: a zero-filling was applied, then a FT of the proper number of points and finally a polynomial baseline correction. A phase correction was applied before the baseline correction only if absolutely necessary and only if the phase of all signals of interest could be properly corrected. ^{19}F NMR spectra were recorded decoupled from proton.

a) KIE

In 1,2-DCE at 80 °C :

Stock solutions of **6'-H-1c** (**SS-6'-H-1c**) and **6'-D-1c** (**SS-6'-D-1c**) were prepared in 1,2-DCE (0.486 M), Stock solution of palladium diacetate (**SS-Pd-I**) was prepared in 1,2-DCE (0.049 M).

Two sealed tubes were charged with 500 µL of either **SS-6'-H-1c** (corresponding to 88.6 mg of **6'-H-1c**, 0.243 mmol, 1 equiv.) or **SS-6'-D-1c** respectively (corresponding to 87.5 mg of **6'-D-1c**, 0.243 mmol, 1 equiv.) and 500 µL of **SS-Pd-I** (corresponding to 5.5 mg of $Pd(OAc)_2$, 0.0245 mmol, 10 mol%). AgOAc (244 mg, 1.458 mmol, 6 equiv.) was added to each tube. The syringes were washed with 100 µL of 1,2-DCE, which was added to the appropriate reaction mixture. Then, 10 µL of 1,4-bis(trifluoromethyl)benzene was added as an internal standard to each reaction mixture. Finally, with a 5 min. interval, 45 µL of methyl acrylate was added along with a magnetic stir bar and the sealed tubes were stirred (750 rpm) at 80 °C.

The sampling (by withdrawing of aliquots) was started after 105 min. (conversion of at least 5 %), and was done at 45 min. intervals as follows: the sealed tube was removed from the oil bath, cooled down in an ice water bath for 20 s. and then allowed to decant for 40 s; 40 µL aliquot was then withdrawn and deposited on a small Celite pad (~2 cm^3) in an oven-dried glass wool plugged Pasteur pipette. The micro syringe was washed with $CDCl_3$ (2 x 50 µL deposited on the Celite pad) and the Celite pad was washed with a further 600 µL of $CDCl_3$. The progress of the reaction was monitored by ^{19}F NMR.

	DCE 80 °C (min x 10^{-1})	**6'-H-1c**	**6'-D-1c**
	0	0	0
t1	10.5	0.134	0.0481
t2	15	0.177	
t3	19.5	0.224	0.086
t4	24	0.256	0.1015
t5	28.5		0.1207
t6	33	0.3238	0.1364
t7	37.5	0.3773	0.1523

KIE = 2.2

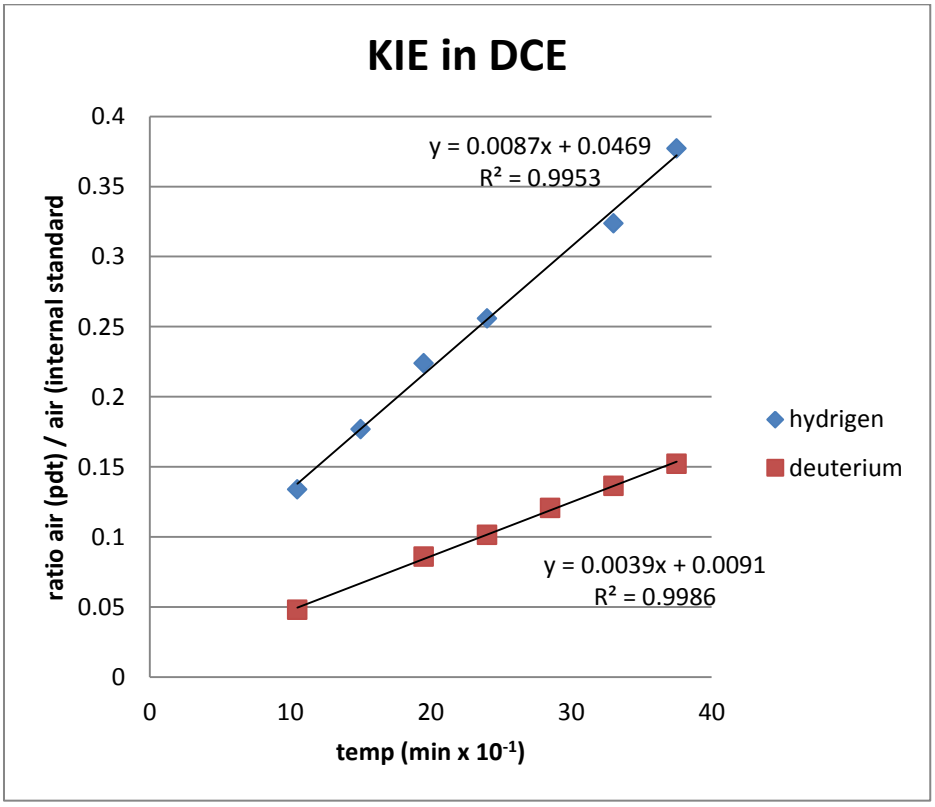

In HFIP at 23 °C :

Stock solutions of **6'-H-1c** (**SS-6'-H-1c**) and **6'-D-1c** (**SS-6'-D-1c**) were prepared in HFIP (0.49 M), Stock solution of palladium diacetate (**SS-Pd-I**) was prepared in HFIP (0.049 M).

Two sealed tubes were charged with 500 µL of either **SS-6'-H-1c** (corresponding to 88.2 mg of **6'-H-1c**, 0.245 mmol, 1 equiv.) or **SS-6'-H-1c** respectively (corresponding to 88.5 mg of **6'-D-1c**, 0.245 mmol, 1 equiv.) and 500 µL of **SS-Pd-I** (corresponding to 5.5 mg of $Pd(OAc)_2$, 0.0245 mmol, 10 mol%). AgOAc (84 mg, 0.50 mmol, 2 equiv.) was added to each tube. The syringes were washed with 100 µL of HFIP, which was added to the appropriate reaction mixture. Then, 10 µL of 1,4-bis(trifluoromethyl)benzene was added as an internal standard to each reaction mixture. Finally, with a 5 min. interval, 45 µL of methyl acrylate was added along with a magnetic stir bar and the sealed tubes were stirred (750 rpm) at 23 °C.

The sampling (by withdrawing of aliquots) was started after 105 min. (conversion of at least 5 %), and was done at 30 min. intervals as follows: the sealed tube was removed from the oil bath, cooled down in an ice water bath for 20 s. and then allowed to decant for 40 s. An 40 µL aliquot was then withdrawn and deposited on a small Celite pad (~2 cm^3) in an oven-dried glass wool plugged Pasteur pipette. The micro syringe was washed with $CDCl_3$ (2 x 50 µL deposited on the Celite pad) and the Celite pad was washed with a further 600 µL of $CDCl_3$. The progress of the reaction was monitored by ^{19}F NMR.

	HFIP 23 °C (min x 10^{-1})	**6'-H-1c**	**6'-D-1c**
t0	0	0	0
t1	10.5	0.164	0.0629
t2	13.5	0.193	0.0696
t3	16.5	0.227	0.076
t4	19.5	0.264	
t5	22.5	0.308	0.0878
t6	25.5	0.3515	0.0971
t7	28.5	0.396	0.104
t8	31.5	0.423	0.107

KIE = 5.9

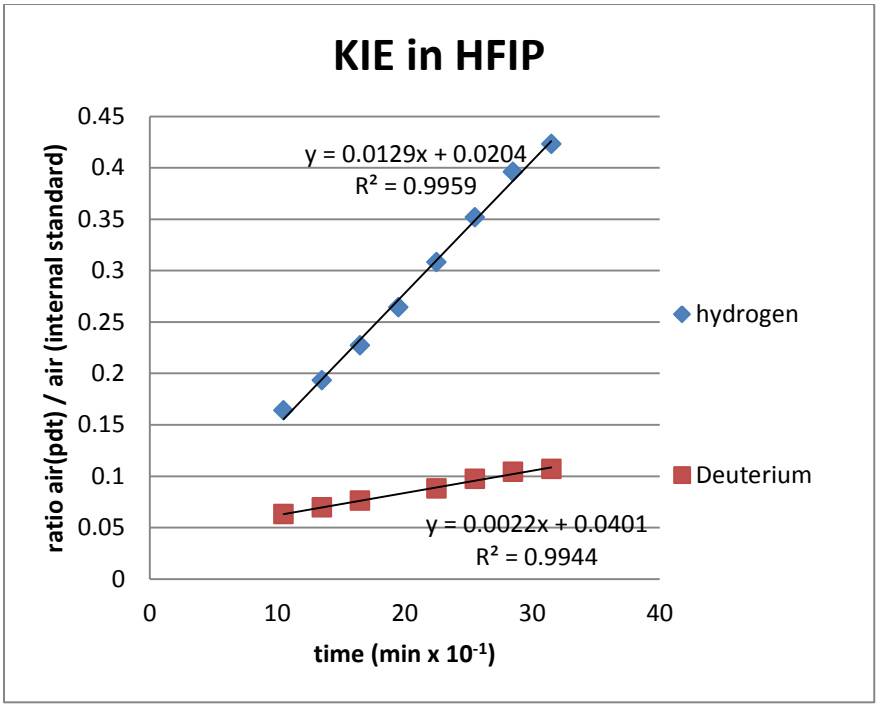

b) Solvent effect

Stock solutions of **1a** (**SS-1a**) (1 equiv, 0.8 M) and $Pd(OAc)_2$ (**SS-Pd-II**) (10 mol%, 0.08 M) were prepared in the appropriate solvent.

Sealed tubes were charged with AgOAC (6.5 mg, 0.04 mmol, 2 equiv), 25 µL of **SS-1a** (corresponding to 6.1 mg, 0.02 mmol, 1 equiv.) and 25 µL of **SS-Pd-II** (corresponding to 0.45 mg, 0.002 mmol, 10 mol%). The reaction mixtures were then diluted with the appropriate solvent(s) to obtain a final concentration of 0.2 M. Finally, methylacrylate (3.6 µL, 0.04 mmol, 2 equiv.) was added with a micro syringe and the reactions were stirred at 25 °C and at 750 rpm for the stated time.

Firstly, a qualitative analysis was performed by means of TLC, using **1a** and **2a** as references: an aliquot was withdrawn with a capillary and directly applied on the TCL plate. The TLC plate was then put in an oven (~100 °C) for at least 10 min. to remove all remaining solvent. If TLC showed more than a trace of the expected product, a quantitative ^1H NMR analysis was peformed: the reaction mixture was filtrated on a Dicalite/silica (40-63 µm) plug and washed with diethyl ether. The solvent was then removed under reduced pressure and the crude mixture dried under vacuum. All the crude mixture was then taken up in $CDCl_3$, and ^1H spectra was recorded to determine the conversion.

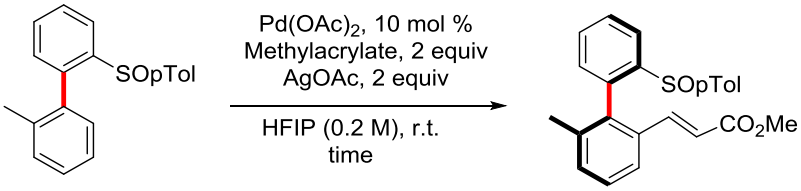

Solvent	**Time**	**Conversion (%)**
*i*PrOH	3 d	-
DCE	2 d	-
$CHCl_3$	3 d	Traces
*i*PrOH / HFIP (9 : 1)	3 d	-
DCE / HFIP (9 : 1)	5 d	98
DCE / AcOH (9 : 1)	2 d	-
DCE / HFIP (1 equiv) (47 : 1 v/v)[a]	16 h	5
DCE / HFIP (5 equiv) (8.5 : 1 v/v) [a]	16 h	10
DCE / HFIP (10 equiv) (3.2 : 1 v/v) [a]	16 h	30
DCE / HFIP (20 equiv) (1.4 : 1 v/v) [a]	**16 h**	**46**
HFIP [a]	**16 h**	**44**

a) at 0.04 mmol scale; indicated conversion is an average value of 2 runs

c) NMR study of H-bonding properties

0.08 M solution of **1a** in $CDCl_3$ as prepared. 0.6 mL of this solution was introduced to the NMR tube and ^1H spectra was recorded (S0). HFIP was added portion wise to this sample and the corresponding NMR spectra were recorded.

Sample	Amount **1a** (mmol)	Amount HFIP	Expected Ratio **1a** / HFIP	Observed ratio **1a** / HFIP
S0	0.048 mmol	-	-	-
S1	0.048 mmol	2 µL, 0.019 mmol	1 : 0.4	1 : 0.4
S2	0.048 mmol	4 µL, 0.038 mmol	1 : 0.8	1 : 1
S3	0.048 mmol	8 µL, 0.076 mmol	1 : 1.6	1 : 1.8
S4	0.048 mmol	24 µL, 0.23 mmol	1 : 5	1 : 6
S5	-	4 µL, 0.038 mmol	-	-

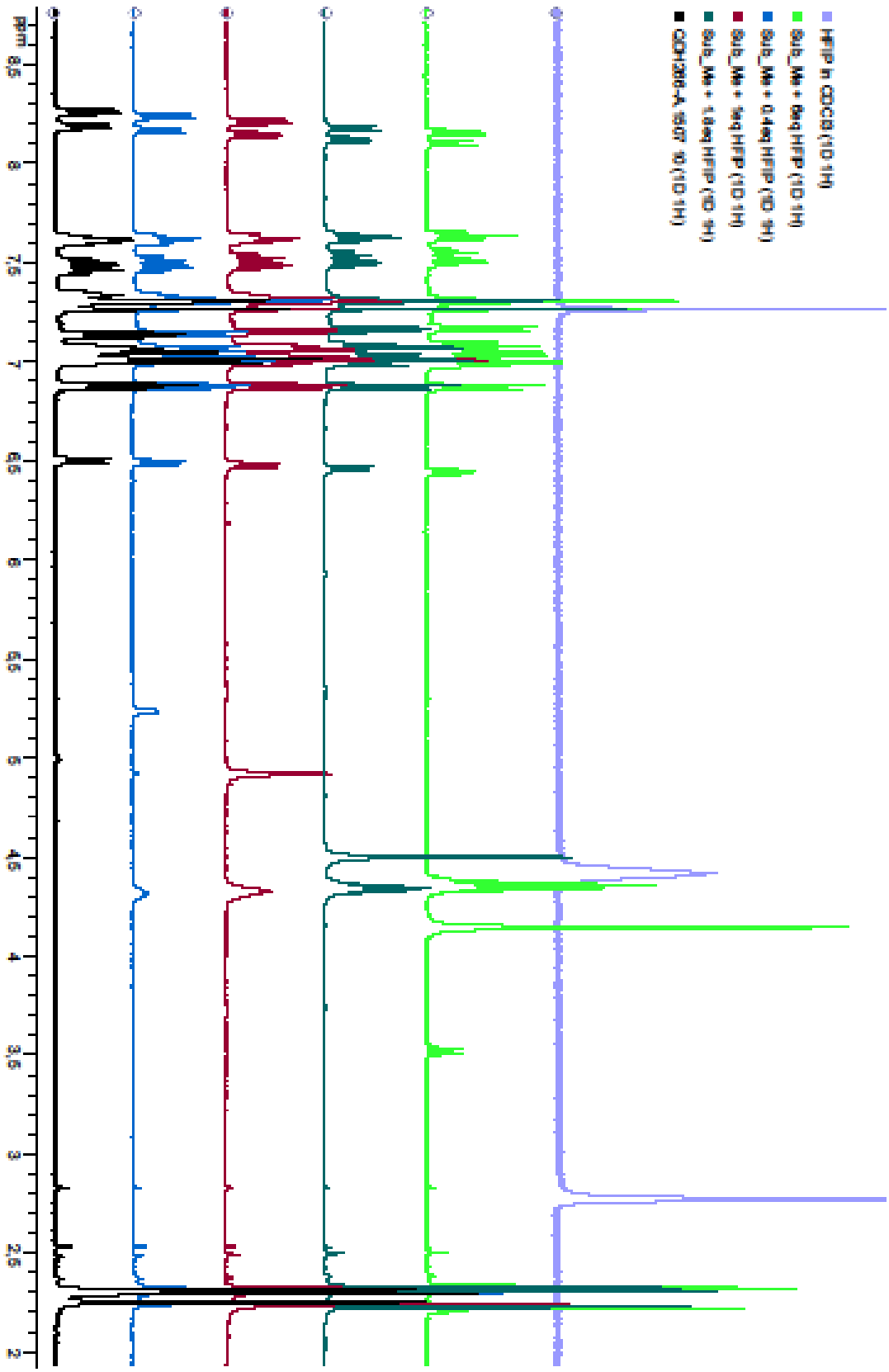

NMR titration of 1a by HFIP

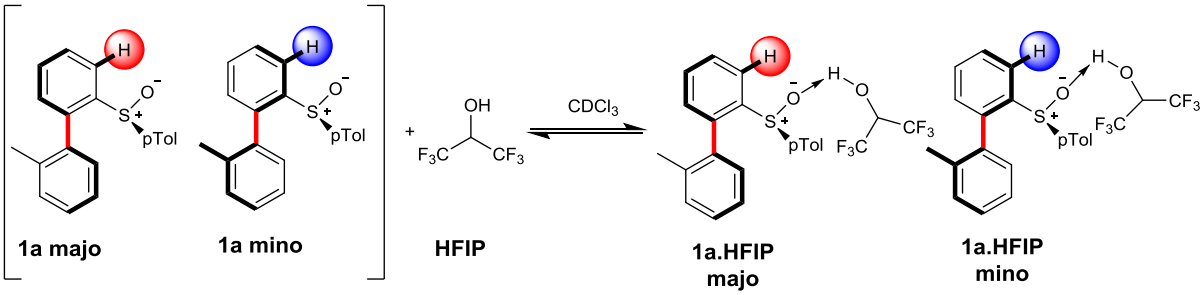

This study concerns formation of Lewis acid-base adduct between the oxygen of the sulfoxyde of (*S*)-(2-(p-tolylsulfinyl)-2'-methyl-1,1-biphenyl (**1a**) and the alcoholic hydrogen of 1,1,1,3,3,3-hexafluoropropan-2-ol (HFIP).

To calculate equilibrium constant of formation of **1a.HFIP** adduct at 20 °C, the concentration of **1a** was kept constant and an increasing amount of HFIP was added, resulting in upfield shift of **3-H 1a** proton (proton *ortho* to the sulfoxyde).

The equilibrium constant of formation of **1a.HFIP** is : $K_{eq} = \frac{[1a.HFIP]}{[1a][HFIP]}$

As the system is under a fast exchange regime, the chemical shift of the afromentioned proton is a mole-fraction weighted average of its chemical shift in free **1a** and its chemical shift in the hydrogen-bond complex **1a.HFIP**.

To ensure the formation of 1:1 complex between **1a** and HFIP the ratio **1a : HFIP** is superior to 2:1.

Following the Benesi-Hildebrand equation, the equilibrium constant can be written [271]:

$$K_{eq} = \frac{\Delta\delta_{obs}}{(\Delta\delta_{excess} - \Delta\delta_{obs})\left([HFIP^0] - \frac{([1a^0]\Delta\delta_{obs})}{\Delta\delta_{excess}}\right)} \quad (eq.1)$$

$\Delta\boldsymbol{\delta_{obs}}$: measured shift of the 3-H 1a proton from its initial value (in absence of HFIP)

$$\Delta\boldsymbol{\delta_{obs}} = \Delta\boldsymbol{\delta_{1a\,(mesured)}} - \Delta\boldsymbol{\delta_{1a\,(initial)}}$$

$\Delta\boldsymbol{\delta_{excess}}$: change in the chemical shift of 3-H 1a proton between the completely complexes 1a and uncomplexed, free **1a**.
$[HFIP^0]$: total concentration of **HFIP**
$[1a^0]$: total concentration of **1a**

$\Delta\delta_{excess}$ and K_{eq} are not known, but these are constant at a given temperature and can be calculated on a basis of series of measurements of $\Delta\boldsymbol{\delta_{obs}}$ as a function of $[HFIP^0]$ and by further curve fitting with eq. 1.

Accordingly: $= \frac{\Delta\delta_{obs}}{\Delta\delta_{excess}}$; $x = \frac{[HFIP^0]}{[1a^0]}$; and $b = K_{eq} \cdot [1a^0]$,

$(eq.1)$ can be rearranged into quadratic form : $0 = \mathrm{b}\,y^2 - (1 + \mathrm{b}(1 + \mathrm{x}))\,\mathrm{y} + \mathrm{bx}$, which can be integrated[287] as

$$y = \frac{\big(1 + b(1 + x)\big) \pm \sqrt{(1 + b(1 + x))^2 - 4b^2 x}}{2b} \; (eq.2)$$

and, with $y = \frac{\Delta\delta_{obs}}{\Delta\delta_{excess}}$, $(eq.2)$ can be written with $\Delta\delta_{obs}$ as a function of the molar ratio

x = $\frac{[HFIP^0]}{[1a^0]}$:

$$\Delta\delta_{obs} = \Delta\delta_{excess} \frac{\big(1 + b(1 + x)\big) - \sqrt{(1 + b(1 + x))^2 - 4b^2 x}}{2b} \; (eq.3)$$

$(eq.3)$ is solved using a non-linear least squares curve fitting program[288].

Procedure :

Abbreviation:

1a majo : signals corresponding to the 3-H proton of the major diastereomer of **1a**

1a mino : signals corresponding to the 3-H proton of the minor diastereomer of **1a**

Sept. HFIP : signal corresponding to OH-C***H***$(CF_3)_2$

A stock solution of **1a** (336.4 mg, 1.098 mmol) in benzene-d6 (10 g, 10.53 mL) was agitated over 3 Å molecular sieves overnight. Similarly HFIP was agitated over 3 Å molecular sieves overnight.

A 1 mL graduated NMR tube was filled the stock solution of **1a** in benzene-d6 (1 mL, 0.104 mmol, 0.104 mol/L), and an ^{1}H NMR spectra was recorded. Then HFIP (by increment of ~1 µL) was added until ~5 µL total were added. An ^{1}H NMR was recorded between each addition.

A zero-filling of 32,768 points was applied to the FID, followed by a Fourrier transform over 65,536 points. Then a polynomial baseline correction was applied, and the relevant signals (**1a** majo, **1a** mino, sept. HFIP) were integrated over $\pm$ 25 Hz.

Results :

NMR integration relative to OH-C***H***$(CF_3)_2$							
1a majo	**1a** mino	**1a**/HFIP	[**1a**]tot (mol/L)	**1a** (mol/L)	majo/**1a**	**1a** (mol/L)	mino/**1a**
3.634	2.992	6.626	0.104	0.548		0.452	
2.224	1.841	4.065		0.547		0.453	
1.620	1.373	2.993		0.541		0.459	
1.386	1.170	2.556		0.542		0.458	
1.042	0.882	1.924		0.542		0.458	
				mean **0.544**		mean **0.456**	

Accordingly:

[**1a**]majo = 0.104 * 0.544 = 0.057

[**1a**]majo = 0.104 * 0.456 = 0.047

H-complex equilibrium constant calculus for the major atropodiastereomer :

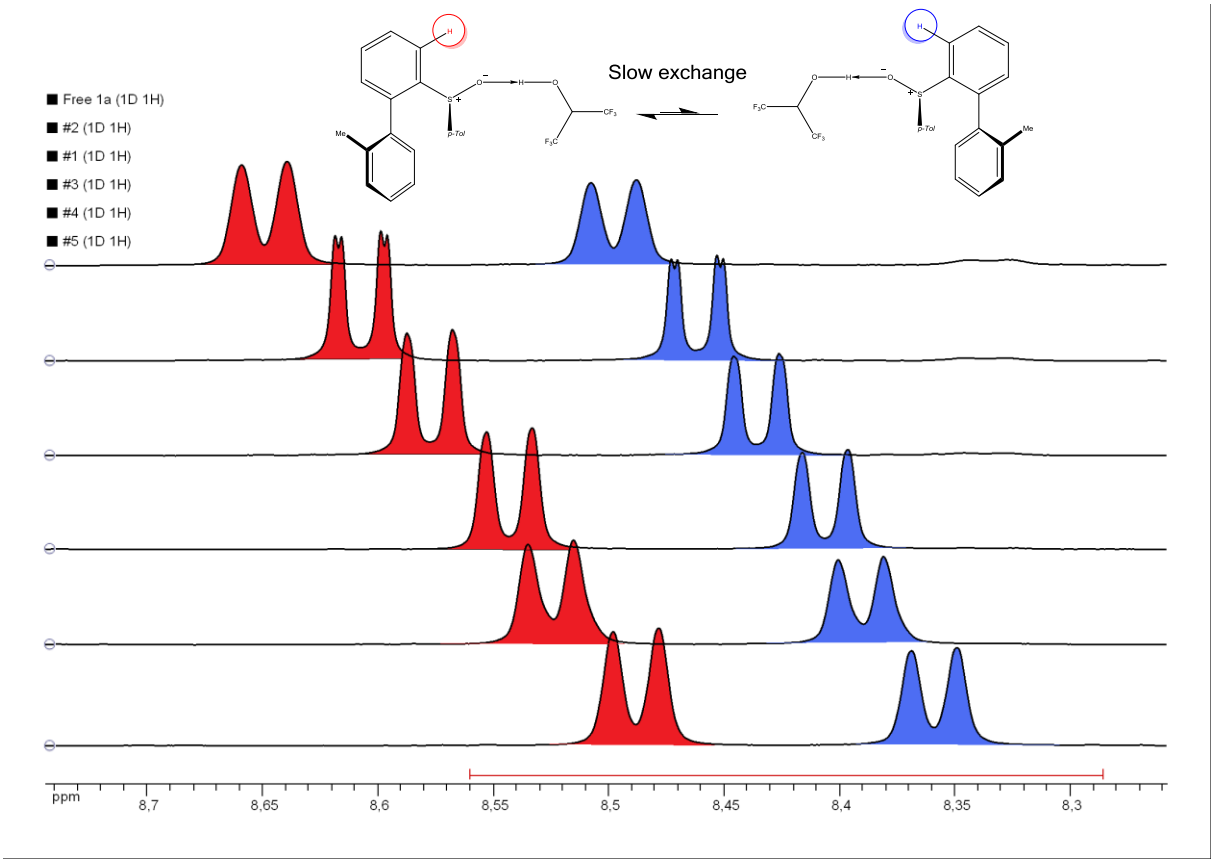

measure #	δ**1a** majo (ppm)	Δδ**1a** **(**ppm)	[**1a**]majo (mol/L)	[HFIP°] (mol/L)	x=[HFIP]°/ [1a]° majo	y = Δδ**1a** majo
0	8.649	0.000	0.057	0.000		
1	8.607	0.042	0.057	0.016	0.277	0.042
2	8.577	0.072	0.057	0.026	0.452	0.072
3	8.542	0.107	0.057	0.035	0.614	0.107
4	8.525	0.124	0.057	0.041	0.719	0.124
5	8.487	0.162	0.057	0.054	0.955	0.162

By entering the x and y value into the MatLab web applet[288] and choosing as rough guesses values of 2 and 4 for the a and b fit parameters (c is indeed zero), we found :

========== Results ==========

a = 0.503 $\pm$ 0.239 and a = $\Delta\delta_{excess}^{majo}$

b = 1.053 $\pm$ 0.27 and $b = K_{eq} \cdot [1a_{majo}^{0}]$, giving :

$$K_{eq}^{majo} = 18.474 \pm 4.74\ L/mol$$

H-complex equilibrium constant calculus for the minor atropodiastereomer :

measure #	δ**1a** mino (ppm)	Δδ**1a** (ppm)	[**1a**]mino (mol/L)	[HFIP°] (mol/L)	x=[HFIP]°/ [1a]° mino	y = Δδ**1a** mino
0	8.498	0.000	0.047	0.000		
1	8.461	0.037	0.047	0.016	0.334	0.042
2	8.435	0.063	0.047	0.026	0.545	0.072
3	8.405	0.093	0.047	0.035	0.740	0.107
4	8.390	0.108	0.047	0.041	0.866	0.124
5	8.358	0.140	0.047	0.054	1.151	0.162

By entering the x and y value into the MatLab web applet[288] and choosing as rough guesses values of 7 and 7 for the a and b fit parameters (c is indeed zero), we found :

========== Results ==========

a = 0.439 $\pm$0.258 and a = $\Delta\delta_{excess}^{mino}$

b = 1.104 $\pm$ 0.46 and $b = K_{eq} \cdot [1a_{mino}^{0}]$, giving :

$$K_{eq}^{mino} = 23.489 \pm 9.78\ L/mol$$

Finally, in order to experimentally confirm the predicted values of $\Delta\boldsymbol{\delta_{obs}}$, a large excess of HFIP was added to the solution of 1a, targeting a complete complexation of 1a with HFIP and the shifts of 3-H 1a proton for both major and minor isomers were measured. Accordingly $\Delta\delta_{excess}^{mino}$ and $\Delta\delta_{excess}^{majo}$ could be estimated and these values are coherent with the estimated values.

	$\Delta\delta_{excess}^{mino}$(ppm)	$\Delta\delta_{excess}^{majo}$(ppm)
Calculated	0.439	0.503
Experimental (~36 equiv. HFIP)	0.407	0.518

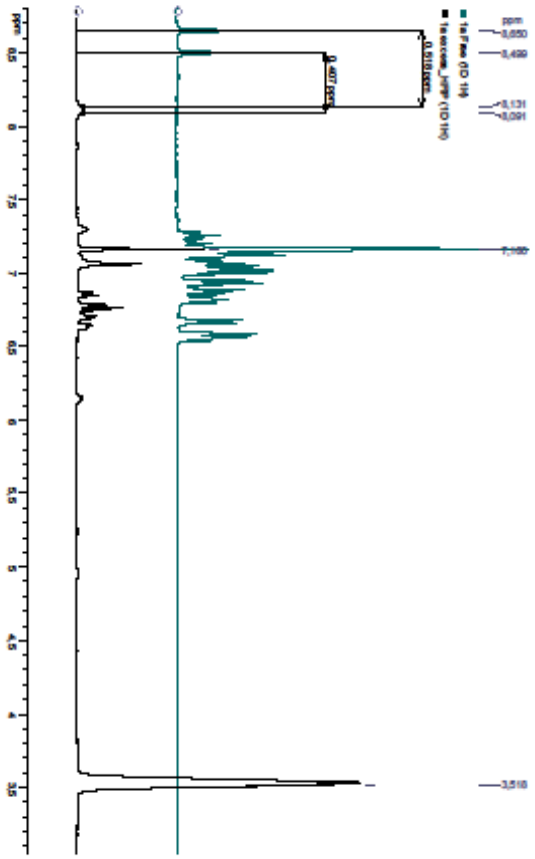

d) FT-IR study of H-bonding properties

1.Equilibrium Studied

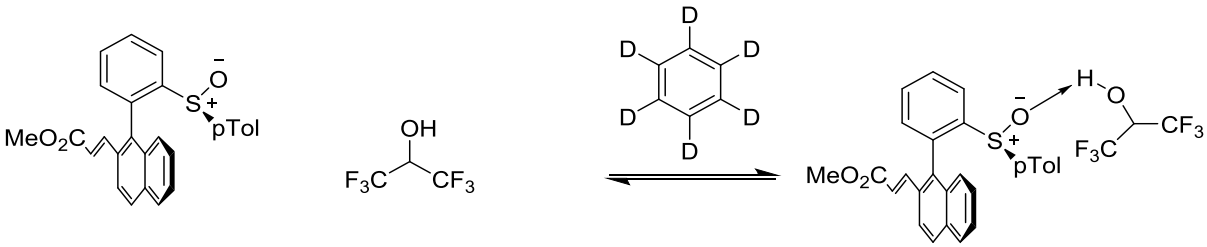

Lewis acid-base adduct between the oxygen of the sulfoxyde of (S)-1-(2-(p-tolylsulfinyl)phenyl)naphthalene (**2c**) and the alcoholic hydrogen of 1,1,1,3,3,3-hexafluoropropan-2-ol (HFIP).

2.Method and apparatus

An NaCl Cell was used, measurement were done with an Perkin-Ellmer Spectrum 2 FT-IR machine and treated with the software Spectrum 2 Each measurement is the average of 8 acquisitions done at 32 °C. HFIP was purchased from Sigma-Aldrich (purity ≥ 99 %), kept over 4 Å molecular sieves and filtered on Celite before use. Benzene-d6 purchased from Armar Chemicals (purity ≥ 99.3 %) and kept over 3 Å molecular sieves. Methyl (*E*)-3-(1-((*aS*)-2-((*S*)-p-tolylsulfinyl)phenyl)naphthalen-2-yl)acrylate (2c) was re-crystallized from dichloromethane/diethylether before use.

3.Preparation of the solutions

Solutions were prepared in volumetric flasks (except for measurements 8 and 9), from mother solutions (except for measurement 9). Mother solutions containing **2c** were briefly heated at 60 °C (water bath) to solubilize the solid.

4. Measurements

Mesurement #		benzene-d6	HFIP	HFIP eq.	2c
0	NaCl cell background	/	/	/	/
1	Solvent backgound	solvent	/		/
2	Zero background	solvent	/		/
3		solvent	0.05 M		/
4		solvent	0.1. M		/
5		solvent	0.1. M	5 eq.	0.02 M
6		solvent	0.1. M	10 eq.	0.01 M
7		solvent	0.1. M	2.5 eq.	0.04 M
8	(software stoppage)	solvent	0.1. M	1.25 eq.	0.08 M
8a		solvent	0.1. M	1 eq.	0.1 M
9		solvent	/		0.08 M
10		solvent	0.1 M	1.25 eq.	0.08 M

S-O bond

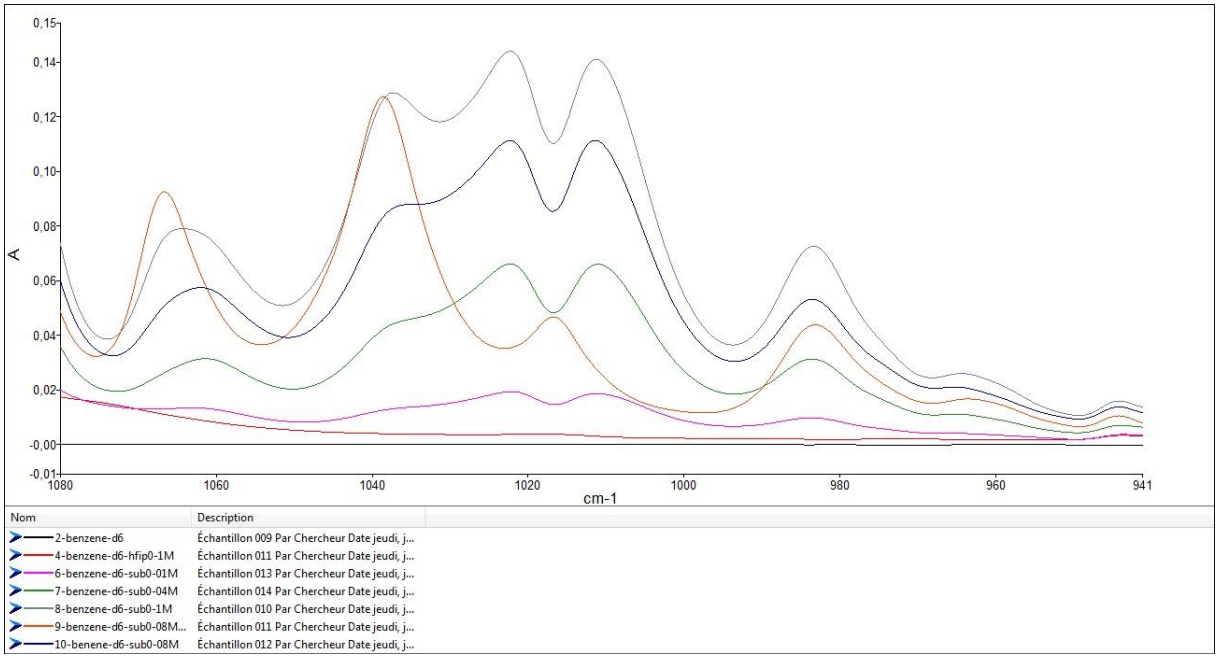

O-H bond of HFIP

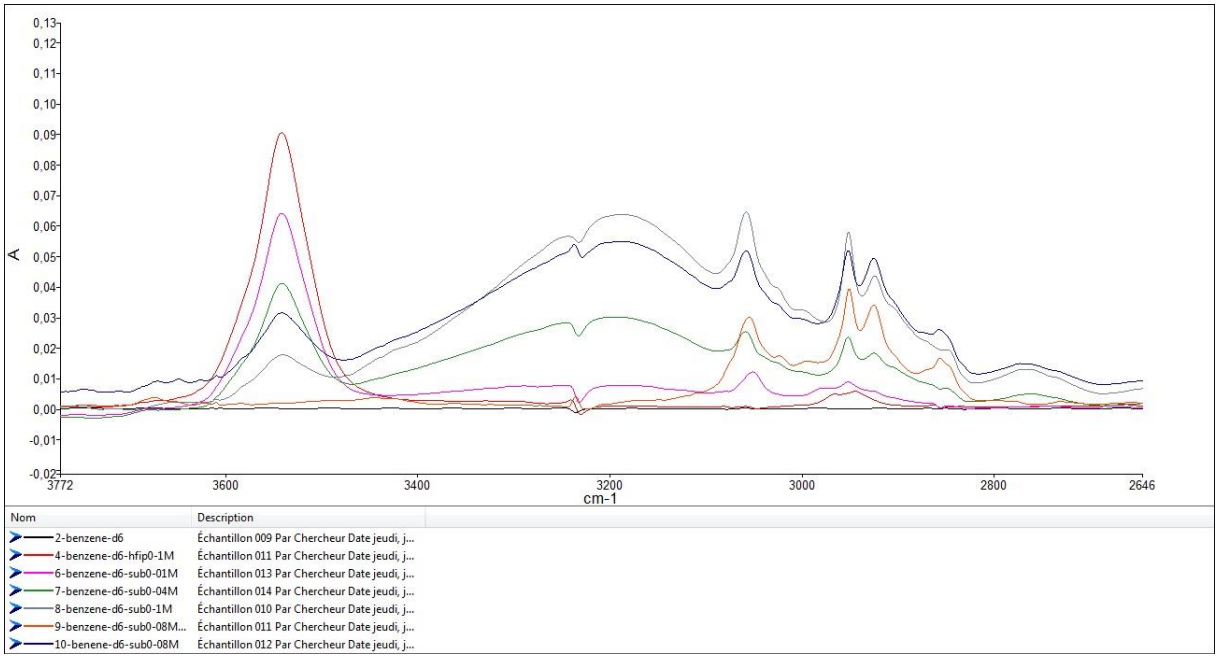

E. References

[239] I. Moritanl, Y. Fujiwara, *Tetrahedron Lett.* **1967**, *8*, 1119–1122.
[240] Y. Fujiwara, I. Moritani, S. Danno, R. Asano, S. Teranishi, *J. Am. Chem. Soc.* **1969**, *91*, 7166–7169.
[241] C. Jia, W. Lu, T. Kitamura, Y. Fujiwara, *Org. Lett.* **1999**, *1*, 2097–2100.
[242] Y. Fujiwara, R. Asano, I. Moritani, S. Teranishi, *J. Org. Chem.* **1976**, *41*, 1681–1683.
[243] Y. Obora, Y. Okabe, Y. Ishii, *Org. Biomol. Chem.* **2010**, *8*, 4071–4073.
[244] Z. She, Y. Shi, Y. Huang, Y. Cheng, F. Song, J. You, *Chem. Commun.* **2014**, *50*, 13914–13916.
[245] E. M. Ferreira, H. Zhang, B. M. Stoltz, in *Mizoroki–Heck React.* (Ed.: rtin Oestreich), John Wiley & Sons, Ltd, **2009**, pp. 345–382.
[246] Y. Fujiwara, C. Jia, *Pure Appl. Chem.* **2001**, *73*, 319–324.
[247] Y. Fuchita, K. Hiraki, Y. Kamogawa, M. Suenaga, K. Tohgoh, Y. Fujiwara, *Bull. Chem. Soc. Jpn.* **1989**, *62*, 1081–1085.
[248] M. D. K. Boele, G. P. F. van Strijdonck, A. H. M. de Vries, P. C. J. Kamer, J. G. de Vries, P. W. N. M. van Leeuwen, *J. Am. Chem. Soc.* **2002**, *124*, 1586–1587.
[249] G. T. Lee, X. Jiang, K. Prasad, O. Repič, T. J. Blacklock, *Adv. Synth. Catal.* **2005**, *347*, 1921–1924.
[250] D.-H. Wang, K. M. Engle, B.-F. Shi, J.-Q. Yu, *Science* **2010**, *327*, 315–319.
[251] K. M. Engle, D.-H. Wang, J.-Q. Yu, *J. Am. Chem. Soc.* **2010**, *132*, 14137–14151.
[252] D. Leow, G. Li, T.-S. Mei, J.-Q. Yu, *Nature* **2012**, *486*, 518–522.
[253] Z. Zhang, K. Tanaka, J.-Q. Yu, *Nature* **2017**, *543*, 538–542.
[254] M. Miura, T. Tsuda, T. Satoh, M. Nomura, *Chem. Lett.* **1997**, *26*, 1103–1104.
[255] M. Miura, T. Tsuda, T. Satoh, S. Pivsa-Art, M. Nomura, *J. Org. Chem.* **1998**, *63*, 5211–5215.
[256] T. Wesch, F. R. Leroux, F. Colobert, *Adv. Synth. Catal.* **2013**, *355*, 2139–2144.
[257] J.-P. Bégué, D. Bonnet-Delpon, B. Crousse, *Synlett* **2004**, *2004*, 18–29.
[258] I. A. Shuklov, N. V. Dubrovina, A. Börner, *Synthesis* **2007**, *2007*, 2925–2943.
[259] T. Sugiishi, M. Matsugi, H. Hamamoto, H. Amii, *RSC Adv.* **2015**, *5*, 17269–17282.
[260] C. Reichardt, *Chem. Rev.* **1994**, *94*, 2319–2358.
[261] C. Reichardt, T. Welton, in *Solvents Solvent Eff. Org. Chem.*, Wiley-VCH Verlag GmbH & Co. KGaA, **2010**, pp. 425–508.
[262] L. Wan, N. Dastbaravardeh, G. Li, J.-Q. Yu, *J. Am. Chem. Soc.* **2013**, *135*, 18056–18059.
[263] G. Chen, T. Shigenari, P. Jain, Z. Zhang, Z. Jin, J. He, S. Li, C. Mapelli, M. M. Miller, M. A. Poss, et al., *J. Am. Chem. Soc.* **2015**, *137*, 3338–3351.
[264] W. Gong, G. Zhang, T. Liu, R. Giri, J.-Q. Yu, *J. Am. Chem. Soc.* **2014**, *136*, 16940–16946.
[265] A. Berkessel, J. A. Adrio, D. Hüttenhain, J. M. Neudörfl, *J. Am. Chem. Soc.* **2006**, *128*, 8421–8426.
[266] K. S. Ravikumar, F. Barbier, J.-P. Bégué, D. Bonnet-Delpon, *J. Fluor. Chem.* **1999**, *95*, 123–125.

[267] D. Vuluga, J. Legros, B. Crousse, A. M. Z. Slawin, C. Laurence, P. Nicolet, D. Bonnet-Delpon, *J. Org. Chem.* **2011**, *76*, 1126–1133.
[268] J. Kiefer, K. Noack, B. Kirchner, *Curr. Phys. Chem.* **2011**, *1*, 340–351.
[269] M. K. D. L. Belarmino, V. F. Cruz, N. B. D. Lima, *J. Mol. Model.* **2014**, *20*, 2477.
[270] A. M. Karachewski, M. M. McNiel, C. A. Eckert, *Ind. Eng. Chem. Res.* **1989**, *28*, 315–324.
[271] F. L. Slejko, R. S. Drago, D. G. Brown, *J. Am. Chem. Soc.* **1972**, *94*, 9210–9216.
[272] K. F. Wong, S. Ng, *Spectrochim. Acta Part Mol. Spectrosc.* **1976**, *32*, 455–456.
[273] P. Ruostesuo, P. Pirilä-Honkanen, S. Kaartinen, *Spectrochim. Acta Part Mol. Spectrosc.* **1988**, *44*, 359–362.
[274] P. Ruostesuo, J. Karjalainen, A. Haaland, S. Samdal, O. Bastiansen, G. Braathen, L. Fernholt, G. Gundersen, C. J. Nielsen, B. N. Cyvin, et al., *Acta Chem. Scand.* **1982**, *36a*, 273–276.
[275] L. S. Gabrielyan, L. G. Melik-Ohanjanyan, S. A. Markarian, *J. Appl. Spectrosc.* **2013**, *80*, 135–137.
[276] J. C. Tai, *J. Comput. Chem.* **1981**, *2*, 161–167.
[277] L. Cazaux, J. D. Bastide, G. Chassaing, P. Maroni, *Spectrochim. Acta Part Mol. Spectrosc.* **1979**, *35*, 15–26.
[278] E. M. Simmons, J. F. Hartwig, *Angew. Chem. Int. Ed.* **2012**, *51*, 3066–3072.
[279] F. H. Westheimer, *Chem. Rev.* **1961**, *61*, 265–273.
[280] M. Gómez-Gallego, M. A. Sierra, *Chem. Rev.* **2011**, *111*, 4857–4963.
[281] Y.-J. Kim, J.-C. Choi, K. Osakada, *J. Organomet. Chem.* **1995**, *491*, 97–102.
[282] G. M. Kapteijn, D. M. Grove, H. Kooijman, W. J. J. Smeets, A. L. Spek, G. van Koten, *Inorg. Chem.* **1996**, *35*, 526–533.
[283] E. Gaster, Y. Vainer, A. Regev, S. Narute, K. Sudheendran, A. Werbeloff, H. Shalit, D. Pappo, *Angew. Chem. Int. Ed.* **2015**, *54*, 4198–4202.
[284] B. Elsler, A. Wiebe, D. Schollmeyer, K. M. Dyballa, R. Franke, S. R. Waldvogel, *Chem. – Eur. J.* **2015**, *21*, 12321–12325.
[285] C. Amatore, A. Jutand, M. J. Medeiros, L. Mottier, *J. Electroanal. Chem.* **1997**, *422*, 125–132.
[286] *Org. Synth.* **1958**, *38*, 22.
[287] C. H. Brubaker, *J. Chem. Educ.* **1966**, *43*, 222.
[288] “Nonlinear Least Squares Curve Fitting,” can be found under http://www.colby.edu/chemistry/PChem/scripts/lsfitpl.html, **n.d.**

Acetoxylation and Iodination

V. Acetoxylation and iodination

A. Foreword

Palladium-catalyzed acetoxylation and iodination reactions of C(sp^2)-H bonds by means of C-H activation share some common features. Indeed they generally occur *via* a Pd^{II}-Pd^{IV} catalytic cycle as strong oxidants are usually present, often in highly acidic medium and/or at elevated temperature. Early evidence of these Pd^{II}-Pd^{IV} catalytic cycles were based on the analogy between Pd and Pt : model reactions using the more stable platinum complexes allowed the isolation of the Pt^{IV} intermediates (Figure V-1a for C-O bond formation[289] and Figure V-1b for C-I bond formation[290]).

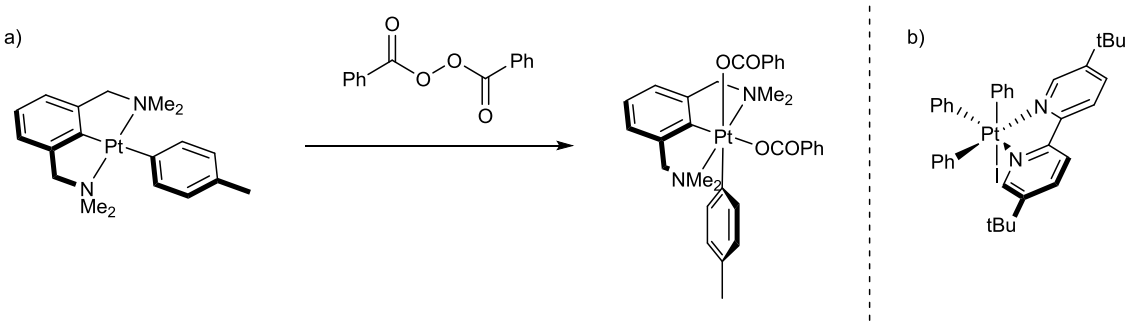

Figure V-1 : high-valent M-O and M-I complexes from group 8

The general mechanism thus starts with coordination of the Pd^{II} active catalytic species with the directing group, followed by insertion into the C-H bond. Then, 2 electrons oxidation of the Pd^{II}-Aryl complex to Pd^{IV} promote the otherwise challenging C-O or C-X reductive elimination, followed by the release of Pd^{II} into the catalytic cycle. Both transformations will be briefly revueed in the following sub-sections.

B. Acetoxylation

1. Introduction

In fact the first report of *directed* Pd-catalyzed acetoxylation showcased the similarity between the two aforementioned transformations, as both C(sp^2)-O (Figure V-2a) and C(sp^2)-X (Figure V-2b) bond formations were reported in 2004 by Dick, Hull and Sanford[291] for substrates bearing a pyridine-type directing group. Good yields of acetoxylated product could be obtained using $PhI(OAc)_2$ (PIDA) as the stoichiometric oxidant, but also as the source of stoichiometric acetoxylating agent. A range of scaffolds could be functionalized using an sp^2-hybridized tertiary nitrogen as the directing group (One should note that the first report of the use of PIDA in conjunction with palladium for the acetoxylation of arenes was made in 1995 by Crab-

tree[292] and already a Pd^{II}/Pd^{IV} catalytic was inferred on the basis of experimental data).

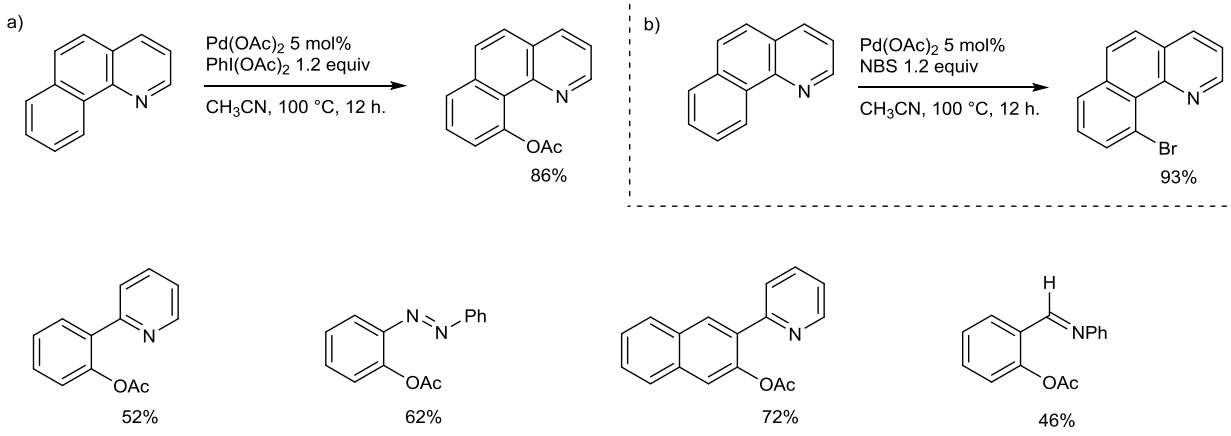

Figure V-2 : first palladium-catalyzed directed acetoxylation

Interestingly, *undirected* palladium-catalyzed acetoxylation using pyridine type-*ligand*, as opposed to *directing group*, had been known for more than 30 years prior to the seminal Sanford report. Indeed when in 1974 Eberson and Jönsson[293] heated a solution of benzene in acetic acid in the presence of a catalytic and equimolar amount of $Pd(OAc)_2$ and 2,2'-bipyridine along with $K_2S_2O_8$ as the oxidant, phenyl acetate was formed, albeit in a low yield of 29%. An early example of C-H activation, the reaction did not carry a lot of synthetic value as substituted benzenes were produced as a mixture of regioisomers along with side-products.

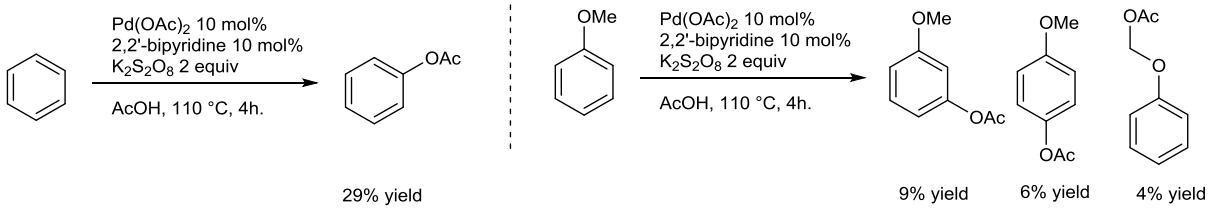

Figure V-3 : early examples of palladium-catalyzed acetoxylation

The combination of inorganic peroxides as the oxidant and acetic acid as the acetoxylating agent was practical and cheap compared to the previously mentioned hypervalent iodine reagents. Therefore in 2006 Desai, Malik and Sanford[294] managed to tame the catalytic system by performing a directed acetoxylation using their nitrogen-based directing group strategy. Thus it was shown that *N*-methoxy phenylimines could be cleanly acetoxylated *ortho* to the directing group by a combination of acetic acid and either $K_2S_2O_8$ or Oxone (Figure V-4 : scope of oxidants).

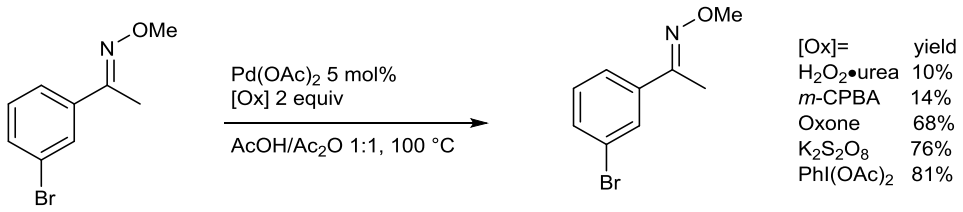

Figure V-4 : scope of oxidants

Furthermore, other directing groups were found to be compatible with this system: probably because of the presence of acetic anhydride, only tertiary anilides derivatives were originally evaluated, but in 2008 Wang, Yuan and Wu[295] showed that by using a AcOH/DCE solvent system acetanilide and secondary anilides derivatives could also underdo this C-O coupling (thus by coordination *via* the oxygen atom).

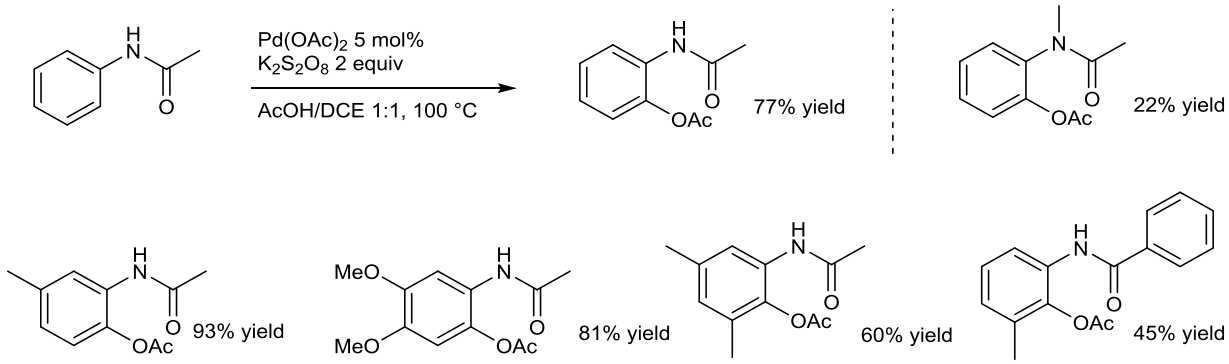

Figure V-5 : examples of acetanilides directed acetoxylation

Another example disclosed by Vickers, Mei and Yu in 2010[296] concerns the functionalization of biologically important phenyl ethylamine scaffolds when the amino group is protected as a triflamide with moderate yield. Remarquably more elaborate substrates were acetoxylated in better yields (Figure V-6a), and N-Tf protected (-)-ephedrine was functionalized with a good yield of 71% with *in-situ* protection of the free hydroxyl group.

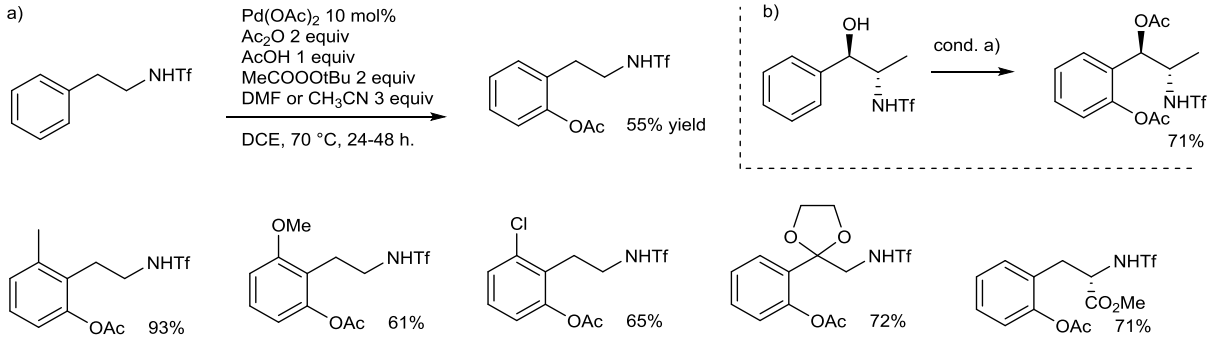

Figure V-6 : other DG for the acetoxylation reaction

More recently, the potential of the directed acetoxylation was expanded to *meta*-selective functionalization. The use of an elaborate template allowed Tang, Li and Yu

in 2013[297] to functionalize with moderate yields and good regioselectivity several aromatic N-methylamines.

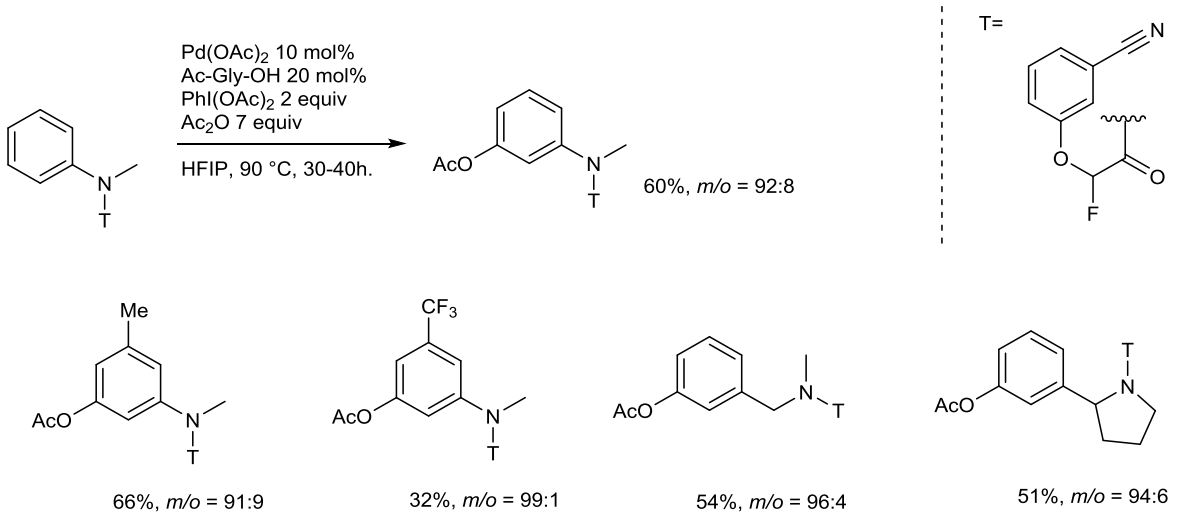

Figure V-7 *meta*-selective acetoxylation

As computational work was undertaken in collaboration with Jean-Pierre Djukic to unveil the mechanism of the atroposelective C(sp^2)-H acetoxylation developed in our laboratory, we will explore in some details the mechanistic aspects concerning palladium-catalyzed C(sp^2)-H acetoxylation.

Most of the later detailed mechanistic work has been conducted on 2-phenylpyridine-type substrate[298] , and thus similar cyclopalladated intermediate were inferred on the basis of results presented Figure V-8.

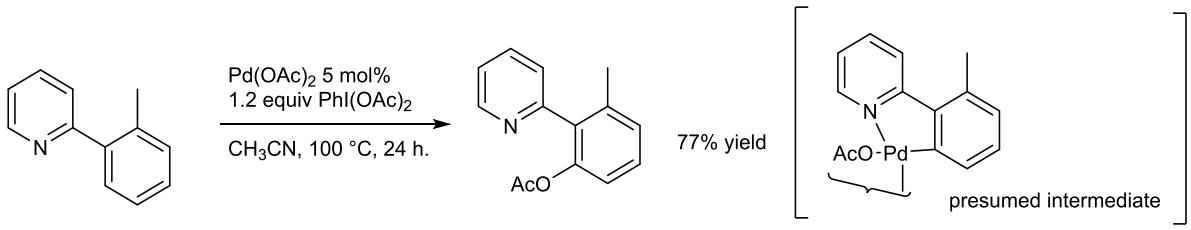

Figure V-8: model reaction for mechanistic studies

For the phenylpyridine substrates the C-H insertion step was found to be the turnover-limiting step, as indicated by the intermolecular, inter-reactional measured KIE of 4.3, and accordingly the palladation step was studied first.

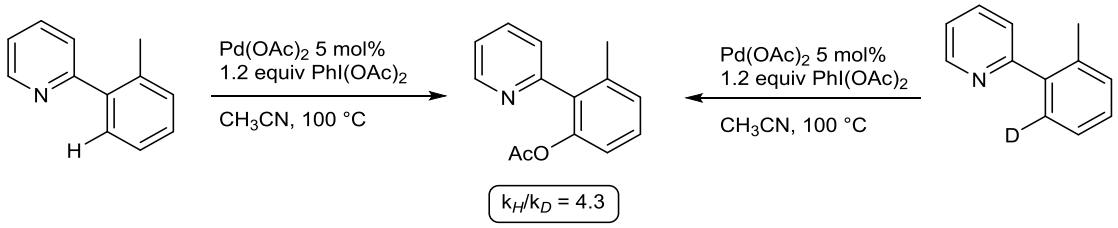

Figure V-9 : kinetic isotope effect

Sanford and co-workers then determined the kinetic order of each reaction component, and found:

- 1.5 order in $Pd(OAc)_2$, which might indicate competing pathway between different complexes prior to the C-H cleavage.

- inverse 1 order in substrate, that indicates equilibrium dissociation of the substrate from the catalyst resting state, prior to the C-H cleavage.

- zero order in oxidant (as expected as the C-H cleavage is the limiting step).

Next, a Hammett plot was realized using substituted *pyridines* (and not substituted phenyls) and the Hammett σ value of +0.89 was measured, indicating that electron-withdrawing substituents on the pyridine ring increase the rate of the cyclopalladation. This is consistent with the electrophilic character of the palladium, as well as with the coordination of the palladium catalyst before the C-H insertion. Indeed, in this view, electron-poor pyridine directing group will make the catalyst more electrophilic and thus facilitate the C-H cleavage.

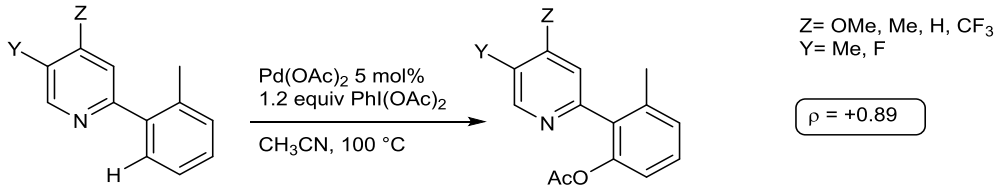

Figure V-10 : Hammett-plot experiment

On the basis of the experimental data, the following mechanism was proposed: $Pd(OAc)_2$ reacts quickly with the substrate **1** to generate the catalyst resting state **2**, which is coordinated by two molecules of **1**. Reversible de-coordination of one the ligand **1** (Figure V-11a), produces the active catalytic specie **3** which undergoes irreversible C-H cleavage delivering the cyclopalladated intermediate **4** (Figure V-11b). However to explain the 1.5 order in $Pd(OAc)_2$ one must take into account that competing pathways from the catalyst resting state leading to the cyclometallated product can exist, and thus a dimeric structure was also proposed for the intermediate **3** (for details see[298]).

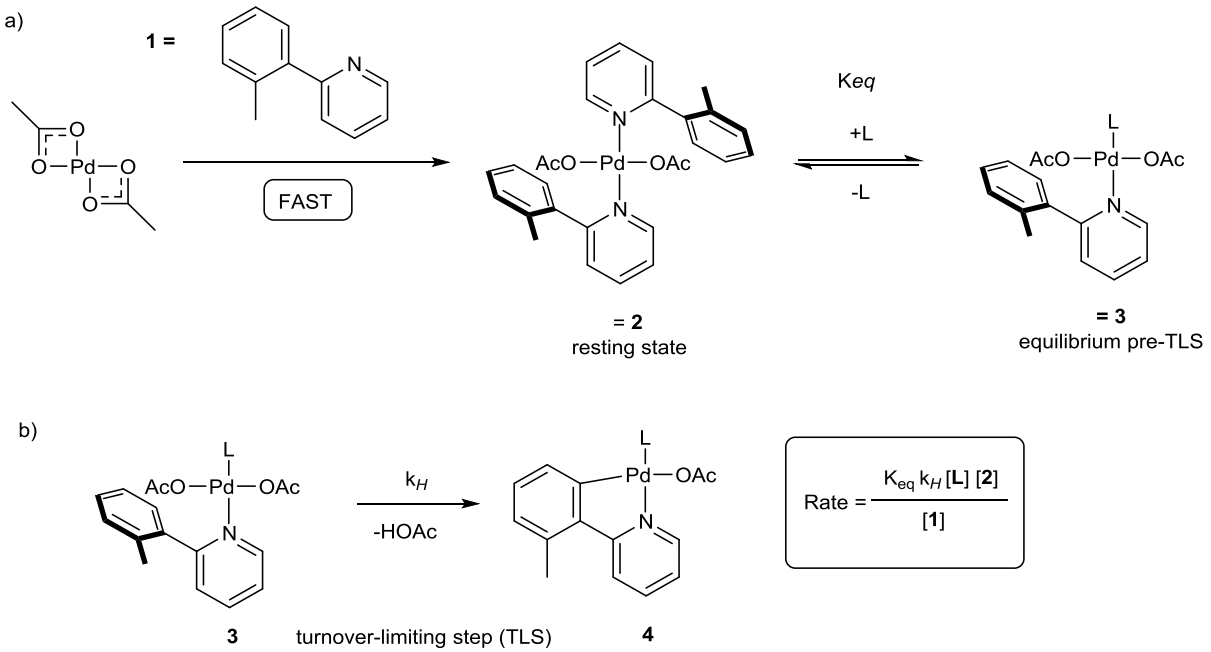

Figure V-11 : mechanistic scenario leading to the TLS

Next the C-O bond forming step was studied as a stable Pd^{IV} complex was isolated after oxidation of the cyclometallated Pd^{II} complex by $PhI(OC(O)Ph)_2$. This Pd^{IV} complex did produce the acetoxylated product upon heating in a range of solvent (Figure V-12a). The relative rates of the reductive elimination (RE) were measured in several solvents, but no correlation between the rates of the RE and the polarity of the solvents (Figure V-12b) could be found. Furthermore, a Hammett plot using substituted benzoates was realized, and a constant of ρ = -1.36 was found, indicating that electron-rich benzoates coupling partners led to an acceleration of the RE (Figure V-12c). These two effects were used to rule out a RE mechanism involving ionic intermediates, i.e. first by dissociation of a benzoate ligand followed by inter- or intra-molecular attack on the phenyl ring. However a limitation of the stoichiometric system studied is that it is under *basic* conditions (benzoate and phenylpyridine ligands), whereas the catalytic system is actually under *acidic* conditions (one equivalent of "H^+" is generated after each C-H cleavage).

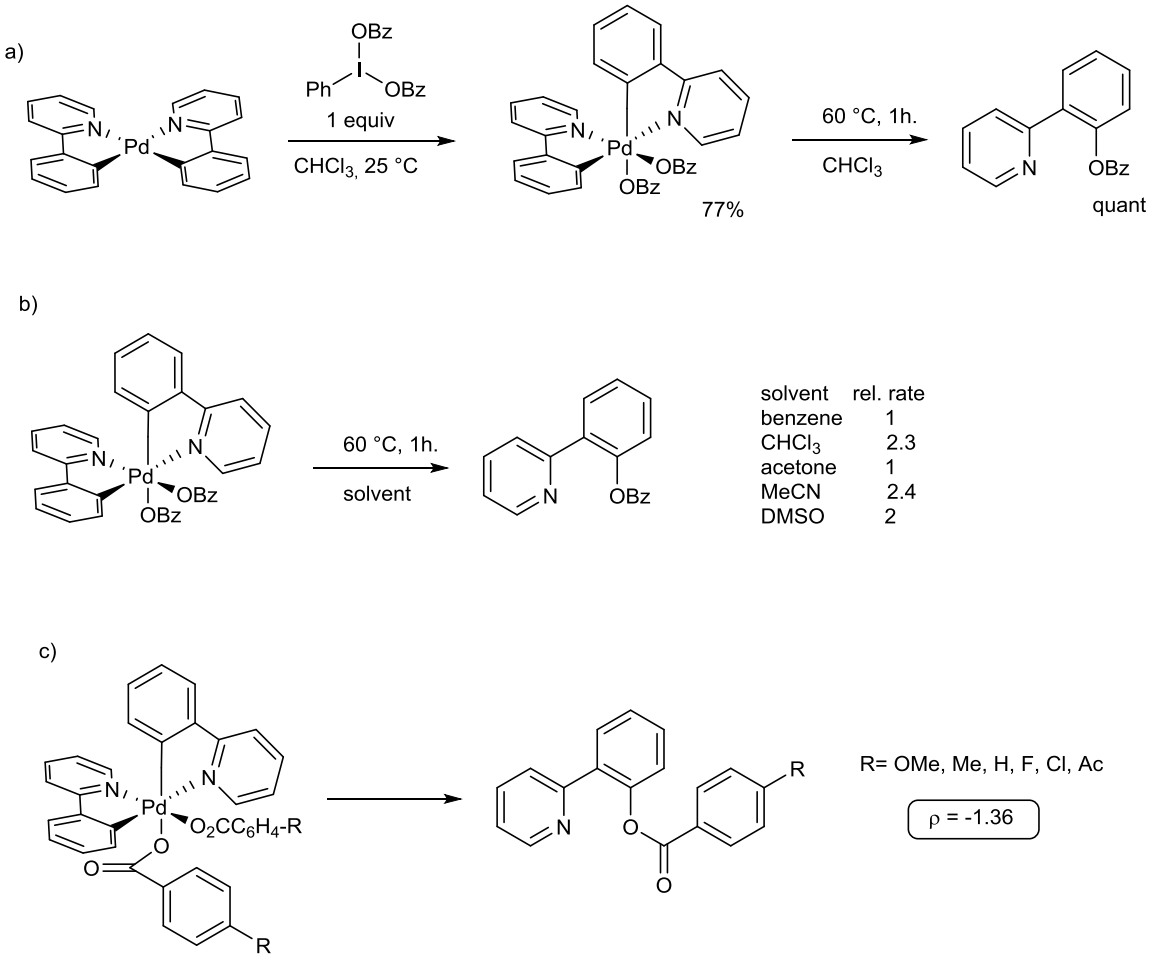

Figure V-12 : reductive elimination from Pd^{IV} complexes

Thus more detailed studies concerning the possibility of a dissociative ionic mechanism were undertaken[299]. It was found, using electrospray mass spectrometry analysis, that the coordinatively saturated Pd^{IV} complex presented actually does exchange an acetate ligand for an acetate-d_3 at room temperature in CH_2Cl_2 (Figure V-13). Being saturated, the ligand exchange must occur through a dissociative mechanism, and thus an ionic intermediate complex. Interestingly, the exchange occurred only *trans* to the σ-aryl ligand. Furthermore it was shown, thanks to the preparation of the Pd^{IV} complex **C,** they showed that C-O reductive elimination occurred only from the acetate *trans* to σ-pyridine ligand. As both acetate are *cis* to the same σ-aryl ligand, this led to the hypothesis that the ligand exchange (or at the very least, the ligand dissociation) are mechanistically linked. Furthermore, when the rate of C-O bond formation and ligand were measured in absence and in presence of acetic acid, it was found that AcOH was accelerating both reactions (3.6 and 4.5 fold acceleration) reinforcing the possibility that they are linked (Figure V-13). The authors finally conclude that the dissociative mechanism was most the likely operating.

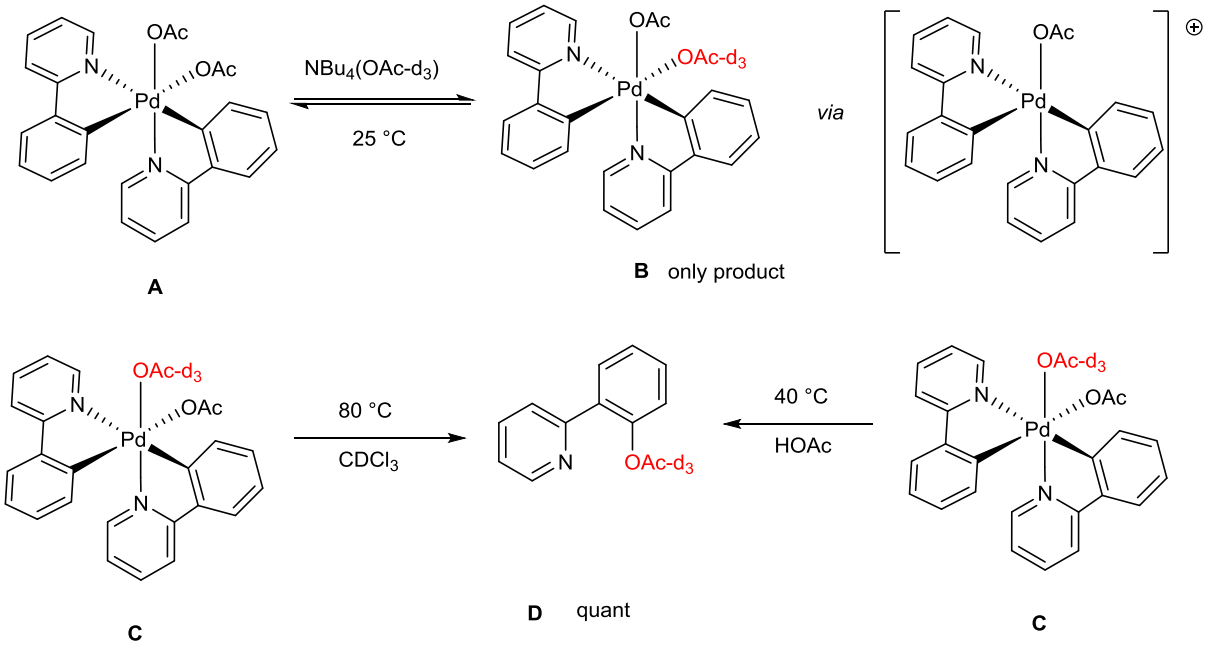

Figure V-13 : dissociative mechanism evidence

Finally, concerning asymmetric transformations, the pioneer work was reported in 2005 by Corey[300] and concerned asymmetric C(sp^3)-H functionalization using a N-protected α-amino amide substituted by an 8-amidoquinoline auxiliary (Figure V-14). This allowed the functionalization of amino acids substrates, and interestingly this transformation was promoted by the of $Mn(OAc)_2$. Concerning the work on asymmetric C(sp^2)-H acetoxylation, only one example had been reported and was revueed the first part of this thesis[34].

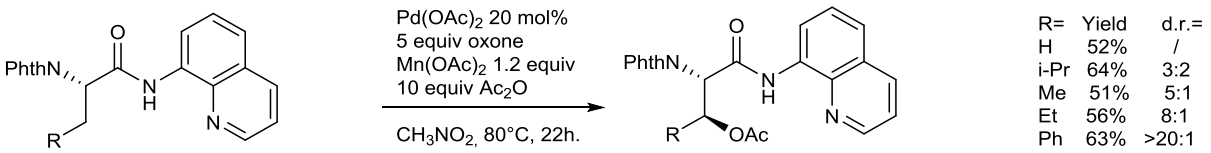

Figure V-14 : pioneer work on asymmetric acetoxylation

Following this pioneering work, the asymmetric acetoxylation remained undeveloped till 2014 when we disclosed our atropo-diastereoselective transformation, presented in this manuscript.

2. Results and discussion

The following work has been conducted during the Master 2 stage in collaboration with the Dr. Chinmoy Kumar Hazra.

Our endeavor towards a mild C-H activation began by investigating the C-O coupling reaction of biaryle substrate **1** (Table V-1). Firstly, a standard substrate **1a**, used as a 55:45 mixture of atropodiastereomers on the ^{1}H NMR time scale, was reacted with $Pd(OAc)_2$ and $PhI(OAc)_2$ (used as both acetoxylating agent and oxidant). Although the desired product **2a** could be isolated in a yield of 50%) with an excellent diastereoselectivity (d.r. > 98:2), a high reaction temperature was required (80 °C, Table V-1, entry 1). Rewardingly, the replacement of $PhI(OAc)_2$ by acetic acid and a persulfate oxidant drastically improved the efficiency of this C-O coupling (Table V-1, entry 2) and the reaction proceeded smoothly even at room temperature (Table V-1, entry 3). The catalytic system was also robust as no precaution towards air and moisture were required. Both the yield and the d.r. were improved by the addition of a small amount of water as **2a** was isolated in 93% yield and 98:2 d.r. (Table V-1, entry 4). This small amount of water might improve the solubility of $(NH_4)_2S_2O_8$ (as the reaction is heterogeneous). The transformation was still efficient in aqueous medium (Table V-1, entry 5). Notable, no acetoxylation of **1a** occurred in the absence of the Pd-catalyst. The structure of **2a** was confirmed by X-ray diffraction analysis and the absolute (*SaR*) configuration was attributed.

Table V-1 : Optimization of the acetoxylation reaction

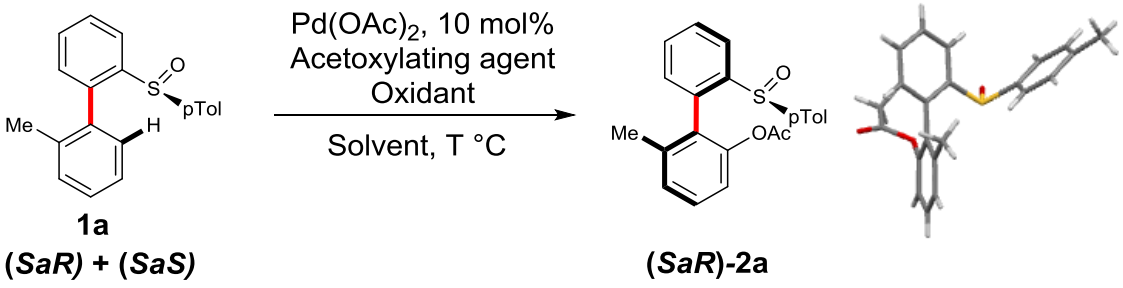

1a
(*SaR*) + (*SaS*)
d.r. = 55:45

(*SaR*)-2a

Entry	"OAc" (X equiv)	Oxidant	Solvent	T(°C)/ t (h)	Yield (%)[a]	dr[b]
1	$PhI(OAc)_2$ (2.4)		HFIP	80/16	41	>98:2
2	AcOH (46)	$K_2S_2O_8$	HFIP	80/24	89	90:10
3	AcOH (46)	$(NH_4)_2S_2O_8$	HFIP	25/14	88	96:4
4[c]	AcOH (46)	$(NH_4)_2S_2O_8$	HFIP	25/14	93	98:2
5	AcOH (46)	$(NH_4)_2S_2O_8$	H_2O	25/16	86	83:17

[a] Isolated yield. [b] Determined by crude ^{1}H NMR. [c] Reaction conducted with 2 equiv of H_2O and under air.

With the optimized reaction condition in hand, the scope of this reaction was explored (Figure V-15).

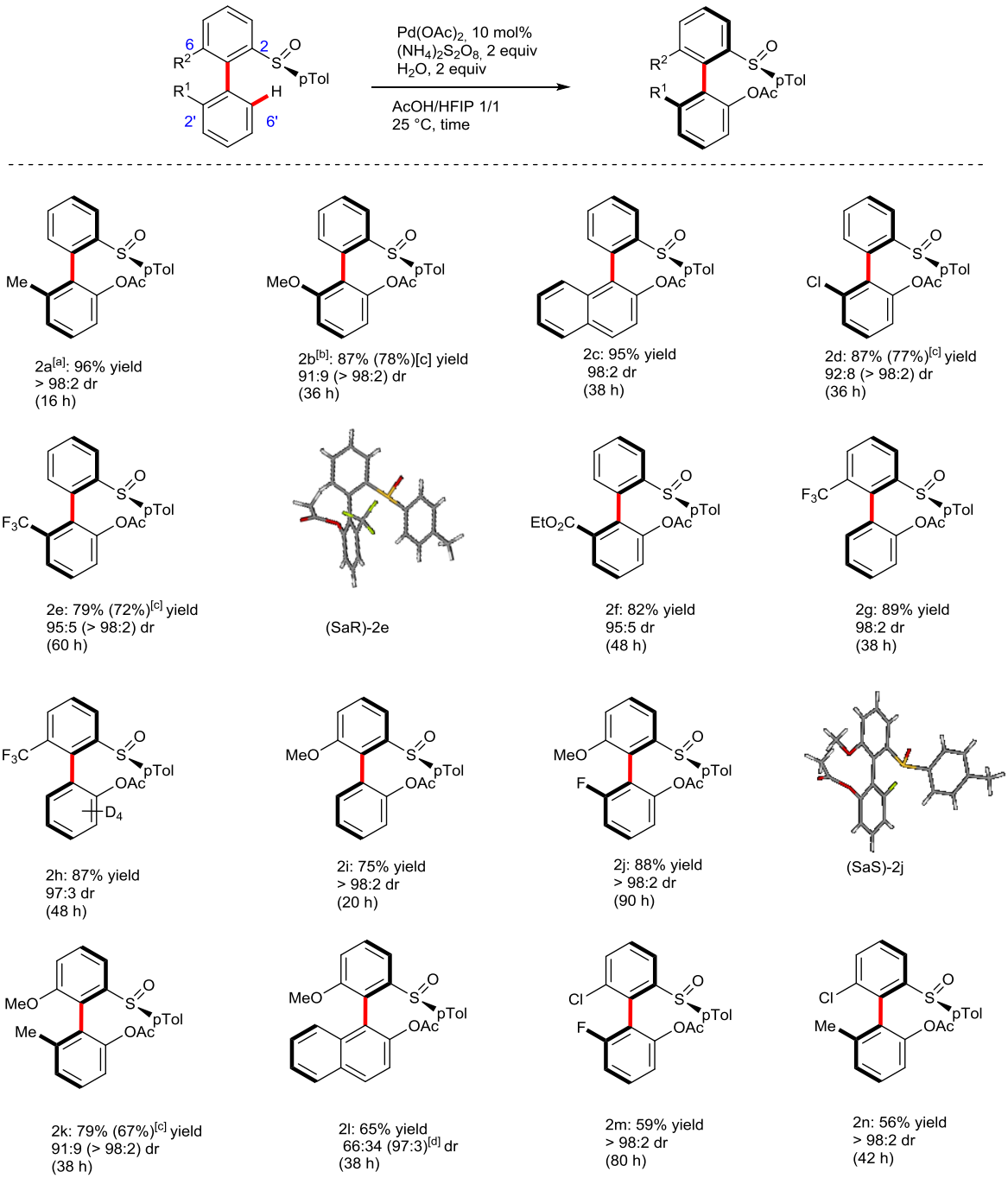

Figure V-15 : substrate scope for asymmetric direct acetoxylation.

Standard reaction conditions: 1 (0.2-0.3 mmol); $Pd(OAc)_2$ (10 mol%); $(NH_4)_2S_2O_8$ (2 equiv), H_2O (2 equiv), HFIP/AcOH 1/1 v/v, air, 25 °C; isolated yields; dr determined by ^1H NMR analysis on the crude mixture. [a] at 1.5 mmol scale. [b] at 10 °C; [c] yield and dr after recrystallization. [d] dr in brackets of product after silica gel column chromatography.

The reaction proceeded smoothly for an array of 2'-substituted biaryls (**2a-f**). A slight decrease in the diastereoselectivity for **2b** was probably due to the less sterically demanding OMe group. Recrystallization of **2b** however enabled to isolate the atropisomerically pure product in 78% yield. Our catalytic system is also compatible with electron-poor substrates (**1d-f**). When **1f**, bearing two possible coordinating groups, *ie*. sulfoxide and ester, was submitted to the reaction conditions, the sulfoxyde-directed C-H activation occurred selectively at the expected 6'-position. Subsequently, 6-substituted biaryls have been tested; such proaxially chiral **1g**-**1i** underwent highly diastereoselective C-O coupling and no diacetoxylation occurred. Finally, our attention turned towards *ortho*-trisubstituted substrates. **1j**, bearing the relatively small OMe and F substituents afforded **2j** in excellent yield and stereoselectivity. In contrast, a decreased chiral induction was observed in the case of the more hindered **1k** and **1l**. Surprisingly, when trisubstituted biaryls bearing a rather bulky Cl substituent at the 6-position and F or Me groups at the 2'-position (**1m**,**n**) were submitted to the reaction conditions, the corresponding acetoxylated products **2m** and **2n** were isolated in atropisomerically pure form but in lower yields. Notably, the remaining substrates **1m**,**n** were recovered as sole diastereomers in respectively 40 and 41% yields.

To get insight on this original C-H activation/DKR transformation, several mechanistic studies were undertaken. First, the reversibility of the metalation was investigated when **6'-D-1j** was reacted with $Pd(OAc)_2$ in an HFIP/AcOH mixture, significant D/H scrambling was observed (Figure V-16b). Besides, a very weak intermolecular intermolecular reactional Kinetic Isotope Effect of 1.09 was measured when **1j** and **6'-D-1j** were submitted to the acetoxylation reaction conditions (Figure V-16a). These results indicate that C-H bond cleavage is not the turnover-limiting step and is coherent with the hypothesis that the overall outcome of this transformation is controlled by the kinetics of reductive elimination and isomerisation. Indeed C-O reductive elimination at palladium(II) is recognized as difficult[301,302] but is facilitated for electron-poor metal. Thus either reductive elimination at Pd^{II} or oxidative addition and reductive elimination at Pd^{IV} are expected to be the slow step of the catalytic cycle[298].

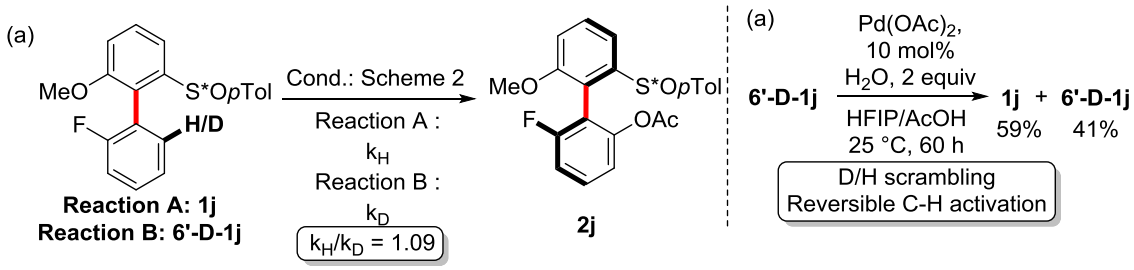

Figure V-16 : KIE and reversibility study

Subsequently, in order to provide experimental evidence for the mechanism of the (dynamic) kinetic resolution pathway, the diastereomeric excess (d.e.) of the substrates of the acetoxylation reactions of **1e, 1j** and **1m** were followed using ^{19}F NMR (Figure V-17). For each substrate, the modification of the diastereomeric excess was

measured in the course of the reaction and as a function of conversion, which allowed us to define 3 different types of substrate.

Type I : when **1e** was submitted to the reaction conditions, its diastereomeric ratio remains constant, indicating that atropisomerization of **1e** is fast compared to the turnover-limiting step (product (*SaR*)-**2e** is isolated in 79% yield and 95:5 d.r.), and therefore that a DKR mechanism is operative.

Type II: In contrast, during the reaction of **1j**, the d.r. changes significantly: this indicates that atropisomerization is slow compared to the turnover-limiting step. However, the isolation of (*SaS*)-**2j** in atropomerically pure form and in 88% yield clearly indicates that atropisomerization did occurred during the course of the reaction, and therefore indicates that a Dynamic Asymmetric Transformation (DYKAT) mechanism is operative.

Type III: Finally, the acetoxylation of **1m** led to full conversion of the (*SaR*)-**1m** atropisomer and the transformation stops when achieving 65% conversion (corresponding to the total consumption of the major diastereomer of the substrate). The increased steric hindrance around the biaryl axis of **1m** might prevent the DKR/DYKAT pathways and a simple Kinetic Resolution (KR) occurs.

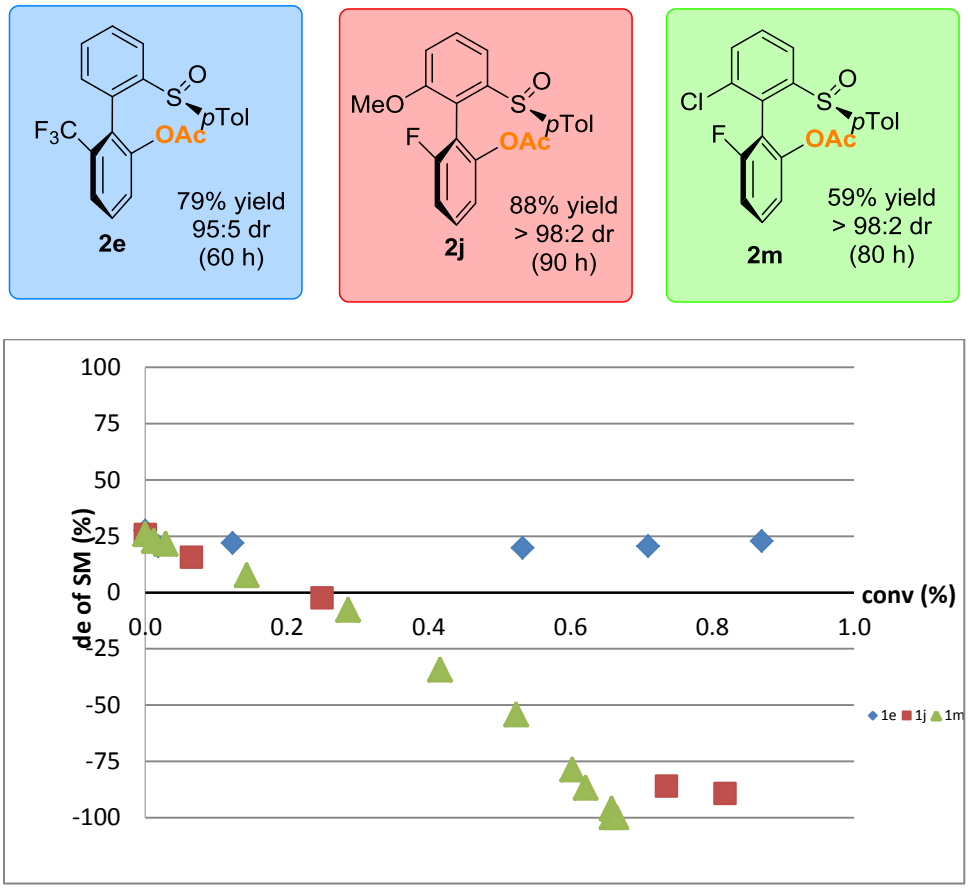

Figure V-17 : Variation of the diastereomeric excess of 1e, 1j and 1m as a function of conversion

Therefore the exact nature of the catalytic cycle will largely depend on the type of substrate used. Nevertheless, based on these findings and the literature, a general, simplified, catalytic cycle can be proposed (Figure V-18). Coordination of the catalyst through the sulfur atom, followed by reversible insertion into the C-H bond yields a 6-membered palladacycle which undergoes persulfate-mediated oxidation to a Pd(IV) intermediate. The Pd(IV) intermediate is expected to rapidly undergo reductive elimination, affording the C-O coupled atropoenriched product **2B.**

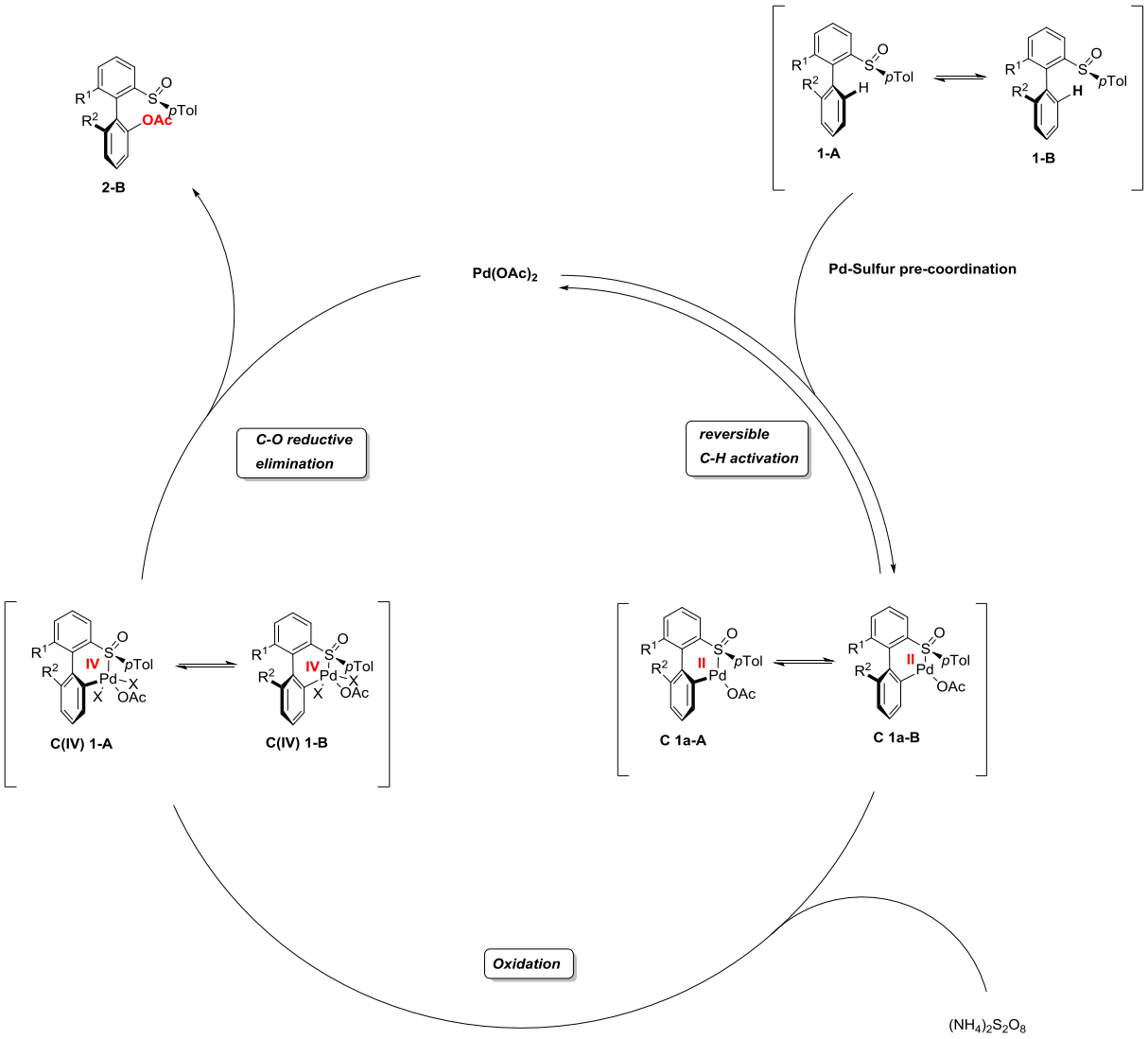

Figure V-18 : general catalytic cycle

To go deeply in the mechanism of this C-H acetoxylation, we performed firstly the determination of rotational barriers, secondly we isolated different palladacycles and thirdly we studied the effect of the expected hydrogen-bond between HFIP and the oxygen of the sulfoxide. Towards this three purposes substrate **1a** was chosen as a type **I** representative and substrate **2j** was chosen as a type **II** representative.

Type I, substrate 1a :

Determination of rotational barrier

First the rotational barrier of **1a** was measured by variable temperature ^{1}H NMR (Figure V-19. A coalescence temperature of 70°C (± 5°C) (343.15K) was found for the protons of the methyl group *ortho* to the biphenyl, and accordingly a $\Delta G^{\ddagger}_{343.15K}$ = 18.30 kcal/mol (±0.3 kcal/mol), which correspond (assuming that $\Delta G^{\ddagger}$ stays constant over this range of temperature) to an half-life of atropisomerization of *t*½ = 2.9 seconds at 25 °C. This value is in good agreement with the calculated barrier of $\Delta G^{\ddagger}_{298.15K}$ = 17 kca/mol. This shows that atropisomerization of **1a-A** to **1a-B** (Figure V-18) can indeed occur at 25 °C through a DKR type reaction.

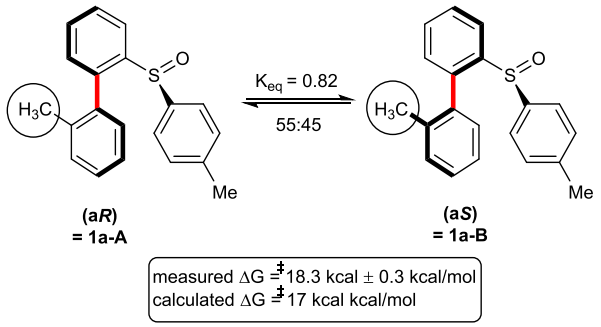

Figure V-19 : rotational berrier of substrate 1a

Next, we endeavor in isolating the putative palladacycle intermediate **C1a** (Figure V-18), in order to elucidate the effect of cyclometallation on the atropisomerization barrier. Indeed it is well known that bridging substituents can significantly modify the rotational barrier of biaryls, either diminishing or increasing it when stereogenic substituants are present on the bridging moeity[303]. Unfortunately, we were unable to isolate **C1a** with an acetate ligand, but reaction of **1a** with stoichiometric $Pd(OAc)_2$ in pure HFIP at 25 °C followed by ligand exchange delivered several palladacycles with differently sized ligands, and each were further studied.

Isolation of palladacycles

Palladacycle **C1**, a bridged dimer (with a relatively small chloride L-type ligand), was isolated, after column chromatography, with a d.r. ~57:43 (extensive broadening of signals because of the bridging chloride ligand and/or fast atropisomerization made a precise d.r. determination difficult).

Palladacycle **C2,** carrying the larger 4-methylpyridine, exhibited a d.r. of 85:15 after column chromatography. Gratifyingly, crystals suitable for X-Ray analysis were grown, confirming the enantiopurity as well as the expected absolute configuration of the biaryl axis. Interestingly, ^{1}H NMR of an enantiopure monocrystal in $CDCl_3$ at 25 °C showed a mixture of two compounds, the same mixture as after chromatography, thus showing that atropisomerization is possible at 25 °C.

Palladacycle **C3**, with a bulky IMe carbene ligand, was obtained with a d.r. >98:2 as shown by ^{1}H NMR analysis.

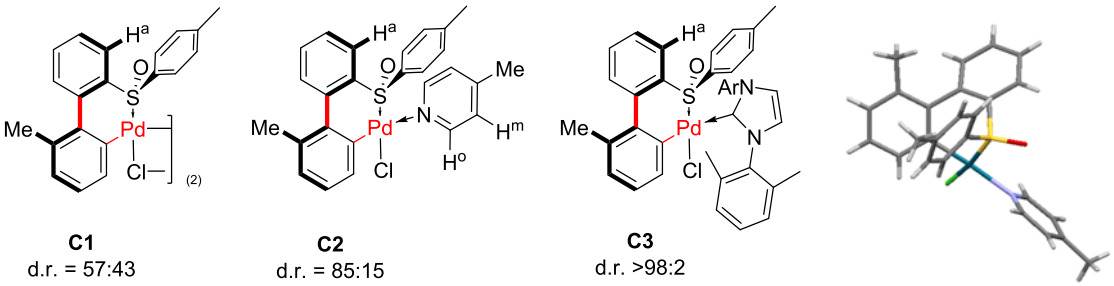

Figure V-20 : isolated palladacycles ; C2 X-ray crystal structure

This effect of the ligand size can on the d.r. be understood by examining the X-Ray structure of **C2.** Indeed it clearly shows that the *p*-tolyl substituent and the 4-Mepyridine ligand are in an *anti* conformation when the biaryl configuration is (a*R*). However, when the biaryl configuration is (a*S*), and because of the square-planar geometry of the Pd^{II} atom, the L ligand and the *p*-tolyl substituent will be forced in a *syn* conformation. Thus, as no bulky ligands are present in our reaction, we can safely assume that palladacycle does not prevent atropisomerization between **C1a-A** and **C1a-B**).

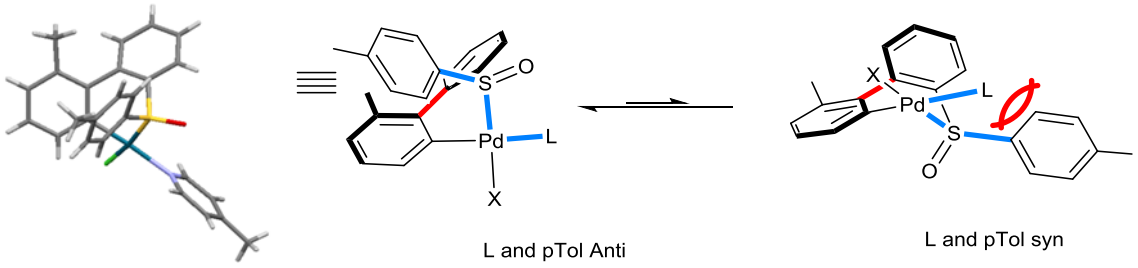

Figure V-21 : stereoselectivy model for the palladacycle intermediate

Influence of HFIP

Next, the effect of the expected hydrogen-bond between HFIP and the oxygen of the sulfoxyde was investigated. Titration of **C2** with HFIP in $CDCl_3$ led to an almost complete reversal of the d.r. measured : from 85:15 to 25:75 (which is coherent if we assume that H-bonding between the oxygen of the sulfoxyde and HFIP is effectively increasing the relative size of the oxygen, thereby diminishing the steric differentiation with the pTol substituent). Extensive peak broadening was also observed, which is characteristic of an accelerated rate of interconvertion between the two atropisomers. This modification of the d.r. in the presence of HFIP shows that the position of the equilibrium between **C1a-A** and **C1a-B** is of little importance towards the stereooutcome of the reaction. This fact hints that a Curtin-Hammett mechanism might be at work: indeed, if two reactants, here **C1a-A** and **C1a-B**, are in a fast equilibrium, and each gave an isomeric product (respectively **2a-A** and **2a-B**) the position of the equilibrium will not be reflected in the product distribution if the product formation is slow compared to the equilibrium.

Thus we set on measuring the effect of the palladacycle formation, with and without HFIP, on the barrier of atropisomerization of **1a**. Accordingly a barrier of 15.7 (±0.6)

kcal/mol was measured for **C2**, whereas a barrier of 15.6 (±0.6) kcal/mol was measured for **C2** in the presence of 4 equivalent of HFIP, a negligible difference. In either case, atropisomerization is extremely facile, and thus might be much more rapid than the oxidative addition and/or reductive elimination (OA/RE) that occur later on in the catalytic cycle (one should also note that the isolated solid palladacycles were stable for weeks under argon. However, slow dehydropalladation occurred for **C2** and **C3** in pure HFIP (few days), whereas dehydropalladation was very fast in the presence of AcOH (minutes).

Additionally, DFT calculations in collaboration with Jean-Pierre Djukic were undertaken to shed some light on the mechanism of the acetoxylation reaction, and especially to determine the stereo-selective step. Therefore, we turned ourselves to the analysis of the calculated reaction profile for **1a** in order to rationalize the overall transformation (DFTcalculation, in the gas phase at 298.15K: assuming a κ^2 carboxylate ligand on the palladium Figure V-22).

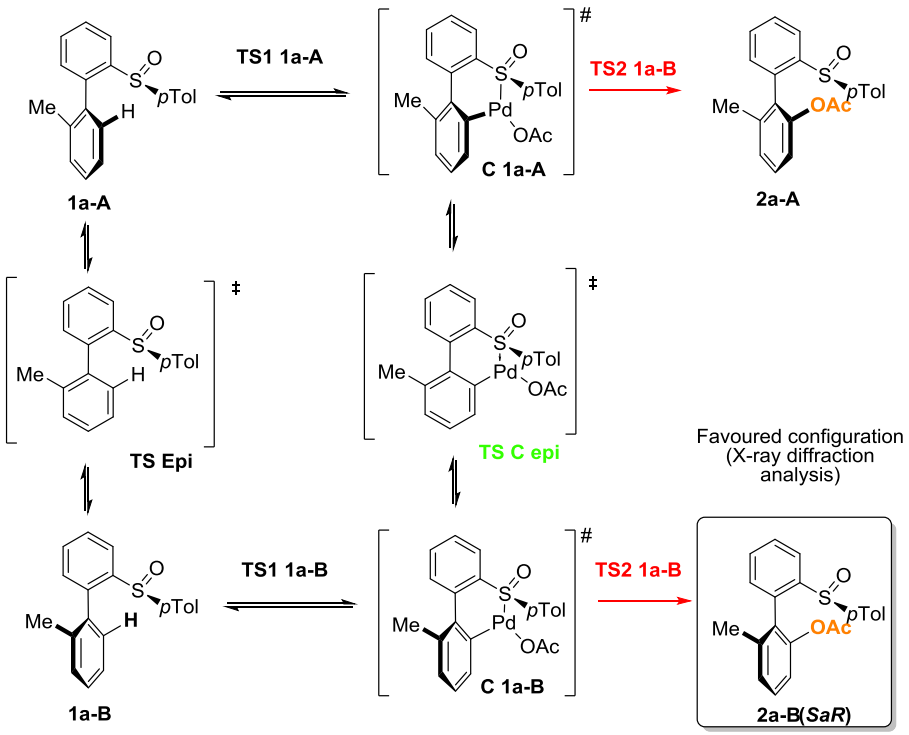

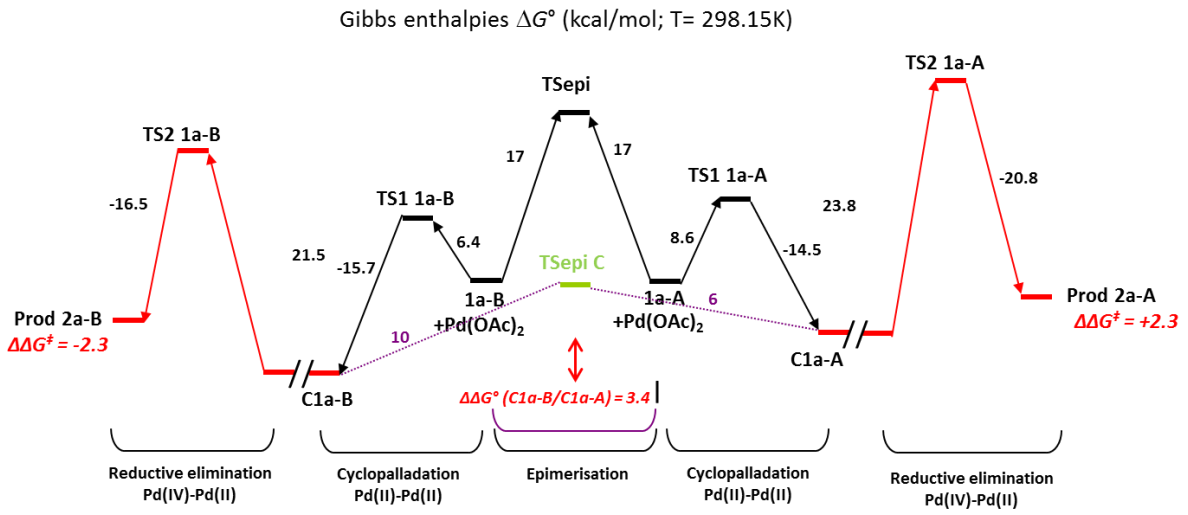

Figure V-22 : 1a reaction profile

Therefore, we turned ourselves to the analysis of the calculated reaction profile for **1a** in order to rationalize the overall transformation (DFT, in the gas phase at 298.15K: assuming a κ^2 carboxylate ligand on the palladium Figure V-22). As expected the C-H insertion is facile and reversible for each atropisomers (**TS1**: 6.4 kcal/mol for **1a-B**; 8.6 kcal/mol for **1a-A**; one should note that the reversibility is further enhanced by the dehydropalladation side-reaction in the presence of acetic acid). Atropisomerization of **1a** is also fast at 25°C (**TSepi**: 17 kcal/mol for both **1a-B** and **1a-B**) but palladacycle formation results in a spectacular reduction of the rotational barrier (**TSepi C**: 10 kcal/mol for both **C1a-B** and 6 kcal/mol **C1a-B**). Thus the pair of atropisomeric intermediates **C1a-B** and **C1a-A** are in rapid (*via* **TSepi C**) equilibrium considering that no bulky ligands are present in our medium. Therefore the stereo-determining step of the overall transformation should occur later in the catalytic cycle.

Indeed it was found that a Pd^{IV}-Pd^{II} C-O bond forming RE would be the turnover-limiting step. Experimental data support an irreversible reductive elimination from a Pd^{IV} intermediate as stoichiometric reaction of **1a** with $Pd(OAc)_2$ did not yield any product in the absence of an oxidant. Neither does reaction of **1a** with Pd^0. Furthermore, the acetoxylated product **2a** was found to be stable in the presence of Pd^{II} and/or Pd^0, thereby showing that acetoxylation is irreversible.

The overall transformation therefore satisfies the boundary Curtin-Hammett conditions[304]. The Curtin-Hammett principle[305] states that when two isomeric reactants (**C1a-B and C1a-A**) are in very fast equilibrium relative to the rates of their irreversible transformation towards two products (respectively **2a-B** and **2a-A**), the relative amount of **2a-B** and **2a-A** depends only on the difference of energy between the two transition states leading to the products ($\Delta\Delta G^{\ddagger}$ (**TS2 1a**) = $\Delta G^{\ddagger}$ (TS2 **1a-B**) - $\Delta G^{\ddagger}$ (TS2 **1a-A**) = -2.3 kcal/mol). Indeed, [**2a-B**]/[**2a-A**] = $e^{(-\Delta\Delta G\ddagger\ (TS2\ \mathbf{1a})/RT)}$: inserting the values calculated by DFT in the previous equation gave [**2a-B**]/[**2a-A**] = 48.5, which corresponds to a d.r.= 98:2. This is in good agreement with the experimental data, as the d.r. of **2A** was found to be ~98:2 (depending on the scale of the reaction).

Type II, substrate 1j.

As previously, we first attempted to measure the rotational barrier of **1j**. However the coalescence temperature was out of reach, as little peak broadening was observed at 100 °C, thus indicating a relatively high rotational barrier. Indeed the value of $\Delta G^{\ddagger}_{298.15K}$ = ~30 kcal/mol was found by calculation, corresponding to an half-life of $t½$ = ~49 years at 25°C. This indicates that a DYKAT mechanism is most probably at works for **1j**, as **2j** was isolated in 88% yield with a d.r. >98:2.

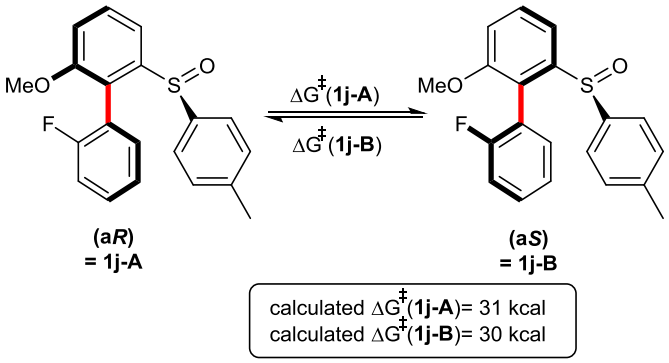

Figure V-23 : 1j rotation barrier

Thus an additional experiment was carried out to estimate the barrier. The acetoxylation was run at around 70% conversion and the catalyst quenched by a simple silica gel filtration. Then, inspection of the ^{19}F NMR spectra of the crude mixture showed the expected d.r. >90:10 in favor of **(aS)-1j-A.** However, after 36 hours at 25 °C in $CDCl_3$, we were surprised to find that equilibration of **1j** to its original d.r. of 60:40 (**(aS)-1j-A/(aR)-1j-b)** had occurred. This is clearly in contradiction with the calculated value of $\Delta G^{\ddagger}_{298.15K}$ = 30 kcal/mol, and the reasons for this discrepancy are unclear at the moment.

Nevertheless, **1j** reaction profile was calculated, and presents the following characteristics (Figure V-24).

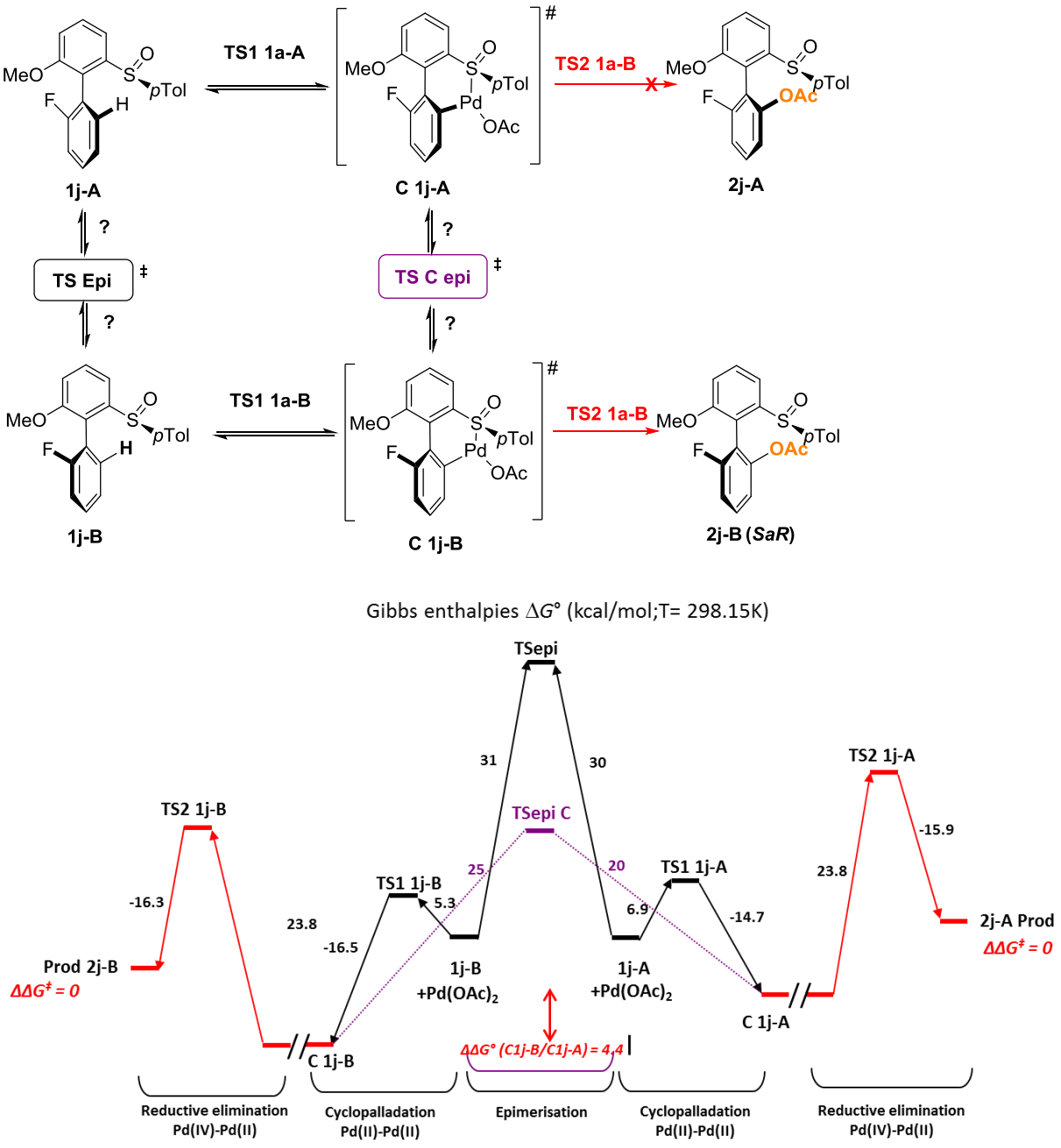

Figure V-24 : 1j reaction profile

First of all, C-H insertion is facile and reversible for both substrates. Then an interesting feature of the calculated reaction profile is that $\Delta G^{\ddagger}$ (**TS2 1j-B**) and $\Delta G^{\ddagger}$ (**TS2 1j-A**) are equal to 23.8 kcal/mol ($\Delta\Delta G^{\ddagger} = 0$). Thus the stereo-determining step must come before the OA/RE events in the catalytic cycle. Accordingly it is effectively seen on the reaction profile that epimerization of **1j**, cyclopalladation of **1j** and palladacycle epimerization of **C1j** all favor, kinetically and thermodynamically the **B** atropisomer. Thus **C1j-B** can be seen as a "thermodynamic and a kinetic sink". Furthermore the large free energy difference between **C 1j-B** and **C 1j-A**, $\Delta\Delta G°$ = -4.4 kcal/mol, indicates the high selectivity in favor of the product **C 1j-B**. This is further supported by the work of Feringa and coworkers on similar trisubstituted biphenyl sulfoxyde in

2016[303] (Figure V-25), where palladacycle formation from **X** led to only one atropisomer being visible on ^{1}H and ^{19}F NMR for palladacycles **C4** and **C5**.

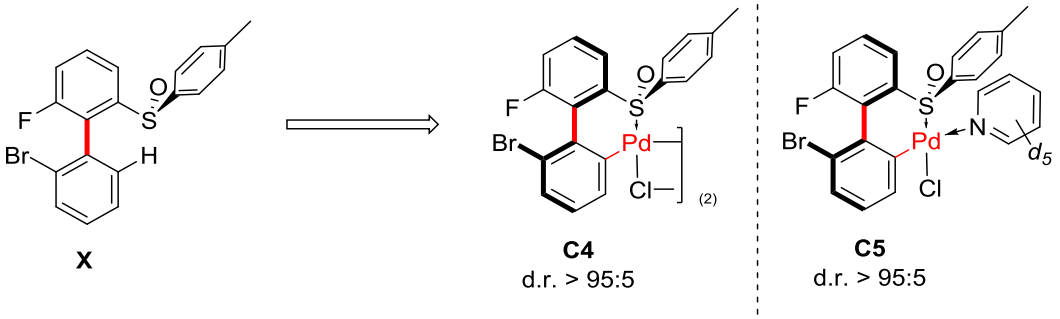

Figure V-25 : literature precedent of biphenylsulfoxyde palladacycles

Encouraged by the efficiency of this diastereoselective acetoxylation reaction, we subsequently focused on proving a more general character of such an original asymmetric C-H activation reaction. Aiming at the construction of synthetically useful axially chiral scaffolds, we turned our attention towards an iodination reaction.

C. Iodination

1. introduction

As previously mentioned, C(sp^2)-O and C(sp^2)-I bond formation share some common mechanistic manifolds and thus iodination using palladium catalysis by means of C-H activation will be briefly revueed.

Halogenation of arenes by means of palladium catalysis was known as early as 1970 when azobenzene was quite efficiently chlorinated by a $PdCl_2/Cl_2$ combination[306] (Figure V-26a). This early result already showcased the complementarity of the palladium catalyzed reaction with the electrophilic aromatic substitution, as different regioisomers were produced in both cases (Figure V-26b).

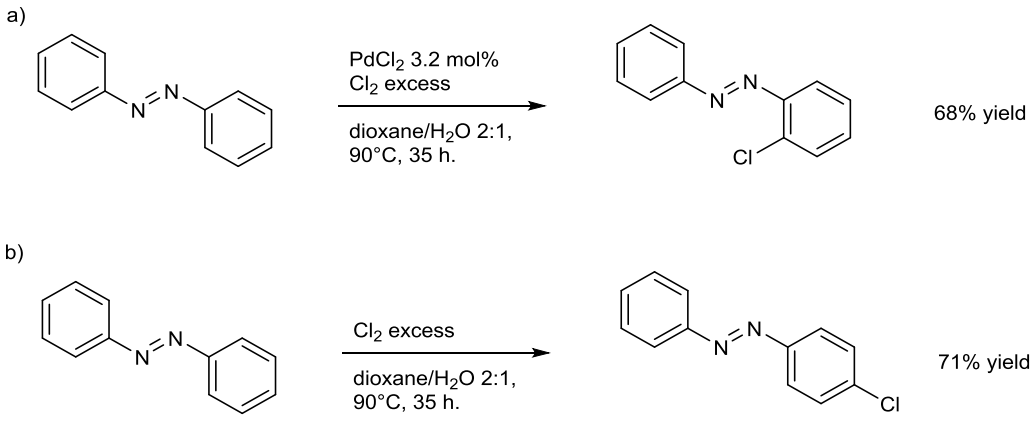

Figure V-26 : early examples of C-X Pd-catalyzed bond formation

However the use of a large excess of chlorine gas probably hampered its widespread acceptation. Accordingly, more practical halogenating agent were sought after, and one of most popular and efficient reagent acting as a source of "I^+" as well as an oxidant became N-iodosuccinimide NIS. In fact its use in combination with $Pd(OAc)_2$ was described in 2001 in a patent (functionalization of benzoic acids[307]) prior to the seminal Sanford article using N-chlorosuccinimide[291] (NCS). Other common oxidant system are (Figure V-27a)[308] : $PhI(OAc)_2/I_2$ (producing *in-situ* IOAc)[309], direct use of IOAc (Suàrez reagent) and molecular iodine I_2[310]. Interestingly, these iodination reactions could be conducted with $Pd(OAc)_2$ in AcOH with very little acetoxylated side-products (Figure V-27b).

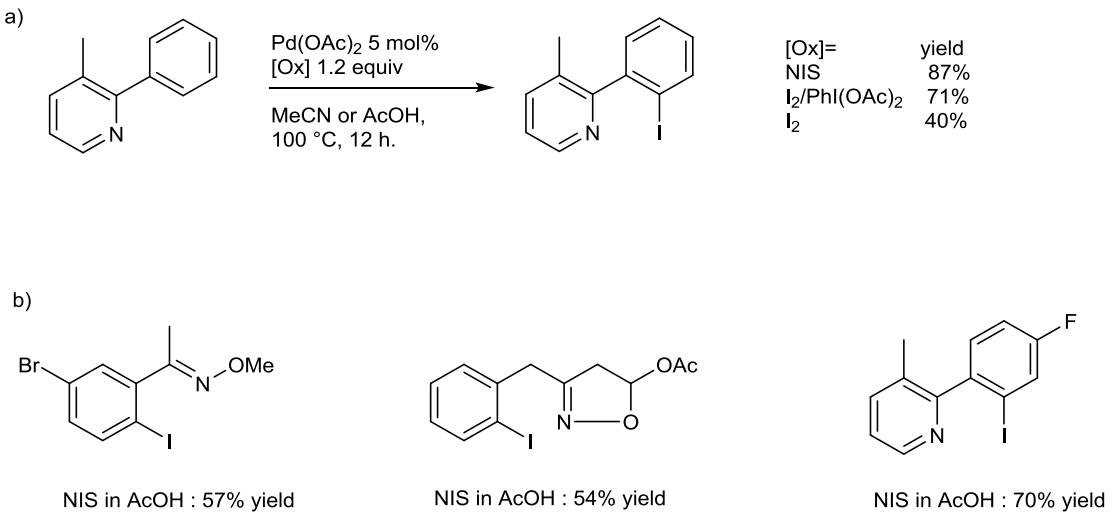

Figure V-27 : first example of directed Pd-catalyzed iodination

The putative Pd^{IV} intermediate was isolated[311] using the related oxidant N-chlorosuccinimide (NCS) (Figure V-28a). Interestingly, reductive elimination from this complex afforded the chlorinated product as the major one when AcOH was used as the solvent, whereas in pyridine the C-C coupling product was the major one (Figure V-28b).

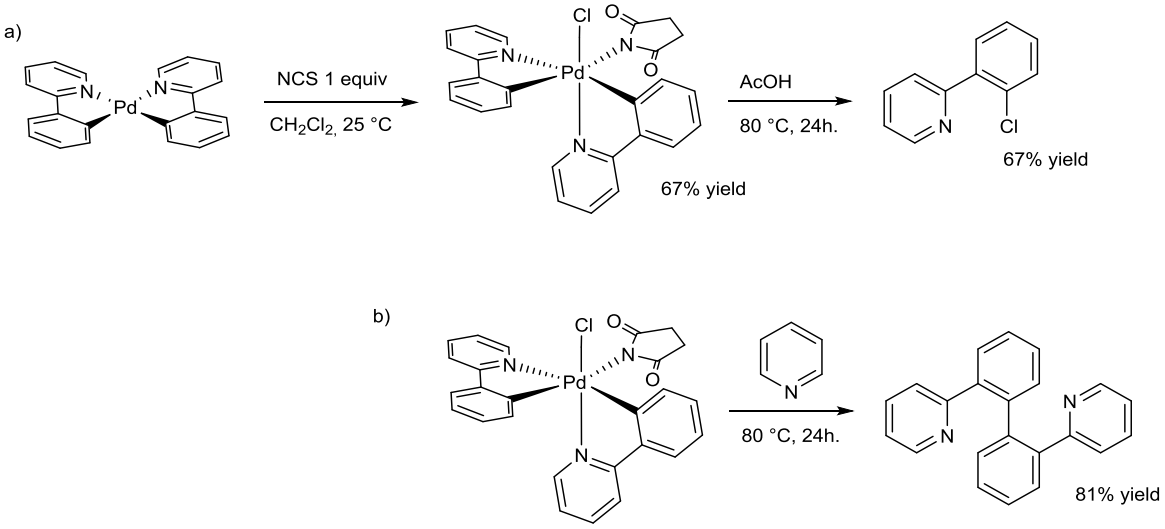

Figure V-28 : reductive C-X elimination from Pd^{IV}

As previously mentioned in the first part of this manuscript, the use of enantiopure MPAAs ligands enabled asymmetric transformations by kinetic resolution, and two examples are presented Figure V-29 : the first in 2014 by Yu and coworkers[36]. The second, more relevant to the subject of this thesis, by You and co-workers[312] also in 2014, where enantioenriched heterobiaryles could be obtained by means of C-H activation. This work was reported independently from our work on atroposelective iodination of biaryles by means of C-H activation a few months later.

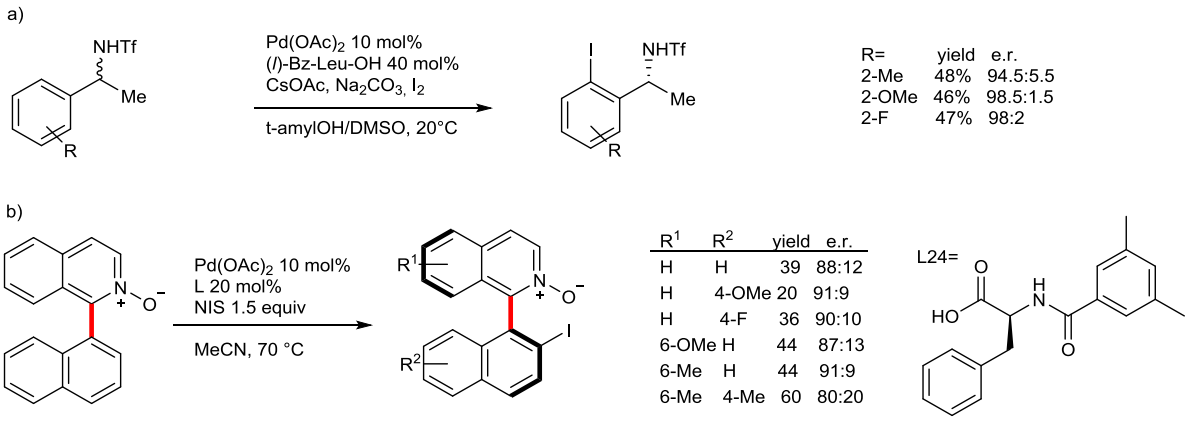

Figure V-29 : asymmetric iodination reaction

2. Results and discussion

Rapidly, compared to the C-H acetoxylation reaction conditions, we discovered that a simple replacement of $(NH_4)_2S_2O_8$ oxidant by NIS (1.3 equiv) led to a complete switch in the reactivity of our catalytic system enabling smooth, mild and highly diastereoselective C-I coupling (Scheme 4). The standard substrate **1a** could thus be converted into atropisomerically pure iodinated **3a** in excellent 98% yield.

The study of the reaction scope revealed that quite similar DKR occurs for this C-I coupling (Figure V-30). Slightly lowered diastereoselectivities were, however, observed and longer reaction times were required to achieve full conversions. Yet, disubstituted biaryls could be converted at room temperature and in good yields into iodinated products with diastereoselectivities ranging from 91:9 to > 98:2 (**3a**-**3i**). The efficiency of this C-I coupling for *ortho*-trisubstituted molecules depends strongly on the steric hindrance generated by the 6- and 2'- substituents. Comparably to the acetoxylation reaction, an excellent atroposelectivity was reached for **3j** bearing unbulky substituents (structure confirmed by X-ray diffraction analysis). Progressive increase of the steric demande around the Ar-Ar axis led, firstly, to a lower level of diastereoselectivity (**3k**, **3l**). Finally, the highly congested substrate **3n** underwent iodination under a simple kinetic resolution scenario. Besides, in the presence of NBS, **1a** could also be converted into the expected brominated **4a**, however a slight decrease in stereocontrol was observed (d.r. of 93:7).

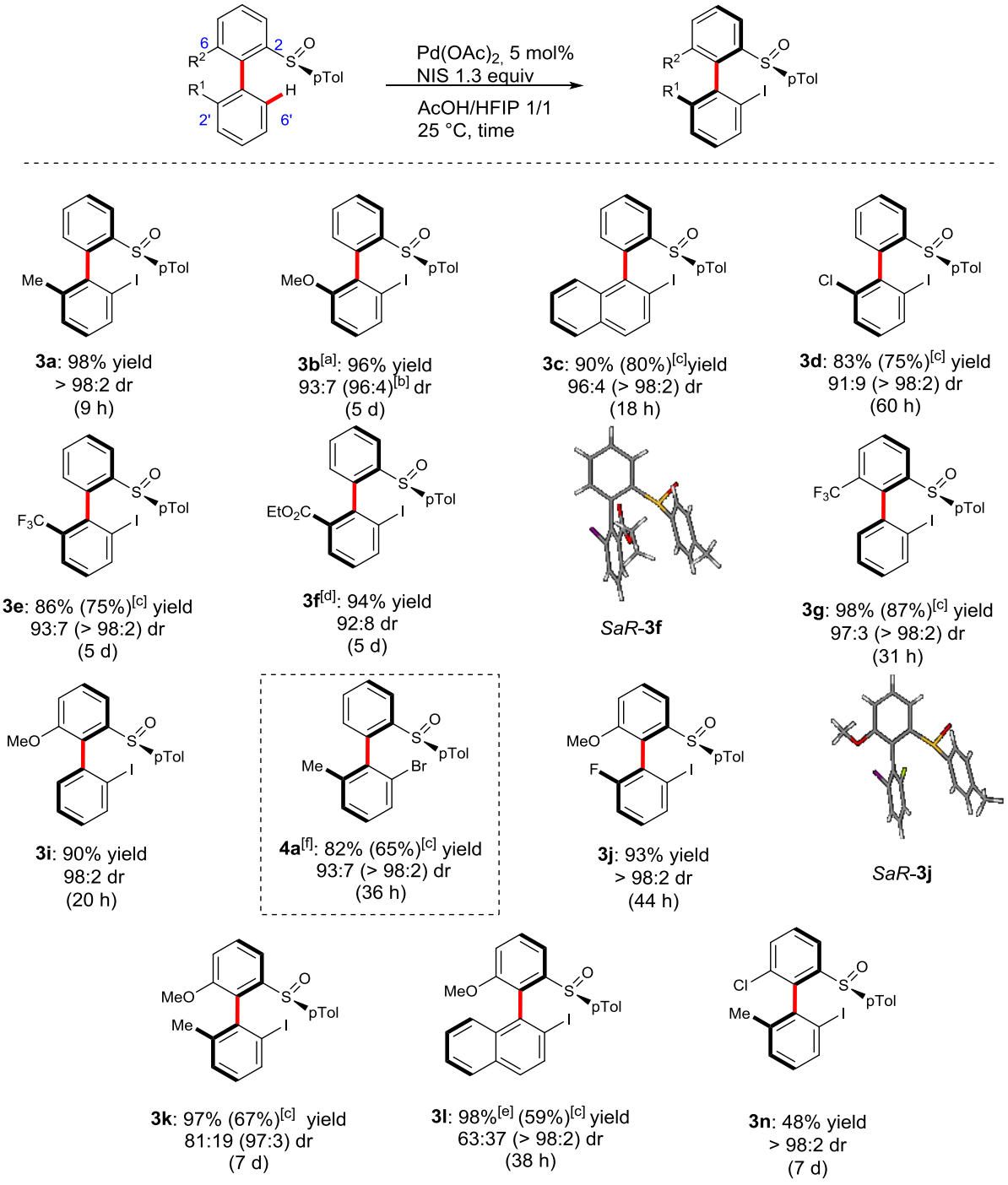

Figure V-30 : Substrate scope for asymmetric iodination occuring *via* KR/DKR

Standard reaction conditions: 1 (0.3 mmol-0.2 mmol); $Pd(OAc)_2$ (5 mol%); NIS (1.3 equiv), HFIP/AcOH 1/1 v/v, air, 25 °C; isolated yields; dr determined by ^1H NMR analysis on the crude mixture. [a] DCE as solvent at 40 °C, 10 mol% of $Pd(OAc)_2$. [b] dr after column. [c] yield and dr after recrystallization. [d] 10 mol% of $Pd(OAc)_2$. [e] conv. and dr measured on crude mixture. [f] NBS was used and the reaction was performed at 40 °C.

D. Post-functionalization

The additional key advantage of the herein presented strategy relies on the traceless character of the chiral sulfoxyde DG, which paves the way toward general application of our transformation (Figure V-31). The DG can be readily removed from the chiral products with retention of axial stereoenrichement via sulfoxyde/lithium exchange followed by electrophilic trapping (various electrophiles are compatible)[313,314]. As a representative example, chiral **2a** (prepared at 1.5 mmol scale in 96% yield and dr ≥ 98:2) was first converted into the protected alcohol **6** (in 89% yield). Subsequently low-temperature exchange with lithium and electrophilic trapping using dry ice afforded chiral carboxylic acid **7** in non-optimized 57% yield and e.r. superior to 99:1.

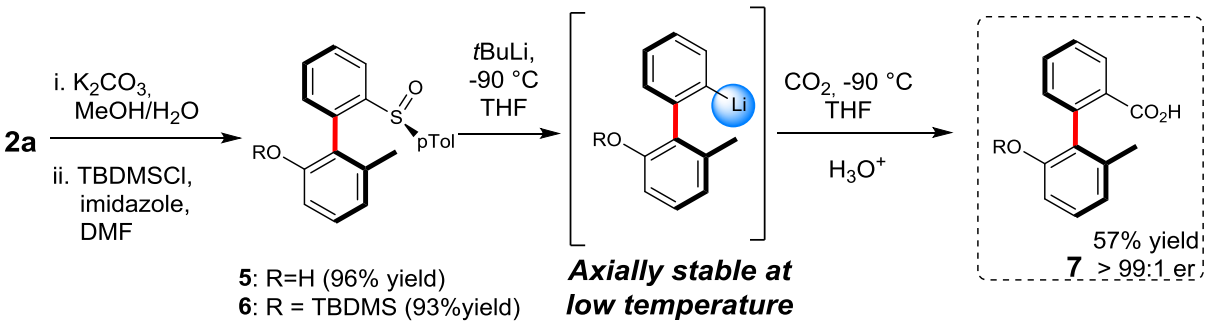

Figure V-31 : traceless character of the sulfoxyde auxilliary

In conclusion original atroposelective diastereoselective C-H activation reactions were developed. The characteristic features of these transformations are the mild conditions, and the possibility to access a large panel of oxygenated, iodinated and olefinated tri-substituted biaryls with high yields and selectivities by a DKR mechanism. Tetra-substituted biphenyls are either obtained *via* a DYKAT mechanism or a simple KR mechanism. This represent an efficient and powerful methodology to access a large panel of enatiopure biaryls scaffolds as the sulfoxyde auxiliary is cheap, readily available in both absolute configuration and interconvertible towards a myriad of functional groups by sulfoxyde/lithium exchange.

The application of the developed methodologies towards the synthesis of a known axially chiral natural product, (-)-steganone, was then undertaken I the next part of this manuscript. Indeed the C-H activation approach should afford the possibility of a more straightforward and economical synthesis.

This work on C-H acetoxylation and iodination has been reported in Angewandte Chemie, International Edition 2014, 53, 13871-13875 and Phosphorus, Sulfur and Silicon and the Related Elements 2015, 190, 1339-1351.

The publication on mechanistic studies and DFT calculations is in preparation.

E. Experimental part

1. General Procedure for acetoxylation reaction (GP3)

Reaction was performed under air. A sealed tube was successively charged with biaryl substrates (1a–1n, 0.2 mmol, 1.0 equiv), $Pd(OAc)_2$ (10 mol%, 4.5 mg, 0.02 mmol), $(NH_4)_2S_2O_8$ (2.0 equiv, 91.3 mg, 0.4 mmol). AcOH (46.5 equiv, 530 µL, 9.3 mmol), HFIP (25.3 equiv, 530 µL, 5.06 mmol), and H_2O (2.0 equiv, 7.2 µL, 0.40 mmol) [large amount of a solution of HFIP/H_2O was prepared separately] were added, and the resulting suspension was stirred at 25 °C until analysis of an aliquot by TLC indicated (near) complete conversion of the biaryl substrates (18–90 h). The reaction was quenched with saturated $NaHCO_3$ solution. Aqueous phase was extracted with EtOAc, the combined organic phase was washed with brine, dried over Na_2SO_4, filtrated and concentrated under vacuum to furnish the crude acetoxylated products 2a–2n. The crude mixture was analyzed by ^{1}H NMR to determine diastereomeric ratio. Purification by flash column chromatography on silica gel afforded the analytically pure acetoxylated products.

2. Characterization Data of the Acetoxylated products 2a–2n

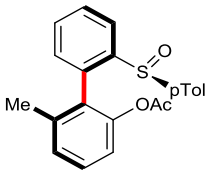

(*R*)-6-methyl-2'-((*S*)-*p*-tolylsulfinyl)-[1,1'-biphenyl]-2-yl acetate
Chemical Formula: $C_{22}H_{20}O_3S$
Molecular Weight: 364,4590

(*SaR*)-6-Methyl-2'-(*p*-tolylsulfinyl)-[1,1'-biphenyl]-2-yl-acetate [(*SaR*)-2a]: Prepared from (*S*)-2-methyl-2'-(*p*-tolylsulfinyl)-1,1'-biphenyl 1a, (1.0 equiv. 450 mg, 1.47 mmol) according to GP3, for 16 h by using $Pd(OAc)_2$ (10 mol%, 33 mg, 0.147 mmol), $(NH_4)_2S_2O_8$ (2.0 equiv, 670 mg, 2.94 mmol), AcOH (46.5 equiv, 3.91 mL, 68.4 mmol), HFIP (25.3 equiv, 3.91 mL, 37.19 mmol), and H_2O (2.0 equiv, 52.9 µL, 2.94 mmol). Purification by flash column chromatography on silica gel using mixture of cyclohexane and ethyl acetate (3/2, v/v) afforded the title compound [(*SaR*)-2a, 515.9 mg, 1.42 mmol, 96%, *dr* > 98:2] as a yellow crystal.

^{1}H-NMR ($CDCl_3$, 400 MHz): δ = 8.27 (dd, *J* = 7.9, 1.1 Hz, 1H), 7.63 (td, *J* = 7.6, 1.2 Hz, 1H), 7.47 (td, *J* = 7.5, 1.3 Hz, 1H), 7.35 (t, *J* = 7.9 Hz, 1H), 7.11–7.02 (m, 4H), 7.02–6.92 (m, 3H), 2.30 (s, 3H), 1.88 (s, 3H), 1.25 (s, 3H) ppm.
^{13}C-NMR ($CDCl_3$, 101 MHz): δ = 169.3, 148.2, 144.5, 142.0, 141.3, 139.3, 133.8, 131.3, 130.6, 130.1, 129.7 (2 C_{pTol}), 129.6, 128.9, 128.1, 126.5 (2 C_{pTol}), 123.1, 120.0, 21.5, 20.6, 19.5 ppm.
R_f (c-Hex : EtOAc = 2:1): 0.33.

Mp. = 168.3–170.3 °C.
IR (ATR): $\tilde{\nu}$ /cm^{-1} = 3053 (w), 2950 (w), 2924 (w), 1769 (s), 1463 (w), 1370 (m), 1198 (s), 1165 (s), 1083 (m), 1044 (s), 1028 (s), 1001 (s), 955 (m), 880 (m), 805 (s), 777 (s), 752 (s), 509 (s).
[α]$^{20}_{D}$ = –210.0 (c = 1, $CHCl_3$).
EA *calcd*. for $C_{22}H_{20}O_3S$: 72.50 (C); 5.53 (H); *found*: 72.14 (C); 5.48 (H).

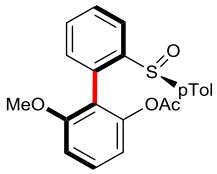

(*R*)-6-methoxy-2'-((*S*)-*p*-tolylsulfinyl)-[1,1'-biphenyl]-2-yl acetate
Chemical Formula: $C_{22}H_{20}O_4S$
Molecular Weight: 380,4580

(*SaR*)-6-Methoxy-2'-(*p*-tolylsulfinyl)-[1,1'-biphenyl]-2-yl-acetate [(*SaR*)-2b]: Prepared from (S)-2-methoxy-2'-(*p*-tolylsulfinyl)-1,1'-biphenyl 1b, (1.0 equiv, 97 mg, 0.3 mmol) according to GP3 at 10 °C for 36 h by using $Pd(OAc)_2$ (10 mol%, 6.7 mg, 0.03 mmol), $(NH_4)_2S_2O_8$ (2.0 equiv, 137 mg, 0.6 mmol), AcOH (46.5 equiv, 800 µL, 13.96 mmol), HFIP (25.3 equiv, 800 µL, 7.59 mmol), and H_2O (2.0 equiv, 10.8 µL, 0.6 mmol). The crude mixture was analyzed by ^{1}H NMR; *dr* = 91: 9. The product was purified by flash column chromatography on silica gel using mixture of cyclohexane and ethyl acetate (1/1, v/v) (87% yield) and recrystallization from *n*-pentane and dichloromethane to afford 2b as a colorless crystal (89.2 mg, 0.234 mmol, 78%, *dr* > 98:2).

^{1}H-NMR ($CDCl_3$, 400 MHz): δ = 8.12 (dd, *J* = 7.9, 1.0 Hz, 1H), 7.58 (td, *J* = 7.6, 1.2 Hz, 1H), 7.46 (td, *J* = 7.5, 1.2 Hz, 1H), 7.39 (t, *J* = 8.3 Hz, 1H), 7.14 (dd, *J* = 7.5, 1.0 Hz, 1H), 7.06 (br s, 4H), 6.86 (d, *J* = 8.2 Hz, 1H), 6.64 (d, *J* = 8.4 Hz, 1H), 3.28 (s, 3H), 2.30 (s, 3H), 1.91 (s, 3H) ppm.
^{13}C-NMR ($CDCl_3$, 101 MHz): δ = 169.2, 157.9, 148.9, 144.6, 142.2, 141.3, 131.9, 131.5, 130.5, 130.3, 129.4 (2 $C_{p\text{Tol}}$), 128.9, 126.3 (2 $C_{p\text{Tol}}$), 124.0, 119.9, 114.8, 108.3, 55.3, 21.5, 20.6 ppm.
R_f (*c*-Hex : EtOAc = 1:1): 0.27.
Mp. = 175.7–177.7 °C.
IR (ATR): $\tilde{\nu}$ /cm^{-1} = 2924 (w), 2847 (w), 1769 (s), 1605 (m), 1580 (m), 1464 (m), 1365 (w), 1270 (m), 1198 (m), 1075 (s), 1040 (s), 778 (s), 530 (s).
[α]$^{20}_{D}$ = –205.0 (c = 1, $CHCl_3$).
EA *calcd*. for $C_{22}H_{20}O_4S$: 69.45 (C); 5.30 (H); *found*: 69.36 (C); 5.32 (H).

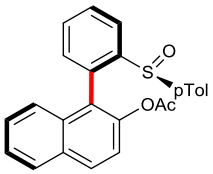

1-(2-((*S*)-*p*-tolylsulfinyl)phenyl)naphthalen-2-yl acetate
Chemical Formula: $C_{25}H_{20}O_3S$
Molecular Weight: 400,4920

(*SaR*)-1-[2-(*p*-Tolylsulfinyl)phenyl]naphthalen-2-yl-acetate [(*SaS*)-2c]: Prepared from (*S*)-1-[2-(*p*-tolylsulfinyl)phenyl]naphthalene (1 equiv, 102 mg, 0.3 mmol) following the GP3 for 38 h, using $(NH_4)_2S_2O_8$ (2 equiv, 136 mg, 0.6 mmol) and $Pd(OAc)_2$ (10 mol%, 6.74 mg, 0.03 mmol) and H_2O (2 equiv, 10.8 µL, 0.6 mmol), in a mixture of AcOH (46.5 equiv, 800 µL, 13.96 mmol), and HFIP (25.3 equiv, 800 µL, 7.59 mmol). The crude mixture was analyzed by ^{1}H NMR; dr = 98:2. The crude product was purified by flash chromatography on triethylamine-neutralized silica gel (EtOAc/*c*-Hex 1:3), giving (*SaR*)-1-[2-(*p*-tolylsulfinyl)phenyl]naphthalen-2-yl-acetate (113 mg, 0.284 mmol, 95 %, *dr* = 98:2), as white solid.

^{1}H-NMR (400 MHz, $CDCl_3$): δ = 8.30 (d, *J* = 7.9 Hz, 1 H), 7.95 (d, *J* = 8.9 Hz, 1 H), 7.80 (d, *J* = 8.2 Hz, 1 H), 7.71 (t, *J* = 7.7 Hz, 1 H), 7.55 (t, *J* = 7.4 Hz, 1 H), 7.39 (d, *J* = 8.8 Hz, 1 H), 7.33 (t, *J* = 7.9 Hz, 1 H), 7.21 (d, *J* = 7.5 Hz, 1 H), 6.98-6.94 (m, 1 H), 6.67–6.59 (m, 5 H), 2.07 (s, 3 H), 2.01 (s, 3 H) ppm.
^{13}C-NMR (101 MHz, $CDCl_3$): δ = 169.2, 145.6, 145.5, 141.3, 140.8, 132.8, 132.6, 131.9, 131.6, 130.4, 130.3, 129.2 (2 $C_{p\text{Tol}}$), 129.1, 127.8, 126.4, 126.0, 125.8 (2 $C_{p\text{Tol}}$), 125.3, 125.1, 123.7, 121.4, 21.1, 20.6 ppm.
R_f (EtOAc/*c*-Hex 3:2) = 0.63.
Mp. = 144.9–147 °C.
IR (ATR): $\tilde{\nu}$ /cm^{-1} = 3055 (w), 2923 (w), 2852 (w), 1763 (s), 1367 (m), 1192 (s), 1041 (s), 1014 (m), 806 (m), 768 (m), 535 (s).
$[\alpha]_D^{21}$= –123.9 (c = 0.75, $CHCl_3$).
EA = *calcd. for* $C_{25}H_{20}O_3S$ 74.98 (C), 5.03 (H), *found* 75.06 (C), 5.23 (H).

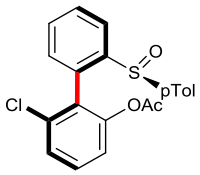

(*S*)-6-chloro-2'-((*S*)-*p*-tolylsulfinyl)-[1,1'-biphenyl]-2-yl acetate
Chemical Formula: $C_{21}H_{17}ClO_3S$
Molecular Weight: 384,8740

(*SaS*)-6-Chloro-2'-(*p*-tolylsulfinyl)-[1,1'-biphenyl]-2-yl-acetate [(*SaS*)-2d]: Prepared from (*S*)-2-chloro-2'-(*p*-tolylsulfinyl)-1,1'-biphenyl 1d, (1.0 equiv, 65.0 mg, 0.2 mmol) according to GP3 for 36 h by using $Pd(OAc)_2$ (10 mol%, 4.5 mg, 0.02 mmol), $(NH_4)_2S_2O_8$ (2.0 equiv, 91.3 mg, 0.4 mmol), AcOH (46.5 equiv, 530 µL, 9.3 mmol), HFIP (25.3 equiv, 530 µL, 5.06 mmol), and H_2O (2.0 equiv, 7.2 µL, 0.4 mmol, 2.0 equiv). The crude mixture was analyzed by ^{1}H NMR; *dr* = 92:8. The product was purified by flash column chromatography on silica gel using mixture of cyclohexane and ethyl acetate (1/1, v/v) (87 % yield) and recrystallization from *n*-pentane and dichloromethane to afford 2d as a colorless crystal (59.0 mg, 0.153 mmol, 77% *dr* > 98:2).

^{1}H-NMR ($CDCl_3$, 400 MHz): δ = 8.13 (d, *J* = 8.1 Hz, 1H), 7.62 (t, *J* = 7.6 Hz, 1H), 7.50 (t, *J* = 7.5 Hz, 1H), 7.41 (t, *J* = 8.1 Hz, 1H), 7.26 (d, *J* = 8.1 Hz, 1H), 7.20 (d, *J* = 7.8 Hz, 1H), 7.19 (d, *J* = 7.6 Hz, 1H), 7.09 (br s, 4H), 2.32 (s, 3H), 1.93 (s, 3H) ppm.

^{13}C-NMR ($CDCl_3$, 101 MHz): δ = 168.9, 149.2, 144.8, 141.9, 141.2, 135.5, 132.2, 131.8, 130.8, 130.3, 130.2, 129.9 (2 C_{pTol}), 129.8, 127.5, 125.9 (2 C_{pTol}), 123.9, 121.4, 21.6, 20.6 ppm.
R_f (*c*-Hex : EtOAc = 1:1): 0.44.
Mp. = 159.1–161.1 °C.
IR (ATR): $\tilde{\nu}$ /cm^{-1} = 2362 (w), 2325 (w), 1771 (s), 1449 (m), 1195 (s), 1174 (s), 1088 (m), 1046 (s), 1015 (s), 935 (s), 776 (s), 741 (s), 531 (s), 507 (s).
$[\alpha]^{20}_D$ = –183.0 (c = 1, $CHCl_3$).
EA *calcd*. for $C_{21}H_{17}ClO_3S$: 65.54 (C); 4.45 (H); *found*: 65.60 (C); 4.45 (H).

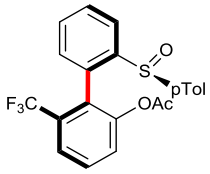

(*R*)-2'-((*S*)-*p*-tolylsulfinyl)-6-(trifluoromethyl)-[1,1'-biphenyl]-2-yl acetate
Chemical Formula: $C_{22}H_{17}F_3O_3S$
Molecular Weight: 418,4302

(*SaR*)-2'-(*p*-Tolylsulfinyl)-6-(trifluoromethyl)-[1,1'-biphenyl]-2-yl-acetate [(*SaR*)-2e]: Prepared from (*S*)-2-(*p*-tolylsulfinyl)-2'-(trifluoromethyl)-1,1'-biphenyl 1e, (1.0 equiv, 108 mg, 0.3 mmol) according to GP3 for 60 h by using $Pd(OAc)_2$ (10 mol%, 6.7 mg, 0.03 mmol), $(NH_4)_2S_2O_8$ (2.0 equiv, 137 mg, 0.6 mmol), AcOH (46.5 equiv, 800 µL, 13.96 mmol), HFIP (25.3 equiv, 800 µL, 7.59 mmol), and H_2O (2.0 equiv, 10.8 µL, 0.6 mmol). The crude mixture was analyzed by ^{1}H NMR; *dr* = 95:5. The product was purification by flash column chromatography on silica gel using mixture of cyclohexane and ethyl acetate (1/1, v/v) (79% yield) and recrystallization from *n*-pentane and dichloromethane to afford 2e as a colorless crystal (90.3 mg, 0.216 mmol, 72% *dr* > 98:2).

^{1}H-NMR ($CDCl_3$, 400 MHz): δ = 8.09 (d, *J* = 7.9 Hz, 1H), 7.69–7.57 (m, 3H), 7.54–7.43 (m, 2H), 7.18 (d, *J* = 7.4 Hz, 1H), 7.09 (d, *J* = 8.2 Hz, 2H), 7.04 (d, *J* = 8.2 Hz, 2H), 2.31 (s, 3H), 1.92 (s, 3H) ppm.
^{13}C-NMR ($CDCl_3$, 101 MHz): δ = 168.9, 149.2, 144.8, 142.1, 140.5, 131.8, 131.1 (q, J_{CF} = 2.0 Hz), 130.6, 130.1, 129.9, 129.7 (2 C_{pTol}), 126.7 (q, J_{CF} = 2.1 Hz), 125.8 (2 C_{pTol}), 124.5 (q, J_{CF} = 5.1 Hz), 124.2, 123.0 (q, J_{CF} = 275.0 Hz), 121.6, 21.5, 20.5 ppm + 1C overlapping.
^{19}F-NMR ($CDCl_3$, 377 MHz): –57.8 ppm.
R_f (*c*-Hex : EtOAc = 1:1): 0.31.
Mp. = 158.3–160.3 °C.
IR (ATR): $\tilde{\nu}$ /cm^{-1} = 3047 (w), 2925 (w), 1770 (s), 1448 (m), 1432 (m), 1371 (m), 1314 (s), 1196 (s), 1164 (s), 1082 (s), 1043 (s), 925 (s), 814 (s), 756 (s), 624 (s), 535 (s).
$[\alpha]^{20}_D$ = –198.7 (c = 1, $CHCl_3$).
EA *calcd*. for $C_{22}H_{17}F_3O_3S$: 63.15 (C); 4.10 (H); *found*: 63.37 (C); 4.00 (H).

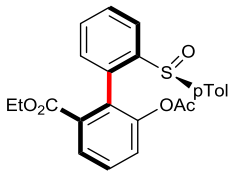

ethyl (*R*)-6-acetoxy-2'-((*S*)-*p*-tolylsulfinyl)-[1,1'-biphenyl]-2-carboxylate
Chemical Formula: $C_{24}H_{22}O_5S$
Molecular Weight: 422,4950

(*SaR*)-Ethyl-6-acetoxy-2'-((S)-*p*-tolylsulfinyl)-[1,1'-biphenyl]-2-carboxylate [(*SaR*)-2f]: Prepared from ethyl (*S*)-2'-(*p*-tolylsulfinyl)-[1,1'-biphenyl]-2-carboxylate 1f, (1.0 equiv, 73 mg, 0.2 mmol) according to GP3 for 48 h by using $(NH_4)_2S_2O_8$ (2.0 equiv, 91 mg, 0.4 mmol), $Pd(OAc)_2$ (10 mol%, 4.5 mg, 0.02 mmol) and H_2O (2.0 equiv, 7 µL, 0.4 mmol), in a mixture of AcOH (46.5 equiv, 530 µL, 9.3 mmol) and HFIP (25.3 equiv, 530 µL, 5.06 mmol). The crude mixture was analyzed by ^{1}H NMR; dr = 95:5. The crude product was purified by flash chromatography on triethylamine-neutralized silica gel (EtOAc/*c*-Hex 1:2), giving (69 mg, 0.163 mmol, 82 %, *dr* = 95 : 5) as yellowish solid.

^{1}H-NMR (400 MHz, $CDCl_3$): δ = 8.10 (dd, *J* = 7.9 Hz, 0.9 Hz, 1 H), 7.93 (dd, *J* = 7.9, 1.2 Hz, 1 H), 7.57-7.50 (m, 2 H), 7.45-7.41 (m, 2 H), 7.43-7.27 (m, 5 H), 3.78 (ABX_3, *J* = 11.1, 7.1 Hz, 1 H), 3.58 (ABX_3, *J* = 11.1, 7.1 Hz, 1 H), 2.30 (s, 3 H), 1.91 (s, 3 H), 0.74 (ABX_3, 7.1 Hz, 3 H) ppm.
^{13}C-NMR (101 MHz, $CDCl_3$): δ = 169.0, 165.1, 148.7, 143.6, 141.5, 141.2, 134.5, 132.2, 131.9, 130.6, 130.2, 129.6 (2 $C_{p\text{Tol}}$), 129.5, 129.0, 128.7, 126.7, 125.8 (2 $C_{p\text{Tol}}$), 123.7, 60.6, 21.4, 20.4, 13.4 ppm.
R_f (EtOAc/*c*-Hex 1:1) = 0.37.
Mp. = 122-124 °C (Et_2O).
IR (ATR): $\tilde{\nu}$ /cm^{-1} = 3053 (w), 2979 (w), 2957 (w), 2925 (w), 1770 (s), 1714 (s), 1461 (m), 1367 (m), 1288 (s), 1195 (s), 1181 (s), 1082 (m), 1042 (s), 1023 (s), 1015 (s), 810 (s), 755 (s), 528 (s).
$[\alpha]_D^{21}$ = –172.2 (c = 0.1, $CHCl_3$).
HRMS (*ESI*) = 445.1084 [M+Na$^+$], *calcd.* for $C_{24}H_{22}NaO_5S^+$ = 445.1080.

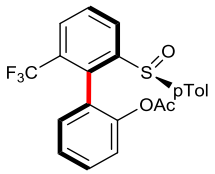

2'-((*S*)-*p*-tolylsulfinyl)-6'-(trifluoromethyl)-[1,1'-biphenyl]-2-yl acetate
Chemical Formula: $C_{22}H_{17}F_3O_3S$
Molecular Weight: 418,4302

(*SaR*)-2'-(*p*-Tolylsulfinyl)-6'-(trifluoromethyl)-[1,1'-biphenyl]-2-yl-acetate [(*SaR*)-2g]: Prepared from (*S*)-2-(*p*-tolylsulfinyl)-6-(trifluoromethyl)-1,1'-biphenyl 1g, (1.0 equiv, 72.0 mg, 0.2 mmol) according to GP3 for 38 h by using $Pd(OAc)_2$ (10 mol%, 4.5 mg, 0.02 mmol), $(NH_4)_2S_2O_8$ (2.0 equiv, 91.3 mg, 0.4 mmol), AcOH (46.5 equiv, 530 µL, 9.3 mmol), HFIP (25.3 equiv, 530 µL, 5.06 mmol), and H_2O (2.0 equiv, 7.2 µL, 0.4 mmol). The crude product was analyzed by ^{1}H NMR, *dr* = 98:2. Purification by

flash column chromatography on silica gel using mixture of cyclohexane and ethyl acetate (1/1, v/v) afforded the title compound [(*SaR*)-2g, 74.2 mg, 0.177 mmol, 89%, *dr* = 98:2] as a colorless thick oil.

^{1}H-NMR ($CDCl_3$, 400 MHz): δ = 8.47 (dd, *J* = 7.9, 0.6 Hz, 1H), 7.87 (d, *J* = 7.6 Hz, 1H), 7.77 (t, *J* = 7.7 Hz, 1H), 7.51–7.38 (m, 2H), 7.07 (d, *J* = 8.0 Hz, 2H), 7.03 (td, *J* = 7.5, 1.0 Hz, 1H), 6.99 (d, *J* = 8.2 Hz, 2H), 6.53 (d, *J* = 7.6 Hz, 1H), 2.32 (s, 3H), 2.02 (s, 3H) ppm.
^{13}C-NMR ($CDCl_3$, 101 MHz): δ = 168.1, 147.9, 147.6, 142.4, 141.2, 133.9 (q, J_{CF} = 1.5 Hz), 132.2 (q, J_{CF} = 1.3 Hz), 130.3 (q, J_{CF} = 30.0 Hz), 130.3, 129.9 (2 $C_{p\text{Tol}}$), 129.3, 128.7 (q, J_{CF} = 5.1 Hz), 127.3, 126.5 (2 $C_{p\text{Tol}}$), 125.6, 125.0, 123.3 (q, J_{CF} = 275.4 Hz), 122.8, 21.5, 20.9 ppm.
^{19}F-NMR ($CDCl_3$, 377 MHz): –58.0 ppm.
R_f (*c*-Hex : EtOAc = 1:1): 0.34.
IR (ATR): $\tilde{\nu}$ /cm^{-1} = 2958 (w), 2922 (w), 2852 (w), 1759 (s), 1448 (m), 1370 (m), 1310 (s), 1185 (s), 1170 (s), 1128 (s), 803 (s), 762 (s), 697 (s), 535 (s), 507 (s).
$[\alpha]^{20}_D$ = –197.5 (c = 0.97, $CHCl_3$).
HRMS: 441.0743 $[M+Na]^+$, *calcd*. for $C_{22}H_{17}NaF_3O_3S$ = 441.0734.

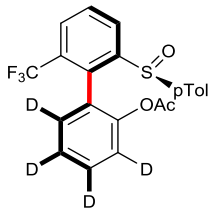

(*R*)-2'-((*S*)-*p*-tolylsulfinyl)-6'-(trifluoromethyl)-[1,1'-biphenyl]-2-yl-3,4,5,6-d_4 acetate
Chemical Formula: $C_{22}H_{13}D_4F_3O_3S$
Molecular Weight: 422,4546

(*SaR*)-2'-(*p*-Tolylsulfinyl)-6'-(trifluoromethyl)-3,4,5,6-d$_4$-[1,1'-biphenyl]-2-yl-acetate [(*SaR*)-2h]: Prepared from (*S*)-2-(*p*-tolylsulfinyl)-6-(trifluoromethyl)-2',3',4',5',6'-d5-1,1'-biphenyl 1h, (1.0 equiv, 36.5 mg, 0.1 mmol) according to GP3 for 48 h by using $Pd(OAc)_2$ (10 mol%, 2.3 mg, 0.01 mmol), $(NH_4)_2S_2O_8$ (2.0 equiv, 45.6 mg, 0.2 mmol), AcOH (46.5 equiv, 270 µL, 4.65 mmol), HFIP (25.3 equiv, 270 µL, 2.53mmol) and H_2O (2.0 equiv, 3.6 µL, 0.2 mmol). The crude product was analyzed by ^{1}H NMR, *dr* = 97:3. Purification by flash column chromatography on silica gel using mixture of cyclohexane and ethyl acetate (1/1, v/v) afforded the title compound [(*SaR*)-2h, 36.8 mg, 0.087 mmol, 87%, *dr* = 97:3] as a colorless oil.

^{1}H-NMR ($CDCl_3$, 400 MHz): δ = 8.47 (d, *J* = 7.8 Hz, 1H), 7.87 (d, *J* = 7.7 Hz, 1H), 7.77 (t, *J* = 7.9 Hz, 1H), 7.08 (d, *J* = 8.0 Hz, 2H), 6.99 (d, *J* = 8.1 Hz, 2H), 2.32 (s, 3H), 2.02 (s, 3H) ppm.
^{13}C-NMR ($CDCl_3$, 101 MHz): δ = 168.1, 147.8, 147.6, 142.4, 141.2, 133.8 (q, J_{CF} = 1.6 Hz), 130.3 (q, J_{CF} = 30.1 Hz), 129.9 (2 $C_{p\text{Tol}}$), 129.3, 128.7 (q, J_{CF} = 5.1 Hz), 127.3, 126.5 (2 $C_{p\text{Tol}}$), 125.5, 123.3 (q, J_{CF} = 275.8 Hz), 21.6, 21.0 ppm.
^{19}F-NMR ($CDCl_3$, 377 MHz): –58.0 ppm.
R_f (*c*-Hex : EtOAc = 1:1): 0.60.

IR (ATR): $\tilde{\nu}$ /cm^{-1} = 3056 (w), 2925 (m), 2869 (w), 1769 (w), 1394 (m), 1369 (m), 1310 (s), 1192 (s), 1141 (s), 1068 (s), 1046 (s), 807 (s), 754 (s), 695 (m). **[α]$^{20}_{D}$** = –183.4 (c = 1.35, $CHCl_3$). **HRMS**: 445.0985 [M+Na]$^+$, *calcd*. for $C_{22}H_{13}D_4NaF_3O_3S$ = 445.0994.

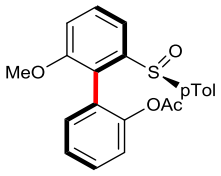

2'-methoxy-6'-((*S*)-*p*-tolylsulfinyl)-[1,1'-biphenyl]-2-yl acetate
Chemical Formula: $C_{22}H_{20}O_4S$
Molecular Weight: 380,4580

(*SaR*)-2'-Methoxy-6'-(*p*-tolylsulfinyl)-[1,1'-biphenyl]-2-yl-acetate [(*SaR*)-2i]: Prepared from (*S*)-2-methoxy-6-(*p*-tolylsulfinyl)-1,1'-biphenyl 1i, (1.0 equiv, 64.4 mg, 0.2 mmol) according to GP3 for 20 h by using $Pd(OAc)_2$ (10 mol%, 4.5 mg, 0.02 mmol), $(NH_4)_2S_2O_8$ (2.0 equiv, 91.3 mg, 0.4 mmol), AcOH (46.5 equiv, 530 µL, 9.28 mmol), HFIP (25.3 equiv, 530 µL, 5.06 mmol), and H_2O (2.0 equiv, 7.2 µL, 0.4 mmol). The crude mixture was analyzed by ^{1}H NMR, *dr* > 98:2. Purification by flash column chromatography on silica gel using mixture of cyclohexane and ethyl acetate (1/1, v/v) afforded the title compound [(*SaR*)-2i, 56.6 mg, 0.149 mmol, 75%, *dr* > 98:2] as a white solid.

^{1}H-NMR ($CDCl_3$, 300 MHz): δ = 7.77 (dd, *J* = 7.9, 1.0 Hz, 1H), 7.56 (t, *J* = 8.1 Hz, 1H), 7.13 (td, *J* = 7.5, 1.2 Hz, 1H), 7.47–7.38 (m, 1H), 7.29 (dd, *J* = 8.1, 1.1 Hz, 1H), 7.16–7.02 (m, 5H), 6.75 (dd, *J* = 7.6, 1.6 Hz, 1H), 3.71 (s, 3H), 2.30 (s, 3H), 2.00 (s, 3H) ppm.
^{13}C-NMR ($CDCl_3$, 75 MHz): δ = 168.9, 157.2, 148.2, 146.4, 142.3, 141.5, 133.0, 130.2, 129.6 (1 C + 2 C_{pTol}), 126.5, 125.9 (2 C_{pTol}), 125.6, 123.7, 122.8, 115.7, 113.6, 56.3, 21.5, 20.8 ppm.
R_f (*c*-Hex : EtOAc = 1:1): 0.22.
IR (ATR): $\tilde{\nu}$ /cm^{-1} = 3013 (w), 2927 (w), 1769 (s), 1587 (m), 1455 (s), 1368 (m), 1260 (s), 1128 (s), 1021 (m), 721 (m). **[α]$^{20}_{D}$** = –269.3 (c = 0.745, $CHCl_3$). **HRMS:** 403.0948 [M+Na]$^+$, *calcd*. for $C_{22}H_{20}NaO_4S$ = 403.0975.

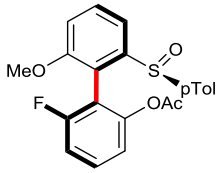

(*S*)-6-fluoro-2'-methoxy-6'-((*S*)-*p*-tolylsulfinyl)-[1,1'-biphenyl]-2-yl acetate
Chemical Formula: $C_{22}H_{19}FO_4S$
Molecular Weight: 398,4484

(*SaS*)-6-Fluoro-2'-methoxy-6'-(*p*-tolylsulfinyl)-[1,1'-biphenyl]-2-yl-acetate [(*SaS*)-2j]: Prepared from (*S*)-2'-fluoro-2-methoxy-6-(*p*-tolylsulfinyl)-1,1'-biphenyl 1j, (1.0

equiv, 102 mg, 0.3 mmol) following the GP3 for 90 h, using $(NH_4)_2S_2O_8$ (2.0 equiv, 136 mg, 0.6 mmol), $Pd(OAc)_2$ (10 mol%, 6.7 mg, 0.03 mmol) and H_2O (2.0 equiv, 10.8 µL, 0.6 mmol), in a mixture of AcOH (46.5 equiv, 800 µL, 13.96 mmol), and HFIP (25.3 equiv, 800 µL, 7.59 mmol). The crude mixture was analyzed by ^{1}H NMR, dr > 95:5. The crude product was purified by flash chromatography on triethylamine-neutralized silica gel (EtOAc/*c*-Hex 1:2), giving (*SaS*)-6-fluoro-2'-methoxy-6'-(*p*-tolylsulfinyl)-[1,1'-biphenyl]-2-yl acetate (105 mg, 0.264 mmol, 88%, *dr* > 98:2) as white powder.

^{1}H-NMR (400 MHz, $CDCl_3$): δ = 7.72 (dd, *J* = 8.0, 0.9 Hz, 1 H), 7.59 (t, *J* = 8.0 Hz, 1 H), 7.42 (td, *J* = 8.3, 6.4 Hz, 1 H), 7.14–7.04 (m, 6 H), 6.88 (td, *J* = 7.6, 0.9 Hz, 1 H), 3.75 (s, 3 H), 2.31 (s, 3 H), 2.01 (s, 3 H) ppm.
^{13}C-NMR (101 MHz, $CDCl_3$): δ = 168.5, 160.9 (d, J_{CF} = 248.7 Hz), 157.6, 149.1 (d, J_{CF} = 6.1 Hz), 146.7, 141.8, 141.7, 131.0, 130.3 (d, J_{CF} = 10.2 Hz), 129.8 (2 C_{pTol}), 125.5 (2 C_{pTol}), 118.5 (d, J_{CF} = 3.5 Hz), 117.6, 115.9, 115.8 (d, J_{CF} = 20 Hz), 113.5, 112.9 (d, J_{CF} = 22.3 Hz), 56.4, 21.5, 20.8 ppm.
^{19}F-NMR (377 MHz, $CDCl_3$): δ = –110.6.
R_f (EtOAc/*c*-Hex 3:2) = 0.44.
Mp. = 145.6–148 °C (EtOAc/*c*-Hex).
IR (ATR): $\tilde{\nu}$ /cm^{-1} = 3006 (w), 2922 (w), 2847 ‘w), 1764 (s), 1587 (m), 1458 (m), 1370 (m), 1201 (s), 1035 (s), 1024 (s), 792 (s), 506 (s).
$[\alpha]_D^{22}$= –285 (c = 0.95, $CHCl_3$).
HRMS (*ESI*) = 421.0893 [M+Na$^+$], *calcd.* for $C_{22}H_{19}FO_4SNa^+$ = 421.0880.

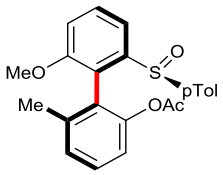

(*R*)-2'-methoxy-6-methyl-6'-((*S*)-*p*-tolylsulfinyl)-[1,1'-biphenyl]-2-yl acetate
Chemical Formula: $C_{23}H_{22}O_4S$
Molecular Weight: 394,4850

(*SaR*)-2'-Methoxy-6-methyl-6'-(*p*-tolylsulfinyl)-[1,1'-biphenyl]-2-yl-acetate [(*SaR*)-2k]: Prepared from (*S*)-2-methoxy-2'-methyl-6-(*p*-tolylsulfinyl)-1,1'-biphenyl 1k, (1.0 equiv, 67.3 mg, 0.2 mmol) according to GP3 for 38 h by using $Pd(OAc)_2$ (10 mol%, 4.5 mg, 0.02 mmol), $(NH_4)_2S_2O_8$ (2.0 equiv, 91.3 mg, 0.4 mmol), AcOH (46.5 equiv, 530 µL, 9.3 mmol), HFIP (25.3 equiv, 530 µL, 5.06 mmol), and H_2O (2.0 equiv, 7.2 µL, 0.4 mmol, 2.0 equiv). The crude mixture was analyzed by ^{1}H NMR, *dr* = 91:9. The product was purification by flash column chromatography on silica gel using mixture of cyclohexane and ethyl acetate (1/1, v/v) (79% yield) and recrystallization from *n*-pentane and dichloromethane to afford (*SaR*)-2k as a white crystal (52.8 mg, 0.134 mmol, 67%, *dr* > 98:2).

^{1}H-NMR ($CDCl_3$, 300 MHz): δ = 7.88 (d, *J* = 7.9 Hz, 1H), 7.61 (t, *J* = 8.0 Hz, 1H), 7.35 (t, *J* = 7.8 Hz, 1H), 7.10 (d, *J* = 8.1 Hz, 1H), 7.05-7.02 (m, 3H), 6.98–6.90 (m, 3H), 3.71 (s, 3H), 2.30 (s, 3H), 1.91 (s, 3H), 1.24 (s, 3H) ppm.

^{13}C-NMR (CDCl$_3$, 75 MHz): δ = 169.0, 157.2, 148.3, 146.1, 141.9, 141.4, 140.8, 130.1, 129.6 (1 C + 2 C_{pTol}), 127.5, 126.4 (2 C_{pTol}), 126.1, 122.0, 120.0, 114.9, 113.3, 56.2, 21.5, 20.7, 18.8 ppm.
R_f (*c*-Hex : EtOAc = 1:1): 0.26.
Mp. = 160.3–162.3 °C.
IR (ATR): $\tilde{\nu}$ /cm^{-1} = 3053 (w), 2924 (w), 2862 (w), 1763 (s), 1587 (m), 1367 (m), 1258 (m), 1197 (s), 1084 (m), 1030 (s), 787 (m), 736 (m), 593 (m), 511 (s).
[α]$^{20}_D$ = –232.1 (c = 1.06, CHCl$_3$).
EA *calcd*. for $C_{23}H_{22}O_4S$: 70.03 (C); 5.62 (H); *found*: 70.15 (C); 5.66 (H).

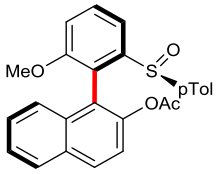

1-(2-methoxy-6-((*S*)-*p*-tolylsulfinyl)phenyl)naphthalen-2-yl acetate
Chemical Formula: $C_{26}H_{22}O_4S$
Molecular Weight: 430,5180

(*SaR*)-1-[2-Methoxy-6-(*p*-tolylsulfinyl)phenyl]naphthalen-2-yl-acetate [(*SaR*)-2l]: Prepared from (*S*)-1-[2-methoxy-6-(*p*-tolylsulfinyl)phenyl]naphthalene 1l, (1.0 equiv, 74.5 mg, 0.2 mmol) according to GP3 for 38 h by using $Pd(OAc)_2$ (10 mol%, 4.5 mg, 0.02 mmol), $(NH_4)_2S_2O_8$ (2.0 equiv, 91.3 mg, 0.4 mmol), AcOH (46.5 mmol, 530 µL, 9.28 mmol), HFIP (25.3 equiv, 530 µL, 5.06 mmol), and H_2O (2.0 equiv, 7.2 µL, 0.4 mmol). The crude mixture was analyzed by ^{1}H NMR, *dr* = 66:34. Purification by flash column chromatography on silica gel using mixture of cyclohexane and ethyl acetate (1/1, v/v) enabled the separation of the two diastereomers; (*SaR*)-2l was isolated as a white crystal (56.4 mg, 65%, dr = 97:3).

^{1}H-NMR (CDCl$_3$, 400 MHz): δ = 7.92 (2 overlapping d, *J* = 7.8, 7,1 Hz, 2H), 7.77 (d, *J* = 8.2 Hz, 1H), 7.69 (t, *J* = 8.1 Hz, 1H), 7.43 (d, *J* = 8.9 Hz, 1H), 7.29 (t, *J* = 7.8 Hz, 1H), 7.12 (d, *J* = 8.2 Hz, 1H), 6.92 (t, *J* = 7.5 Hz, 1H), 6.64–6.51 (m, 5H), 3.60 (s, 3H), 2.06 (s, 3H), 2.04 (s, 3H) ppm.
^{13}C-NMR (CDCl$_3$, 101 MHz): δ = 169.1, 157.9, 147.1, 145.9, 141.4, 140.8, 132.8, 131.4, 130.5, 130.4, 129.2 (2 C_{pTol}), 127.9, 126.2, 125.9 (2 C_{pTol}), 125.4, 125.2, 122.6, 121.6, 121.1, 115.7, 113.5, 56.3, 21.3, 20.9 ppm.
R_f (cyclohexane: ethyl acetate = 1:1): 0.19.
Mp. = 221.7–223.7 °C.
IR (ATR): $\tilde{\nu}$ /cm^{-1} = 3060 (w), 3013 (w), 2964 (w), 2838 (w), 1763 (s), 1458 (m), 1432 (m), 1366 (m), 1258 (s), 1193 (s), 1154 (m), 1037 (s), 1010 (m), 811 (m).
[α]$^{20}_D$ = –180.3 (c = 0.835, CHCl$_3$).
HRMS: 453.1080 [M+Na]$^+$, *calcd*. for $C_{26}H_{22}NaO_4S$ = 453.1131.

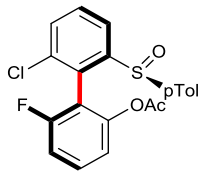

(*R*)-2'-chloro-6-fluoro-6'-((*S*)-*p*-tolylsulfinyl)-[1,1'-biphenyl]-2-yl acetate
Chemical Formula: $C_{21}H_{16}ClFO_3S$
Molecular Weight: 402,8644

(*SaR*)-2'-Chloro-6-fluoro-6'-(*p*-tolylsulfinyl)-[1,1'-biphenyl]-2-yl acetate [(*SaR*)-2m]: Prepared from (*S*)-2-chloro-2'-fluoro-6-(*p*-tolylsulfinyl)-1,1'-biphenyl 1m, (1.0 equiv, 103 mg, 0.3 mmol) following the GP3 for 80 h, using $(NH_4)_2S_2O_8$ (2.0 equiv, 136 mg, 0.6 mmol), $Pd(OAc)_2$ (10 mol%, 6.7 mg, 0.03 mmol) and H_2O (2.0 equiv, 10.8 µL, 0.6 mmol), in a mixture of AcOH (46.5 equiv, 800 µL, 13.96 mmol), and HFIP (25.3 equiv, 800 µL, 7.59 mmol). The crude mixture was analyzed by ^{1}H NMR, mixture of starting material and desired product. The crude product was purified by flash chromatography on triethylamine-neutralized silica gel (EtOAc/*c*-Hex 2:5), giving (*SaS*)-2'-chloro-6-fluoro-6'-(p-tolylsulfinyl)-[1,1'-biphenyl]-2-yl acetate (71 mg, 0.178 mmol, 59%, d.r. > 98:2) as white solid along with (*SaR*)-2-chloro-2'-fluoro-6-(*p*-tolylsulfinyl)-1,1'-biphenyl (41 mg, 0.119 mmol, 40%, *dr* > 98:2).

^{1}H-NMR (400 MHz, $CDCl_3$): δ = 8.13–8.08 (m, 1 H), 7.62–7.57 (m, 2 H), 7.47 (td, *J* = 8.3, 6.4 Hz, 1 H), 7.18 (td, *J* = 8.2, 0.9 Hz, 1 H), 7.09 (d, *J* = 8.3 Hz, 2 H), 7.02 (d, *J* = 8.3 Hz, 2 H), 6.86 (td, *J* = 8.5, 0.6 Hz, 1 H), 2.32 (s, 3 H), 2.02 (s, 3 H) ppm. **^{13}C-NMR (101 MHz, $CDCl_3$):** δ = 168.2, 160.4 (d, J_{CF} = 249.8 Hz), 148.8 (d, J_{CF} = 5.5 Hz), 147.6, 142.3, 141.0, 135.9 (d, J_{CF} = 1.1 Hz), 131.9, 131.2 (d, J_{CF} = 10.0 Hz), 130.7, 129.9, 127.6, 125.9, 122.5, 118.8 (d, J_{CF} = 3.8 Hz), 116.6 (d, J_{CF} = 19.4 Hz), 113.1 (d, J_{CF} = 22.0 Hz), 21.6, 20.7 ppm. **R_f** (EtOAc/*c*-Hex 1:1) = 0.45. **IR (ATR):** $\tilde{\nu}$ /cm^{-1} = 3075 (w), 3053 (w), 2927 (w), 1765 (s), 1619 (m), 1575 (m), 1459 (s), 1369 (m), 1189 (s), 1083 (m), 1048 (s), 1017 (m), 874 (m), 791 (s). **$[\alpha]_D^{20}$**= –342 (c = 0.8, $CHCl_3$). **HRMS** (*ESI*) = [M+Na$^+$] 425.0363, *calcd.* for $C_{21}H_{16}ClFNaO_3S^+$ = 425.0385.

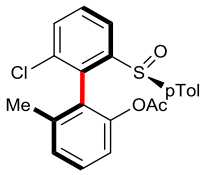

(*S*)-2'-chloro-6-methyl-6'-((*S*)-*p*-tolylsulfinyl)-[1,1'-biphenyl]-2-yl acetate
Chemical Formula: $C_{22}H_{19}ClO_3S$
Molecular Weight: 398,9010

(*SaS*)-2'-Chloro-6-methyl-6'-(*p*-tolylsulfinyl)-[1,1'-biphenyl]-2-yl-acetate [(*SaS*)-2o]: Prepared from (*S*)-2-chloro-2'-methyl-6-(*p*-tolylsulfinyl)-1,1'-biphenyl 1n, (1.0 equiv, 34 mg, 0.1 mmol) according to GP3 for 42 h by using $Pd(OAc)_2$ (10 mol%, 2.3 mg, 0.01 mmol), $(NH_4)_2S_2O_8$ (2.0 equiv, 45.6 mg, 0.2 mmol), AcOH (46.5, equiv, 270 µL, 4.65 mmol), HFIP (25.3 equiv, 270 µL, 2.53 mmol), and H_2O (2.0 eqiov, 3.6 µL, 0.2 mmol). The crude mixture was analyzed by ^{1}H NMR, mixture of 1n and 2n; *dr* of

2n > 98:2) Purification by flash column chromatography on silica gel using mixture of cyclohexane and ethyl acetate (6.5/3.5, v/v) afforded the title compound [(*SaS*)-2n, 22.1 mg, 0.555 mmol, 56%, *dr* > 98:2] as a colorless oil along with (*SaR*)-2-chloro-2'-methyl-6-(*p*-tolylsulfinyl)-1,1'-biphenyl (14 mg, 0.041 mmol, 41%, dr > 98:2).

^{1}H-NMR ($CDCl_3$, 300 MHz): δ = 8.23 (dd, *J* = 7.3, 1.7 Hz, 1H), 7.64–7.54 (m, 2H), 7.40 (t, *J* = 8.0 Hz, 1H), 7.16 (d, *J* = 8.1 Hz, 1H), 7.06 (d, *J* = 8.1 Hz, 2H), 6.97 (d, *J* = 7.6 Hz, 1H), 6.92 (d, *J* = 8.1 Hz, 2H), 2.32 (s, 3H), 1.94 (s, 3H), 1.19 (s, 3H) ppm.
^{13}C-NMR ($CDCl_3$, 75 MHz): δ = 168.7, 148.0, 147.0, 142.5, 140.6, 140.3, 135.4, 132.3, 131.7, 130.1, 129.9, 129.7 (2 $C_{p\text{Tol}}$), 127.6, 126.8 (2 $C_{p\text{Tol}}$), 126.7, 121.8, 120.3, 21.6, 20.7, 18.5 ppm.
R_f (*c*-Hex : EtOAc = 6.5:3.5): 0.17.
IR (ATR): $\tilde{\nu}$ /cm^{-1} = 3049 (w), 2922 (w), 2853 (w), 1765 (s), 1460 (m), 1417 (m), 1367 (m), 1195 (s), 1088 (s), 1049 (s), 951 (m), 874 (m), 814 (m), 784 (s), 505 (s).
$[\alpha]^{20}_D$ = –265 (c = 0.755, $CHCl_3$).
HRMS: 421.0633 $[M+Na]^+$, *calcd*. for $C_{22}H_{19}ClNaO_3S$ = 421.0636.

3. General Procedure for iodination reaction (GP4).

The reactions were performed under air. A sealed tube was successively charged with biaryl substrates 1a–1n, (1.0 equiv, 0.2 mmol), $Pd(OAc)_2$ (5 mol%, 2.3 mg, 0.01 mmol), NIS (1.3 equiv, 58.5 mg, 0.26 mmol). AcOH (69.8 equiv, 800 µL, 13.96 mmol) and HFIP (38 equiv, 800 µL, 7.59 mmol) were added, and the resulting mixture was stirred at 25 °C until analysis of an aliquot by TLC indicates complete conversion of the biaryl substrates (12 h–7 d). The mixture was quenched with saturated $NaHCO_3$ solution. Aqueous phase was extracted with ethyl acetate, the combined organic phase was washed with brine, dried over Na_2SO_4, filtrated and concentrated under vacuum to furnish the crude iodinated products 3a–3n. The crude mixture was analyzed by ^1H NMR to determine diastereoselectivity. Purification by flash column chromatography on silica gel using yielded the analytically pure iodinated products.

4. Characterization Data of Iodinated Products 3a–3n

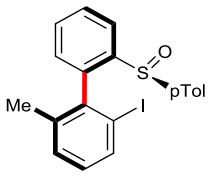

(*R*)-2-iodo-6-methyl-2'-((*S*)-*p*-tolylsulfinyl)-1,1'-biphenyl
Chemical Formula: $C_{20}H_{17}IOS$
Molecular Weight: 432,3195

(*SaR*)-2-Iodo-6-methyl-2'-(*p*-tolylsulfinyl)-1,1'-biphenyl [(*SaR*)-3a]: [Reaction performed at large scale]. Prepared from (*S*)-2-methyl-2'-(*p*-tolylsulfinyl)-1,1'-biphenyl 1a, (1.0 equiv, 460 mg, 1.5 mmol) according to GP4 for 12 h by using $Pd(OAc)_2$ (5 mol%, 16.8 mg, 0.075 mmol), NIS (1.3 equiv, 438.7 mg, 1.95 mmol), AcOH (69.8 equiv, 6.0 mL, 103.2 mmol), and HFIP (38 equiv, 6.0 mL, 57.0 mmol). The crude mixture was analyzed by ^1H NMR; *dr* = 98:2. Purification by flash column chromatography on silica gel using mixture of cyclohexane, dichloromethane, and ethyl acetate (from 5/1/1 to 2/1/1, v/v/v) afforded the title compound [(*SaR*)-3a, 615.7 mg, 95%, *dr* = 98:2] as a needle like yellow crystal.

^{1}H-NMR ($CDCl_3$, 400 MHz): δ = 8.36 (dd, *J* = 7.8, 1.0 Hz, 1H), 7.73 (td, *J* = 7.6, 1.3 Hz, 1H), 7.69 (td, *J* = 7.5, 1.3 Hz, 1H), 7.53 (t, *J* = 7.9 Hz, 1H), 7.06 (d, *J* = 8.1 Hz, 2H), 7.03–6.97 (m, 5H), 2.31 (s, 3H), 1.14 (s, 3H) ppm.
^{13}C-NMR ($CDCl_3$, 101 MHz): δ = 143.8, 142.2, 141.2, 140.9, 139.5, 137.0, 130.9, 130.2, 130.1, 129.9, 129.7 (2 C_{pTol}), 129.3, 126.9 (2 C_{pTol}), 123.7, 101.6, 21.6, 21.1 ppm + 1 C overlapping.
R_f (*c*-Hex : EtOAc : DCM = 2:1:1): 0.55.
Mp. = 154.3–157.3 °C.
IR (ATR): $\tilde{\nu}$ /cm^{-1} = 3047 (w), 2917 (w), 1593 (vw), 1440 (m), 1081 (s), 1062 (m), 1038 (s), 810 (s), 769 (s), 755 (s), 623 (m), 545 (m), 508 (s).
$[\alpha]^{20}_D$ = –147.8 (c = 0.8, $CHCl_3$).
HRMS: 454.9942 $[M+Na]^+$, *calcd*. for $C_{20}H_{17}INaOS$ = 454.9937.

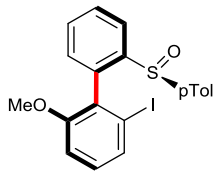

(*R*)-2-iodo-6-methoxy-2'-((*S*)-*p*-tolylsulfinyl)-1,1'-biphenyl
Chemical Formula: $C_{20}H_{17}IO_2S$
Molecular Weight: 448,3185

(*SaR*)-2-Iodo-6-methoxy-2'-(*p*-tolylsulfinyl)-1,1'-biphenyl [(*SaR*)-3b]: Prepared from (*S*)-2-methoxy-2'-(*p*-tolylsulfinyl)-1,1'-biphenyl 1b, (1.0 equiv, 64.4 mg, 0.2 mmol) according to GP4 for 5 d at 40 °C by using $Pd(OAc)_2$ (10 mol%, 4.5 mg, 0.02 mmol), NIS (1.3 equiv, 58.6 mg, 0.26 mmol), DCE (50 equiv, 800 µL, 10.0 mmol). The crude mixture was analyzed by 1H NMR, *dr* = 93:7. Purification by flash column chromatography on silica gel using mixture of cyclohexane, dichloromethane, and ethyl acetate (from 5/1/1 to 2/2/1, v/v/v) afforded the title compound [(*SaR*)-3b, 86.0 mg, 0.192 mmol, 96%, *dr* = 96:4] as a white solid.

^{1}H-NMR ($CDCl_3$, 400 MHz): δ = 8.21 (d, *J* = 7.9 Hz, 1H), 7.65 (t, *J* = 7.6 Hz, 1H), 7.57 (d, *J* = 7.9 Hz, 1H), 7. 53 (t, *J* = 7.4 Hz, 1H), 7.15–7.01 (m, 6H), 6.66 (d, *J* = 8.3 Hz, 1H), 3.13 (s, 3H), 2.31 (s, 3H) ppm.
^{13}C-NMR ($CDCl_3$, 101 MHz): δ = 157.5, 143.8, 141.8, 141.5, 139.1, 131.1, 131.0 (2 C overlapping), 130.8 (2 C overlapping), 129.4 (2 $C_{p\text{Tol}}$), 129.2, 126.8 (2 $C_{p\text{Tol}}$), 124.4, 110.1, 102.1, 54.9, 21.5 ppm.
R_f (*c*-Hex : DCM : EtOAc = 2:2:1): 0.4.
IR (ATR): $\tilde{\nu}$ /cm^{-1} = 3029 (w), 2924 (w), 2853 (w), 1558 (m), 1455 (s), 1422 (s), 1256 (s), 1082 (m), 1020 (s), 810 (m), 769 (s), 623 (m), 514 (s).
$[\alpha]^{20}_D$ = –123.9 (c = 0.615, $CHCl_3$).
HRMS: 470.9836 $[M+Na]^+$, *calcd*. for $C_{20}H_{17}INaO_2S$ = 470.9886.

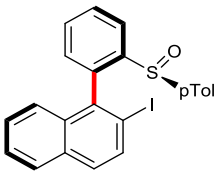

2-iodo-1-(2-((*S*)-*p*-tolylsulfinyl)phenyl)naphthalene
Chemical Formula: $C_{23}H_{17}IOS$
Molecular Weight: 468,3525

(*SaR*)-2-Iodo-1-[2-(*p*-tolylsulfinyl)phenyl]naphthalene [(*SaR*)-3c]: Prepared from (*S*)-1-[2-(*p*-tolylsulfinyl)phenyl]naphthalene 1c, (1.0 equiv, 68.5 mg, 0.2 mmol) according to GP4 for 18 h by using $Pd(OAc)_2$ (5 mol%, 2.3 mg, 0.01 mmol), NIS (1.3 equiv, 58.6 mg, 0.26 mmol), AcOH (69.8 equiv, 800 µL, 13.96 mmol), and HFIP (38 equiv, 800 µL, 7.59 mmol). The crude mixture was analyzed by ^{1}H NMR, *dr* = 96:4. Purification by flash column chromatography on silica gel using mixture of cyclohexane, ethyl acetate, and dichloromethane (from 5/1/1 to 2/1/1, v/v/v) (90% yield) and rapid recrystallization from dichloromethane and pentane afforded the title compound [(*SaR*)-3c, 74.9 mg, 0.160 mmol, 80%, *dr* > 98:2] as a white solid.

^{1}H-NMR ($CDCl_3$, 400 MHz): δ = 8.39 (d, *J* = 7.9 Hz, 1H), 8.01 (d, *J* = 8.7 Hz, 1H), 7.76 (t + d overlapping, *J* = 8.8, 7.8 Hz, 2H), 7.61 (t + d, *J* = 8.5, 7.3 Hz, 2H), 7.32 (dd, *J* = 7.5, 6.2 Hz, 1H), 7.12 (d, *J* = 7.3, 1H), 6.82 (t, *J* = 7.8 Hz, 1H), 6.63 (d, *J* = 8.1 Hz, 2H), 6.58 (d, *J* = 8.2 Hz, 2H), 6.42 (d, *J* = 8.6 Hz, 1H), 2.08 (s, 3H) ppm.
^{13}C-NMR ($CDCl_3$, 101 MHz): δ = 144.9, 141.6, 140.4, 140.3, 139.7, 135.6, 133.5, 132.6, 130.8, 130.8, 130.1, 129.6, 129.2 (2 $C_{p\text{Tol}}$), 127.8, 126.7, 126.3 (2 $C_{p\text{Tol}}$), 126.2, 125.9, 124.2, 99.7, 21.3 ppm.
R_f (cyclohexane: ethyl acetate: dichloromethane = 2:1:1): 0.68.
IR (ATR): $\tilde{\nu}$ /cm^{-1} = 3059 (w), 1575 (w), 1498 (w), 1377 (w), 1085 (m), 1066 (m), 1034 (s), 805 (s), 770 (s), 739 (s), 626 (s), 542 (s), 509 (s).
$[\alpha]^{20}_D$ = –30.5 (c = 0.61, $CHCl_3$).
EA *calcd*. for $C_{23}H_{17}IOS$: 58.98 (C); 3.66 (H); *found*: 58.63 (C); 3.84 (H).

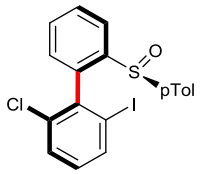

(*R*)-2-chloro-6-iodo-2'-((*S*)-*p*-tolylsulfinyl)-1,1'-biphenyl
Chemical Formula: $C_{19}H_{14}ClIOS$
Molecular Weight: 452,7345

(*SaR*)-2-Chloro-6-iodo-2'-(*p*-tolylsulfinyl)-1,1'-biphenyl [(*SaR*)-3d]: Prepared from (*S*)-2-chloro-2'-(*p*-tolylsulfinyl)-1,1'-biphenyl 1d, (1.0 equiv, 65.4 mg, 0.2 mmol) according to GP4 for 60 h by using $Pd(OAc)_2$ (5 mol%, 2.3 mg, 0.01 mmol), NIS (1.3 equiv, 58.6 mg, 0.26 mmol), AcOH (69.8 equiv, 800 µL, 13.96 mmol) and HFIP (38 equiv, 800 µL, 7.59 mmol). The crude mixture was analyzed by ^{1}H NMR; *dr* = 91:9. The product was purified by flash column chromatography on silica gel using mixture of cyclohexane and ethyl acetate (1/1, v/v) (83% yield) and recrystallization from *n*-pentane and dichloromethane to afford the title compound (*SaR*)-3d, as a needle like yellow crystal (68.3 mg, 0.151 mmol, 75% *dr* > 98:2).

^{1}H-NMR ($CDCl_3$, 400 MHz): δ = 8.22 (dd, *J* = 7.9, 0.8 Hz, 1H), 7.92 (d, *J* = 7.8 Hz, 1H), 7.68 (td, *J* = 7.7, 0.8 Hz, 1H), 7.55 (td, *J* = 7.5, 0.8 Hz, 1H), 7.28 (t, *J* = 7.9 Hz, 1H), 7.15–7.02 (m, 6H), 2.32 (s, 3H) ppm.
^{13}C-NMR ($CDCl_3$, 101 MHz): δ = 143.9, 142.1, 140.7, 140.7, 140.1, 137.9, 134.9, 131.1, 131.0, 130.3, 129.9, 129.8 (2 $C_{p\text{Tol}}$), 129.6, 126.5 (2 $C_{p\text{Tol}}$), 124.4, 101.7, 21.6 ppm.
R_f (*c*-Hex : EtOAc = 1:1): 0.48.
Mp. = 169.5–171.5 °C.
IR (ATR): $\tilde{\nu}$ /cm^{-1} = 3072 (w), 3047 (w), 1595 (w), 1547 (m), 1492 (m), 1422 (s), 1195 (m), 1082 (s), 1062 (s), 1038 (s), 809 (s), 772 (s), 763 (s), 742 (s), 733 (s), 724 (s), 532 (s).
$[\alpha]^{20}_D$ = –129.4 (c = 1, $CHCl_3$).
EA *calcd*. for $C_{19}H_{14}ClIOS$: 50.41 (C); 3.12 (H); *found*: 50.25 (C); 3.19 (H).

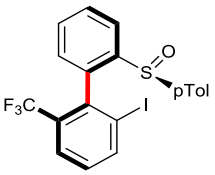

(*R*)-2-iodo-2'-((*S*)-*p*-tolylsulfinyl)-6-(trifluoromethyl)-1,1'-biphenyl
Chemical Formula: $C_{20}H_{14}F_3IOS$
Molecular Weight: 486,2907

(*SaR*)-2-Iodo-2'-(*p*-tolylsulfinyl)-6-(trifluoromethyl)-1,1'-biphenyl [(*SaR*)-3e]: Prepared from (*S*)-2-methoxy-2'-(*p*-tolylsulfinyl)-1,1'-biphenyl 1e, (1.0 equiv, 72.0 mg, 0.2 mmol) according to GP4 for 5 d by using $Pd(OAc)_2$ (5 mol%, 2.3 mg, 0.01 mmol), NIS (1.3 mmol, 58.6 mg, 0.26 mmol), AcOH (69.8 equiv, 800 µL, 13.96 mmol), and HFIP (38 equiv, 800 µL, 7.59 mmol). The crude mixture was analyzed by ^{1}H NMR, *dr* = 93:7. The product was purified by flash column chromatography on silica gel using mixture of cyclohexane and ethyl acetate (1/1, v/v) (86% yield) and recrystallization from *n*-pentane and dichloromethane to afford the title compound (*SaR*)-3e, as a colorless crystal (72.8 mg, 0.150 mmol, 75% *dr* = 97:3).

^{1}H-NMR ($CDCl_3$, 300 MHz): δ = 8.25 (d, *J* = 7.9 Hz, 1H), 8.19 (dd, *J* = 7.9, 1.3 Hz, 1H), 7.68 (overlapping t+d, *J* = 7.7, 1.4, 8.0 Hz, 2H), 7.54 (td, *J* = 7.6, 1.4 Hz, 1H), 7.27 (td, *J* = 8.0, 0.9 Hz, 1H), 7.13–7.00 (m, 5H), 2.32 (s, 3H) ppm.
^{13}C-NMR ($CDCl_3$, 101 MHz): δ = 144.1, 143.2, 142.3, 140.2 (q, *J* = 1.5 Hz), 139.9, 139.6, 131.0 (q, *J* = 29.9 Hz), 130.8, 130.2, 130.1, 129.8 (q, *J* = 2 Hz), 129.7 (2 $C_{p\text{Tol}}$), 126.6 (q, *J* = 5.0 Hz), 126.3 (2 $C_{p\text{Tol}}$), 124.5, 122.5 (q, *J* = 276 Hz), 104.7, 21.5 ppm.
^{19}F-NMR ($CDCl_3$, 377 MHz): δ = –58.7 ppm.
R_f (*c*-Hex : ethyl acetate = 1:1): 0.5.
Mp. = 158.3–160.5 °C.
IR (ATR): $\tilde{\nu}$ /cm^{-1} = 3060 (w), 2923 (w), 1595 (m), 1426 (m), 1302 (s), 1202 (s), 1172 (s), 1145 (s), 1129 (s), 1084 (s), 1053 (s), 1029 (s), 1014 (s), 802 (s), 757 (s), 682 (s), 626 (s), 530 (s), 512 (s).
$[\alpha]^{20}_D$ = –134.0 (c = 1, $CHCl_3$).
EA *calcd*. for $C_{20}H_{14}F_3IOS$: 49.40 (C); 2.90 (H); *found*: 49.29 (C); 2.82 (H).

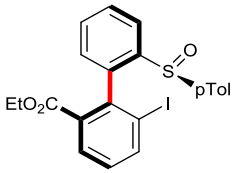

ethyl (*R*)-6-iodo-2'-((*S*)-*p*-tolylsulfinyl)-[1,1'-biphenyl]-2-carboxylate
Chemical Formula: $C_{22}H_{19}IO_3S$
Molecular Weight: 490,3555

(*SaR*)-Ethyl-6-iodo-2'-(*p*-tolylsulfinyl)-[1,1'-biphenyl]-2-carboxylate [(*SaR*)-3f]: Prepared from (*S*)-ethyl-2'-(*p*-tolylsulfinyl)-[1,1'-biphenyl]-2-carboxylate 1f, (1.0 equiv, 36.4 mg, 0.1 mmol) according to GP4 for 5 d by using $Pd(OAc)_2$ (10 mol%, 2.3 mg, 0.01 mmol), NIS (1.3 equiv, 29.3 mg, 0.13 mmol), AcOH (69.8 equiv, 400 µL, 6.98 mmol), and HFIP (38 equiv, 400 µL, 3.8 mmol). The crude mixture was analyzed by

^{1}H NMR, *dr* = 92:8. Purification by flash column chromatography on silica gel using mixture of cyclohexane and ethyl acetate (1/1, v/v) afforded the title compound (*SaR*)-3f, [46.0 mg, 0.094 mmol, 94%, *dr* = 92:8] as a yellow crystal. For major isomer:

^{1}H-NMR ($CDCl_3$, 400 MHz): δ = 8.22 (two overlapping d, *J* = 7.1, 6.7 Hz, 2H), 8.02 (d, *J* = 7.5 Hz, 1H), 7.66 (t, *J* = 7.7 Hz, 1H), 7.51 (t, *J* = 7.6 Hz, 1H), 7.28–7.22 (m, 1H), 7.08 (aq, *J* = 8.3, Hz, 4H), 7.01 (d, *J* = 7.6 Hz, 1H), 3.74–3.58 (m, 1H), 3.54–3.40 (m, 1H), 2.30 (s, 3H), 0.72 (t, *J* = 7.1 Hz, 3H) ppm.
^{13}C-NMR ($CDCl_3$, 101 MHz): δ = 164.5, 143.4, 142.8, 142.6, 142.5, 141.8, 140.8, 132.3, 130.9, 130.5, 130.0, 129.8, 129.6 (2 $C_{p\text{Tol}}$), 129.3, 126.4 (2 $C_{p\text{Tol}}$), 124.0, 103.9, 60.8, 21.5, 13.4 ppm.
R_f (*c*-Hex : EtOAc = 1:1): 0.44.
Mp. = 117.2–119.2 °C.
IR (ATR): $\tilde{\nu}$ /cm^{-1} = 2980 (w), 2923 (w), 1707 (s), 1421 (w), 1362 (w), 1288 (s), 1194 (m), 1082 (s), 1039 (s), 1012 (s), 810 (m), 760 (s), 701 (m), 620 (m), 533 (s).
$[\alpha]^{20}_D$ = –107.6 (c = 1.465, $CHCl_3$).
HRMS: 512.9981 $[M+Na]^+$, *calcd*. for $C_{22}H_{19}F_3NaIO_3S$ = 512.9992.

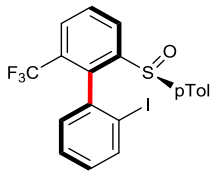

2'-iodo-2-((*S*)-*p*-tolylsulfinyl)-6-(trifluoromethyl)-1,1'-biphenyl
Chemical Formula: $C_{20}H_{14}F_3IOS$
Molecular Weight: 486,2907

(*SaR*)-2'-Iodo-2-(*p*-tolylsulfinyl)-6-(trifluoromethyl)-1,1'-biphenyl [(*SaR*)-3g]: Prepared from (*S*)-2-(*p*-tolylsulfinyl)-6-(trifluoromethyl)-1,1'-biphenyl 1g, (1.0 equiv, 72.0 mg, 0.2 mmol) according to GP4 for 31 h by using $Pd(OAc)_2$ (5 mol%, 2.3 mg, 0.01 mmol), NIS (1.3 equiv, 58.6 mg, 0.26 mmol), AcOH (69.8 equiv, 800 µL, 13.96 mmol), and HFIP (38 equiv, 800 µL, 7.59 mmol). The crude mixture was analyzed by ^{1}H NMR, *dr* = 97:3. The product was purified by flash column chromatography on silica gel using mixture of cyclohexane and ethyl acetate (13/7, v/v) and recrystallization from *n*-pentane and dichloromethane to afford the title compound (*SaR*)-3g, as a colorless solid (84.5 mg, 0.174 mmol, 87% *dr* = 97:3).

^{1}H-NMR ($CDCl_3$, 400 MHz): δ = 8.54 (d, *J* = 7.7 Hz, 1H), 7.99 (d, *J* = 7.5 Hz, 1H), 7.89 (d, *J* = 7.8 Hz, 1H), 7.82 (t, *J* = 7.9 Hz, 1H), 7.17–7.04 (m, 4H), 6.99 (d, *J* = 8.4 Hz, 2H), 6.46 (d, *J* = 6.7 Hz, 1H), 2.32 (s, 3H) ppm.
^{13}C-NMR ($CDCl_3$, 75 MHz): δ = 147.0, 142.5, 140.9, 140.1, 139.2, 138.1, 132.0 (q, *J* = 1.6 Hz), 130.4, 129.9 (2 $C_{p\text{Tol}}$), 129.7, 129.5 (q, *J* = 30 Hz), 128.6 (q, *J* = 5.0 Hz), 127.7, 127.4, 126.9 (2 $C_{p\text{Tol}}$), 126.0 (q, *J* = 276 Hz), 100.9, 21.6 ppm.
^{19}F NMR ($CDCl_3$, 377 MHz): δ = -58.32.
R_f (*c*-Hex : EtOAc = 6.5:3.5): 0.27.
Mp. = 149.5–151.5 °C.

IR (ATR): $\tilde{\nu}$ /cm^{-1} = 3056 (w), 2955 (w), 2923 (w), 2852 (w), 1431 (m), 1306 (s), 1170 (m), 1134 (s), 1090 (m), 1066 (s), 1042 (s), 999 (m), 804 (s), 755 (s), 530 (s), 506 (s). **[α]$^{20}_{D}$** = –178.0 (c = 1, $CHCl_3$). **HRMS:** 508.9655 [M+Na]$^+$, *calcd*. for $C_{20}H_{14}F_3NaIOS$ = 508.9654.

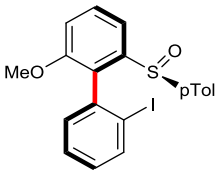

2'-iodo-2-methoxy-6-((*S*)-*p*-tolylsulfinyl)-1,1'-biphenyl
Chemical Formula: $C_{20}H_{17}IO_2S$
Molecular Weight: 448,3185

(*SaR*)-2'-Iodo-2-methoxy-6-(*p*-tolylsulfinyl)-1,1'-biphenyl [(*SaR*)-3i]: Prepared from (*S*)-2-methoxy-6-(*p*-tolylsulfinyl)-1,1'-biphenyl 1i, (1.0 equiv, 64.4 mg, 0.2 mmol) according to GP4 for 20 h by using $Pd(OAc)_2$ (5 mol%, 2.3 mg, 0.01 mmol, 0.05 equiv), NIS (1.3 equiv, 58.6 mg, 0.26 mmol), AcOH (69.8 equiv, 800 µL, 13.96 mmol), and HFIP (38 equiv, 800 µL, 7.59 mmol). The crude product was analyzed by ^{1}H NMR, *dr* = 98:2. Purification by flash column chromatography on silica gel using mixture of cyclohexane and ethyl acetate (7/3, v/v) afforded the title compound (*SaR*)-3i, [80.2 mg, 0.179 mmol, 90%, *dr* = 98:2] as a white solid.

^{1}H-NMR ($CDCl_3$, 400 MHz): δ = 7.98 (dd, *J* = 7.9, 1.0 Hz, 1H), 7.86 (dd, *J* = 8.0, 1.0 Hz, 1H), 7.64 (t, *J* = 8.1 Hz, 1H), 7.17 (td, *J* = 7.5, 1.2 Hz, 1H), 7.13–7.03 (m, 6H), 6.49 (dd, *J* = 7.6, 1.6 Hz, 1H), 3.72 (s, 3H), 2.32 (s, 3H) ppm. **^{13}C-NMR** ($CDCl_3$, 101 MHz): δ = 156.6, 145.4, 141.9, 141.9, 139.3, 138.7, 132.3, 130.9, 130.4, 129.7 (2 $C_{p\text{Tol}}$), 129.7, 127.7, 126.6 (2 $C_{p\text{Tol}}$), 115.9, 113.6, 101.3, 56.3, 21.6 ppm. **Mp**. = 221.7–223.7 °C. **R_f** (*c*-Hex : EtOAc = 7:3): 0.27. **IR** (ATR): $\tilde{\nu}$ /cm^{-1} = 2964 (m), 2918 (m), 2850 (m), 1732 (m), 1568 (m), 1459 (m), 1433 (m), 1263 (s), 1153 (m), 1011 (s), 790 (s), 761 (s), 738 (m). **[α]$^{20}_{D}$** = –178.2 (c = 0.95, $CHCl_3$). **HRMS**: 470.9836 [M+Na]$^+$, *calcd.* for $C_{20}H_{17}INaO_2S$ = 470.9886.

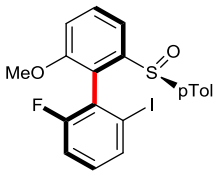

(*R*)-2-fluoro-6-iodo-2'-methoxy-6'-((*S*)-*p*-tolylsulfinyl)-1,1'-biphenyl
Chemical Formula: $C_{20}H_{16}FIO_2S$
Molecular Weight: 466,3089

(*SaR*)-2-Fluoro-6-iodo-2'-methoxy-6'-(-*p*-tolylsulfinyl)-1,1'-biphenyl [(*SaR*)-3j]: Prepared from (*S*)-2'-fluoro-2-methoxy-6-(-*p*-tolylsulfinyl)-1,1'-biphenyl 1j, (1.0 equiv, 114 mg, 0.335 mmol), following GP4 for 44 h, using NIS (1.3 equiv, 98.2 mg, 0.436 mmol) and $Pd(OAc)_2$ (5 mol%, 3.8 mg, 0.017 mmol) in a mixture of HFIP (38 equiv, 1

mL, 12.71 mmol) and AcOH (69.8 equiv, 1 mL, 23.38 mmol). The crude mixture was analyzed by 1H NMR, *dr* = 97:3. The crude product was purified by flash chromatography on silica gel (Et_2O/*n*-Pentane from 4:3 to 2:1) and afforded *(SaR)*-2-fluoro-6-iodo-2'-methoxy-6'-(-p-tolylsulfinyl)-1,1'-biphenyl (145 mg, 0.312 mmol, 93 %, *dr* = 98:2) as white powder.

^{1}H-NMR (400 MHz, $CDCl_3$): δ = 7.81 (dd, *J* = 7.9, 0.8 Hz, 1 H), 7.78 (d, *J* = 7.9 Hz, 1 H), 7.66 (t, *J* = 8.1 Hz, 1 H), 7.13–7.04 (m, 6 H), 6.89 (dt, *J* = 8.6, 0.8 Hz, 1 H), 3.73 (s, 3 H), 2.32 (s, 3 H) ppm.
^{13}C-NMR (101 MHz, $CDCl_3$): δ = 160.0 (d, J_{CF} = 250.9 Hz), 156.9 (d, J_{CF} = 0.9 Hz), 146.0 (d, J_{CF} = 0.7 Hz), 142.0, 141.4, 135.0 (d, J_{CF} = 3.5 Hz), 131.6 (d, J_{CF} = 8.6 Hz), 131.2, 129.8, 127.4 (d, J_{CF} = 19.1 Hz), 126.3 (d, J_{CF} = 0.9 Hz), 125.0, 116.4, 115.4 (d, J_{CF} = 22.7 Hz), 113.6, 102.1 (d, J_{CF} = 1.8 Hz), 56.4, 21.6 ppm.
^{19}F-NMR (377 MHz, $CDCl_3$): δ = –150.7 ppm.
R_f **(**EtOAc/DCM/*c*-Hex 3:1:2) = 0.60.
IR (ATR): $\tilde{\nu}$ /cm^{-1} = 3055 (w), 3015 (w), 2922 (w), 2834 (w), 1727 (m), 1585 (m), 1558 (m), 1430 (s), 1264 (s), 1252 (s), 1176 (m), 1155 (m), 1083 (m), 1023 (s), 1012 (s), 855 (s), 779 (s), 515 (s).
[α]$_D^{20}$= –169 (c = 0.9, $CHCl_3$).
HRMS (*ESI*) = 488.9774 [M+Na$^+$], *calcd.* for $C_{20}H_{16}FIO_2SNa^+$ = 488.9792.

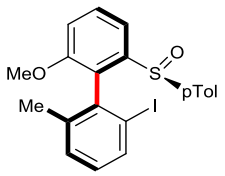

(*R*)-2-iodo-2'-methoxy-6-methyl-6'-((*S*)-*p*-tolylsulfinyl)-1,1'-biphenyl
Chemical Formula: $C_{21}H_{19}IO_2S$
Molecular Weight: 462,3455

(*SaR*)-2-Iodo-6-methyl-2'-(*p*-tolylsulfinyl)-1,1'-biphenyl [(*SaR*)-3k]: Prepared from (*S*)-2-methyl-2'-(*p*-tolylsulfinyl)-1,1'-biphenyl 1k, (1.0 equiv, 67.3 mg, 0.2 mmol) according to GP4 for 7 d by using $Pd(OAc)_2$ (5 mol%, 2.3 mg, 0.01 mmol), NIS (1.3 equiv, 58.6 mg, 0.26 mmol), AcOH (69.8 equiv, 800 µL, 13.96 mmol), and HFIP (38 equiv, 800 µL, 7.59 mmol). The crude mixture was analyzed by ^{1}H NMR, *dr* = 81:19. The product was purified by flash column chromatography on silica gel using mixture of cyclohexane and ethyl acetate (1/1, v/v) (97% yield) and recrystallization from *n*-pentane and dichloromethane to afford the title compound (*SaR*)-3k, as a needle like crystal (62.1 mg, 0.134 mmol, 67%, *dr* = 97:3).

^{1}H-NMR ($CDCl_3$, 300 MHz): δ = 7.96 (dd, *J* = 7.9, 1.0 Hz, 1H), 7.86 (dd, *J* = 8.0, 1.0 Hz, 1H), 7.67 (t, *J* = 8.1 Hz, 1H), 7.12–6.95 (m, 7H), 3.72 (s, 3H), 2.31 (s, 3H), 1.12 (s, 3H) ppm.
^{13}C-NMR ($CDCl_3$, 75 MHz): δ = 156.3, 145.3, 142.2, 140.9, 140.7, 137.7, 136.9, 130.2, 130.1, 130.0, 129.6, 129.6 (2 C_{pTol}), 127.0 (2 C_{pTol}), 115.6, 113.4, 102.2, 56.3, 21.6, 20.3 ppm.
R_f **(***c*-Hex : EtOAc = 1:1): 0.44.

Mp. = 187.5–189.5 °C.
IR (ATR): $\tilde{\nu}$ /cm^{-1} = 3047 (w), 2961 (w), 2922 (w), 2835 (w), 1585 (m), 1462 (m), 1428 (m), 1253 (s), 1171 (m), 1152 (m), 1082 (m), 1052 (s), 1029 (s), 815 (s), 765 (s), 626 (m), 511 (s)
[α]$^{20}_{D}$ = –111.2 (c = 0.545, $CHCl_3$).
HRMS: 485.0000 [M+Na]$^+$, *calcd.* for $C_{21}H_{19}INaO_2S$ = 485.0040.

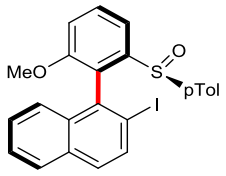

2-iodo-1-(2-methoxy-6-((*S*)-*p*-tolylsulfinyl)phenyl)naphthalene
Chemical Formula: $C_{24}H_{19}IO_2S$
Molecular Weight: 498,3785

(*SaR*)-2-Iodo-1-[2-methoxy-6-(*p*-tolylsulfinyl)phenyl]naphthalene [(*SaR*)-3l]: Prepared from (*S*)-1-[2-methoxy-6-(*p*-tolylsulfinyl)phenyl]naphthalene 1l, (1.0 equiv, 74.5 mg, 0.2 mmol) according to GP4 for 38 h by using $Pd(OAc)_2$ (5 mol%, 2.3 mg, 0.01 mmol), NIS (1.3 equiv, 58.6 mg, 0.26 mmol), AcOH (69.8 equiv, 800 µL, 13.96 mmol), and HFIP (38 equiv, 800 µL, 7.59 mmol). The crude mixture was analyzed by ^{1}H NMR, *dr* = 63:37. The product was purified by flash column chromatography on silica gel using mixture of cyclohexane and ethyl acetate (1/1, v/v) (98% yield) and recrystallization from *n*-pentane and dichloromethane to afford the title compound (*SaR*)-3l, as a colorless crystal (58.7 mg, 0.118 mmol, 59%, *dr* > 98:2).

^{1}H-NMR ($CDCl_3$, 400 MHz): δ = 8.00 (t+d, *J* = 8.6, 7.9 Hz, 2H), 7.76 (d, *J* = 8.1 Hz, 1H), 7.72 (d, *J* = 8.6 Hz, 1H), 7.60 (d, *J* = 8.7 Hz, 1H), 7.29 (t, *J* = 7.6 Hz, 1H), 7.16 (d, *J* = 8.3 Hz, 1H), 6.78 (dd, *J* = 7.9, 7.4 Hz, 1H), 6.58 (brs, 4H), 6.40 (d, *J* = 8.5 Hz, 1H), 3.63 (s, 3H), 2.09 (s, 3H) ppm.
^{13}C-NMR ($CDCl_3$, 101 MHz): δ = 157.0, 146.2, 141.5, 140.3, 136.6, 135.7, 133.4, 132.4, 130.7, 130.1, 129.2, 129.2 (2 $C_{p\text{Tol}}$), 127.8, 126.6, 126.3 (2 $C_{p\text{Tol}}$), 125.9, 125.7, 116.1, 113.6, 100.2, 56.4, 21.3 ppm.
R_f (*c*-Hex : EtOAc = 1:1): 0.42.
Mp. = 224.4–226.4 °C.
IR (ATR): $\tilde{\nu}$ /cm^{-1} = 2998 (w), 2961 (w), 2832 (w), 1584 (w), 1460 (m), 1431 (m), 1263 (s), 1153 (m), 1050 (m), 1028 (s), 806 (s), 776 (s), 735 (s).
[α]$^{20}_{D}$ = –108.5 (c = 1.2, $CHCl_3$).
HRMS: 521.0000 [M+Na]$^+$, *calcd.* for $C_{24}H_{19}INaO_2S$ = 521.0043.

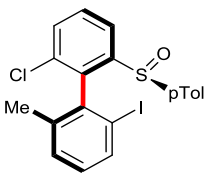

(*S*)-2-chloro-2'-iodo-6'-methyl-6-((*S*)-*p*-tolylsulfinyl)-1,1'-biphenyl
Chemical Formula: $C_{20}H_{16}ClIOS$
Molecular Weight: 466,7615

(*SaR*)-2-Chloro-2'-iodo-6'-methyl-6-(*p*-tolylsulfinyl)-1,1'-biphenyl [(*SaS*)-3n]: Prepared from (*S*)-2-chloro-2'-methyl-6-(*p*-tolylsulfinyl)-1,1'-biphenyl 1o, (1.0 equiv, 34 mg, 0.1 mmol) according to GP4 for 7 d by using $Pd(OAc)_2$ (5 mol%, 1.1 mg, 0.005 mmol), NIS (1.3 equiv, 29.3 mg, 0.13 mmol), AcOH (69.8 equiv, 400 µL, 6.98 mmol), and HFIP (38 equiv, 400 µL, 3.8 mmol). The crude mixture was analyzed by ^{1}H NMR, mixture of starting material and product. Purification by flash column chromatography on silica gel using mixture of cyclohexane, ethyl acetate, and dichloromethane (3/1/3, v/v/v) afforded the title compound (*SaS*)-3n, [22.4 mg, 0.048 mmol, 48%, *dr* > 98:2] as a colorless solid.

^{1}H-NMR ($CDCl_3$, 300 MHz): δ = 8.29 (dd, *J* = 7.6, 1.5 Hz, 1H), 7.86 (dd, *J* = 7.6, 1.4 Hz, 1H), 7.66 (t, *J* = 8.0 Hz, 1H), 7.60 (dd, *J* = 8.0, 1.2 Hz, 1H), 7.12–6.96 (m, 6H), 2.33 (s, 3H), 1.11 (s, 3H) ppm.
^{13}C-NMR ($CDCl_3$, 75 MHz): δ = 146.2, 142.7, 140.5, 140.2, 139.4, 138.3, 137.1, 134.3, 131.7, 130.7, 130.3, 130.0, 129.8 (2 $C_{p\text{Tol}}$), 127.2 (2 $C_{p\text{Tol}}$), 122.5, 100.9, 21.6, 20.1 ppm.
R_f (cyclohexane: ethyl acetate: dichloromethane = 3:1:3): 0.38.
IR (ATR): $\tilde{\nu}$ /cm^{-1} = 3049 (w), 2921 (w), 2853 (w), 1556 (m), 1439 (m), 1406 (m), 1259 (m), 1095 (s), 1082 (s), 1044 (s), 1018 (m), 800 (m), 762 (m), 741 (s), 623 (m), 503 (s).
$[\alpha]^{20}_D$ = –168.7 (c = 1.115, $CHCl_3$).
HRMS: 488.9550 $[M+Na]^+$, *calcd*. for $C_{20}H_{16}ClINaOS$ = 488.9550.

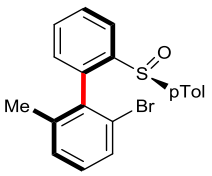

(*R*)-2-bromo-6-methyl-2'-((*S*)-*p*-tolylsulfinyl)-1,1'-biphenyl
Chemical Formula: $C_{20}H_{17}BrOS$
Molecular Weight: 385,3190

(*SaR*)-2-Bromo-6-methyl-2'-(*p*-tolylsulfinyl)-1,1'-biphenyl [(*SaR*)-4a]: Prepared from (*S*)-2-methyl-2'-(*p*-tolylsulfinyl)-1,1'-biphenyl 1a. A sealed tube was successively charged with (*S*)-2-methyl-2'-(*p*-tolylsulfinyl)-1,1'-biphenyl 1a, (1.0 equiv, 30.6 mg, 0.1 mmol), $Pd(OAc)_2$ (5 mol%, 1.1 mg, 0.005 mmol), NBS (1.3 equiv, 23.1 mg, 0.13 mmol). AcOH (69.8 equiv, 400 µL, 6.98 mmol), and HFIP (38 equiv, 400 µL, 3.8 mmol), were added, and the resulting mixture was stirred at 40 °C until analysis of an aliquot by TLC indicated complete conversion of the biaryl substrate (36 h). The mixture was quenched with saturated $NaHCO_3$ solution. Aqueous phase was extracted with ethyl acetate, the combined organic phase was washed with brine, dried over Na_2SO_4, filtrated and concentrated under vacuum to furnish the crude product. The crude mixture was analyzed by ^{1}H NMR; *dr* = 93:7. The product was purified by flash column chromatography on silica gel using mixture of cyclohexane and ethyl acetate (1/1, v/v) (82% yield) and recrystallization from *n*-pentane and dichloromethane to afford (*SaR*)-4a, as a white solid. (25.1 mg, 0.065 mmol, 65% *dr* > 98:2).

^{1}H-NMR ($CDCl_3$, 400 MHz): δ = 8.34 (d, *J* = 8.02 Hz, 1H), 7.67 (t, *J* = 7.5 Hz, 1H), 7.62–7.48 (m, 2H), 7.18 (t, *J* = 7.8 Hz, 1H), 7.09–6.96 (m, 6H), 2.30 (s, 3H), 1.16 (s, 3H) ppm.
^{13}C-NMR ($CDCl_3$, 101 MHz): δ = 144.2, 142.1, 141.2, 140.1, 137.9, 137.6, 130.9, 130.5, 130.0, 129.9, 129.6 (2 C_{pTol}), 129.2, 129.2, 126.8 (2 C_{pTol}), 124.7, 123.6, 21.6, 20.5 ppm.
R_f (cyclohexane: ethyl acetate = 1:1): 0.2.
Mp. = 122.1–124.1 °C.
IR (ATR): $\tilde{\nu}$ /cm^{-1} = 3051 (w), 2955 (w), 2921 (w), 1444 (m), 1084 (m), 1061 (m), 1037 (s), 806 (m), 771 (s), 743 (m), 621 (m), 546 (s), 520 (s).
$[\alpha]^{20}_D$ = –124.5 (c = 1, $CHCl_3$).
HRMS: 409.0038 $[M+Na]^+$, *calcd.* for $C_{20}H_{17}BrNaOS$ = 409.0056.

5. Palladacycles synthesis

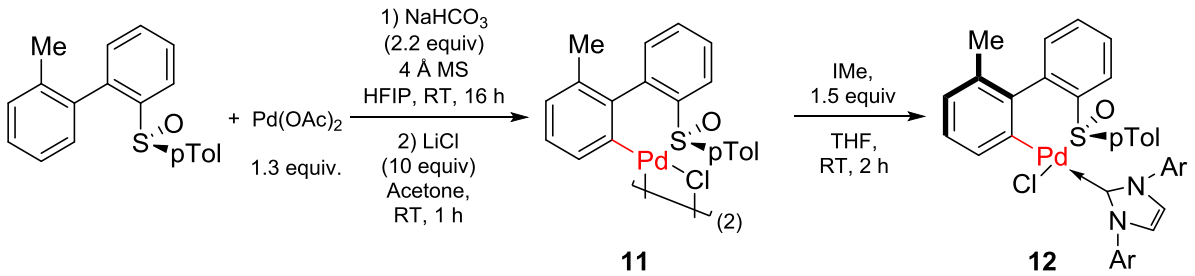

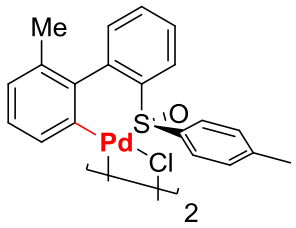

[[(6-methyl-2'-((*S*)-p-tolylsulfinyl)-[1,1'-biphenyl]-2-yl)Cl][Palladium^{II}] dimer

C1 (*S*)-2-methyl-2'-(p-tolylsulfinyl)-1,1'-biphenyl (1 equiv, 215 mg, 0.702 mmol), along with $Pd(OAc)_2$ (1.3 equiv, 205 mg, 0.913 mmol), $NaHCO_3$ (2.21 equiv, 130 mg, 1.55 mmol) and 4 Å MS were loaded in a sealed vial under air. Anhydrous HFIP (7 mL) was then added and the resulting heterogenous mixture was stirred for 16 hours at room temperature. It was then diluted with DCM, filtrated on a celite plug and the filtrate was evaporated to dryness. Then LiCl (10 equiv, 298 mg, 0.145 mL, 7.03 mmol) was added followed by acetone (21 mL) and the reaction mixture was stirred at 25 °C for 1 hour, when the solvent was removed under reduced pressure and the resulting solid was finally dissolved in DCM (sonication might bu used), and filtrated over a celite plug. The crude product was purified by flash chromatography

(CyH/AcMe 80 : 20; streaking, caused by slow decomposition to the starting material and an unkown by-product, however the title compound is isolated with c.a. 95% purity), affording [[(6-methyl-2'-((*S*)-p-tolylsulfinyl)-[1,1'-biphenyl]-2-yl)Cl][Palladium^{II}] dimer (232 mg, 0.519 mmol, 74 %) as a light yellow powder. *Fast exchange caused by the bridging chlorides caused extensive broadening of peaks at 25 °C on the ^{1}H NMR spectra and coalescence of the majority of signals. However, an atropisomeric ratio of 1 : 1.3 (using the broad doublet at 8.22 ppm) can be tentatively proposed.*
^{1}**H-NMR** ($CDCl_3$, 400 MHz) : δ = 8.22 (brd d, 1H), 7.75 – 7.28 (m, 6H), 6.97 (s, 2H), 6.79 (s, 1H), 6.65 (d, J = 7.3 Hz, 1H), 2.24 (s, 3H), 1.98 (s, 3H) ppm.

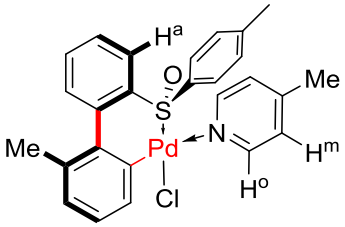

C2 [[($_a$*S*)-(6-methyl-2'-((*S*)-p-tolylsulfinyl)-[1,1'-biphenyl]-2-yl)(4-MePy)Cl][Palladium^{II}]
To a solution of [[(6-methyl-2'-((S)-p-tolylsulfinyl)-[1,1'-biphenyl]-2-yl)Cl][PalladiumII] dimer (1 equiv, 72 mg, 0.161 mmol) in DCM (2000 µL) was added 4-methylpyridine (1.14 equiv, 17.1 mg, 18 µL, 0.184 mmol) . The mixture was stirred at room temperature for 30 min, then the volatiles were remover under reduced pressure. Chromatography (AcMe/CyH) gave [[(aS)-(6-methyl-2'-((S)-p-tolylsulfinyl)-[1,1'-biphenyl]-2-yl)(4-MePy)Cl][PalladiumII] (83 mg, 0.154 mmol, 95%) as a yellowish solid. Recrystallization by gaseous diffusion of n-Pentane in a concentrated $CHCl_3$ solution at 4-6 °C gave monocrystals of the title compound (53 mg, 0.0803 mmol, 50%). The ^{1}H NMR of the solid isolated after flash chromatography and the ^{1}H NMR of the monocrystals are identical.

mixture of two atropisomers on the NMR time scale, only the major is reported for the ^{13}C NMR.
^{1}**H-NMR** ($CDCl_3$, 400 MHz) :
major dia : δ = 8.67 (d, J = 6.1 Hz, 2H), 8.19 – 8.06 (m, 1H), 7.67 (d, J = 7.7 Hz, 1H), 7.62 – 7.53 (m, 2H), 7.55 – 7.47 (m, 1H), 7.38 (d, J = 8.3 Hz, 2H), 7.17 (d, J = 5.8 Hz, 2H), 6.99 (d, J = 8.1 Hz, 2H), 6.86 (t, J = 7.6 Hz, 0H), 6.66 (d, J = 7.2 Hz, 1H), 2.36 (s, 3H), 2.26 (s, 3H), 1.95 (s, 3H) ppm
minor dia : δ = 8.55 (d, J = 5.5 Hz, 2H), 8.37 (d, J = 6.8 Hz, 1H), 7.66 – 7.61 (m, 1H), 7.60 – 7.54 (m, 1H), 7.55 – 7.48 (m, 1H), 7.45 – 7.39 (m, 2H), 7.26 (d, J = 1.3 Hz, 1H), 7.08 (d, J = 5.6 Hz, 2H), 6.94 (d, J = 7.9 Hz, 2H), 6.69 – 6.62 (m, 2H), 2.36 (s, 3H), 2.23 (s, 3H), 2.02 (s, 3H) ppm
^{13}**C NMR** (101 MHz, $CDCl_3$) : δ =151.14 (2C), 149.76, 143.18, 142.61, 141.51, 140.19, 136.23, 135.49, 135.34, 133.73, 132.79, 131.09, 129.13 (2C), 128.54, 127.88, 127.12, 126.60 (2C), 125.30 (2C), 123.47, 22.20, 21.38, 21.10 ppm.

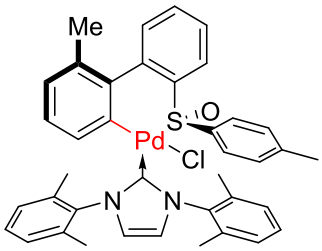

C3 [[($_a$*S*)-(6-methyl-2'-((*S*)-p-tolylsulfinyl)-[1,1'-biphenyl]-2-yl)(IMe)Cl][Palladium^{II}]

A mixture of IMeHCl (1.5 equiv, 148 mg, 0.476 mmol) and KOtBu (3 equiv, 107 mg, 0.954 mmol) in THF (15 mL) was allowed to react 1 hour, at room temp, when it was added by a syringe fitted with a 0.2 µm PTFE filter to a solution of [[(6-methyl-2'-((*S*)-p-tolylsulfinyl)-[1,1'-biphenyl]-2-yl)][PalladiumII](Cl)-μ-(Cl)] dimer (1 equiv, 142 mg, 0.317 mmol) in THF (3 mL). The resulting mixture was stirred for 2 hours and the pale yellow solution turned deep orange-red. The solvent was then removed under reduced pressure and flash chromatography afforded [[(6-methyl-2'-((*S*)-p-tolylsulfinyl)-[1,1'-biphenyl]-2-yl)(IMe)Cl][Palladium^{II}] (193 mg, 0.266 mmol, 84%) as a yellow powder. In solution at room temperature, significant decomposition occurs over few days, however in the solid state it is stable at 4-6 °C under argon for weeks. Recrystallization by layering a concentrated THF solution with Et_2O in a narrow container and letting the resulting biphasic mixture equilibrating at 4-6 °C gave monocrystals of the title compound (62 mg, 0.0854 mmol, 44% of the amount engaged in the recrystallization). The ^{1}H NMR of the solid isolated after flash chromatography and the ^{1}H NMR of the monocrystals are identical. ^{1}**H-NMR** ($CDCl_3$, 600 MHz) : δ = 7.66 (dd, J = 7.7, 1.3 Hz, 1H), 7.43 – 7.40 (m, 1H), 7.39 (td, J = 7.5, 1.5 Hz, 1H), 7.37 (t, J = 7.2 Hz, 1H), 7.35 (dq, J = 7.4, 1.4 Hz, 1H), 7.30 (dd, J = 7.5, 1.2 Hz, 1H), 7.18 – 7.14 (m, 2H), 7.13 (d, J = 1.7 Hz, 1H), 7.08 (d, J = 6.8 Hz, 2H), 7.06 (d, J = 1.8 Hz, 1H), 6.93 (d, J = 7.5 Hz, 1H), 6.76 – 6.73 (***AA'***BB', 2H), 6.72 – 6.69 (AA'***BB'***, 2H), 6.65 (t, J = 7.5 Hz, 1H), 6.40 (d, J = 7.3 Hz, 1H), 2.65 (s, 3H), 2.34 (s, 3H), 2.25 (s, 3H), 2.20 (s, 3H), 2.17 (s, 3H), 1.80 (s, 3H).

6. Post-modification of 2a

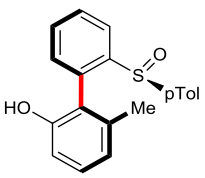

(*R*)-6-methyl-2'-((*S*)-*p*-tolylsulfinyl)-[1,1'-biphenyl]-2-ol
Chemical Formula: $C_{20}H_{18}O_2S$
Molecular Weight: 322,4220

(*SaR*)-6-Methyl-2'-(*p*-tolylsulfinyl)-[1,1'-biphenyl]-2-ol [(*SaR*)-5]: Prepared from (*SaR*)-6-methyl-2'-(*p*-tolylsulfinyl)-[1,1'-biphenyl]-2-yl-acetate [(*SaR*)-2a]. A round bottom flask was charged with (*S*)-6-methyl-2'-(*p*-tolylsulfinyl)-[1,1'-biphenyl]-2-yl-acetate (*SaR*)-2a, (1.0 equiv, 330 mg, 0.905 mmol), and K_2CO_3 (5.0 equiv, 626 mg, 4.5 mmol). MeOH (37 mL), and H_2O (23.2 mL) were added and the resulting mixture was stirred at room temperature until analysis of an aliquot by TLC indicated complete conversion of the starting material (1 h). The mixture was quenched with saturated NH_4Cl (40 mL) solution. Aqueous phase was extracted with ethyl acetate, the combined organic phase was washed with brine, dried over Na_2SO_4, filtrated and concentrated under vacuum to furnish the crude hydroxylated product (*SaR*)-5. Purification by flash column chromatography on silica gel using mixture of cyclohexane and ethyl acetate (2/3, v/v) afforded the title compound [(*SaR*)-5, 280.5 mg, 0.87 mmol, 96%, *dr* > 98:2] as a white solid.

^{1}H-NMR ($CDCl_3$, 400 MHz): δ = 8.23 (brd, 1H), 8.29 (dd, *J* = 7.8, 1.1 Hz, 1H), 7.56 (td, *J* = 7.7, 1.0 Hz, 1H), 7.49 (td, *J* = 7.5, 1.1 Hz, 1H), 7.15 (dd, *J* = 7.4, 1.1 Hz, 1H), 7.08 (t, *J* = 7.7 Hz, 3H), 7.02 (d, *J* = 8.2 Hz, 2H), 6.84 (d, *J* = 8.1 Hz, 1H), 6.61 (d, *J* = 7.5 Hz, 1H), 2.32 (s, 3H), 1.29 (s, 3H) ppm.
^{13}C-NMR ($CDCl_3$, 101 MHz): δ = 153.9, 144.2, 141.9, 140.9, 138.3, 135.3, 131.3, 131.1, 129.7, 129.6 (2 $C_{p\text{Tol}}$), 128.7, 126.3 (2 $C_{p\text{Tol}}$), 124.1, 123.5, 121.6, 113.9, 21.6, 19.7 ppm.
R_f (*c*-Hex : EtOAc = 2:3): 0.36.
IR (ATR): $\tilde{\nu}$ /cm^{-1} = 3665 (w), 3158 (brd), 2988 (w), 2921 (w), 2954 (w), 1584 (w), 1461 (m), 1291 (m), 1082 (m), 1021 (m), 999 (s), 804 (m), 764 (s), 774 (s), 745 (s), 531 (s), 506 (s).
$[\alpha]^{20}_D$ = –153.0 (c = 1, $CHCl_3$).
HRMS: 345.0874 $[M+Na]^+$, *calcd*. for $C_{20}H_{18}NaO_2S$ = 345.0925.

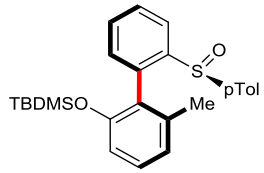

tert-butyldimethyl(((*R*)-6-methyl-2'-((*S*)-*p*-tolylsulfinyl)-[1,1'-biphenyl]-2-yl)oxy)silane
Chemical Formula: $C_{26}H_{32}O_2SSi$
Molecular Weight: 436,6850

(*SaR*)-*tert*-Butyldimethyl{[6-methyl-2'-(*p*-tolylsulfinyl)-[1,1'-biphenyl]-2-yl]oxy}silane [(*SaR*)

-6]: Prepared from (*SaR*)-6-methyl-2'-(*p*-tolylsulfinyl)-[1,1'-biphenyl]-2-ol [(*SaR*)-5]. A round bottom flask was successively charged with (*SaR*)-6-methyl-2'-(*p*-tolylsulfinyl)-[1,1'-biphenyl]-2-ol (*SaR*)-5, (1.0 equiv, 310 mg, 0.96 mmol), TBDMSCl (1.40 equiv, 203 mg, 1.35 mmol), and Imidazole (2.5 equiv, 164 mg, 2.4 mmol). DMF (10 mL) was added, and the resulting mixture was maintained first at 0 °C and then allowed to stir at room temperature (25 °C) overnight. Analysis of an aliquot by TLC indicated complete conversion of the starting material (12 h). The mixture was quenched with satu-

rated NH_4Cl (30 mL) solution. Aqueous phase was extracted with ethyl acetate, the combined organic phase is washed with brine, dried over Na_2SO_4, filtrated and concentrated under vacuum to furnish the crude product (*SaR*)-6. Purification by flash column chromatography on silica gel using mixture of cyclohexane and ethyl acetate (1/1, v/v) afforded the title compound (*SaR*)-6, [390 mg, 0.896 mmol, 93%, *dr* > 98:2] as a white solid.

^{1}H-NMR ($CDCl_3$, 400 MHz): δ = 8.26 (dd, *J* = 7.9, 1.0 Hz, 1H), 7.57 (td, *J* = 7.6, 1.0 Hz, 1H), 7.44 (td, *J* = 7.4, 1.2 Hz, 1H), 7.18 (t, *J* = 7.8 Hz, 1H), 7.04 (dd, *J* = 7.4, 0.8 Hz, 1H), 7.01 (d, *J* = 8.0 Hz, 2H), 6.92 (d, *J* = 8.0 Hz, 2H), 6.79 (d, *J* = 8.0 Hz, 1H), 6.67 (d, *J* = 7.6 Hz, 1H), 2.28 (s, 3H), 1.16 (s, 3H), 0.68 (s, 9H), 0.23 (s, 3H), –0.09 (s, 3H) ppm.
^{13}C-NMR ($CDCl_3$, 101 MHz): δ = 152.7, 145.3, 142.0, 141.5, 139.1, 135.8, 130.9, 130.2, 129.4 (2 $C_{p\text{Tol}}$), 129.3, 128.7, 128.2, 126.5 (2 $C_{p\text{Tol}}$), 123.1, 122.9, 116.5, 25.4, 21.5, 19.7, 17.9, –3.8, –4.7 ppm.
R_f (*c*-Hex : EtOAc = 1:1): 0.2.
IR (ATR): $\tilde{\nu}$ /cm^{-1} = 2958 (w), 2924 (w), 2954 (w), 1598 (w), 1575 (m), 1482 (w), 1462 (s), 1268 (s), 1289 (s), 1082 (m), 1062 (m), 1041 (s), 964 (m), 836 (s), 811 (s), 774 (s), 744 (s), 620 (m), 545 (m), 519 (s).
$[\alpha]^{20}_D$ = –180.4 (c = 0.75, $CHCl_3$).
HRMS: 459.1723 $[M+Na]^+$, *calcd*. for $C_{26}H_{32}NaO_2SSi$ = 459.1784.

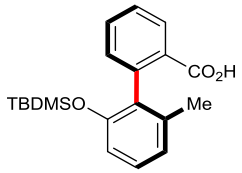

(*R*)-2'-((*tert*-butyldimethylsilyl)oxy)-6'-methyl-[1,1'-biphenyl]-2-carboxylic acid
Chemical Formula: $C_{20}H_{26}O_3Si$
Molecular Weight: 342,5100

(*R*)-2'-[(*tert*-Butyldimethylsilyl)oxy]-6'-methyl-[1,1'-biphenyl]-2-carboxylic-acid [(*R*)-7a]: Prepared from (*SaR*)-*tert*-butyldimethyl{[6-methyl-2'-(*p*-tolylsulfinyl)-[1,1'-biphenyl]-2-yl]oxy}-silane [(*SaR*)-6]. A flame dried schlenk tube was charged with (*SaR*)-*tert*-butyldimethyl{[6-methyl-2'-(*p*-tolylsulfinyl)-[1,1'-biphenyl]-2-yl]oxy}silane (*SaR*)-6, (1.0 equiv, 29.6 mg, 0.068 mmol). Dry THF (1.5 mL) was added and the reaction mixture was cooled down to -90 °C. After 15 min, 1.67 M solution of *t*-BuLi (2.1 equiv, 85 µL, 0.142 mmol) was added. After 15 min CO_2 (from dry ice; excess) was bubbled into the reaction mixture while maintaining the reaction temperature at –90 °C. After 15 min at –90 °C the whole reaction mixture was allowed to reach room temperature over 30 min. The mixture was quenched with HCl (1 N) solution. Aqueous phase was extracted with ethyl acetate, the combined organic phase was washed with brine, dried over Na_2SO_4, filtrated and concentrated under vacuum to furnish the crude product. Purification by flash column chromatography on silica gel using mixture of cyclohexane and ethyl acetate (5/3, v/v) afforded the title compound [(*S*)-7, 13.2 mg, 0.039 mmol, 57%, *er* > 98:2] as a white solid.

^{1}H-NMR ($CDCl_3$, 400 MHz): δ = 8.03 (dd, *J* = 7.8, 1.0 Hz, 1H), 7.55 (td, *J* = 7.6, 1.2 Hz, 1H), 7.39 (td, *J* = 6.6, 1.0 Hz, 1H), 7.18 (d, *J* = 7.2 Hz, 1H), 7.11 (t, *J* = 7.9 Hz, 1H), 6.86 (d, *J* = 7.5 Hz, 1H), 6.68 (d, *J* = 8.1 Hz, 1H), 1.99 (s, 3H), 0.61 (s, 9H), 0.02 (s, 3H), –0.03 (s, 3H) ppm.
^{13}C-NMR ($CDCl_3$, 101 MHz): δ = 171.4, 152.3, 140.0, 137.3, 132.8, 132.4, 131.9, 131.0, 130.2, 127.9, 127.2, 122.8, 116.0, 25.3, 20.6, 17.8, –4.3, –4.4 ppm.
R_f (*c*-Hex : EtOAc = 5:3): 0.38.
IR (ATR): $\tilde{\nu}$ /cm^{-1} = 2954 (w), 2928 (w), 2857 (w), 1695 (s), 1679 (s), 1571 (m), 1463 (s), 1392 (m), 1289 (s), 1259 (s), 1053 (s), 970 (m), 837 (s), 777 (s), 757 (s), 687 (m).
$[\alpha]^{20}_D$ = –71.0 (c = 0.15, $CHCl_3$).
HRMS: 365.1506 $[M+Na]^+$, *calcd*. for $C_{20}H_{26}NaO_3Si$ = 365.1543.

Analysis of the chiral purity; chiral HPLC: (AD-H, 95:5 hex/*i*PrOH; 0.5 mL/min, c = 0.1 mg/mL, (*S*) r_t = 8.63 min, (*R)* r_t = 9.15 min). Rg: The small modifications of the r_t might be observed.

A racemic sample was prepared from rac-1a using the same synthetic pathway.

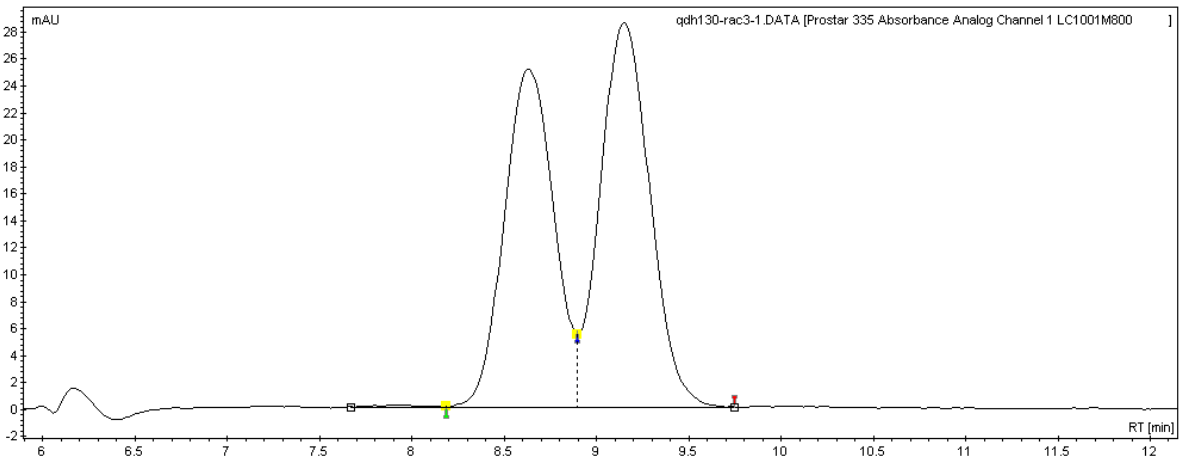

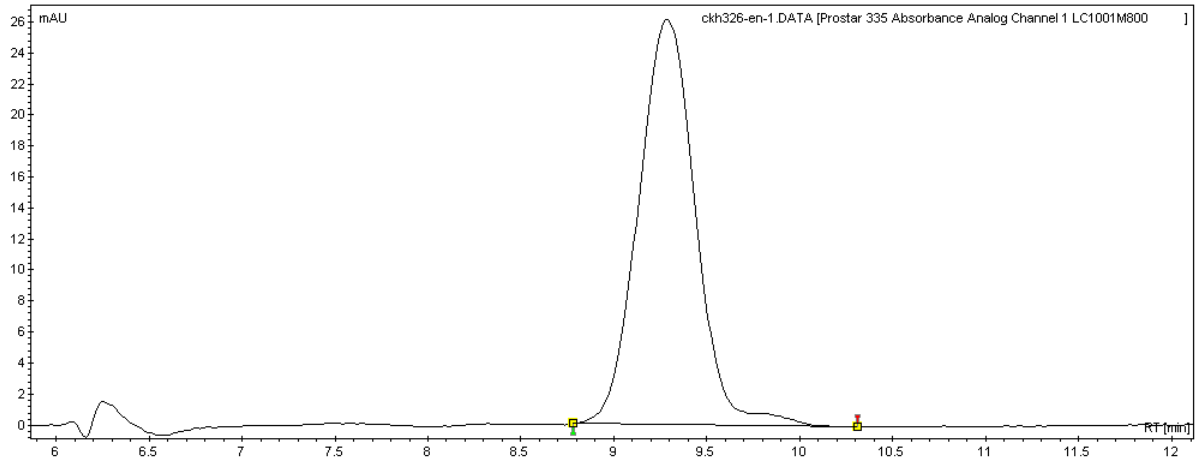

7. Mechanistic studies

a) KIE

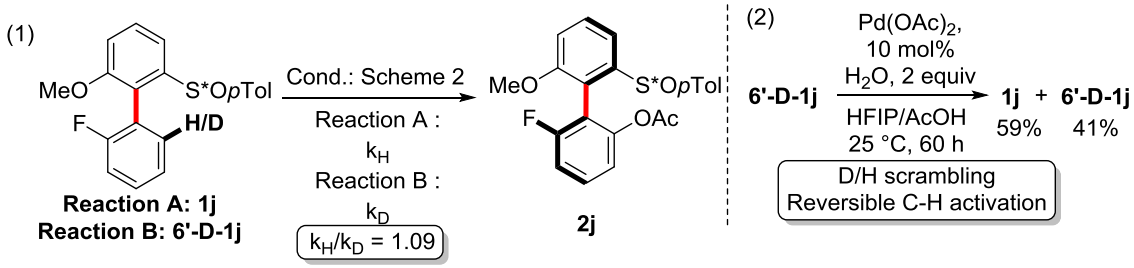

The reactions were performed using fluorobenzene as internal standard and the kinetic was followed using ^{19}F NMR. Reactions A and B were performed in parallel.

Reaction A

Microwave reactor was charged with 1j, (1.0 equiv, 60 mg, 0.176 mmol), $(NH_4)_2S_2O_8$ (2.0 equiv, 80.4 mg, 0.352 mmol), $Pd(OAc)_2$ (10 mol%, 4.0 mg, 0.017 mmol). HFIP (440 µL), AcOH (440 µL), H_2O (6.4 µL) and fluorobenzene (0.4 equiv, 6.6 µL, 0.07 mmol). The reactor was sealed with septum-cap and the reaction mixture was stirred at 25 °C for 7.5 h.

Sampling: A sample of 30 µL of the reaction mixture was taken, diluted with 0.5 mL of $CDCl_3$ and filtrated over celite. Conversion was determined by ^{19}F NMR.

Sampling: 0 min; 3 h; 3.5 h; 4 h; 4.45 h; 5.5 h; 6.5 h; 7.5 h.

Reaction B

Microwave reactor was charged with 6'-D-1j, (1.0 equiv, 60 mg, 0.176 mmol), $(NH_4)_2S_2O_8$ (2.0 equiv, 80.4 mg, 0.352 mmol), $Pd(OAc)_2$ (10 mol%, 4.0 mg, 0.017 mmol). HFIP (440 µL), AcOH (440 µL), H_2O (6.4 µL) and fluorobenzene (0.4 equiv, 6.6 µL, 0.07 mmol). The reactor was sealed with septum-cap and the reaction mixture was stirred at 25 °C for 7.5 h.

Sampling: A sample of 30 µL of the reaction mixture was taken, diluted with 0.5 mL of $CDCl_3$ and filtrated over celite. Conversion was determined by ^{19}F NMR.

Sampling: 0 min; 3 h; 3.5 h; 4 h; 4.45 h; 5.5 h; 6.5 h; 7.5 h.

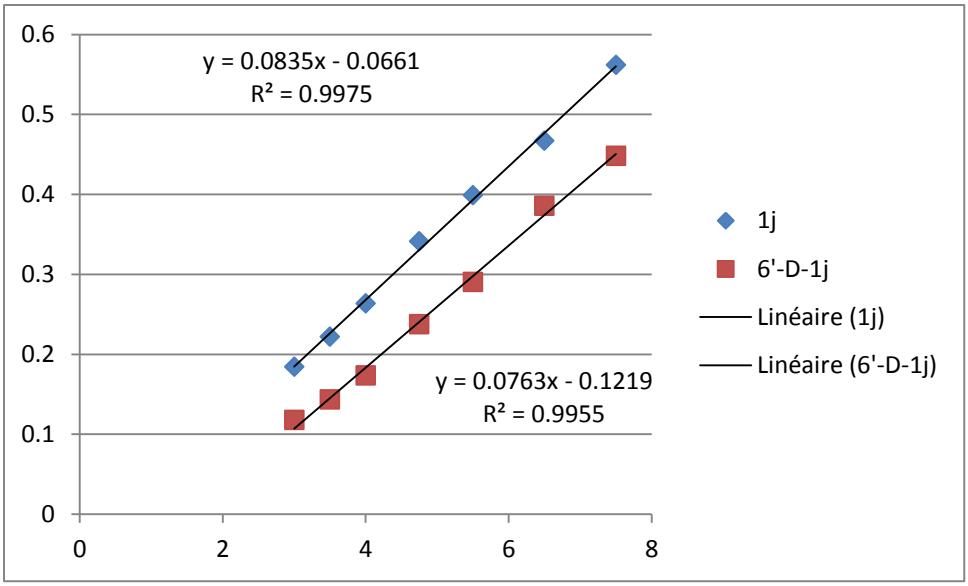

$$\frac{kH}{kD} = \frac{0.0835}{0.0763} = 1.09$$

b) Study of the reversibility of the reaction:

Red-cap sealed tube was charged with 6'-D-1j, (1.0 equiv, 15.2 mg, 0.042 mmol) and $Pd(OAc)_2$ (10 mol%, 1 mg, 0.0042 mmol). HFIP (0.2 mL), HFIP (0.2 mL) and H_2O (1.6 µL) were added, the tube was sealed and the reaction mixture was stirred for 60 h at 25 °C. The reaction mixture was diluted with EtOAc and $NaHCO_3$ was added. The phases were separated and the aqueous phase was extracted 3 times with EtOAc. The combine organic phase was washed with brine, dried over Na_2SO_4, filtrated and concentrated under vacuum. The crude product was purified by flash silica gel chromatography (*c*-Hex/EtOAc 7/3). The product (14 mg, 0.038 mmol%) was isolated as mixture of 1j and 6'-D-1j in 59/41 ratio, determined by ^{1}H NMR.

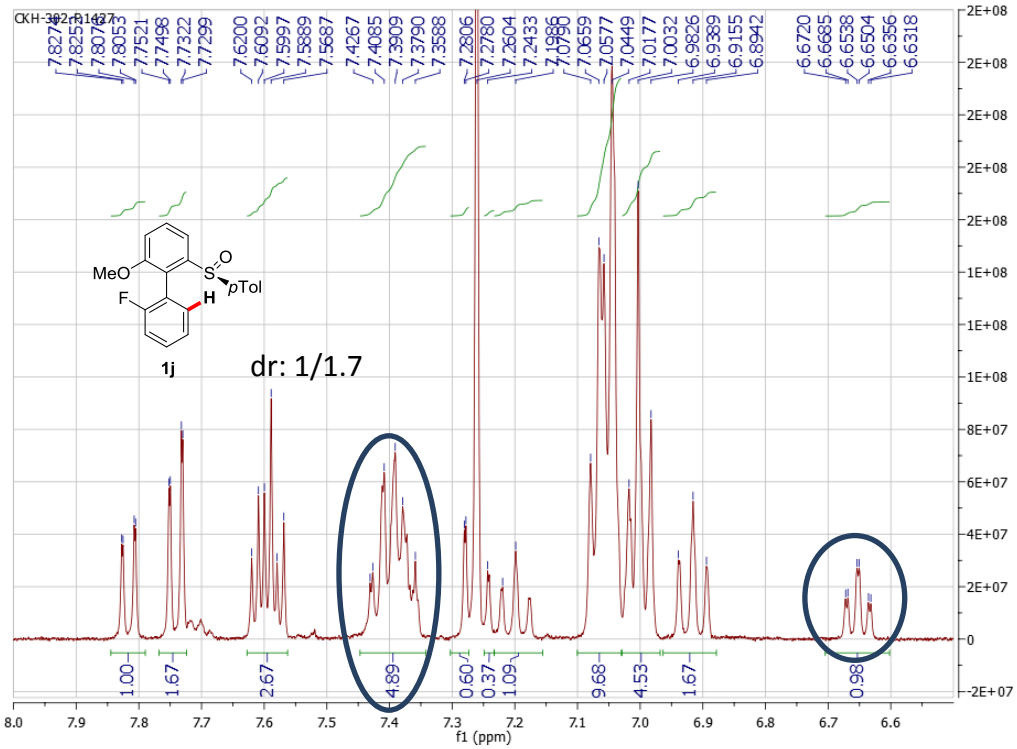
CKH-302-P1427
MeO
F
S
O
pTol
H
1j
dr: 1/1.7
f1 (ppm)

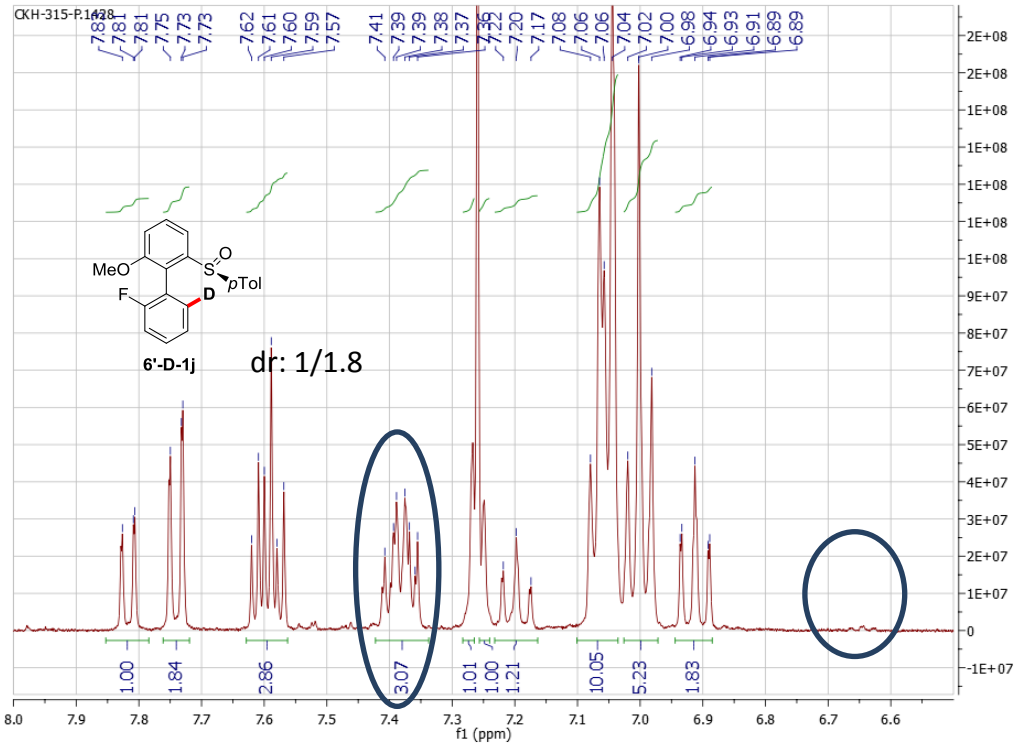
CKH-315-P1428
MeO
F
S
O
pTol
D
6'-D-1j
dr: 1/1.8
f1 (ppm)

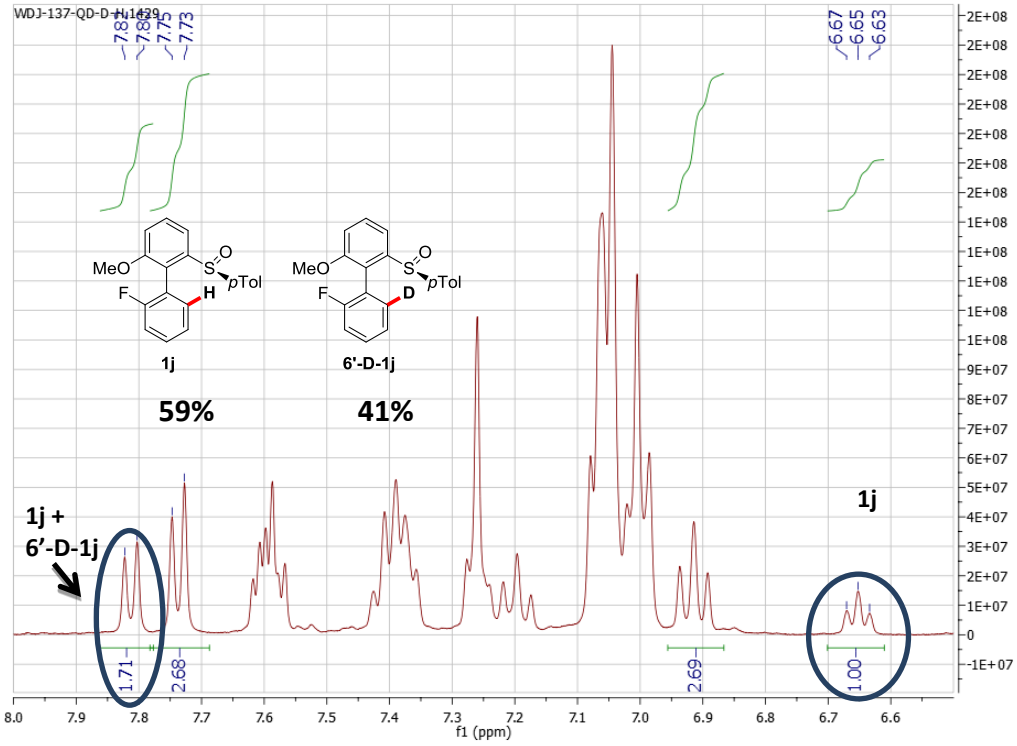

c) Study of the modification of the diastereomeric ration of 1e, 1j and 1m

The reactions were performed using trifluoromethylbenzene or fluorobenzene as internal solvents. The reactions were followed using ^{19}F NMR (two diastereomers of 1e, 1j and 1m have separated signals in ^{19}F NMR).

1e:

Microwave reactor was charged with 1e, (1.0 equiv, 150 mg, 0.416 mmol), $(NH_4)_2S_2O_8$ (2.0 equiv, 190.0 mg, 0.832 mmol), $Pd(OAc)_2$ (10 mol%, 9.3 mg, 0.042 mmol). HFIP (1040 µL), AcOH (1040 µL), H_2O (15 µL) and trifluoromethylbenzene (0.4 equiv. 20.5 µL, 0.166 mmol). The reactor was sealed and the reaction mixture was stirred at 25 °C.

Sampling: A sample of 30 µL of the reaction mixture was taken, diluted with 0.5 mL of $CDCl_3$ and filtrated over celite. The ration between two diastereomers of 1e was determined by ^{19}F NMR.

Sampling: 0 h; 3 h; 8 h; 22 h; 34 h; 46.5 h

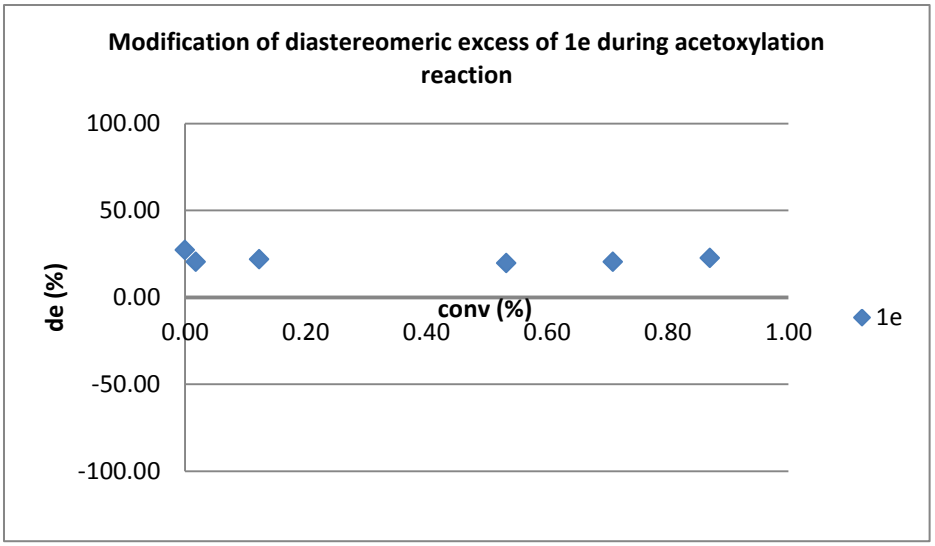

1j:

Microwave reactor was charged with 1j, (1.0 equiv. 140 mg, 0.411 mmol), $(NH_4)_2S_2O_8$ (2.0 equiv. 187.0 mg, 0.822 mmol), $Pd(OAc)_2$ (10 mol%, 9.2 mg, 0.041 mmol). HFIP (1030 µL), AcOH (1030 µL), H_2O (15 µL) and fluorobenzene (0.4 equiv, 15.5 µL, 0.165 mmol). The reactor was sealed and the reaction mixture was stirred at 25 °C.

Sampling: A sample of 30 µL of the reaction mixture was taken, diluted with 0.5 mL of $CDCl_3$ and filtrated over celite. The ration between two diastereomers of 1j was determined by ^{19}F NMR.

Sampling: 0 h; 4 h; 8 h; 22 h; 34 h.

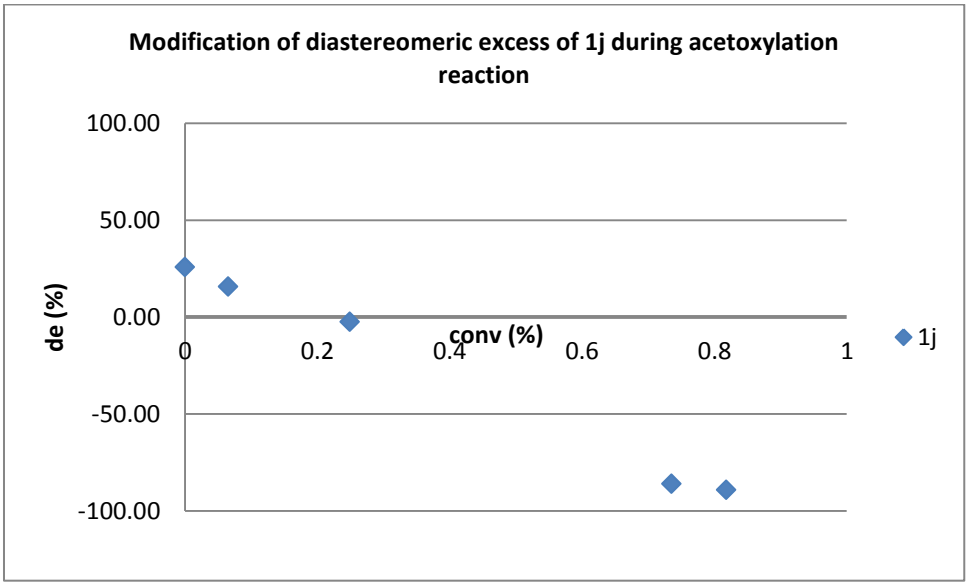

1m:

Microwave reactor was charged with 1m, (1.0 equiv, 100 mg, 0.29 mmol), $(NH_4)_2S_2O_8$ (2.0 equiv, 132.4 mg, 0.58 mmol), $Pd(OAc)_2$ (10 mol%, 6.5 mg, 0.029 mmol). HFIP (726 µL), AcOH (726 µL), H_2O (10.5 µL) and fluorobenzene (0.6 equiv, 16.4 µL, 0.174 mmol). The reactor was sealed and the reaction mixture was stirred at 25 °C.

Sampling: A sample of 30 µL of the reaction mixture was taken, diluted with 0.5 mL of $CDCl_3$ and filtrated over celite. The ration between two diastereomers of 1m was determined by ^{19}F NMR.

Sampling: 0 h; 4 h; 8 h; 20 h; 30 h; 44 h; 54 h; 72 h; 80 h; 92.5 h; 104 h; 127 h

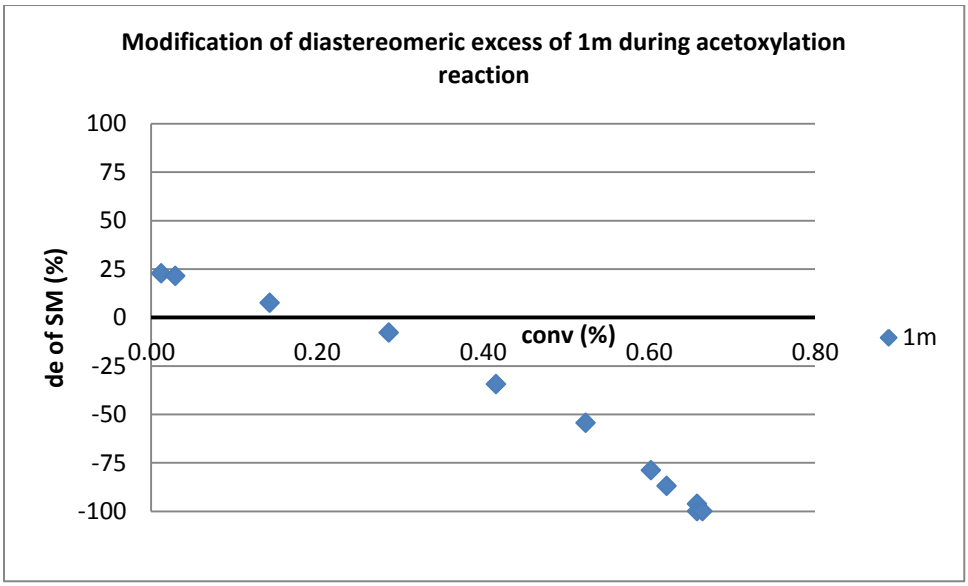

8. Rotational Barrier determination by D-NMR

a) Substrate 1a

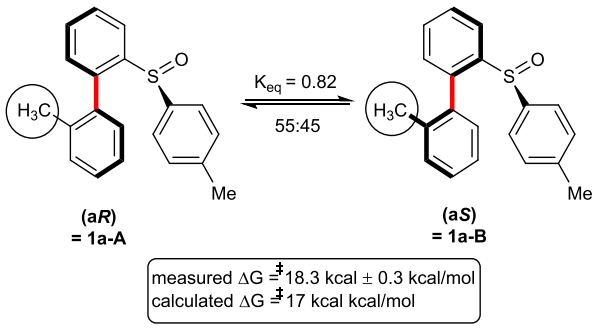

$$k = \frac{\pi}{\sqrt{2}} v_{AB}$$

v_{AB}= 7.08 Hz

$$k = 15.76\ s^{-1}$$

Eyring equation gives

$$k = \frac{k_B T}{h} e^{\frac{-\Delta G‡}{RT}}$$

which gives

$$\Delta G‡ = R \cdot T\left(\frac{h}{k_B} + \ln(k/T)\right)$$

2-Me-2'-pTolsulfinyl[1,1']Biphenyl

C2Cl2D4

T (K)	ΔvAB (Hz)	k (s-1)	ΔG‡
343.15	7.08	15.7176	18.3

$\Delta G^{‡}$ = 18.3 kcal/mole at 70 °C in $C_2Cl_2D_4$ (+/- 5K, i.e. +/- 0.3 kcal)

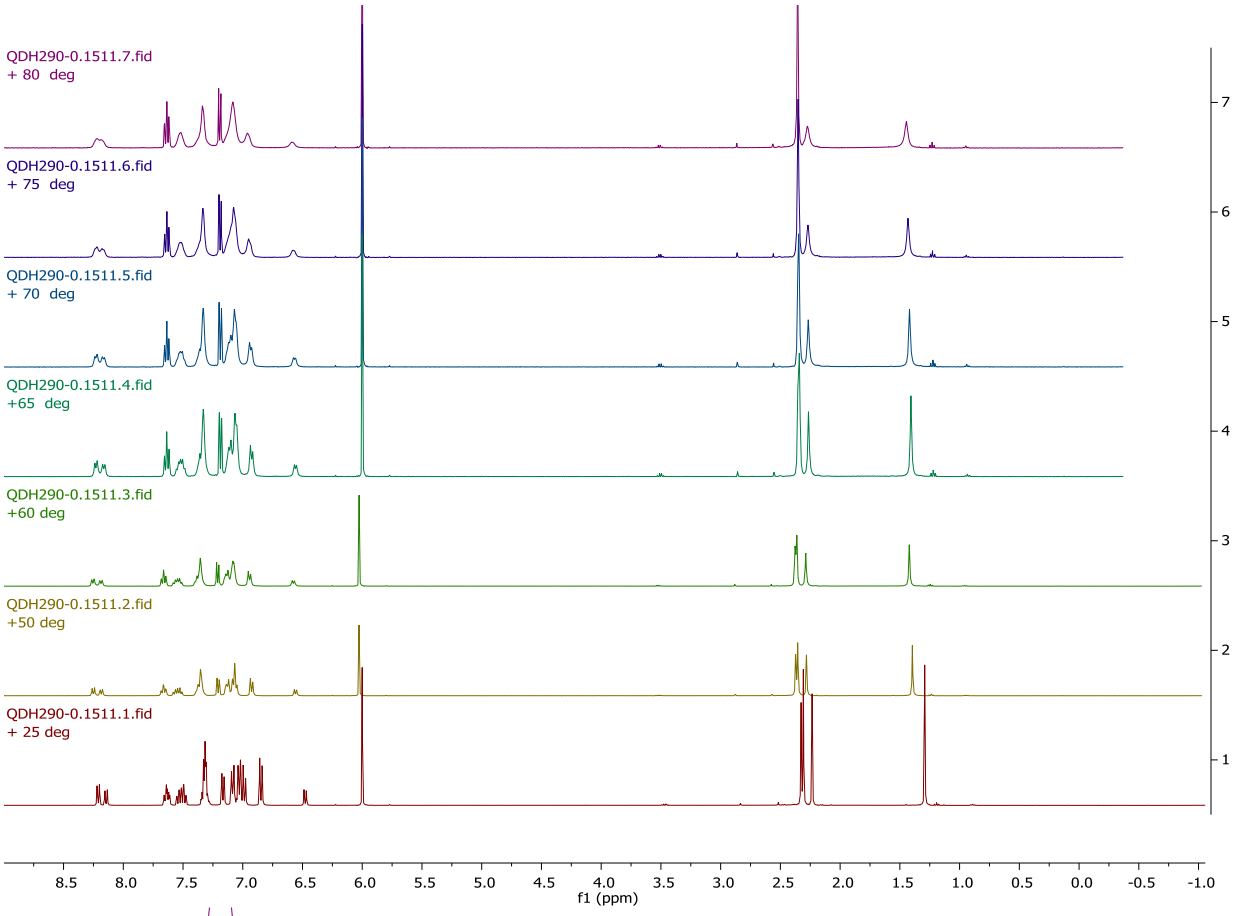
QDH290-0.1511.7.fid
+ 80 deg
QDH290-0.1511.6.fid
+ 75 deg
QDH290-0.1511.5.fid
+ 70 deg
QDH290-0.1511.4.fid
+65 deg
QDH290-0.1511.3.fid
+60 deg
QDH290-0.1511.2.fid
+50 deg
QDH290-0.1511.1.fid
+ 25 deg
8.5 8.0 7.5 7.0 6.5 6.0 5.5 5.0 4.5 4.0 3.5 3.0 2.5 2.0 1.5 1.0 0.5 0.0 -0.5 -1.0
f1 (ppm)
7
6
5
4
3
2
1

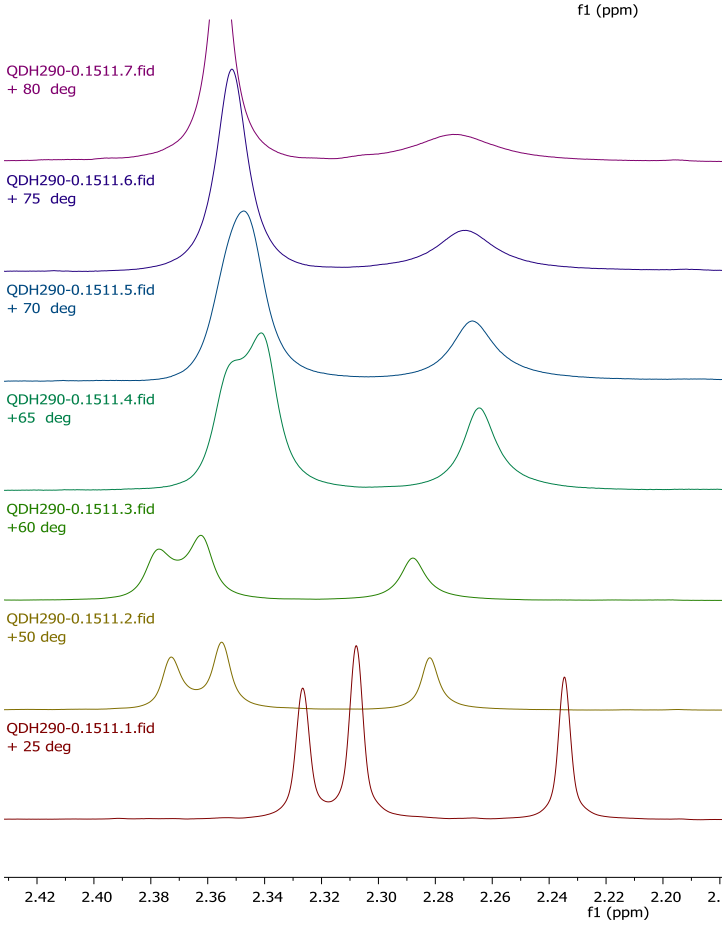
QDH290-0.1511.7.fid
+ 80 deg
QDH290-0.1511.6.fid
+ 75 deg
QDH290-0.1511.5.fid
+ 70 deg
QDH290-0.1511.4.fid
+65 deg
QDH290-0.1511.3.fid
+60 deg
QDH290-0.1511.2.fid
+50 deg
QDH290-0.1511.1.fid
+ 25 deg
2.42 2.40 2.38 2.36 2.34 2.32 2.30 2.28 2.26 2.24 2.22 2.20 2.
f1 (ppm)

b) C2 palladacycle

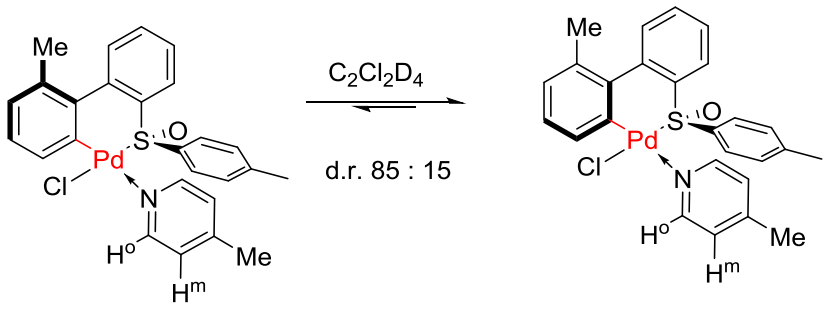

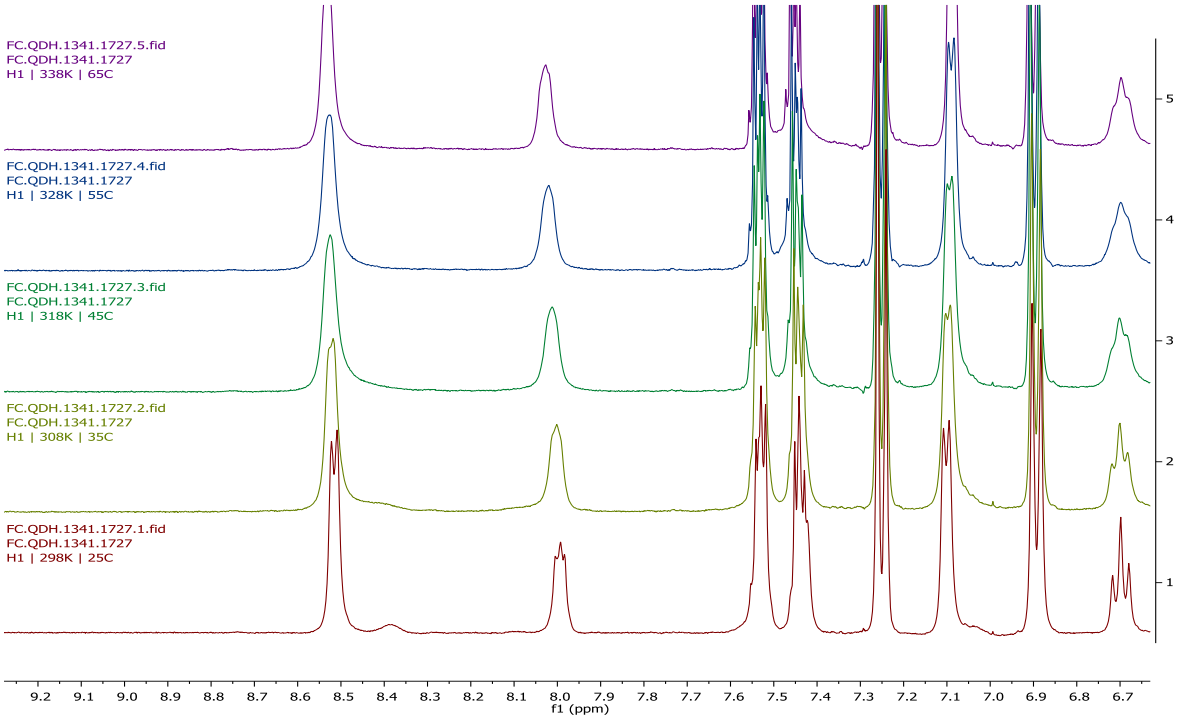

	(2-Me-2'-pTolsulfinyl[1,1']Biphenyl-6-yl)PdCl-4-MePy

C2Cl2D4

T (K)	ΔvAB (Hz)	k (s-1)	ΔG‡
318.15	52.8	117.216	15.7

$\Delta G^{\ddagger}$ = 15.7 kcal/mole at 45 °C in $C_2Cl_2D_4$ (+/- 10K, i.e. +/- 0.6 kcal)

c) C2 palladacycle + 4 equiv HFIP

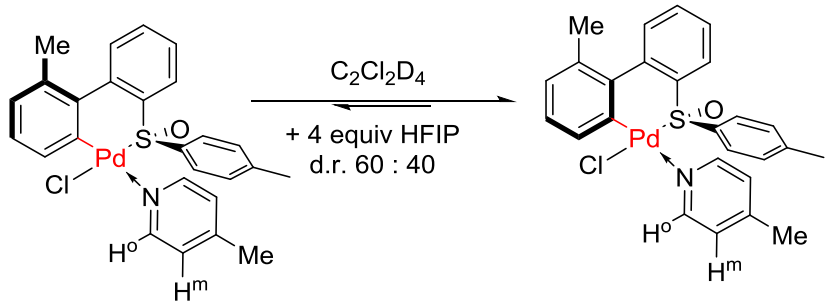

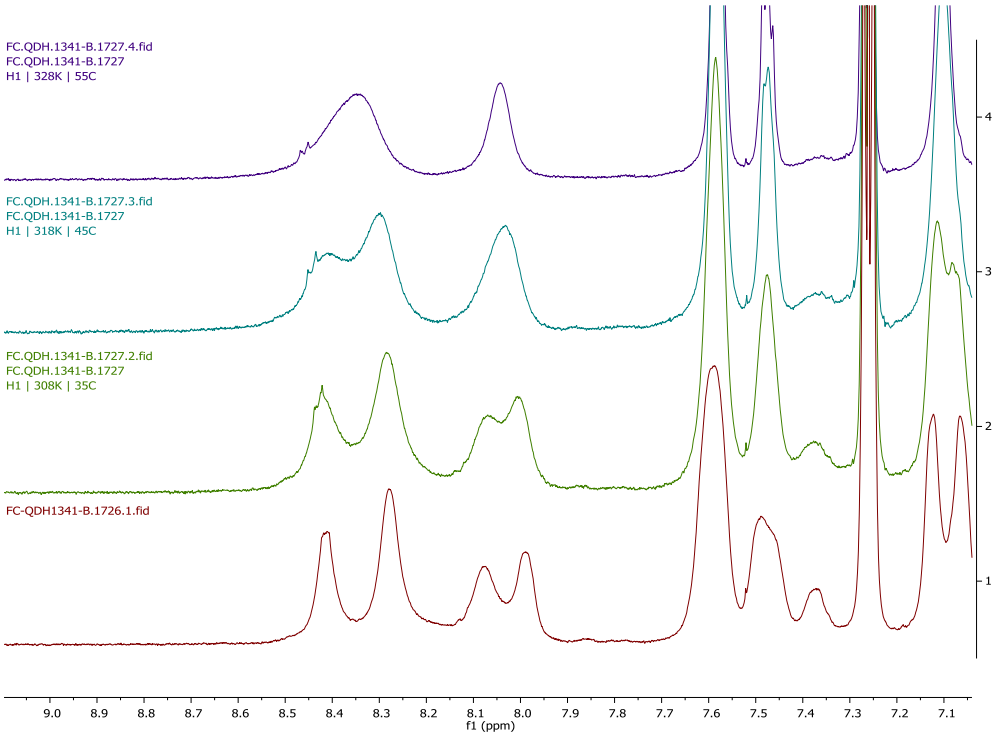

	(2-Me-2'-pTolsulfinyl[1,1']Biphenyl-6-yl)PdCl-4-MePy			
C2Cl2D4 HFIP (4eq)	T (K)	ΔvAB (Hz)	k (s-1)	ΔG‡
	318.15	53.7	119.214	15.64

$\Delta G^{\ddagger}$ = 15.6 kcal/mole at 45 °C in $C_2Cl_2D_4$ (+/- 10K, i.e. +/- 0.6 kcal)

d) NMR titration of C2 with HFIP

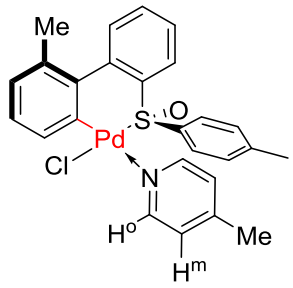

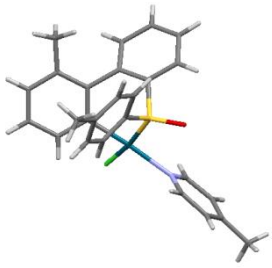

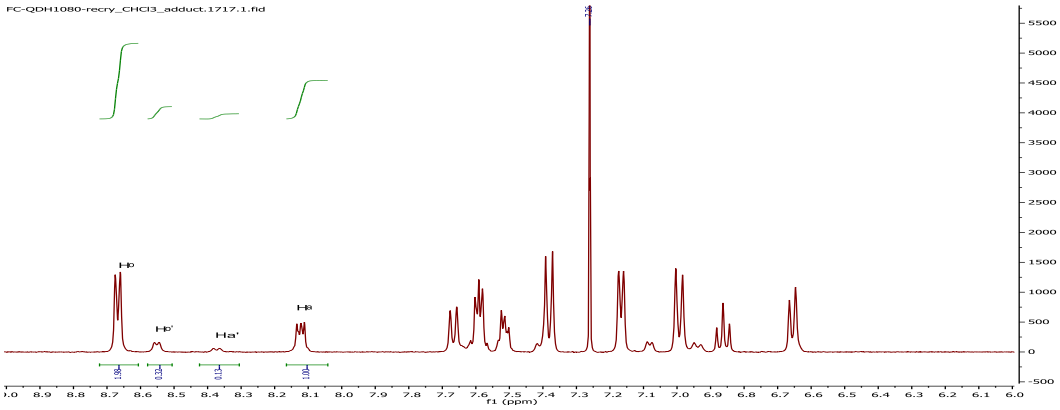

from bottom to top : **1a**-4-MePyPdCl in $CDCl_3$ + x equiv HFIP with x = 0, 1, 1.5, 2, 10, 30. d.r. of red spectra (0 equiv HFIP) = 85 : 15; d.r. of violet spectra (30 equiv HFIP) = 25 :75

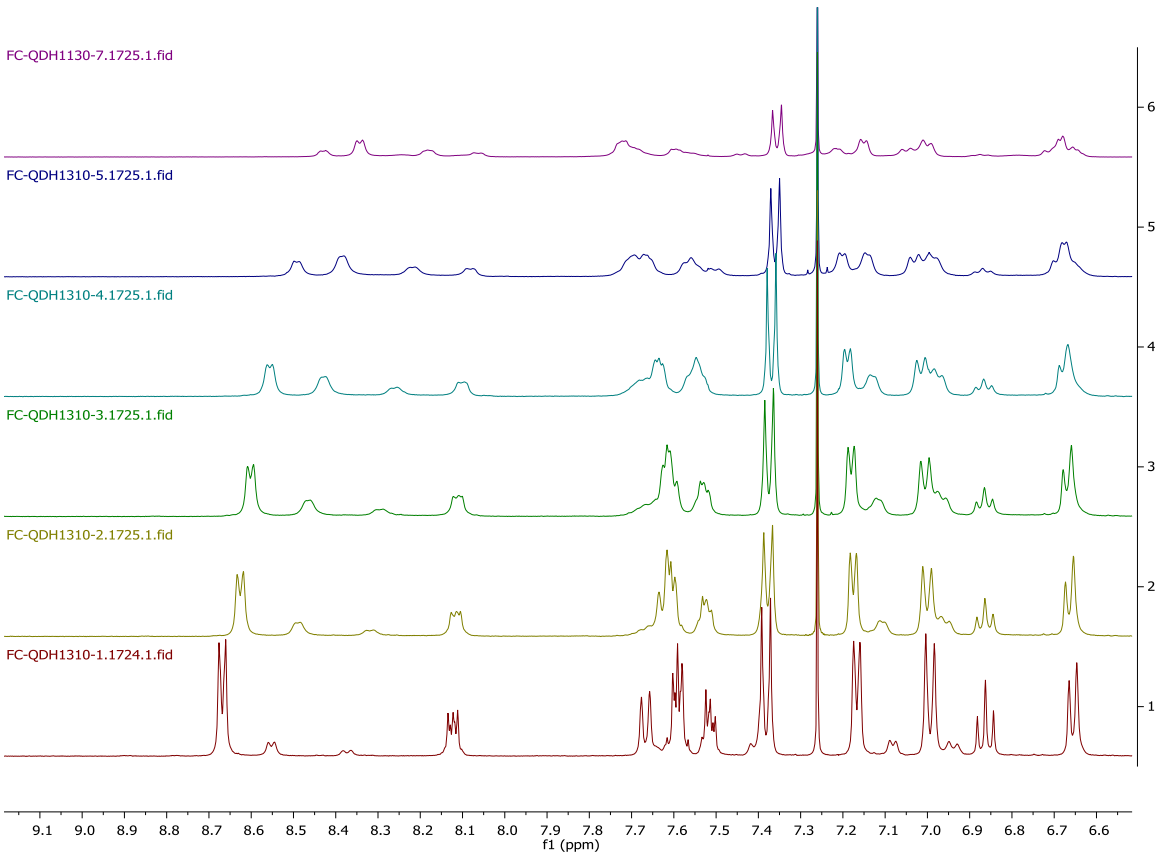

9. Control experiments

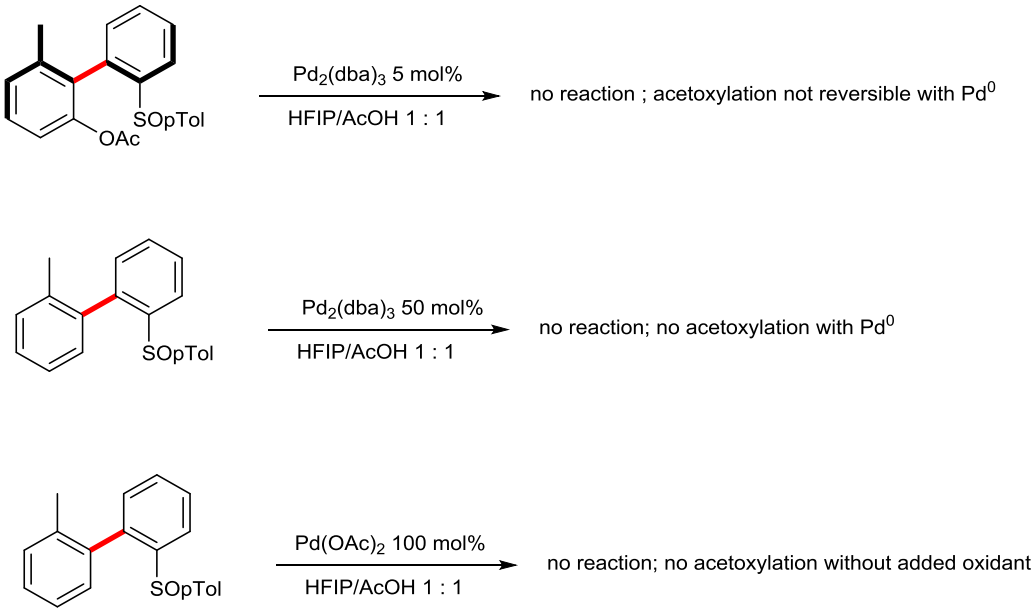

F. References

[289] A. J. Canty, M. C. Denney, G. van Koten, B. W. Skelton, A. H. White, *Organometallics* **2004**, *23*, 5432–5439.
[290] A. J. Canty, J. Patel, T. Rodemann, J. H. Ryan, B. W. Skelton, A. H. White, *Organometallics* **2004**, *23*, 3466–3473.
[291] A. R. Dick, K. L. Hull, M. S. Sanford, *J. Am. Chem. Soc.* **2004**, *126*, 2300–2301.
[292] T. Yoneyama, R. H. Crabtree, *J. Mol. Catal. Chem.* **1996**, *108*, 35–40.
[293] L. Eberson, L. Jönsson, *J. Chem. Soc. Chem. Commun.* **1974**, *0*, 885–886.
[294] L. V. Desai, H. A. Malik, M. S. Sanford, *Org. Lett.* **2006**, *8*, 1141–1144.
[295] G.-W. Wang, T.-T. Yuan, X.-L. Wu, *J. Org. Chem.* **2008**, *73*, 4717–4720.
[296] C. J. Vickers, T.-S. Mei, J.-Q. Yu, *Org. Lett.* **2010**, *12*, 2511–2513.
[297] R.-Y. Tang, G. Li, J.-Q. Yu, *Nature* **2014**, *507*, 215–220.
[298] K. J. Stowers, M. S. Sanford, *Org. Lett.* **2009**, *11*, 4584–4587.
[299] J. M. Racowski, A. R. Dick, M. S. Sanford, *J. Am. Chem. Soc.* **2009**, *131*, 10974–10983.
[300] B. V. S. Reddy, L. R. Reddy, E. J. Corey, *Org. Lett.* **2006**, *8*, 3391–3394.
[301] J. F. Hartwig, *Inorg. Chem.* **2007**, *46*, 1936–1947.
[302] R. A. Widenhoefer, H. A. Zhong, S. L. Buchwald, *J. Am. Chem. Soc.* **1997**, *119*, 6787–6795.
[303] B. S. L. Collins, J. C. M. Kistemaker, E. Otten, B. L. Feringa, *Nat. Chem.* **2016**, *8*, 860–866.
[304] J. I. Seeman, *J. Chem. Educ.* **1986**, *63*, 42.
[305] J. I. Seeman, *Chem. Rev.* **1983**, *83*, 83–134.
[306] D. R. Fahey, *J. Organomet. Chem.* **1971**, *27*, 283–292.
[307] H. Kodama, T. Katsuhira, T. Hino, K. Tsubata, *K. Chem. Abstr.* **2001**, *135*, 344284.
[308] D. Kalyani, A. R. Dick, W. Q. Anani, M. S. Sanford, *Org. Lett.* **2006**, *8*, 2523–2526.
[309] R. Giri, X. Chen, J.-Q. Yu, *Angew. Chem. Int. Ed.* **2005**, *44*, 2112–2115.
[310] X.-C. Wang, Y. Hu, S. Bonacorsi, Y. Hong, R. Burrell, J.-Q. Yu, *J. Am. Chem. Soc.* **2013**, *135*, 10326–10329.
[311] S. R. Whitfield, M. S. Sanford, *J. Am. Chem. Soc.* **2007**, *129*, 15142–15143.
[312] D.-W. Gao, Q. Gu, S.-L. You, *ACS Catal.* **2014**, *4*, 2741–2745.
[313] F. R. Leroux, A. Berthelot, L. Bonnafoux, A. Panossian, F. Colobert, *Chem. – Eur. J.* **2012**, *18*, 14232–14236.
[314] P. B. Hitchcock, G. J. Rowlands, R. Parmar, *Chem. Commun.* **2005**, *0*, 4219–4221.

.

Steganone

VI. Steganone

A. Introduction

(-)-Steganone is part of the stegane family of natural product which is in turn part of the large class of lignans natural products (lignan should not be confused with lignin which is an organic polymer made of hydroxycinnamyl alcohols monomers and is the main component of the cell walls of plants, making it the second most abundant organic material on earth behind cellulose). Lignans are dimers made of phenyl propanoid units which are usually oxygenated at the C9-C9' positions[315] (Figure VI-1a). The stegane natural products are part of the dibenzocyclooctadienes sub-family (Figure VI-1b).

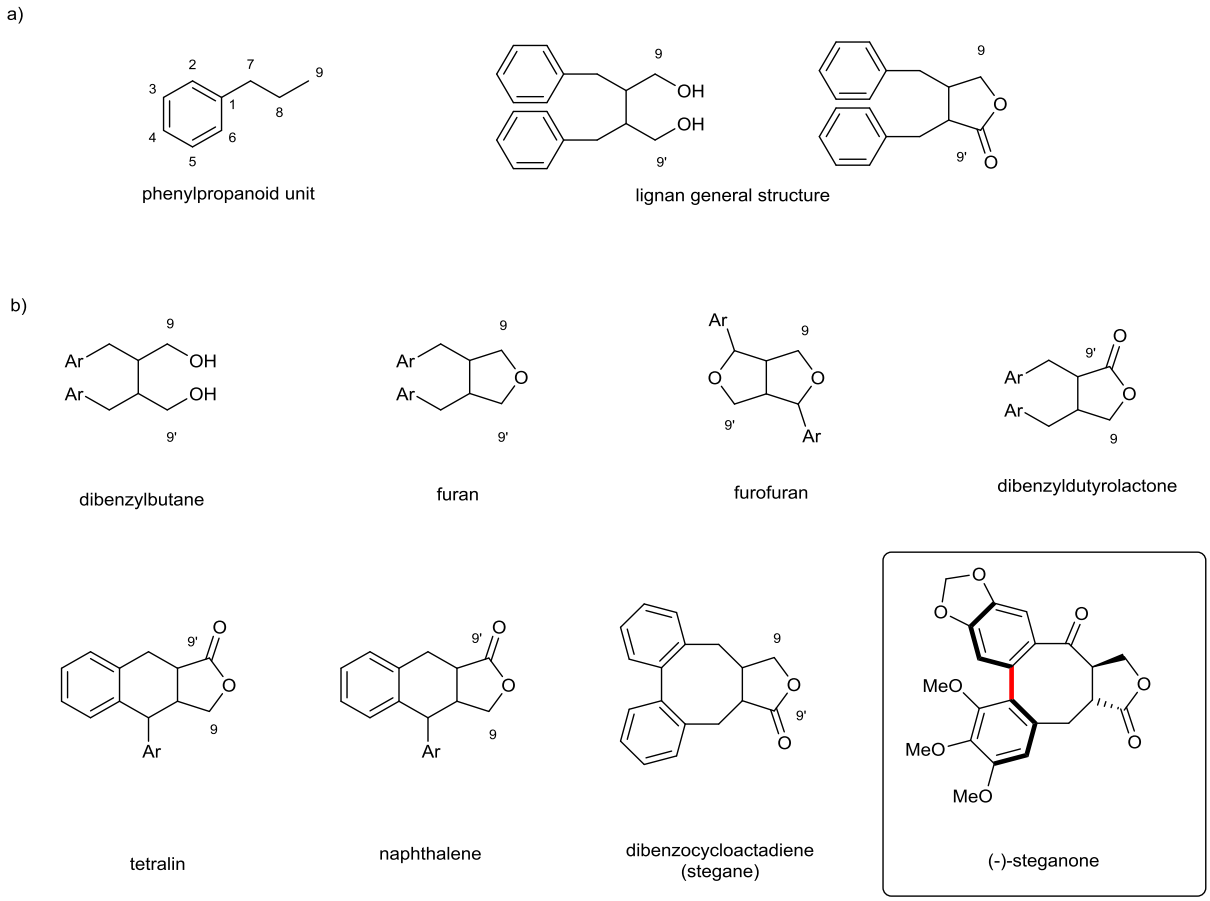

Figure VI-1 : lignans natural products

The stegane family contains several natural products that were isolated in 1973[316] from *Steganotaenia araliacea* extracts, yielding steganacin steganangin, steganol and steganone (Figure VI-2a). At that time, only the schizandrins[317] (Figure VI-2b) natural products were known in the dibenzocyclooctadiene family. Since then, more than 70 natural compounds were found to belong to this dibenzocyclooctadiene family[318]. Stegane natural products were found to have some activity against the P-388

leukemia *in vivo* in mice and *in vitro* against cells derived from human carcinoma of the nasopharynx. Indeed they inhibit the assembly of tubulin into microtubules, and thereby exhibit a cytotoxic effect. They bind to the colchicine site in tubulin and their polyoxygenated biaryl framework has been shown to be essential for their activity[319]. Noteworthy, only the a*R* atropisomers of stegane natural products are capable of binding to tubulin[318]. Consequently steganone and its derivatives, due to their relatively simple structure and their biological activity, have become a popular target to illustrate the potential of new atroposelective Ar-Ar coupling methodologies[320].

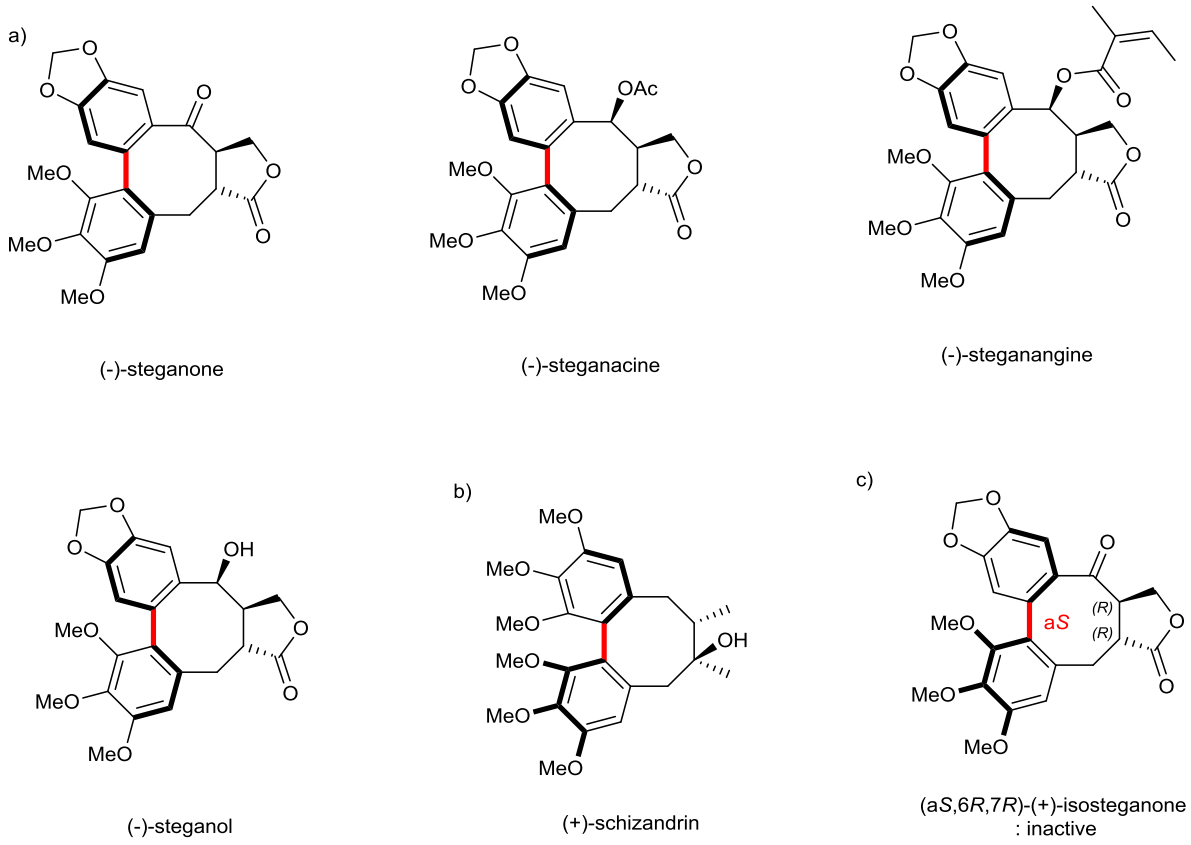

Figure VI-2 : stegane natural products

The first total synthesis of (±)-steganone (Figure VI-3), by Kende and coworkers in 1976[321] (concomitantly with Raphael and Schlessinger[320]), used an intramolecular oxidative cyclization in the presence of VOF_3 to construct the biaryl axis. Once the biaryl axis was installed, saponification and decarboxylation of the malonate ester produced only one diastereomer. Subsequent lactone formation using formaldehyde under basic conditions also resulted in the isolation of only one diastereomer, (±)-steganone. Remarquably, this sequence of reaction, without any chiral information, produced only one pair of enantiomers between the 4 possible.

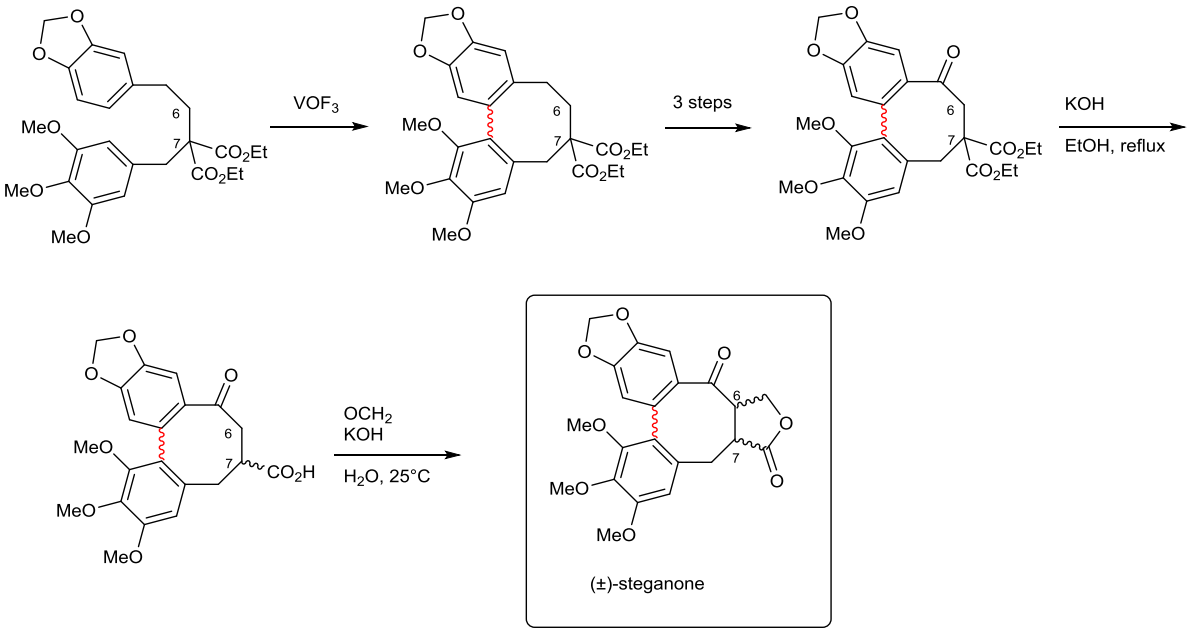

Figure VI-3 : first total synthesis of steganone

However, it was found later on that a non-identified by-product had contaminated the final product. The same year, the Kende group identified (+)-isosteganone as the by-product[322]. It was then discovered that (+)-isosteganone would quantitatively isomerize to (-)-steganone, either under high temperature or under basic conditions (Figure VI-4). This shows that (a*R)* atropisomers of the stegane family are the thermodynamically favored ones. The thermodynamic driving force towards (-)-steganone is the conjugation of the carbonyl of the ketone with the aromatic ring, as shown by the reduced stretching frequency in (-)-steganone (1667 cm^{-1}) compared to (+)-isosteganone (1707 cm^{-1}). A number of groups would later use these properties to conduct asymmetric total synthesis of (-)-steganone.

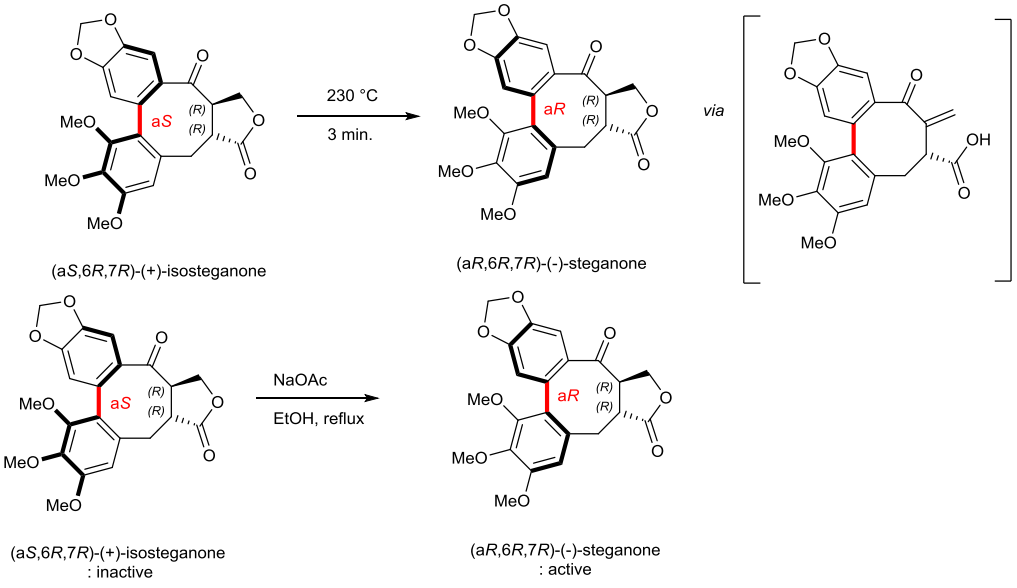

Figure VI-4 : steganone isomerization

The first asymmetric total synthesis of (-)-steganone was accomplished by Robin and coworkers[323] in 1980 (Figure VI-5). They realized that the control of the absolute configuration of the C7-carbon was the key to obtain an enantiopur product. Indeed, with enantiopur **1Aa** in hand, an Ullmann coupling afforded **2A** with uncontrolled axial chirality. Cyclization to **3A** under kinetic control yielded **3A** as a sole atropisomer, albeit with the wrong configuration. Then lactone formation following Kende procedure gave **4A** (+)-isosteganone as a sole diastereomer, and isomerization of the biaryl axis under thermodynamic control in refluxing xylenes led to (-)-steganone, thereby showing that the control of the absolute configuration of the C7-position is sufficient to achieve an asymmetric synthesis of steganone.

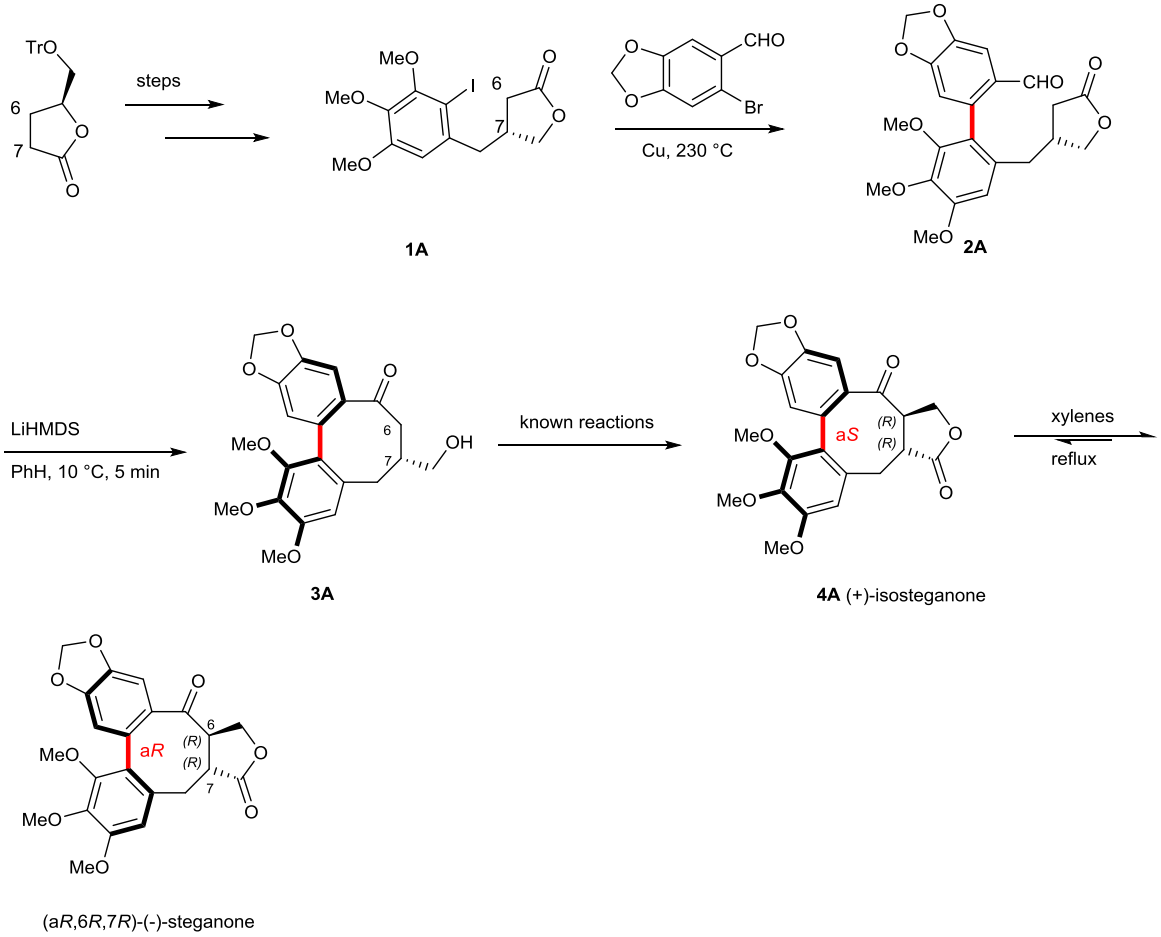

Figure VI-5 : first asymmetric synthesis

Interestingly, Meyers and coworkers[80] in 1987 (Figure VI-6) introduced a new strategy to perform the asymmetric steganone synthesis. The key step consists in the atropodiastereoselective Grignard S_NAr coupling which afforded the **1B** biaryloxazoline with a d.r. of 87:13 and an 85% crude yield (isolated in an atropopure form in 63% yield). After several steps the intermediate **2B** was obtained and cyclized to **3B** with retention of the axial chirality. At this point a remarkable sequence of hydrolysis, decarboxylation and methylation of the C7-position substituent occurred with axial-to-central chirality transfer, as the newly created C7 chiral center was enantiopur and as racemization of the birayl axis occurred. Nevertheless, diasteromers of **4B** were sep-

arated by chromatography (the “wrong” **(a*S*)-4B** could be recycled by thermal isomerization), and know reactions led to the (a*R*,6*R*,7*R*)-(-)-steganone, with a longest linear sequence of 10 steps and a 0.6% total yield. An optical purity of 80-84% was measured and the authors supposed that epimerization occurred along the path leading from **4B** to steganone however, with hindsight it seems more plausible that it occurred between **1B** and **2B**.

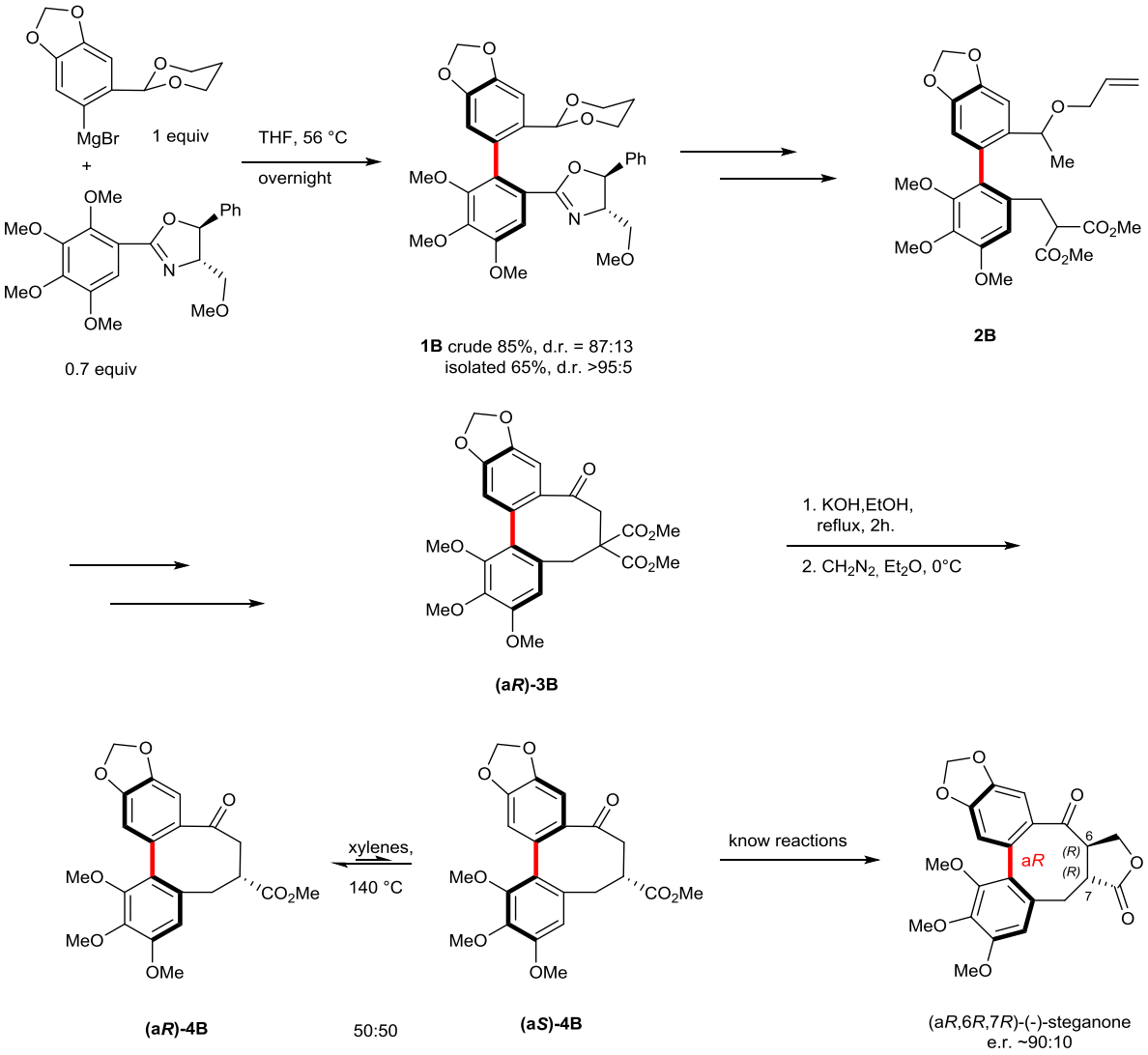

Figure VI-6 : first atroposelective synthesis

The total asymmetric synthesis by Molander and coworkers[324] (Figure VI-7a) in 2000 also used axial-to-central chirality transfer, as their samarium-promoted 8-endo ketyl-olefin cyclization of atropopure **1C** afforded the cyclized intermediate **2C,** where all 3 chiral centers are thought to be controlled by the axial chirality (**2C** has been confirmed to be identical to the known isopicrosteganol **3C**). At this point the oxidation of the benzylic alcohol (and *in-situ* removal of the chromium auxiliary) yielded **4C** as a mixture of atropisomers at room temperature. Indeed the thermodynamic driving force towards (-)-steganone is the conjugation of the carbonyl of the ketone with the aromatic ring. This is only possible if both the C6-carbon and the C7-carbon absolute

configuration are (*R*). Indeed, epimerization of the C6 carbon using DBU in THF yielded (-)-steganone with an e.r. >99:1. However, when the epimerization of the C6 carbon was attempted with NaOAc in refluxing EtOH (Figure VI-7b), (-)-steganone was obtained but with an e.r. = 83:17, meaning that partial epimerization of the C7 carbon occurred. This shows that the *relative* configuration of all three stereocenters is under thermodynamic control, and further that it is controlled by the *absolute* configuration of the C7 carbon : under isomerization conditions, (*R*)-C7 yields (-)-steganone, whereas (*S*)-C7 yields (+)-steganone. Furthermore, in the Meyers[80] and in the Molander[324] syntheses the absolute configuration of the C7 stereocenter is controlled by the absolute configuration of the biaryl axis. Thus the atropisomeric axis can *in fine* be the source of the asymmetry, and therefore its control is sufficient to obtain enantiopur (-)-steganone.

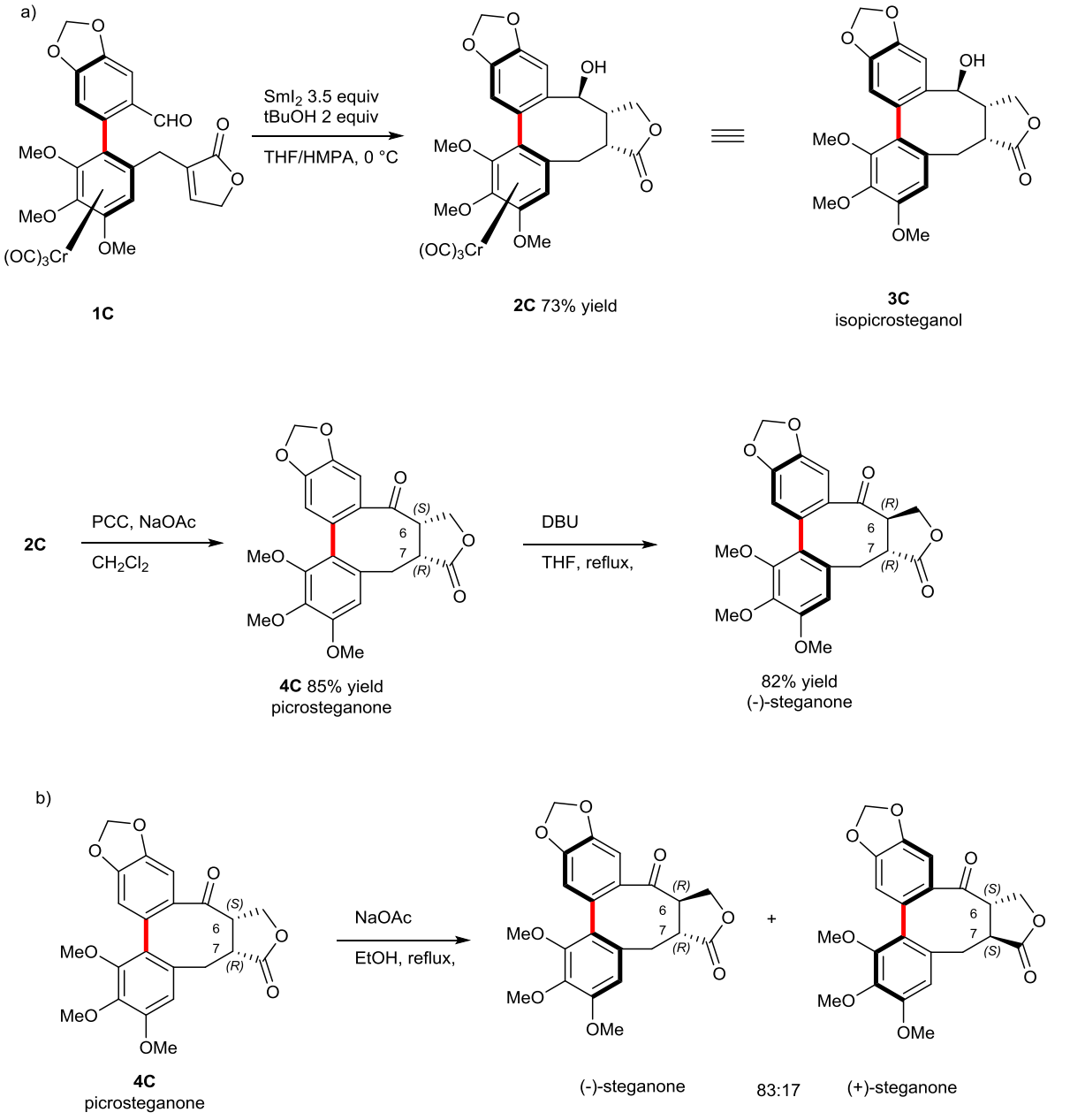

Figure VI-7 : total synthesis and studies on isomerization

Actually, the Molander synthesis was based on Uemura and coworkers work[325,326]. They performed in 1995 an atroposelective formal synthesis of (-)-steganone *via* a diastereoselective Suzuki coupling of an enantioenriched planar chiral (arene)chromium coupling partner **2D** (no yield is given for the transformation of **1D** to **2D** (Figure VI-8). The atropodiastereoselective Suzuki coupling yielded **3D** as a sole atropisomer, and protection of the benzylic alcohol afforded **4D**, obtained in 9 steps and 12% yield with a d.r. >95:5. The formal synthesis was accomplished by 6 more steps to afford **5D**.

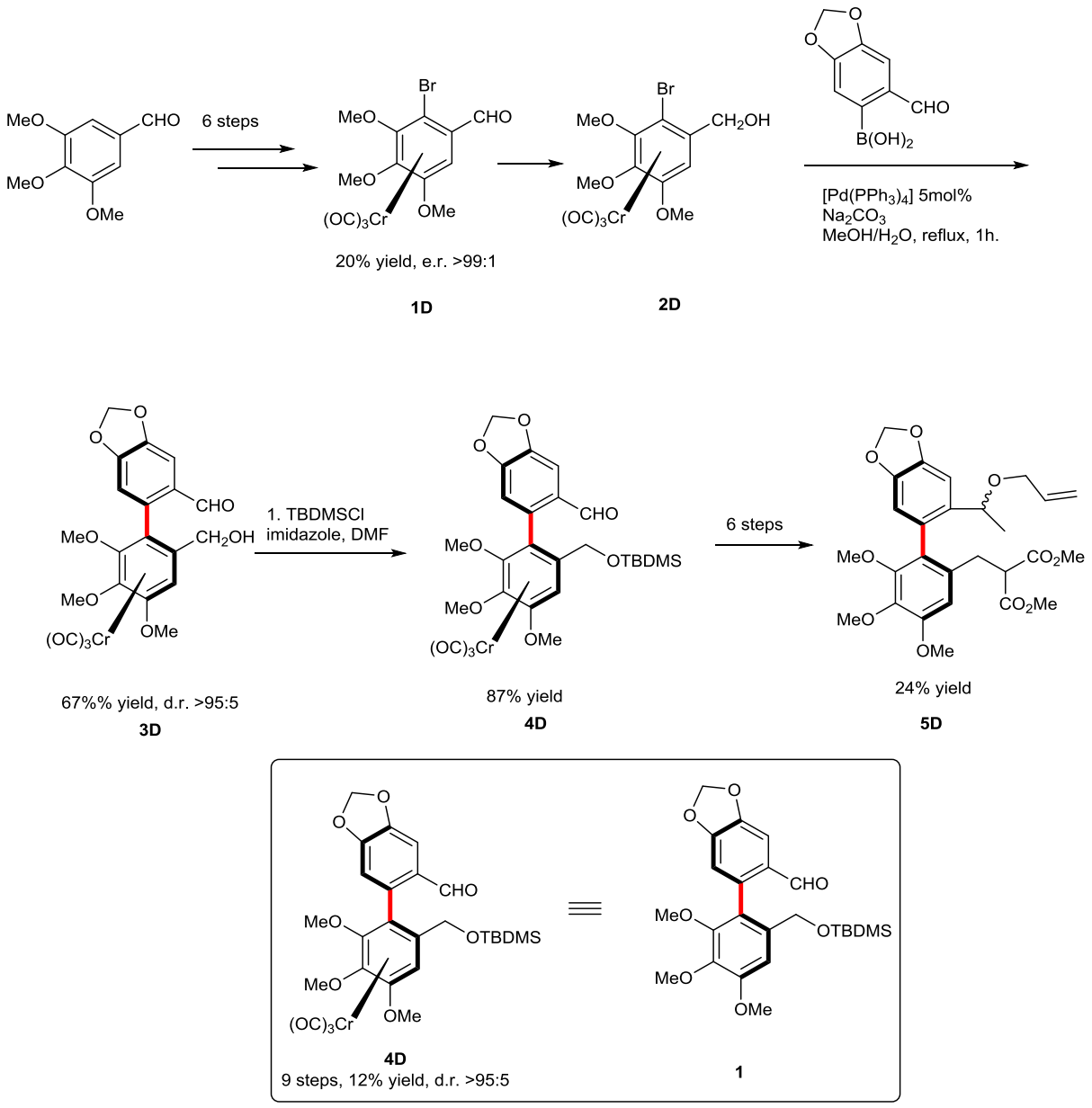

Figure VI-8 : formal synthesis through diastereoselective Suzuki coupling using planar chiral (arene)chromium partner

The next formal synthesis by Abe, Harayama and coworkers in 2004 is based on Bringmann's lactone concept[327]. The commercially available piperonyl alcohol was transformed into the lactone **1E (**Figure VI-9**)**, which underwent direct arylation to **2E**

with 63% yield. Enantioselective opening of the lactone-bridge of the non-atropisomeric biaryl was performed with the enaniopur Me-(*R*)-CBS borane–oxazaborolidine affording **3E** with an excellent yield and a good enantiomeric ratio. Two more steps were necessary to obtain the key intermediate **1**, which can be transformed to the known **4E** with two more steps (**4E** is linked to the Meyers' intermediate **2B** Figure VI-6**).**

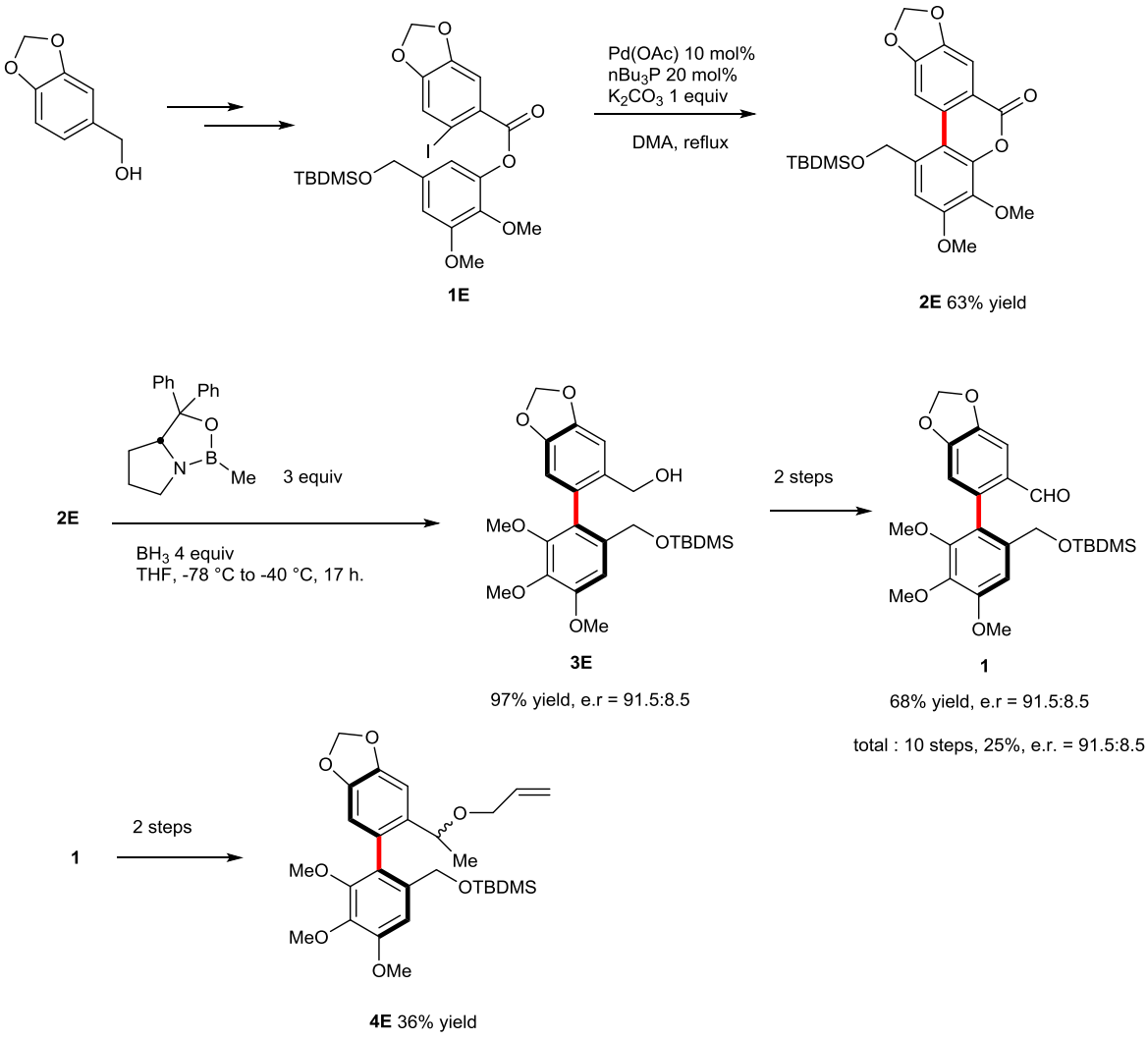

Figure VI-9 : formal synthesis using the lactone concept developed by G. Bringmann

In 2003[328], 2006[329] and 2007[330], Baudoin and coworkers published a series of papers showcasing the diastereoselective Suzuki coupling strategy towards stegane natural products (Figure VI-10). In a very straightforward synthesis, enantioselective reduction of ketone **1F** with the (*S*)-CBS borane–oxazaborolidine followed by iodination afforded **2F** which underwent atropodiastereoselective Suzuki coupling to form **3F** with a d.r. of 92:8 and a moderate yield of 41%. Although not a strict formal synthesis, intermediate **3F** is closely related to intermediates from Uemura[326] and Abe and Harayama[327] syntheses, showing why the atroposelective Ar-Ar coupling is probably the most efficient and versatile synthetic approach towards such scaffolds,offering the most convergent way towards atropoenriched molecules.

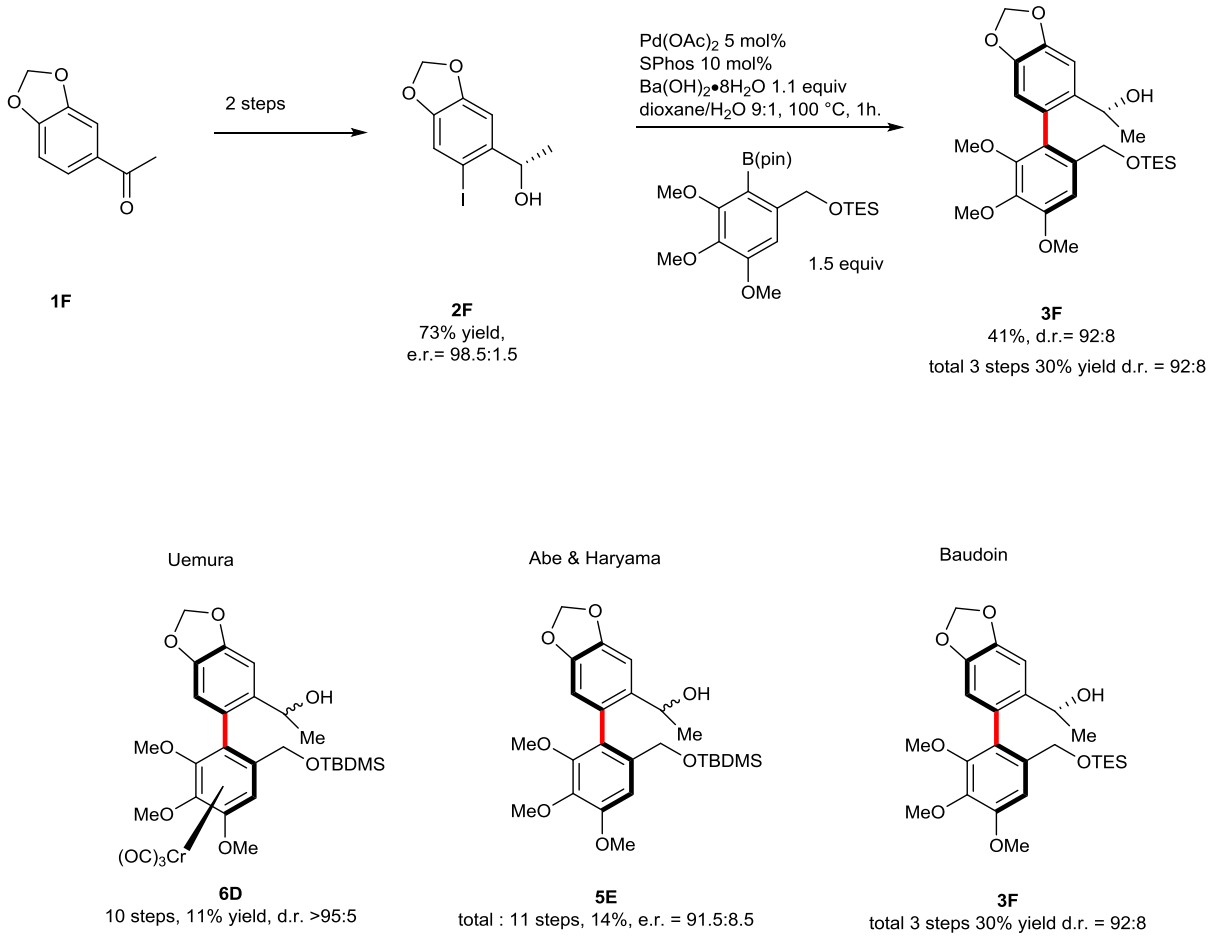

Figure VI-10 : formal synthesis through diastereoselective Suzuki coupling

In 2014 Yalcouye, Leroux and Colobert[331] applied the diastereoselective Suzuki-Miyaura coupling strategy using an enantiopure sulfinyl auxiliary. The β-acetoxysulfoxyde **4G** was installed by condensation of the anion of the (*R*)-methyl *para*-tolylsulfoxyde on the benzoate **1G** followed by chelation-controlled diastereoselective reduction and acylation to afford **4G** in 7 steps and 24% overall yield as a sole diastereomer. Suzuki coupling using XPhos palladacycle proved to be completely atropodiastereoselective and gave **5G** with a yield of 68%. The sulfoxyde auxiliary was removed by a Pummerer rearrangement to afford **6G**, and two more steps were necessary to obtain the intermediate **7G** whose enantiomeric ratio was ascertain by chiral HPLC (e.r. >99:1). However the last step to the known **8G** showed some erosion of the enantiopurity as **8G** was isolated with an 88% yield and e.r.= 97:3. Thus this 15 steps sequence afforded the target compound with an 9% overall yield and an e.r. of 97:3.

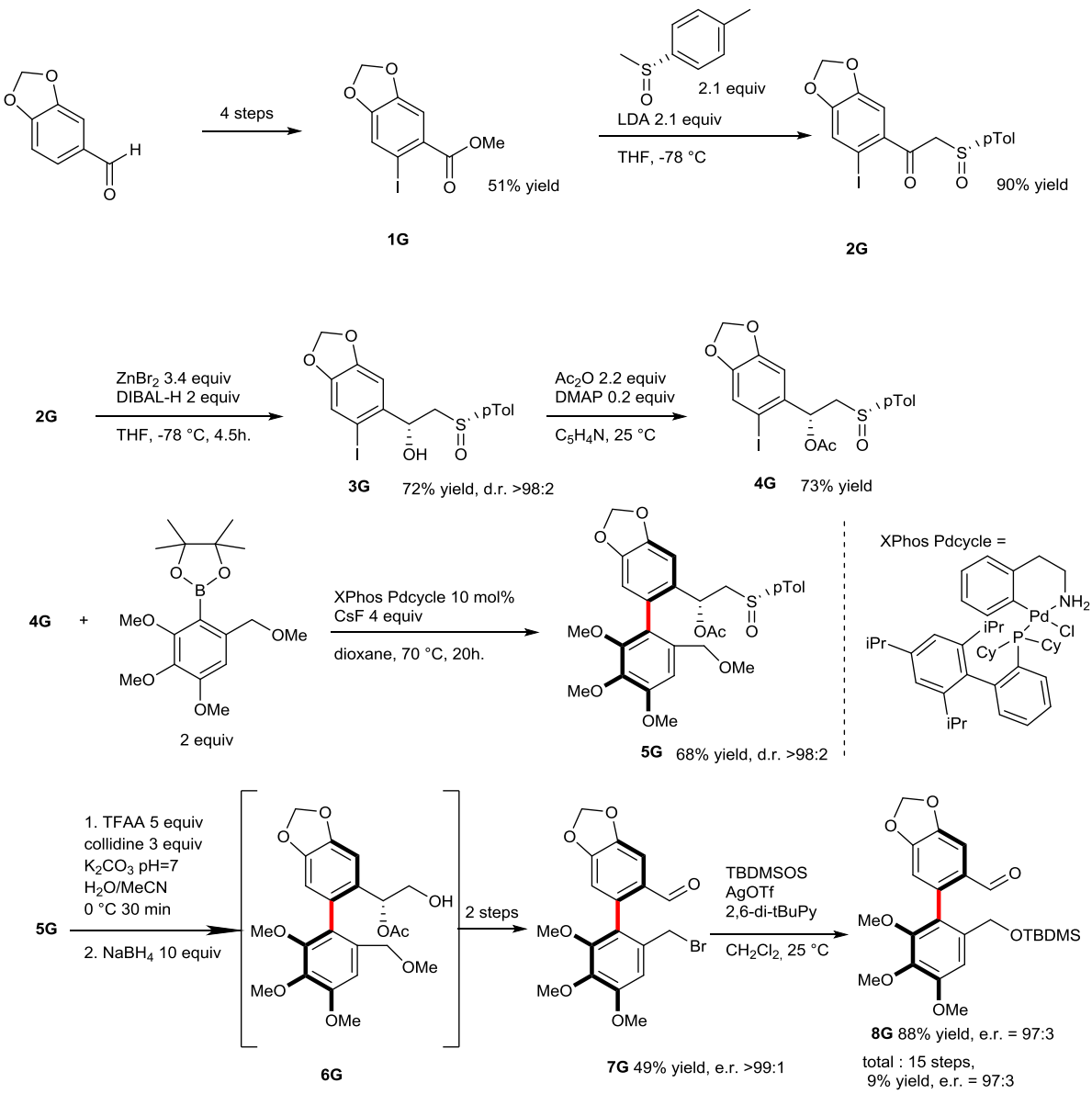

Figure VI-11 : formal synthesis through atropodiastereoselective Suzuki coupling reaction

In 2017 Augros, Panossian and Leroux[332] applied a transition-metal-free methodology to the (-)-steganone formal synthesis. A previously developed diastereoselective aryne coupling[333] product was transformed into the known intermediate of Abe and Harayama (compound **1** Figure VI-12). The atropodiastereoselective aryne coupling using an enatiopure oxazoline as auxiliary gave **1H** with a good yield but a low d.r. of 56:44 in favor of the opposite atropisomer to complete the (-)-steganone formal synthesis. However the diastereomers could be separated, and **2H** was obtained in diastereopur form with a 33% yield. Removal of the $SiMe_3$ protecting groups followed by reductive removal of the oxazoline and protection of the benzylic alcohol occurred with 90% yield. Lithium/halogen exchange and trapping of the resulting anion at low temperature gave the known **4H** with 85% yield and an e.r >99:1. In total, **4H** was obtained in 8 steps with a 19% yield and a e.r. > 99:1.

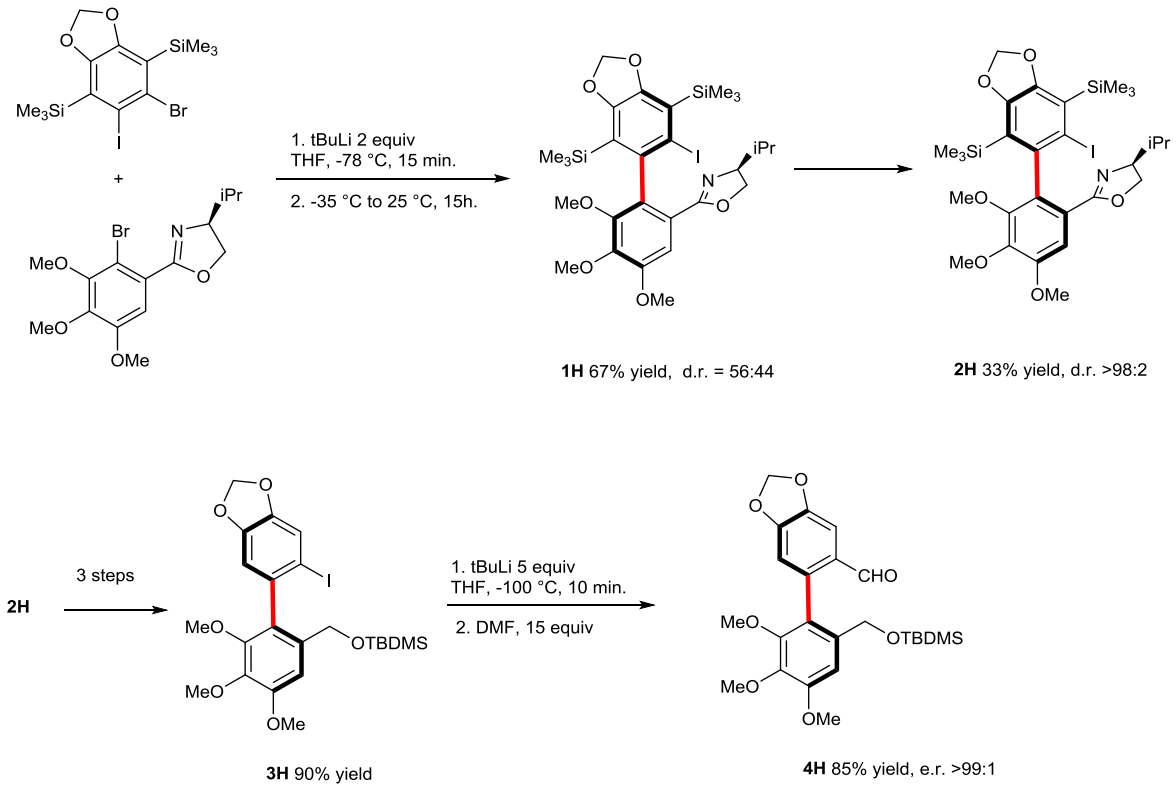

Figure VI-12 :formal synthesis through diastereoselective aryne coupling

Despite the large body of work present in the literature on the synthesis of (-)-steganone, no strategy based on C-H functionalization was applied in this context Indeed, over the last decade organic chemistry and more particularly transition metal-based homogenous catalysis has been profoundly impacted by the development of the C-H activation field[334–338]. In particular, the synthetic value of the C-H activation field has been beautifully illustrated by an elegant implementation of this strategy in the total synthesis of numerous biologically active compounds like (-)-Incarviatone[339], Verruculogen[340], (+)-Linoxepin[341], and Dictyodendrin[342] for example. In the majority of cases the C-H functionalization approach is utilized either to functionalize (hetero)aromatic cores or to construct cyclic moieties by means of intramolecular transformations. In contrast, related stereoselective reactions remain highly challenging and their implementation into multi-step synthesis is clearly less documented. Considering the advantages of our atropodiastereoselective; sulfoxyde-directed C-H activation (i.e. excellent efficiency, mild conditions and traceless character of the sulfoxyde moiety leading to a variety of product), we embarked on the design of an original synthetic route towards steganone, based on our asymmetric C-H activation.

A. Results and discussion

The key step of such retrosynthetic pathway would consist on blocking the axial chirality by introducing, *via* an atropo-diastereoselective C-H activation, an additional substituent on the optically active biaryl precursor with uncontrolled axial chirality (Figure VI-13). Accordingly, the direct asymmetric C-C is requested and the newly introduced alkyl substituent should be straightforwardly converted into a benzylic alcohol via simple functional group manipulations.

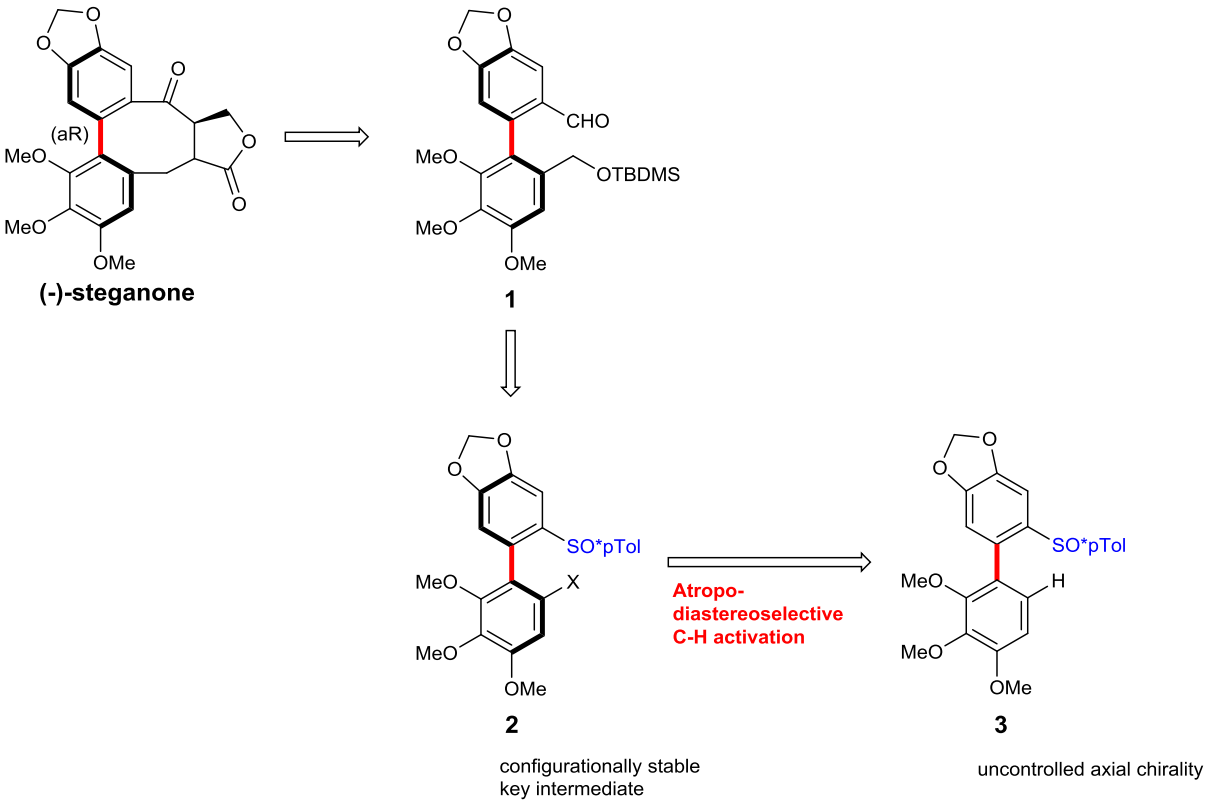

Figure VI-13 : retrosynthetic strategy

Following such hypothesis, a first retrosynthetic pathway implying an atropodiastereoselective C-H alkylation key step was designed (Figure VI-14). A stereoselective introduction of the methyl substituent at the 6' position, followed by its hydroxylation should lead to the formation of a configurationally stable biaryl benzylic alcohol **4** in only 7 steps.

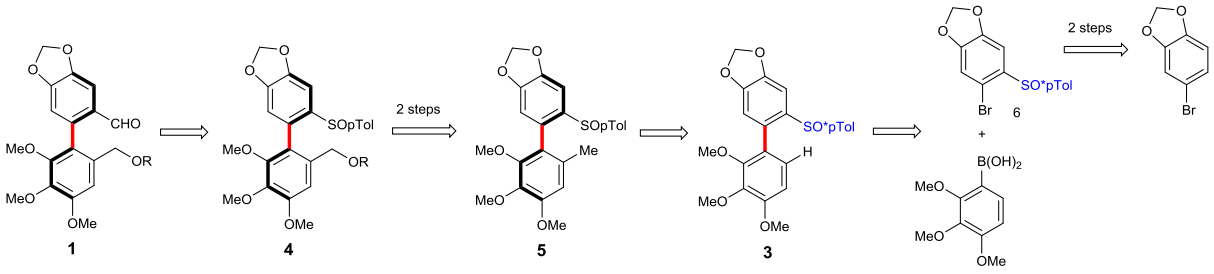

Figure VI-14 : atroposelective alkylation retrosynthetic scheme

Encouraged by our previous work on the Pd-catalyzed atropodiastereoselective direct olefination, we hypothesized that a closely related alkylation, although much more challenging[343–345], could also be achieved using iodomethane as coupling partner. Disappointingly, the coupling failed when using reaction conditions previously optimized for the oxidative Heck reaction. As distinguish mechanistic scenarios operate in both cases, we hypothesized that addition of a ligand could be required to boost the reactivity of our catalytic system. Accordingly, drawing inspiration from the recent publications by Yu[346], we performed the targeted reaction using more electrophilic $Pd(TFA)_2$ catalyst in combination with pyridine-derived ligand (L1), silver pivalate salt as iodide scavenger in HFIP and DCE solvents, but any product was obtained either at 80°C nor at 100°C (Table 1, entry 1-2). No reactivity was also observed when carbene ligands such as IMes (L2) and IPr (L3) were tested in combination with acidic additives (Table 1, entry 3-6). Subsequently, we turned our attention to other alkylating agents such as boronic acid derivatives. Indeed, Yu disclosed an efficient direct alkylation reaction compatible with these organometallic alkyl sources. Disappointingly, the desired compound could not be obtained with a reasonable efficiency neither using methyl boronic acid (Table 1, entry 7-8), nor potassium methyltrifluoroborate alkylating agents (Table 1, entry 9-10), even when ligands such as 2,6-lutidine (L1), NHC (L2) and monoprotected amino acid (L3) were added to the reaction mixture. Finally, the lack of any reactivity for these C-C couplings forced us to reconsider the retrosynthetic pathway to access **1**.

Table VI-1 : optimization of the alkylation reaction

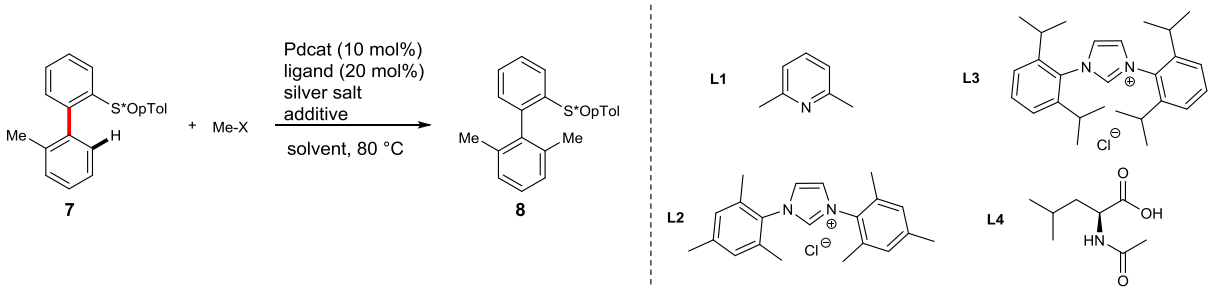

Entry	Me-X	Ligand	Pd_{cat}	Ag salt (equiv)	Additive (equiv)	Solvent	Conv. (%)
1	Me-I	L1	$Pd(TFA)_2$	AgOPiv (3.5 equiv)	-	HFIP	nr
2	Me-I	L1	$Pd(TFA)_2$	AgOPiv (3.5 equiv)	-	DCE	nr
3	Me-I	L2	$Pd(OAc)_2$	Ag_2CO_3 (2 equiv)	TFA (0.4 equiv)	HFIP	nr
4	Me-I	L3	$Pd(OAc)_2$	Ag_2CO_3 (2 equiv)	PivOH (0.5 equiv)	HFIP	nr
5	Me-I	L3	$Pd(OAc)_2$	AgTFA (4 equiv)	TFA (0.4 equiv)	HFIP	nr
6	Me-I	L3	$Pd(OAc)_2$	AgOAc (4 equiv)	TFA (0.4 equiv)	HFIP	nr
7	Me-$B(OH)_2$	L2	$Pd(OAc)_2$	Ag_2CO_3 (2 equiv)	TFA (0.4 equiv)	HFIP	nr
8	Me-$B(OH)_2$	L2	$Pd(OAc)_2$	Ag_2CO_3 (2 equiv)	TFA (0.4 equiv)	DCE	nr
9[a]	Me-BF_3K	L2	$Pd(OAc)_2$	Ag_2CO_3 (2 equiv)	-	HFIP	nr
10[a]	Me-BF_3K	L4	$Pd(OAc)_2$	Ag_2CO_3 (2 equiv)	-	HFIP	nr

An alternative route to prepare an axially chiral precursor of **1** is directly based on the oxidative Heck reaction, previously developed in our laboratory (Figure VI-15). Indeed, an oxidative cleavage of the double bond of the C-H olefination product **9**, followed by a reduction of the corresponding aldehyde would deliver the targeted intermediate **4**.

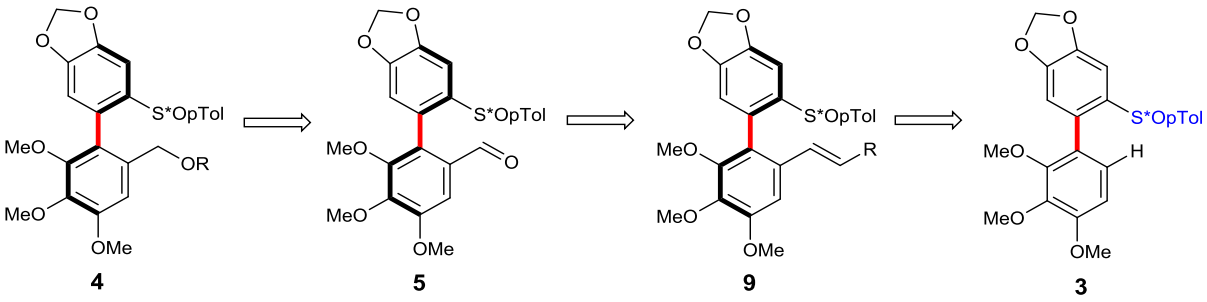

Figure VI-15 : atroposelective Fujiwara-Moritani retrosynthetic scheme

We commenced our synthetic efforts by preparing the biaryl sulfoxyde substrate **3** (Figure VI-16). This compound may be obtained via Suzuki-Miyaura coupling between the enantiomerically pure (S)-bromo-6-(p-tolylsulfinyl)benzo[*d*](1,3)dioxole **6** and the commercially available 2,3,4-trimethoxyphenyl boronic acid. To access **6**, iodination of 1-bromo-3,4-(methylenedioxy)benzene was firstly performed using iodine and silver trifluoroacetate[347]. The corresponding bromo-iodo derivative was reacted with *i*-PrMgCl and a following trapping with the optically pure and the less expensive (1*R*,2*S*,5*R*)-(*S*) enantiomer of the menthysulfinate afforded the desired aryl-sulfoxyde **6** in enantiomerically pure form and quantitative yield. The first attempt to build up the biaryl scaffold via Suzuki coupling using $Pd(OAc)_2$ catalyst, sodium carbonate base and *tert*-butyl ammonium bromide, in water and under microwave heating was rather disappointing as the desired product was isolated in 55% yield. We speculated that the electron-richness of both coupling partners might account for this moderate efficiency. Pd-PEPPSI complex was therefore tested but no improvement of this Ar-Ar coupling was observed. Finally, we were pleased to discover that applying Buchwald's conditions[348] for the Suzuki coupling the desired biaryl **3** was obtained in quantitative yield. Importantly, this reaction worked perfectly well also at 2g scale. As expected, this axially chiral compound was obtained as a mixture of two atropodiastereomers in a relatively rapid equilibrium, as indicated by NMR analysis (broad signals in ^{1}H NMR confirm that the coalescence temperature of **3** is close to RT). **3** was subsequently submitted to our oxidative Heck reactions conditions, employing methyl acrylate coupling partner, $Pd(OAc)_2$ catalyst, silver acetate oxidant and HFIP medium. As foreseen based on our previous work, this C-H functionalization could be performed under extremely mild reaction conditions (25 °C), affording **9** quantitatively and the yield of both diastereomers of 95:4 was evaluated by ^{1}H NMR. Importantly, atropopure **9** could be isolated in 92% yield by recrystallization.

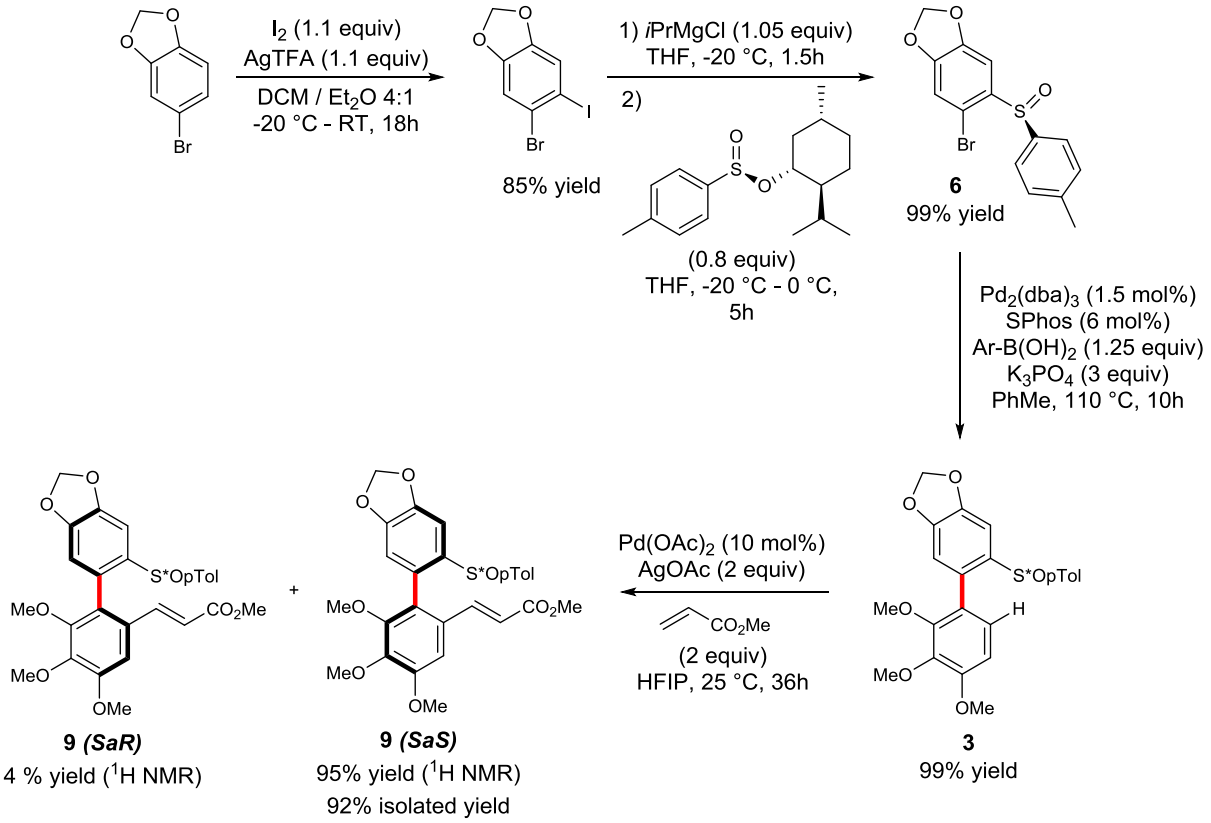

Figure VI-16 : synthesis of 9 with controlled axial chirality

The stereoselective outcome of this transformation is believed to be controlled by a distinct steric environment of the two atropodiastereomeric palladacyclic intermediates influenced by the stereogenic character of the sulfoxyde moiety (Figure VI-17). Based on the X-Ray structures of the closely related products previously obtained via such sulfoxyde-directed atroposelective C-H activation, it can be assumed that the functionalization occurs from the opposite site of the pTol-substituent of the sulfoxyde. Indeed the two atropisomers of **3** are in equilibrium, formation of **Pd-IntA** is favored because of the reduced steric hindrance between the Pd atom coordination sphere and the p-Tol substituent of the stereogenic DG: indeed the square planar geometry of the palladacycle forces one of the Pd ligand and the pTol substituent in a *syn* conformation on the disfavored **Pd-IntB**, whereas they are in a *anti* conformation on the favored **Pd-IntA**. Consequently, the configuration of the major **9** diastereomer can be assigned as a*S*. Noteworthy, because two atropisomers of **3** are converted into (*Sa*S)-**9**, this asymmetric C-H activation follows a dynamic kinetic resolution scenario. However, epimerization of the two atropisomeric palladacycles (and thus a dynamic kinetic transformation resolution scenario) cannot be excluded.

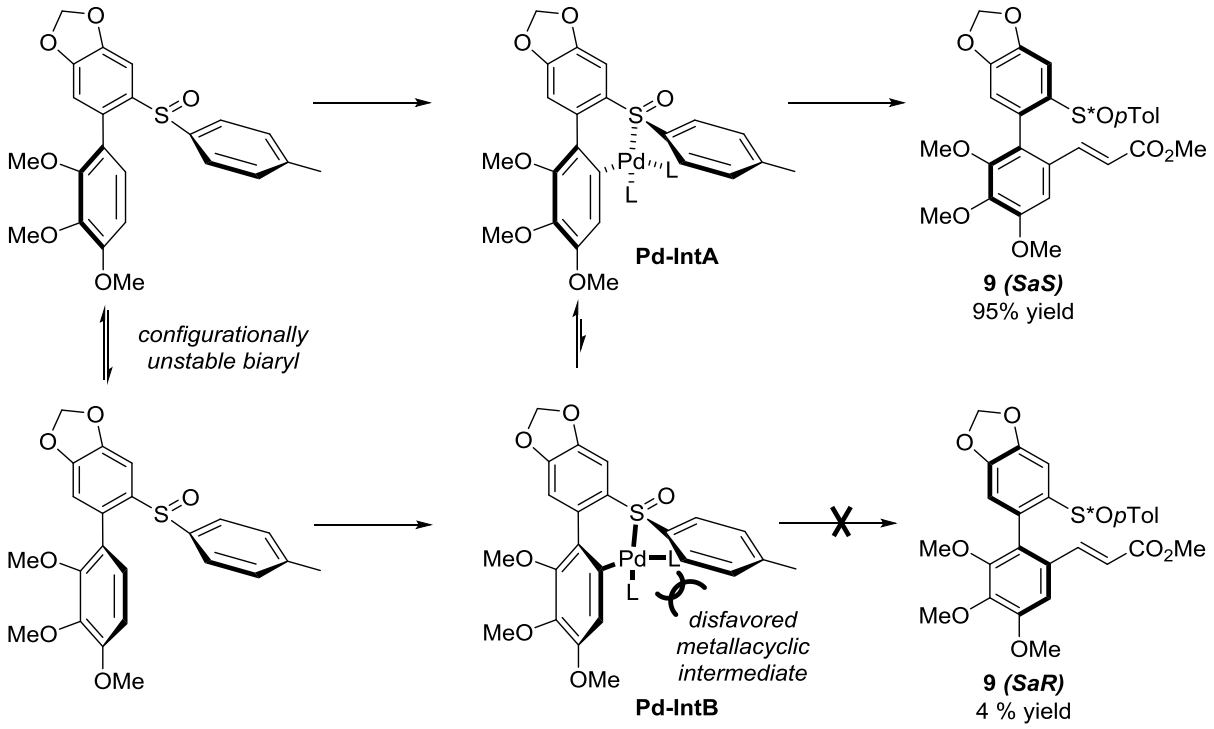

Figure VI-17 : stereoselectivity rationale

Once the axial chirality of the biaryl scaffold installed, the functional group interconversion process is undertaken to access steganone precursor **4** (Figure VI-18). Initially, ozonolysis of the alkene moiety was targeted but a complex crude mixture was obtained when performing the reaction in a mixture of CCl_4 and CH_2Cl_2 at -20°C. Subsequently, we explored the OsO_4-catalyzed oxidative cleavage. Deceivingly, although several different oxidants (hydrogen peroxide, oxone, NMO, NaIO4) and solvents (DMF, acetonitrile, water/dioxane) were tested, a clean reaction was not achieved. Addition of a weak base, such as 2,6-lutidine[349], or phenyl boronic acid[350] (to convert the double bond into bulky phenylboronic ester) did not produce the expected results neither.

In light of these difficulties, we reasoned that the electron withdrawing character of the ester substituent of the olefin moiety accounts for the moderate reactivity of this oxidative cleavage and hence reduction of the ester group into alcohol should be beneficial. Following this hypothesis, DIBAL-H reduction of **9** was performed and the corresponding benzylic alcohol was isolated together with a small amount of the remaining starting material (9:1 mixture of **10** and **9**). This mixture was directly engaged in the oxidative cleavage using OsO_4 catalyst and NMO oxidant in acetone/water medium. Rewardingly, the starting material was fully consumed but a complex stereoisomeric mixture of **11** and **12** was observed on TLC and LC-MS. Fortunately, this crude could be successfully converted into the desired aldehyde **5** by means of $Pb(OAc)_4$ mediated oxidative cleavage of the diol moiety. Reduction of the crude **5** and subsequent protection of the corresponding alcohol delivered the atropodiastereomerically pure **4** (R = TBDMS) in an exceptional 92% yield over 5 steps.

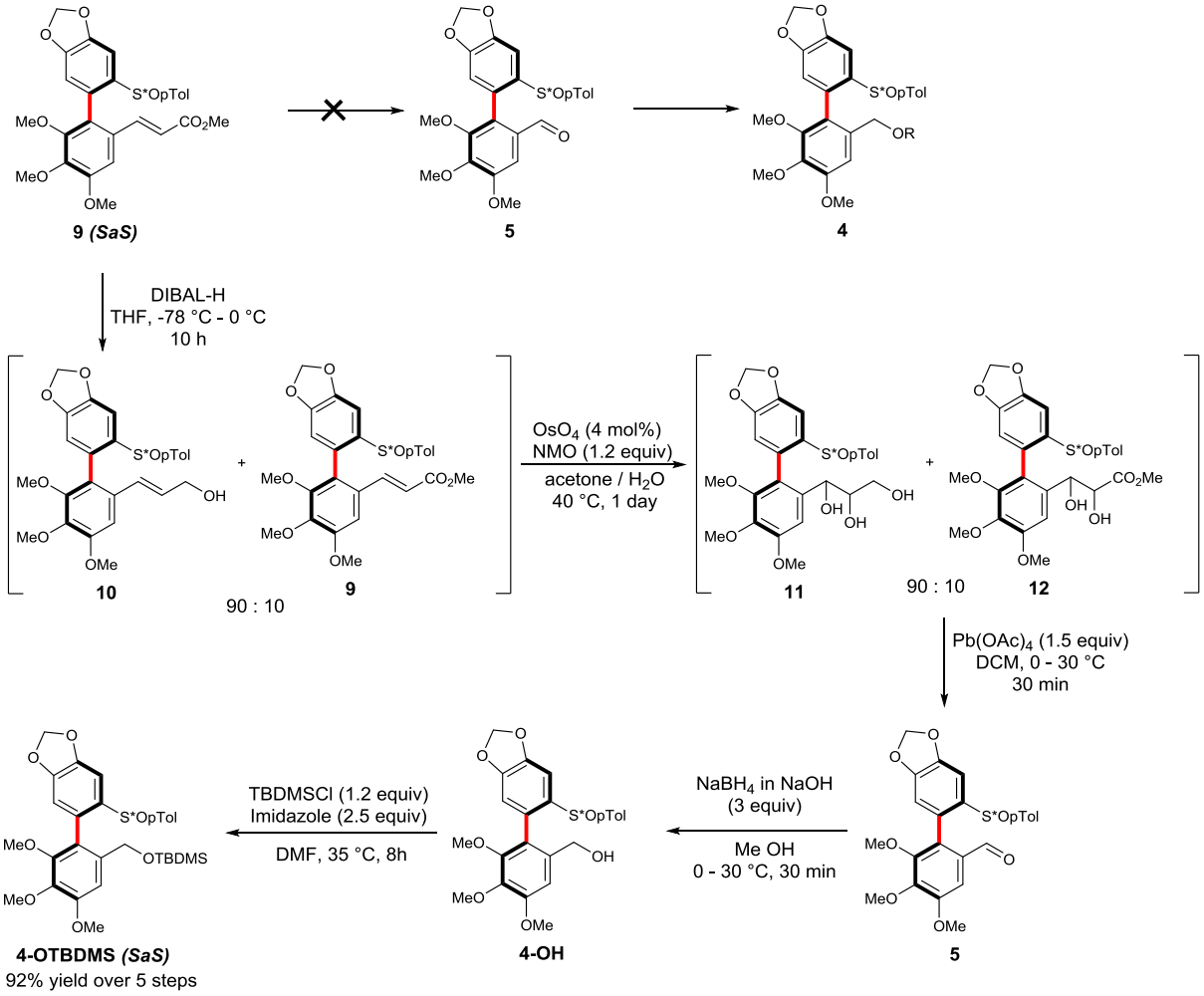

Figure VI-18 : synthesis of 4-OTBDMS

Completion of the targeted synthesis consists on removal of the sulfoxyde directing group and concomitant installation of the aldehyde motif (Figure VI-19). A cleavage of the Ar-SO*p*Tol bond in presence of lithium bases followed by an electrophilic trapping is well described in literature. In the context of the synthesis of atropoenantiopure biaryl scaffolds, a major difficulty may arise from the possible atropimerization when an Ar-Li intermediate is formed[313]. Aware of this sensitive step, we performed the targeted sulfoxyde/lithium exchange followed by the electrophilic trapping implying methyle formate as the aldehyde precursor, using 4.09 equiv. of *t*-BuLi in THF at -94 °C[314]. We were delighted to see that the targeted molecule **1** could be synthesized in a fair yield of 60%. Importantly, the optical purity of **1** was maintained as confirmed by chiral HPLC analysis.

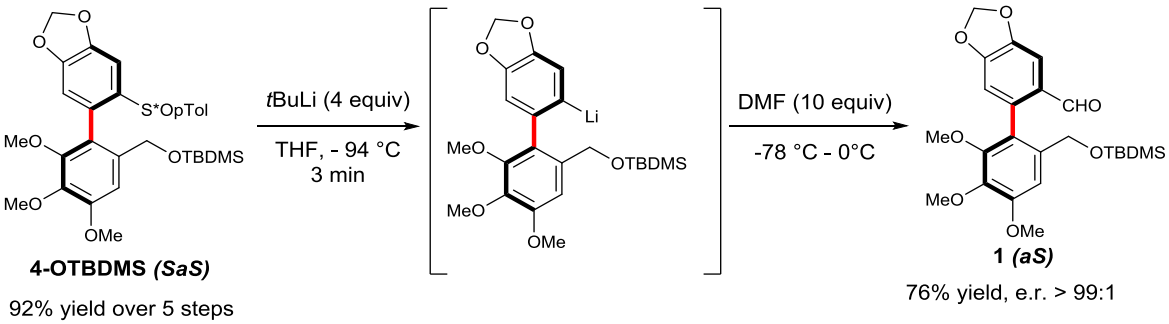

Figure VI-19 : synthesis of 1

In summary, we have successfully executed a formal synthesis of (+)-steganone. The herein described approach is very straightforward as the targeted scaffold is afforded in only 10 steps, amongst which **5** of them are performed without isolation of the crude products. Accordingly, the final product **1** is isolated in remarkable overall yield of 42.3% and with an enantiomeric ratio above 99:1. Importantly, the key step of this synthesis allowing induction of the chiral information implies an asymmetric C-H activation reaction. Important to note is also the fact that this synthesis does not require any expensive chemicals and catalysts and all catalytic steps may be performed on multigram scale. We note that using (*S*)-sulfoxyde directing group, the enantiomer of the precursor of the naturally occurring (-)-steganone is prepared. However, strictly identical synthetic approach would deliver (a*R*)-1 if (*R*)-sulfoxide is embedded on the biaryl substrate at the beginning of this synthesis.

Accordingly, we illustrate herein that thanks to its excellent stereoselectivity, efficiency, robustness and traceless character of the DG, the sulfoxyde-directed asymmetric C-H activation can be astutely employed to construct natural products, allowing design of unprecedented and very efficient synthetic strategies.

This work towards the synthesis of steganone has been published in Tetrahedron 2016, 72, 5238-5245 in a special issue dedicated to axial chirality.

B. Experimental data

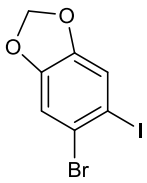

5-bromo-6-iodobenzo[*d*][1,3]dioxole
Chemical Formula: $C_7H_4BrIO_2$
Molecular Weight: 326,9155

6-bromo-5-iodobenzo[*d*][1,3]dioxole: :
To a vigorously stirred solution of 5-bromobenzo[*d*][1,3]dioxole (1 equiv, 8 g, 4.82 mL, 39.8 mmol) and silver trifluoroacetate (1.1 equiv, 9.67 g, 43.8 mmol) in DCM (100 mL) at -20 °C was added dropwise over 1 h. a solution of iodine (1.1 equiv, 11.1 g, 10.9 mL, 43.8 mmol) in a mixture of DCM (200 mL) and diethylether (100 mL). The mixture was then allowed back to room temperature and stirred overnight. The reaction mixture was quenched with a 10 % (w/w) solution of sodium thiosulfate, the phases were separated and the aqueous phase was extracted with diethylether. The combined organic phases were washed with a saturated $NaHCO_3$ solution, brine, and dried over sodium sulfate. The solvent was removed under reduced pressure and the crude product was recrystallized from methanol yielding 6-bromo-5-iodobenzo[*d*][1,3]dioxole (11.1 g, 33.9 mmol, 85 %).

^{1}**H-NMR** ($CDCl_3$, 400 MHz) : 7.24 (s, 1H), 7.08 (s, 1H), 5.99 (s, 2H) ppm. ^{13}**C-NMR** ($CDCl_3$, 101 MHz): δ = 149.1, 147.9, 120.7, 119.1, 112.7, 102.3, 89.3 ppm. **EA :** *see*[331].

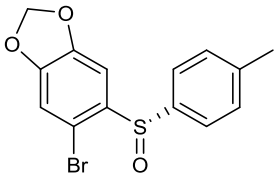

(*S*)-5-bromo-6-(*p*-tolylsulfinyl)benzo[*d*][1,3]dioxole
Chemical Formula: $C_{14}H_{11}BrO_3S$
Molecular Weight: 339,2030

(*S*)-5-bromo-6-(p-tolylsulfinyl)benzo[*d*][1,3]dioxole .
To a solution of 6-bromo-5-iodobenzo[*d*][1,3]dioxole (1.2 equiv, 7.81 g, 23.9 mmol) in THF (33 mL) at -20 °C was added dropwise a solution of *i-Pr*MgCl (1.21 equiv, 2 M in THF, 12 mL, 24 mmol). The resulting mixture was stirred at -20 °C for 1.5 hour. The Grignard solution was cannulated to a solution of (1*R*,2*S*,5*R*)-(−)-menthyl (*S*)-*p*-toluenesulfinate (1 equiv, 5.86 g, 19.9 mmol) in THF (100 mL) at -20 °C and stirred at this temperature for 2 hours. The reaction mixture was then allowed back to 0°C over 1 hour and stirred for another hour at this temperature. The reaction was diluted with diethylether and quenched by a saturated solution of

ammonium chloride. The phases were separated and the aqueous phase extracted with diethylether. After removal of the solvent under reduced pressure, the crude product was charged in a sublimator and placed under vacuum at 40 °C overnight in order to sublimate the menthol out of the crude product. The resuting solid was purified by crystallization by liquid/liquid diffusion of *n*-pentane into DCM, yielding (*S*)-5-bromo-6-(p-tolylsulfinyl)benzo[*d*][1,3]dioxole (6.7 g, 19.8 mmol, 99 %), with an enantiomeric ratio > 95 : 5.

^{1}H-NMR ($CDCl_3$, 400 MHz) : 7.62 (AA'BB'm, 2H), 7.43 (s, 1H), 7.25 (AA'BB'm, 2H), 6.95 (s, 1H), 6.06 (dd, J = 16.1, 1.2 Hz, 2H), 2.37 (s, 3H) ppm. **^{13}C-NMR** ($CDCl_3$, 101 MHz): δ = 150.9, 148.8, 142.0, 142.0, 138.4, 130.1, 125.8, 113.0, 111.8, 106.1, 102.7, 21.6 ppm. $[\alpha]_D^{20}$ = -16.5 ° (c = 2.32, $CHCl_3$). **EA** : *Calcd. for* : (C) 49.57, (H) 3.27 ; *found* : (C) 49.50, (H) 3.32.

Determination of the enantiomeric ratio of (*S*)-5-bromo-6-(p-tolylsulfinyl)benzo[*d*][1,3]dioxole .

Preparation of racemic 5-bromo-6-(p-tolylsulfinyl)benzo[d][1,3]dioxole : to a solution of (*S*)-5-bromo-6-(p-tolylsulfinyl)benzo[*d*][1,3]dioxole (1 equiv, 43 mg, 0.127 mmol) in acetone (1 mL) was successively added TFAA (4.03 equiv, 107 mg, 71 µL, 0.51 mmol) and NaI (3 equiv, 57 mg, 0.38 mmol) at 0 °C. The reaction mixture was stirred at 25 °C for 5 min. and quenched by a 10 % (w/w) sodium thiosulfate solution. The phases were separated and the organic phase was dried over sodium sulfate. The solvent was removed under reduced pressure, and the crude product was dissolved in DCM (2.5 mL). To this solution was added at 0 °C m-CPBA (1.12 equiv, 35 mg, 62.5 µL, 0.142 mmol), and the reaction mixture was stirred at 25 °C for 30 min., when the reaction was quenched by an 1 M NaOH solution. Flash chromatography (c-Hex/EtOAc) yielded racemic 5-bromo-6-(*p*-tolylsulfinyl)benzo[*d*][1,3]dioxole (38.7 mg, 0.114 mmol, 90 %).

Proton NMR determination of the e.r. : to an NMR tube containing a solution of racemic 5-bromo-6-(*p*-tolylsulfinyl)benzo[*d*][1,3]dioxole (1 equiv, 10 mg, 0.0295 mmol) in CDCl3 (0.6 mL) was added (1*R*)-1-(anthracen-9-yl)-2,2,2-trifluoroethan-1-ol (2 equiv, 16.3 mg, 0.059 mmol). To an NMR tube containing a solution of enantioenriched 5-bromo-6-(*p*-tolylsulfinyl)benzo[*d*][1,3]dioxole (1 equiv, 11 mg, 0.0324 mmol) in CDCl3 (0.6 mL) was added (1*R*)-1-(anthracen-9-yl)-2,2,2-trifluoroethan-1-ol (2.01 equiv, 18 mg, 0.0652 mmol). Comparison of the two spectra gave an e.r. > 95 : 5 for (*S*)-5-bromo-6-(p-tolylsulfinyl)benzo[*d*][1,3]dioxole**.**

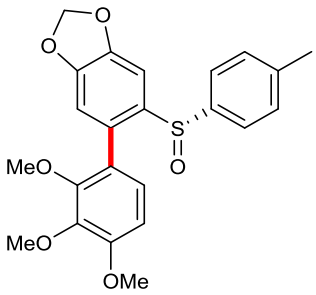

(*S*)-5-(*p*-tolylsulfinyl)-6-(2,3,4-trimethoxyphenyl)benzo[*d*][1,3]dioxole
Chemical Formula: $C_{23}H_{22}O_6S$
Molecular Weight: 426,4830

(*S*)-5-(*p*-tolylsulfinyl)-6-(2,3,4-trimethoxyphenyl)benzo[*d*][1,3]dioxole.

A sealed tube, flushed with argon, was charged with (*S*)-5-bromo-6-(*p*-tolylsulfinyl)benzo[*d*][1,3]dioxole (1 equiv, 1000 mg, 2.95 mmol), dicyclohexyl[2-(2,6-dimethoxyphenyl)phenyl]phosphane (6.03 %, 73 mg, 0.178 mmol) and Tris(dibenzylideneacetone) dipalladium (1.52 %, 41 mg, 0.0448 mmol), along with K_3PO_4 (3.04 equiv, 1900 mg, 8.95 mmol). Anhydrous toluene (20 mL) was added, followed by a solution of 2,3,4- trimethoxyphenylboronic acid (1.25 equiv, 780 mg, 3.68 mmol) in anhydrous toluene (10 mL) The reaction mixture was stirred at 110 °C for 10 hours.The reaction mixture was cooled down to room temperature and filtrated over celite. The filtrate was diluted with diethylether and washed with a 1M NaOH solution to remove unreacted boronic acid, and the aqueous phase was extracted with diethylether. After removal of the solvent under pressure the crude product is pure enough for most application. Nevertheless, flash chromatographiy (c-Hex/EtOAC) yielded analytically pure (*S*)-5-(*p*-tolylsulfinyl)-6-(2,3,4-trimethoxyphenyl)benzo[*d*][1,3]dioxole (1244 mg, 2.92 mmol, 99 %)**.**

Note : because we are near the coalescence temperature for most of the signals in ^{1}H-NMR and ^{13}C-NMR at room temperature, some signals are split (~50 : 50) between the two atropisomers in the ^{1}H spectra, whereas some are not ; however the majority of the signals are very broad. In the ^{13}C spectra some signal are even too broad to be detected (thus some carbon might be missing).
^{1}H-NMR ($CDCl_3$, 400 MHz) : 7.42 (brd, 0.5H), 7.31 (Brd, 0.5H), 7.18 (Brd, 1.5 H), 7.13 (s, 2H), 7.11 (s, 1H), 6.70 (brd, 2H), 6.54 (Brd, 0.5H), 6.01 (d, J = 8.07 Hz, 2H), 3.91 (s, 3H), 3.85 (Brd, 3H), 3.79 (Brd, 1.5H), 3.32 (Brd, 1.5H), 2.30 (s, 3H) ppm.
^{13}C-NMR ($CDCl_3$, 101 MHz): δ = 154.2, 151.3, 149.8, 148.2, 142.4, 141.0, 129.6, 126.2, 125.4, 124.4, 110.9, 110.9, 107.0, 105.2, 104.3, 102.0, 61.1, 56.2, 21.4 ppm.
HRMS (ESI): *calc. for $C_{23}H_{23}O_6S^+$* 427.120 ; found 427.121.

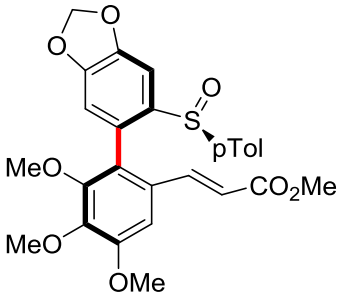

methyl (*E*)-3-(3,4,5-trimethoxy-2-((a*S*)-6-((*S*)-*p*-tolylsulfinyl)benzo[*d*][1,3]dioxol-5-yl)phenyl)acrylate

$C_{27}H_{26}O_8S$

510,5570

methyl (*E*)-3-(3,4,5-trimethoxy-2-((a*S*)-6-((*S*)-p-tolylsulfinyl)benzo[*d*][1,3]dioxol-5-yl)phenyl)acrylate.

To a solution of (*S*)-5-(*p*-tolylsulfinyl)-6-(2,3,4-trimethoxyphenyl)benzo[*d*][1,3]dioxole (1 equiv, 1244 mg, 2.92 mmol), palladium diacetate (10 %, 65.5 mg, 0.292 mmol) and silver acetate (2.03 equiv, 990 mg, 0.305 mL, 5.93 mmol) in hfip (10 mL) was added methyl acrylate (1.9 equiv, 478 mg, 0.5 mL, 5.55 mmol). The resulting mixture was stirred at 25 °C for 36 hours. The reaction mixture was diluted with diethylether and filtrated over celite. The organic phase was washed with water, the phases were separated and the aqueous phase extracted with ethylacetate. The combined organic phases were filtrated over a silica plug and the solvent was removed under reduced pressure. Proton NMR showed the presence of two atropodiastereomers : methyl (*E*)-3-(3,4,5-trimethoxy-2-((a*S*)-6-((*S*)-p-tolylsulfinyl)benzo[*d*][1,3]dioxol-5-yl)phenyl)acrylate (1420 mg, 2.78 mmol, 95 %), and methyl (*E*)-3-(3,4,5-trimethoxy-2-((a*R*)-6-((*S*)-p-tolylsulfinyl)benzo[*d*][1,3]dioxol-5-yl)phenyl)acrylate (62 mg, 0.121 mmol, 4 %). In order to obtain pure methyl (*E*)-3-(3,4,5-trimethoxy-2-((a*S*)-6-((*S*)-p-tolylsulfinyl)benzo[*d*][1,3]dioxol-5-yl)phenyl)acrylate, the crude mixture of both atropisomers was dissolved at room temperature in a 10 : 1 mixture of diethylether/DCM; slow evaporation of this solution yielded methyl (*E*)-3-(3,4,5-trimethoxy-2-((a*S*)-6-((*S*)-p-tolylsulfinyl)benzo[*d*][1,3]dioxol-5-yl)phenyl)acrylate (1370 mg, 2.68 mmol, 92 %) as colorless small prisms.

^{1}**H-NMR** ($CDCl_3$, 400 MHz) : 7.42 (d, J = 15.9 Hz, 1H), 7.32 (s, 1H), 7.26 (***AA'***BB'm, 2H), 7.16 (AA'***BB'***m, 2H), 7.00 (s, 1H), 6.62 (s, 1H), 6.30 (d, J = 15.9 Hz, 1H), 6.08 (dd, J = 12.5, 1.3 Hz, 2H), 3.96 (s, 3H), 3.81 (s, 3H), 3.72 (s, 3H), 3.38 (s, 3H), 2.32 (s, 3H) ppm.
^{13}**C-NMR** ($CDCl_3$, 101 MHz): δ = 167.0, 154.1, 151.6, 150.0, 148.8, 143.6, 142.1, 141.9, 141.3, 138.9, 129.8 (2 $C_{p\text{Tol}}$), 129.7, 129.3, 125.6 (2 $C_{p\text{Tol}}$), 125.6, 119.6, 111.1, 105.7, 104.9, 102.2, , 61.0, 60.4, 56.2, 51.8, 21.5 ppm.
$[\alpha]_D^{20}$ = -70.4 ° (c = 0.9, $CHCl_3$).
EA : *Calcd. for* : (C) 63.52, (H) 5.13; *found* : (C) 63.40, 5.15 (H).

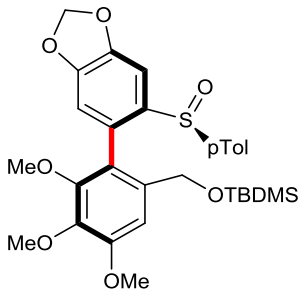

tert-butyldimethyl((3,4,5-trimethoxy-2-((*S*)-6-((*S*)-*p*-tolylsulfinyl)benzo[*d*][1,3]dioxol-5-yl)benzyl)oxy)silane
Chemical Formula: $C_{30}H_{38}O_7SSi$
Molecular Weight: 570,7720

tert-butyldimethyl((3,4,5-trimethoxy-2-((a*S*)-6-((*S*)-p-tolylsulfinyl)benzo[*d*][1,3]dioxol-5-yl)benzyl)oxy)silane.

-Step 1. To a solution of methyl (*E*)-3-(3,4,5-trimethoxy-2-((a*S*)-6-((*S*)-p-tolylsulfinyl)benzo[*d*][1,3]dioxol-5-yl)phenyl)acrylate (1 equiv, 451 mg, 0.8834 mmol) in THF (2.5 mL) at -78 °C was added dropwise DIBAL (3.51 equiv, 1 M in THF, 3.10 mL, 3.10 mmol). The reaction mixture was stirred at - 78°C for 4 hours (TLC analysis showed low conversion), and was then allowed back to 0°C over 6 hours. The mixture diluted with ether and was quenched by an ice-cold 1M HCL solution. The phases were separated and the aqueous phase was extracted with diethylether. The combined organic phases were washed with an 1M HCl solution, a saturated $NaHCO_3$ solution, and dried over sodium sulfate. The solvent was removed under reduced pressure, yielding a ~ 90 : 10 mixture of (*E*)-3-(3,4,5-trimethoxy-2-((a*S*)-6-((*S*)-p-tolylsulfinyl)benzo[*d*][1,3]dioxol-5-yl)phenyl)prop-2-en-1-ol / methyl (*E*)-3-(3,4,5-trimethoxy-2-((a*S*)-6-((*S*)-p-tolylsulfinyl)benzo[*d*][1,3]dioxol-5-yl)phenyl)acrylate which was directly engaged in the next step.

- Step 2. The ~90 : 10 mixture of product/substrate was dissolved in acetone (6 mL), and OsO4 (3.98 %, 0.08 M (2.5 % w/w) in *t*-BuOH, 440 µL, 0.0352 mmol) was added. The resulting mixture was stirred 5 min. at 25 °C, when a solution of NMO (1.2 equiv, 124 mg, 1.06 mmol) in water (1.5 mL) was added. The reaction was stirred at 35/40 °C for 20 hours, when TLC analysis (cHex/EtOAC/AcOH 3 : 7 : 0.5) and proton NMR showed complete conversion. The reaction was diluted with diethyl ether and quenched by the addition of a saturated sodium sulfite solution (8 mL) and vigorously stirred at 35 °C for 30 min. The phases were separated, and the pH of the aqueous phase was adjusted to ~1/2 with an 1 M sulfuric acid solution. The aqueous phase was then extracted with EtOAc, and the combined organic phases were washed with a saturated $NaHCO_3$ solution, dried over sodium sulfate, and the solvent was removed under reduced pressure.

-Step 3. (*The crude product from step 2 was dried by addition of toluene (2 x ~10 mL) and removal of the solvent under reduced pressure at 60 °C.*)
Under an inert atmosphere, the crude product was dissolved in anhydrous DCM (30

mL), to which was added portion wise $Pb(OAc)_4$ (1.55 equiv, 608 mg, 1.37 mmol) at 0 °C. The ice bath was removed, and the mixture was stirred at 25 °C for 30 min, when TLC analysis (*c*-Hex/EtOAc/AcOH 3 : 7 : 0.2 ; revealed with 2,4-DNPH) showed complete conversion and only one aldehyde/ketone product. The reaction mixture was filtrated over a silica/celite plug (washed with DCM) and the solvent was removed under reduced pressure. The crude product was directly engaged in the next step.

-Step 4. To the crude product was added methanol (8 mL) and the resulting mixture was cooled down to 0 °C. A freshly prepared solution of $NaBH_4$ (2.99 equiv, 3 M in 1 M NaOH aqueous solution, 880 µL, 2.64 mmol) was then added drop wise to the methanol solution at 0 °C. The reaction was stirred at 30 °C for 30 min., diluted with diethylether and water, and quenched by careful addition of an 1 M sulfuric acid solution. The phases were separated, and the aqueous phase was extracted with EtOAc. The combined organic phases were washed with a saturated $NaHCO_3$ solution, the solvent was removed under reduced pressure and the crude product was directly engaged in the next step.

-Step 5. To a solution of the crude product and imidazole (2.5 equiv, 150 mg, 2.203 mmol) in DMF (4 mL) was added portion wise at 0 °C TBDMSCl (1.25 equiv, 167 mg, 0.19 mL, 1.108 mmol). The mixture was stirred at 35 °C for 8 h, quenched by an 1 M NaOH solution, and diluted with EtOAc. The phases were separated and the aqueous phase was extracted with EtOAc. The combined organic phases were washed with brine and dried over sodium sulfate. After removal of the solvent under reduced pressure, flash chromatography (*c*-Hex/EtOAc), yielded, over five steps, *tert*-butyldimethyl((3,4,5-trimethoxy-2-((a*S*)-6-((*S*)-p-tolylsulfinyl)benzo[*d*][1,3]dioxol-5-yl)benzyl)oxy)silane (462 mg, 0.8094 mmol, 92 %).

^{1}**H-NMR** ($CDCl_3$, 400 MHz) : 7.36 (***AA'***BB'm, 2H), 7.19 (AA'***BB'***m, 2H), 7.19 (s, 1H), 7.04 (s, 1H), 6.63 (s, 1H), 6.04 (dd, J = 10.6, 1.4 Hz, 2H), 4.63, (d, J = 13.8 Hz, 1H), 4.42 (d, J = 13.8 Hz, 1H), 3.94 (s, 3H), 3.81 (s, 3H), , 3.52 (s, 3H), 2.34 (s, 3H), 0.93 (s, 9H), 0.07 (s, 3H), 0.03 (s, 3H) ppm.
^{13}**C-NMR** ($CDCl_3$, 101 MHz): δ = 153.9, 151.1, 150.1, 148.4, 142.0, 140.9, 140.5, 138.8, 135.8, 130.6, 129.7 (2 $C_{p\text{-}Tol}$), 125.2 (2 $C_{p\text{-}Tol}$), 121.6, 110.4, 105.7, 105.7, 102.0, 62.9, 60.8, 60.6, 56.0, 26.0, 21.4, 18.4 (3 $C_{t\text{-}Bu}$), -5.2, -5.3 ppm.
$[\alpha]_D^{20}$ = -102.45 ° (c = 1, $CHCl_3$).
HRMS (ESI): *calc. for* $C_{30}H_{38}LiO_7SSi^+$ 577.227 ; found 577.225.

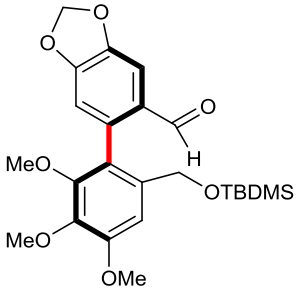

(*S*)-6-(6-(((*tert*-butyldimethylsilyl)oxy)methyl)-2,3,4-trimethoxyphenyl)benzo[*d*][1,3]dioxole-5-carbaldehyde
Chemical Formula: $C_{24}H_{32}O_7Si$
Molecular Weight: 460,5980

(a*S*)-6-(6-(((*tert*-butyldimethylsilyl)oxy)methyl)-2,3,4-trimethoxyphenyl)benzo[*d*][1,3]dioxole-5-carbaldehyde.

Anhydrous conditions. To a solution of *tert*-butyldimethyl((3,4,5-trimethoxy-2-((a*S*)-6-((*S*)-*p*-tolylsulfinyl)benzo[*d*][1,3]dioxol-5-yl)benzyl)oxy)silane (1 equiv, 107 mg, 0.187 mmol) in THF (2.5 mL) was added quickly *tert*-BuLi (3.96 equiv, 1.65 M in pentane, 0.45 mL, 0.742 mmol) at -78 °C. The color of the reaction mixture changed from pale yellow to a strong yellow/orange, and, when no more color change was evident (which took 3 min. at – 78 °C), DMF (10.3 equiv, 141 mg, 0.15 mL, 1.94 mmol) was immediately added in one portion. The mixture was then stirred for 30 min at -78 °C then allowed to warm up in air to 0°C. The reaction was quenched by a saturated ammonium chloride solution, diluted with diethylether and the phases were separated. The aqueous phase was extracted with EtOAc; the combined organic phases were dried over sodium sulfate. Flash chromatography (*c*-Hex/EtOAC from 10 : 90 to 30 : 70) yielded (a*S*)-6-(6-(((*tert*-butyldimethylsilyl)oxy)methyl)-2,3,4-trimethoxyphenyl)benzo[*d*][1,3]dioxole-5-carbaldehyde (57.7 mg, 0.123 mmol, 67%)

^{1}**H-NMR** ($CDCl_3$, 400 MHz) : 9.50 (s, 1H), 7.46 (s, 1H), 6.96 (s, 1H), 6.68 (s, 1H), 6.10 (d, J = 7.43 Hz, 2H), 4.34 (d, J = 13.2 Hz, 1H), 4.25 (d, J = 13.2 Hz, 1H), 3.92 (s, 3H), 3.88 (s, 3H), 3.61 (s, 3H), 0.88 (s, 9H), -0.03 (s, 3H), -0.03 (s, 3H) ppm. ^{13}**C-NMR** ($CDCl_3$, 101 MHz): δ = 190.5, 153.8, 152.4, 151.4, 148.1, 140.9, 137.2, 135.6, 129.7, 121.8, 111.0, 106.4, 106.1, 102.2, 63.0, 61.1, 61.0, 56.1, 26.0, 18.4 (3 $C_{t\text{-}Bu}$), -5.3, -5.3 ppm. $[\alpha]_D^{20}$ = +2.04 ° (c = 1, $CHCl_3$).
HRMS (ESI): *calc. for* $C_{24}H_{32}LiO_7SSi^+$ 467.208 ; found 467.209.

Chiral HPLC analysis of (a*S*)-6-(6-(((*tert*-butyldimethylsilyl)oxy)methyl)-2,3,4-trimethoxyphenyl)benzo[*d*][1,3]dioxole-5-carbaldehyde :

A racemic sample of (a*S*)-6-(6-(((*tert*-butyldimethylsilyl)oxy)methyl)-2,3,4-trimethoxyphenyl)benzo[*d*][1,3]dioxole-5-carbaldehyde was prepared by thermal isomerization of the chiral axis at 200 °C for 45 min.

Chiral-HPLC conditions : column : Daicel ChiralCel IB, n-Hexane/i-PrOH 98:2, 0.5 mL/min, 1 µL of 0.1 mg/mL mother solution injected.

LCM UMR7509
COHA
Chiral analysis report

<Sample Information>

Sample Name : qdh437-rac
Data Filename : qdh437-rac_03.lcd
Method Filename : Hex_IPA_9802_0-5ml.lcm
Batch Filename : 2016-01-25.lcb
Vial # : 1-3
Injection Volume : 1 uL
Date Acquired : 25/01/2016 16:04:03 Acquired by : User-Adv
IB hex/iproh 98/2 0.5ml

<PDA Chromatogram>

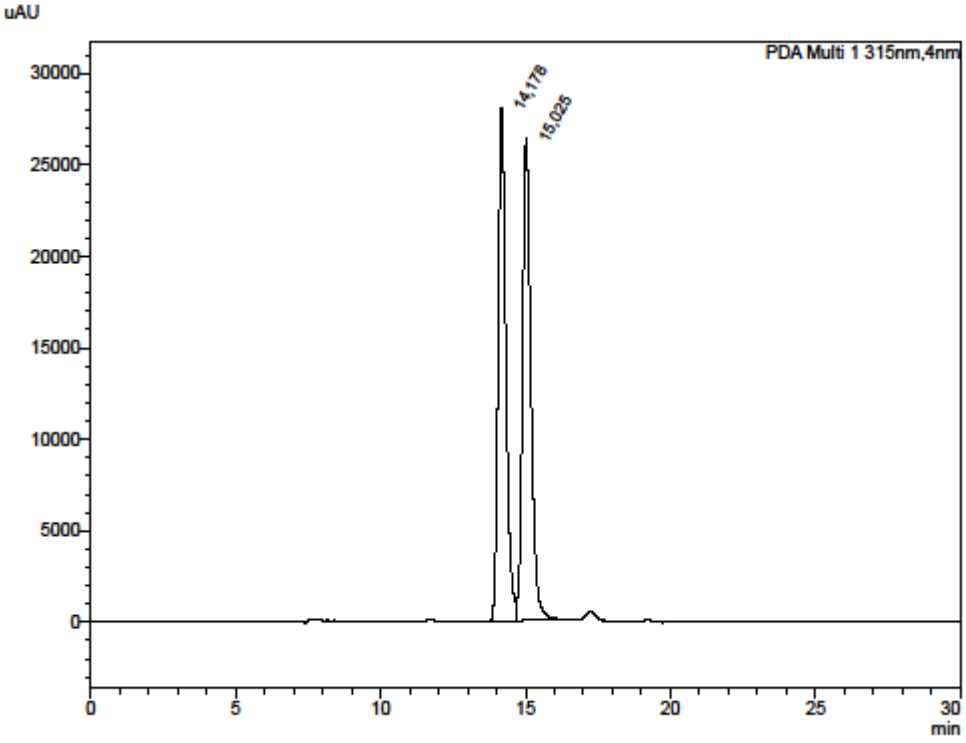

<PDA Chromatogram>

Peak Table

PDA Ch1 315nm

Peak#	Ret. Time	Area	Height	Area%	Capacity Factor(k')	Resolution(USP)	Lambda max
1	14,178	523032	28093	49,767	–	–	205/234/272/311/649
2	15,025	527925	26374	50,233	0,060	1,696	205/234/272/311/569
Total		1050957	54467	100,000			

C:\LabSolutions\Data\2016\2016-01-25\qdh437-rac_03.lcd

LCM UMR7509
COHA
Chiral analysis report

<Sample Information>

Sample Name : qdh437-rac
Data Filename : qdh437-rac_03.lcd
Method Filename : Hex_IPA_9802_0-5ml.lcm
Batch Filename : 2016-01-25.lcb
Vial # : 1-3
Injection Volume : 1 uL
Date Acquired : 25/01/2016 16:04:03 Acquired by : User-Adv
IB hex/iproh 98/2 0.5ml

<PDA Chromatogram>

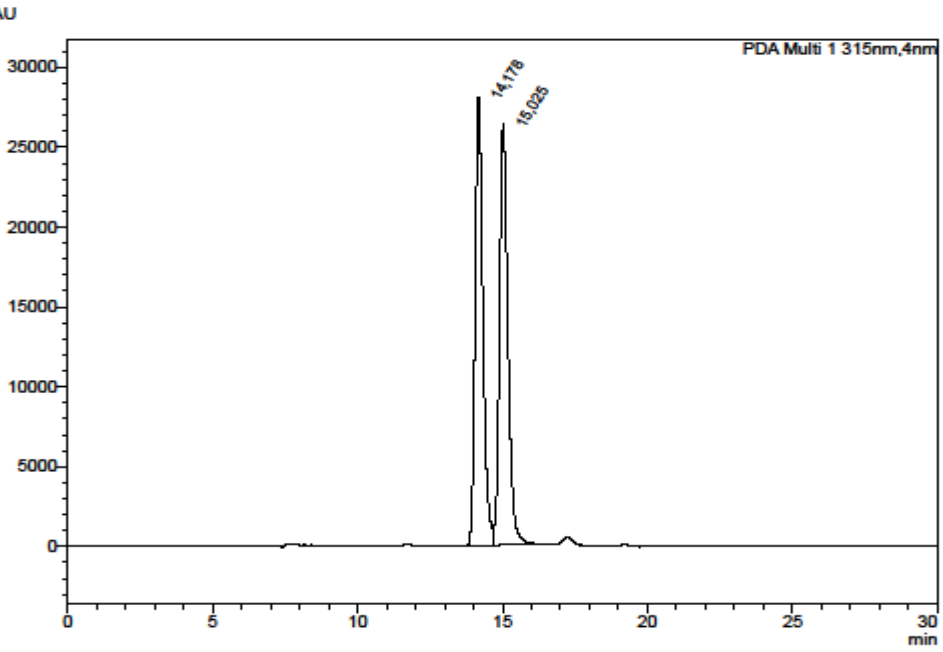

<PDA Chromatogram>

Peak Table

PDA Ch1 315nm

Peak#	Ret. Time	Area	Height	Area%	Capacity Factor(k')	Resolution(USP)	Lambda max
1	14.178	523032	28093	49.767	-	-	205/234/272/311/649
2	15.025	527925	26374	50.233	0.060	1.696	205/234/272/311/569
Total		1050957	54467	100.000			

C:\LabSolutions\Data\2016\2016-01-25\qdh437-rac_03.lcd

LCM UMR7509
COHA
Chiral analysis report

<Sample Information>

Sample Name : qdh441-en01
Data Filename : qdh441-en01_02.lcd
Method Filename : Hex_IPA_9802_0-5ml.lcm
Batch Filename : 2016-01-26.lcb
Vial # : 1-2
Injection Volume : 1 uL
Date Acquired : 26/01/2016 15:13:18 Acquired by : User-Adv
IB hex/iproh 98/2 0.5ml

<PDA Chromatogram>

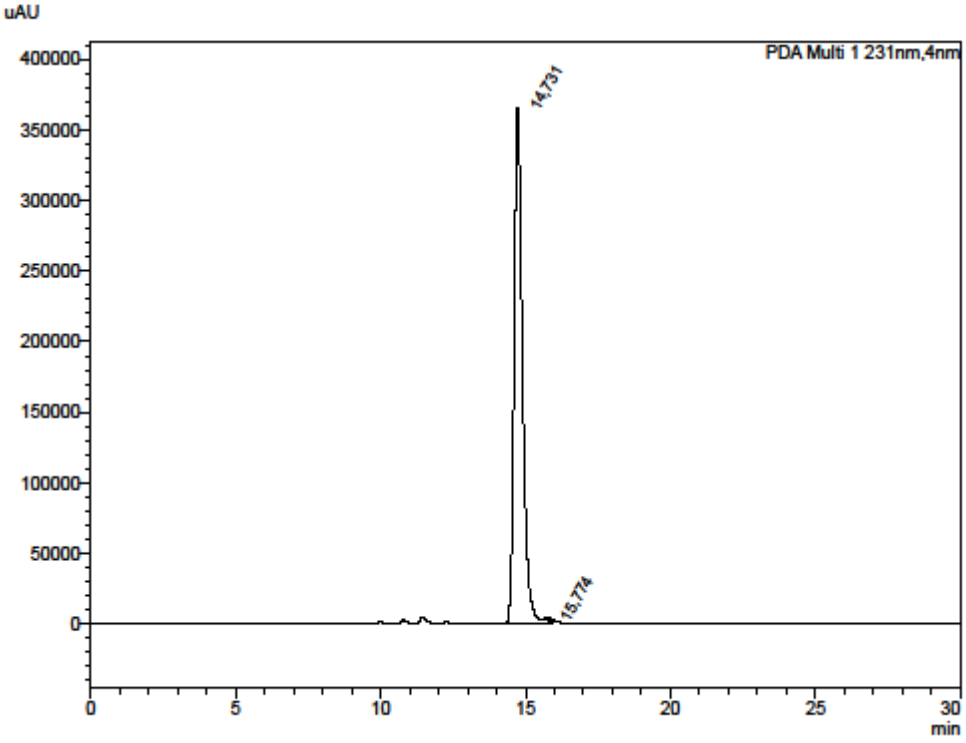

<PDA Chromatogram>

Peak Table

PDA Ch1 231nm

Peak#	Ret. Time	Area	Height	Area%	Capacity Factor(k')	Resolution(USP)	Lambda max
1	14.731	7301711	365497	99.660	-	-	205/234/272/311/655
2	15.774	24896	1573	0.340	0.071	2.190	205/234/269/312/655
Total		7326607	367070	100.000			

C:\LabSolutions\Data\2016\2016-01-26\qdh441-en01_02.lcd

C. References

[315] "Lignans chemical biological and clinical properties | Plant science," can be found under http://www.cambridge.org/fr/academic/subjects/life-sciences/plant-science/lignans-chemical-biological-and-clinical-properties, **n.d.**

[316] S. M. Kupchan, R. W. Britton, M. F. Ziegler, C. J. Gilmore, R. J. Restivo, R. F. Bryan, *J. Am. Chem. Soc.* **1973**, *95*, 1335–1336.

[317] N. K. Kochetkov, A. Khorlin, O. S. Chizhov, V. I. Sheichenko, *Tetrahedron Lett.* **1961**, *2*, 730–734.

[318] J. Chang, J. Reiner, J. Xie, *Chem. Rev.* **2005**, *105*, 4581–4609.

[319] T. L. Nguyen, C. McGrath, A. R. Hermone, J. C. Burnett, D. W. Zaharevitz, B. W. Day, P. Wipf, E. Hamel, R. Gussio, *J. Med. Chem.* **2005**, *48*, 6107–6116.

[320] O. Baudoin, F. Guéritte, in *Stud. Nat. Prod. Chem.* (Ed.: Atta-ur-Rahman), Elsevier, **2003**, pp. 355–417.

[321] A. S. Kende, L. S. Liebeskind, *J. Am. Chem. Soc.* **1976**, *98*, 267–268.

[322] A. S. Kende, L. S. Liebeskind, C. Kubiak, R. Eisenberg, *J. Am. Chem. Soc.* **1976**, *98*, 6389–6391.

[323] J. P. Robin, O. Gringore, E. Brown, *Tetrahedron Lett.* **1980**, *21*, 2709–2712.

[324] L. G. Monovich, Y. Le Huérou, M. Rönn, G. A. Molander, *J. Am. Chem. Soc.* **2000**, *122*, 52–57.

[325] K. Kamikawa, T. Watanabe, A. Daimon, M. Uemura, *Tetrahedron* **2000**, *56*, 2325–2337.

[326] M. Uemura, A. Daimon, Y. Hayashi, *J. Chem. Soc. Chem. Commun.* **1995**, *0*, 1943–1944.

[327] H. Abe, S. Takeda, T. Fujita, K. Nishioka, Y. Takeuchi, T. Harayama, *Tetrahedron Lett.* **2004**, *45*, 2327–2329.

[328] O. Baudoin, A. Décor, M. Cesario, F. Guéritte, *Synlett* **2003**, *2003*, 2009–2012.

[329] A. Joncour, A. Décor, S. Thoret, A. Chiaroni, O. Baudoin, *Angew. Chem. Int. Ed.* **2006**, *45*, 4149–4152.

[330] A. Joncour, A. Décor, J.-M. Liu, M.-E. Tran Huu Dau, O. Baudoin, *Chem. – Eur. J.* **2007**, *13*, 5450–5465.

[331] B. Yalcouye, S. Choppin, A. Panossian, F. R. Leroux, F. Colobert, *Eur. J. Org. Chem.* **2014**, *2014*, 6285–6294.

[332] D. Augros, B. Yalcouye, S. Choppin, M. Chessé, A. Panossian, F. R. Leroux, *Eur. J. Org. Chem.* **2017**, *2017*, 497–503.

[333] B. Yalcouye, A. Berthelot-Bréhier, D. Augros, A. Panossian, S. Choppin, M. Chessé, F. Colobert, F. R. Leroux, *Eur. J. Org. Chem.* **2016**, *2016*, 725–732.

[334] L. McMurray, F. O'Hara, M. J. Gaunt, *Chem. Soc. Rev.* **2011**, *40*, 1885–1898.

[335] T. Newhouse, P. S. Baran, *Angew. Chem. Int. Ed.* **2011**, *50*, 3362–3374.

[336] J. Yamaguchi, A. D. Yamaguchi, K. Itami, *Angew. Chem. Int. Ed.* **2012**, *51*, 8960–9009.

[337] D. Y.-K. Chen, S. W. Youn, *Chem. – Eur. J.* **2012**, *18*, 9452–9474.

[338] J. Wencel-Delord, F. Glorius, *Nat. Chem.* **2013**, *5*, 369–375.

[339] B. Hong, C. Li, Z. Wang, J. Chen, H. Li, X. Lei, *J. Am. Chem. Soc.* **2015**, *137*, 11946–11949.

[340] Y. Feng, D. Holte, J. Zoller, S. Umemiya, L. R. Simke, P. S. Baran, *J. Am. Chem. Soc.* **2015**, *137*, 10160–10163.
[341] H. Weinstabl, M. Suhartono, Z. Qureshi, M. Lautens, *Angew. Chem. Int. Ed.* **2013**, *52*, 5305–5308.
[342] A. K. Pitts, F. O'Hara, R. H. Snell, M. J. Gaunt, *Angew. Chem. Int. Ed.* **2015**, *54*, 5451–5455.
[343] O. Daugulis, J. Roane, L. D. Tran, *Acc. Chem. Res.* **2015**, *48*, 1053–1064.
[344] X. Chen, K. M. Engle, D.-H. Wang, J.-Q. Yu, *Angew. Chem. Int. Ed.* **2009**, *48*, 5094–5115.
[345] L. Ackermann, *Chem. Commun.* **2010**, *46*, 4866–4877.
[346] R.-Y. Zhu, J. He, X.-C. Wang, J.-Q. Yu, *J. Am. Chem. Soc.* **2014**, *136*, 13194–13197.
[347] H.-K. Chang, S. Datta, A. Das, A. Odedra, R.-S. Liu, *Angew. Chem. Int. Ed.* **2007**, *46*, 4744–4747.
[348] T. E. Barder, S. D. Walker, J. R. Martinelli, S. L. Buchwald, *J. Am. Chem. Soc.* **2005**, *127*, 4685–4696.
[349] W. Yu, Y. Mei, Y. Kang, Z. Hua, Z. Jin, *Org. Lett.* **2004**, *6*, 3217–3219.
[350] S. Chiba, M. Kitamura, K. Narasaka, *J. Am. Chem. Soc.* **2006**, *128*, 6931–6937.

Arylation

VII. Arylation

A. Introduction

Considering the mild conditions under which we were able to perform atroposelectives olefination, acetoxylation and iodination, we envisioned to adapt our methodology towards an atroposelective arylation reaction to build-up interesting *ortho*-terphenyl bearing one chiral axis (Figure VII-1a).

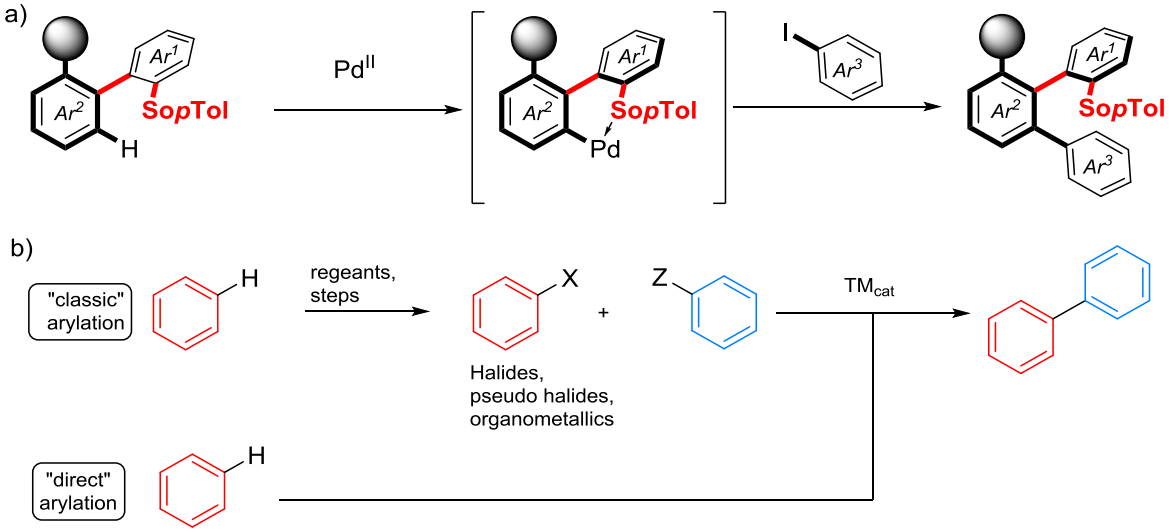

Figure VII-1: arylation of biphenyl sulfoxide and classic and direct arylation

Regarding the large body of work existing in the literature, palladium-catalyzed direct arylation reaction can be classified along broad guidelines[66,351]. Considering the prefuntionalized coupling partner, organometallic, halide, pseudo-halide or acid (*via* decarboxylation) derived arenes may be used (Figure VII-2a). Due to the clear mechanistic differences (transmetallation step using organometallic partners, oxidative addition for halides and decarboxylation event for carboxylic acids) we will focus exclusively on halide/pseudo halide aromatics. Finally the factors controlling the regioselectivity are another important parameter, as it will lead to distinct mechanistic scenario. To this end three general strategies exist: regioselectivity arising from the substrate innate reactivity, intramolecular reactions and the use of DG (Figure VII-2b).

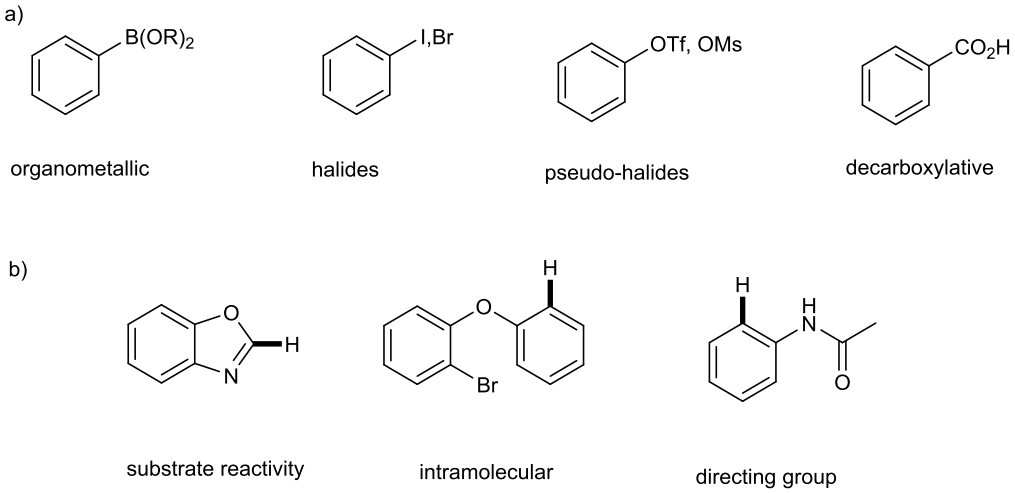

Figure VII-2: classification of palladium catalyzed direct arylation reactions

An important feature of these directed, pallado-catalyzed direct arylation with haloarenes, is that two distinct mechanistic scenario are possible. The first is based on a Pd^{0}-Pd^{II} catalytic cycle (Figure VII-3a): implying 1) oxidative addition of the haloarene to produce a σ-aryl palladium intermediate that 2) initiate the C-H cleavage of the coupling partner (by one of the mechanism viewed in the first part of this manuscript). 3) Reductive elimination affords the product and the Pd^{0} catalyst.

The other possibility is a Pd^{II}-Pd^{IV} cycle (Figure VII-3b), where 1) a Pd^{II} catalyst undergoes insertion into the C-H bond of the non pre-functionalized coupling partner. 2) The σ-arylPd^{II} intermediate undergoes oxidative addition to a Pd^{IV} complex and 3) reductive elimination yields the product along with the catalyst.

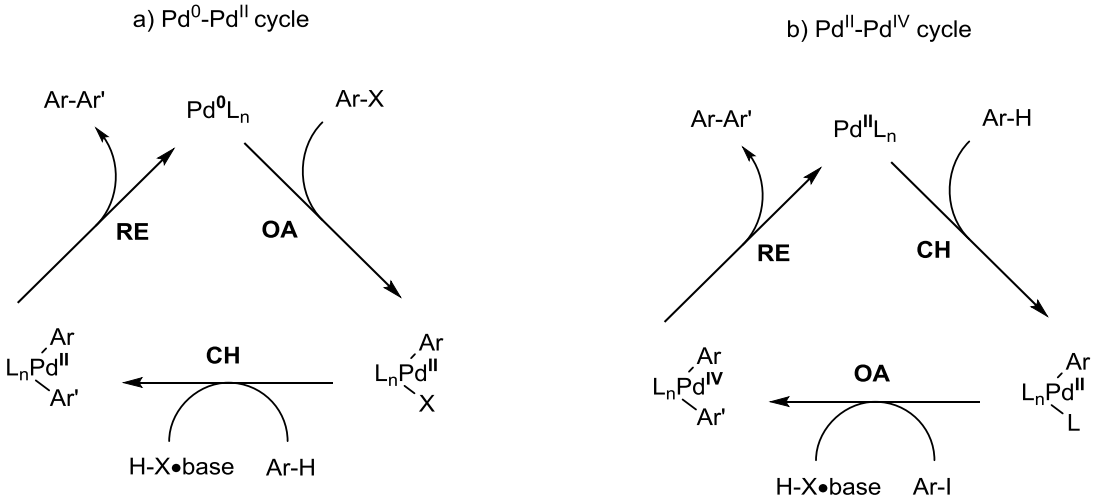

Figure VII-3 : possible catalytic cycles

Historically, the Pd^{0} -Pd^{II} cycle has been associated with intramolecular direct arylations. Indeed these reactions often used strong σ-donating phosphines ligands in combination with aryl bromides and a base (typically carbonates). In these conditions, OA would be facile and hence initiate the catalytic cycle. Then the C-H cleav-

age would occur, and several distinct mechanisms have been proposed: σ-bond methathesis, S_EAr and CMD/AMLA. These early examples often showed a large primary KIE (Fagnou 2006[352], Figure VII-4a) and were facilitated by electron-withdrawing substituents on the aromatic rings of electronically biased substrates (Echavarren 2006[353,354] Figure VII-4b). On these bases, a S_EAr mechanism was disqualified, and “proton abstraction mechanism” was initially proposed by Echavarren in 2006.

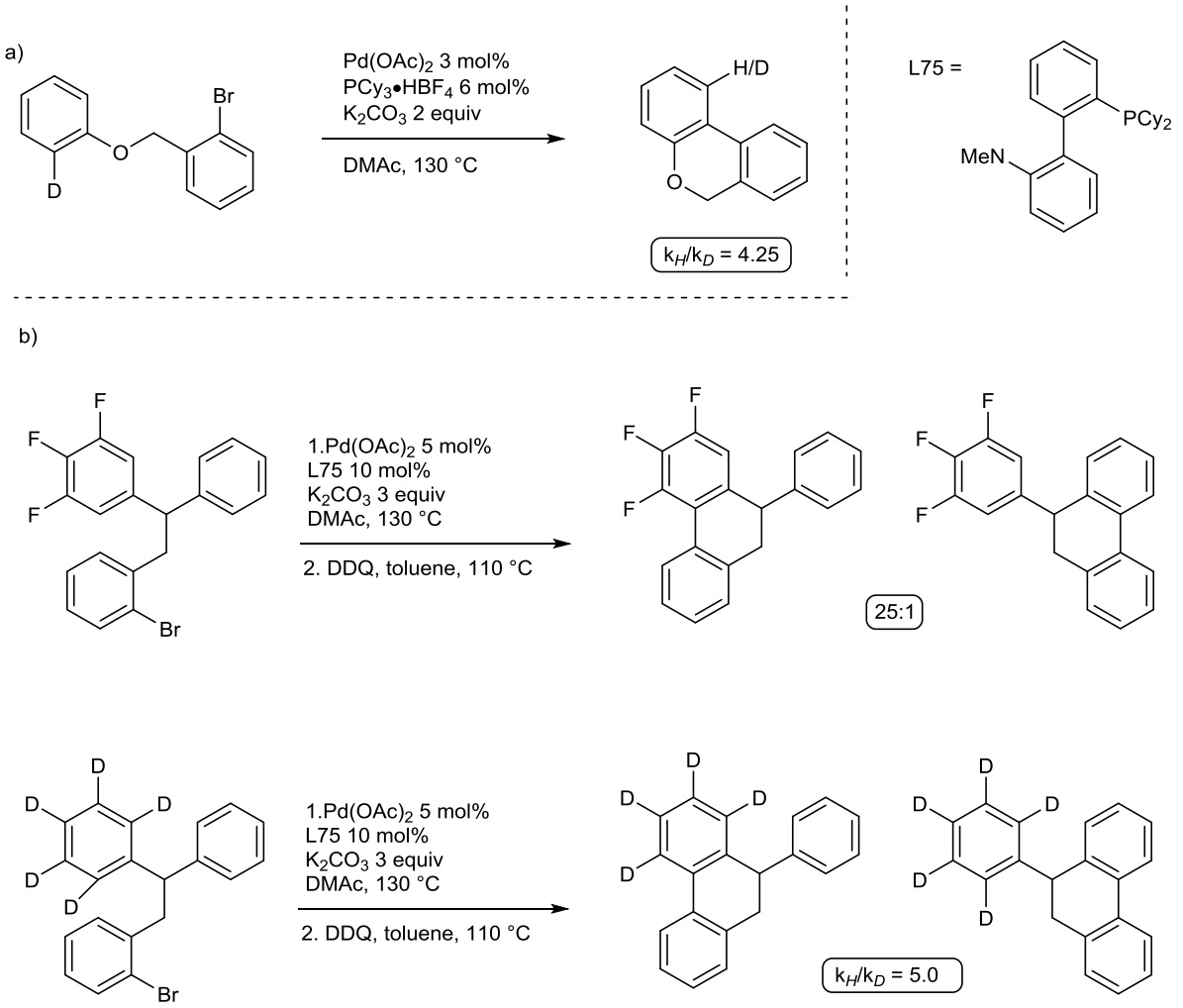

Figure VII-4: mechanistic studies on intramolecular direct arylation

Importantly, similar features where observed on intermolecular reaction by Fagnou in 2006[355] (Figure VII-5a: electron deficient substrates more reactive towards the C-H cleavage limiting step). Moreover, a common feature of these reactions is the use of $Pd(OAc)_2$ as pre-catalyst, and, as discovered slightly later, carboxylate-type ligands strongly improves the efficiency of the catalytic system. Fagnou and coworkers[356] (Figure VII-5b) found out that the nature of the carboxylate moiety might enhanced the C-H cleavage. Indeed the intermolecular direct arylation of *para*-tolylbromide with benzene was more efficient when using pivalic acid as an additive (Figure VII-5b).

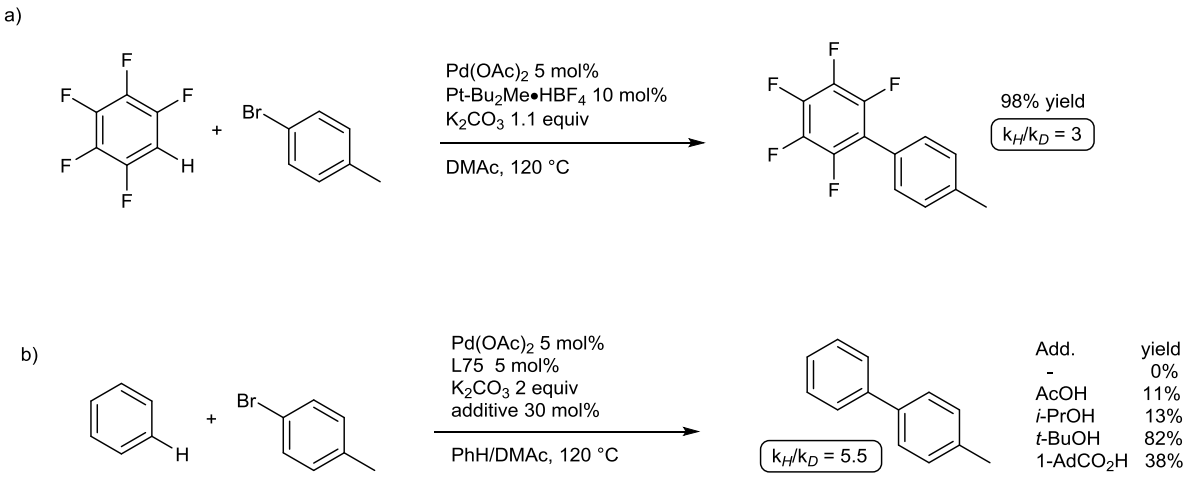

Figure VII-5 : mechanistic studies on intermolecular direct arylation

Following these studies, the general concept of the participation of carboxylate ligands, dubbed, Concerted Metallation Deprotanation[24] (CMD) was developed[14], then later refined[16] and retrospectively extended to other metals[22,357,358].

However, it is important to note that, although sharing the CMD/AMLA C-H cleavage mechanism, these *undirected* direct arylation reactions (Figure VII-4and Figure VII-5), exhibit an important difference from *directed* direct arylation.

Indeed, in directed C-H activation reactions, pre-coordination with the substrate is expected in order to direct the palladium catalyst towards the *ortho* C-H bond. Thus one can say that the substrate is acting as a ligand, and additional ligands that coordinate strongly at palladium might saturate the catalyst. Therefore, these reactions have usually relied on the combination of a “ligand-free” electrophilic palladium pre-catalyst capable of conducting a CMD/AMLA C-H insertion ($Pd(OAc)_2$, $Pd(OPiv)_2$, $Pd(TFA)_2$), along with an aryl iodide. Indeed, coordination with the directing group followed by C-H insertion, would result in a σ-aryl complex more electron-rich and capable of undergoing oxidative addition with an aryl iodide.

The earliest report of this type of catalytic cycle was made in 1984 by Tremont and co-workers[359] (however with an alkyl iodide). Acetanilide was reacted with 1.5 equivalent of palladium diacetate in the presence of methyl iodide to afford the *ortho*-methylated product in quantitative yield (Figure VII-6a). They proposed that the alkylation of the acetanilide-palladium acetate intermediate occurred by an oxidative addition/reductive elimination reaction rather than by an electrophilic attack of the Pd-C bond or by a radical mechanism based on the fact that MeI reacted faster than EtI (primary vs secondary iodide) and because MeOTf and Me_2SO_4 also alkylated the cyclopalladated complex. Furthermore, they discovered that the iodide produced was poisoning the catalyst (as PdI_2 was inefficient in this reaction Figure VII-6b) and that the use of a silver salt to trap the iodide produced made the reaction catalytic (Figure VII-6c).

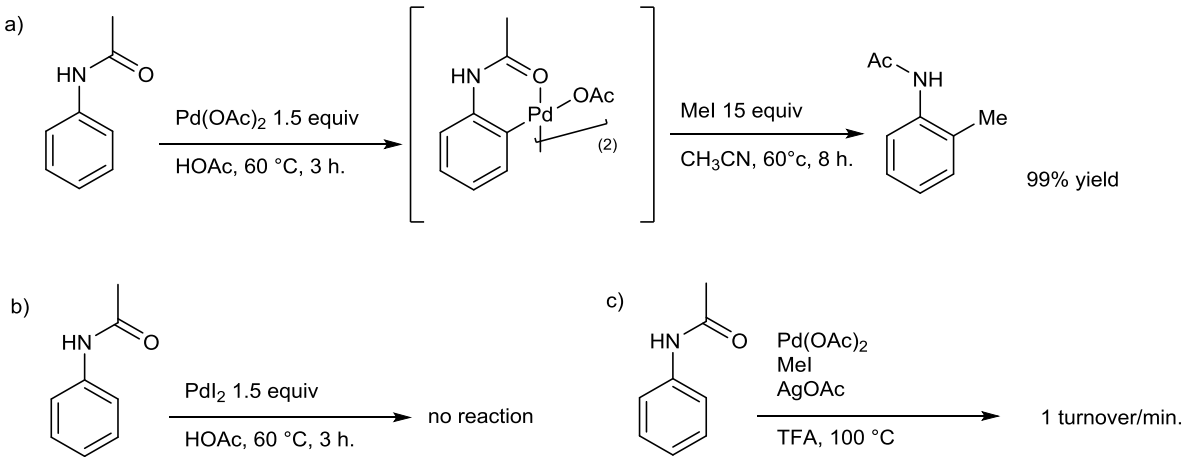

Figure VII-6 : palladium-catalyzed acetanilide functionalization

This early report inspired Daugulis and co-workers when, in 2005[360] they managed to conduct the arylation of anilide derivatives in similar conditions. Nitrogen-based directing groups were also used (Figure VII-7a), then later amines at elevated temperature (Daugulis 2006[361] Figure VII-7b).

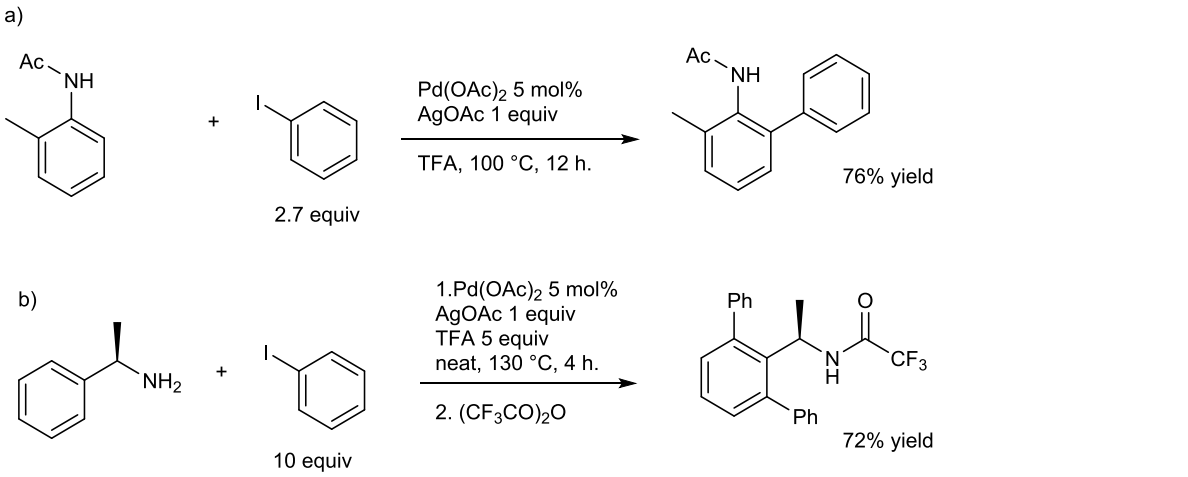

Figure VII-7 : early Pd^{II}-Pd^{IV} arylations

A number of directing groups were found compatible with these conditions[362]: benzamides[363] (Figure VII-8a), benzoic acids[364] (Figure VII-8b), benzyl amines[361] (Figure VII-8c), 2-substituted pyridines[365,366] (Figure VII-8d).

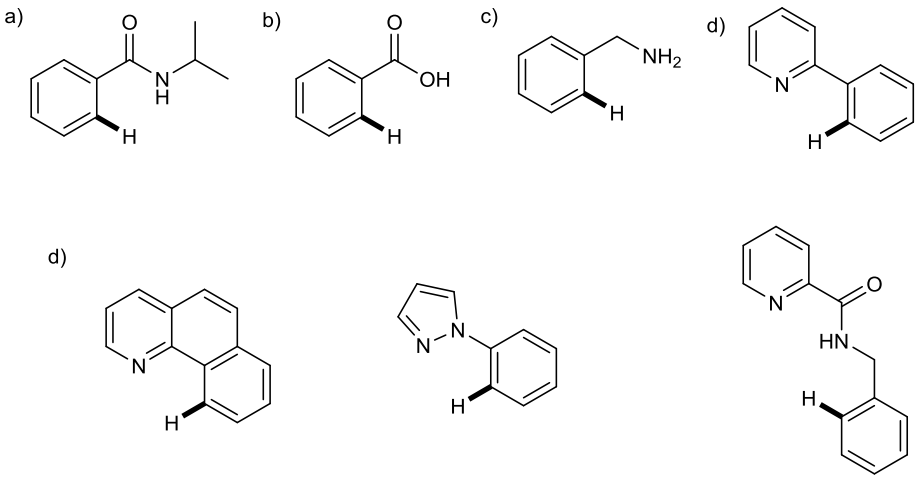

Figure VII-8 : directing groups in palladium catalyzed arylation

N-methoxy arylimines were also found to be suitable substrates, and a tandem direct-arylation/Heck reaction could be performed to obtained fluorenone derivatives[367] (Figure VII-9a). The concept was later extended to the use of a sub-stoichiometric amount of an amine derivative in order to form a transient directing group *via* a reversible imine formation[368] (Figure VII-9b).

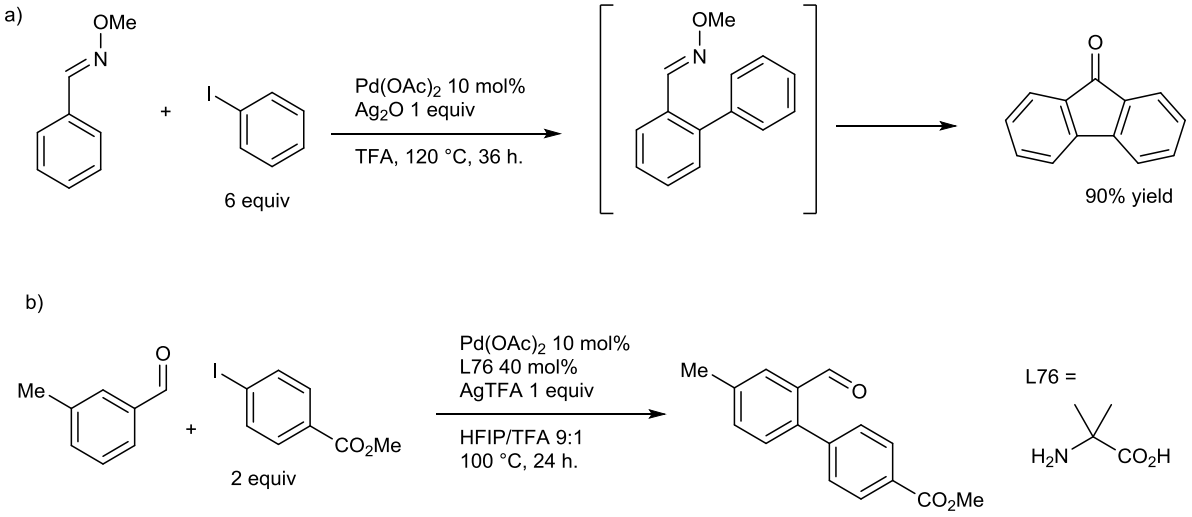

Figure VII-9 : arylation of benzaldehyde derivatives

Concerning the work on biaryles functionalization an early example of these direct arylations was reported in 1997 by the Miura group[369] (Figure VII-10 : arylation of biphenyls derivatives (Figure VII-10).

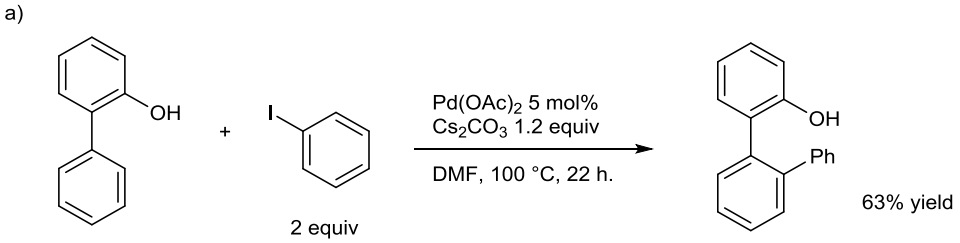

Figure VII-10 : arylation of biphenyls derivatives

Furthermore only the report of Lassaletta[370] on atroposelective biaryl arylation in 2013 existed prior to our work, and this example was reviewed in the introduction part of this manuscript.

B. Towards original scaffolds

During our work, it occurred to us that by increasing the steric hindrance around the coupling partner, an *ortho*-terphenyl bearing two chiral axes, would be produced. An interesting feature of such an *ortho*-geometry would be the shared stereogenic environment between the two external aromatic rings (for example position and steric hindrance of Ar^1 will directly impact positioning of Ar^3). To exhibit double atropisomeric features, both axes should be at least tri-substitued, and thus two possibilities exist: type **A** products (Figure VII-11a) or type **B** products (Figure VII-11b). As the control of the second chiral axis is expected to depend on the steric differentiation between the two *ortho''* positions of the aryliodide, strategy **A** seemed more promising. Furthermore, we anticipated that strategy **A** would yield products with the absolute sense of chirality depicted in Figure VII-11a in a reliable way. Indeed the stereo-determining OA/RE steps for the Ar^2-Ar^3 axis would be much more favorable with the bulky *ortho''* substituent of Ar^3 pointing away from encumbered face of the biaryl, i.e. away from the *p*-tolyl substituent of the stereogenic sulfur atom.

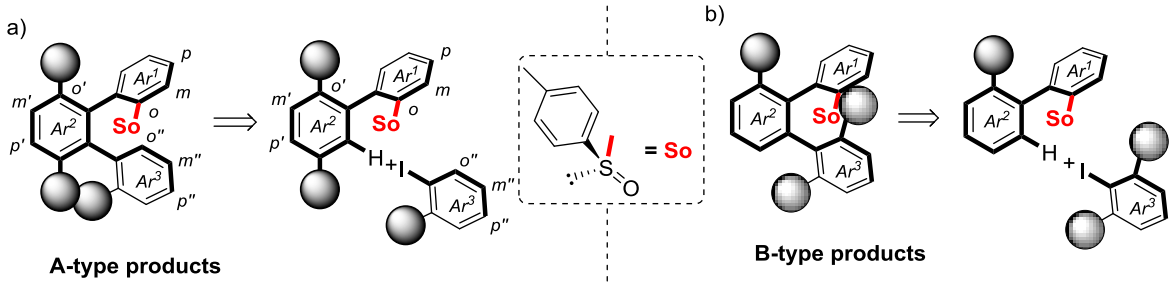

Figure VII-11 : strategies towards an *o*-terphenyl with two axes of chirality by direct arylation

Then, if such a challenging asymmetric direct arylation succeeded, the newly obtained scaffolds could be used as original stereogenic ligands. However, in order to build up such triaryles promising ligands, additional points need to be considered. Indeed the presence of two chiral axes is obviously not a sufficient condition to ensure chiral induction. As an example, if we consider the phosphine **1A** (Figure VII-12a); readily obtained from the corresponding sulfoxide after SO/Li exchange), although it will possess two axes of chirality, the "locked" conformation of Ar^3 causes the Ar^3-Me group to always point away from the phosphine-metal complex coordination sphere. Furthermore, the Ar^2-methoxy group is relatively far from the catalytic site. Therefore it stands to reason that it should not exhibit a much different chirality induction than the *o*-terphenyl **0A**. Thereby we developed the hypothesis that the asymmetric induction would not come directly from the presence of the two chiral axes, but rather from their substitution pattern considering an additional coordination site.

Type **A** *o*-terphenyls, with their Ar^1 and Ar^3 aromatic rings locked in their respective conformation exhibit a unique property : the possibility of *pseudo*-planar chirality. Considering the achiral [2.2]cyclophane introduction of an *ortho*-substituent gives the

planar chiral, *ortho*-substitued, [2.2]cyclophane (Figure VII-12b). This structure is similar to our general *o*-terphenyl structure. However, as seen before, just one substituent is not enough for chiral induction. A popular planar chiral ligand based on the cyclophane scaffold, phanephos exhibits the pseudo *ortho*-substitution pattern to achieve excellent chiral induction. Accordingly compound **2A**, with its *ortho/meta''*, pattern could be our *pseudo* planar chiral mimic (Figure VII-12).

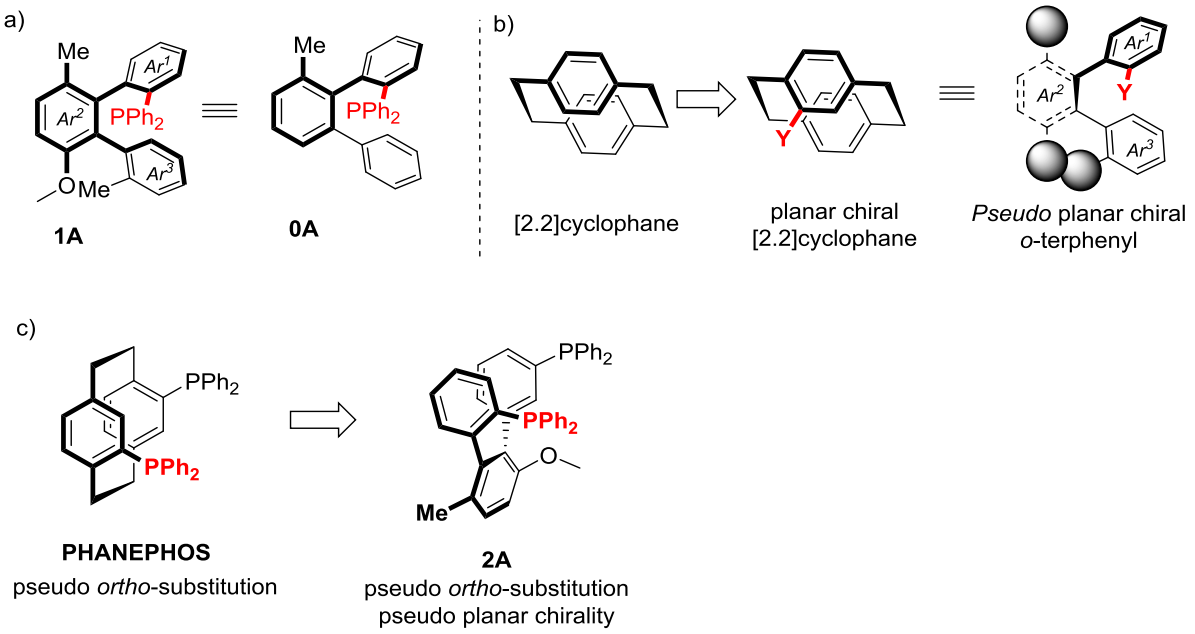

Figure VII-12 : *o*-terphenyls, cyclophane and pseudo planar chirality

Moreover preparation of such terphenyl scaffolds based on the convergent synthesis of three aromatic rings is highly advantageous. Indeed our goal is not only to design a *pseudo*-planar chiral equivalent of phanephos, but to go a step further by overcoming the limitation of the phanephos scaffold (*i.e*. restricted modularity on the phanephos scaffold; enantiopur ligands other than the diphosphine are difficult to obtain). By introducing different heteroatoms at the *meta''* position, followed by SO/Li exchange we could envisioned to access a large panel of hetero or homobidentate ligands. Furthermore varied substituents at the *para* and *para''* positions would permit the fine tuning of the electronic/steric properties of our ligands. A large library of a new class of enantioenriched ligands could be rapidly constructed (Figure VII-13).

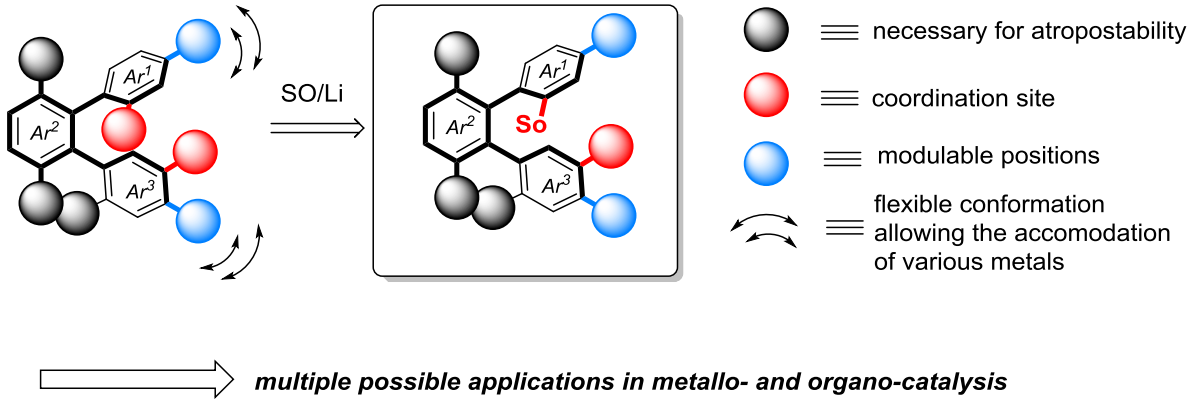

Figure VII-13 : stereogenic multi-functional bidentate scaffold

To build up such stereogenic terphenyl scaffolds, several synthetic challenges need however to be overcome, as testified by the scarcity of the literature examples related to such structures (Figure VII-14):

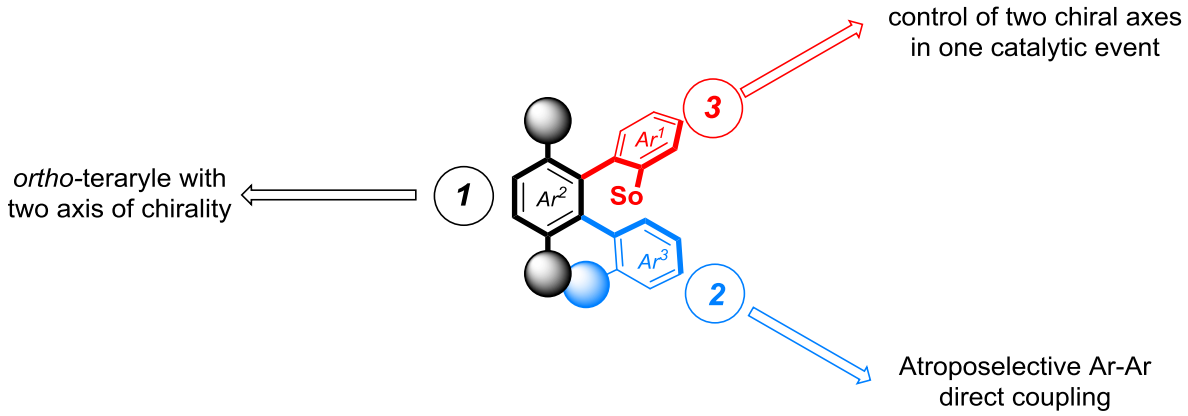

Figure VII-14 : specific challenges of bis-atropisomeric *o*-teraryls

challenge 1 (Figure VII-14): the first example of atroposelective synthesis of a teraryl with two axis of chirality was reported in 2004 by Takagi, Shibata and coworkers[371]. They astutely applied a three-component [2+2+2] cycloaddition of alkynes catalyzed by an iridium- enantiopur phosphine complex to a tethered dienyne symmetrically substituted by *ortho*-encumbered aromatics (Figure VII-15). Cycloaddition with a symmetrically substituted alkyne thus yielded *para*-teraryles in good yields and essentially perfect stereoselectivity. Furthermore the high (20 mol%) catalytic loading in Ir could be reduced to less than 1 mol% on the optimized reaction. This concept was extended to the synthesis of a noviaryl with eight (!) axis of chirality in 2004[372]. If these results are impressive, the relatively high temperature and the need for symmetrical substitution limit their general synthetic utility.

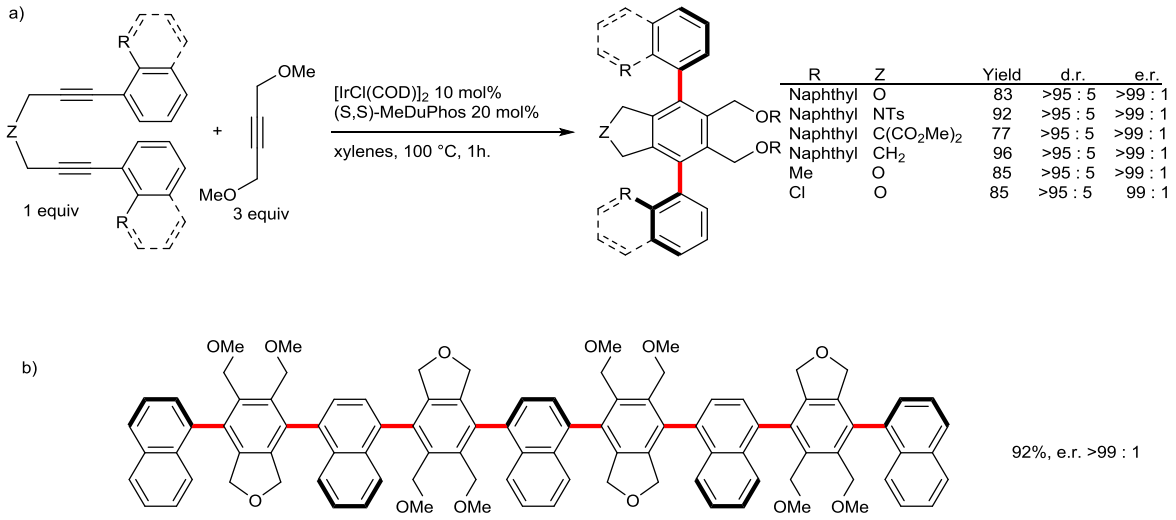

R	Z	Yield	d.r.	e.r.
Naphthyl	O	83	>95 : 5	>99 : 1
Naphthyl	NTs	92	>95 : 5	>99 : 1
Naphthyl	$C(CO_2Me)_2$	77	>95 : 5	>99 : 1
Naphthyl	CH_2	96	>95 : 5	>99 : 1
Me	O	85	>95 : 5	>99 : 1
Cl	O	85	>95 : 5	99 : 1

Figure VII-15 : iridium catalyzed *para*-teraryl formation

A similar strategy from Tanaka and coworkers in 2007[373] allowed the synthesis of *para*-teraryls with excellent enantioselectivities but deceiving diastereoselectivities (Figure VII-16). The use of rhodium allows the reaction to proceed at room temperature

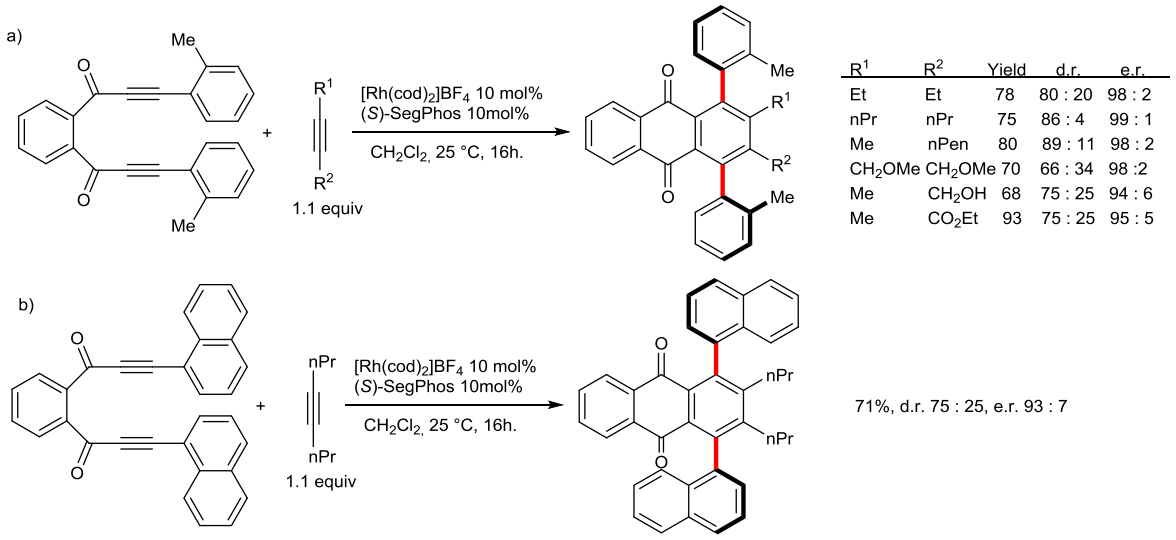

R^1	R^2	Yield	d.r.	e.r.
Et	Et	78	80 : 20	98 : 2
nPr	nPr	75	86 : 4	99 : 1
Me	nPen	80	89 : 11	98 : 2
CH_2OMe	CH_2OMe	70	66 : 34	98 :2
Me	CH_2OH	68	75 : 25	94 : 6
Me	CO_2Et	93	75 : 25	95 : 5

Figure VII-16 : rhodium catalyzed *para*-teraryl formation

An interesting *para*-teraryl bearing two chirality axes was reported in 2016 by Sun, Kürti and Xu (Figure VII-17). O-alkylation of a 1,2-dihydroxynaphthalene by an N-tosyl iminoquinone produced a centrally chiral intermediate that rearranges with central-to-axial chirality transfer towards a BINOL-type product. A second reaction yielded a *para*-teraryl with two axes of chirality, excellent yield and e.r.

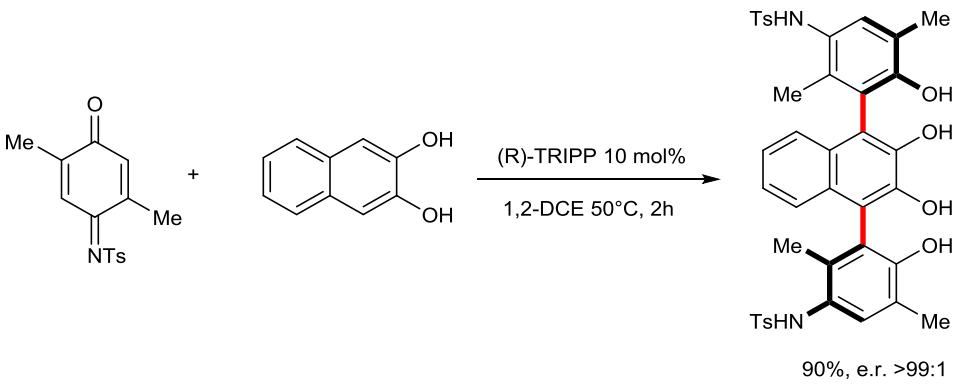

Figure VII-17 : organocatalytic synthesis of a *para*-teraryl

Concerning examples more closely related to the work presented in this manuscript, the synthesis of *ortho*-teraryls, only two examples, to the best of our knowledge, are known. In 2006 Shibata, Tsuchikama and Otsuka[374] used their iridum/DuPhos catalyst on a trienyne doubly tethered and substituted at the terminal alkynes by aromatics (Figure VII-18). Doubly atropisomeric terphenyls were thus obtained, with good to excellent yields, d.r. and e.r. Once again, the major limitation of this work resides in the preparation of only symmetrical scaffolds. However, it seems that careful construction of the trienyne might yield more diversified products, but the authors did not explore this possibility.

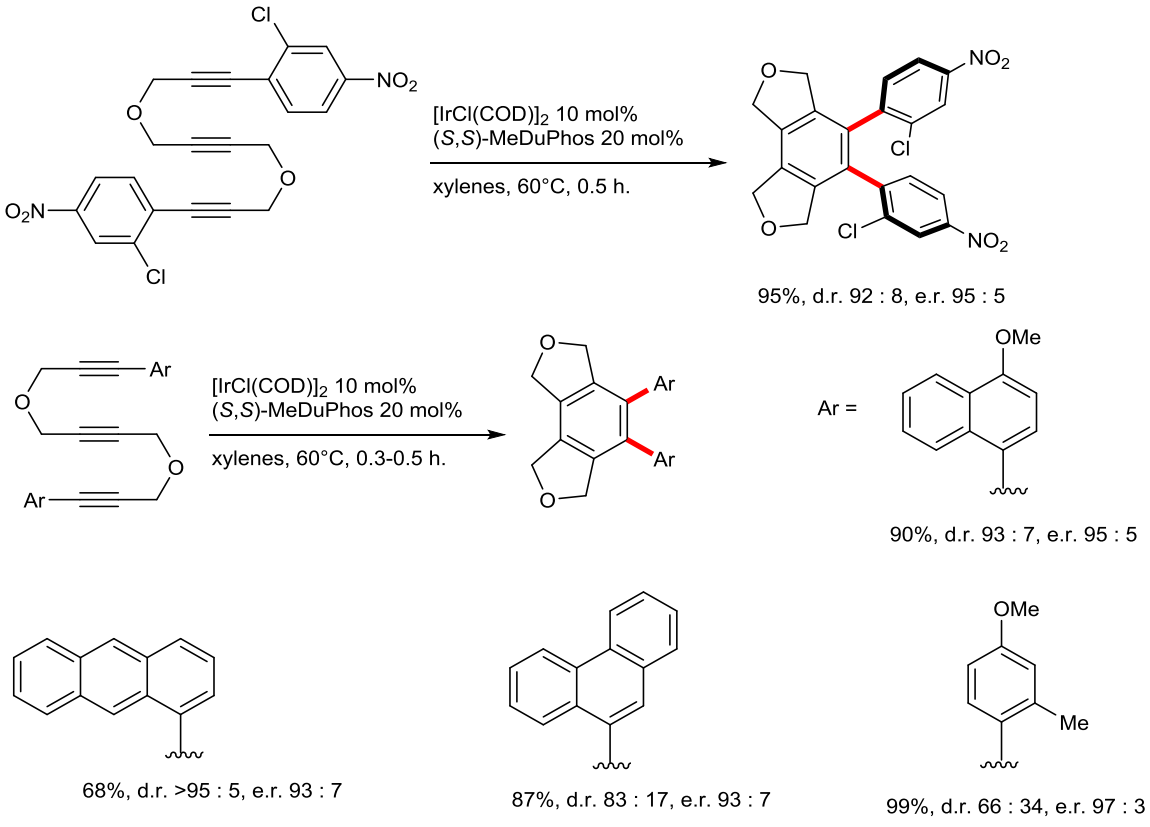

Figure VII-18 : enantioselective *ortho*-terphenyls formation

Finally in 2016 Lotter, Sparr and coworkers[375] report the second example of atroposelective synthesis of an *ortho*-teraryl (Figure VII-19). Their step by step, organocatalytic approach utilizes sequences of: 1) double alcohol oxidation to aldehydes 2) asymmetric organocatalytic aldol condensation mediated by L-*iso*leucine resulting in cyclization and aromatization. Very good yield and excellent d.r. were obtained.

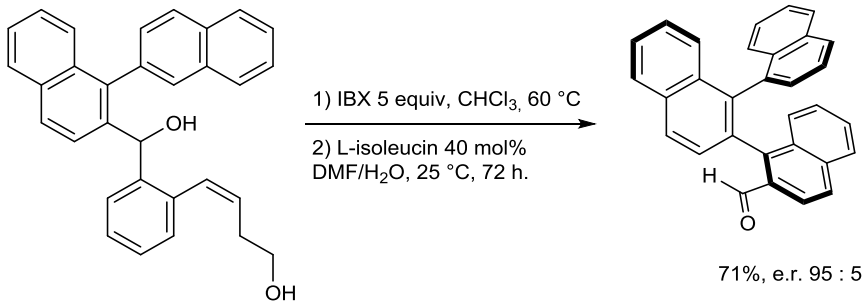

Figure VII-19 : organocatalytic *ortho*-teraryl formation

challenge 2 (Figure VII-14): A direct highly atroposelective coupling. No examples of higly (≥95:5) atroposelective Ar-Ar coupling by C-H activation were at the time reported in the literature. Only the work of Itami and coworkers on parented *undirected* direct arylation of thiophene yielded at best a product with 86:14 e.r.[68,376]. Since, Antonchick and coworkers[69] reported an atroposelective directed arylation *via* α-diazoketones with good yields and high e.r., but their methodology is not strictly speaking a direct arylation, and thus allowed little structural variation of the coupling partners.

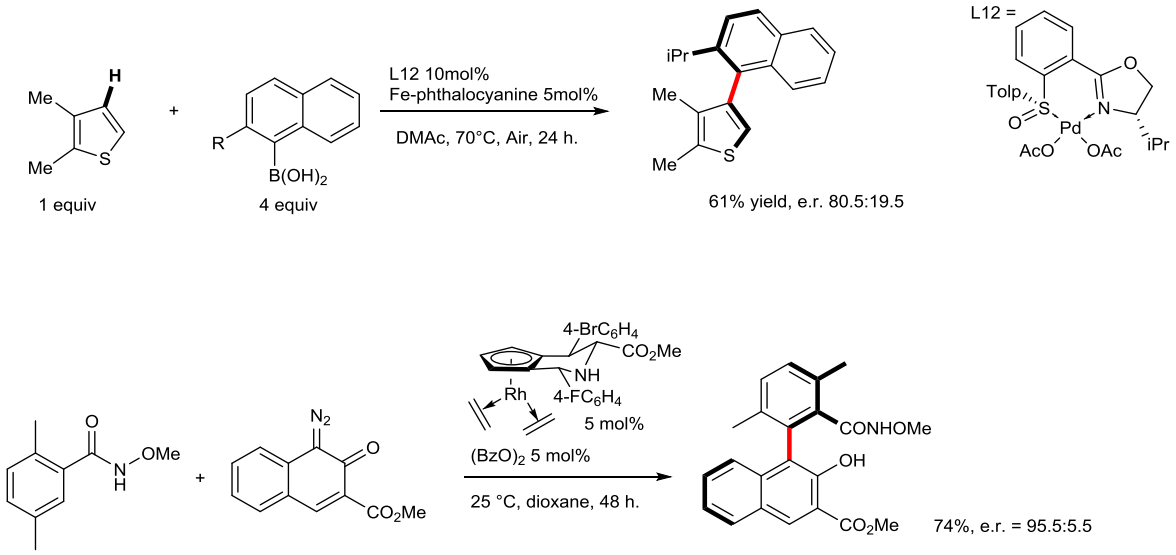

Figure VII-20 : atroposelective direct arylation

challenge 3 (Figure VII-14): The last challenge would reside in the need for the control of both chiral axes during the same catalytic event. Besides the work already presented, two other examples should be highlighted. In 2007, Hsung and coworkers report[377] (Figure VII-21) a rhodium catalyzed cycloaddition of an N-alkyne substituted oxazolidinone with a dienyne to afford products exhibiting both a C-C and a C-N chiral axis.

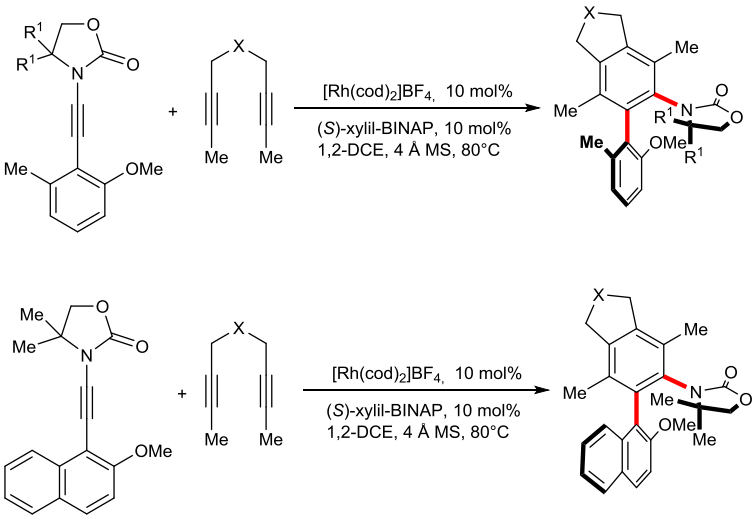

R^1	X	Yield	d.r.	e.r.
Me	$C(CO_2Me)_2$	93	86 : 14	>99 : 1
Me	O	92	83 : 17	>99 : 1
Ph	O	68	50 : 50	91 : 9

X	Yield	d.r.	e.r.
$C(CO_2Me)_2$	93	86 : 14	>99 : 1
O	92	83 : 17	99 : 1

Figure VII-21 : control of C-C and C-N axes in one event

In 2008 Tanaka and coworkers[378] (Figure VII-22) reported a closely related reaction delivering products with a C-C Ar-Ar atropisomeric axis and a C-C Ar-amide atropisomeric axis, with essentially perfect selectivities.

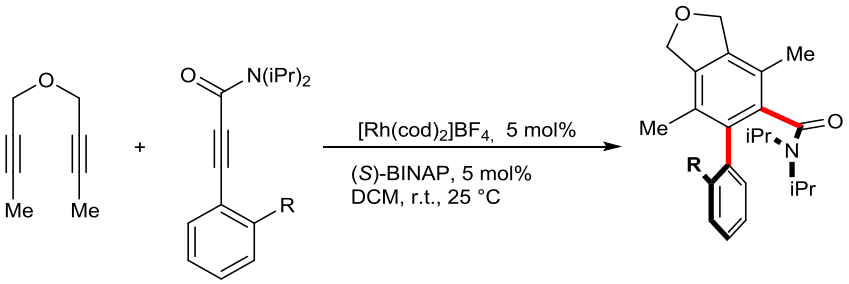

R	Yield	d.r.	e.r.
Me	91	>95 : 5	>99 : 1
Br	86	>95 : 5	>99 : 1

Figure VII-22 : control of two chiral axes in one event

C. Results and discussion

Considering the challenges in building a bis-atropisomeric *ortho*-terphenyl by means of an atroposelective direct arylation, the outset of our experimental work consisted in developing a robust method for the non-atroposelective direct arylation of biaryl-sulfoxide **1a**. No reaction occurred using a simple, ligand-free catalytic system (Table 1, entry 1) and only traces of the expected product were formed when adding a ligand (2,6-lutidine, **L77**)[263] and trifluoroacetic acid (TFA), together with a silver salt (Ag_2CO_3) in a mixed HFIP/DCE (1:1) solvent system (Table 1, entry 2). However, while performing the reaction in HFIP and at higher temperature (115 °C), high conversion of the starting material was observed (Table 1, entry 3). Replacement of 2,6-lutidine by a stronger **σ**–donor N-heterocyclic carbene precursors such as IMeHCl (**L78**) or commercially available IPrHCl **(L79)** allowed formation of **3aA** in very high yields and with excellent diastereo- and enantioselectivity (Table 1, entry 4-5, for details, see experimental section).

Table 2 : Optimisation of the direct arylation of 1a

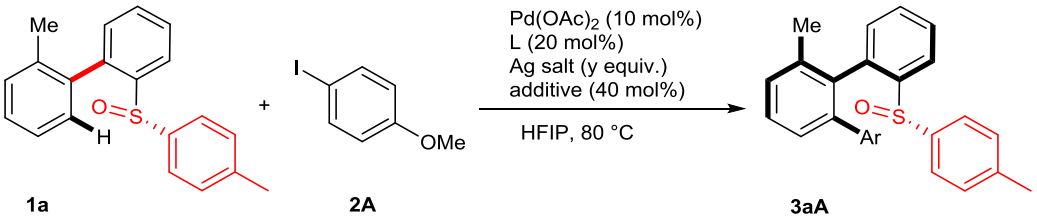

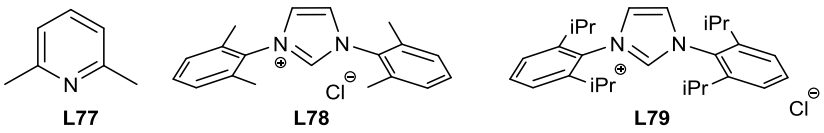

entry	L	Ag_{salt}	Additive	Conv. (%)	d.r. / e.r
1	-	AgOAc (2)	-	n.d.	n.d. / n.d.
2	L77	Ag_2CO_3 (1.5)	-	Traces	n.d. / n.d.
3	L77	Ag_2CO_3 (2)	TFA	80	95:5 / n.d.
4	L78	Ag_2CO_3 (2)	TFA	90	≥ 98:2 / >99:1
5	L79	Ag_2CO_3 (2)	TFA	> 90	98:2 / > 99:1

[a] : determined by ^{1}H NMR of the crude reaction mixture [b] : determined by chiral HPLC

With the optimized protocol in hands, the scope of this coupling was evaluated ([a] : for details see experimental section

Figure VII-23). Deceivingly, other electron rich or neutral Ar-I such as *p*-iodotoluene (**2B**) or iodobenzene (**2C**) performed poorly (less than 50% conversion). The addition of ethyl iodoacetate **4** as an additive restored the desired reactivity. Arguably, **4** acts as an organic oxidant rendering the catalytic system much more robust (regeneration of Pd(II)–catalyst from "deactivated" Pd(0) species, for details see experimental section). In presence of **4**, a highly efficient coupling between **1a** and both electron-rich and electron-poor Ar-I occurred, delivering targeted molecules with excellent atropoinduction (d. r. > 95 : 5). **3aA-3aF** were isolated in high yields (80 – 95%) but longer reaction times (14 h) were required to complete the reaction with arenes bearing electron-withdrawing substituents (**3aD**, **3aE**). Subsequently, the tolerance of our catalytic system towards different substituents of the biaryl-sulfoxide precursor was investigated. As foreseen, the arylation of **1b** worked well, but the desired product **3bA** was isolated in a significantly decreased optical purity of 61:39, certainly due to its partial atropo-racemization under the reaction conditions. In contrast, an excellent diastereoselectivity was observed for **3cA** and **3dA**, bearing respectively chloro- and trifluoromethyl-substituents. The absolute (*Sa*R) configuration of **3aE** was determined based on X-ray analysis and the configuration of all other compounds was attributed accordingly.

Following our initial goal of assembling the terphenyl scaffolds with two chiral axes, the coupling with sterically demanding *ortho*-substituted Ar-I was investigated. Encouragingly this challenging C-C bond formation still performed well with *o*-iodoanisole (**2I**), *o*-iodotoluene (**2J**), 1-iodonaphthalene (**2K**) and methyl 2-iodobenzoate (**2L**) delivering **3aI**-**3aL** in high yields (73 – 90%) ([a] : for details see experimental section

Figure VII-23). Importantly, these newly synthesized terphenyls contain already two chiral axis, ie. Ar^1-Ar^2 and Ar^2-Ar^3, but Ar^2-Ar^3 is not atropisomeric under reaction conditions.

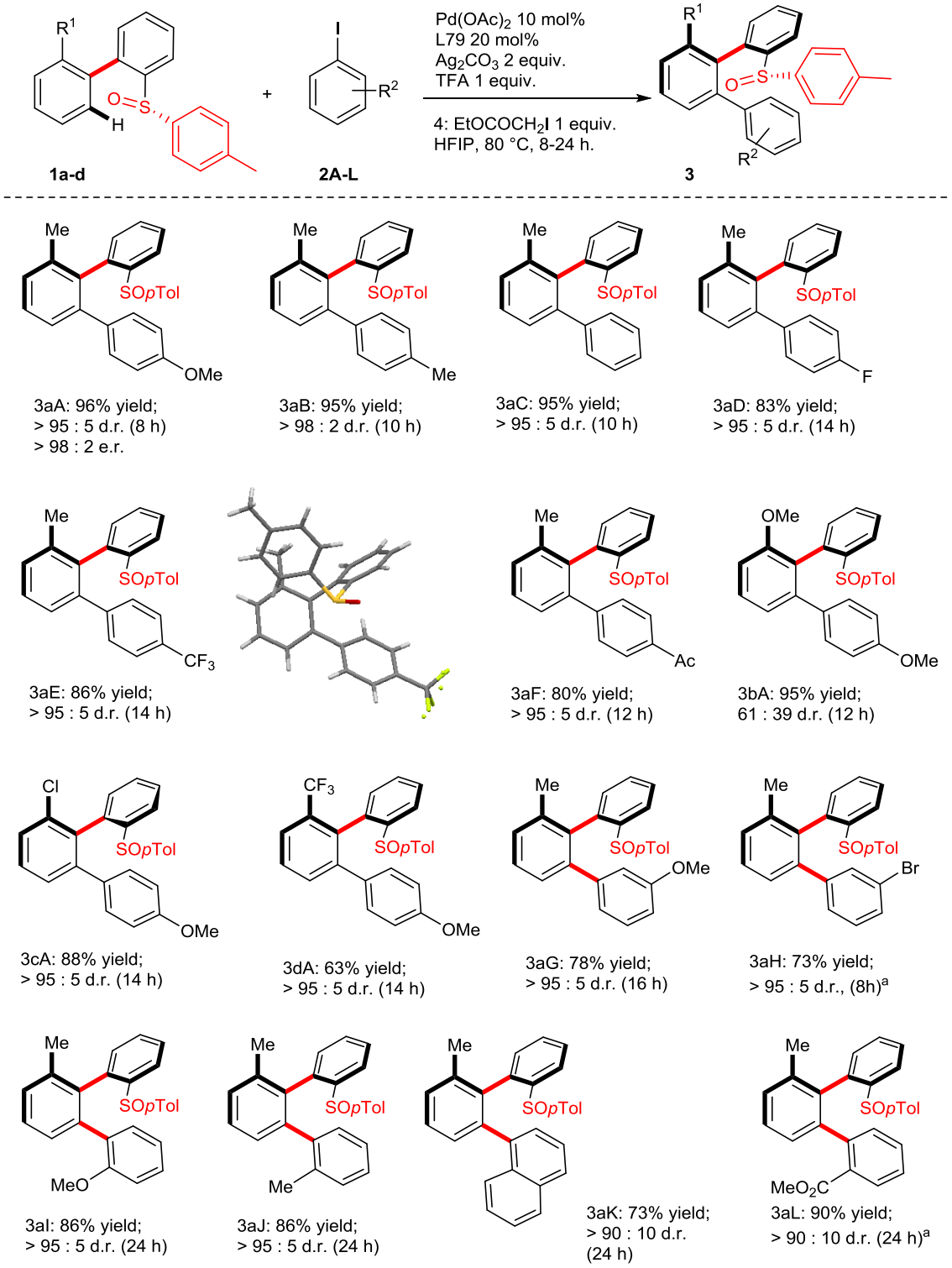

[a] : for details see experimental section

Figure VII-23 : Scope of direct arylation of biaryl sulfoxides 1a-1d.

Increased steric hindrance around the Ar^2-Ar^3 axis should warrant its atropostability. Following considerations presented in the introduction of this chapter, we selected the *meta*-OMe-substituted **1e** (the limited steric demand of OMe group, its electron-donating features and a possible "secondary-directing group" behavior) as a test substrate (Table 3). **1e** was therefore submitted to the standard reaction conditions in combination with *ortho*-iodotoluene **2J**, but only trace amount of the expected product was detected in LC-MS even after few days of reaction (Table 3, entry 1). Significantly increased catalyst loading (40 mol%) and a large excess of **2J** (6 equivalents) allowed formation of **3eJ**, albeit in a low 30% yield (Table 3, entry 2). Besides, the use of a large amount of $Pd(OAc)_2$ resulted in the generation of an undesired, acetoxylated product **5eOAc**, whereas under the "acetate-free" protocol (use of a well-defined NHC-Pd complex, $[IMePdCl]_2$) only trace amount of **3eJ** was formed (Table 3, entry 3). Likewise, $Pd(OPiv)_2$ precatalyst furnished C-O coupling product **5eOPiv** predominantly (Table 2, entry 4). Unexpectedly, the addition of more soluble silver salt such as AgTFA, AgOTf and $AgBF_4$ hampered the formation of this side product (it has been previously demonstrated that silver salts promote C-C coupling over C-O coupling in σ-aryl palladacycle intermediates bearing carboxylate ligands[299]), and when employing $Pd(TFA)_2$ catalyst, together with AgTFA additive, the expected terphenyl was delivered in 70% yield (Table 3, entry 5). Excitingly, ^{1}H NMR analysis of **3eJ** clearly indicates its high diastereopurity, demonstrating that both chiral axis might be set in a single step (dr > 10 : 1). Further optimization of the reaction conditions revealed: 1) the detrimental impact of water (Table 3, entry 6); 2) the negative effect of an increased concentration of both, the coupling partner **2J** and the catalyst (Table 3, entry 7); 3) suppression of the direct alkylation side reaction by replacing ethyl iodoacetate **4a** by ethyl bromoacetate **4b** (Table 3, entry 8 vs. 9). Consequently, **3eJ** was isolated in satisfactory yield of 64% and as a sole atropisomer (d.r. = 25.6 : 1, Table 3; entry 9 ; after recrystallization d.r. > 98 : 2), albeit using large catalyst loading (25 mol% of palladium). Significantly more reliable catalytic system was obtained adding an optimized amount of molecular sieves (MS) (Table 3, entry 10). Under this modified protocol not only reproducibility was guaranteed, but also the amount of silver salts could be significantly reduced. Accordingly, using $Pd(TFA)_2$ (25 mol%), AgTFA (1 equiv.) and Ag_2CO_3 (2.5 equiv.) and adding 25 mg/mL of molecular sieves, the desired terphenyl product was isolated after 4 hours, as an atropoisomerically pure product in a yield of 49% (Table 3, entry 10). Importantly, this optimized amount of MS allowed the catalyst loading to be reduce for more reactive coupling partners (for details see experimental section).

Table 3 : Optimisation of the arylation between two ortho-substituted partners.

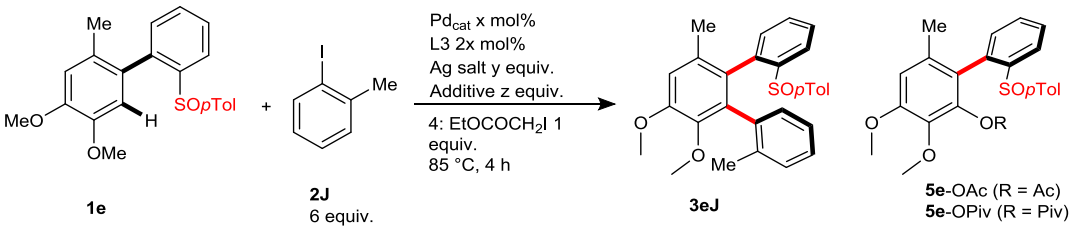

Entry	Pd (x mol%)	Ag salt (y equiv.)	Additive	3 (%)[a]	d.r.[b]
1[c]	$Pd(OAc)_2$ (10)	Ag_2CO_3 (2)	TFA (40)	< 5	-
2[d]	$Pd(OAc)_2$ (40)	Ag_2CO_3 (2)	TFA (40)	30	nd
3[e]	$(IMe\text{-}PdCl)_2$ (20)	Ag_2CO_3	TFA (40)	< 5	-
4[f]	$Pd(OPiv)_2$ (40)	Ag_2CO_3	TFA (40)	10	-
5	$Pd(TFA)_2$ (40)	Ag_2CO_3 (2) AgTFA (1)	-	70	≥ 10:1
6	$Pd(TFA)_2$ (40)	Ag_2CO_3 (2) AgTFA (1)	H_2O (5%)	< 5	-
7[g]	$Pd(TFA)_2$ (40)	Ag_2CO_3 (2) AgTFA (4)	3 Å MS	30	nd
8[h]	$Pd(TFA)_2$ (25)	Ag_2CO_3 (2) AgTFA (5)	3 Å MS[i]	55	> 10:1
9[h,j]	$Pd(TFA)_2$ (25)	Ag_2CO_3 (2) AgTFA (5)	3 Å MS[i]	64	> 26:1[k]
10[c,l]	$Pd(TFA)_2$ (25)	Ag_2CO_3 (2.5) AgTFA (1)	4 Å MS[m] (25 mg/mL)	49	> 20:1

a) determined by ^{1}H NMR; b) d.r. of Ar^2-Ar^3 axis was determined on crude mixture by ^{1}H NMR; c) 2 equivalents of **2I**; d) **5e-OAc** was isolated in 30% yield; e) IMe-HCl (40 mol%) was added; f) **5e-OPiv** was isolated in 60% yield; g) 5 equivalents of EtO-$COCH_2Br$, 10 equivalents of 2I; h) 3.5 equivalents of **2I**; i) beads; j) $EtOCOCH_2Br$ (3.5 equiv.) was used instead of $EtOCOCH_2I$ (3.5 equiv); k) d.r. of isolated product = 25.6 : 1; l) reaction conducted for 4 hours at 85 °C; m) powder.

Once the feasibility of this challenging transformation validated, its scope was explored (Figure VII-24). The coupling of **1e** with electron-rich 2-iodotoluene derivatives **2J**, **2M** and **2N** occurred smoothly delivering **3eJ**, **3eM** and **3eN** in moderate to good yields, with no loss of the atroposelection. Importantly, introduction of an additional electron-donating substituent *para* to the iodide on **2** increased the reactivity of this coupling partner and therefore **3eM** and **3eN** were prepared using a decreased catalytic loading of 15 mol%. Introduction of a third electron-donating substituent (as with 2,3,4-trimethoxyiodobenzene) was detrimental. In contrast, less electron-rich biaryl substrate **1f** was more effective than **1e** as the desired arylation could be achieved with only 10 mol% of Pd (**3fJ**, **3fM-N**). This higher reactivity can be tentatively at-

tributed to the increased electron density at C'2 position due to the disappearance of the inductive effect of the C'4-OMe group, resulting in an higher reactivity of the palladacycle intermediate. This coupling tolerates well the presence of a Cl-atom (**2P**), leading to the formation of **3fP**, product suitable for further functionalization, in 70 % yield. Likewise, isolation of brominated scaffolds **3fQ** and **3fR** in decent yields of 49 and 51%, is remarkable. Worth of highlightening is also formation of potentially bi-coordinating skeletons such as **3fS** and **3fT**, bearing N-phthalamide (Phth) and OMe groups respectively. Besides, the *ortho*-position of the aryl-iodide may also be substituted by other motifs, such as a Cl-atom or an OMe group (products **3fU** and **3fI, 3fV**). The decreased steric hindrance around the Ar^2-Ar^3 axis for **3fI** and **3fV** resulted, however, in a slight decrease of the atroposelectivity. Outstandingly, even more sterically demanding Me substituent could be introduced at the key, *meta* position of Ar^2. In this case the coupling is clearly more challenging, bar **3gT** and **3gI** could still be isolated as atropoisomerically pure compounds, but needed a higher reaction temperature (115 °C). Finally, biaryls precursors bearing both electron-donating and electron-withdrawing substituents on Ar^1 (*meta* to the sulfoxide auxiliary) performed well under the standard reaction conditions, delivering **3hR**, **3iR**, **3jR**, **3kR** and **3lR** in 44-67% yields. Noteworthy, recrystallization of **3eN** provided an analytically suitable crystal and the X-ray diffraction analysis allowed determination of its absolute configuration. The absolute configuration of other coupling products was attributed accordingly.

Figure VII-24 : Scope of the terphenyls with two chirality axes; (4 diastereomers could be potentially obtained and 3 of them were identified on crude ^{1}H NMR)

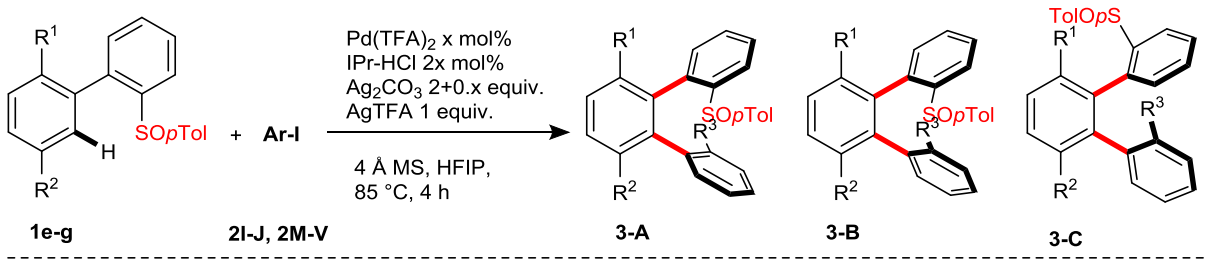

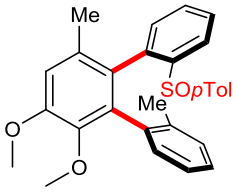

3eJ: 83% conv. (25 mol% Pd)
49 : 2 : 1 d. r. (crude)
49% yield; 98 : 2 d. r.

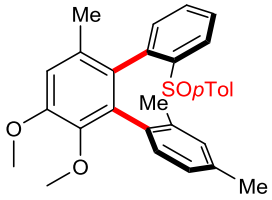

3eM: 96% conv. (15 mol% Pd)
22 : 1 : 1 d. r. (crude)
73% yield; 98 : 2 d. r.

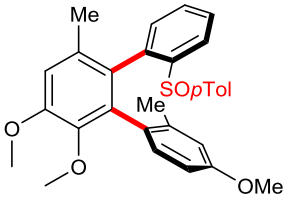

3eN: 90% conv. (15 mol% Pd)
21 : 1 : 0 d. r. (crude)
65% yield; 98 : 2 d.r.

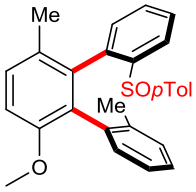

3fJ: 56% conv. (10 mol% Pd)
23 : 2 : 1 d. r. (crude)
44% yield ; 98 : 2 d. r.

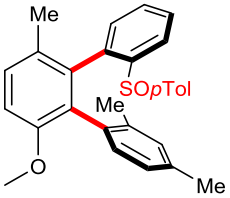

3fM: 80% conv. (10 mol% Pd)
45 : 2 : 1 d. r. (crude)
62% yield; 98 : 2 d. r.

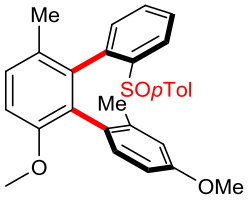

3fN: 96% conv. (10 mol% Pd)
213 : 4 : 1 d. r. (crude)
63% yield; 98 : 2 d. r.

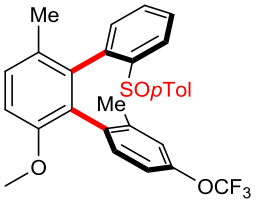

3fO: 76% conv. (15 mol% Pd)
62 : 2 : 0 d. r. (crude)
49% yield; 98 : 2 d. r.

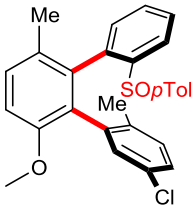

3fP: 95% conv. (20 mol% Pd)
53 : 2 : 1 d. r. (crude)
70% yield; 97 : 3 d. r.

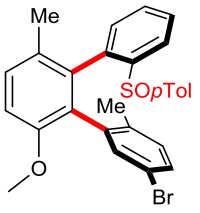

3fQ: >95% conv. (25 mol% Pd)
20.4 : -[b] : 1 d. r. (crude)
49% yield; > 98 : 2 d. r.

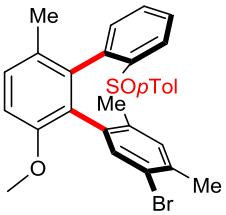

3fR: >95% conv. (20 mol% Pd)
22.4 : - [b]:1 d. r. (crude)
51% yield; 97 : 3 d. r.

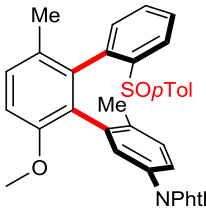

3fS: 95% conv. (35 mol% Pd)

59% yield[a]; 98 : 2 d. r.

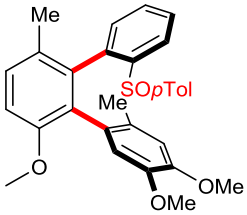

3fT: 97% conv. (15 mol% Pd)
29 : 2 : 1 d. r. (crude)
53% yield; 98 : 2 d. r.

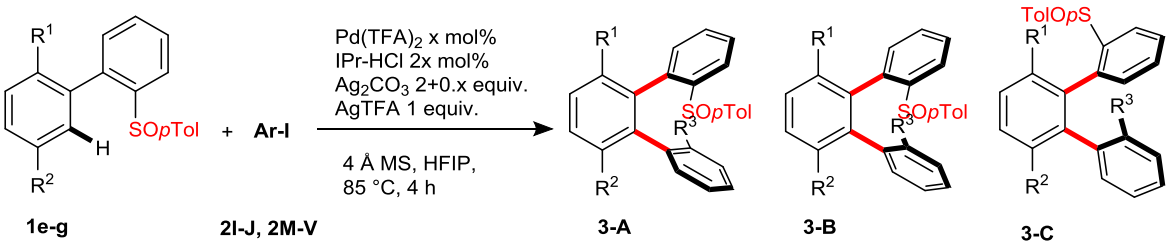

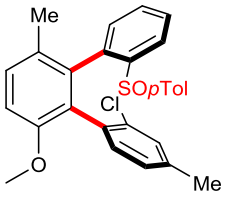

3fU: 89% conv. (20 mol% Pd)
625 : 1 : 10 d. r. (crude)
69% yield.; 97 : 3 d. r.

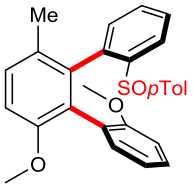

3fI: 84% conv. (10 mol% Pd)
6 : 1 : 1 d. r. (crude)
66% yield; 97 : 3 d. r.

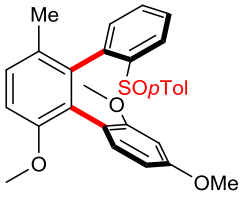

3fV: 76% conv. (10 mol% Pd)
78 : 16 : 1 d. r. (crude)
33% yield; 94 : 6 d. r.

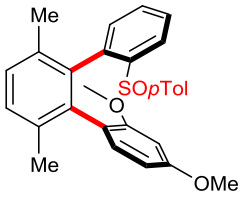

3gV: 55% conv. (30 mol% Pd)
15 : 2 : 0 d. r. (crude)
24% yield; 94 : 6 d. r.

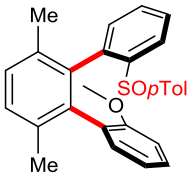

3gI: 39% conv. (30 mol% Pd)
24 : 2 : 0 (crude)
16% yield; 98 : 2 d. r.

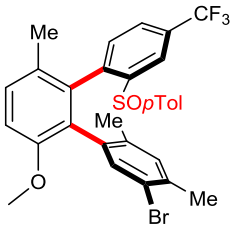

3hR: >95% conv. (20 mol% Pd)
64 : 2 : 3 (crude)
49% yield; 98 : 2 d. r.

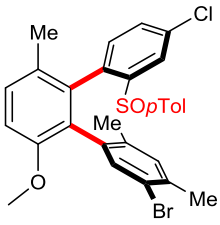

3iR: >95% conv. (20 mol% Pd)
223 : 4 : 1 d. r. (crude)
67% yield; 98 : 2 d. r.

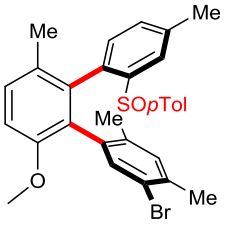

3jR: >95% conv. (20 mol% Pd)
54 : 1 : 0 d. r. (crude)
68% yield; 98 : 2 d. r.

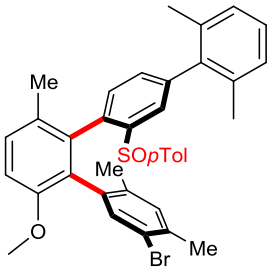

3lR: >95% conv. (20 mol% Pd)
37 : 1 : 0 d. r. (crude)
44% yield; 98 : 2 d. r.

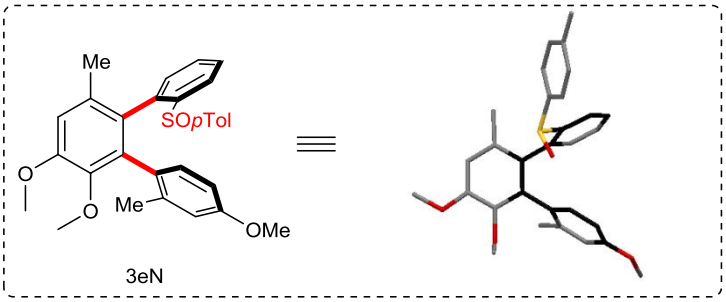

a : For details see experimental part; b : not determined due to overlapping signals; crude d.r. = A/B/(C+D) diastereomers; isolated d.r. = A/(B+C+D) diastereomers

The unique stereoselective outcome of this transformation arises from the fact that two chiral axis can be perfectly controlled in a single transformation delivering one

diastereomer out of eight possible. In order to unambiguously prove the optical purity of the obtained products and characterize these unique scaffolds, few fundamental tests were performed and the rotational barriers for several compounds were determined. Firstly, the diastereomeric and enantiomeric purity of **3aA** was proved by chiral HPLC analysis. As **3aA** is atropostable even at 200 °C (Figure VII-25a; no significant modification of its d.r. was evidenced after thermal treatment), the rotational barrier for the Ar^1-Ar^2 axis could not be determined experimentally. The DFT studies allowed however to calculate a very high rotational barrier of 37.1 kcal/mol for a related product **3aC;** this translate to an half-life of racemization $t^{1/2}$ = ~3 hours at 200 °C. Importantly, as both atropodiastereomers of **3aA** are equally stable and as the rotation around the Ar^1-Ar^2 axis cannot occur under the reaction condition, the stereoinduction observed is kinetically controlled. Furthermore, this very high rotational barrier allowed us to study the thermal epimerization of the Ar^2-Ar^3 axial without interference from Ar^1-Ar^2. Atropodiastereomerically pure **3fM** was therefore subjected to thermal treatment (heating at 200 °C in mesitylene) and after 30 min racemization of the Ar^2-Ar^3 axis was evidenced. Thus, the kinetics of atropisomerization of the Ar^2-Ar^3 axis of product **3fM** were followed at 140 °C in $C_2Cl_4D_2$ until equilibration (K_{eq} = 0.92; Figure VII-25b). The rotational barrier of 32.5 kcal/mol was thus measured experimentally, which translate to $t^{1/2}$ = ~39 days at 85°C. Importantly, the computed value of $\Delta G^{\ddagger}$ of 32.7 kcal/mol for this compound was found, proving excellent correlation between experimental measurements and DFT calculations. In case of **3gI**, a slightly lower energy of 28.8 kcal/mol is required for atroporacemization ($t^{1/2}$ = ~ 10 hours at 85°C Figure VII-25b). Finally, as both atropodiastereomers of **3fM** and **3gI** are equally stable (DFT calculation), and as their atropimerization half-life are relatively long compared to the reaction time, the chiral induction during Ar^2-Ar^3 bond formation is under kinetic control.

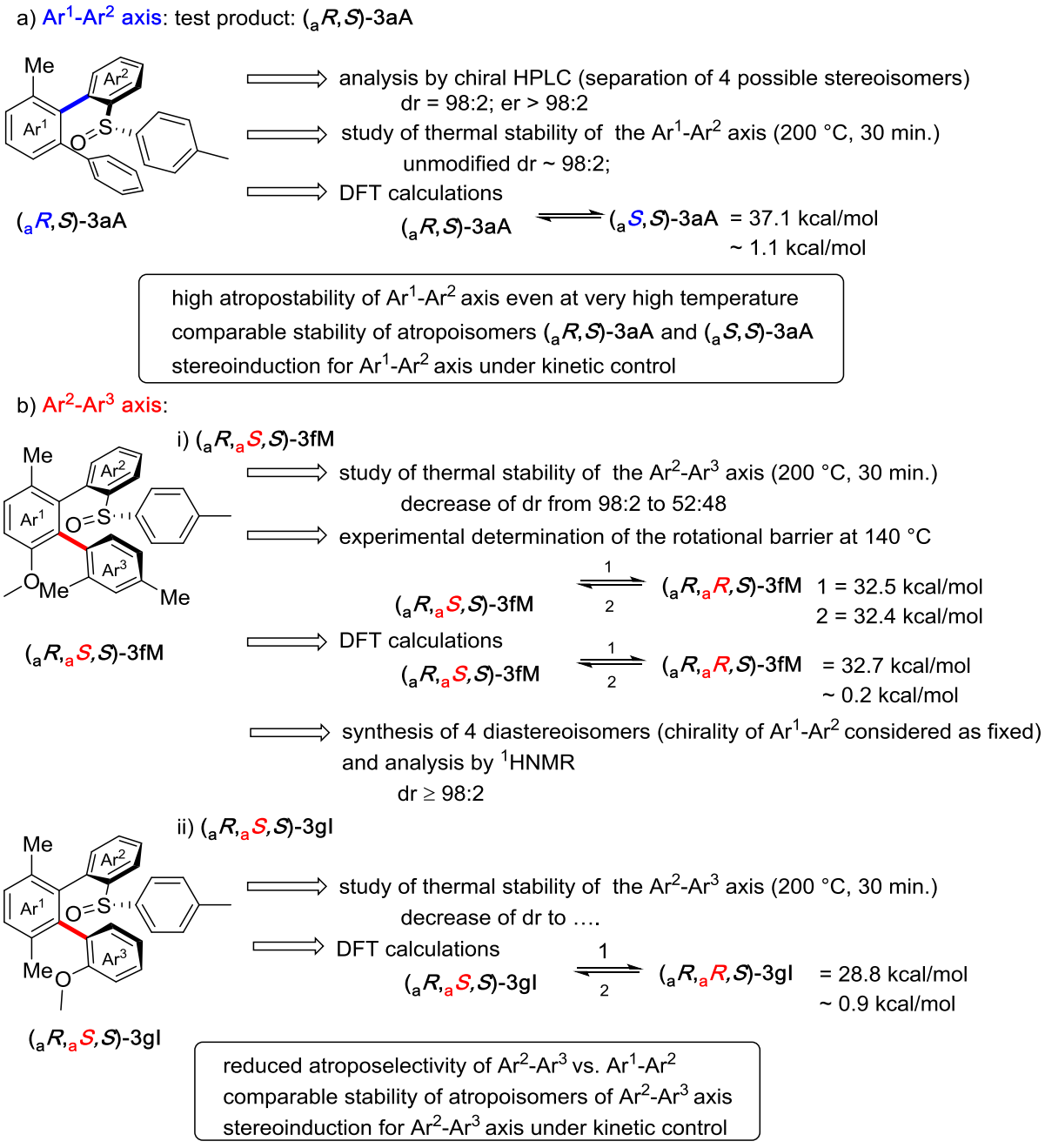

Figure VII-25 : atropostability study

To complete this study some mechanistic investigations have also been conducted. Firstly, crossed mechanistic experiments concerning the C-H cleavage step were undertaken, as we used two different set of conditions on two different types of substrates (Conditions **A** (non-anhydrous) from [a] : for details see experimental section

Figure VII-23 for substrate **1a**. Conditions **B** (anhydrous) from Figure VII-24 for substrate **1f**). Thus the deuterated substrates **1a** and **1f** were prepared and the reversibility of the C-H cleavage step was examined (Figure VII-26a) in the two different reaction settings. As we expected, significant D/H scrambling occurred under non-anhydrous conditions regardless of the substrate used. Indeed water, generated as a

side-product generated during reaction accelerates dehydropalladation[199]. In contrast D/H scrambling was negligible in anhydrous conditions. Next intermolecular competition KIE experiments were conducted for substrate **1a** and **1j** with coupling partner **2M,** both in conditions **B** (irreversible C-H cleavage). Similar values of KIE (1.66 for arylation of **1a** and 1.58 for arylation of **1f**) were measured (Figure VII-26b). These values indicate that the palladation step is not-turnover limiting, and that the turnover limiting step should occur later in the catalytic cycle[278] (probably either oxidative addition step or reductive elimination step). In conclusion, substrates **1a** and **1j** exhibit similar comportments in reversibility and KIE experiments, and therefore probably undergo closely related catalytic cycle when submitted to the same conditions.

+

Figure VII-26 : KIE and reversibility test

Subsequently, in order to characterize the key intermediates, we endeavored on preparation of the metallacyclic species (Figure VII-27). Rewardingly, reaction between **1a** and a stoichiometric amount of $Pd(OAc)_2$, in presence of base, followed by ligand exchange, delivered a dimeric metallacyclic complex **6**. In presence of the NHC, **6** was easily converted into the well-defined, atropisomeric Pd-NHC complex **7** isolated by chromatography. The X-Ray structure of **7** clearly illustrates formation of the palladacyclic intermediate via coordination of the catalyst by the S-atom. Interestingly, the crystalline structure of **7** indicates that the Ar^1-Ar^2 axis has the same configuration as the product, indicating that the axial chirality could be controlled at this step. Indeed when monocrystals of **7** were dissolved in $CDCl_3$ and an ^1H NMR spectra showed only one atropisomer at 25 °C. Furthermore, low- and high-temperature NMR of **7** did not reveal any atropisomerization, thereby showing that the rotational barrier of **7** is augmented compared to **1a** which is not atropisomeric at 25 °C. However, when **7** was used as the catalyst in the reaction of **1f** with **2N** in conditions **B** (anhydrous) little product formation was observed, showing that **7** is not a true catalytic intermediate. Nevertheless, in order to support the role of a close analogue of **7** as a key intermediate of the catalytic transformation, reductive elimination from **7** was explored. In absence of silver salt only small amount of the terphenyl product was obtained and reactions using only one source of Ag were low yielding. **3aA** was formed quantitatively when both additives were introduced simultaneously. Quite surprisingly, metallacyclic intermediate resulting from the palladation of **1f** could not be obtained although several different reaction conditions were tested (for details on experiment on the palladacycles, see the experimental section).

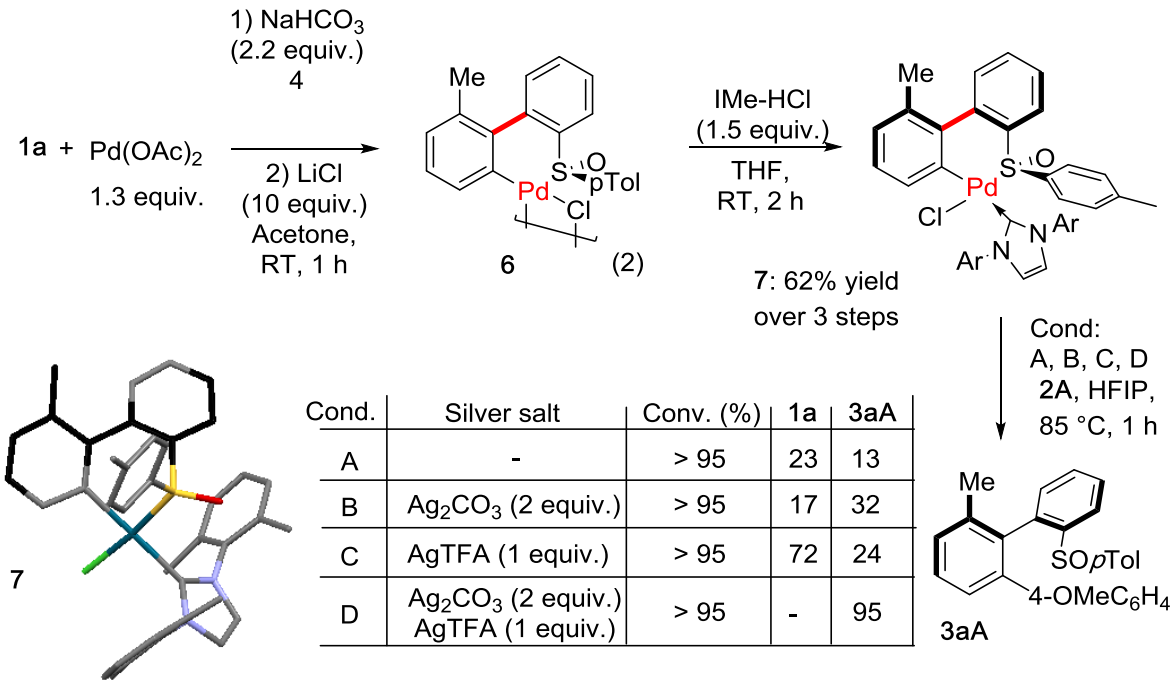

Cond.	Silver salt	Conv. (%)	1a	3aA
A	-	> 95	23	13
B	Ag_2CO_3 (2 equiv.)	> 95	17	32
C	AgTFA (1 equiv.)	> 95	72	24
D	Ag_2CO_3 (2 equiv.) AgTFA (1 equiv.)	> 95	-	95

Figure VII-27 : Synthesis and reactivity of palladacyclic intermediate

Based on these experiments and literature precedents, it can be reasonably speculated that a general catalytic cycle of this transformation implies 4 fundamental steps, ie. 1) precoordination of the Pd-catalyst by the sulfoxide moiety, 2) low-energy demanding direct metallation of the C-H bond, 3) oxidative addition of the coupling partner (**2**) generating Pd(IV)[379–382] intermediates and 4) reductive elimination delivering the desired coupling product along with the regenerated catalyst. These initial studies suggest oxidative addition or reductive elimination to be the rate determining step.

The originality of this transformation comes from the unique possibility to control both axial chiralities in a single transformation (Figure VII-28). Isolation of the atropisomerically pure palladacyclic intermediate **7** clearly suggests that the stereoselectivity of Ar^1-Ar^2 axis is induced during the C-H cleavage. Indeed, under the reaction conditions biaryls substrates are not configurationally stable and the rotation around Ar^1-Ar^2 axis occurs. In contrast, variable temperature studies of **7** suggest that the formation of the palladacyclic intermediate bearing a NHC ligand significantly increases the rotational barrier of Ar^1-Ar^2 axis rendering racemization unlikely. The stereochemical outcome of this step can be rationalized considering steric hindrance during the formation of the palladacycle intermediate. When diastereomer (a*R*,*S*)-**1** reacts with the NHC-Pd catalyst, the interactions between the chiral auxiliary and the NHC ligand are minimized (*p*-tolyl moiety above the plane vs. NHC ligand underneath the plane). In contrast, palladation of (a*R*,*S*)-**1** would require accommodation of the bulky ligand and *p*-tolyl group in the same plane. Accordingly, taking into account 1) rapid interconversion of (a*R*,*S*)-**1** and (a*S*,*S*)-**1**, 2) irreversibility of the C-H activation step and 3) high atropostability of the palladacyclic intermediate, it can be reasonably surmised that palladiation of (a*S*,*S*)-**1** is strongly disfavored and the transformations implies Dynamic Kinetic Resolution. In contrast, chirality of the Ar^2-Ar^3 linkage arises

from the favored oxidative addition of the Ar-I coupling partner from a sterically less congested face of the metallacyclic intermediate, ie. by minimizing the steric hindrance between the SO*p*Tol moiety and the *ortho*-substituent of the Ar-I coupling partner. In addition, reductive elimination from such a sterically less congested Pd(IV) intermediates seems also enhanced.

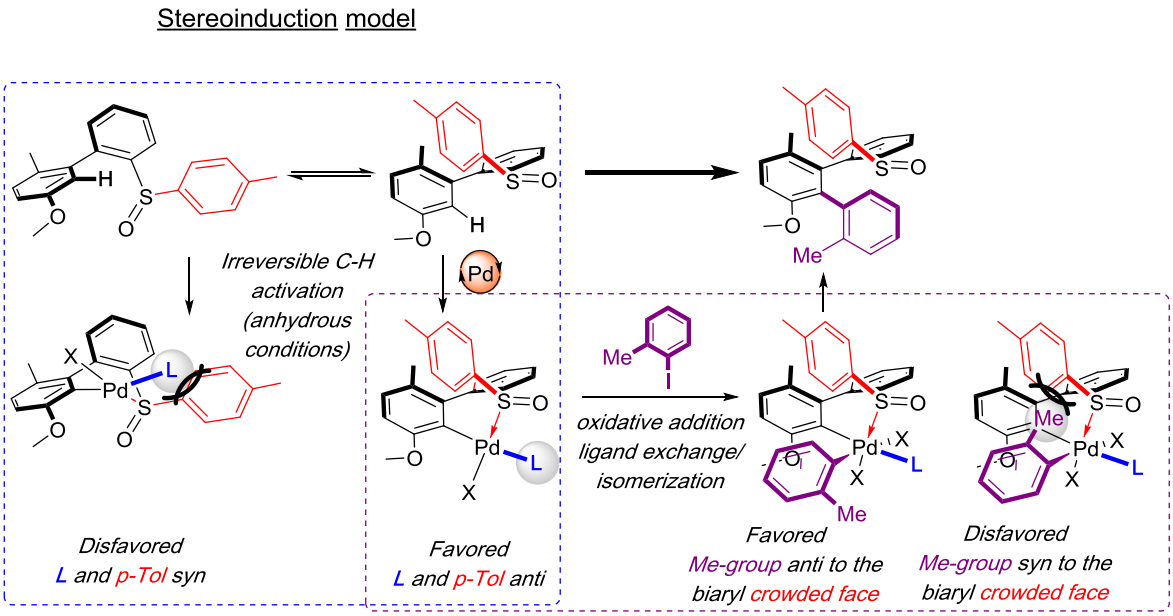

Figure VII-28 : stereoinduction model

To demonstrate the synthetic value of this unprecedented transformation we further focused on a large-scale synthesis of the bis-atropisomeric **3fP** (Figure VII-29). Enantiopure substrate **1f** was firstly prepared at gram scale, in 3 steps (53% overall yield) from inexpensive precursors, ie. 3-bromo-4-methylphenol and 1-bromo-2-iodobenzene, using only cheap reactants and catalysts and without the need for column chromatography. The large scale direct atroposelective arylation with **2P** occurred smoothly, furnishing 774 mg of optically pure **3fP** (65% yield).

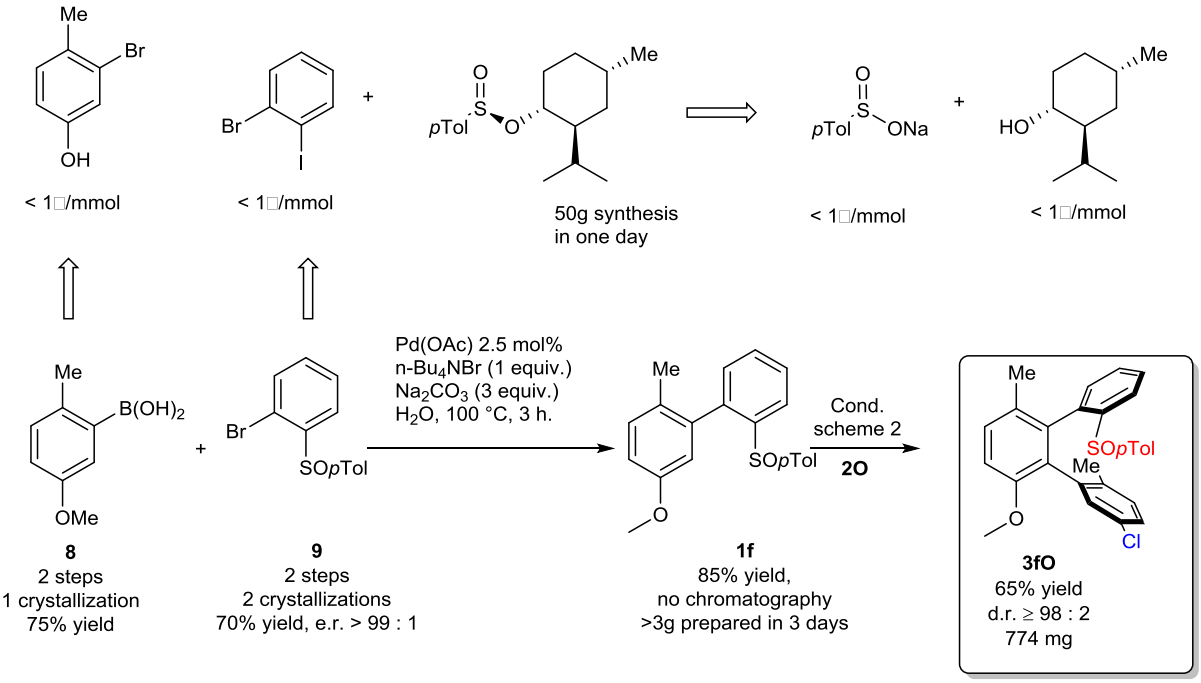

Figure VII-29 : large scale synthesis of 3fP

Subsequently, benefiting from a traceless character of the sulfoxide moiety, post-modifications of **3fP** were undertaken (Figure VII-30). Rewardingly, removal of the directing group *via* sulfoxide/lithium exchange and subsequent trapping with CO_2, HCO_2Et or PPh_2Cl went smoothly, delivering the corresponding enantiomerically pure products **8**, **9** and **10** in moderate to high yields. Importantly, the diastereomeric ratio and the enantiomeric ratio of **10** were confirmed to be >98 : 2, and its absolute configuration proved by X-ray analysis, yet confirming that our methodology is well-suited to offer optically pure, diverse and unique scaffolds.

Indeed the key application of the newly obtained terphenyls with two chiral axis concerns their use as unprecedented, chiral ligands exhibiting a pseudo-planar chirality. Towards this goal bromo-substituted **3aI**, **3fQ** and **3fR** were subjected to a double lithiation reaction followed by electrophilic trapping with PPh_2Cl (Figure VII-30). The simultaneous sulfoxide and bromine exchanges occurred smoothly and the desired diphosphine ligands DoaxPhos (**13a-c**) were isolated in good to fair yields (75, 54 and 57%). DoaxPhos ligands constitute the first example of a new class of chiral ligands presenting this original tridimensional structure.

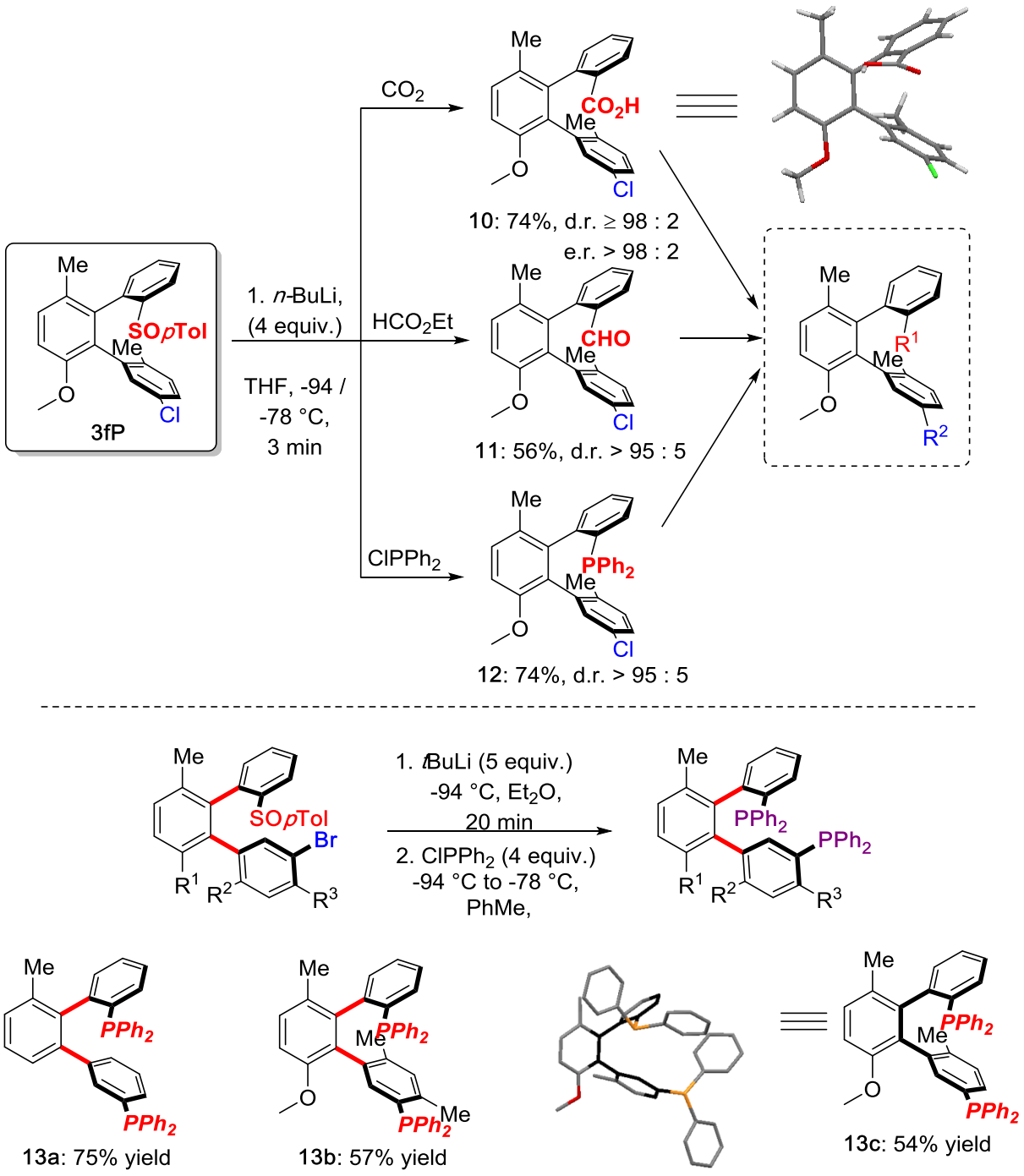

Figure VII-30 : Post-functionalization of terphenyl scaffolds.

In order to evaluate the catalytic activity of these ligands in an industrially relevant transformation, we embarked on Rh-catalyzed hydrogenation of olefins, and more precisely on the hydrogenation of amino acids precursor, a standard test for new chelating diphosphines (Table 4). Reduction of disubstitued alkene **14a** was achieved using terphenyl diphosphines exhibiting only one atropisomeric axis (**13a**), but a racemic product was obtained. This might be due to the conformational freedom of the Ar^2–Ar^3 in **13a** which will result in the formation of a bridged complex rather than a chelate one, as it is known for diphosphines that can form a 10 membered ring[383]. In contrast, the rigid structure of **13b** and **13c** ensured by the presence of the second

chiral axis resulted in good stereoinduction delivering products with 92:8 and 97.5:2.5 enantiomeric ratios. Even more promising results were obtained for the trisubstituted substrate **14b**. In this case hydrogenation occurred with >99:1 e.r., using **13c**. Worth noting is that the hydrogenation could also be conducted at 50 °C with no significant loss of selectivity.

Table 4 : hydrogenation of α-(acylamino)acrylic esters

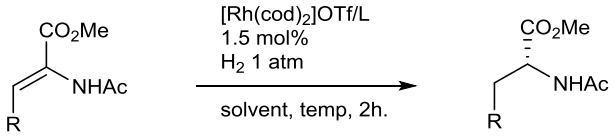

14a : R=H
14b : R=Ph

15a : R=H
15b : R=Ph

entry	14	L	Solvent	Temp. (°C)	Conv. (%)[a]	e.r[b]
1	**14a**	**13a**	EtOH	25	> 99	50:50
2	**14a**	**13b**	EtOH	25	> 99	80:20
3[c]	**14a**	**13b**	DCM	25	> 99	92:8
4	**14a**	**13c**	DCM	25	> 99	97.5:2.5
5	**14b**	**13b**	EtOH	25	> 99	98:2
6	**14b**	**13c**	EtOH	25	> 99	99.5:0.5

a) determined by ^{1}H NMR; b) determined by chiral HPLC; c) 5h

Thus, this new family of enantiopure skeletons, terphenyls exhibiting two atropisomeric Ar-Ar axis are original compounds built up via a challenging asymmetric C-H activation strategy. Importantly, this direct coupling is not only the first example of an highly atroposelective direct Ar-Ar bond formation, but also two chiral elements are perfectly stereocontrolled during one synthetic event. Hence accessed terphenyls present a unique, tridimensional structure and by means of functional group modifications they can be easily converted into an array of unique bicoordinating ligands. Accordingly, a diphosphine ligand DoaxPhos was prepared and its activity as chiral ligand in asymmetric hydrogenation was explored.

D. Experimental data

1. Description of the procedure

a) GP1 : Arylation with simple control of axial chirality

In an oven-dried tube and under air, the substrate (1 equiv), the iodoarene (2 equiv), Ag_2CO_3 (2 equiv), $Pd(OAc)_2$ (10 mol%), and IPrHCl (20 mol%) were added, followed by HFIP (C [substrate] = 0.2 mol/L) , ethyl iodoacetate (1 equiv) and finally TFA (1 equiv). The resulting mixture was stirred at room temperature for 10 min. and was then put in an oil bath (care should be taken that most of the tube is into the oil) at 80 °C with stirring. The reaction was followed by TLC *(caution should be exercise when opening the tube due to the inside built-up pressure)*. After the stated time, the reaction was diluted with Et_2O and filtered over a short pad of silica (washed with Et_2O). The volatiles were removed under reduced pressure and the product was isolated by flash chromatography (*n*-pentane/Et_2O).

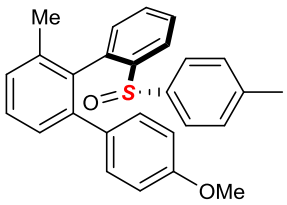

(*R*)-4''-methoxy-6'-methyl-2-((*S*)-*p*-tolylsulfinyl)-1,1':2',1''-terphenyl
Chemical Formula: $C_{27}H_{24}O_2S$
Molecular Weight: 412,5470

3aA. The general procedure **GP1** was followed for 8 hours, from (*S*)-2-methyl-2'-(p-tolylsulfinyl)-1,1'-biphenyl (1 eq., 100 mg, 0.326 mmol) and *p*-iodoanisole (1.98 eq., 151 mg, 0.645 mmol).and yielded ($_a$*R*)-4''-methoxy-6'-methyl-2-((*S*)-p-tolylsulfinyl)-1,1':2',1''-terphenyl (129 mg, 0.313 mmol, 96%) as a light yellow oil with a d.r. >95 : 5 and an e.r. > 98 : 2.
^{1}**H-NMR** ($CDCl_3$, 400 MHz) : δ = 7.99 (dd, J = 7.6, 1.6 Hz, 1H), 7.50 (td, J = 7.5, 1.6 Hz, 1H), 7.46 (td, J = 7.4, 1.8 Hz, 1H), 7.37 (t, J = 7.6 Hz, 1H), 7.31 – 7.27 (m, 2H), 7.13 – 7.05 (***A₁A₁'***B_1B_1', 2H), 7.02 (d, J = 5.0 Hz, 1H), 7.00 – 6.96 (***A₂A₂'***B_2B_2', 2H), 6.88 – 6.82 (A_2A_2'***B₂B₂'***, 2H), 6.73 – 6.66 (A_1A_1'***B₁B₁'***, 2H), 3.73 (s, 3H), 2.29 (s, 3H), 1.20 (s, 3H) ppm
^{13}**C-NMR** ($CDCl_3$, 101 MHz): δ = 158.17, 142.85, 141.53, 141.33, 140.94, 137.66, 137.62, 134.70, 133.02, 131.76, 130.91 (2C), 129.62, 129.18 ($2C_{pTol}$), 128.87, 128.45, 128.01, 127.80, 126.22 ($2C_{pTol}$), 122.85, 112.96 (2C), 54.87, 21.19, 19.91 ppm.
$[\alpha]_D^{20}$ = -45.6° (c =0.158, $CHCl_3$).
HRMS (ESI): *calc. for* $C_{27}H_{25}O_2S^+$ 413.1570 ; found 413.1577.

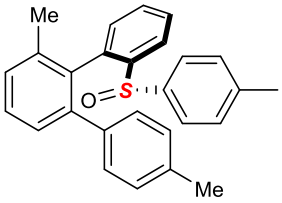

(*R*)-4'',6'-dimethyl-2-((*S*)-*p*-tolylsulfinyl)-1,1':2',1''-terphenyl
Chemical Formula: $C_{27}H_{24}OS$
Molecular Weight: 396,5480

3aB. The general procedure **GP1** was followed for 10 hours, from (*S*)-2-methyl-2'-(p-tolylsulfinyl)-1,1'-biphenyl (1 eq., 70 mg, 0.228 mmol) and *p*-iodotoluene (1.99 eq., 99 mg, 0.454 mmol) and yielded (*aR*)-4'',6'-dimethyl-2-((*S*)-p-tolylsulfinyl)-1,1':2',1''-terphenyl (86.1 mg, 0.217 mmol, 95 %) as yellow solid with a d.r. >95 : 5. ^{1}**H-NMR** ($CDCl_3$, 400 MHz) : δ = 7.91 (d, J = 7.4 Hz, 1H), 7.41 (p, J = 7.3 Hz, 2H), 7.30 (t, J = 7.6 Hz, 1H), 7.22 (d, J = 7.5 Hz, 2H), 6.99 (d, J = 8.0 Hz, 2H), 6.95 (d, J = 8.0 Hz, 2H), 6.93 – 6.86 (m, 3H), 6.77 (d, J = 8.0 Hz, 2H), 2.22 (s, 3H), 2.17 (s, 3H), 1.11 (s, 3H). ^{13}**C-NMR** ($CDCl_3$, 101 MHz): δ = 142.86, 141.82, 141.57, 141.00, 137.74 (2C), 137.67, 136.29, 134.76, 131.84, 129.77 (2C), 129.62, 129.26 (2C), 129.05, 128.53, 128.39 (2C), 128.09, 127.98, 126.42 (2C), 122.97, 21.34, 21.05, 20.01 ppm. $[\alpha]_D^{20}$ = -14.9 ° (c = 1 , $CHCl_3$).
HRMS (ESI): *calc. for* $C_{27}H_{25}OS^+$ 397.1621 ; found 397.1642.

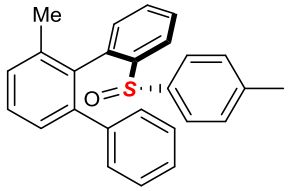

(*R*)-6'-methyl-2-((*S*)-*p*-tolylsulfinyl)-1,1':2',1''-terphenyl
Chemical Formula: $C_{26}H_{22}OS$
Molecular Weight: 382,5210

3aC. The general procedure **GP1** was followed for 10 hours, from (*S*)-2-methyl-2'-(p-tolylsulfinyl)-1,1'-biphenyl (1 eq., 80 mg, 0.261 mmol) and iodobenzene (2 eq., 0.522 mmol) and yielded ($_a$*R*)-6'-methyl-2-((*S*)-p-tolylsulfinyl)-1,1':2',1''-terphenyl (95 mg, 0.248 mmol, 95%) as an orange oil with a d.r. >95 : 5. ^{1}**H-NMR** ($CDCl_3$, 400 MHz) : δ = 7.98 (d, J = 7.2 Hz, 1H), 7.58 – 7.45 (m, 2H), 7.41 (t, J = 7.6 Hz, 1H), 7.38 – 7.29 (m, 2H), 7.23 – 7.12 (m, 5H), 7.07 (d, J = 7.4 Hz, 1H), 7.06 – 6.99 (***AA'***BB', 2H), 6.93 – 6.83 (AA'***BB'***, 2H), 2.32 (s, 3H), 1.24 (s, 3H) ppm ^{13}**C-NMR** ($CDCl_3$, 101 MHz): δ = 142.95, 141.81, 141.54, 140.99, 140.63, 137.71, 137.47, 134.77, 131.77, 129.87 (2C), 129.61, 129.24 (2C), 129.23, 128.52, 128.13, 127.87, 127.54 (2C), 126.68, 126.34 (2C), 122.92, 21.30, 19.97 ppm. $[\alpha]_D^{20}$ = - 36.1° (c = 0.870 , $CHCl_3$).
HRMS (ESI): *calc. for* $C_{26}H_{23}O_2S^+$ *383.1464* ; found 383.1473 .

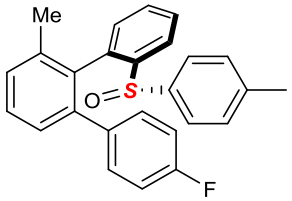

(*R*)-4''-fluoro-6'-methyl-2-((*S*)-*p*-tolylsulfinyl)-1,1':2',1''-terphenyl
Chemical Formula: $C_{26}H_{21}FOS$
Molecular Weight: 400,5114

3aD. The general procedure **GP1** was followed for 14 hours, from (*S*)-2-methyl-2'-(p-tolylsulfinyl)-1,1'-biphenyl (1 eq., 80 mg, 0.261 mmol) and *p*-fluoroiodobenzene (1.99 eq., 115 mg, 60 µL, 0.52 mmol) and yielded ($_aR$)-4''-fluoro-6'-methyl-2-((*S*)-p-tolylsulfinyl)-1,1':2',1''-terphenyl (87 mg, 0.217 mmol, 83%) as a yellow solid with a d.r. of >95 : 5.
^{1}**H-NMR** ($CDCl_3$, 400 MHz) : δ = 7.91 (dd, J = 7.7, 1.4 Hz, 1H), 7.44 (td, J = 7.6, 1.6 Hz, 1H), 7.39 (td, J = 7.3, 1.6 Hz, 1H), 7.32 (t, J = 7.6 Hz, 1H), 7.27 – 7.16 (***A₁A₁'***B_1B_1', 2H), 7.11 – 7.02 (m, 2H), 6.99 (d, J = 7.4 Hz, 1H), 6.97-6.90 (***A₂A₂'***B_2B_2', 2H), 6.84 – 6.73 (A_1A_1'***B₁B₁'*** + A_2A_2'***B₂B₂'***, 4H), 2.23 (s, 3H), 1.14 (s, 3H) ppm.
^{13}**C-NMR** ($CDCl_3$, 101 MHz): δ = 161.61 (d, *J* = 246.4 Hz), 142.81, 141.68, 140.77 (2C), 137.84, 137.32, 136.61 (d, *J* = 3.4 Hz), 134.79, 131.67, 131.48, 131.37, 129.59 (d, *J* = 29.3 Hz, 2C), 129.29 ($2C_{pTol}$) , 128.60, 128.29, 127.79, 126.33 ($2C_{pTol}$) , 123.09, 114.58 (d, *J* = 21.4 Hz, 2C), 21.31, 19.96 ppm.
^{19}**F-NMR** ($CDCl_3$, 125.6 MHz): δ = -115.59 ppm.
$[\alpha]_D^{20}$ = -18.9 ° (c = 0.342 , $CHCl_3$).
HRMS (ESI): *calc. for* $C_{26}H_{21}NaOS^+$ 423.1189 ; found 423.1159.

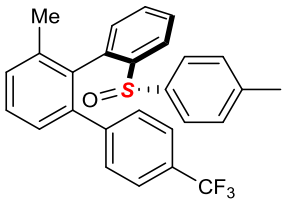

(*R*)-6'-methyl-2-((*S*)-*p*-tolylsulfinyl)-4''-(trifluoromethyl)-1,1':2',1''-terphenyl
Chemical Formula: $C_{27}H_{21}F_3OS$
Molecular Weight: 450,5192

3aE. The general procedure **GP1** was followed for 14 hours, from (*S*)-2-methyl-2'-(p-tolylsulfinyl)-1,1'-biphenyl (1 eq., 81 mg, 0.264 mmol) *p*-trifluoromethyliodobenzene (2.01 eq., 144 mg, 78 µL, 0.531 mmol) and yielded ($_aR$)-6'-methyl-2-((*S*)-p-tolylsulfinyl)-4''-(trifluoromethyl)-1,1':2',1''-terphenyl (103 mg, 0.229 mmol, 86%) with a d.r. > 95 : 5.
^{1}**H-NMR** ($CDCl_3$, 400 MHz) : δ = 7.98 (dd, J = 7.4, 1.7 Hz, 1H), 7.52 (td, J = 7.4, 1.4 Hz, 1H), 7.48 (td, J = 7.5, 1.8 Hz, 1H), 7.43 (d, J = 8.1 Hz, 2H), 7.41 (t, J = 7.6 Hz, 1H), 7.34 – 7.26 (m, 4H), 7.09 (d, J = 7.6 Hz, 1H), 7.05 – 7.00 (m, 2H), 6.89 – 6.83 (m, 2H), 2.30 (s, 3H), 1.21 (s, 3H) ppm.
^{13}**C-NMR** ($CDCl_3$, 101 MHz): δ = 144.44 (q, J = 1.2 Hz), 142.75, 141.84, 140.66, 140.40, 138.12, 136.95, 134.63, 131.61, 130.09 (2C), 130.00, 129.84, 129.35 (2C), 128.73, 128.53, 128.22 (q, J = 32.4 Hz), 127.80, 126.41 (2C), 124.56 (q, J = 3.7 Hz),

124.04 (q, J = 272.1 Hz, 2C), 123.26, 21.32, 19.88 ppm. **^{19}F-NMR** ($CDCl_3$, 125.6 MHz): δ = -62.39 ppm. $[\alpha]_D^{20}$ = -17.8 ° (c = 0.71, $CHCl_3$). **HRMS (ESI):** *calc. for $C_{27}H_{21}F_3KOS^+$ 489.0897* ; found 489.0868 . 81 mg, 0.264 mmol) *p*-

^{1}H-NMR ($CDCl_3$, 400 MHz) : δ = 7.98 (dd, J = 7.4, 1.7 Hz, 1H), 7.52 (td, J = 7.4, 1.4 Hz, 1H), 7.48

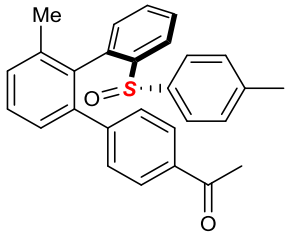

1-((*R*)-3'-methyl-2''-((*S*)-*p*-tolylsulfinyl)-[1,1':2',1''-terphenyl]-4-yl)ethan-1-one
Chemical Formula: $C_{28}H_{24}O_2S$
Molecular Weight: 424,5580

3aF. The general procedure **GP1** was followed for 12 hours, from (*S*)-2-methyl-2'-(p-tolylsulfinyl)-1,1'-biphenyl (1 eq., 81 mg, 0.264 mmol) and *p*-iodoacetophenone (2 eq., 130 mg, 0.528 mmol) and yielded 1-((*aR*)-3'-methyl-2''-((*S*)-p-tolylsulfinyl)-[1,1':2',1''-terphenyl]-4-yl)ethan-1-one (90 mg, 0.212 mmol, 80%) as a yellow powder. **^{1}H-NMR** ($CDCl_3$, 400 MHz) : δ = 7.96 (dd, J = 6.88, 1.93 Hz, 1H), 7.77 (*AA'*BB', 2H), 7.53-7.46 (m, 2H), 7.42 (t, J = 7.61 Hz, 1H), 7.32-7.29 (m, 2H), 7.28 (AA'*BB'*, 2H), 7.10 (d, J = 7.52 Hz, 1H), 7.02 (*AA'*BB', 2H), 6.85 (AA'*BB'*, 2H), 2.54 (s, 3H), 2.30 (s, 3H), 1.23 (s, 3H) ppm. **^{13}C-NMR** ($CDCl_3$, 101 MHz): δ = 197.70, 145.71, 142.81, 141.79, 140.71, 140.70, 138.06, 137.03, 135.16, 134.66, 131.69, 130.07 (2C), 129.99, 129.84, 129.35 (2C), 128.72, 128.52, 127.72 (2C), 127.70, 126.36 (2C), 123.18, 26.50, 21.34, 19.93 ppm. $[\alpha]_D^{20}$ = -18.7 ° (c = 1.27, $CHCl_3$). **HRMS (ESI):** *calc. for $C_{28}H_{24}NaO_2S^+$* 447.1394 ; found 447.1389.

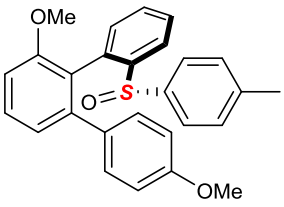

(*S*)-4'',6'-dimethoxy-2-((*S*)-*p*-tolylsulfinyl)-1,1':2',1''-terphenyl
Chemical Formula: $C_{27}H_{24}O_3S$
Molecular Weight: 428,5460

3bA. The general procedure **GP1** was followed for 12 hours, using (*S*)-2-methoxy-2'-(p-tolylsulfinyl)-1,1'-biphenyl (1 eq., 90 mg, 0.279 mmol) and *p*-iodoanisole (1.99 eq., 130 mg, 0.555 mmol) and yielded ($_a$*R*)-6'-methyl-2-((*S*)-p-tolylsulfinyl)-4''-(trifluoromethyl)-1,1':2',1''-terphenyl (113 mg, 0.264 mmol, 95%) with a d.r. of 61 : 39. **^{1}H-NMR** ($CDCl_3$, 400 MHz) : (mixture of atropisomers; attribution of all major/minor (1.57 : 1) signals was not possible, total integration 61.68) δ = 8.13 (dd, J = 7.9, 1.1

Hz, 1H minor), 7.85 – 7.77 (m, 1.57H major), 7.52 – 7.37 (m, 7.01H), 7.25 – 7.19 (m, 1.64H), 7.16 (td, J = 7.5, 1.2 Hz, 1H), 7.14 – 7.09 (m, 3.28H), 7.09 – 7.00 (m, 11.02H), 7.00 – 6.95 (m, 3.23H), 6.75 – 6.65 (m, 5.78H), 6.43 – 6.35 (m, 2H minor), 6.05 – 5.96 (m, 2H minor), 3.90 (s, 3H minor), 3.73 (s, 4.94H), 3.67 (s, 3H minor), 3.26 (s, 4.79H), 2.31 (s, 4.86H), 2.22 (s, 3H minor) ppm.
^{13}**C-NMR** ($CDCl_3$, 101 MHz): (mixture of atropisomers) δ = 158.45, 158.16, 156.85, 156.15, 145.53, 143.56, 142.86, 142.51, 141.94, 141.66, 141.25, 140.93, 135.84, 134.93, 132.62, 132.53, 132.46, 131.91, 130.98, 130.19, 130.16, 129.90, 129.70, 129.61, 129.56, 129.18, 128.15, 128.11, 126.35, 125.86, 124.59, 124.49, 124.23, 123.09, 122.52, 122.52, 113.24, 112.68, 109.76, 108.82, 55.94, 55.07, 55.05, 54.81, 21.36, 21.34 ppm.
(due to the high number of peaks, the 8 carbons integrating each for 2 from the p-tolyl group and the p-methoxyphenyl group could not be identified.)
^{1}**H-NMR** ($CDCl_3$, 400 MHz) : δ = 7.86 – 7.78 (m, 1H), 7.44 (dt, J = 7.3, 1.6 Hz, 1H), 7.40 (dt, J = 5.1, 1.7 Hz, 1H), 7.40 (t, J = 7.3 Hz, 1H), 7.25 – 7.19 (m, 1H), 7.14 – 7.08 (***A₁A₁'***B_1B_1', 2H), 7.07 (dd, J = 6.4, 1.0 Hz, 1H), 7.06 – 7.00 (***A₂A₂'B₂B₂'***, 4H), 6.74 – 6.68 (A_1A_1'***B₁B₁'***, 2H), 6.67 (dd, J = 6.5, 0.9 Hz, 1H), 3.73 (s, 3H), 3.27 (s, 3H), 2.31 (s, 3H) ppm.
^{13}**C-NMR** ($CDCl_3$, 101 MHz): δ = 158.37, 156.77, 143.49, 142.79, 141.87, 140.86, 135.76, 132.54, 132.46, 130.90 (2C), 129.82, 129.54, 129.11 (2C), 128.07, 126.27 (2C), 124.51, 124.15, 122.45, 113.17 (2C), 108.75, 54.97, 54.73, 21.29 ppm.
HRMS (ESI): *calc. for* $C_{27}H_{25}O_3S^+$ *429.1519* ; found 429.1521.

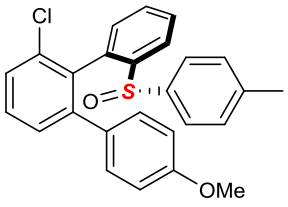

(*S*)-6'-chloro-4''-methoxy-2-((*S*)-*p*-tolylsulfinyl)-1,1':2',1''-terphenyl
Chemical Formula: $C_{26}H_{21}ClO_2S$
Molecular Weight: 432,9620

3cA. The general procedure **GP1** was followed for 14 hours, using (*S*)-2-chloro-2'-(p-tolylsulfinyl)-1,1'-biphenyl (1 eq., 85 mg, 0.26 mmol) and *p*-iodoanisole (1.99 eq., 121 mg, 0.517 mmol) and yielded ($_a$*S*)-6'-chloro-4''-methoxy-2-((*S*)-p-tolylsulfinyl)-1,1':2',1''-terphenyl (99 mg, 0.229 mmol, 88 %) with a d.r. > 95 : 5.
^{1}**H-NMR** ($CDCl_3$, 400 MHz) : δ = 7.88 (dd, J = 7.4, 1.7 Hz, 1H), 7.50 (td, J = 7.3, 1.5 Hz, 1H), 7.47 (td, J = 7.4, 1.6 Hz, 1H), 7.42 – 7.31 (m, 3H), 7.26 (dd, J = 7.1, 2.0 Hz, 1H), 7.14 – 7.08 (***A₁A₁'***B_1B_1', 2H), 7.08 – 7.03 (***A₂A₂'***B_2B_2', 2H), 7.03 – 6.97 (A_1A_1'***B₁B₁'***, 2H), 6.77 – 6.65 (A_2A_2'***B₂B₂'***, 2H), 3.73 (s, 3H), 2.31 (s, 3H) ppm.
^{13}**C-NMR** ($CDCl_3$, 101 MHz): δ = 158.67, 143.66, 143.21, 141.52, 140.73, 136.06, 135.16, 134.28, 132.23, 131.89, 130.85 (2C), 129.85, 129.55, 129.47 (2C), 128.81, 128.75, 128.08, 125.91 (2C), 123.75, 113.29 (2C), 54.96, 21.34 ppm.

$[\alpha]_D^{20}$ = -47.7 ° (c = 0.680, $CHCl_3$).
HRMS (ESI): *calc. for* $C_{26}H_{21}NaClO_2S^+$ 455.0843; found 455.0845.

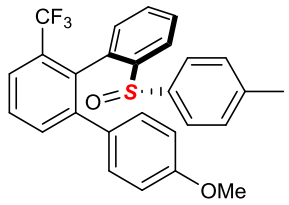

(*S*)-4''-methoxy-2-((*S*)-*p*-tolylsulfinyl)-6'-(trifluoromethyl)-1,1':2',1''-terphenyl
Chemical Formula: $C_{27}H_{21}F_3O_2S$
Molecular Weight: 466,5182

3dA. The general procedure **GP1** was followed for 12 hours, from (*S*)-2-(p-tolylsulfinyl)-2'-(trifluoromethyl)-1,1'-biphenyl (1 eq., 94 mg, 0.261 mmol) and *p*-iodoanisole (2 eq., 122 mg, 0.521 mmol) and yielded ($_a$*S*)-4''-methoxy-2-((S)-p-tolylsulfinyl)-6'-(trifluoromethyl)-1,1':2',1''-terphenyl (77 mg, 0.165 mmol, 63%) as an off-white solid with a d.r. of >95 : 5.
Crystals suitable for X-Ray analysis were grown by layering a concentrated DCM solution with *n*-pentane in a narrow container and letting the resulting biphasic mixture equilibrate at 4-6 °C.
^{1}**H-NMR** ($CDCl_3$, 400 MHz) : δ = 7.90 (dd, J = 7.6, 1.5 Hz, 1H), 7.68 – 7.63 (m, 1H), 7.63 – 7.58 (m, 2H), 7.51 (td, J = 7.6, 1.6 Hz, 1H), 7.46 (td, J = 7.4, 1.5 Hz, 1H), 7.39 (d, J = 7.4 Hz, 1H), 7.12 – 7.05 (***A₁A₁'***B_1B_1', 2H), 7.04 – 6.98 (***A₂A₂'***B_2B_2', 2H), 6.89 – 6.82 (A_2A_2'***B₂B₂'***, 2H), 6.76 – 6.68 (A_1A_1'***B₁B₁'***, 2H), 3.74 (s, 3H), 2.29 (s, 3H) ppm.
^{13}**C-NMR** ($CDCl_3$, 101 MHz): δ = 158.70, 143.60, 142.92, 141.80, 140.12, 135.30, 134.07, 133.54 (q), 131.47 (q, J = 2.8 Hz), 131.45, 131.23 (2C), 130.01 (q, J = 29.3 Hz), 129.48, 129.28 (2C), 129.01, 128.69, 125.93 (2C), 125.24 (q, J = 5.4 Hz), 123.30, 123.19 (q, J = 274.7 Hz), 113.28 (2C), 54.94, 21.26 ppm.
^{19}**F-NMR** ($CDCl_3$, 125.6 MHz): δ = -57.47 ppm.
$[\alpha]_D^{20}$ = -18.2 ° (c = 0.398 , $CHCl_3$).
HRMS (ESI): *calc. for* $C_{27}H_{21}F_3NaO_2S^+$ *489.1112* ; found 489.1100.

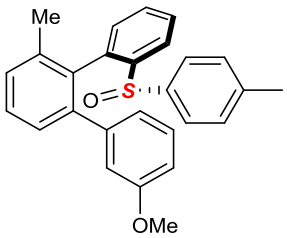

(*R*)-3''-methoxy-6'-methyl-2-((*S*)-*p*-tolylsulfinyl)-1,1':2',1''-terphenyl
Chemical Formula: $C_{27}H_{24}O_2S$
Molecular Weight: 412,5470

3aG. The general procedure **GP1** was followed for 16 hours, using (*S*)-2-methyl-2'-(p-tolylsulfinyl)-1,1'-biphenyl (1 eq., 80 mg, 0.261 mmol) and *m*-iodoanisole (1.99 eq., 121 mg, 62 µL, 0.519 mmol) and yielded (a*R*)-3''-methoxy-6'-methyl-2-((*S*)-p-tolylsulfinyl)-1,1':2',1''-terphenyl (84 mg, 0.204 mmol, 78%) as an orange oil with a

d.r. >95 : 5.
^{1}H-NMR ($CDCl_3$, 400 MHz) : 8.00 (d, J= 8.9 Hz ; 1H), 7.52-7.44 (m, 2H), 7.39 (t, J= 7.6 Hz, 1H), 7.33 (d, J= 7.1 Hz, 1H), 7.29 (d, J = 8.4 Hz, 1H), 7.11 (t, J= 7.9 Hz, 1H), 7.06 (d, J= 7.2 Hz, 1H), 7.01 (AA'BB', 2H), 6.87 (AA'BB', 2H), 6.83 (d, J= 7.6 Hz, 1H), 6.71-6.67 (m, 2H), 3.61 (3H), 2.30 (3H), 1.22 (3H) ppm.
^{13}C-NMR ($CDCl_3$, 101 MHz): δ = 158.65, 143.19, 141.98, 141.62, 141.57, 141.04, 137.77, 137.62, 134.76, 131.72, 129.62, 129.32, 129.28 (2C), 128.66, 128.55, 128.19, 127.83, 126.34 (2C), 123.11, 122.51, 115.34, 112.91, 55.07, 21.33, 20.04 ppm.
$[\alpha]_D^{20}$ = -18.8 ° (c = 1.02, $CHCl_3$).
HRMS (ESI): *calc. for* $C_{27}H_{25}O_2S^+$ 413.1570 ; found 413.1577.

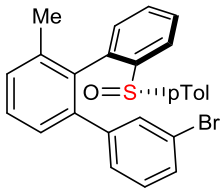

(*R*)-3''-bromo-6'-methyl-2-((*S*)-*p*-tolylsulfinyl)-1,1':2',1''-terphenyl
Chemical Formula: $C_{26}H_{21}BrOS$
Molecular Weight: 461,4170

3aH. Under air, (*S*)-2-methyl-2'-(p-tolylsulfinyl)-1,1'-biphenyl (1 eq., 950 mg, 3.1 mmol) was loaded in a Ace pressure tube along with 3-bromoiodobenzene (2.02 eq., 1768 mg, 800 µL, 6.25 mmol), AgTFA (1.02 eq., 700 mg, 3.17 mmol), Ag_2CO_3 (1.42 eq., 1215 mg, 4.41 mmol), IPrHCl (12 %, 158 mg, 0.372 mmol), $Pd(TFA)_2$ (6.02 %, 62 mg, 0.186 mmol) and powdered activate 4 Å MS (500 mg). HFIP (21 mL) was added and the mixture stirred 15 min at room temperature. After completion of the reaction (TLC and LC-MS), the crude was filtered on a silica gel plug and subsequent flash chromatography afforded (R)-3''-bromo-6'-methyl-2-((S)-p-tolylsulfinyl)-1,1':2',1''-terphenyl (1038 mg, 2.25 mmol, 73%) with a d.r. >95 : 5.
^{1}H-NMR ($CDCl_3$, 400 MHz) : δ = ongoing ppm.
^{13}C-NMR ($CDCl_3$, 101 MHz): δ = ongoing ppm.
$[\alpha]_D^{20}$ =ongoing.
HRMS (ESI): *ongoing*

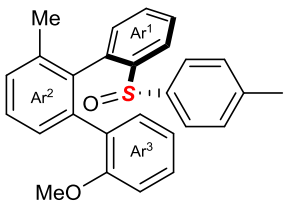

(*R*)-2-methoxy-3'-methyl-2''-((*S*)-*p*-tolylsulfinyl)-1,1':2',1''-terphenyl
Chemical Formula: $C_{27}H_{24}O_2S$
Molecular Weight: 412,5470

3aI. The general procedure **GP1** was followed for 16 hours, from (*S*)-2-methyl-2'-(p-tolylsulfinyl)-1,1'-biphenyl (1 eq., 87 mg, 0.284 mmol) and *o*-iodoanisole (1.99 eq., 132 mg, 74 µL, 0.566 mmol)

and yielded ($_aR$)-2-methoxy-3'-methyl-2''-((*S*)-p-tolylsulfinyl)-1,1':2',1''-terphenyl (89 mg, 0.216 mmol, 76 %) with a d.r. >95 : 5 about Ar^1-Ar^2. *(two atropisomers are present on the ^{1}H NMR spectra at 25 °C, so a high temperature spectra was recorded under the reasonable assumption that the Ar^3-Ar^2 chiral axis, less hindered than the Ar^1-Ar^2 chiral axis, will thus be in fast rotation on the NMR time scale, thereby showing: 1) the d.r. of the Ar^1-Ar^2 chiral axis-sulfoxide diastereomeric pair; 2) that in the reaction conditions the Ar^2-Ar^3 chiral axis is not stable). Slow rotation about the Ar^2-Ar^3 chiral axis on the NMR time scale caused peaks broadening, to the point that not all signals are present on the ^{13}C spectra.*
^{1}**H-NMR** ($CDCl_3$, 500 MHz) : δ = 7.93 (dd, J = 7.6, 1.0 Hz, 1H), 7.42 (dt, J = 7.4, 1.0 Hz, 1H), 7.38 (t, J = 6.9 Hz, 1H), 7.59 – 7.20 (brd, 2.5H), 7.23 (dd, J = 7.4, 1.2 Hz, 1H), 7.14 (t, J = 7.3 Hz, 1H), 7.08 – 7.03 (brd, 1H), 7.03 – 6.97 (***AA'***BB', 2H), 6.96 – 6.89 (AA'***BB'***, 2H), 7.03 – 6.32 (brd, 2.5H), 4.00 – 3.02 (brd, 3H), 2.30 (s, 3H), 1.19 (s, 3H).ppm.
^{1}**H-NMR** (CD_3CN, 400 MHz, 80°C) : δ = 7.87 – 7.78 (m, 1H), 7.50 – 7.37 (m, 3H), 7.37 – 7.23 (m, 2H), 7.23 – 7.15 (m, 2H), 7.15 – 7.12 (m, 1H), 7.12 – 7.06 (***AA'***BB', 2H), 6.98 – 6.89 (AA'***BB'***, 2H), 6.90 – 6.82 (m, 1H), 6.79 – 6.68 (m, 1H), 3.55 (s, 3H), 2.31 (s, 3H), 1.25 (s, 3H) ppm.
^{13}**C-NMR** ($CDCl_3$, 101 MHz, 80°C): δ = 157.82, 157.16, 144.80, 142.97, 142.81, 139.37, 138.83, 138.12, 137.41, 133.02, 132.57, 131.00, 130.31 ($2C_{p\text{Tol}}$), 130.19, 130.00, 129.64, 129.21, 129.01, 128.77, 126.86 ($2C_{p\text{Tol}}$), 122.80, 120.57, 55.32, 21.13, 20.16 ppm.
HRMS (ESI): *calc. for $C_{27}H_{25}O_2S^+$ 413.1570* ; found 413.1593 .

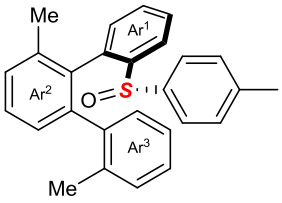

(*R*)-2,3'-dimethyl-2''-((*S*)-*p*-tolylsulfinyl)-1,1':2',1''-terphenyl
Chemical Formula: $C_{27}H_{24}OS$
Molecular Weight: 396,5480

3aJ. The general procedure **GP1** was followed for 24 hours, using (*S*)-2-methyl-2'-(p-tolylsulfinyl)-1,1'-biphenyl (1 eq., 109 mg, 0.356 mmol) and *o*-iodotoluene (2.01 eq., 155 mg, 91 µL, 0.714 mmol) and yielded ($_aR$)-2,3'-dimethyl-2''-((*S*)-p-tolylsulfinyl)-1,1':2',1''-terphenyl (121 mg, 0.305 mmol, 86 %) with a d.r. >95 : 5 about Ar^1-Ar^2 and as a 50 : 50 mixture of atropisomers about Ar^2-Ar^3 on the NMR time scale. *(two atropisomers are present on the ^{1}H NMR spectra at 25 °C, so a high temperature spectra was recorded under the reasonable assumption that the Ar^3-Ar^2 chiral axis, less hindered than the Ar^1-Ar^2 chiral axis, will thus be in fast rotation on the NMR time scale, thereby causing the coalescence of some signals showing: 1) the d.r. of the Ar^1-Ar^2 chiral axis-sulfoxide diastereomeric pair; 2) that in the reaction conditions the Ar^2-Ar^3 chiral axis is not stable).*
^{1}**H-NMR** ($CDCl_3$, 400 MHz) : (mixture of two atropisomers 1 : 1) δ = 8.00 (dd, J = 7.9,

1.0 Hz, 1H), 7.96 (dd, J = 7.4, 1.7 Hz, 1H), 7.59 (d, J = 6.6 Hz, 1H), 7.51 – 7.38 (m, 3H), 7.36 (d, J = 7.9 Hz, 2H), 7.36 – 7.27 (m, 1H), 7.29 – 7.22 (m, 3H), 7.18 (t, J = 7.5 Hz, 1H), 7.16 – 7.10 (m, 2H), 7.10 – 7.03 (m, 6H), 7.04 – 6.97 (m, 4H), 6.93 (dd, J = 7.1, 5.2 Hz, 3H), 6.76 (t, J = 7.3 Hz, 1H), 6.67 (d, J = 7.8 Hz, 1H), 2.57 (s, 3H), 2.32 (s, 3H), 2.31 (s, 3H), 1.89 (s, 3H), 1.19 (s, 3H), 1.16 (s, 3H) ppm. ^{1}**H-NMR** (CD_3CN, 400 MHz, 80 °C) : δ = 7.98 – 7.81 (brd, 1H), 7.64 – 7.54 (brd, 0.5H), 7.54 – 7.35 (brd, 3H), 7.36 – 7.22 (brd, 2H), 7.22 – 7.04 (brd, 5H), 7.05 – 6.92 (brd, 2.5H), 6.87 – 6.66 (brd, 1H), 2.56 (brd, 1.5H), 2.32 (s, 3H), 1.92 (brd, 1.5H), 1.26 (s, 3H). ^{13}**C-NMR** ($CDCl_3$, 101 MHz): δ = 143.20, 143.11, 141.69, 141.59, 141.33, 141.17, 140.97, 140.53, 140.25, 138.79, 138.26, 137.63, 137.47, 137.30, 135.88, 135.66, 135.49, 135.03, 132.31, 131.40, 131.10, 130.08, 129.62, 129.54, 129.41, 129.39 (2C$_{p\text{Tol}}$), 129.31 (2C$_{p\text{Tol}}$), 129.03 (2C), 128.85, 128.66, 128.40, 128.18, 127.87, 127.78, 127.52, 127.28, 126.85, 126.62 (2C$_{p\text{Tol}}$), 126.35 (2C$_{p\text{Tol}}$), 125.15, 124.26, 122.73, 122.51, 21.33, 21.32, 20.78, 20.18, 20.15, 19.84 ppm. **HRMS (ESI):** *calc. for $C_{27}H_{25}OS^+$ 397.1621* ; found 397.1648.

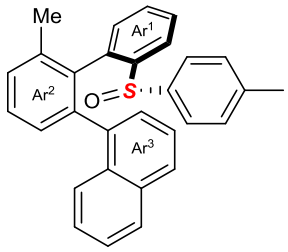

1-((*R*)-6-methyl-2'-((*S*)-*p*-tolylsulfinyl)-[1,1'-biphenyl]-2-yl)naphthalene
Chemical Formula: $C_{30}H_{24}OS$
Molecular Weight: 432,5810

3aK. The general procedure **GP1** was followed for 24 hours, using (*S*)-2-methyl-2'-(p-tolylsulfinyl)-1,1'-biphenyl (1 eq., 109 mg, 0.356 mmol) and 1-iodonaphthalene (2 eq., 180 mg, 104 µL, 0.712 mmol) and yielded 1-(($_a$*R*)-6-methyl-2'-((*S*)-p-tolylsulfinyl)-[1,1'-biphenyl]-2-yl)naphthalene (113 mg, 0.261 mmol, 73%) with a d.r. >90 : 10 about Ar^1-Ar^2 and as a 61 : 39 mixture of atropisomers about Ar^2-Ar^3 on the NMR time scale. ^{1}**H-NMR** ($CDCl_3$, 500 MHz) : (mixture of atropisomers 1 : 2.4; *calc. integration 24 + 24*2.4 =81.6*, found 82.9) δ = 8.25 (d, J = 8.6 Hz, 1H), 7.87 (dd, J = 7.7, 1.4 Hz, 1.2H), 7.85 (d, J = 7.9 Hz, 2.3H), 7.82 – 7.77 (m, 3.3H), 7.69 – 7.65 (m, 4.5H), 7.63 (d, J = 8.2 Hz, 1.3H), 7.54 – 7.49 (m, 1.4H), 7.49 – 7.43 (m, 8.7H), 7.43 – 7.39 (m, 2.1H), 7.36 – 7.33 (m, 2.5H), 7.33 – 7.28 (m, 5.9H), 7.26 (dt, J = 8.3, 1.4 Hz, 2.3H), 7.21 – 7.16 (m, 4.6H), 7.15 – 7.12 (m, 1.3H), 7.11 – 7.06 (m, 6H), 7.07 – 7.02 (m, 6.7H), 7.00 – 6.95 (m, 6.6H), 6.90 (dd, J = 7.2, 1.2 Hz, 1.2H), 2.33 (s, 6.7H), 2.32 (s, 3.3H), 1.23 (s, 9.9H) ppm. ^{13}**C-NMR** ($CDCl_3$, 126 MHz): (mixture of atropisomers) δ = 143.80, 142.86, 141.75, 141.62, 141.34, 141.13, 140.01, 139.53, 138.78, 138.66, 137.63, 137.38, 137.30, 137.17, 136.44, 136.37, 134.16, 132.85, 132.39, 131.66, 131.48, 130.53, 129.80, 129.47, 129.46 (2C$_{p\text{Tol}}$, major), 129.45, 129.41, 129.34, 129.27, 129.19, 128.55,

128.53, 128.44, 127.99, 127.83, 127.82, 127.65, 127.57, 127.49, 126.99, 126.69, 126.66 ($2C_{pTol}$, major), 126.50, 126.19, 125.94, 125.58, 125.18, 125.18, 124.96, 124.07, 122.84, 122.56, 21.39, 21.38, 20.26, 19.83 ppm. *(due to the high number of peaks, the carbons integrating each for 2 from the p-tolyl group could not be identify.)*
HRMS (ESI): *calc. for $C_{30}H_{25}OS^+$ 433.1621* ; found 433.1637.

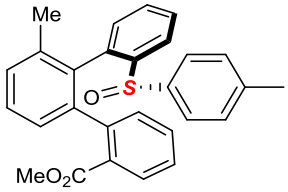

methyl (*R*)-3'-methyl-2''-((*S*)-*p*-tolylsulfinyl)-[1,1':2',1''-terphenyl]-2-carboxylate
Chemical Formula: $C_{28}H_{24}O_3S$
Molecular Weight: 440,5570

3aL. The general procedure **GP2** was followed for 4 hours from (*S*)-2-methyl-2'-(p-tolylsulfinyl)-1,1'-biphenyl (1 eq., 70 mg, 0.228 mmol) and methyl-2-iodobenzoate (2.02 eq., 121 mg, 70 µL, 0.462 mmol) methyl 2-(3-methyl-2-{2-[(S)-(4-methylphenyl)sulfinyl]phenyl}phenyl)benzoate (91 mg, 0.207 mmol, 90%) and yielded methyl ($_aR$)-3'-methyl-2''-((*S*)-p-tolylsulfinyl)-[1,1':2',1''-terphenyl]-2-carboxylate with a d.r. > 90 : 10 about Ar^1-Ar^2 and as a 80 : 20 mixture of atropisomers about Ar^2-Ar^3 on the NMR time scale.
(only the signals of the major diastereomer are reported)
^{1}**H-NMR** ($CDCl_3$, 400 MHz) : δ = 7.90 (d, J = 7.4 Hz, 1H), 7.67 (d, J = 7.6 Hz, 1H), 7.62 (d, J = 7.8 Hz, 1H), 7.55 (t, J = 7.5 Hz, 1H), 7.46 – 7.37 (m, 2H), 7.31 (t, J = 6.9 Hz, 1H), 7.26 – 7.20 (m, 2H), 7.09 (d, J = 7.9 Hz, 1H), 7.07 – 7.03 (***AA'***BB', 2H), 7.01 (d, J = 7.2 Hz, 1H), 6.98 – 6.93 (AA'***BB'***, 2H), 3.65 (s, 3H), 2.31 (s, 3H), 1.17 (s, 3H) ppm.
^{13}**C-NMR** ($CDCl_3$, 101 MHz): δ = 167.07, 142.90, 142.27, 141.72, 141.42, 140.91, 137.32, 136.93, 134.50, 131.90, 131.69, 130.99, 129.71, 129.52, 129.43, 129.41, 129.24, 128.42, 128.25, 127.25, 126.66, 126.49, 122.79, 51.56, 21.35, 19.82 ppm.
HRMS (ESI): *calc. for $C_{28}H_{25}O_3S^+$ 441.1519* ; found 441.1545

b) Arylation with double control of axial chirality :

(1) Iodoarenes Preparation :

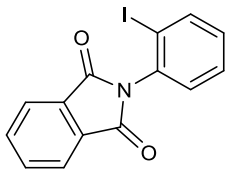

2-(2-iodophenyl)isoindoline-1,3-dione
Chemical Formula: $C_{14}H_8INO_2$
Molecular Weight: 349,1275

2-iodoaniline (1 eq., 1.5 g, 6.85 mmol) and phthalic anhydride (1 eq., 1.01 g, 6.85 mmol) were loaded in a microwave vial. Acetic acid (15 mL) was then added and the vial was heated at 160 °C for 30 min. The resulting mixture was diluted with water and DCM, the phases were separated and the organic phase was washed with a saturated solution of $NaHCO_3$ and then a 1M HCL soltion. The crude product was recrystallized by liquid/liquid diffusion of *n*-petane into DCM at 4-6 °C, affording 2-(2-iodophenyl)isoindoline-1,3-dione (1.49 g, 4.27 mmol, 62 %) as square crystals.

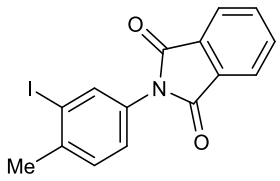

2-(3-iodo-4-methylphenyl)isoindoline-1,3-dione
Chemical Formula: $C_{15}H_{10}INO_2$
Molecular Weight: 363,1545

(a) General procedure for the regioselective S_EAr iodination :

The substrate (1equiv) and NIS (1.1 equiv) were dissolved in acetonitrile (0.25M). Then, TFA (10 mol%) was added and the reaction was stirred at room temperature until almost full consumption of the starting material (usually 4-6 hours). The reactions were quenched by adding first a 1M NaOH solution and a 1M $Na_2S_2O_3$ solution, under vigourous stirring, until complete discoloration of the reaction mixture. The crude product was extracted with DCM and purified as stated bellow.

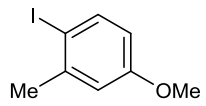

1-iodo-4-methoxy-2-methylbenzene
Chemical Formula: C_8H_9IO
Molecular Weight: 248,0635

From 3-methylanisole (1 eq., 2.4 g, 2.5 mL, 19.6 mmol), application of the general procedure for 6 hours gave a crude product as a 90 : 10 mixture of regioisomers that was recrystallized twice from ethanol (reflux to -18 °C) to afford pure 1-iodo-4-

methoxy-2-methylbenzene 1-iodo-4-methoxy-2-methylbenzene (2.2 g, 8.87 mmol, 45%) as colorless crystals.
^{1}**H-NMR** ($CDCl_3$, 400 MHz) : δ = 7.12 (d, J = 8.4 Hz, 1H), 7.10 (d, J = 2.6 Hz, 1H), 6.77 (dd, J = 8.4, 2.7 Hz, 1H), 3.77 (s, 3H), 2.33 (s, 3H) ppm.
Spectral data matched the litterature.

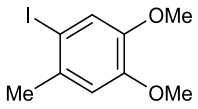

1-iodo-4,5-dimethoxy-2-methylbenzene
Chemical Formula: $C_9H_{11}IO_2$
Molecular Weight: 278,0895

From 4,5-dimethoxy-2-methylbenzene (1 eq., 5.49 g, 5.23 mL, 36.1 mmol) application of the general procedure gave a crude product that was recrystallized from a Et_2O/*n*-Pen (1 : 1) mixture (reflux to -18°C) to yield 1-iodo-4,5-dimethoxy-2-methylbenzene (4.965 g, 17.9 mmol, 49%).
^{1}**H-NMR** ($CDCl_3$, 400 MHz): δ = 7.21 (s, 1H), 6.76 (s, 1H), 3.85 (s, 3H), 3.84 (s, 3H), 2.37 (s, 3H).
Spectral data matched the literature.

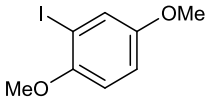

2-iodo-1,4-dimethoxybenzene
Chemical Formula: $C_8H_9IO_2$
Molecular Weight: 264,0625

From 1,3-dimethoxybenzene (1 eq., 10.5 g, 10 mL, 76 mmol) application of the general procedure gave a crude product that was recrystallized from Et_2O (reflux to -18°C, two batches) to afford colorless crystals of 1-iodo-2,4-dimethoxybenzene (10 g, 38 mmol, 50%)
^{1}**H-NMR** ($CDCl_3$, 400 MHz) : δ = 7.62 (d, J = 8.6 Hz, 1H), 6.43 (d, J = 2.7 Hz, 1H), 6.32 (dd, J = 8.6, 2.7 Hz, 1H), 3.86 (s, 3H), 3.80 (s, 3H) ppm.
Spectral data matched the literature.

3-iodo-4-methylaniline (1 eq., 1 g, 4.29 mmol) and phthalic anhydride (1 eq., 0.636 g, 4.29 mmol) were loaded in a microwave vial and DMF (15 mL) was added. The resulting mixture was heated at 200 °C for 30 min. After cooling down to room temperature, it was poured onto water, and the off-white solid was filtrated. The solid was dissolved in DCM, dried with Na_2SO_4 and recrystallized by slow evaporation of a saturated solution of diethyl ether, affording 2-(4-iodo-3-methylphenyl)isoindoline-1,3-dione (1.25 g, 3.44 mmol, 80 %).
^{1}**H-NMR** ($CDCl_3$, 400 MHz) : δ = 7.99 – 7.92 (m, 2H), 7.89 (d, J = 1.8 Hz, 1H), 7.83 – 7.77 (m, 2H), 7.42 – 7.29 (m, 2H), 2.49 (s, 3H) ppm.

(2) GP2: for arylation with double control of axial chirality

Under air, the substrate (1 equiv., loaded as a solution in HFIP), was added to an oven-dried pressure tube containing Ag_2CO_3 (2+0.x equiv.), AgTFA (1 equiv.), $Pd(TFA)_2$ (x mol%), IPrHCl (2x mol%), 4 Å MS (25mg/mL of HFIP) and the iodoarene (2 equiv). Then an additional portion of HFIP was added to wash the walls of the reaction vessel and to achieve a concentration of [Pd] = 0.019 M to 0.010 M. The resulting heterogeneous mixture was stirred at room temperature for c.a. 10 min., and was submerge in a glycerol bath at 85 °C. The color of the reaction changed from greenish to yellowish to dark brown in a time frame of half an hour, depending on the iodoarene used. After 4 hours, the reaction was cooled down to room temperature (*CAUTION : inside build-up of pressure if not properly cooled down*), diluted with Et_2O and filtrated over a small silica gel pad (washed with Et_2O), and the solvent removed under reduced pressure. Then a filtration (using c.a. 100 equiv (w/w) of silica gel relative to the substrate), using pure Et_2O or EtOAC as eluent, was carried out in order to be able to record a good quality ^1H NMR spectra and to determine the diastereoselectivity of the reaction by removing very polar impurities whose signals overlap with the product signal. This “crude after filtration” was diluted in $CDCl_3$, CH_2Br_2 was added as an internal standard, and ^1H NMR spectra were recorded. Finally, the crude product was purified by flash chromatography using Et_2O/*n*-Pen solvent mixture.
Note : important information impacting the safety and the reproducibility of the reaction and concerning the use of the pressure tube, the handling of reagents (and more) along with pictures of the reaction set-up are given hereafter.

(3) General remarks:

Due to the sensitiveness of the reaction, the following guidelines have to be respected to ensure **reproducibility** as well as the **safety** of the operator (reactions conducted **above the boiling point** of the solvent) :

-The reaction were conducted -and the reagents were loaded- under air; however the reaction vessels were dried overnight in an oven (~110 °C) and dry solvents were used.

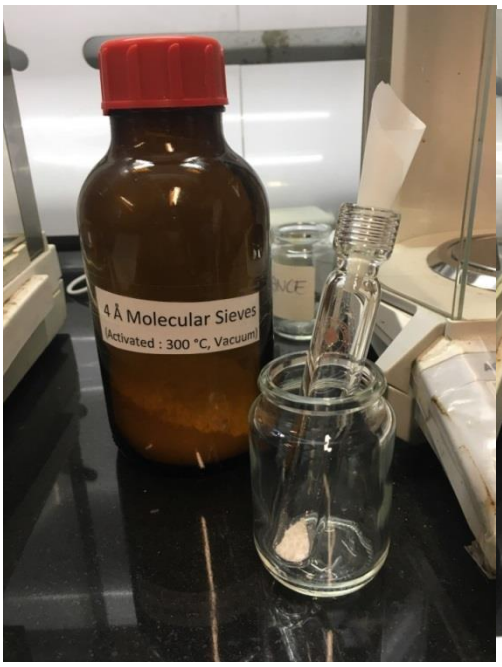

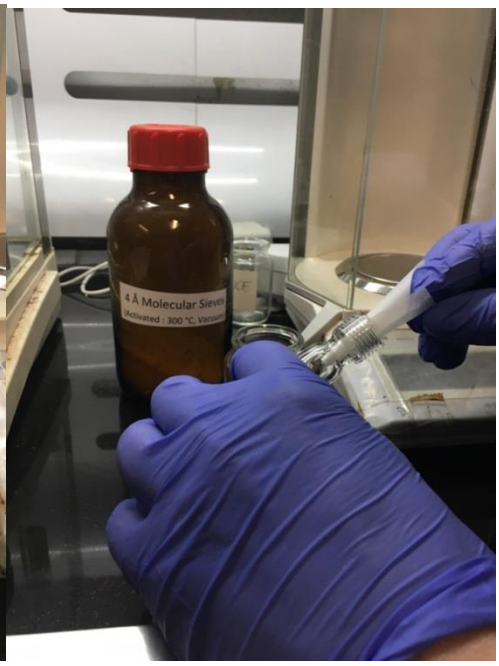

-**<u>Reaction vials:</u>** the reactions were conducted in Ace pressure tubes #7 Ace-Thred (102 mm lenght, 19 mm outside diameter, ~9 mL). However the FETFE front seal **can't be used,** as HFIP will slowly dissolve it, leading to catastrophic failure after some reactions. Also, to ensure proper lifetime and a good seal, one must take care not befouling the threads. In both case, it is possible to wash the threads with HFIP. However, the threads have to be clean when the seal is closed: otherwise the reactor might not hold pressure. Reactors and seals were cleaned between each reaction by fully submerging them in an aqua regia solution for several hours, followed by washing with distilled water, ethanol and acetone. Then both the reaction and the seal were loaded in an oven (~110 °C) overnight, and allowed to cool down to room temperature in a silica gel desiccator.


-HFIP : HFIP was dried by 2 sequential static drying on 3 Å molecular sieves (20% m/v). Plastic syringes should not be reused when using HFIP.

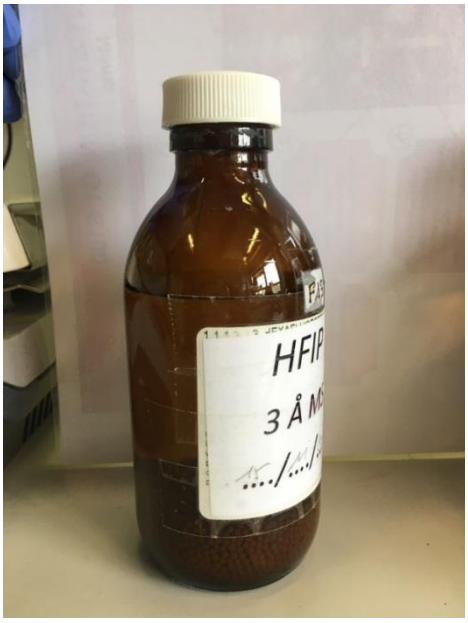

-Ag_2CO_3: the appearance (from yellow to green powder), as well of the supplier, of silver carbonate had little influence on the reaction. It was nonetheless kept in a container protected from light (aluminum foil wrapping) and dried under vacuum overnight before use.

-AgTFA : the silver trifluoroacetate source was essential to attain good yields. Using 98% AgTFA from Sigma-Aldrich (5 g bottle) that were immediately protected from light with aluminum foil when received, as well as flushed with Argon before and after use, allowed us to achieve reproducible results.

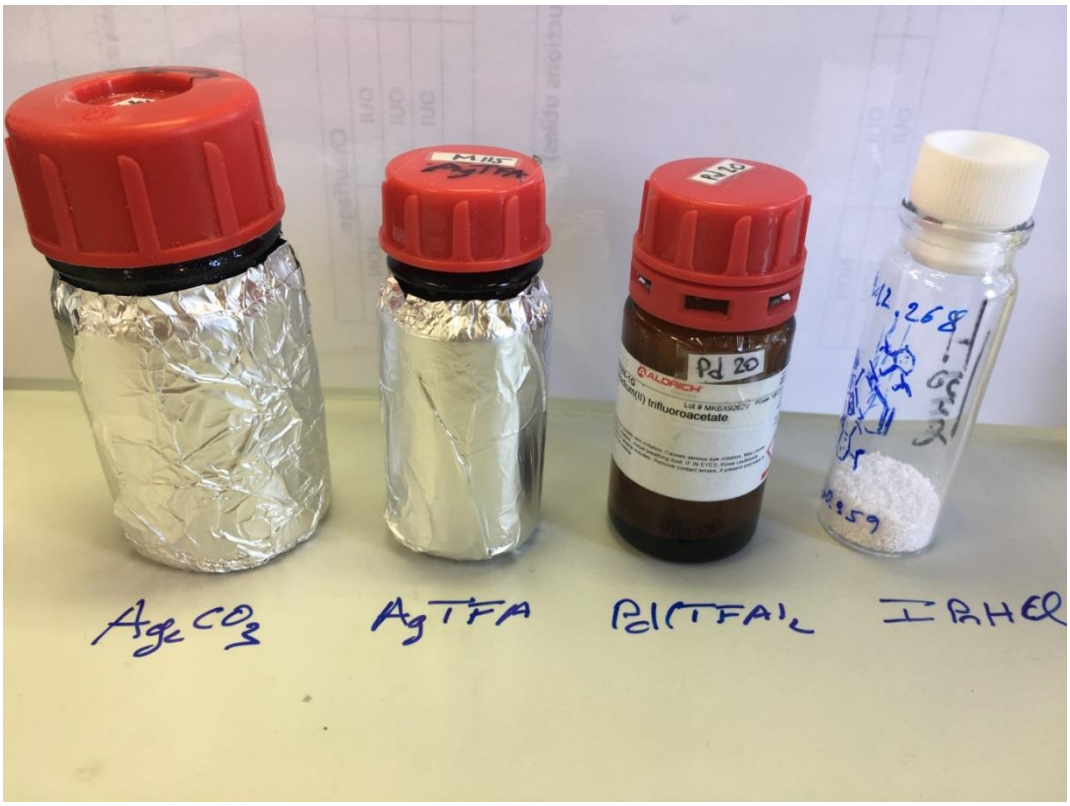

-Molecular Sieves : powdered 4 Å MS were used : it is important to properly active them; first they should be dried overnight in an oven, then loaded in a round-bottom flask that will be heated under vacuum at ~300 °C overnight (heating past 300 °C might results in melting the glass). After use, they should be periodically put under vacuum and back-filled with argon.

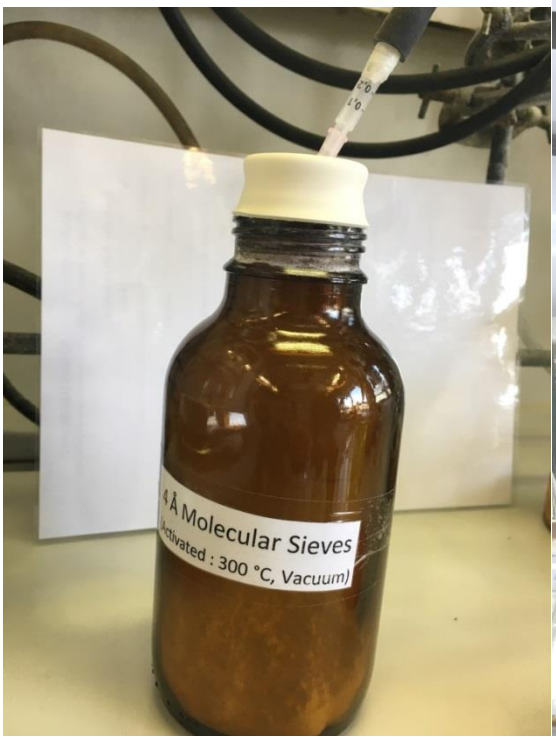

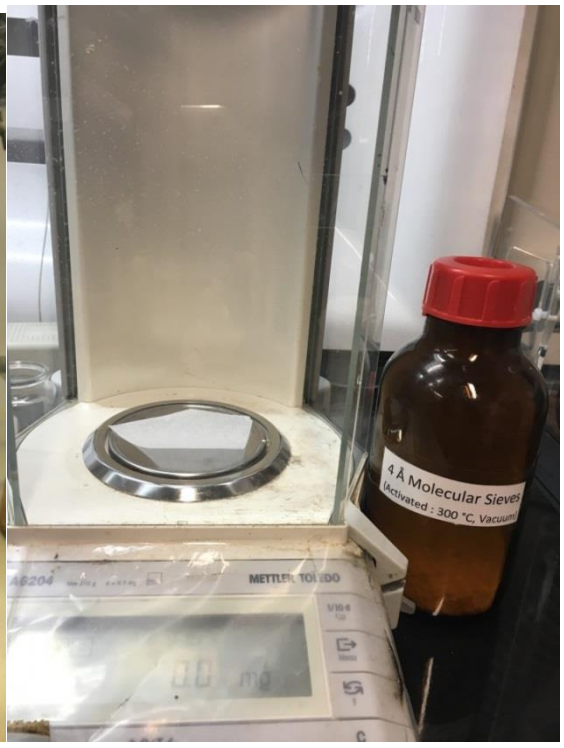

-Substrates : the substrates were mostly in the form of a sticky oil. Stock solutions in chloroform were prepared, the required amount was transferred to a flask, the solvent remove under reduce pressure and dried under vacuum for several hours. Then an HFIP solution was prepared under argon and transferred by means of a syringe to the reaction vessel.

-Aryliodides : the commercial iodides were used as received from several different suppliers.

-NHC precursor : the NHC precursor were prepared in the laboratory. The one used in a crystalline or microcrystalline form.

-Stirring the reactions : as these reactions are heterogeneous, a proper sized stir bar has to be used (2 mm ovoid for the reactors described before).

-Heating the reactions : the reactors were deeply submerged in a glycerol or in an oil bath.

-Monitoring the reactions : care should be taken that the pressure reactors have thick walls, so they should be cooled for some time under a cool stream of water and then exposed to room temperature for some time. A small pressure release (resulting from the evolved CO_2) will occur when the reactors are opened. Samples for TLC and/or LC-MS can be taken under air several times without affecting the reaction.

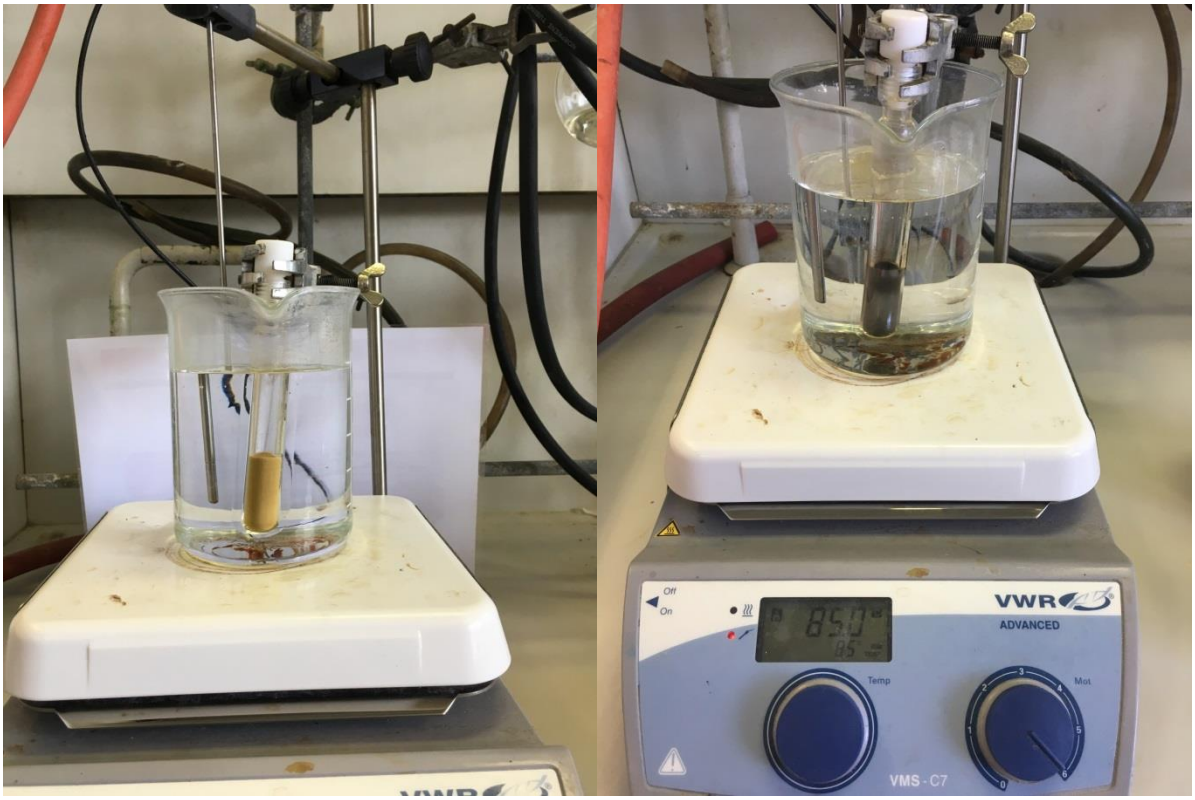

-Work-up: after having cooled down to room temperature, the reactions were diluted with Et_2O (small exotherm) and stirred for ~15 min. The resulting mixture was filtrated

on a small silica gel plug (washed with Et_2O). The volatiles were removed under reduced pressure, and a crude ^1H NMR was recorded. As a reliable diastereomeric ratio could not be determine on the crude NMR (broad and/or overlapping signals, uneven baseline), a thorough filtration was performed (100 equiv (w/w) of silica gel relative to crude product, crude mixture loaded as a DCM solution, large fractions collected), using pure Et_2O or EtOAC as the eluent, to remove left-over reagents and/or by-products : all the fractions were combined after no more compounds eluted in pure Et_2O or EtOAc (as a visual cue, the first organic-containing fraction are marked by a dark coloration. The end of the filtration can be spotted when the color of the eluent stays constant. Usually 4 to 6 fractions contain all the eluting organic material). Another ^1H NMR was then recorded (for d.r. determination), and the crude product was purified by column chromatography (either CyH/EtOAc or *n*-pentane/Et_2O solvent system – with a 200 : 1 (w/w) ratio of silica gel to crude product). Usually, the first (diluted) fractions were not collected in order to obtain a cleaner product.

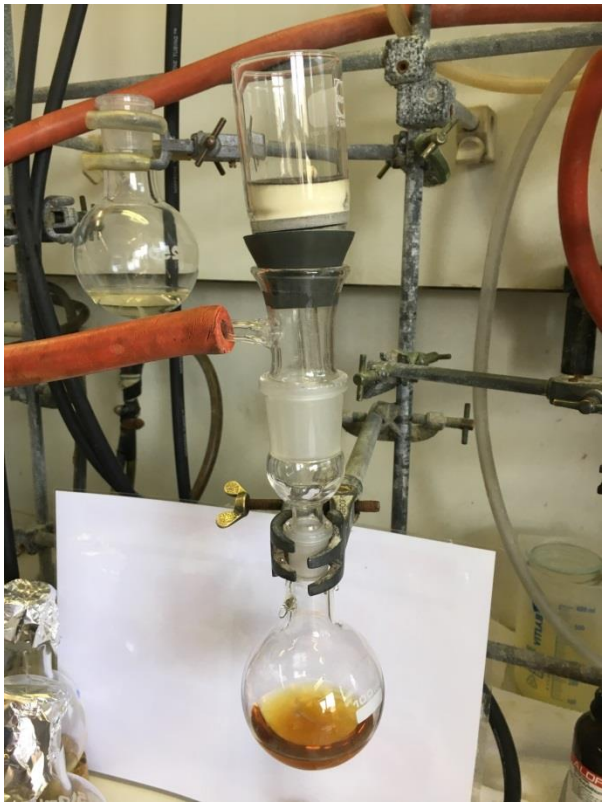

-Quantitative NMR: dibromomethane was used as an internal standard when needed – a stock solution of 50 µL of CH_2Br_2 in $CDCl_3$ was prepared in a 5 mL volumetric flask, and 1 mL was added to the crude mixture: c.a. 0.142 mmol of CH_2Br_2 for reactions where the scale varied between 0.15 and 0.3 mmol.

(4) Scope limitations :

The following substrate were either found unreactive under the standard conditions, or afforded complex mixtures with complete conversion of the starting material:

-of interest is the profound deactivating effect of the C'4-OMe (*meta* to the metallated position), whereas 1l and 1n reached complete conversion in less than 2 hours, their analogs 1r and 1s did not react at all.

-also worth noting is the good reactivity of 1i and 1j : we suspect that the side reactions yielding a complex mixture are explained by the, somewhat, activated benzylic positions in HFIP solvent and with a relatively electron-rich aryl (the aryliodide coupling partner) present in the reaction mixture (see Vuković, V. D.; Richmond, E.; Wolf, E.; Moran, J. *Angew. Chem. Int. Ed.* **2017**, *56*, 3085-3089 for further information).

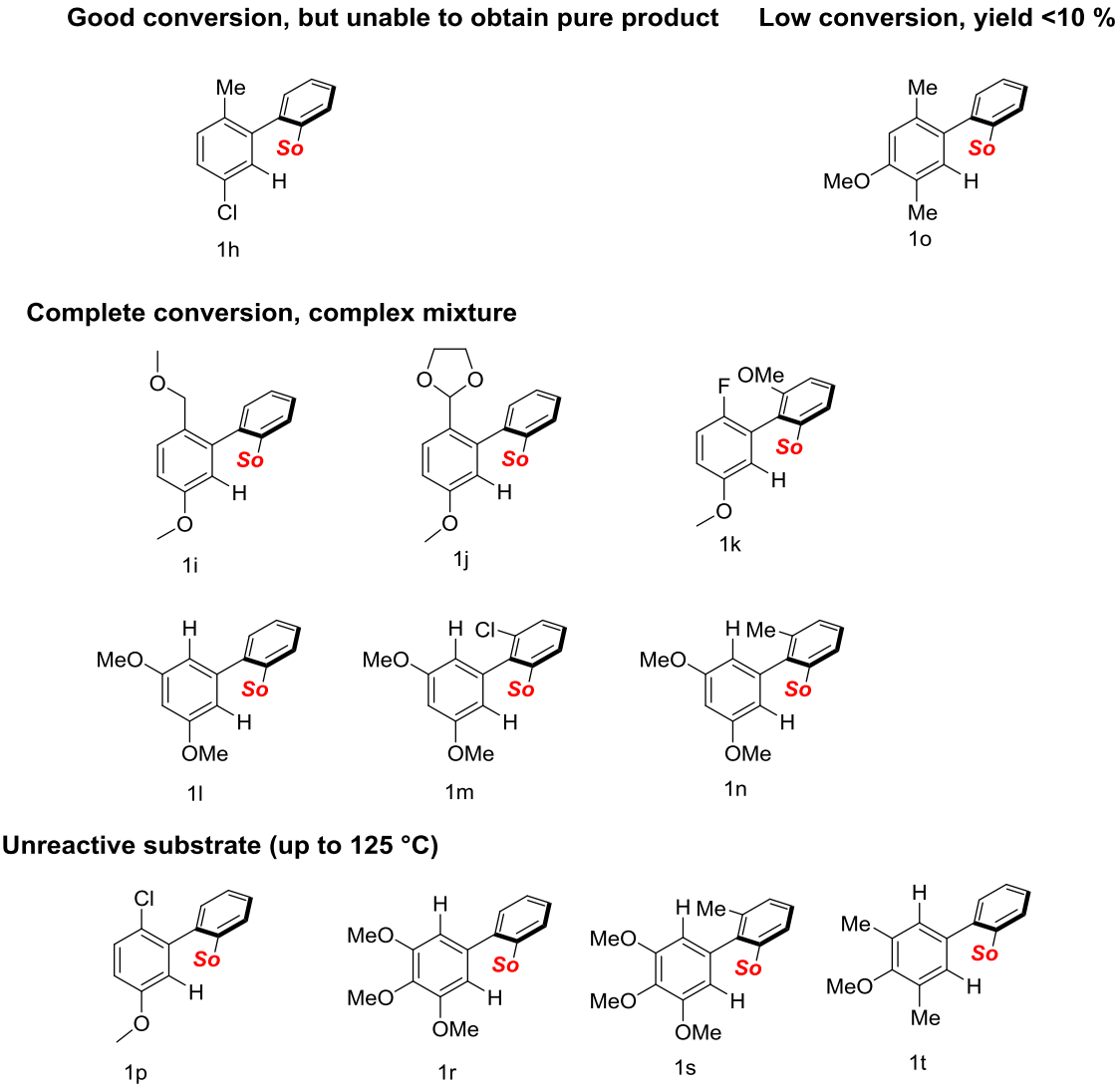

Figure VII-31 : scope limitations

(5) Product characterization

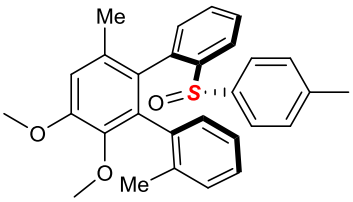

(1'*R*,2'*S*)-3',4'-dimethoxy-2'',6'-dimethyl-2-((*S*)-*p*-tolylsulfinyl)-1,1':2',1''-terphenyl
Chemical Formula: $C_{29}H_{28}O_3S$
Molecular Weight: 456,6000

3eJ. The general procedure **GP2** was followed for 4 hours at 85 °C with **x = 25**, from (*S*)-4,5-dimethoxy-2-methyl-2'-(p-tolylsulfinyl)-1,1'-biphenyl (1 eq., 56 mg, 0.153 mmol) and *o*-iodotoluene (2 eq., 66.7 mg, 39 µL, 0.306 mmol) in HFIP (2050 µL), yielding (1' $_a$*R*,2'$_a$*S*)-3',4'-dimethoxy-2'',6'-dimethyl-2-((*S*)-p-tolylsulfinyl)-1,1':2',1''-terphenyl (34 mg, 0.0745 mmol, 49%) as a yellowish powder, with a d.r. ≥98 : 2 (83% conversion, crude d.r. = 49 : 2 : 1).

^{1}**H-NMR** ($CDCl_3$, 400 MHz) : δ = 7.94 (dd, J = 7.9, 1.1 Hz, 1H), 7.57 (dd, J = 7.6, 1.3 Hz, 1H), 7.37 (td, J = 7.7, 1.3 Hz, 1H), 7.25 (td, J = 7.4, 1.4 Hz, 1H), 7.20 – 7.08 (m, 5H), 7.05 (td, J = 7.5, 1.4 Hz, 1H), 6.99 (dd, J = 7.5, 1.1 Hz, 1H), 6.95 (d, J = 7.5 Hz, 1H), 6.65 (s, 1H), 3.95 (s, 3H), 3.57 (s, 3H), 2.34 (s, 3H), 1.94 (s, 3H), 1.13 (s, 3H) ppm.

^{13}**C-NMR** ($CDCl_3$, 101 MHz): δ = 152.81, 144.70, 143.55, 141.68, 141.19, 137.66, 135.97, 135.50, 135.34, 133.07, 130.19, 129.78, 129.70, 129.45 ($2C_{pTol}$), 129.06, 128.76, 128.12, 127.29, 126.77 ($2C_{pTol}$), 125.00, 123.06, 112.72, 60.63, 55.80, 21.40, 20.13, 19.87 ppm.

$[\alpha]_D^{20}$ = -152.24 ° (c = 0.364, $CHCl_3$).

HRMS (ESI): *calc. for* $C_{29}H_{29}O_3S^+$ *457.1832* ; found 457.1846

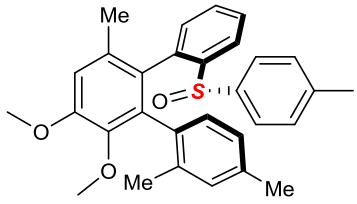

(1'*S*,2'*R*)-5',6'-dimethoxy-2,3',4-trimethyl-2''-((*S*)-*p*-tolylsulfinyl)-1,1':2',1''-terphenyl
Chemical Formula: $C_{30}H_{30}O_3S$
Molecular Weight: 470,6270

3eM. The general procedure **GP2** was followed for 4 hours at 85 °C with **x = 15**, from (*S*)-4,5-dimethoxy-2-methyl-2'-(p-tolylsulfinyl)-1,1'-biphenyl (1 eq., 73 mg, 0.199 mmol) and 1-iodo-2,4-dimethylbenzene (2.01 eq., 92.8 mg, 57 µL, 0.4 mmol) in HFIP (2500), yielding (1'$_a$*S*,2'$_a$*R*)-5',6'-dimethoxy-2,3',4-trimethyl-2''-((*S*)-p-tolylsulfinyl)-1,1':2',1''-terphenyl (68.4 mg, 0.145 mmol, 73 %) as a yellow powder with a d.r. ≥98 : 2 (96% conversion, crude d.r. = 22 : 1 : 1).

^{1}**H-NMR** ($CDCl_3$, 400 MHz) : δ = 7.96 (dd, J = 8.0, 1.2 Hz, 1H), 7.45 (d, J = 7.8 Hz, 1H), 7.38 (td, J = 7.7, 1.3 Hz, 1H), 7.27 (td, J = 7.4, 1.3 Hz, 1H), 7.15 – 7.04 (***AA'BB'***,

4H), 7.00 (dd, J = 7.6, 1.2 Hz, 1H), 6.95 (dd, J = 7.9, 1.2 Hz, 1H), 6.75 (s, 1H), 6.63 (s, 1H), 3.94 (s, 3H), 3.57 (s, 3H), 2.33 (s, 3H), 2.19 (s, 3H), 1.89 (s, 3H), 1.10 (s, 3H).ppm.

^{13}**C-NMR** ($CDCl_3$, 101 MHz): δ = 152.74, 144.84, 143.41, 141.63, 141.14, 137.71, 136.56, 135.53, 134.95, 132.98, 132.88, 130.23, 129.86, 129.72, 129.52, 129.39 (2C$_{p\text{Tol}}$), 128.90, 128.01, 126.73 (2C$_{p\text{Tol}}$), 125.77, 122.92, 112.61, 60.58, 55.75, 21.36, 21.02, 20.02, 19.82 ppm.

$[\alpha]_D^{20}$ = -80.4 ° (c = 0.730, $CHCl_3$).

HRMS (ESI): *calc. for $C_{30}H_{31}O_3S^+$ 471.1988* ; found 471.1982

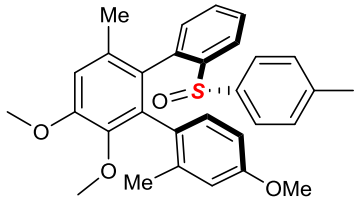

(1'*S*,2'*R*)-4,5',6'-trimethoxy-2,3'-dimethyl-2''-((*S*)-*p*-tolylsulfinyl)-1,1':2',1''-terphenyl
Chemical Formula: $C_{30}H_{30}O_4S$
Molecular Weight: 486,6260

3eN. The general procedure **GP2** was followed for 4 hours at 85 °C with **x = 15**, from (*S*)-4,5-dimethoxy-2-methyl-2'-(p-tolylsulfinyl)-1,1'-biphenyl (1 eq., 73 mg, 0.199 mmol) and 1-iodo-4-methoxy-2-methylbenzene (2 eq., 99 mg, 0.399 mmol) in HFIP (2500 µL), yielding (1'$_a$*S*,2'$_a$*R*)-4,5',6'-trimethoxy-2,3'-dimethyl-2''-((*S*)-p-tolylsulfinyl)-1,1':2',1''-terphenyl (63 mg, 0.129 mmol, 65 %) as a yellow powder with a d.r. ≥98 : 2 (90% conversion, crude d.r. = 21 : : 0).

Crystals suitable for X-Ray analysis were grown by layering a concentrated $CHCl_3$ solution by *n*-pentane in a narrow container and letting the resulting biphasic mixture equilibrate at 4-6 °C.

^{1}**H-NMR** ($CDCl_3$, 400 MHz) : δ = 7.95 (dd, J = 7.9, 1.2 Hz, 1H), 7.48 (d, J = 8.5 Hz, 1H), 7.38 (td, J = 7.7, 1.3 Hz, 1H), 7.27 (td, J = 7.4, 1.3 Hz, 1H), 7.16 – 7.06 (***AA'BB'***, 4H), 6.99 (dd, J = 7.6, 1.1 Hz, 1H), 6.70 (dd, J = 8.5, 2.8 Hz, 1H), 6.63 (s, 1H), 6.50 (d, J = 2.6 Hz, 1H), 3.94 (s, 3H), 3.71 (s, 3H), 3.55 (s, 3H), 2.34 (s, 3H), 1.91 (s, 3H), 1.12 (s, 3H) ppm.

^{13}**C-NMR** ($CDCl_3$, 101 MHz): δ = 158.44, 152.76, 145.10, 143.43, 141.67, 141.15, 137.86, 136.83, 135.26, 132.99, 130.71, 130.25, 129.82, 129.42, 129.25, 128.38, 128.07, 126.75, 123.10, 115.05, 112.67, 109.83, 60.59, 55.80, 54.83, 21.40, 20.36, 19.89 ppm.

$[\alpha]_D^{20}$ = -89.3 ° (c = 0.376, $CHCl_3$).

HRMS (ESI): *calc. for $C_{30}H_{31}O_4S^+$ 487.1938* ; found 487.1886

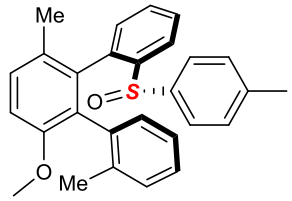

(1'*R*,2'*S*)-3'-methoxy-2'',6'-dimethyl-2-((*S*)-*p*-tolylsulfinyl)-1,1':2',1''-terphenyl
Chemical Formula: $C_{28}H_{26}O_2S$
Molecular Weight: 426,5740

3fJ. The general procedure **GP2** was followed for 4 hours at 85 °C with **x = 10**, from (*S*)-5-methoxy-2-methyl-2'-(p-tolylsulfinyl)-1,1'-biphenyl (1 eq., 61 mg, 0.181 mmol) and (o-iodotoluene (2.16 eq., 85.5 mg, 50 µL, 0.392 mmol) in HFIP (1800 µL), yielding (1'$_a$*R*,2 $_a$*S*)-3'-methoxy-2'',6'-dimethyl-2-((*S*)-p-tolylsulfinyl)-1,1':2',1''-terphenyl (34 mg, 0.0797 mmol, 44%) as a yellowish powder with a d.r. = 98 : 2 (56% conversion, crude d.r. = 23 : 2 : 1).

^{1}**H-NMR** ($CDCl_3$, 400 MHz) : δ = 7.98 (dd, J = 7.9, 1.0 Hz, 1H), 7.53 (dd, J = 7.6, 1.4 Hz, 1H), 7.37 (td, J = 7.7, 1.3 Hz, 1H), 7.25 (td, J = 7.5, 1.4 Hz, 1H), 7.18 – 7.08 (m, 5H), 7.06 (dd, J = 8.4, 0.6 Hz, 1H), 7.04 (td, J = 7.4, 1.4 Hz, 1H), 7.02 – 6.93 (m, 2H), 6.97 (ddd, J = 1237.4, 6.3, 1.0 Hz, 1H), 3.76 (s, 3H), 2.34 (s, 3H), 1.90 (s, 3H), 1.08 (s, 3H) ppm.

^{13}**C-NMR** ($CDCl_3$, 101 MHz): δ = 155.19, 143.03, 141.73, 141.07, 137.94, 137.00, 136.26, 135.53, 129.81, 129.61 (2C), 129.45 (2C), 129.37, 129.17, 129.03, 128.13, 127.19, 126.79 (2C), 125.17, 111.26, 55.91, 21.39, 19.94, 19.11.ppm.

$[\alpha]_D^{20}$ = -20.9 ° (c = 0.225, $CHCl_3$).

HRMS (ESI): *calc. for $C_{28}H_{27}O_2S^+$ 427.1726* ; found 427.1731

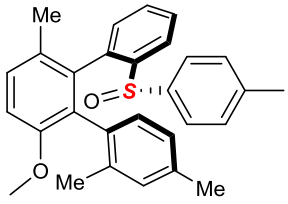

(1'*S*,2'*R*)-6'-methoxy-2,3',4-trimethyl-2''-((*S*)-*p*-tolylsulfinyl)-1,1':2',1''-terphenyl
Chemical Formula: $C_{29}H_{28}O_2S$
Molecular Weight: 440,6010

3fM. The general procedure **GP2** was followed for 4 hours at 85 °C with **x = 10**, from (*S*)-5-methoxy-2-methyl-2'-(p-tolylsulfinyl)-1,1'-biphenyl (1 eq., 75 mg, 0.223 mmol) and 1-iodo-2,4-dimethylbenzene (2 eq., 103 mg, 63.9 µL, 0.447 mmol) in HFIP (2250 µL), yielding (1'$_a$*S*,2'$_a$*R*)-6'-methoxy-2,3',4-trimethyl-2''-((*S*)-p-tolylsulfinyl)-1,1':2',1''-terphenyl (61 mg, 0.138 mmol, 62%) as a yellow powder with a d.r. ≥98 : 2 (80% conversion, crude d.r. = 45 : 2 : 1).

^{1}**H-NMR** ($CDCl_3$, 400 MHz) : δ = 7.99 (dd, *J* = 7.9, 1.6 Hz, 1H), 7.41 (d, *J* = 7.6 Hz, 1H), 7.38 (dd, *J* = 7.6, 1.1 Hz, 1H), 7.26 (td, J = 7.4, 1.6 Hz, 1H), 7.12 (***AA'***BB', 2H), 7.09 (AA'***BB'***, 2H), 7.03 (d, *J* = 8.5 Hz, 1H), 6.98 (dd, J = 7.4, 1.4 Hz, 1H), 6.97 (d, J

= 8.5 Hz, 1H), 6.95 (d, J = 7.4 Hz, 1H), 6.77 (s, 1H), 3.76 (s, 3H), 2.33 (s, 3H), 2.18 (s, 3H), 1.86 (s, 3H), 1.06 (s, 3H) ppm.

^{13}**C-NMR** ($CDCl_3$, 101 MHz): δ = 155.4, 142.9, 141.7, 141.0, 138.0, 137.2, 136.5, 135.2, 133.2, 129.9, 129.8, 129.6, 129.5, 129.5, 129.4, 129.4 (2$C_{p\text{Tol}}$), 129.1, 128.1, 126.8 (2$C_{p\text{Tol}}$), 126.0, 122.9, 111.2, 55.9, 21.4, 21.1, 19.9, 19.1 ppm.

$[\alpha]_D^{20}$ = -102.1 ° (c = 0.740, $CHCl_3$).

HRMS (ESI): *calc. for $C_{29}H_{29}O_2S^+$ 441.1883* ; found 441.1873

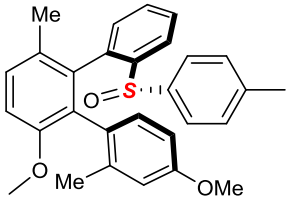

(1'*S*,2'*R*)-4,6'-dimethoxy-2,3'-dimethyl-2''-((*S*)-*p*-tolylsulfinyl)-1,1':2',1''-terphenyl
Chemical Formula: $C_{29}H_{28}O_3S$
Molecular Weight: 456,6000

3fN. The general procedure **GP2** was followed for 4 hours at 85 °C with **x = 10**, from (*S*)-5-methoxy-2-methyl-2'-(p-tolylsulfinyl)-1,1'-biphenyl (1 eq., 119 mg, 0.355 mmol) and 1-iodo-4-methoxy-2-methylbenzene (2.01 eq., 177 mg, 0.715 mmol) in HFIP (3500 µL), yielding (1'$_a$*S*,2'$_a$*R*)-4,6'-dimethoxy-2,3'-dimethyl-2''-((*S*)-p-tolylsulfinyl)-1,1':2',1''-terphenyl (102 mg, 0.223 mmol, 63%) as an orange powder with a d.r. ≥98 : 2 (96% conversion, crude d.r. = 213 : 4 : 1).

^{1}**H-NMR** ($CDCl_3$, 400 MHz) : δ = 7.99 (dd, J = 7.9, 1.2 Hz, 1H), 7.45 (d, J = 8.4 Hz, 1H), 7.38 (td, J = 7.7, 1.3 Hz, 1H), 7.26 (td, J = 7.6, 1.3 Hz, 1H), 7.17 – 7.06 (***AA'BB'***, 4H), 7.04 (d, J = 8.6 Hz, 1H), 6.98 (d, J = 8.2 Hz, 1H), 6.96 (d, J = 6.8 Hz, 1H), 6.69 (dd, J = 8.5, 2.7 Hz, 1H), 6.52 (d, J = 2.6 Hz, 1H), 3.76 (s, 3H), 3.69 (s, 3H), 2.33 (s, 3H), 1.87 (s, 3H), 1.07 (s, 3H) ppm.

^{13}**C-NMR** ($CDCl_3$, 101 MHz): δ = 158.32, 155.57, 142.93, 141.74, 141.04, 138.18, 137.51, 137.04, 130.55, 129.89, 129.55, 129.45, 129.42 (2$C_{p\text{Tol}}$), 129.34, 129.17, 128.67, 128.10, 126.78 (2$C_{p\text{Tol}}$), 123.04, 115.16, 111.22, 109.95, 55.94, 54.79, 21.40, 20.19, 19.17 ppm.

$[\alpha]_D^{20}$ = -128.3 ° (c = 0.9, $CHCl_3$).

HRMS (ESI): *calc. for $C_{29}H_{28}NaO_3S^+$ 479.1651* ; found 479.1643

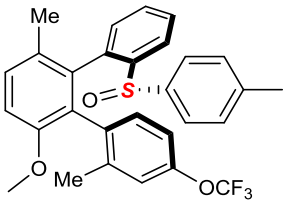

(1'*S*,2'*R*)-6'-methoxy-2,3'-dimethyl-2''-((*S*)-*p*-tolylsulfinyl)-4-(trifluoromethoxy)-1,1':2',1''-terphenyl
Chemical Formula: $C_{29}H_{25}F_3O_3S$
Molecular Weight: 510,5712

3fO. The general procedure **GP2** was followed for 4 hours at 85 °C with **x = 15**, from (*S*)-5-methoxy-2-methyl-2'-(p-tolylsulfinyl)-1,1'-biphenyl (1 eq., 62 mg, 0.184 mmol)

and 1-iodo-2-methyl-4-(trifluoromethoxy)benzene (2.01 eq., 112 mg, 63 µL, 0.371 mmol) in HFIP (2500 µL) , yielding (1'$_a$*S*,2'$_a$*R*)-6'-methoxy-2,3'-dimethyl-2''-((*S*)-p-tolylsulfinyl)-4-(trifluoromethoxy)-1,1':2',1''-terphenyl (46 mg, 0.09 mmol, 49%) as a yellowish powder with a d.r. ≥98 : 2 (76% conversion, crude d.r. 31 : 1 : 0).
^{1}**H-NMR** ($CDCl_3$, 400 MHz) : δ = 7.95 (dd, J = 7.8, 1.1 Hz, 1H), 7.53 (d, J = 8.4 Hz, 1H), 7.38 (td, J = 7.7, 1.3 Hz, 1H), 7.26 (td, J = 7.5, 1.3 Hz, 1H), 7.18 – 7.10 (***AA'BB'***, 4H), 7.08 (dd, J = 8.5, 0.7 Hz, 1H), 6.98 (d, J = 8.5 Hz, 1H), 7.00 – 6.93 (m, 1H), 6.94 (dd, J = 7.6, 1.0 Hz, 1H), 6.81 (s, 1H), 3.76 (s, 3H), 2.34 (s, 3H), 1.91 (s, 3H), 1.13 (s, 3H) ppm.
^{13}**C-NMR** ($CDCl_3$, 101 MHz): δ = 155.13, 148.09 (q, J_{C-F} = 1.6 Hz), 142.98, 141.85, 140.84, 137.95, 137.82, 137.10, 134.98, 130.91, 130.04, 130.03, 129.52 (2C), 129.28, 129.20, 128.34, 128.31, 126.75 (2C), 123.39, 121.05 (q, J_{C-F} = 0.9 Hz), 120.36 (q, J_{C-F} = 256.6 Hz), 117.41, 111.24, 55.84, 21.40, 20.02, 19.14 ppm.
^{19}**F-NMR** ($CDCl_3$, 125.6 MHz): δ = -57.57 ppm.
$[\alpha]_D^{20}$ = -98.6 ° (c = 0.3, $CHCl_3$).
HRMS (ESI): *calc. for $C_{29}H_{26}F_3O_3S^+$ 511.1549* ; found 511.1536

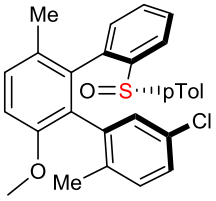

(1'*S*,2'*R*)-5-chloro-6'-methoxy-2,3'-dimethyl-2''-((*S*)-*p*-tolylsulfinyl)-1,1':2',1''-terphenyl
Chemical Formula: $C_{28}H_{25}ClO_2S$
Molecular Weight: 461,0160

3fP. The general procedure **GP2** was followed for 4 hours at 85 °C with **x = 20**, from (*S*)-5-methoxy-2-methyl-2'-(p-tolylsulfinyl)-1,1'-biphenyl (1 eq., 75 mg, 0.223 mmol) and 4-chloro-2-iodo-1-methylbenzene (1.99 eq., 112 mg, 70 µL, 0.444 mmol) in HFIP (3000 µL), yielding (1'$_a$*S*,2'$_a$*R*)-5-chloro-6'-methoxy-2,3'-dimethyl-2''-((*S*)-p-tolylsulfinyl)-1,1':2',1''-terphenyl (72 mg, 0.156 mmol, 70%) as a yellow powder with a d.r. = 97 : 3 (95% conversion, crude d.r. = 53 : 2 : 1).
^{1}**H-NMR** ($CDCl_3$, 400 MHz) : δ = 8.00 (dd, J = 8.0, 1.1 Hz, 1H), 7.55 (d, J = 2.3 Hz, 1H), 7.39 (td, J = 7.7, 1.3 Hz, 1H), 7.26 (dd, J = 7.5, 1.4 Hz, 1H), 7.16 – 7.09 (***AA'BB'***, 4H), 7.08 (dd, J = 8.3, 0.7 Hz, 1H), 7.00 (dd, J = 8.3, 2.3 Hz, 1H), 6.98 (d, J = 8.9 Hz, 1H), 6.96 (dd, J = 7.1, 1.2 Hz, 1H), 6.88 (d, J = 8.2 Hz, 1H), 3.76 (s, 3H), 2.33 (s, 3H), 1.86 (s, 3H), 1.14 (s, 3H) ppm.
^{13}**C-NMR** ($CDCl_3$, 101 MHz): δ = 154.98, 143.28, 141.65, 141.15, 137.94, 137.51, 136.98, 134.19, 130.65, 130.25, 130.10, 129.95, 129.82, 129.43 (2C), 129.40, 129.23, 128.38, 128.24, 127.18, 126.53 (2C), 123.37, 111.22, 55.84, 21.37, 19.40, 19.19 ppm.
$[\alpha]_D^{20}$ = -40.5 ° (c =0.540, $CHCl_3$).
HRMS (ESI): *calc. for $C_{28}H_{25}ClNaO_2S^+$ 483.1156* ; found 483.1103

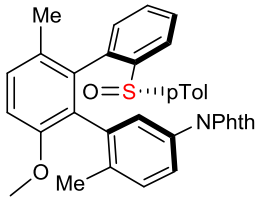

2-((1'*S*,2'*R*)-6'-methoxy-3',6-dimethyl-2''-((*S*)-*p*-tolylsulfinyl)-[1,1':2',1''-terphenyl]-3-yl)isoindoline-1,3-dione
Chemical Formula: $C_{36}H_{29}NO_4S$
Molecular Weight: 571,6910

3fQ. The general procedure **GP2** was followed for 4 hours at 85 °C with **x = 20**, from (*S*)-5-methoxy-2-methyl-2'-(p-tolylsulfinyl)-1,1'-biphenyl (1 eq., 75 mg, 0.223 mmol) and 2-(4-iodo-3-methylphenyl)isoindoline-1,3-dione (1 eq., 81 mg, 0.223 mmol) in HFIP (2400 µL), yielding 2-(1'*S*,2'*R*)-6'-methoxy-3',6-dimethyl-2''-((*S*)-p-tolylsulfinyl)-[1,1':2',1''-terphenyl]-3-yl)isoindoline-1,3-dione (18 mg, 0.0315 mmol, 14%) with a d.r. = 98 : 2 (52% conversion, crude d.r. = n.d., overlapping signals).
An optimized procedure was conducted, giving a more synthetically useful yield, from (S)-5-dimethoxy-2-methyl-2'-(p-tolylsulfinyl)-1,1'-biphenyl (1 eq., 287 mg, 0.853 mmol), AgTFA (0.998 eq., 188 mg, 0.851 mmol), Ag2CO3 (2.34 eq., 551 mg, 2 mmol), 2-(4-iodo-3-methylphenyl)isoindoline-1,3-dione (1.28 eq., 396 mg, 1.09 mmol), 4 Å powdered molecular sieves (200 mg), Pd(TFA)2 (30 %, 85 mg, 0.256 mmol), 1,3-bis(2,6-diisopropylphenyl)-1H-imidazol-3-ium chloride (30.1 %, 109 mg, 0.256 mmol) in hfip (9000 µL) for 5 hours. After cooling down to room temperature the mixture was diluted with CH2Cl2, filtered on a silica gel pad (eluted with Et2O) and the volatiles were removed under reduced pressure. Subsequent chromatography yielded, affording 2-(1'S,2'R)-6'-methoxy-3',6-dimethyl-2''-((S)-p-tolylsulfinyl)-[1,1':2',1''-terphenyl]-3-yl)isoindoline-1,3-dione (358 mg, 0.626 mmol, 73%) as an off-white powder and with a d.r. ≥98 : 2 (95% conversion, crude d.r. = n.d., overlapping signals). A ^{1}H NMR spectra centered on the ($C^{3''}$)-H of the isolated compound with the improved procedure is given.

^{1}H-NMR ($CDCl_3$, 400 MHz) : δ = 8.05 (dd, J = 7.9, 1.3 Hz, 1H), 7.94 – 7.87 (m, 2H), 7.75 – 7.70 (m, 2H), 7.69 (d, J = 2.2 Hz, 1H), 7.43 (td, J = 7.7, 1.3 Hz, 1H), 7.28 (td, J = 7.5, 1.3 Hz, 1H), 7.18 (dd, J = 8.2, 2.3 Hz, 1H), 7.09 (d, J = 8.3 Hz, 1H), 7.07 – 7.04 (m, 4H), 7.03 (d, J = 15.7 Hz, 1H), 7.01 (dd, J = 7.5, 1.2 Hz, 1H), 6.97 (d, J = 4.3 Hz, 1H), 3.79 (s, 3H), 2.31 (s, 3H), 1.94 (s, 3H), 1.05 (s, 3H) ppm.

^{13}C-NMR ($CDCl_3$, 101 MHz) : δ = 167.17 (2C), 155.26, 143.16, 141.51, 141.31, 137.39, 137.03 (2C), 135.78, 133.92 (2C), 131.93, 130.05, 129.69, 129.67, 129.43 (2C), 129.27 (2C), 128.84, 128.66, 128.29, 127.87, 126.82 (2C), 125.45, 124.88, 123.55 (2C), 123.32, 111.43, 56.00, 21.37, 19.78, 19.09 ppm.

$[\alpha]_D^{20}$ = -5.54 ° (c = 0.148, CHCl3).

HRMS (ESI): calc. for $C_{36}H_{29}NNaO_4S^+$ 594.1701 ; found 594.1685

^{1}H-NMR ($CDCl_3$, 400 MHz) : δ = 8.05 (dd, J = 7.9, 1.3 Hz, 1H), 7.94 – 7.87 (m, 2H),

7.75 – 7.70 (m, 2H), 7.69 (d, J = 2.2 Hz, 1H), 7.43 (td, J = 7.7, 1.3 Hz, 1H), 7.28 (td, J = 7.5, 1.3 Hz, 1H), 7.18 (dd, J = 8.2, 2.3 Hz, 1H), 7.09 (d, J = 8.3 Hz, 1H), 7.07 – 7.04 (m, 4H), 7.03 (d, J = 15.7 Hz, 1H), 7.01 (dd, J = 7.5, 1.2 Hz, 1H), 6.97 (d, J = 4.3 Hz, 1H), 3.79 (s, 3H), 2.31 (s, 3H), 1.94 (s, 3H), 1.05 (s, 3H) ppm. ^{13}**C-NMR** ($CDCl_3$, 101 MHz): δ = 167.17 (2C), 155.26, 143.16, 141.51, 141.31, 137.39, 137.03 (2C), 135.78, 133.92 (2C), 131.93, 130.05, 129.69, 129.67, 129.43 (2C), 129.27 (2C), 128.84, 128.66, 128.29, 127.87, 126.82 (2C), 125.45, 124.88, 123.55 (2C), 123.32, 111.43, 56.00, 21.37, 19.78, 19.09 ppm.

$[\alpha]_D^{20}$ = -5.54 ° (c = 0.148 , $CHCl_3$).

HRMS (ESI): *calc. for $C_{36}H_{29}NNaO_4S^+$ 594.1701* ; found 594.1685

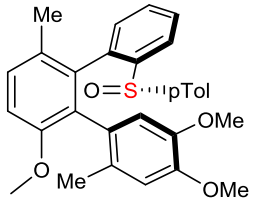

(1'*S*,2'*R*)-4,5,6'-trimethoxy-2,3'-dimethyl-2''-((*S*)-*p*-tolylsulfinyl)-1,1':2',1''-terphenyl
Chemical Formula: $C_{30}H_{30}O_4S$
Molecular Weight: 486,6260

3fR. The general procedure **GP2** was followed for 4 hours at 85 °C with **x = 15**, from (*S*)-5-methoxy-2-methyl-2'-(p-tolylsulfinyl)-1,1'-biphenyl (1 eq., 75 mg, 0.223 mmol) and 1-iodo-4,5-dimethoxy-2-methylbenzene (2.5 eq., 154 mg, 0.557 mmol) in HFIP (3000 µL), yielding (1'S,2'R)-4,5,6'-trimethoxy-2,3'-dimethyl-2''-((S)-p-tolylsulfinyl)-1,1':2',1''-terphenyl (58 mg, 0.119 mmol, 53%) as an orange oil with a d.r. = 98 : 2 (97% conversion, crude d.r. = 29 : 2 : 1).

^{1}**H-NMR** ($CDCl_3$, 400 MHz) : δ = 7.93 (dd, J = 8.0, 1.1 Hz, 1H), 7.34 (td, J = 7.7, 1.3 Hz, 1H), 7.22 (td, J = 7.3, 1.3 Hz, 1H), 7.21 – 7.18 (***AA'***BB', 2H), 7.15 – 7.11 (AA'***BB'***, 2H), 7.08 (dd, J = 8.4, 0.6 Hz, 1H), 7.06 (s, 1H), 6.98 (d, J = 8.5 Hz, 1H), 6.91 (dd, J = 7.6, 1.0 Hz, 1H), 6.49 (s, 1H), 3.88 (s, 3H), 3.78 (s, 3H), 3.75 (s, 3H), 2.34 (s, 3H), 1.86 (s, 3H), 1.18 (s, 3H) ppm.

^{13}**C-NMR** ($CDCl_3$, 101 MHz): δ = 155.38, 147.34, 146.17, 143.21, 141.64, 141.00, 138.46, 137.59, 129.98, 129.46, 129.44 (2$C_{p\text{Tol}}$), 129.39, 129.12, 128.98, 128.21, 128.11, 127.57, 126.52 (2$C_{p\text{Tol}}$), 123.40, 112.62, 111.99, 111.11, 55.95, 55.87, 55.35, 21.35, 19.38, 19.33 ppm.

$[\alpha]_D^{20}$ = -79.5 ° (c = 0.28 , $CHCl_3$).

HRMS (ESI): *calc. for $C_{30}H_{31}O_4S^+$ 487.1938* ; found 487.1939

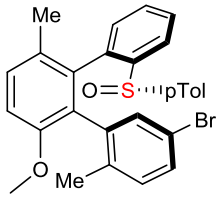

(1'*S*,2'*R*)-5-bromo-6'-methoxy-2,3'-dimethyl-2''-((*S*)-*p*-tolylsulfinyl)-1,1':2',1''-terphenyl
Chemical Formula: $C_{28}H_{25}BrO_2S$
Molecular Weight: 505,4700

3fS. The general procedure **GP2** was followed for 4 hours at 85 °C with **x = 25**, from (*S*)-5-methoxy-2-methyl-2'-(p-tolylsulfinyl)-1,1'-biphenyl (1 eq., 120 mg, 0.357 mmol), 4-bromo-2-iodo-1-methylbenzene (1.98 eq., 210 mg, 105 µL, 0.707 mmol) in hfip (3400 µL), yielding (1'S,2'R)-5-bromo-6'-methoxy-2,3'-dimethyl-2''-((S)-p-tolylsulfinyl)-1,1':2',1''-terphenyl (92 mg, 0.182 mmol, 51 %) as yellow powder with a d.r. ≥98:2 (>95% conversion, crude d.r. = 20.4:?:1 overlapping signals).

^{1}**H-NMR** ($CDCl_3$, 400 MHz) : δ = 8.00 (dd, J = 8.0, 1.1 Hz, 1H), 7.69 (d, J = 2.1 Hz, 1H), 7.39 (td, J = 7.7, 1.3 Hz, 1H), 7.26 (td, J = 7.8, 1.4 Hz, 1H), 7.15 (td, J = 8.3, 2.0 Hz, 1H), 7.15 – 7.04 (m, 5H), 6.98 (d, J = 8.5 Hz, 1H), 6.96 (dd, J = 7.5, 1.1 Hz, 1H), 6.82 (d, J = 8.2 Hz, 1H), 3.76 (s, 3H), 2.33 (s, 3H), 1.84 (s, 3H), 1.14 (s, 3H) ppm.
^{13}**C-NMR** ($CDCl_3$, 101 MHz): δ = 154.92, 143.28, 141.61, 141.14, 138.32, 136.95, 134.72, 132.78, 130.57, 130.11, 130.03, 129.79, 129.39 (2C), 129.37, 129.19, 128.34, 128.05, 126.45 (2C), 123.30, 118.54, 111.17, 55.78, 21.34, 19.44, 19.16 ppm. (1C overlapping not identified)
$[\alpha]_D^{20}$ = -6.4° (C = 0.54, $CHCl_3$)
HRMS (ESI): *calc. for $C_{28}H_{26}BrO_2S^+$ 505.0831* ; found 55.0822

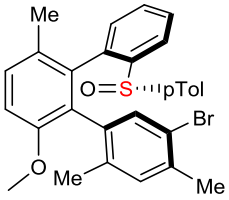

(1'*S*,2'*R*)-5-bromo-6'-methoxy-2,3',4-trimethyl-2''-((*S*)-*p*-tolylsulfinyl)-1,1':2',1''-terphenyl
Chemical Formula: $C_{29}H_{27}BrO_2S$
Molecular Weight: 519,4970

3fR. The general procedure **GP2** was followed for 4 hours at 85 °C with **x = 20**, from (*S*)-5-methoxy-2-methyl-2'-(p-tolylsulfinyl)-1,1'-biphenyl ((1 eq., 50 mg, 0.149 mmol) and 1-bromo-5-iodo-2,4-dimethylbenzene (1.51 eq., 70 mg, 0.225 mmol) in yielding (1'*S*,2'*R*)-5-bromo-6'-methoxy-2,3',4-trimethyl-2''-((*S*)-p-tolylsulfinyl)-1,1':2',1''-terphenyl (25.3 mg, 0.0753 mmol, 51%) as an yellowish powder with a d.r. = 98 : 2 (>95% conversion, crude d.r. = 22.35 : - : 1 overlapping signals).

^{1}**H-NMR** ($CDCl_3$, 400 MHz) : δ = 8.01 (dd, J = 7.9, 1.1 Hz, 1H), 7.71 (s, 1H), 7.39 (td, J = 7.8, 1.3 Hz, 1H), 7.26 (td, J = 7.4, 1.3 Hz, 1H), 7.14 – 7.04 (m, 5H), 6.97 (dd, J = 7.5, 1.1 Hz, 1H), 6.96 (d, J = 8.5 Hz, 1H), 6.81 (s, 1H), 3.76 (s, 3H), 2.32 (s, 3H), 2.23 (s, 3H), 1.81 (s, 3H), 1.11 (s, 3H) ppm.

^{13}**C-NMR** ($CDCl_3$, 101 MHz): δ = 155.17, 143.28, 141.60, 141.23, 137.58, 137.21, 136.19, 135.46, 134.79, 133.55, 131.48, 129.99, 129.74, 129.49, 129.40 (2C), 129.22, 128.31, 128.05, 126.50 (2C), 123.29, 121.12, 111.16, 55.87, 25.30, 22.39, 19.38, 19.21 ppm.

$[\alpha]_D^{20}$ = -3.75 (c = 0.208, $CHCl_3$)

HRMS (ESI): *calc. for $C_{29}H_{28}BrO_2S^+$ 519.0988* ; found 519.0999

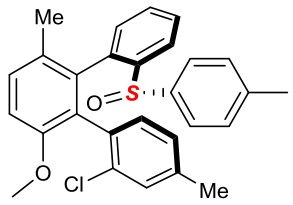

(1'*S*,2'*R*)-2-chloro-6'-methoxy-3',4-dimethyl-2''-((*S*)-*p*-tolylsulfinyl)-1,1':2',1''-terphenyl
Chemical Formula: $C_{28}H_{25}ClO_2S$
Molecular Weight: 461,0160

3fU. The general procedure **GP2** was followed for 4 hours at 85 °C with **x = 20**, from (*S*)-5-methoxy-2-methyl-2'-(p-tolylsulfinyl)-1,1'-biphenyl (1 eq., 62 mg, 0.184 mmol) and 2-chloro-1-iodo-4-methylbenzene (2.58 eq., 120 mg, 75 µL, 0.475 mmol) in HFIP (2500), yielding (1'$_a$*S*,2'$_a$*R*)-2-chloro-6'-methoxy-3',4-dimethyl-2''-((*S*)-p-tolylsulfinyl)-1,1':2',1''-terphenyl (59 mg, 0.128 mmol, 69%) as a yellow powder with a d.r. = 97 : 3 (89% conversion, crude d.r. = 625 : 1 : 10).

^{1}**H-NMR** ($CDCl_3$, 400 MHz) : δ = 7.95 (dd, J = 7.9, 1.3 Hz, 1H), 7.51 (d, J = 7.8 Hz, 1H), 7.40 (td, J = 7.6, 1.4 Hz, 1H), 7.30 (td, J = 7.4, 1.3 Hz, 1H), 7.21 (dd, J = 7.5, 1.3 Hz, 1H), 7.16 – 7.09 (***AA'BB'***, 4H), 7.08 (d, J = 8.0 Hz, 1H), 7.03 (dd, J = 7.8, 1 Hz, 1H), 6.99 (d, J = 8.5 Hz, 1H), 6.98 (s, 1H), 3.77 (s, 3H), 2.34 (s, 3H), 2.20 (s, 3H), 1.10 (s, 3H) ppm.

^{13}**C-NMR** ($CDCl_3$, 101 MHz): δ = 155.29, 142.49, 141.77, 140.83, 138.53, 137.54, 137.24, 132.90, 132.62, 131.03, 130.23, 130.17, 129.89, 129.45 (2C$_{p\text{Tol}}$), 129.22, 129.12, 128.26, 127.54, 127.18, 126.66 (2C$_{p\text{Tol}}$), 122.75, 111.40, 56.07, 21.36, 20.81, 19.01 ppm.

$[\alpha]_D^{20}$ = -151.9 ° (c = 0.575 , $CHCl_3$).

HRMS (ESI): *calc. for $C_{28}H_{25}ClO_2S^+$ 461.1337* ; found 461.1312

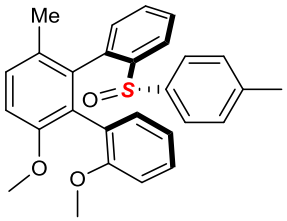

(1'*S*,2'*R*)-2,6'-dimethoxy-3'-methyl-2''-((*S*)-*p*-tolylsulfinyl)-1,1':2',1''-terphenyl
Chemical Formula: $C_{28}H_{26}O_3S$
Molecular Weight: 442,5730

3fl. The general procedure **GP2** was followed for 4 hours at 85 °C with **x = 10**, from (*S*)-5-methoxy-2-methyl-2'-(p-tolylsulfinyl)-1,1'-biphenyl (1 eq., 70 mg, 0.208 mmol) and *o*-iodoanisole (2.02 eq., 98.5 mg, 55 µL, 0.421 mmol) in HFIP (2000 µL) , yielding (1'$_a$*S*,2'$_a$*R*)-2,6'-dimethoxy-3'-methyl-2''-((*S*)-p-tolylsulfinyl)-1,1':2',1''-terphenyl (61 mg, 0.138 mmol, 66%) as a yellow powder with a d.r. = 97 : 3 (84% conversion, crude d.r. = 6 : 1 : 1).

^{1}**H-NMR** ($CDCl_3$, 400 MHz) : δ = 7.82 (dd, J = 7.8, 1.4 Hz, 1H), 7.43 (dd, J = 7.5, 1.8 Hz, 1H), 7.29 (td, J = 7.6, 1.4 Hz, 1H), 7.23 (td, J = 7.4, 1.4 Hz, 1H), 7.09 – 7.02 (m, 1H), 7.03 (dd, J = 7.0, 1.3 Hz, 1H), 7.02 – 6.89 (m, 6H), 6.90 (td, J = 7.5, 1.1 Hz, 1H), 6.46 (dd, J = 8.3, 0.9 Hz, 1H), 3.69 (s, 3H), 3.39 (s, 3H), 2.23 (s, 3H), 1.02 (s, 3H) ppm.

^{13}**C-NMR** ($CDCl_3$, 101 MHz): δ = 155.51, 155.20, 142.70, 141.51, 141.31, 137.73, 137.70, 132.27, 130.97, 129.83, 129.29 (2C), 128.99, 128.82, 128.73, 127.87, 126.63, 126.53 (2C), 124.83, 121.96, 119.90, 111.61, 109.70, 55.98, 54.51, 21.34, 19.06 ppm.

$[\alpha]_D^{20}$ = -146.0 ° (c = 0.802, $CHCl_3$).

HRMS (ESI): *calc. for $C_{28}H_{27}O_3S^+$ 443.1675* ; found 443.1665

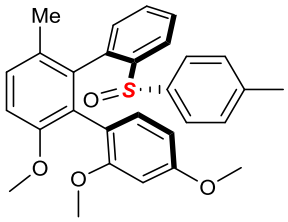

(1'*S*,2'*R*)-2,4,6'-trimethoxy-3'-methyl-2''-((*S*)-*p*-tolylsulfinyl)-1,1':2',1''-terphenyl
Chemical Formula: $C_{29}H_{28}O_4S$
Molecular Weight: 472,5990

3fV. The general procedure **GP2** was followed for 4 hours at 85 °C with **x = 10**, from (*S*)-5-methoxy-2-methyl-2'-(p-tolylsulfinyl)-1,1'-biphenyl (1 eq., 75 mg, 0.223 mmol) and 1-iodo-2,4-dimethoxybenzene (2 eq., 117 mg, 0.446 mmol) in HFIP (2300 µL), yielding (1'$_a$*S*,2'$_a$*R*)-2,4,6'-trimethoxy-3'-methyl-2''-((*S*)-p-tolylsulfinyl)-1,1':2',1''-terphenyl (35 mg, 0.0741 mmol, 33%) as an orange oil with a d.r. = 94 : 6 (99% conversion, crude d.r. = 78 : 16 : 1).

^{1}**H-NMR** ($CDCl_3$, 400 MHz) : δ = 7.92 (dd, J = 7.9, 1.2 Hz, 1H), 7.41 (d, J = 8.4 Hz, 1H), 7.38 (dt, J = 7.7, 1.5, 1.3 Hz, 1H), 7.31 (td, J = 7.4, 1.4 Hz, 1H), 7.12 (dd, J = 7.5, 1.2 Hz, 1H), 7.08 – 6.97 (m, 6H), 6.51 (dd, J = 8.4, 2.4 Hz, 1H), 6.12 (d, J = 2.4 Hz, 1H), 3.77 (s, 3H), 3.73 (s, 3H), 3.44 (s, 3H), 2.31 (s, 3H), 1.07 (s, 3H) ppm.

^{13}**C-NMR** ($CDCl_3$, 101 MHz): δ = 160.11, 156.59, 155.54, 141.53, 138.15, 132.60, 131.09, 129.72, 129.30 (2C), 129.03, 128.77, 127.84, 126.57 (2C), 126.45, 122.09, 117.45, 111.61, 103.47, 98.02, 56.05, 55.04, 54.54, 21.34, 19.10 ppm.

(3 carbons, integrating each for 2C, could not be identified)

$[\alpha]_D^{20}$ = -160.2 ° (c = 0.220, $CHCl_3$).

HRMS (ESI): *calc. for $C_{29}H_{29}O_4S^+$* 473.1781 ; found 473.1776

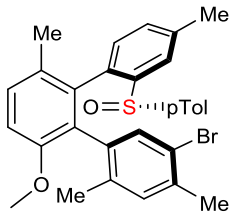

(1'*S*,2'*R*)-5-bromo-6'-methoxy-2,3',4,4''-tetramethyl-2''-((*S*)-*p*-tolylsulfinyl)-1,1':2',1''-terphenyl
Chemical Formula: $C_{30}H_{29}BrO_2S$
Molecular Weight: 533,5240

3jR. The general procedure **GP2** was followed for 4 hours at 85 °C with **x = 20**, from (S)-5'-methoxy-2',4-dimethyl-2-(p-tolylsulfinyl)-1,1'-biphenyl (1 eq., 150 mg, 0.428 mmol) and 1-bromo-5-iodo-2,4-dimethylbenzene(2 eq., 266 mg, 0.856 mmol) in HFIP (4000 µL), yielding (1'*S*,2'*R*)-5-bromo-6'-methoxy-2,3',4,4''-tetramethyl-2''-((*S*)-p-tolylsulfinyl)-1,1':2',1''-terphenyl (155 mg, 0.291 mmol, 68%) as an yellowish powder with a d.r. ≥98 : 2 (>95% conversion, crude d.r. = 54 : 1 : 0).

^{1}**H-NMR** ($CDCl_3$, 400 MHz) : δ = 7.82 (s, 1H), 7.71 (s, 1H), 7.16 – 7.07 (m, 4H), 7.05 (d, J = 8.0 Hz, 2H), 6.95 (d, J = 8.4 Hz, 1H), 6.87 (d, J = 7.7 Hz, 1H), 6.82 (s, 1H), 3.75 (s, 3H), 2.36 (s, 3H), 2.32 (s, 3H), 2.24 (s, 3H), 1.81 (s, 3H), 1.10 (s, 3H) ppm.
^{13}**C-NMR** ($CDCl_3$, 101 MHz): δ = 155.15, 142.63, 141.50, 141.29, 138.33, 137.21, 136.10, 135.58, 134.76, 134.50, 133.62, 131.52, 130.62, 129.92, 129.48 (2C), 129.43, 129.35, 128.19, 126.41 (2C), 123.40, 121.09, 111.03, 55.85, 22.41, 21.37, 21.25, 19.40, 19.25 ppm.
$[\alpha]_D^{20}$ = +89.95 (c = +89.95, c = 0.22)
HRMS (ESI): *calc. for $C_{30}H_{30}BrO_2S^+$ 533.1144* ; found 533.1149

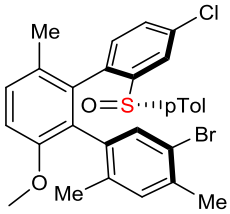

(1'*S*,2'*R*)-5-bromo-4''-chloro-6'-methoxy-2,3',4-trimethyl-2''-((*S*)-*p*-tolylsulfinyl)-1,1':2',1''-terphenyl
Chemical Formula: $C_{29}H_{26}BrClO_2S$
Molecular Weight: 553,9390

3iI. The general procedure **GP2** was followed for 4 hours at 85 °C with **x = 20**, from (1 eq., 132 mg, 0.356 mmol) and 1-bromo-5-iodo-2,4-dimethylbenzene (2 eq., 221 mg, 0.711 mmol) in HFIP (3400 µL), yielding (1'*S*,2'*R*)-5-bromo-4''-chloro-6'-methoxy-2,3',4-trimethyl-2''-((*S*)-p-tolylsulfinyl)-1,1':2',1''-terphenyl (132 mg, 0.238 mmol, 67%) as an yellowish powder with a d.r. = 98 : 2 (>95% conversion, crude d.r. = 223 : 4 : 1).

^{1}**H-NMR** ($CDCl_3$, 400 MHz) : δ = 8.02 (d, J = 2.2 Hz, 1H), 7.69 (s, 1H), 7.24 (dd, J = 8.1, 2.2 Hz, 1H), 7.14 – 7.05 (AA'BB'm, 4H), 7.05 (d, J = 8.6 Hz, 1H), 6.97 (d, J = 8.5 Hz, 1H), 6.93 (d, J = 8.1 Hz, 1H), 6.85 (s, 1H), 3.76 (s, 3H), 2.34 (s, 3H), 2.27 (s, 3H), 1.78 (s, 3H), 1.05 (s, 3H).ppm.
^{13}**C-NMR** ($CDCl_3$, 101 MHz): δ = 155.22, 145.27, 142.08, 140.43, 136.46, 135.98,

135.77, 135.16, 134.63, 133.47, 131.71, 130.91, 130.16, 129.98, 129.50 (2C), 129.16, 127.99, 126.47 (2C), 123.27, 121.15, 111.42, 55.83, 22.40, 21.39, 19.33, 19.06 ppm.

$[\alpha]_D^{20}$ = +155.65 (c = 0.276, $CHCl_3$)

HRMS (ESI): *calc. for $C_{29}H_{27}BrClO_2S^+$ 553.0598* ; found 553.0605

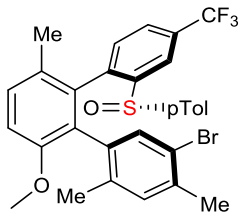

(1'*S*,2'*R*)-5-bromo-6'-methoxy-2,3',4-trimethyl-2''-((*S*)-*p*-tolylsulfinyl)-4''-(trifluoromethyl)-1,1':2',1''-terphenyl
Chemical Formula: $C_{30}H_{26}BrF_3O_2S$
Molecular Weight: 587,4952

3hR. The general procedure **GP2** was followed for 4 hours at 85 °C with **x = 20**, from (1 eq., 212 mg, 0.524 mmol) and 1-bromo-5-iodo-2,4-dimethylbenzene (2 eq., 325 mg, 1.05 mmol) in HFIP (5200 µL) yielding (1'*S*,2'*R*)-5-bromo-6'-methoxy-2,3',4-trimethyl-2''-((*S*)-p-tolylsulfinyl)-4''-(trifluoromethyl)-1,1':2',1''-terphenyl (152 mg, 0.26 mmol, 50%) as an yellowish powder with a d.r. =98 : 0 : 2 (>95% conversion, crude d.r. = 64 : 2 : 3). Some decomposition impurities were present after chromatography, but crystallization by layering concentrated EtOAc solution with pentane gave c.a. 70% yield of previous isolated solid as fluffy off-white needles.

^{1}**H-NMR** ($CDCl_3$, 400 MHz) : δ = 8.36 (dd, J = 1.3, 0.5 Hz, 1H), 7.70 (s, 1H), 7.53 (dd, J = 7.9, 1.3 Hz, 1H), 7.13 (d, J = 7.9 Hz, 1H), 7.12 – 7.08 (m, 2H), 7.08 – 7.03 (m, 4H), 7.00 (d, J = 8.5 Hz, 1H), 3.77 (s, 3H), 2.34 (s, 3H), 2.25 (s, 3H), 1.79 (s, 3H), 1.01 (s, 3H).ppm.

^{13}**C-NMR** ($CDCl_3$, 101 MHz): δ = 155.31, 144.99, 142.26, 141.15, 140.29, 136.68, 135.88, 134.87, 134.58, 133.52, 131.74, 130.74 (q, J = 33.3 Hz), 130.34, 130.27, 129.59 (2C), 128.88, 127.77, 126.57 (2C), 126.43 (q, J = 3.5 Hz), 123.57 (q, J = 272.8 Hz), 121.21, 120.51 (q, J = 3.8 Hz), 111.65, 55.88, 22.39, 21.41, 19.34, 19.02, 14.00 ppm.

$[\alpha]_D^{20}$ = +52.6 (c = 0.312, $CHCl_3$)

HRMS (ESI): *calc. for $C_{29}H_{27}BrClO_2S^+$ 587.0862* ; found 587.0880

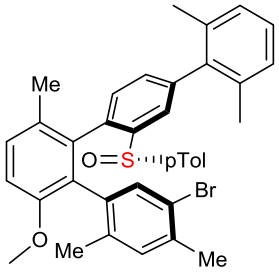

(1'*S*,2'*R*)-5-bromo-6'-methoxy-2,2''',3',4,6'''-pentamethyl-2''-((*S*)-*p*-tolylsulfinyl)-1,1':2',1'':4'',1'''-quaterphenyl
Chemical Formula: $C_{37}H_{35}BrO_2S$
Molecular Weight: 623,6490

3IR. The general procedure **GP2** was followed for 4 hours at 85 °C with **x = 20**, from (1 eq., 125 mg, 0.284 mmol) and 1-bromo-5-iodo-2,4-dimethylbenzene (1.99 eq., 176 mg, 0.566 mmol) in HFIP (2800 µL) yielding (1'$_a$*S*,2'$_a$*R*)-5-bromo-6'-methoxy-2,2''',3',4,6'''-pentamethyl-2''-((*S*)-*p*-tolylsulfinyl)-1,1':2',1'':4'',1'''-quaterphenyl (77.3 mg, 0.124 mmol, 44%) as an yellowish powder with a d.r. ≥98 : 2 (>95% conversion, crude d.r. = 37 : 1 : 0).

^{1}**H-NMR** ($CDCl_3$, 400 MHz) : δ = 7.72 (d, J = 1.4 Hz, 1H), 7.69 (s, 1H), 7.19 (d, J = 8.3 Hz, 2H), 7.13 (d, J = 8.1 Hz, 4H), 7.10 – 7.03 (m, 2H), 7.02 – 6.93 (m, 3H), 6.83 (s, 1H), 3.80 (s, 3H), 2.35 (s, 3H), 2.22 (s, 3H), 2.03 (s, 3H), 1.86 (s, 3H), 1.69 (s, 3H), 1.34 (s, 3H).ppm.
^{13}**C-NMR** ($CDCl_3$, 101 MHz): δ = 155.07, 143.88, 141.54, 141.51, 141.19, 140.43, 137.47, 136.36, 136.18, 136.01, 135.77, 135.17, 134.99, 133.41, 131.19, 130.53, 129.83, 129.46 (2C), 129.39, 128.90, 128.45, 127.30, 127.25, 127.03, 126.63 (2C), 124.19, 121.11, 111.12, 55.80, 22.21, 21.35, 20.72, 20.05, 19.38, 19.27 ppm.
$[\alpha]_D^{20}$ = +158.49 (c = 0.106, $CHCl_3$)
HRMS (ESI): *calc. for* $C_{37}H_{36}BrO_2S^+$ 623.1614; found 623.1612

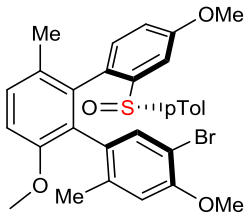

(1'*S*,2'*R*)-5-bromo-4,4'',6'-trimethoxy-2,3'-dimethyl-2''-((*S*)-*p*-tolylsulfinyl)-1,1':2',1''-terphenyl
Chemical Formula: $C_{30}H_{29}BrO_4S$
Molecular Weight: 565,5220

3IR. The general procedure **GP2** was followed for 4 hours at 85 °C with **x = 10**, from (S)-4,5'-dimethoxy-2'-methyl-2-(p-tolylsulfinyl)-1,1'-biphenyl (1 eq., 90 mg, 0.246 mmol) and 1-bromo-5-iodo-2-methoxy-4-methylbenzene (2 eq., 160 mg, 0.491 mmol) in HFIP (2345 µL) yielding (1'$_a$*S*,2'$_a$*R*)-5-bromo-4,4'',6'-trimethoxy-2,3'-dimethyl-2''-((*S*)-*p*-tolylsulfinyl)-1,1':2',1''-terphenyl (65.6 mg, 0.116 mmol, 47% however some impurities resulting from the decomposition of the starting material could not be removed by column chromatography) as a yellowish powder with a d.r. ≥ 98 : 2 (>95% conversion, crude d.r. = 58 : 1 : n.d.).

^{1}**H-NMR** ($CDCl_3$, 400 MHz) : δ = 7.62 (s, 1H), 7.49 (d, J = 2.7 Hz, 1H), 7.08 – 6.94 (m, 7H), 6.85 (dd, J = 8.4, 2.7 Hz, 1H), 6.43 (s, 1H), 3.86 (s, 3H), 3.77 (s, 3H), 3.44 (s, 3H), 2.31 (s, 3H), 2.29 (s, 3H), 1.06 (s, 3H) ppm.
^{13}**C-NMR** ($CDCl_3$, 101 MHz): δ = 159.36, 155.07, 154.66, 143.75, 141.50, 141.18, 137.67, 137.61, 135.64, 132.34, 130.10, 129.63, 129.53, 129.22 (2C), 126.30 (2C), 125.37, 124.20, 116.08, 114.45, 112.41, 111.28, 105.51, 55.88, 55.44, 54.71, 23.11, 21.32, 19.06 ppm.
$[\alpha]_D^{20}$ = +46.8 (c = 0.783, $CHCl_3$)
HRMS (ESI): *calc. for* $C_{30}H_{30}BrO_4S^+$ 565.1043; found 565.1042

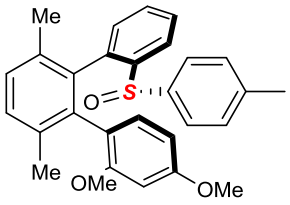

(1'*R*,2'*R*)-2,4-dimethoxy-3',6'-dimethyl-2''-((*S*)-*p*-tolylsulfinyl)-1,1':2',1''-terphenyl
Chemical Formula: $C_{29}H_{28}O_3S$
Molecular Weight: 456,6000

3gV. The general procedure **GP2** was followed for 2 hours at 115 °C with **x = 30**, from (*S*)- 2,5-dimethyl-2'-(p-tolylsulfinyl)-1,1'-biphenyl (1 eq., 50 mg, 0.156 mmol) and 1-iodo-2,4-dimethoxybenzene (2.01 eq., 83 mg, 0.314 mmol) in HFIP (2500 µL), yielding (1'$_a$*R*,2'$_a$*R*)-2,4-dimethoxy-3',6'-dimethyl-2''-((*S*)-p-tolylsulfinyl)-1,1':2',1''-terphenyl (17.4 mg, 0.038 mmol, 24.4 %) as a yellow powder with a d.r. = 94 : 6 (55% conversion, crude d.r. = 15 : 2 : 0).
^{1}**H-NMR** ($CDCl_3$, 400 MHz) : 7.93 (dd, J = 7.9, 1.0 Hz, 1H), 7.42 – 7.33 (m, 1H), 7.35 (d, J = 8.3 Hz, 1H), 7.28 (td, J = 7.4, 1.4 Hz, 1H), 7.25 (d, J = 7.6 Hz, 1H), 7.08 (ddd, J = 7.3, 1.3, 0.3 Hz, 1H), 7.10 – 7.00 (**AA'BB'**, 4H), 7.00 – 6.93 (m, 1H), 6.49 (dd, J = 8.4, 2.4 Hz, 1H), 6.14 (d, J = 2.4 Hz, 1H), 3.73 (s, 3H), 3.47 (s, 3H), 2.32 (s, 3H), 2.11 (s, 3H), 1.07 (s, 3H) ppm.
^{13}**C-NMR** ($CDCl_3$, 101 MHz): δ = 159.98, 156.45, 142.49, 141.55, 141.15, 138.60, 137.03, 136.87, 134.60, 134.27, 131.25, 130.70, 130.12, 129.33 (2C), 128.89, 128.82, 127.75, 126.69 (2C), 122.16, 120.88, 103.42, 98.04, 55.04, 54.59, 21.34, 20.60, 19.52 ppm.
$[\alpha]_D^{20}$ = -92.5 ° (c = 0.309 , $CHCl_3$).
HRMS (ESI): *calc. for* $C_{29}H_{29}O_3S^+$ 457.1832; found 457.1830

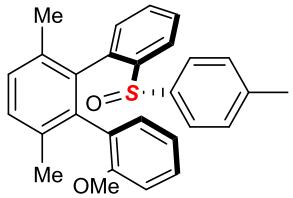

(1'*R*,2'*R*)-2-methoxy-3',6'-dimethyl-2''-((*S*)-*p*-tolylsulfinyl)-1,1':2',1''-terphenyl
Chemical Formula: $C_{28}H_{26}O_2S$
Molecular Weight: 426,5740

3gl. The general procedure **GP2** was followed for 2 hours at 115 °C with **x = 30**, from (*S*)- 2,5-dimethyl-2'-(p-tolylsulfinyl)-1,1'-biphenyl (1 eq., 50 mg, 0.156 mmol) and *o*-iodoanisole (2.01 eq., 73.4 mg, 41 µL, 0.314 mmol) in HFIP (2500 µL), yielding (1'$_a$*R*,2'$_a$*R*)-2-methoxy-3',6'-dimethyl-2''-((*S*)-p-tolylsulfinyl)-1,1':2',1''-terphenyl (10.7 mg, 0.025 mmol, 16 %) as a yellow powder with a d.r. ≥98 : 2 (39% conversion, crude d.r. 12 : 1 : 0).

^{1}**H-NMR** ($CDCl_3$, 400 MHz) : δ = 7.91 (dd, J = 7.9, 1.1 Hz, 1H), 7.46 (dd, J = 7.4, 1.7 Hz, 1H), 7.36 (td, J = 7.6, 1.4 Hz, 1H), 7.28 (dt, J = 7.4, 1.4, 1.3 Hz, 1H), 7.28 (d, J = 7.9 Hz, 1H), 7.15 – 7.02 (m, 6H), 6.98 (d, J = 7.7 Hz, 1H), 6.96 (td, J = 7.4, 1.1 Hz, 1H), 6.56 (dd, J = 8.3, 0.8 Hz, 1H), 3.50 (s, 3H), 2.32 (s, 3H), 2.11 (s, 3H), 1.09 (s, 3H) ppm.

^{13}**C-NMR** ($CDCl_3$, 101 MHz): δ = 155.41, 142.68, 141.59, 141.20, 138.42, 137.28, 136.45, 134.30, 134.11, 131.01, 130.72, 130.23, 129.38 ($2C_{pTol}$), 128.94, 128.88, 128.69, 128.12, 127.82, 126.72 ($2C_{pTol}$), 122.15, 120.19, 109.78, 54.59, 21.37, 20.59, 19.53 ppm.

$[\alpha]_D^{20}$ = -137.3 ° (c = 0.285, $CHCl_3$).

HRMS (ESI): *calc. for* $C_{28}H_{27}O_2S^+$ 427.1726; found 457.1805

A. Large scale reaction and post-functionalization:

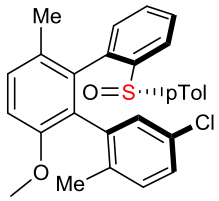

(1'*S*,2'*R*)-5-chloro-6'-methoxy-2,3'-dimethyl-2''-((*S*)-*p*-tolylsulfinyl)-1,1':2',1''-terphenyl
Chemical Formula: $C_{28}H_{25}ClO_2S$
Molecular Weight: 461,0160

3fP. To a 35 mL oven-dried Ace pressure tube and under air were added, in that order, Ag_2CO_3 (2.31 eq., 1635 mg, 5.93 mmol), $Pd(TFA)_2$ (20.4 mol%, 174 mg, 0.523 mmol), IPrHCl (39.9 %, 435 mg, 1.02 mmol), AgTFA (1.04 eq., 588 mg, 2.66 mmol), 4 Å powdered MS (1.04 eq., 600 mg, 2.68 mmol), 4-chloro-2-iodo-1-methylbenzene (2.22 eq., 1440 mg, 900 µL, 5.7 mmol), and (*S*)-5-methoxy-2-methyl-2'-(p-tolylsulfinyl)-1,1'-biphenyl (1 eq., 864 mg, 2.57 mmol, as a stock solution in HFIP), further HFIP (24 mL total) was added to rinse the walls of the reaction vessel, and the resulting mixture was put at 85 °C for 4 hours. It was worked-up as described in the **GP2**, and subsequent flash chromatography yielded (1'$_a$*S*,2'$_a$*R*)-5-chloro-6'-methoxy-2,3'-dimethyl-2''-((*S*)-p-tolylsulfinyl)-1,1':2',1''-terphenyl (774 mg, 1.68 mmol, 65.4%) as a yellowish powder with a d.r. ≥98 : 2 (crude d.r. = 63 : 1 : 0).

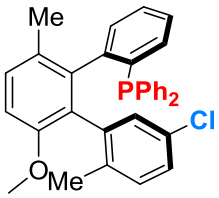

((1'*R*,2'*S*)-5''-chloro-3'-methoxy-2'',6'-dimethyl-[1,1':2',1''-terphenyl]-2-yl)diphenylphosphane
$C_{33}H_{28}ClOP$
507,0098

*Caution **:** as phosphines are readily oxidized by oxygen when heated or in presence of a catalyst, removal of the volatiles under reduced pressure should be done at 40 °C maximum, and the vacuum should be broken with argon. Likewise, argon should be used to drive the eluent during flash chromatography.*

8. To a solution of (1*S*,1''*R*)-5-chloro-6'-methoxy-2,3'-dimethyl-2''-((*S*)-p-tolylsulfinyl)-1,1':2',1''-terphenyl (1 eq., 98 mg, 0.213 mmol) in THF (2000 µL) at -94 °C (acetone slush bath) was added dropwise n-BuLi (4.14 eq., 1.6 M, 550 µL, 0.88 mmol). The mixture was stirred 5 min. at -94 °C (color changed from light yellow to darker green/orange), when neat, freshly distilled $ClPPh_2$ was added in one portion, causing instant discoloration (care should be taken to add $ClPPh_2$ directly into the reaction mixture as it will freeze on the walls of the reaction vessel). The resulting mixture was stirred and allowed to come back to -78 °C over 30 min. It was then quenched by a MeOH solution in Et_2O (1mL, MeOH/Et_2O 1 : 10 v/v), diluted with further Et_2O and

filtrated on a silica gel plug. Volatiles were removed under reduced pressure and flash chromatography (*n*-Pen/Et_2O 90 : 10; the crude mixture was loaded as a 80 : 20 *n*-Pen/DCM solution) afforded ((1'*R*,2'*S*)-5''-chloro-3'-methoxy-2'',6'-dimethyl-[1,1':2',1''-terphenyl]-2-yl)diphenylphosphane (80 mg, 0.158 mmol, 74 %) as a white powder with a d.r. >95 : 5 by ^{1}H NMR.

^{1}**H-NMR** ($CDCl_3$, 400 MHz) : δ = 7.45 (t, J = 1.8 Hz, 1H), 7.37 – 7.27 (m, 5H), 7.27 – 7.22 (m, 3H), 7.23 – 7.17 (m, 1H), 7.17 – 7.12 (m, 2H), 7.12 – 7.08 (m, 2H), 7.06 (d, J = 8.6 Hz, 1H), 7.00 (dd, J = 8.2, 2.2 Hz, 1H), 6.97 – 6.89 (m, 3H), 3.72 (s, 3H), 2.00 (s, 3H), 1.28 (s, 3H).

^{13}**C-NMR** ($CDCl_3$, 101 MHz): δ = 154.62, 146.23 (d, J = 34.1 Hz), 141.03 (d, J = 6.5 Hz), 139.44, 138.54 (d, J = 12.3 Hz), 136.90 (d, J = 11.9 Hz), 136.29 (d, J = 13.1 Hz), 135.05, 135.04 (d, J = 22.0 Hz), 134.09 (d, J = 2.3 Hz), 132.71 (d, J = 17.3 Hz), 130.16 (d, J = 3.1 Hz), 129.47, 129.43, 129.41, 129.35 (d, J = 8.8 Hz), 128.92 (d, J = 0.7 Hz), 128.68 (d, J = 6.4 Hz), 128.45 (d, J = 0.9 Hz), 128.26 (d, J = 8.8 Hz), 128.20 (d, J = 6.2 Hz), 127.57, 127.49 (d, J = 0.8 Hz), 127.05, 126.84, 110.25, 55.71, 19.51, 19.39 (d, J = 1.5 Hz).ppm.

^{31}**P-NMR** ($CDCl_3$, 162 MHz): δ = -15.02 ppm.

$[\alpha]_D^{20}$ = -13.5 ° (c = 1.45, $CHCl_3$).

HRMS (ESI): *calc. for $C_{33}H_{29}ClOP^+$ 507.1639* ; found 507.1625

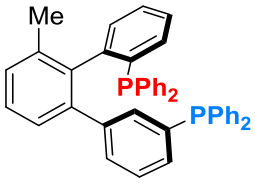

(*R*)-(6'-methyl-[1,1':2',1''-terphenyl]-2,3''-diyl)bis(diphenylphosphane)

$C_{43}H_{34}P_2$

612,6925

13a A solution of (*R*)-3''-bromo-6'-methyl-2-((*S*)-p-tolylsulfinyl)-1,1':2',1''-terphenyl (1 eq., 898 mg, 1.95 mmol) in Et_2O (20 mL) was stirred at -94 °C, when *t*-BuLi (4.28 eq., 1.7 M in pentane, 4.9 mL, 8.33 mmol) was added dropwise (color dark blue/maroon, precipitate). After 20 min., $ClPPh_2$ (3.01 eq., 1290 mg, 1.05 mL, 5.85 mmol) in toluene (1 mL) was added and the resulting mixture allowed to reach 25 °C (color lightened, off-white precipitate appeared as the temperature rose). The crude mixture was filtered under argon, and the solid was triturated and washed with small portion of water (2 times) and MeOH (3 times). After drying under vacuum, the crude off-white solid contained little (c.a. 5%) phosphine oxide impurities, that were removed by dissolving the solid in DCM filtration on a silica gel pad. Recrystallization in degassed acetone (reflux to 0 °C) removed mono-phosphine impurities white microcrystals of (*R*)-(6'-methyl-[1,1':2',1''-terphenyl]-2,3''-diyl)bis(diphenylphosphane) (833 mg, 1.36 mmol, 70%). (low solubility in most organic solvent)

^{1}**H-NMR** ($CDCl_3$, 400 MHz) : δ = 7.33 – 6.95 (m, 28H), 6.66 – 6.53 (m, 3H), 1.53 (s, 3H) ppm.

^{13}**C-NMR** ($CDCl_3$, 101 MHz): δ = 146.07, 145.74, 142.31, 142.25, 141.29, 141.27, 139.32, 139.25, 138.36, 138.23, 137.18, 137.16, 137.03, 136.93, 136.77, 136.69, 136.65, 136.59, 136.45, 135.51, 135.41, 135.35, 134.57, 134.35, 134.24, 134.21, 134.03, 133.84, 133.78, 133.59, 132.53, 132.35, 131.77, 131.54, 131.49, 131.43, 131.12, 131.10, 128.87, 128.61, 128.45, 128.42, 128.31, 128.25, 128.18, 128.16, 128.09, 128.00, 127.94, 127.75, 127.67, 127.52, 127.40, 127.22, 20.56 ppm.
^{31}**P-NMR** ($CDCl_3$, 162 MHz): δ = -5.46, -14.94.ppm.
$[\alpha]_D^{20}$ =ongoing
HRMS (ESI): *calc. for*; found

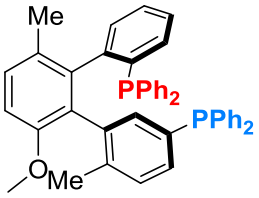

((1'*R*,2'*S*)-3'-methoxy-6',6''-dimethyl-[1,1':2',1''-terphenyl]-2,3''-diyl)bis(diphenylphosphane)
$C_{45}H_{38}OP_2$
656,7455

13b : *Anhydrous conditions:* A solution of (1'*S*,2'*R*)-5-bromo-6'-methoxy-2,3'-dimethyl-2''-((*S*)-p-tolylsulfinyl)-1,1':2',1''-terphenyl (1 eq., 300 mg, 0.594 mmol) in Et_2O (6 mL) was cooled to -94 °C. A solution of *t*-BuLi (5 eq., 1.55 M in pentane, 1.91 mL, 2.97 mmol) was then added dropwise (color changed to dark blue/maroon, some precipitate). The resulting mixture was stirred at -94 °C for 20 min., when a solution of $ClPPh_2$ (4.22 eq., 553 mg, 0.45 mL, 2.51 mmol) in toluene (0.5 mL) was slowly cannulated. The resulting mixture was allowed to reach -78 °C over 30 min., and was quenched by filtration over a silica gel pad under argon (washed with Et_2O, some DCM can be added to solubilize the reaction mixture before cannulation). Solvent was removed under reduced pressure, and flash chromatography (Et_2O/*n*-pentane 10:90, product loaded as 20:80 DCM/*n*-pentane solution) afforded ((1'*R*,2'*S*)-3'-methoxy-6',6''-dimethyl-[1,1':2',1''-terphenyl]-2,3''-diyl)bis(diphenylphosphane) (doax-phos) (210 mg, 0.32 mmol, 54%) as a white powder. Recrystallization by layering a concentrated 80:20 $CHCl_3$/Et_2O solution with *n*-pentane afforded colorless crystals suitable for X-Ray analysis.

^{1}**H-NMR** ($CDCl_3$, 400 MHz) : δ = 7.69 (dd, J = 10.7, 1.5 Hz, 1H), 7.36 – 6.94 (m, 29H), 6.92 (d, J = 8.4 Hz, 1H), 6.80 – 6.73 (m, 1H), 3.72 (s, 3H), 2.03 (s, 3H), 1.25 (s, 3H) ppm.
^{13}**C-NMR** ($CDCl_3$, 101 MHz): δ = 154.88, 146.42, 146.09, 140.97, 140.91, 138.42, 138.40, 138.37, 138.29, 138.25, 137.78, 137.71, 137.58, 137.28, 137.15, 137.12, 137.05, 136.75, 136.68, 136.52, 136.38, 135.22, 135.00, 133.85, 133.83, 133.80, 133.60, 133.21, 133.09, 133.06, 133.03, 132.91, 132.88, 131.92, 131.82, 131.56, 131.53, 129.65, 129.63, 129.54, 129.52, 129.20, 129.03, 128.97, 128.75, 128.47,

128.18, 128.16, 128.14, 128.11, 128.04, 128.00, 127.95, 127.79, 127.44, 126.79, 110.51, 55.83, 20.07, 19.41, 19.40 ppm.
^{31}**P-NMR** ($CDCl_3$, 162 MHz): δ = -6.94, -14.90 ppm.
$[\alpha]_D^{20}$ = -31.1 (c = 1, $CHCl_3$)
HRMS (ESI): *calc. for $C_{46}H_{40}OP_2^+$ 657.2471*; found 657.2463

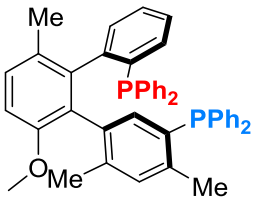

((1'*R*,2'*S*)-3'-methoxy-4'',6',6''-trimethyl-[1,1':2',1''-terphenyl]-2,3''-diyl)bis(diphenylphosphane)
$C_{46}H_{40}OP_2$
670,7725

13c : *Anhydrous conditions:* A solution of (1'*S*,2'*R*)-5-bromo-6'-methoxy-2,3',4-trimethyl-2''-((*S*)-p-tolylsulfinyl)-1,1':2',1''-terphenyl (1 eq., 240 mg, 0.462 mmol) in Et_2O (4 mL) was cooled to -94 °C. A solution of *t*-BuLi (5.15 eq., 1.7 M in pentane, 1.4 mL, 2.38 mmol) was then added dropwise (color changed to dark blue/maroon, some precipitate). The resulting mixture was stirred at -94 °C for 20 min., when a solution of $ClPPh_2$ (4.22 eq., 430 mg, 0.35 mL, 1.95 mmol) in toluene (2 mL) was slowly cannulated. The resulting mixture was allowed to reach -78 °C over 30 min., and was quenched by filtration over a silica gel pad under argon (washed with Et_2O, some DCM can be added to solubilize the reaction mixture before cannulation). Solvent was removed under reduced pressure, and flash chromatography (Et_2O/*n*-pentane 10:90, product loaded as 20:80 DCM/*n*-pentane solution) afforded ((1'*R*,2'*S*)-3'-methoxy-6',6''-dimethyl-[1,1':2',1''-terphenyl]-2,3''-diyl)bis(diphenylphosphane) (*o''*-Me-doaxphos) ((175 mg, 0.261 mmol, 57%)as a white powder.

^{1}**H-NMR** ($CDCl_3$, 400 MHz) : δ = 7.25 – 7.07 (m, 16H), 7.08 – 6.96 (m, 5H), 6.93 (d, J = 8.7 Hz, 1H), 6.89 (d, J = 4.6 Hz, 1H), 6.85 (d, J = 8.4 Hz, 1H), 6.80 – 6.71 (m, 2H), 6.57 – 6.49 (m, 2H), 3.66 (s, 3H), 2.26 (s, 3H), 1.95 (s, 3H), 1.18 (s, 3H) ppm.
^{13}**C-NMR** ($CDCl_3$, 101 MHz): δ = 155.30, 146.37, 146.04, 140.97, 140.91, 139.89, 139.67, 138.20, 137.34, 136.87, 136.16, 136.00, 135.31, 135.08, 134.57, 134.37, 133.62, 133.61, 133.59, 133.40, 132.19, 132.04, 131.28, 130.56, 130.50, 129.50, 129.12, 128.81, 128.20, 128.13, 128.08, 128.00, 127.94, 127.90, 127.87, 127.78, 127.74, 126.97, 111.41, 56.40, 20.93, 20.74, 20.32, 19.60 ppm.
$[\alpha]_D^{20}$ =ongoing
HRMS (ESI): *calc. for $C_{46}H_{40}OP_2^+$ 671.2627*; found 671.2628

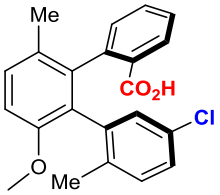

(1'R,2'S)-5''-chloro-3'-methoxy-2'',6'-dimethyl-[1,1':2',1''-terphenyl]-2-carboxylic acid
Chemical Formula: $C_{22}H_{19}ClO_3$
Molecular Weight: 366,8410

9. To a solution of (1*S*,1''*R*)-5-chloro-6'-methoxy-2,3'-dimethyl-2''-((*S*)-p-tolylsulfinyl)-1,1':2',1''-terphenyl (1 eq., 80 mg, 0.174 mmol) in THF (2000 µL) at -78 °C was added dropwise n-BuLi (4.15 eq., 1.6 M, 450 µL, 0.72 mmol). The mixture was stirred 3 min. at -78 °C (color changed from light yellow to darker orange), when gaseous CO_2 was bubbled into the reaction mixture, causing discoloration after few minutes. The resulting mixture was stirred at -78 °C for 30 min. with continuous CO_2 bubbling. It was quenched at -78 °C by addition of a MeOH solution in Et_2O, allowed back to room temperature, acidified to pH 1 by the addition of 1M HCl solution. The phases were separated and the organic phase was dried over Na_2SO_4. The volatiles were removed under reduced pressure and flash chromatography (CyH/EtOAc/AcOH 70 : 30 : 1) afforded (1'R,2'S)-5''-chloro-3'-methoxy-2'',6'-dimethyl-[1,1':2',1''-terphenyl]-2-carboxylic acid (47 mg, 0.128 mmol, 74%) as a yellowish solid with a d.r. >95 : 5 by ^{1}H NMR.
Crystals suitable for X-ray analysis were grown in a round-bottom flask by layering a diluted DCM solution with *n*-pentane and letting the resulting mixture equilibrate at 4-6 °C.
^{1}**H-NMR** ($CDCl_3$, 400 MHz) : δ = 10.96 (brd s, 1H), 7.93 (dd, J = 7.8, 1.2 Hz, 1H), 7.30 (td, J = 7.5, 1.4 Hz, 1H), 7.25 – 7.18 (m, 2H), 7.02 – 6.96 (m, 1H), 6.96 – 6.89 (m, 2H), 6.87 (d, J = 8.2 Hz, 2H), 3.75 (s, 3H), 2.02 (s, 3H), 1.96 (s, 3H) ppm.
^{13}**C-NMR** ($CDCl_3$, 101 MHz): δ = 171.49, 154.62, 141.97, 141.51, 139.06, 134.87, 132.19, 130.59, 130.48, 129.99, 129.95, 129.76, 129.47, 129.18, 127.68, 127.20, 126.93, 126.61, 109.37, 55.60, 19.87, 19.33 ppm.
$[\alpha]_D^{20}$ = -42.3 ° (c = 0.230, $CHCl_3$).
HRMS (ESI): *calc. for* $C_{22}H_{19}NaO_3^+$ *389.0915* ; found 389.0892.

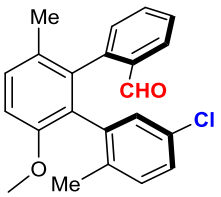

(1'R,2'S)-5''-chloro-3'-methoxy-2'',6'-dimethyl-[1,1':2',1''-terphenyl]-2-carbaldehyde
Chemical Formula: $C_{22}H_{19}ClO_2$
Molecular Weight: 350,8420

10. To a solution of (1S,1''R)-5-chloro-6'-methoxy-2,3'-dimethyl-2''-((S)-p-tolylsulfinyl)-1,1':2',1''-terphenyl (1 eq., 80 mg, 0.174 mmol) in THF (2000 µL) at -78 °C was added dropwise n-BuLi (4.15 eq., 1.6 M, 450 µL, 0.72 mmol). The mixture was stirred 3 min.

at -78 °C (color changed from light yellow to darker orange), when neat ethyl formate (17.8 eq., 229 mg, 250 µL, 3.09 mmol), kept over K_2CO_3, was added in one portion, causing instant discoloration. The resulting mixture was stirred at -78 °C for 15 min. It was then quenched by a MeOH solution in Et_2O (1mL, MeOH/Et_2O 1 : 10 v/v), diluted with further Et_2O and filtrated on a silica gel plug. Volatiles were removed under reduced pressure and flash chromatography (*n*-Pen/Et_2O 80 : 20) afforded (1'R,2'S)-5''-chloro-3'-methoxy-2'',6'-dimethyl-[1,1':2',1''-terphenyl]-2-carbaldehyde (34 mg, 0.0969 mmol, 56%) as a white solid, with a d.r. >95 : 5 (possible diastereomer, using the aldehyde proton as a probe, account for less than the ^{13}C satellites integration on the ^1H NMR spectra, thereby giving a d.r. >95 : 5).

^{1}**H-NMR** ($CDCl_3$, 400 MHz) : δ = 9.89 (s, 1H), 7.86 (dd, J = 7.7, 1.4 Hz, 1H), 7.35 (td, J = 7.4, 1.5 Hz, 1H), 7.31 – 7.23 (m, 2H), 6.99 – 6.91 (m, 3H), 6.89 (dd, J = 7.5, 1.1 Hz, 1H), 6.65 (d, J = 1.8 Hz, 1H), 3.76 (s, 3H), 2.06 (s, 3H), 1.95 (s, 3H) ppm.

^{13}**C-NMR** ($CDCl_3$, 101 MHz): δ = 191.91, 154.87, 143.44, 138.50, 137.89, 135.16, 133.77, 133.50, 130.49, 130.31, 129.91, 129.47, 129.34, 128.64, 128.51, 127.61, 127.28, 126.83, 110.43, 55.65, 20.19, 19.35 ppm.

$[\alpha]_D^{20}$ = -38.8 ° (c = 1.4, $CHCl_3$).

HRMS (ESI): *calc. for $C_{22}H_{20}ClO_2^+$ 351.1146;* found 351.1144.

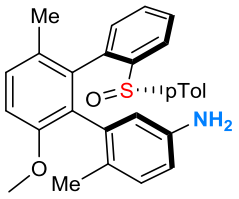

(1'*S*,2'*R*)-6'-methoxy-3',6-dimethyl-2''-((*S*)-*p*-tolylsulfinyl)-[1,1':2',1''-terphenyl]-3-amine
Chemical Formula: $C_{28}H_{27}NO_2S$
Molecular Weight: 441,5890

2-(1'*S*,2'*R*)-6'-methoxy-3',6-dimethyl-2''-((*S*)-*p*-tolylsulfinyl)-[1,1':2',1''-terphenyl]-3-yl)isoindoline-1,3-dione (1 eq., 136 mg, 0.238 mmol) was dissolved in THF (5 mL) and EtOH (5 mL) at 0 °C. Hydrazine monohydrate (50.4 eq., 600 mg, 0.6 mL, 12 mmol) was added dropwise and the cooling bath was removed. The mixture was stirred 1 hour at room temperature (TLC showed completion). Most of the solvent was removed under reduced pressure and the residue (~1mL) was dissolved in CH_2Cl_2/NaOH 3M and extracted twice with CH_2Cl_2. The volatiles were removed under reduced pressure and column chromatography in EtOAc with 1% Et_3N gave (1'*S*,2'*R*)-6'-methoxy-3',6-dimethyl-2''-((*S*)-*p*-tolylsulfinyl)-[1,1':2',1''-terphenyl]-3-amine (96 mg, 0.217 mmol, 91%) as an off-white solid

^{1}**H-NMR** ($CDCl_3$, 400 MHz) : δ = 7.88 (dd, J = 7.9, 1.1 Hz, 1H), 7.28 (td, J = 7.8, 1.3 Hz, 1H), 7.17 (dd, J = 6.7, 1.3 Hz, 1H), 7.16 – 7.10 (m, 2H), 7.09 – 7.04 (m, 2H), 7.02 (d, J = 8.4 Hz, 1H), 6.91 (d, J = 8.4 Hz, 1H), 6.89 (dd, J = 7.5, 1.2 Hz, 1H), 6.85 (d, J = 2.4 Hz, 1H), 6.66 (d, J = 8.1 Hz, 1H), 6.31 (dd, J = 8.0, 2.4 Hz, 1H), 3.70 (s, 3H), 3.52 (brd s, 2H), 2.26 (s, 3H), 1.72 (s, 3H), 1.17 (s, 3H) ppm.

^{13}**C-NMR** ($CDCl_3$, 101 MHz): δ = 158.10, 146.48, 146.43, 144.58, 144.38, 141.21, 140.29, 139.97, 132.91, 132.76, 132.63, 132.52 (2C), 132.41, 132.34, 131.79,

131.22, 129.26 (2C), 128.57, 126.30, 120.32, 117.51, 114.21, 58.89, 24.37, 22.45, 21.91 ppm.

$[\alpha]_D^{20}$ = -41.1 ° (c = 1.4, $CHCl_3$).

HRMS (ESI): *calc. for $C_{28}H_{27}NO_2S^+$ 442.1821;* found 442.1835

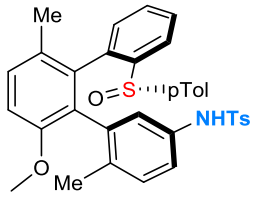

N-((1'*S*,2'*R*)-6'-methoxy-3',6-dimethyl-2''-((*S*)-*p*-tolylsulfinyl)-[1,1':2',1''-terphenyl]-3-yl)-4-methylbenzenesulfonamide
Chemical Formula: $C_{35}H_{33}NO_4S_2$
Molecular Weight: 595,7720

To mixture a of (1'*S*,2'*R*)-6'-methoxy-3',6-dimethyl-2''-((*S*)-*p*-tolylsulfinyl)-[1,1':2',1''-terphenyl]-3-amine (1 eq., 48 mg, 0.109 mmol) and pyridine (2.27 eq., 19.6 mg, 0.02 mL, 0.247 mmol) was added a solution of tosyl chloride (1.06 eq., 22 mg, 0.115 mmol) in $CHCl_3$ (1 mL). After 2 hours TLC showed completion, and the reaction was quenched with MeOH followed by 1M H_2SO_4, and diluted with EtOAC the organic phase was separated and washed with 1 M H_2SO_4. Flash chromatography in Et_2O afforded *N*-((1'*S*,2'*R*)-6'-methoxy-3',6-dimethyl-2''-((*S*)-*p*-tolylsulfinyl)-[1,1':2',1''-terphenyl]-3-yl)-4-methylbenzenesulfonamide (44 mg, 0.0739 mmol, 68%).

^{1}**H-NMR** ($CDCl_3$, 400 MHz) : δ = 7.74 (dd, J = 7.9, 1.2 Hz, 1H), 7.66 (d, J = 8.3 Hz, 2H), 7.29 (s, 1H), 7.27 – 7.10 (m, 8H), 7.07 (dd, J = 8.2, 2.4 Hz, 1H), 6.96 (t, J = 7.9 Hz, 1H), 6.93 (d, J = 2.4 Hz, 2H), 6.89 – 6.83 (m, 2H), 3.69 (s, 3H), 2.38 (s, 3H), 2.35 (s, 3H), 1.84 (s, 3H), 1.37 (s, 3H) ppm.

^{13}**C-NMR** ($CDCl_3$, 101 MHz): δ = 154.93, 142.72, 141.90, 140.39, 138.28, 137.30, 137.11, 136.83, 133.86, 132.74, 130.29, 129.92, 129.86, 129.66 (2C), 129.28 (2C), 129.16, 128.97, 128.80, 128.16, 127.35 (2C), 126.10 (2C), 125.23, 123.99, 123.43, 120.38, 111.40, 55.80, 21.47, 21.38, 19.52, 19.19 ppm.

$[\alpha]_D^{20}$ = -33.6 ° (c = 0.154, $CHCl_3$).

HRMS (ESI): *calc. for $C_{35}H_{33}LiNO_4S_2^+$ 602.2006;* found 602.1991.

c) Hydrogenation

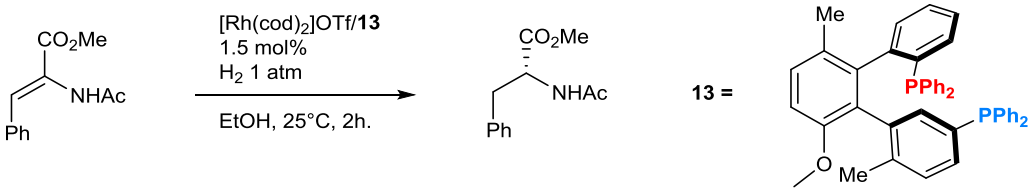

General procedure : in a oven-dried tube closed with a septum was loaded the substrate (1equiv). Similarly an oven-dried schlenk closed with a septum was loaded with

the metal (1.5-2 mol%) along with the ligand (2-2.5 mol%). Both vessels were evacuated under vacuum and back-filled with argon (4 times). Then the schlenk was put under vacuum, the stopcock closed and the vacuum was carefully broken with an hydrogen balloon. The required solvent was then added by mean of a syringe (~0.01 M) and the catalyst stock solution was stirred for 15 min in order to properly activate the complex. Meanwhile the required solvent was added to the substrate under argon, a hydrogen balloon fitted with a needle was inserted in the septum, vigorous stirring was started, and the required amount of the solution of the catalyst was added to the substrate (final concentration 0.1 M). The reaction was followed by ^{1}H NMR and upon completion the solvent was removed under reduced pressure, the solid residue dissolved in DCM and filtrated over a silica gel plug to remove the catalyst (eluting with Et_2O or EtOAc) affording the pure, by ^{1}H NMR, product. Enantiomeric ratio determination was carried out by HPLC on a chiral stationary phase against a racemic reference prepared by hydrogenation of the same substrate over Pd/C ([Pd] 10 mol%) in MeOH. Absolute configuration was attributed by comparison of the specific rotation sign with literature value[163].

Chiral HPLC conditions: ODH column, *n*-Hex/*i*PrOH 90 : 10, 0.5 mL/min, 1 µL of a 4 mg/mL injected.

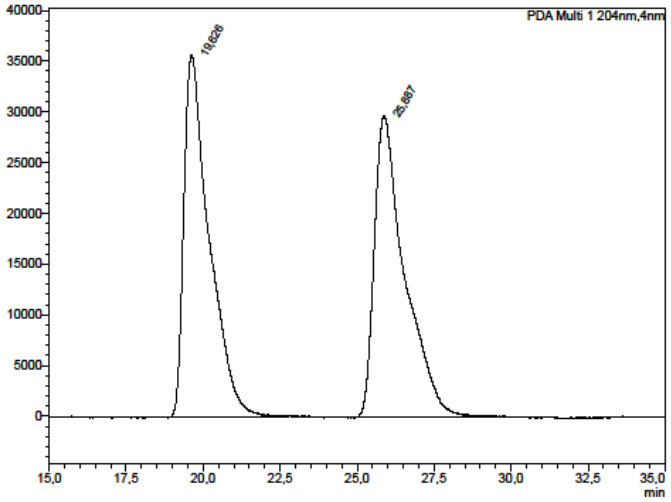

<PDA Chromatogram>

Peak Table

PDA Ch1 204nm

Peak#	Ret. Time	Area	Height	Area%	Capacity Factor(k')	Resolution(USP)	Lambda max
1	19,626	2038222	33733	49,889	-	-	206/238/655/631
2	25,887	2047298	29750	50,111	0,319	3,857	206/238/655/630/489
Total		4085520	63483	100,000			

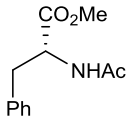

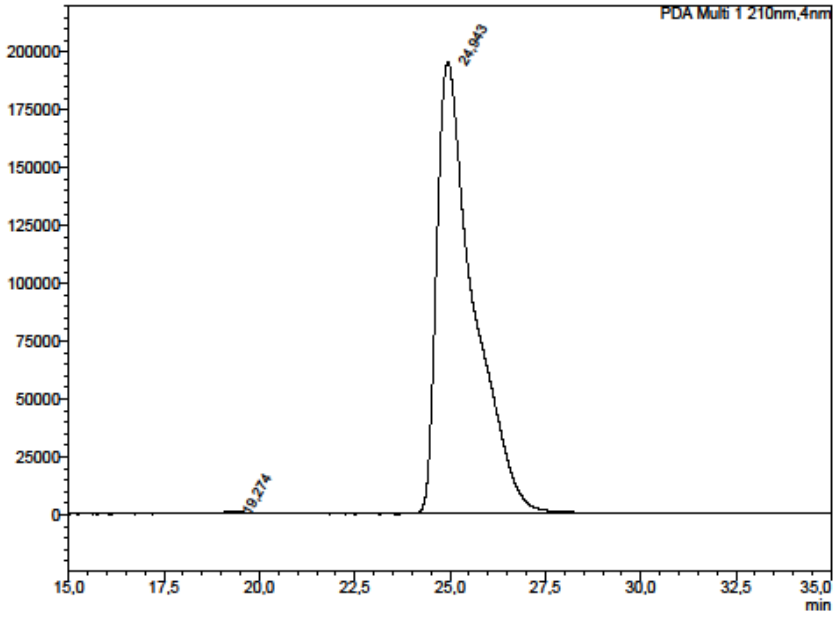

<PDA Chromatogram>

Peak Table

PDA Ch1 210nm

Peak#	Ret. Time	Area	Height	Area%	Capacity Factor(k')	Resolution(USP)	Lambda max
1	19,274	63674	1227	0,484	-	-	206/288/569/482/679
2	24,943	13084152	195327	99,516	0,294	4,449	206/238/485/441/593
Total		13147826	196554	100,000			

d) Aldehyde alkylation

A litterature procedure was followed: *J. Org. Chem.* **2002**, *67*, 1346. E.r. was determined by chiral HPLC, against a racemic sample prepared by alkylation of the same substrate with EtMgBr at 0 °C in THF.

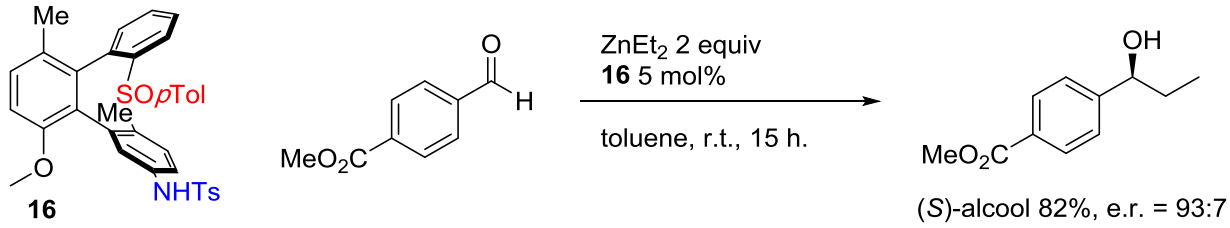

(*S*)-alcool 82%, e.r. = 93:7

Chiral HPLC conditions: ODH column, *n*-Hex/*i*PrOH 90 : 10, 0.5 mL/min, 1 µL of a 2 mg/mL injected

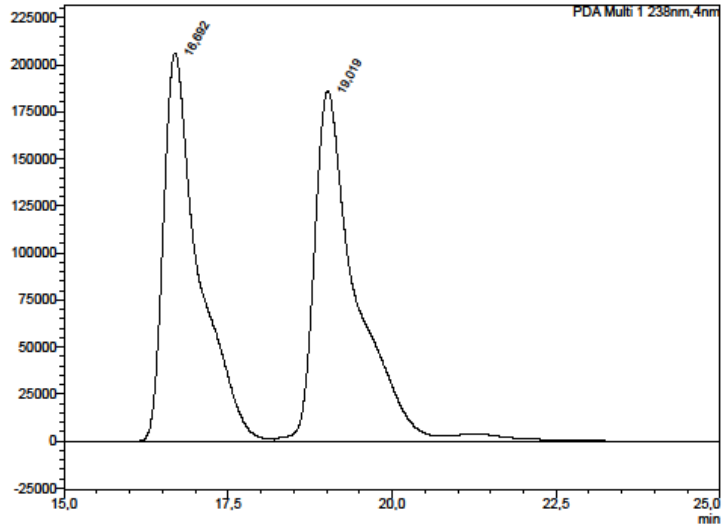

<PDA Chromatogram>

Peak Table

PDA Ch1 238nm

Peak#	Ret. Time	Area	Height	Area%	Capacity Factor(k')	Resolution(USP)	Lambda max
1	16,692	7663393	206000	47,896	-	-	236/204/659/488/405
2	19,019	8336789	185918	52,104	0,139	2,704	236/204/488
Total		16000182	391918	100,000			

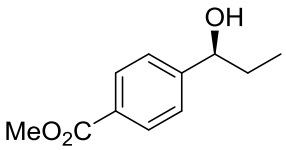

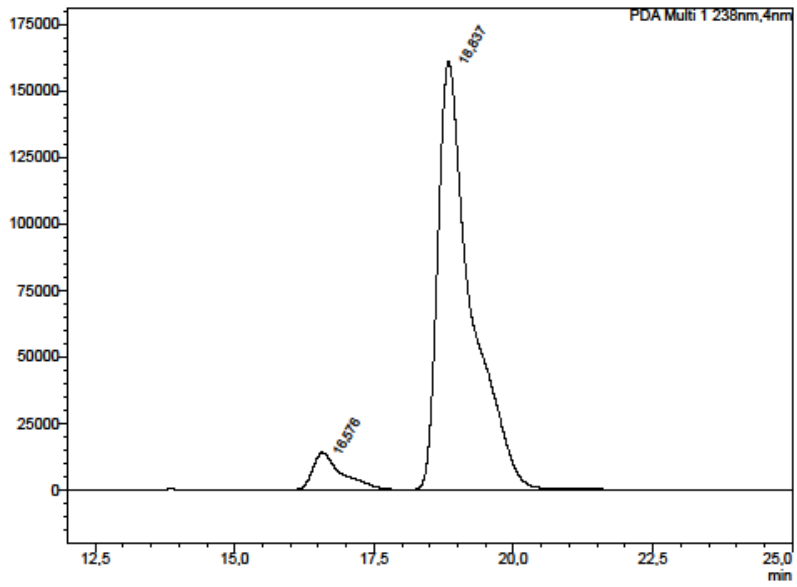

<PDA Chromatogram>

Peak Table

PDA Ch1 238nm

Peak#	Ret. Time	Area	Height	Area%	Capacity Factor(k')	Resolution(USP)	Lambda max
1	16,576	503264	13913	7,042	-	-	236/204/658/486/387
2	18,837	6643749	160833	92,958	0,136	2,701	236/204/655/486/381
Total		7147014	174746	100,000			

e) Synthesis of Palladacycle intermediate

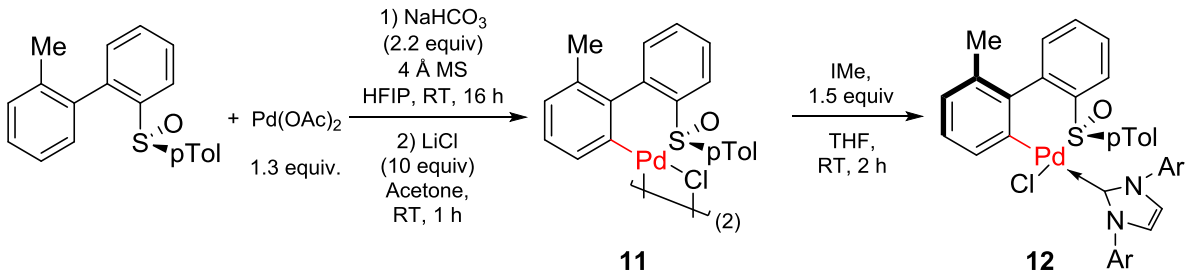

figureVII-32 : d) Synthesis of Palladacycle intermediate

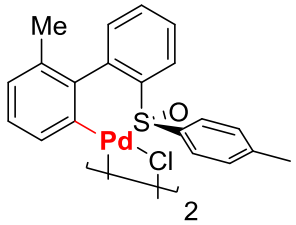

[[(6-methyl-2'-((*S*)-p-tolylsulfinyl)-[1,1'-biphenyl]-2-yl)Cl][Palladium^{II}] dimer

11. (*S*)-2-methyl-2'-(p-tolylsulfinyl)-1,1'-biphenyl (1 eq., 215 mg, 0.702 mmol), along with $Pd(OAc)_2$ (1.3 eq., 205 mg, 0.913 mmol), $NaHCO_3$ (2.21 eq., 130 mg, 1.55 mmol) and 4 Å MS were loaded in a sealed vial under air. Anhydrous HFIP (7 mL) was then added and the resulting heterogenous mixture was stirred for 16 hours at room temperature. It was then diluted with DCM, filtrated on a celite plug and the filtrate was evaporated to dryness. Then LiCl (10 eq., 298 mg, 0.145 mL, 7.03 mmol) was added followed by acetone (21 mL) and the reaction mixture was stirred at 25 °C for 1 hour, when the solvent was removed under reduced pressure and the resulting solid was finally dissolved in DCM (sonication might bu used), and filtrated over a celite plug. The crude product was purified by flash chromatography (CyH/AcMe 80 : 20; streaking, caused by slow decomposition to the starting material and an unkown by-product, however the title compound is isolated with c.a. 95% purity), affording [[(6-methyl-2'-((*S*)-p-tolylsulfinyl)-[1,1'-biphenyl]-2-yl)Cl][Palladium^{II}] dimer (232 mg, 0.519 mmol, 74 %) as a light yellow powder.

Fast exchange caused by the bridging chlorides caused extensive broadening of peaks at 25 °C on the ^{1}H NMR spectra and coalescence of the majority of signals. However, an atropisomeric ratio of 1 : 1.3 (using the broad doublet at 8.22 ppm) can be tentatively proposed.

^{1}**H-NMR** ($CDCl_3$, 400 MHz) : δ = 8.22 (brd d, 1H), 7.75 – 7.28 (m, 6H), 6.97 (s, 2H), 6.79 (s, 1H), 6.65 (d, J = 7.3 Hz, 1H), 2.24 (s, 3H), 1.98 (s, 3H) ppm.

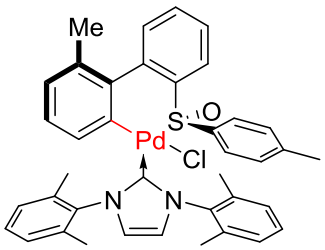

[[($_a$*S*)-(6-methyl-2'-((*S*)-p-tolylsulfinyl)-[1,1'-biphenyl]-2-yl)(IMe)Cl][Palladium^{II}]

12. A mixture of IMeHCl (1.5 eq., 148 mg, 0.476 mmol) and KOtBu (3 eq., 107 mg, 0.954 mmol) in THF (15 mL) was allowed to react 1 hour, at room temp, when it was added by a syringe fitted with a 0.2 µm PTFE filter to a solution of [[(6-methyl-2'-((*S*)-p-tolylsulfinyl)-[1,1'-biphenyl]-2-yl)][PalladiumII](Cl)-µ-(Cl)] dimer (1 eq., 142 mg, 0.317 mmol) in THF (3 mL). The resulting mixture was stirred for 2 hours and the pale yellow solution turned deep orange-red. The solvent was then removed under reduced pressure and flash chromatography afforded [[(6-methyl-2'-((*S*)-p-tolylsulfinyl)-[1,1'-biphenyl]-2-yl)(IMe)Cl][Palladium^{II}] (193 mg, 0.266 mmol, 84%) as a yellow powder. In solution at room temperature, significant decomposition occurs over few days, however in the solid state it is stable at 4-6 °C under argon for weeks. Recrystallization by layering a concentrated THF solution with Et_2O in a narrow container and letting the resulting biphasic mixture equilibrating at 4-6 °C gave monocrystals of the title compound (62 mg, 0.0854 mmol, 44% of the amount engaged in the recrystallization). The ^{1}H NMR of the solid isolated after flash chromatography and the ^{1}H NMR of the monocrystals are identical.

^{1}**H-NMR** ($CDCl_3$, 600 MHz) : δ = 7.66 (dd, J = 7.7, 1.3 Hz, 1H), 7.43 – 7.40 (m, 1H), 7.39 (td, J = 7.5, 1.5 Hz, 1H), 7.37 (t, J = 7.2 Hz, 1H), 7.35 (dq, J = 7.4, 1.4 Hz, 1H), 7.30 (dd, J = 7.5, 1.2 Hz, 1H), 7.18 – 7.14 (m, 2H), 7.13 (d, J = 1.7 Hz, 1H), 7.08 (d, J = 6.8 Hz, 2H), 7.06 (d, J = 1.8 Hz, 1H), 6.93 (d, J = 7.5 Hz, 1H), 6.76 – 6.73 (***AA'***BB', 2H), 6.72 – 6.69 (AA'***BB'***, 2H), 6.65 (t, J = 7.5 Hz, 1H), 6.40 (d, J = 7.3 Hz, 1H), 2.65 (s, 3H), 2.34 (s, 3H), 2.25 (s, 3H), 2.20 (s, 3H), 2.17 (s, 3H), 1.80 (s, 3H).

f) Synthesis of NHC Ligand

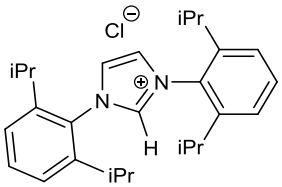

1,3-bis(2,6-diisopropylphenyl)-imidazolium chloride; **IPrHCl**
Chemical Formula: $C_{27}H_{37}ClN_2$
Molecular Weight: 425,0565

Step 1 : Glyoxal (1 eq., 6.2 M, 4.2 mL, 26 mmol) in MeOH (15 mL) was added to a solution of 2,6-diisopropylaniline (2.04 eq., 9400 mg, 10 mL, 53 mmol) in MeOH (15

mL) and AcOH (0.15 mL) previously warmed to ~60 °C. The resulting solution was stirred at room temp. immediatly after addition, soon started to crystallized (~15 min.), and was stirred for 12 more hours at room temperature.
The resulting solution was put in the fridge for 1-2 hours and the bright yellow solid was filtered, washed with small portions of MeOH until the color of the filtrate did not change (bright yellow). Drying on vacuum afforded (1*E*,2*E*)-N^1,N^2-bis(2,6-diisopropylphenyl)ethane-1,2-diimine (8.56 g, 22.7 mmol, 87 %).

Step 2 : to a solution of (1*E*,2*E*)-N^1,N^2-bis(2,6-diisopropylphenyl)ethane-1,2-diimine (1 eq., 8.56 g, 22.7 mmol) and paraformaldehyde (1.03 eq., 2.1 g, 1.79 mL, 23.3 mmol) in ethyl acetate (150 mL) at 70 °C was added dropwise a solution of TMSCl (1.03 eq., 2.55 g, 3 mL, 23.5 mmol) in ethyl acetate (30 mL). The resulting solution was stirred for 2 hours after addition at 70 °C.
After having cooled down to room temp, the yellow-orange solution was put in the fridge for 2-3 hours. Filtration yielded off-white microcrystals, and ^{1}H NMR showed impurities from technical 2,6-di-isopropylaniline. So the solid was recrystallized by dissolved it in warm acetone, followed by hot filtration and cooling down first at room temperature, then in the fridge and finally at -18 °C; 3 batches of equal purity were collected, yielding 1,3-bis(2,6-diisopropylphenyl)imidazolium chloride (8.69 g, 20.04 mmol, 90 %).
^{1}**H-NMR** ($CDCl_3$, 400 MHz) : δ = 10.14 (s, 1H), 8.15 (d, J = 1.6 Hz, 2H), 7.58 (t, J = 7.9 Hz, 2H), 7.35 (d, J = 7.8 Hz, 4H), 2.45 (hept, J = 6.8 Hz, 4H), 1.29 (d, J = 6.8 Hz, 12H), 1.25 (d, J = 6.9 Hz, 12H) ppm.
Spectral data matched the literature[384].

Other NHCs were synthesized following literature procedure[384] :

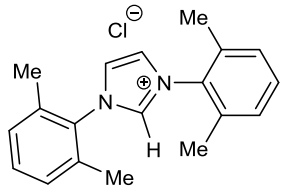

IMeHCl

2. Diastereomeric and Enantiomeric ratio determination, Chiral HPLC

a) Enantiomeric ratio of arylation with simple control of axial chirality

To determine the enantiomeric ratio of, as well as the retention time of each isomer on chiral HPLC, the following procedure was followed :

a. A racemic mixture of **1a** was prepared by reduction and reoxydation of the sulfoxide of the biaryls substrate.

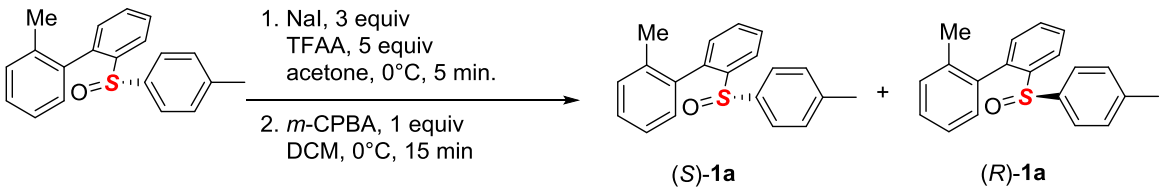

FigureVII-33 : reduction/oxidation of the sulfoxide

b. The optimized arylation reaction was conducted using racemic **1a** to obtained two enantiomers of **3aA.**

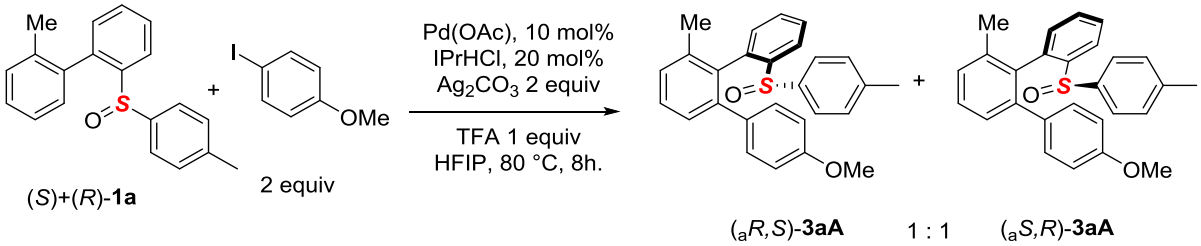

FigureVII-34 : direct arylation on a racemic substrate

c. A ^{1}H NMR, using a chiral shift reagent (3 equiv of Pirkle's alcohol) was recorded to ascertain the ($_a$*R*,*S*)-**3aA** /($_a$*S*,*R*)-**3aA** ratio = 1 : 1

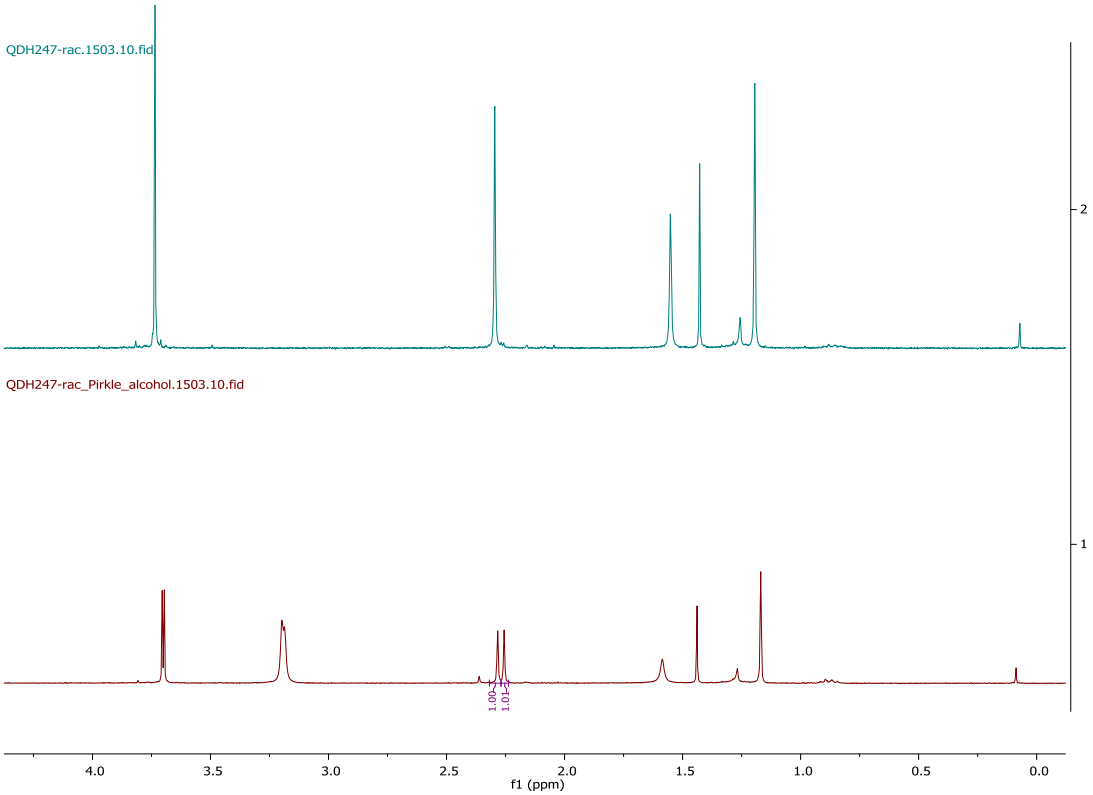

Figure VII-35 : ^{1}H NMR with ($_{a}$*R*,*S*)-3aA**/($_{a}$*S*,*R*)-**3aA** with 3 equivalent of Pirkle's alcohol**

d. Then the 1 : 1 ($_{a}$*R*,*S*)-**3aA** / ($_{a}$*S*,*R*)-**3aA** mixture was reduced and re-oxidized (racemization of the sulfoxide moiety), to provide 4 diastereomers. However, the oxidation was diastereoselective in favor of the new diastereomer (produced by the reaction when using the (*R*)-sulfoxide, by ^{1}H NMR) : thus, the ($_{a}$*R*,*S*)-**3aA** /($_{a}$*S*,*R*)-**3aA** enantiomers pair is present with 1 : 2 ratio over the ($_{a}$*R*,*R*)-**3aA** / ($_{a}$*S*,*S*)-**3aA** enantiomers pair.

e. This ratio made possible the determination of the retention time of each enantiomeric pair on the chiral HPLC chromatogram, as well as the determination of the diastereomeric and the enantiomeric ratio of **3aA**.

f. The process is resumed in this flow chart (FigureVII-36):

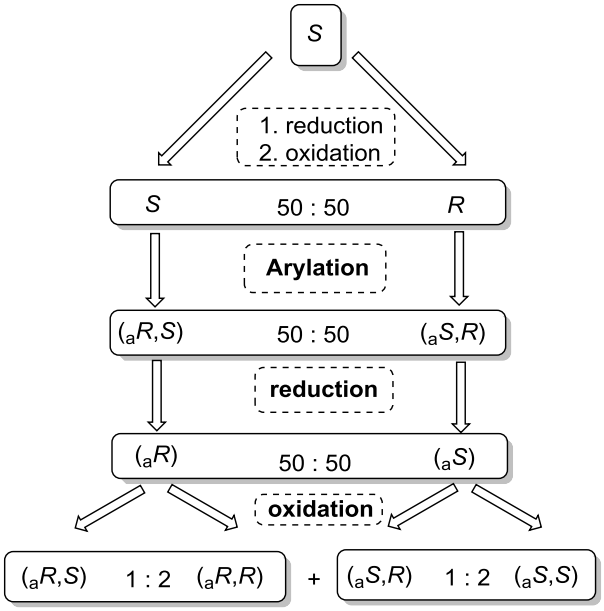

FigureVII-36 : diastereomers preparation scheme

g. The e.r. (and d.r.) of the product **3aA** was determined by injecting 2 different crude reaction mixtures on 2 sets of HPLC conditions : *conditions A: column AD-H; 1 mL/min; 20 µL injected; 95 : 5 n-Hex/i-PrOH*
conditions B: column AD-H; 0.5 mL/min; 20 µL injected; 95 : 5 n-Hex/i-PrOH

In both cases dr of 98 : 2 and er of 99% were measured as indicated on the following chromatograms (these results are also reported in the chiral HPLC optimization section).

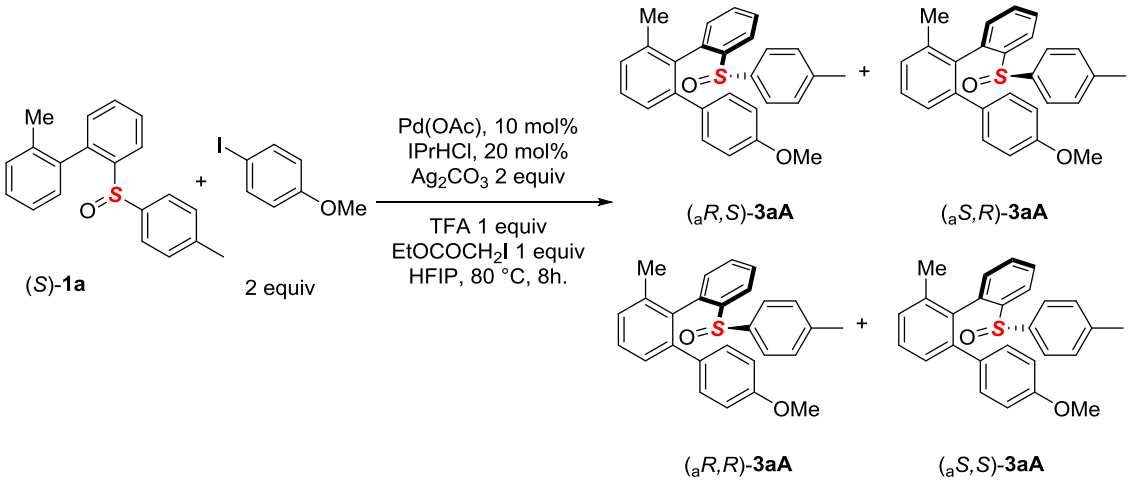

Figure VII-37 : 4 diastereomers, condition A

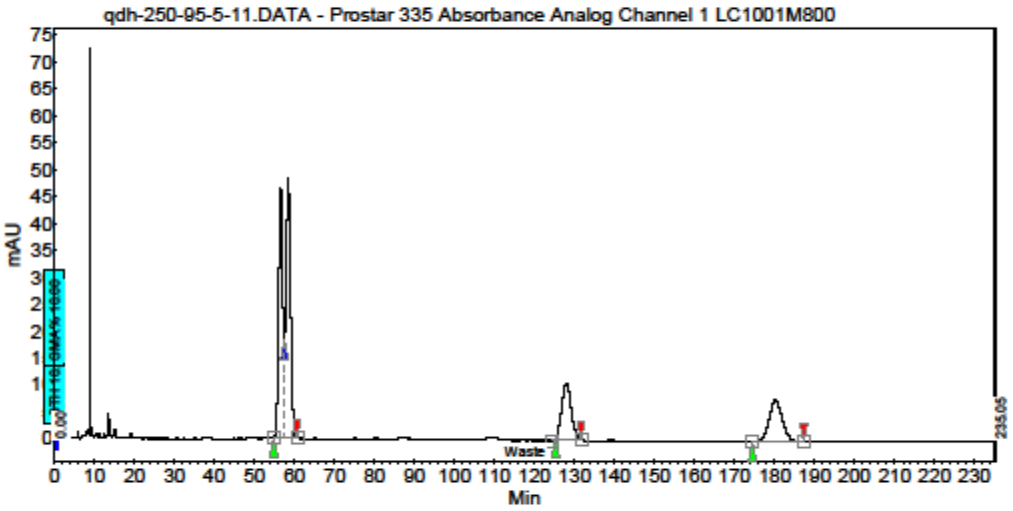

Peak results :

Index	Name	Time [Min]	Quantity [% Area]	Height [mAU]	Area [mAU.Min]	Area % [%]
1	UNKNOWN	56.49	32.09	46.6	57.4	32.089
2	UNKNOWN	58.43	35.17	48.2	62.9	35.170
3	UNKNOWN	127.93	16.16	10.5	28.9	16.163
4	UNKNOWN	180.20	16.58	7.8	29.7	16.578
Total			100.00	113.0	178.9	100.000

4 diastereomers, condition B

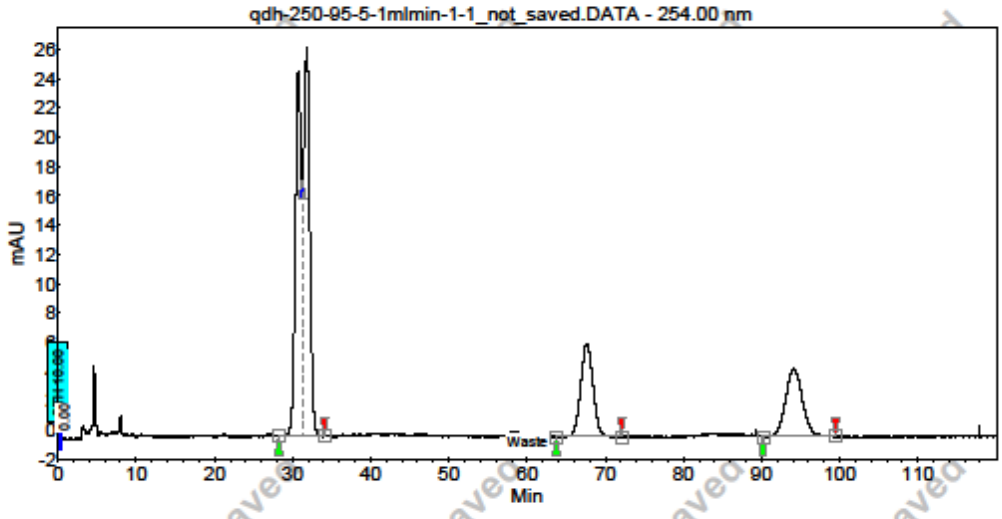

Peak results :

Index	Name	Time [Min]	Quantity [% Area]	Height [mAU]	Area [mAU.Min]	Area % [%]
1	UNKNOWN	30.75	31.57	24.9	22.2	31.572
2	UNKNOWN	31.82	35.73	26.6	25.1	35.734
3	UNKNOWN	67.63	16.45	6.4	11.6	16.447
4	UNKNOWN	94.15	16.25	4.6	11.4	16.247
Total			100.00	62.5	70.3	100.000

Crude reaction mixture 1, condition A

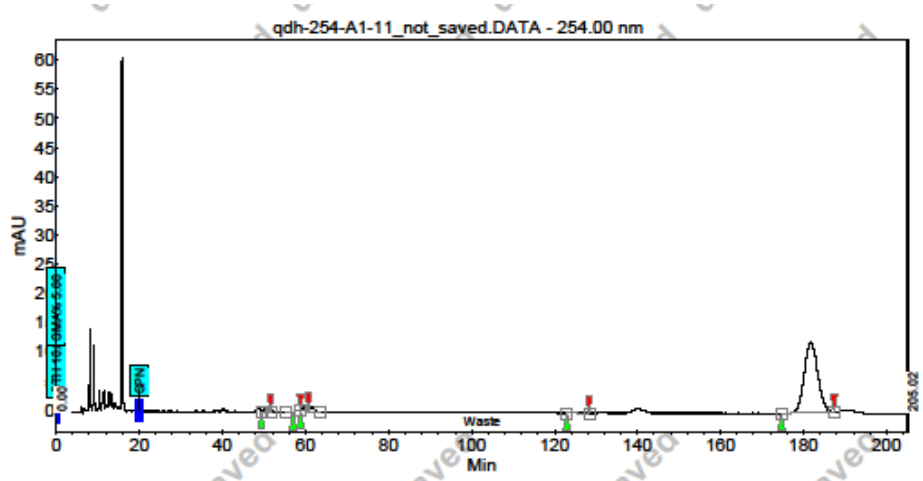

Peak results :

Index	Name	Time [Min]	Quantity [% Area]	Height [mAU]	Area [mAU.Min]	Area % [%]
1	UNKNOWN	50.57	0.65	0.4	0.3	0.648
2	UNKNOWN	57.08	0.05	0.1	0.0	0.048
5	UNKNOWN	59.72	1.52	0.7	0.7	1.516
4	UNKNOWN	125.58	1.32	0.3	0.6	1.323
3	UNKNOWN	181.71	96.47	12.1	45.5	96.466
Total			100.00	13.5	47.2	100.000

Crude reaction mixture 2, condition B

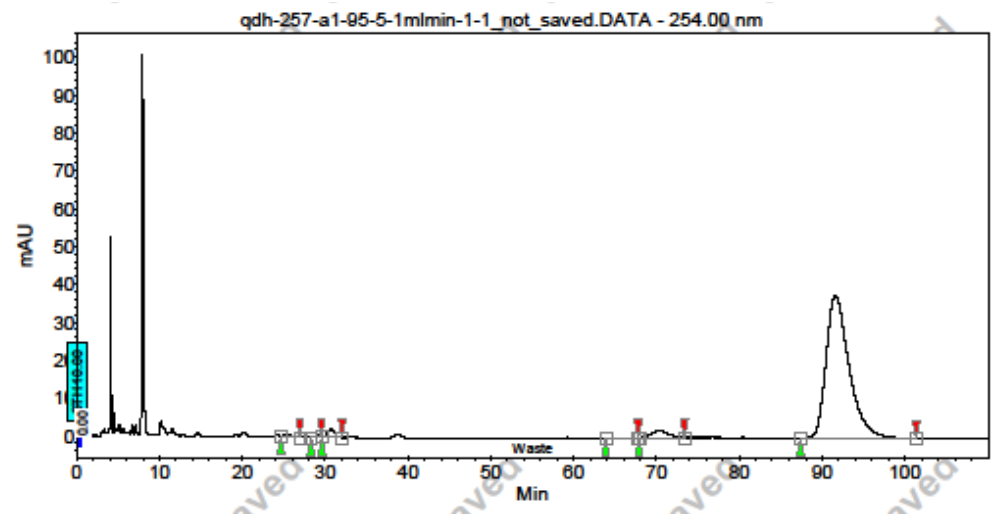

Peak results :

Index	Name	Time [Min]	Quantity [% Area]	Height [mAU]	Area [mAU.Min]	Area % [%]
4	UNKNOWN	25.22	0.44	0.7	0.6	0.436
6	UNKNOWN	28.96	0.15	0.4	0.2	0.152
5	UNKNOWN	30.67	1.56	2.3	2.0	1.558
2	UNKNOWN	65.67	0.21	0.2	0.3	0.206
3	UNKNOWN	70.36	3.51	1.9	4.6	3.513
1	UNKNOWN	91.58	94.14	37.9	122.7	94.135
Total			100.00	43.3	130.3	100.000

b) Diastereomeric ratio of arylation with double control of axial chirality

(1) General Procedure

The diastereomeric ratio determination should concern, for the model substrate, the following 4 diastereomers, (It was previously demonstrated that the sulfoxide does not epimerize under the reaction conditions):

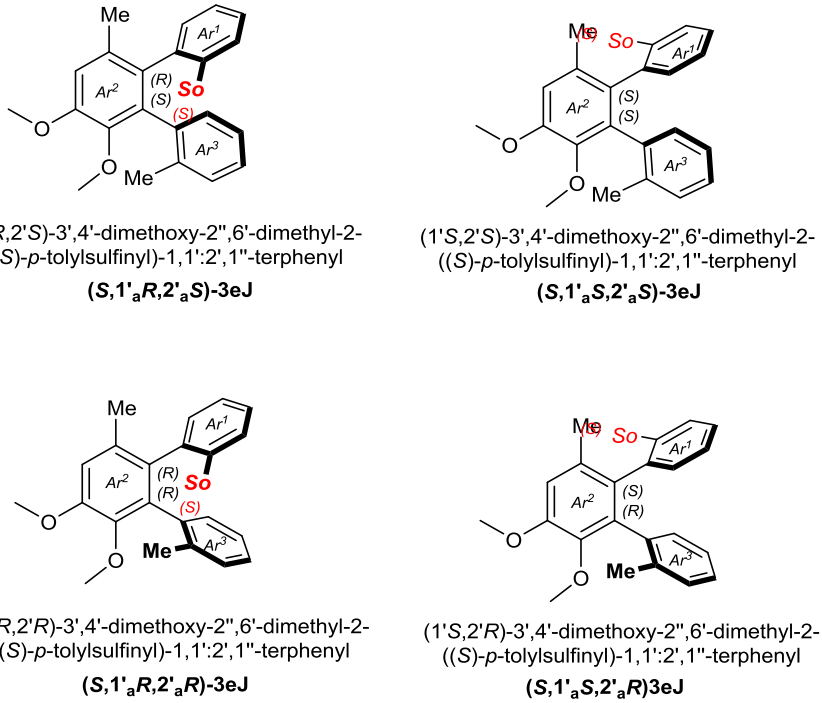

figureVII-38 : diastereomers of ($_s$S)-3eM

The X-Ray crystallography structure of **3eN** allows to determine the absolute configuration of the major, isolated, product is assigned as (*S*,1'*aR*,2'*aS*)-**3eN**.

Step 1: Products **3aI** (the -2',1''- axis is chiral but not atropisomeric) and **3aA** (the -2',1''- axis is not chiral) were submitted to the heating at 200 °C for 1h. This thermic treatment did not revealed any modification of the ^{1}H NMR spectra, in particular regarding the signal of the proton *ortho* to the sulfoxide moiety, clearly indicating that the Ar_1-Ar_2 axis does not epimerize under these conditions when substituted with a (2S)-*p*-tolylsufinyl, a 2'-phenyl and a 6'-methyl groups.

Step 2: Product **3eI**, bearing two chiral, atropisomeric axis, was submitting to the thermal conditions. Epimerization of the less hindered axis (i.e. -2',1''-) occurred under these thermic conditions, as indicated by ^{1}H NMR. Accordingly, mixture of **two diastereomers (*S*,1'*aR*,2'*aS*) and (*S*,1'*aR*,2'*aR*) was obtained**.

Step 3: **(*S*,1'*aR*,2'*aS*) was submitted to reduction/oxidation conditions in order**

to racemize the sulfoxide moiety. Accordingly, a mixture of 3 stereoisomer (*S*,1'*aR*,2'*aS*), (*R*,1'*aR*,2'*aS*), (*S*,1'*aR*,2'*aR*) and (*R*,1'*aR*,2'*aR*) was obtained. Stereoisomer (*R*,1'*aR*,2'*aS*) is not expected to be present in the crude reaction mixture, its spectra is identical to its enantiomer : (S,1'aS,2'aR)-**3eJ**; which is possibly present in the reaction mixture.

Such procedure allows us therefore to identify **3 of the 4 possible diastereomers formed during the reaction**.
Detailed analysis of the crude ^{1}H NMR spectra (region of 7.80 – 8.00 ppm, characteristic for proton signals *ortho*- to the sulfoxide moiety) shows 3 types of signals: one major one, corresponding to the diastereoisomer of the isolated product, and two very minor signals, which could be attributed to the signals of other diastereomers, characterized previously. The integration of these three signals allows determination of the diastereoselectivity of the reaction.

Step 4: Notably, close comparison between the spectra of each diastereomer and the spectra of crude mixture did not allow identification of the 4th, missing diastereomer.

Step 5: Finally, in order to further confirm that the sulfoxide moiety does not racemize under the reaction conditions and that its enantiopurity does not need to be taken into consideration while characterizing different diastereomers obtained during the reaction, the standard reaction was conducted at *c.a.* ~50% conversion and the recovered substrate **1f** was analyzed by chiral HPLC. Accordingly, **e.r. of recovered substrate > 98 : 2 was measured.**

In consequence, the d.r. of the reaction is given as a ratio between 3 different diastereomers, as indicated on 6:

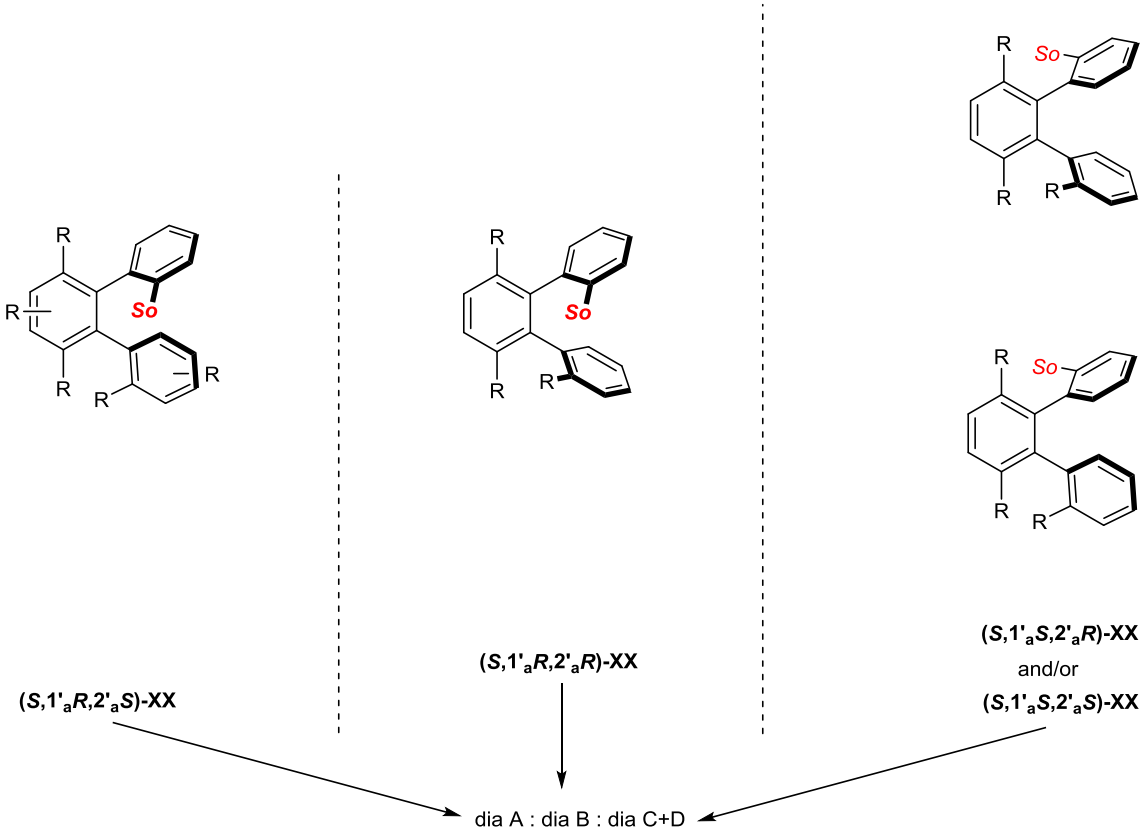

FigureVII-39 : general classification of diastereomers of the products

The overall protocol applied to prepare and characterize different diastereomers of **3eJ** is summarized on FigureVII-40 and the corresponding NMR spectra and chiral HPLC chromatograms are indicated below.

Notably, the same protocol was used to prepare and analyze different possible diastereomers for **3fM**. Comparable results have been obtained.

Furthermore, the thermal epimerization procedure was conducted on several other product showing that the minor diastereomers always present the same pattern on the ^{1}H NMR spectra when the substituents *ortho* the newly form axis (Ar^{2}-Ar^{3}) are identical for a given substrate.

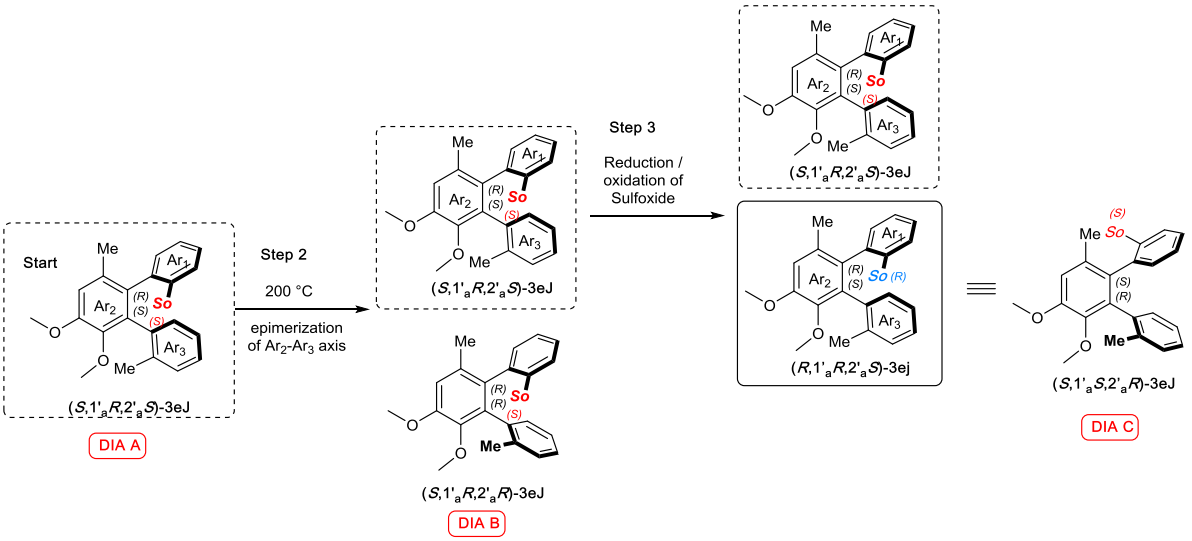

FigureVII-40 : scheme for the preparation and identification of 3eJ diastereomers

(2) General procedure applied to the model substrate product 3e

Step 1 : Study of the thermal stability of Ar^1-Ar^2 axis

a) After a thermal treatment of **3al** at 200 °C for 1h, no significant modification of the ^{1}H NMR spectra was observed indicating that the atropisomeric axis Ar^1-Ar^2 does not epimerize.

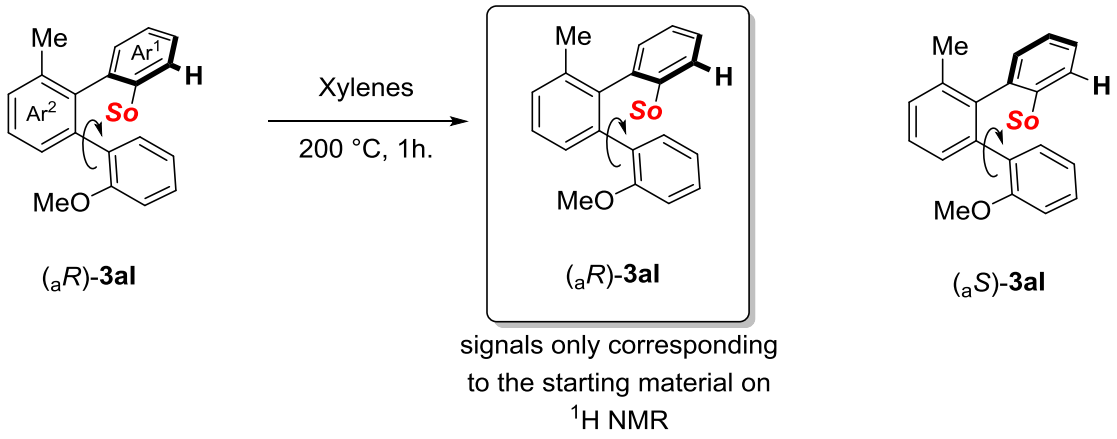

Top spectra : **($_a$*R*)-3al before the thermal treatment; *bottom spectra* : ($_a$*R*)-3al after the thermal threatment**

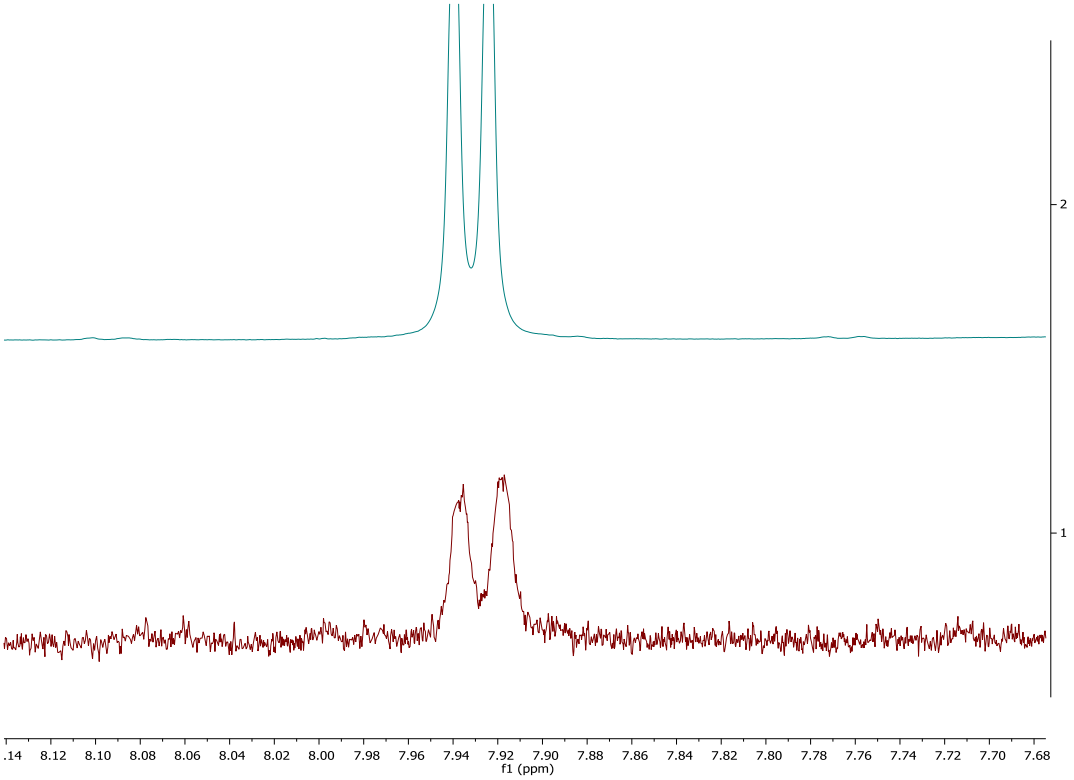

Figure VII-41 : Study of the thermal stability of Ar^1-Ar^2 axis of 3al

b) Thermal treatment of **3aA** indicated that the atropisomeric axis does not epimerize at 200 °C over 1h.

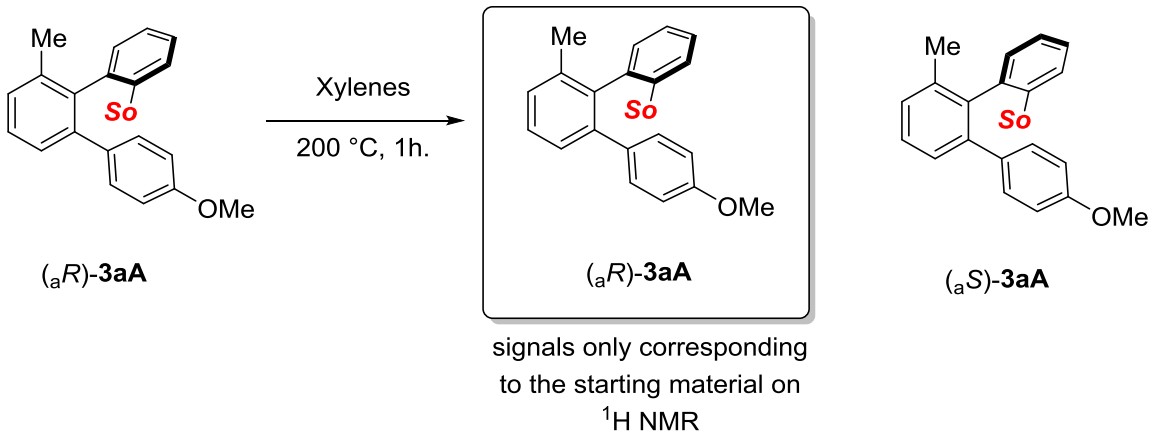

Top spectra : **($_a$*R*)-3aA before the thermal treatment; *bottom spectra* : ($_a$*R*)-3aA after the thermal treatment**

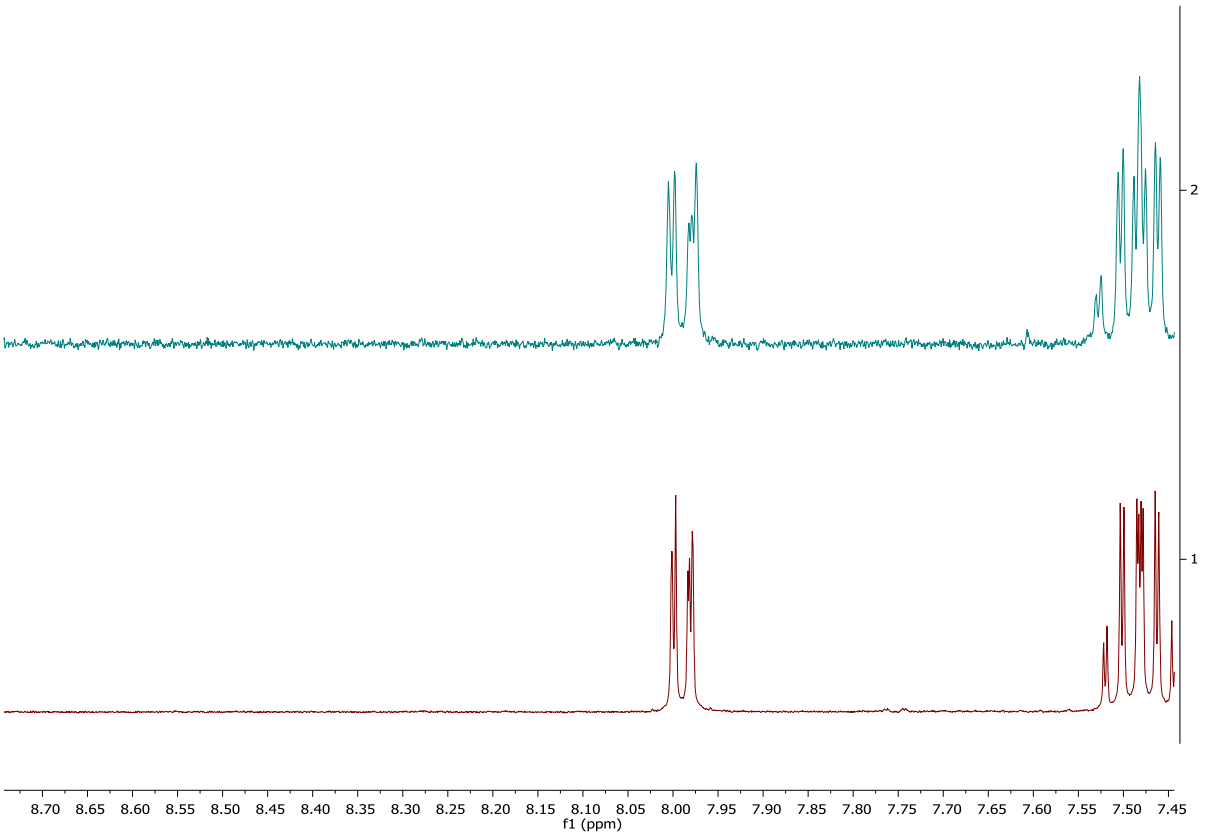

Figure VII-42 : Study of the thermal stability of Ar^1-Ar^2 axis of 3aA

Step 2 : Thermal epimerization of Ar^2-Ar^3 axis.

(1'aS,2'aR)-**3eI** was submitter to heating in xylenes solution (10 mg/ 1mL) at 200 °C for 1 hour in a microwave oven. Comparison of the initial spectra of **(1'aS,2'aR)-3eJ** (green spectra) and the spectra recorded after heating (red spectra) shows new signal in a characteristic region at 7.94 ppm (7.94 (dd, J = 7.9, 1.61 Hz)). This signal was attributed to the proton at ($C^{3''}$) of the assumed **(1'aR,2'aR)-3eJ** diastereomer.

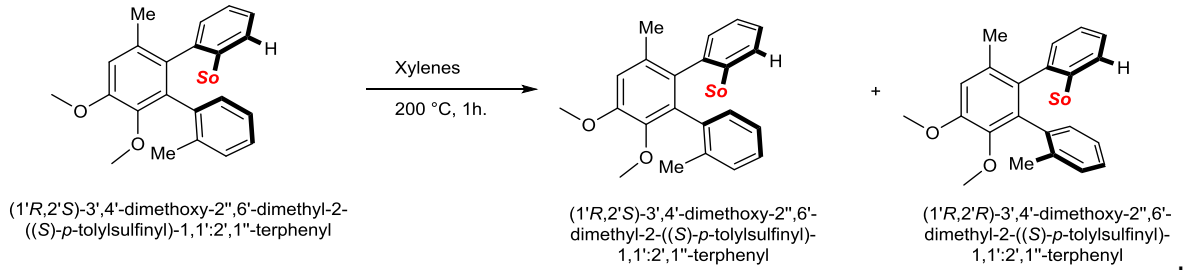

(1'*R*,2'*S*)-3',4'-dimethoxy-2'',6'-dimethyl-2-((*S*)-*p*-tolylsulfinyl)-1,1':2',1''-terphenyl

(1'*R*,2'*S*)-3',4'-dimethoxy-2'',6'-dimethyl-2-((*S*)-*p*-tolylsulfinyl)-1,1':2',1''-terphenyl

(1'*R*,2'*R*)-3',4'-dimethoxy-2'',6'-dimethyl-2-((*S*)-*p*-tolylsulfinyl)-1,1':2',1''-terphenyl

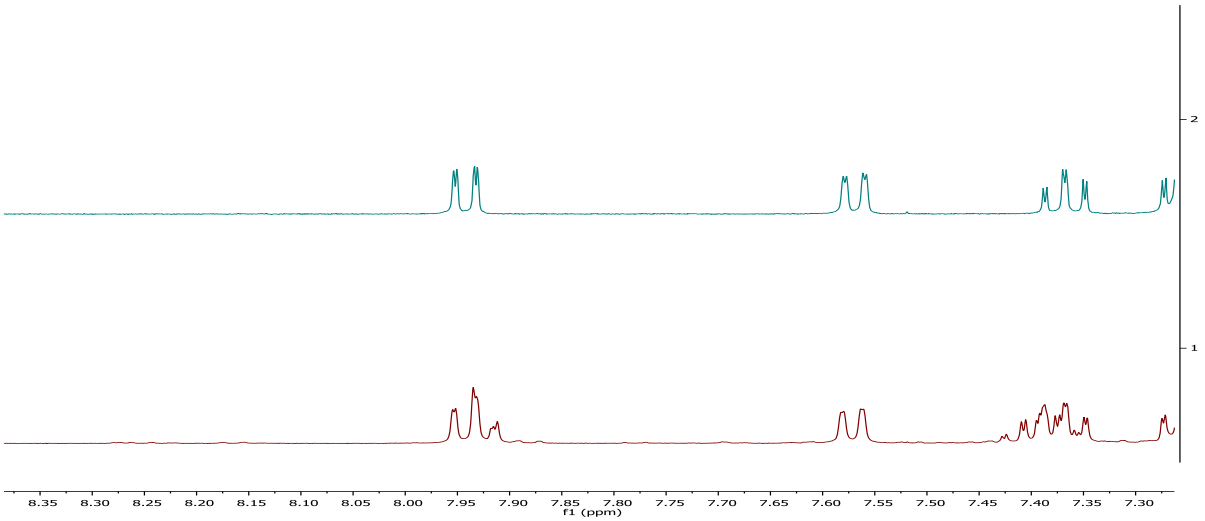

Figure VII-43 : Thermal epimerization of Ar2-Ar3 axis of 3eJ

Step 3 : Racemization of the sulfoxide group

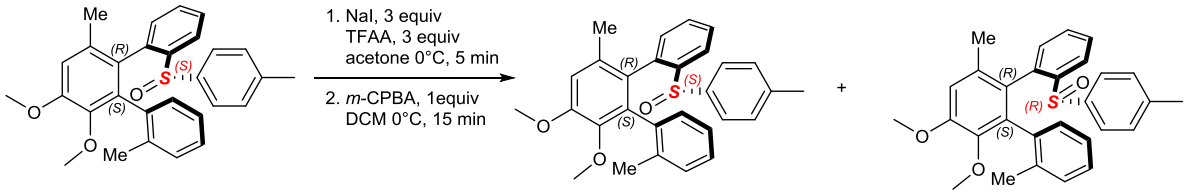

quant. (*S*,1'*R*,2'*S*)-**3eJ**/(*R*,1'*R*,2'*S*)-**3eJ**, 1.5 : 1

Top spectra: **3eJ before the Ox/Red treatment; *bottom spectra* : 3eJ after the Ox/Red treatment**

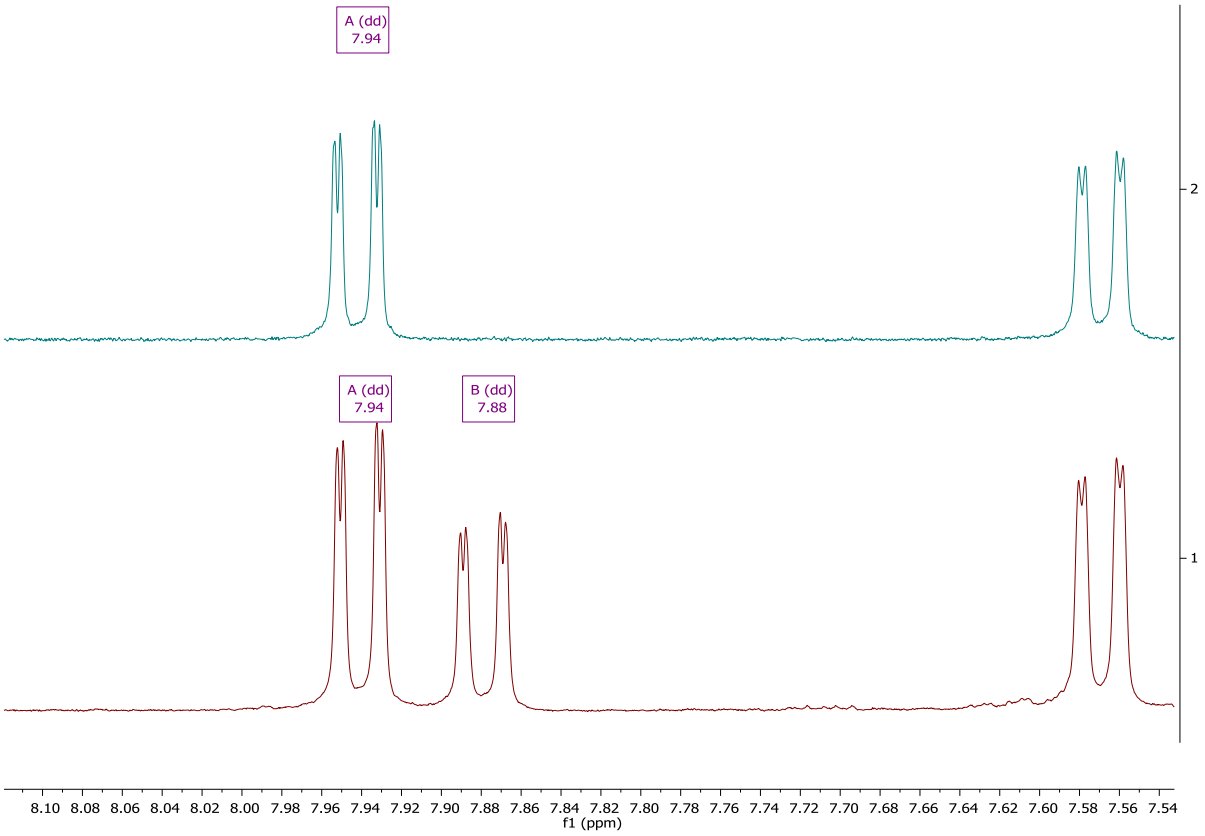

Figure VII-44 : Racemization of the sulfoxide group of 3eJ

Step 5 : Confirmation of the optical stability of the sulfoxide moiety under reaction conditions

Preparation of a sample of racemic **1f** by reduction / oxidation sequence

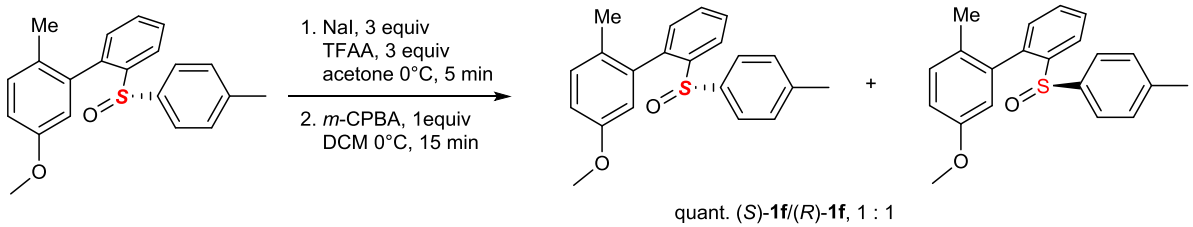

FigureVII-45 : preparation of racemic 1f

Subsequently, standard arylation using enantiopure **1f** substrate was conducted till 50% conversion and the optical purity of the remaining starting material was analyzed by chiral HPLC.

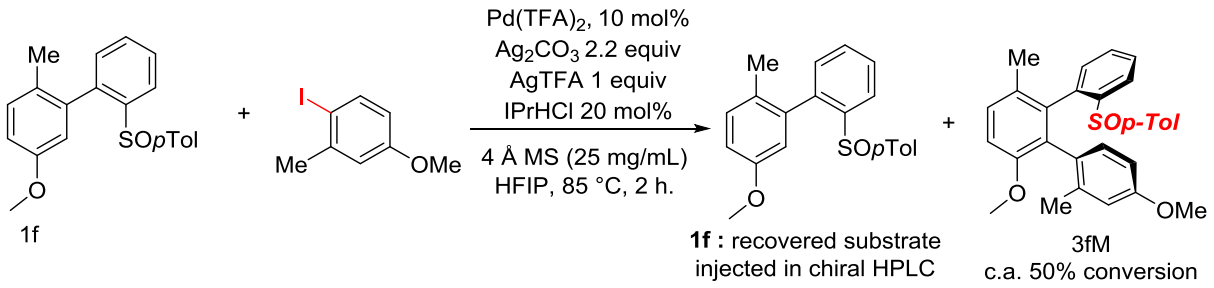

FigureVII-46: arylation of racemic 1f

Chiral HPLC conditions: ADH column, 0.5 mL/min, 1µL injected, 95 : 5 n-Hex/i-PrOH

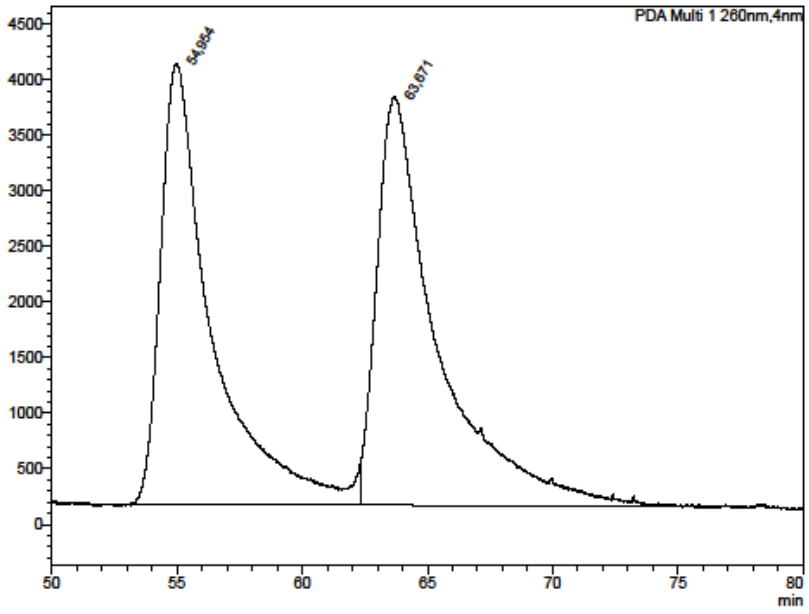

<PDA Chromatogram>

Peak Table

PDA Ch1 260nm

Peak#	Ret. Time	Area	Height	Area%	Capacity Factor(k')	Resolution(USP)	Lambda max
1	54,954	564221	3969	47,731	-	-	204/638/499
2	63,671	617853	3676	52,269	0,159	2,389	204/638/486
Total		1182074	7644	100,000			

Figure VII-47 : Racemic 3f chiral HPLC

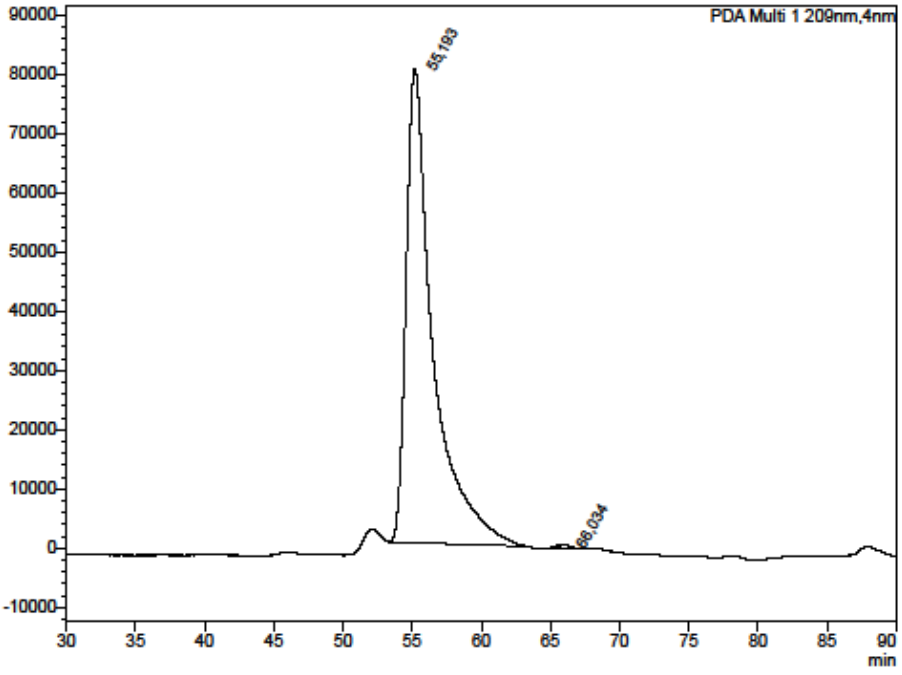

<PDA Chromatogram>

Peak Table

PDA Ch1 209nm

Peak#	Ret. Time	Area	Height	Area%	Capacity Factor(k')	Resolution(USP)	Lambda max
1	55,193	10809440	80107	99,500	-	-	205/485/584/441/420
2	66,034	54362	662	0,500	0,196	4,208	213/236/265/485/291
Total		10863802	80768	100,000			

Figure VII-48 : Recovered 3f chiral HPLC

Results on the crude NMR of compound 3eN:

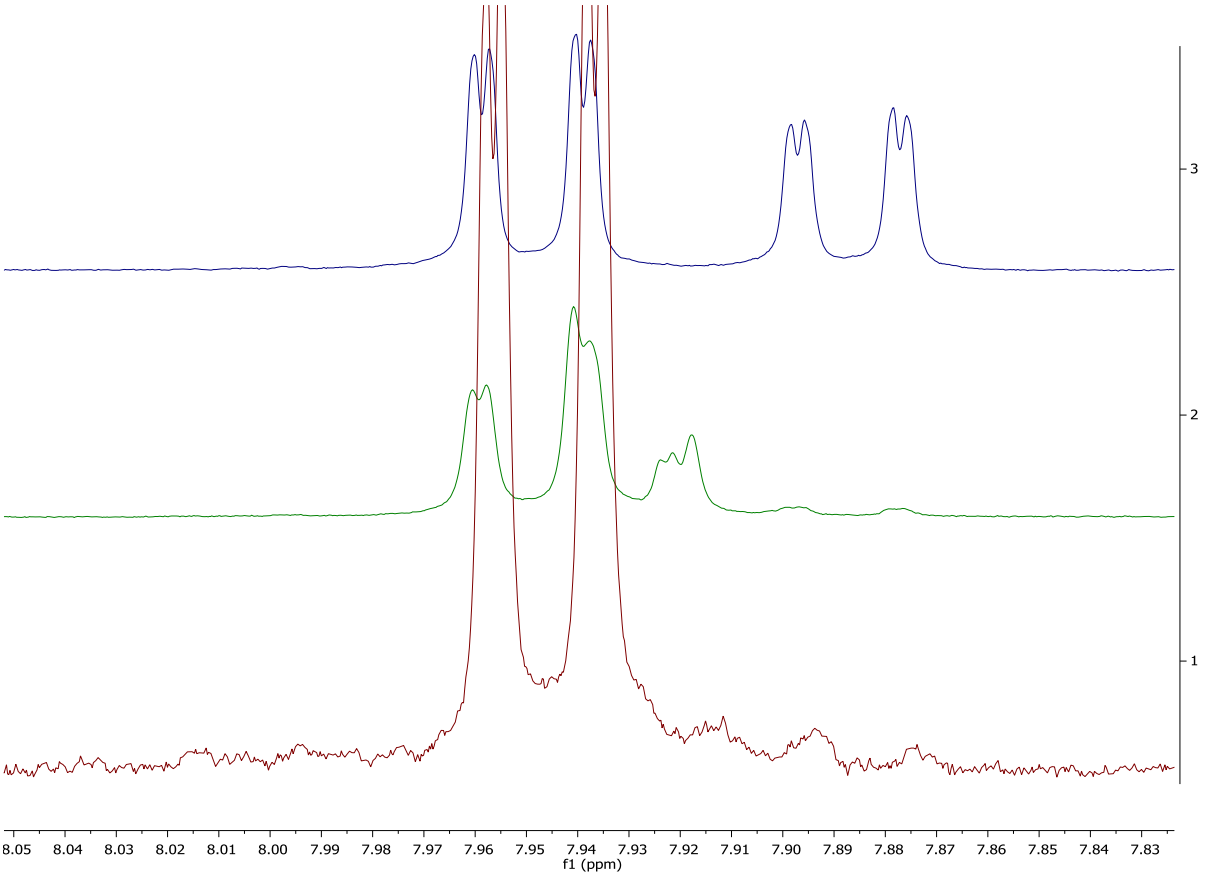

Figure VII-49 : top spectra : Step 3; middle spectra : Step 2; bottom spectra crude reaction mixture

(3) Thermal epimerization of 3eM

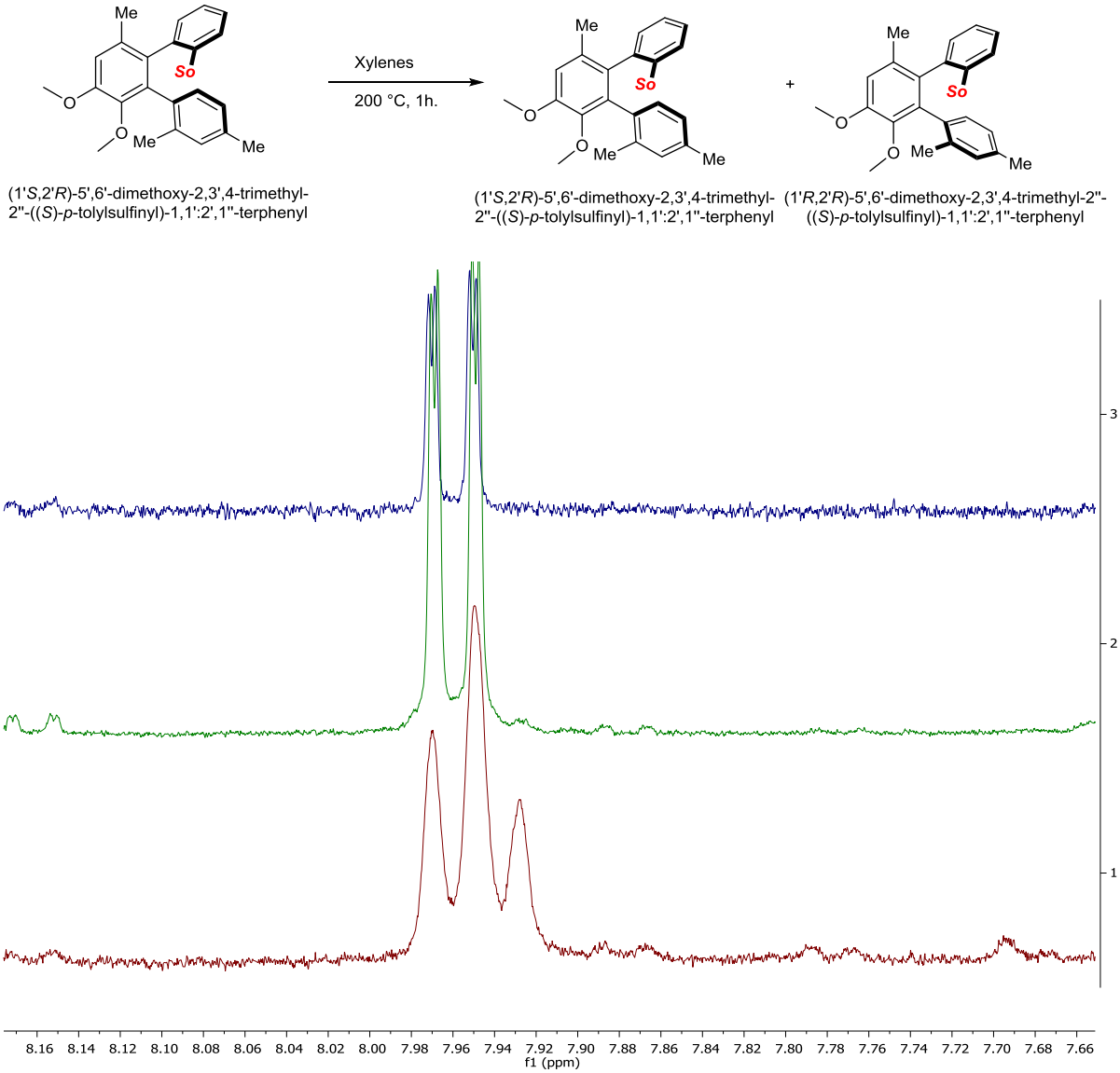

Figure VII-50 : thermal epimerization of 3eM : Top isolated product; middle crude mixture ; bottom crude mixture after thermal epimerization

(4) General procedure for analysis of 3fN diastereomers

Step 2: Thermal epimerization around Ar_2-Ar_3 axis.

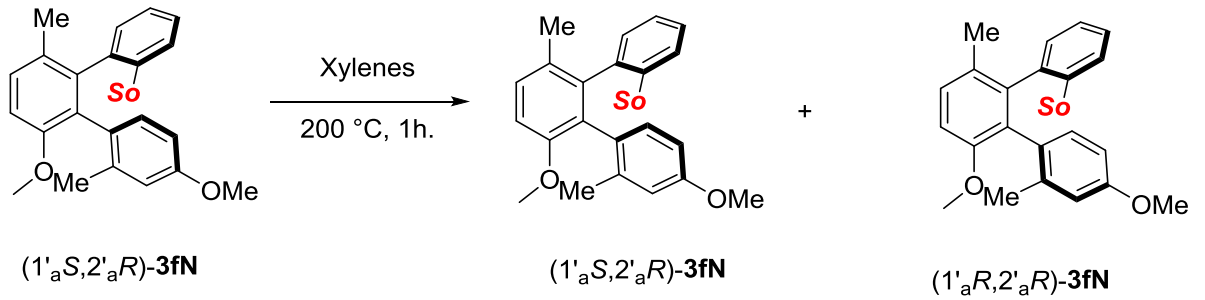

$(1'_aS,2'_aR)$-**3fN** $(1'_aS,2'_aR)$-**3fN** $(1'_aR,2'_aR)$-**3fN**

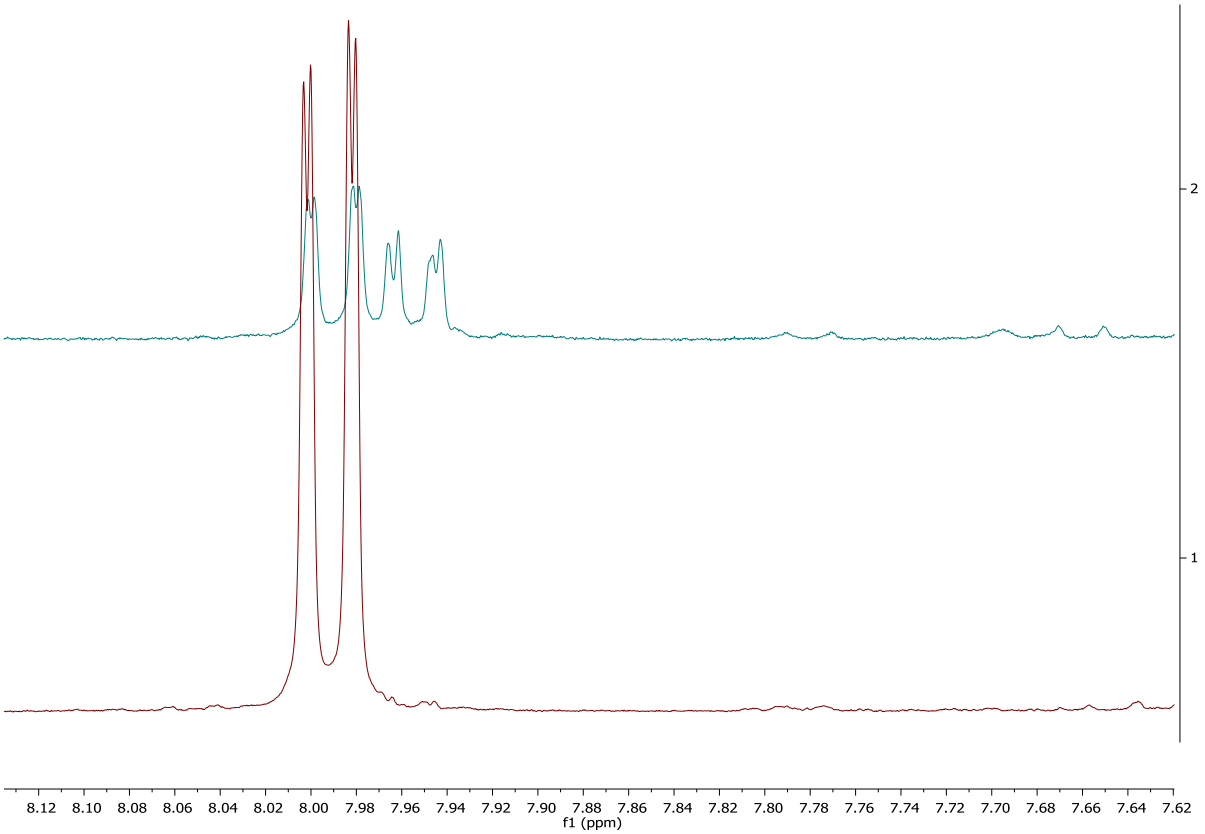

Figure VII-51 : thermal epimerization of 3fN : top crude mixture after thermal treatment; bottom isolated product

Step 3: Reduction/oxidation sequence to racemize the sulfoxide moiety.

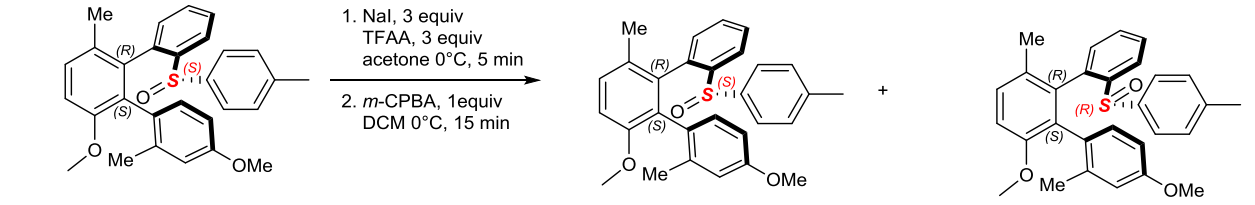

(1'*S*,2'*R*)-4,6'-dimethoxy-2,3'-dimethyl-2''-((*S*)-*p*-tolylsulfinyl)-1,1':2',1''-terphenyl

(1'*S*,2'*R*)-4,6'-dimethoxy-2,3'-dimethyl-2''-((*S*)-*p*-tolylsulfinyl)-1,1':2',1''-terphenyl

(1'*S*,2'*R*)-4,6'-dimethoxy-2,3'-dimethyl-2''-((*R*)-*p*-tolylsulfinyl)-1,1':2',1''-terphenyl

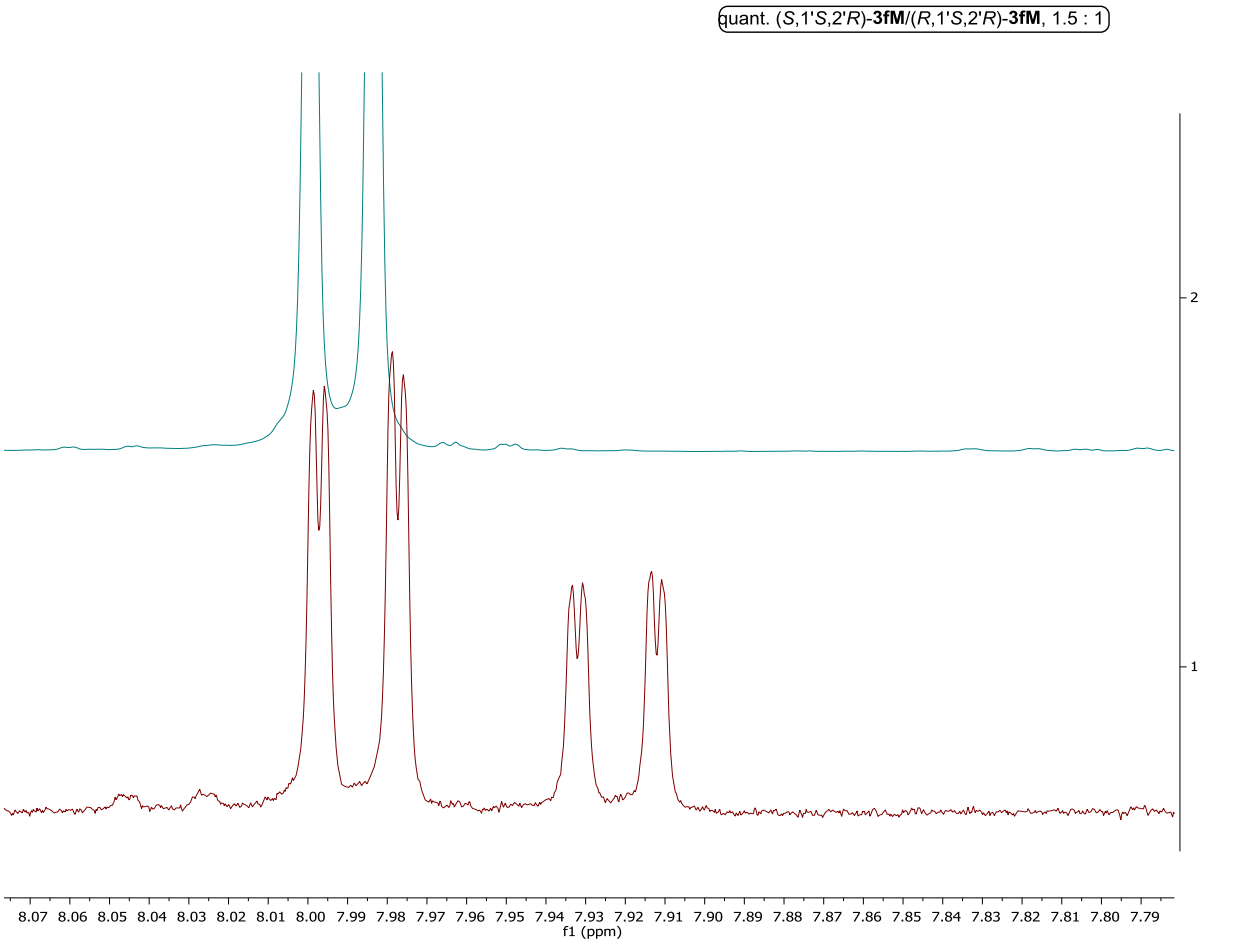

Figure VII-52 : epimerization od the sulfoxide moiety of 3fN; Top spectra substrate; bottom spectra crude ^{1}H NMR after reduction/oxidation

Results on crude ^{1}H NMR of compound 3fN:

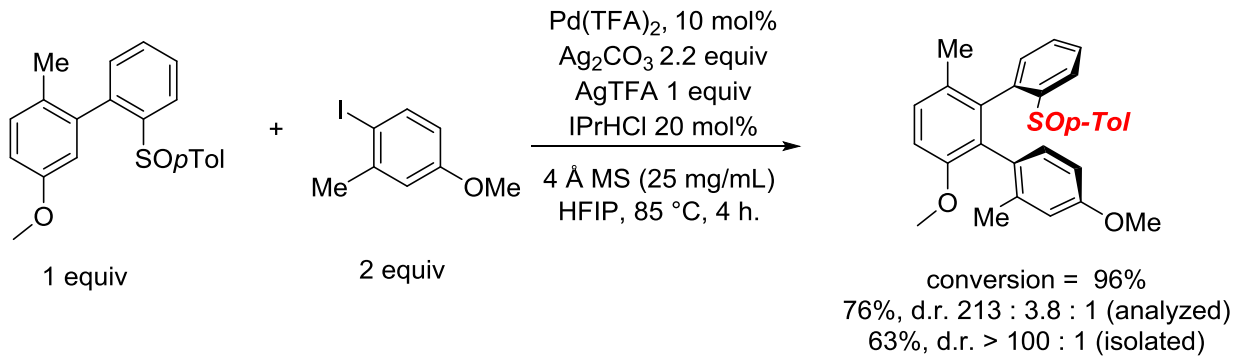

conversion = 96%
76%, d.r. 213 : 3.8 : 1 (analyzed)
63%, d.r. > 100 : 1 (isolated)

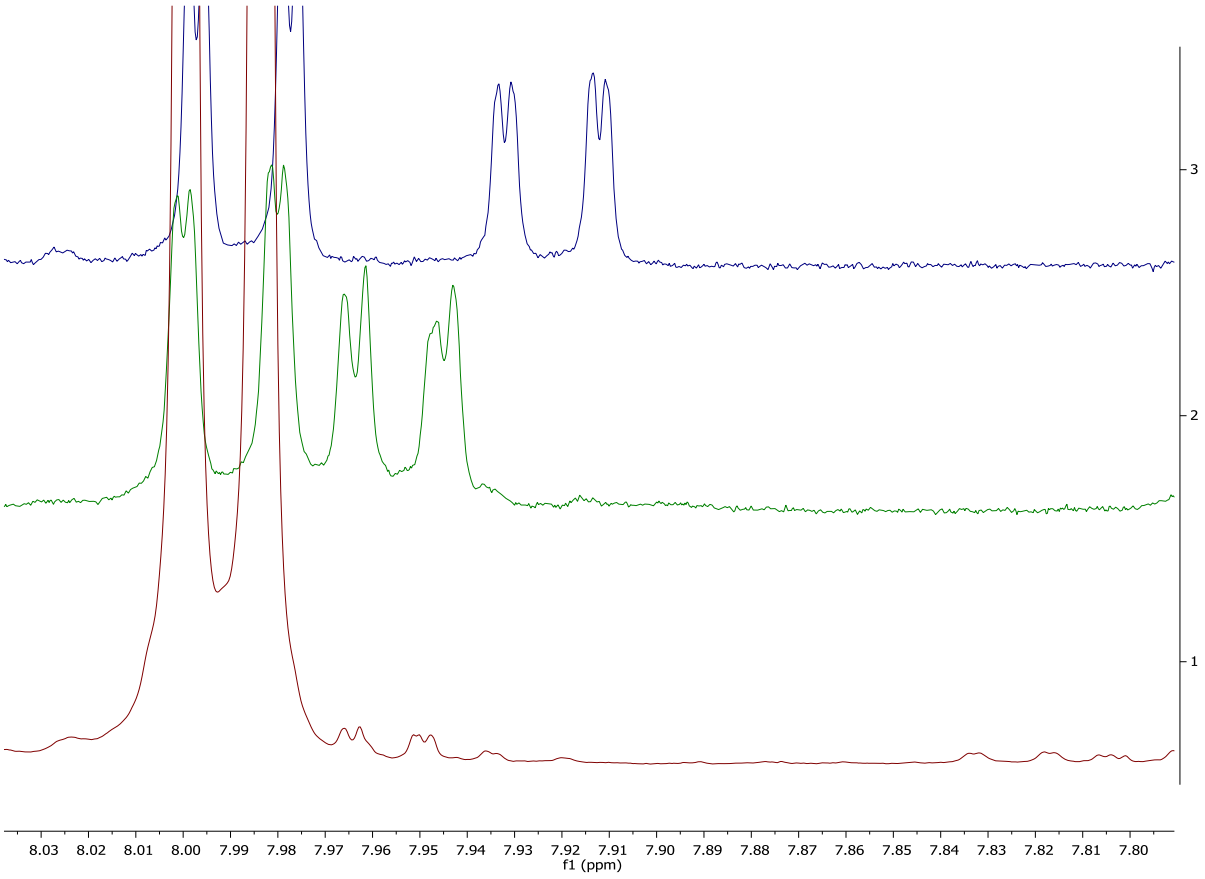

Figure VII-53 : identification of 3fN diastereomers; Top spectra : epi red/ox ; middle spectra thermal epi ; bottom spectra crude ^{1}H NMR

(5) Thermal epimerization of 3fP

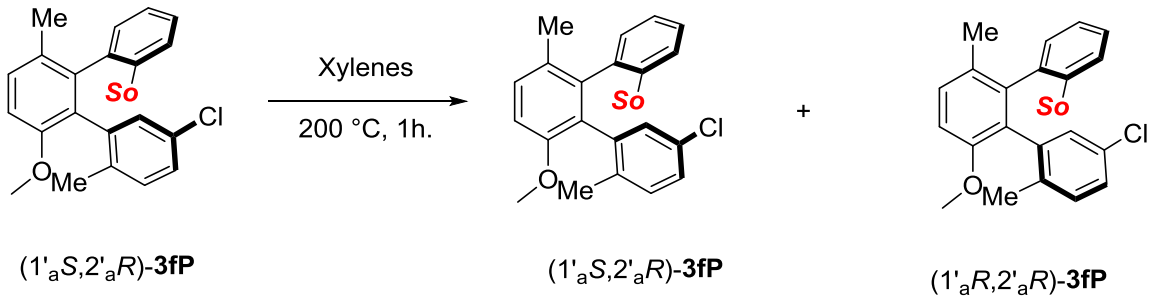

$(1'_aS,2'_aR)$-**3fP** $(1'_aS,2'_aR)$-**3fP** $(1'_aR,2'_aR)$-**3fP**

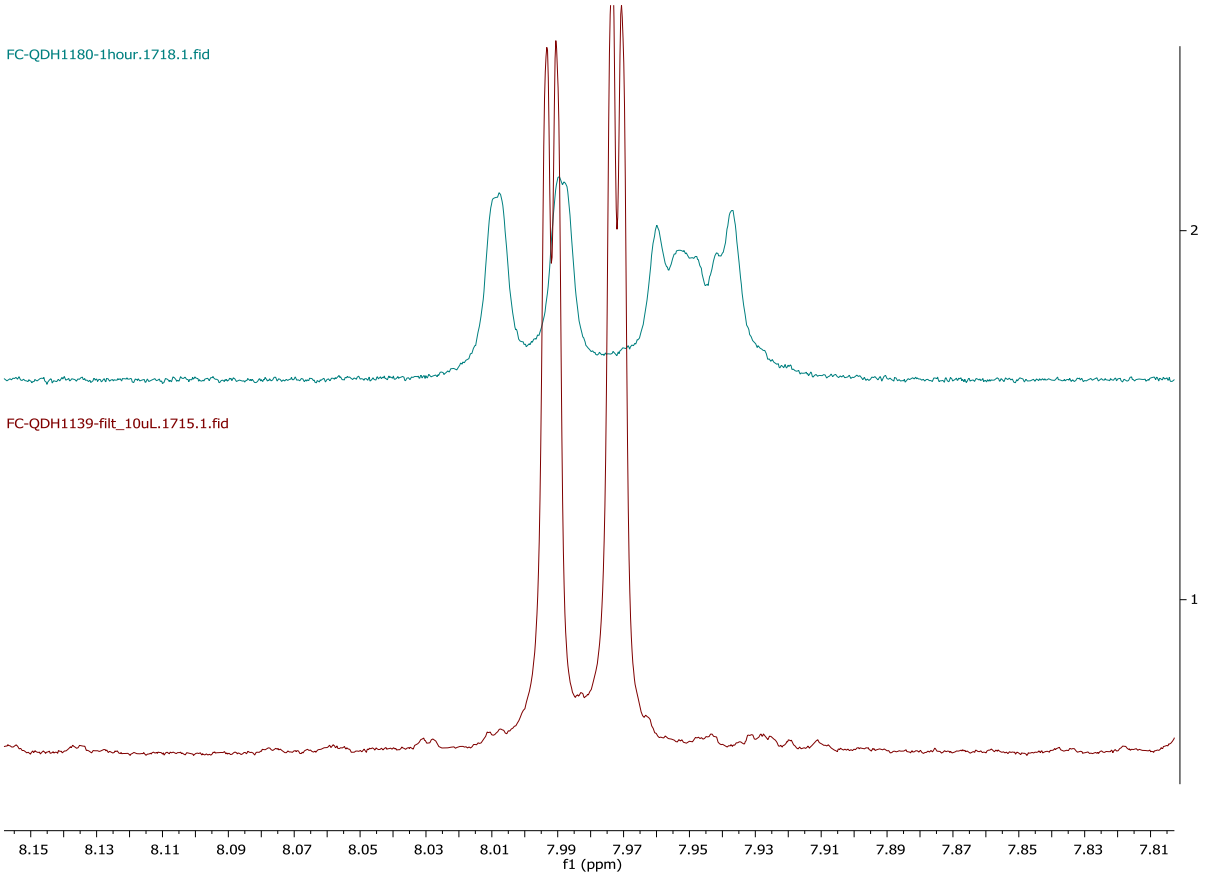

Figure VII-54 : thermal epimerization of 3fP; Top spectra : thermal epimerization ; Bottom spectra crude ^{1}H NMR

(6) Thermal epimerization of 3fU

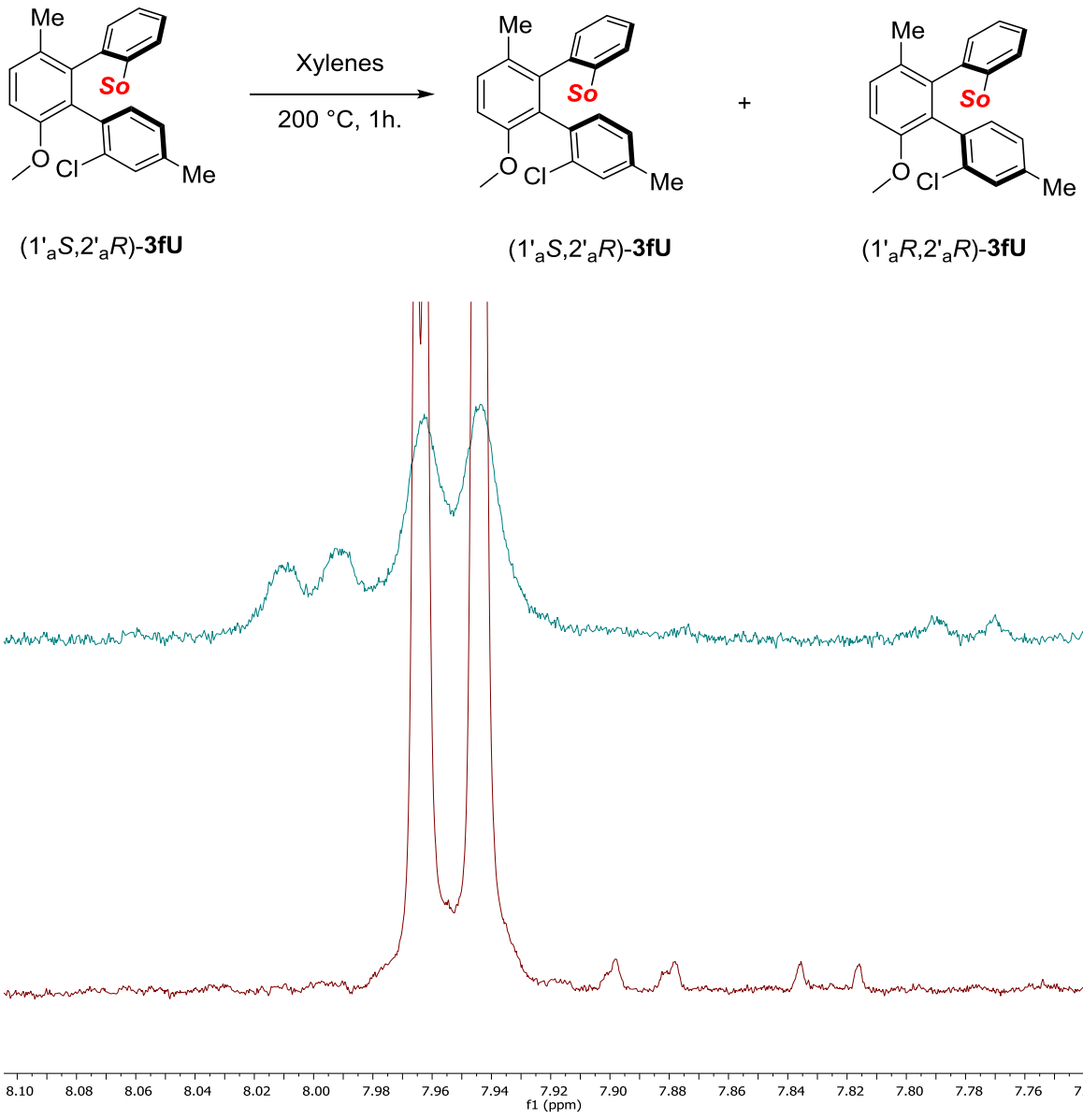

Figure VII-55 :thermal epimerization of 3fU; Top spectra : thermal epimerization ; Bottom spectra : crude reaction mixture

(7) Thermal epimerization of 3fl

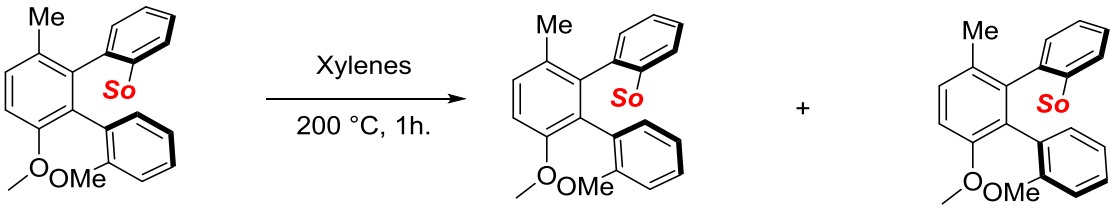

(1'$_a$*S*,2'$_a$*R*)-**3fl** (1'$_a$*S*,2'$_a$*R*)-**3fl** (1'$_a$*R*,2'$_a$*R*)-**3fl**

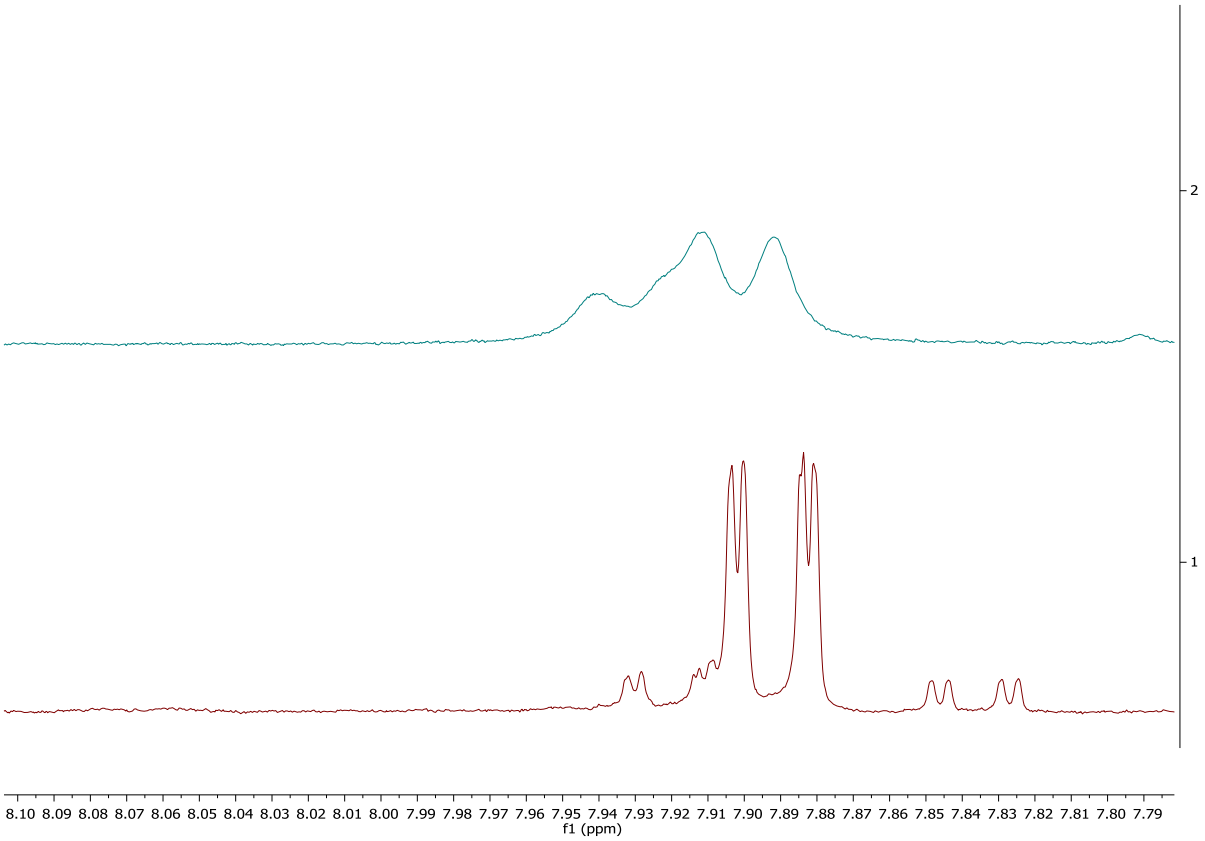

Figure VII-56 : thermal epimerization of 3fl. Top spectra : thermal epimerization ; Bottom spectra : crude reaction mixture

(8) Thermal epimerization of 3gI

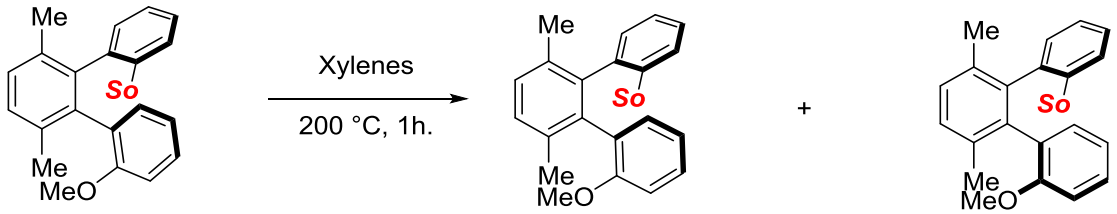

(1'$_a$*S*,2'$_a$*R*)-**3gI** (1'$_a$*S*,2'$_a$*R*)-**3gI** (1'$_a$*R*,2'$_a$*R*)-**3gI**

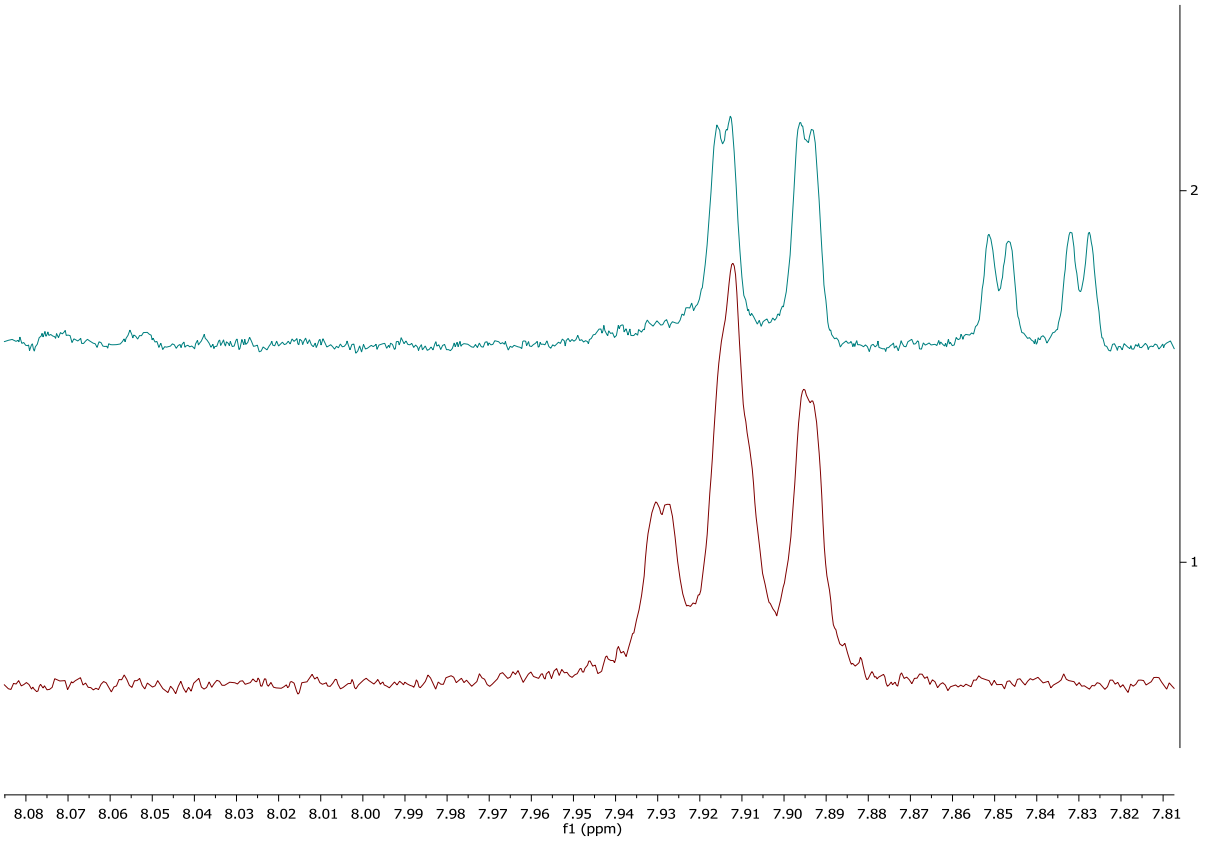

Figure VII-57 thermal epimarizatio o f 3gI.Top spectra : crude reaction mixture; Bottom spectra : thermal epimerization

(9) Thermal epimerization of 3gV

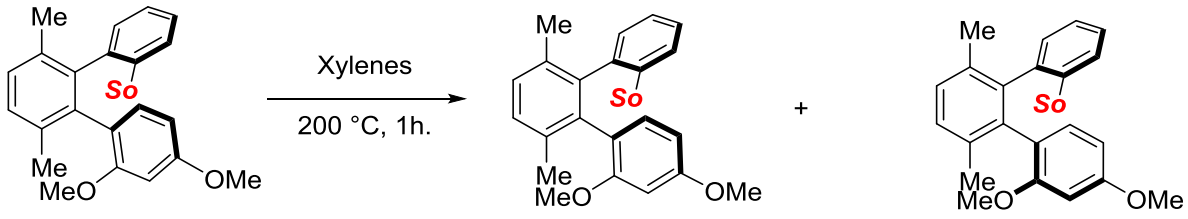

(1'$_a$*R*,2'$_a$*R*)-**3gV** (1'$_a$*S*,2'$_a$*R*)-**3gV** (1'$_a$*S*,2'$_a$*R*)-**3gV**

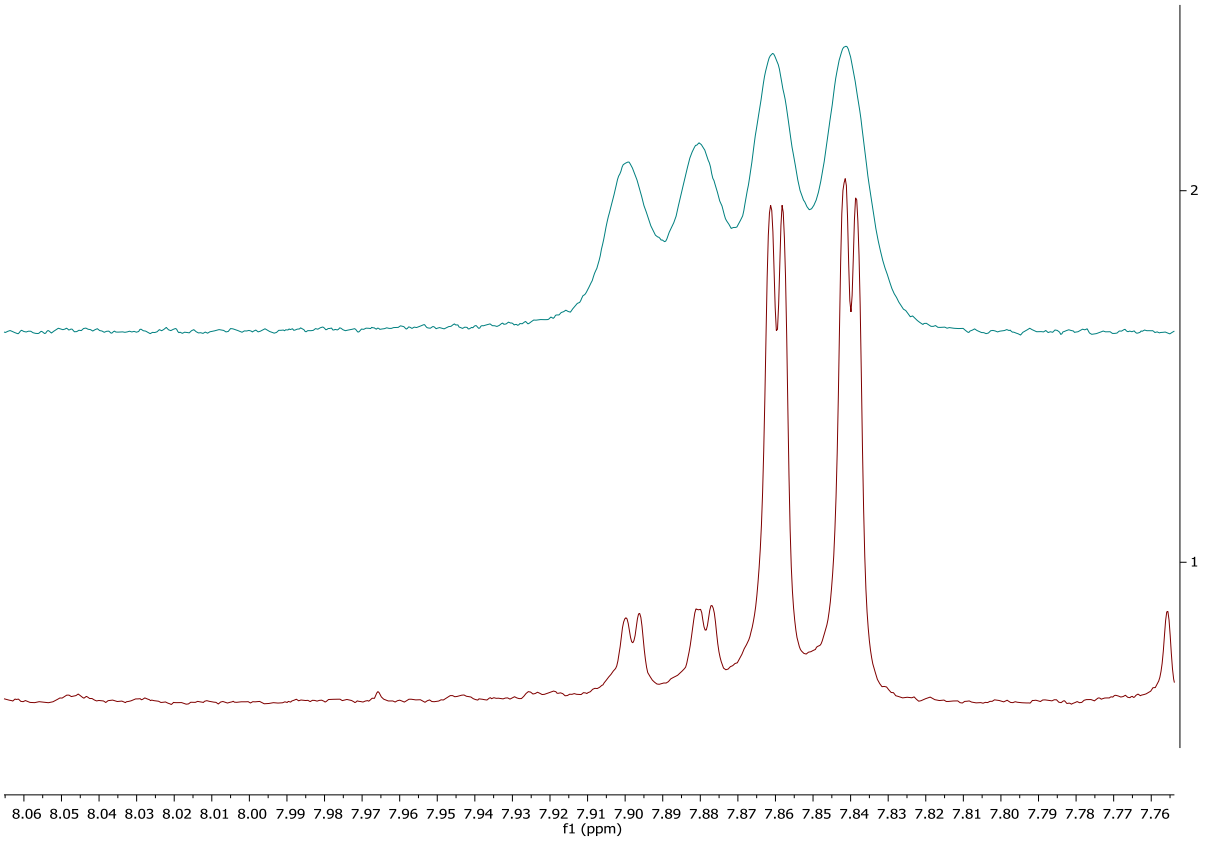

Figure VII-58 thermal epimerization of 3gV. Top spectra : thermal epimerization ; Bottom spectra : crude reaction mixture

c) *Diastereomeric and enantiomeric ratio of product 8*

In order to determine the diastereomeric ratio of **8**, substrate **3fP** was epimerized about the Ar^2-Ar^3 biaryl axis :

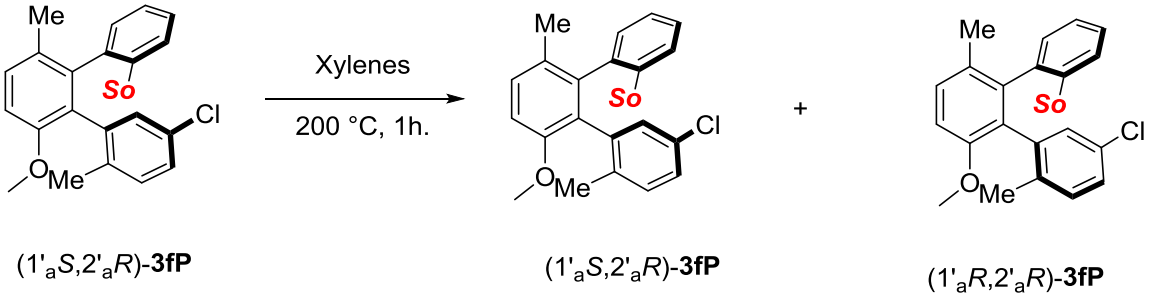

$(1'_aS,2'_aR)$-**3fP** $(1'_aS,2'_aR)$-**3fP** $(1'_aR,2'_aR)$-**3fP**

FigureVII-59 : thermal epimerization of 3fP

Then the diastereomeric mixture was submitted to the conditions used for the preaparation of **8**, thus yielding the following diastereomer mixture :

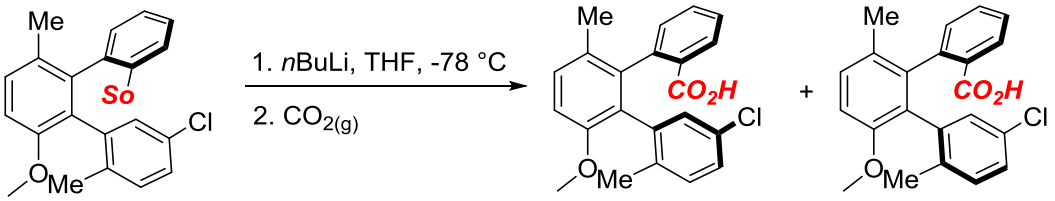

$(1'_aR,2'_aS)$-**8** $(1'_aR,2'_aR)$-**8**

FigureVII-60 : functionalization of epimerized 3fP

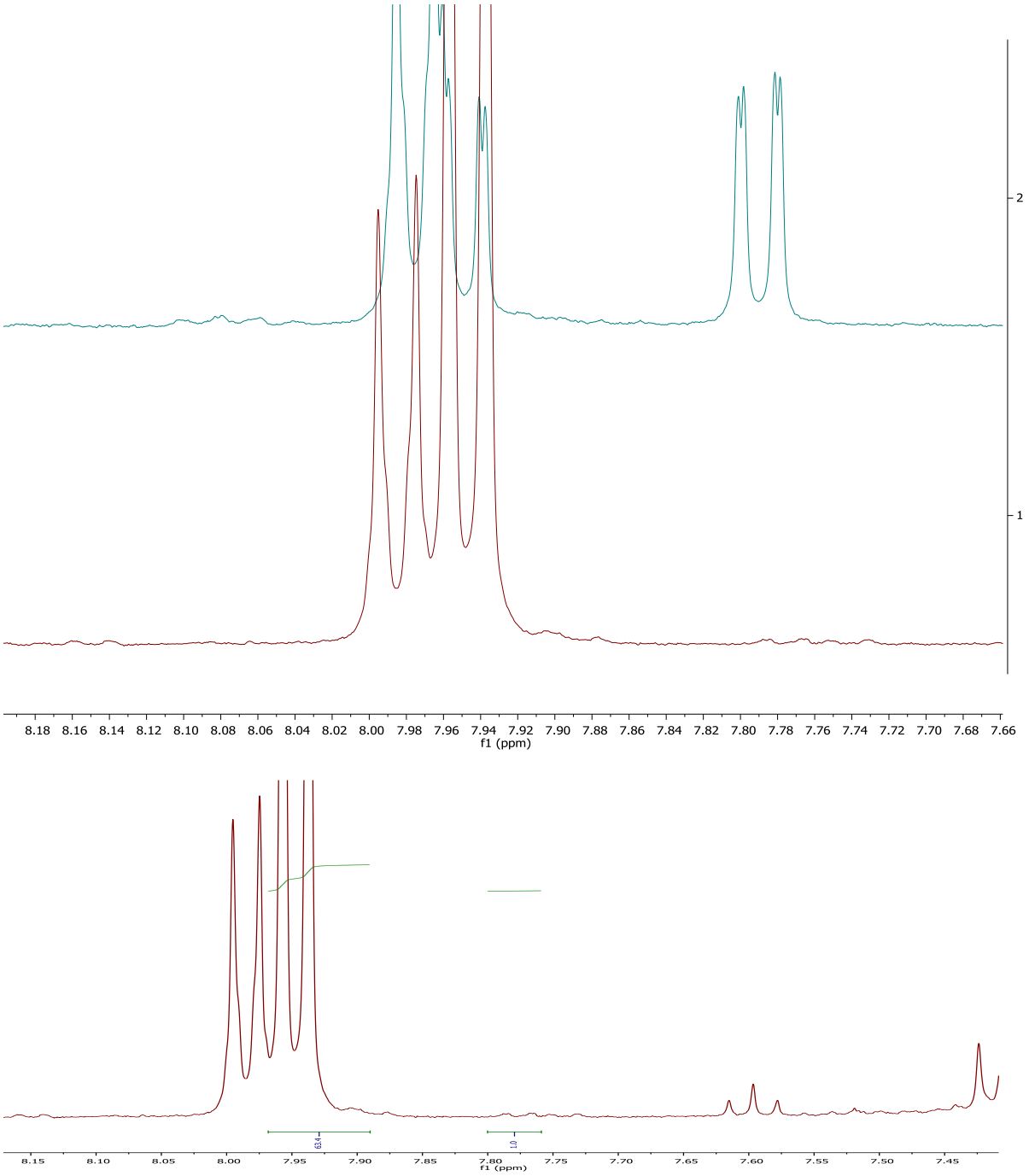

Figure VII-61 : determination of the d.r. of 8 on ^{1}H NMR; Top spectra diastereomeric mixture of 8, bottom spectra : crude reaction mixture on atropopure substrate; integration on crude mixture : 63.4 : 1

Then, to determine the e.r. of **8**, the arylation with double control of axial chirality was conducted on a racemic substrate **1f**, in order to afford both enantiomers of the product **3fO**.

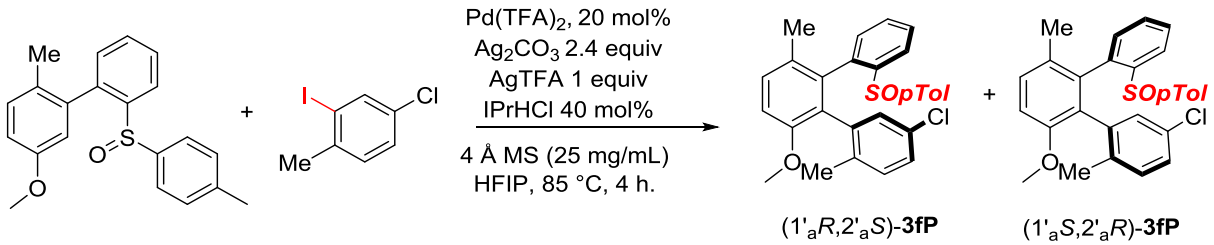

FigureVII-62: arylation of racemic 3fO

Racemic mixture of **3fP** was submitted to standard sulfoxide/lithium exchange followed by trapping with CO_2, affording racemic mixture of **8 (**1 : 1 ratio).

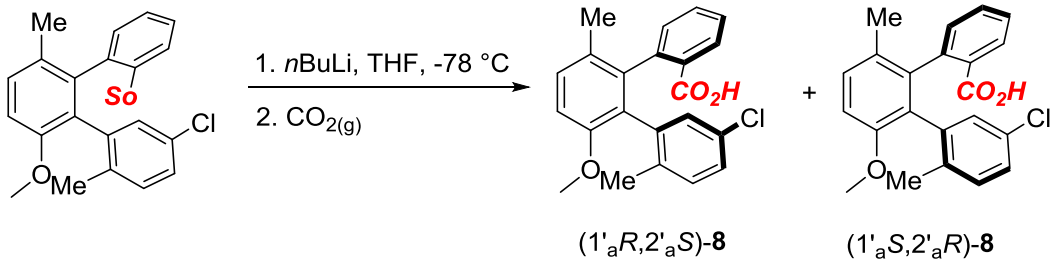

FigureVII-63 : functionalization of epimerized 3fO

Chiral HPLC analysis then allowed us to determine the e.r. of (1'$_a$R,2'$_a$S)-**8 : e.r. >98 : 2.**

Chiral HPLC conditions: ADH column, 0.5 mL/min, 1µL injected, 95 : 5 n-Hex/i-PrOH

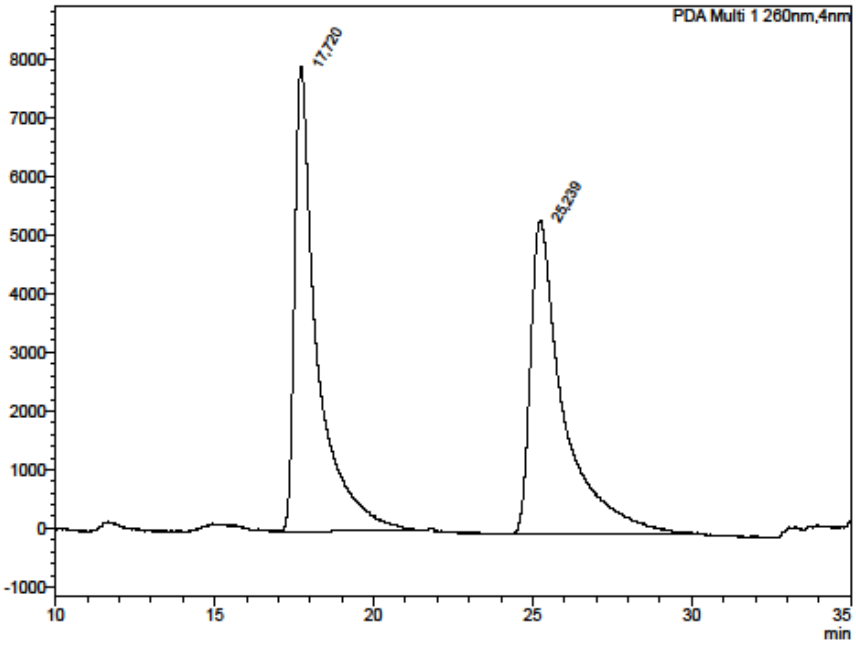

<PDA Chromatogram>

Peak Table

PDA Ch1 260nm

Peak#	Ret. Time	Area	Height	Area%	Capacity Factor(k')	Resolution(USP)	Lambda max
1	17,720	386862	7937	50,205	-	-	205/282/483/409
2	25,239	383702	5360	49,795	0,424	5,934	205/282/655/485
Total		770564	13298	100,000			

Figure VII-64 : (1'aR,2'aS)-8/(1'aS,2'aR)-8 pair chiral HPLC

Isolated (1'$_a$R,2'$_a$S)-8 chiral HPLC

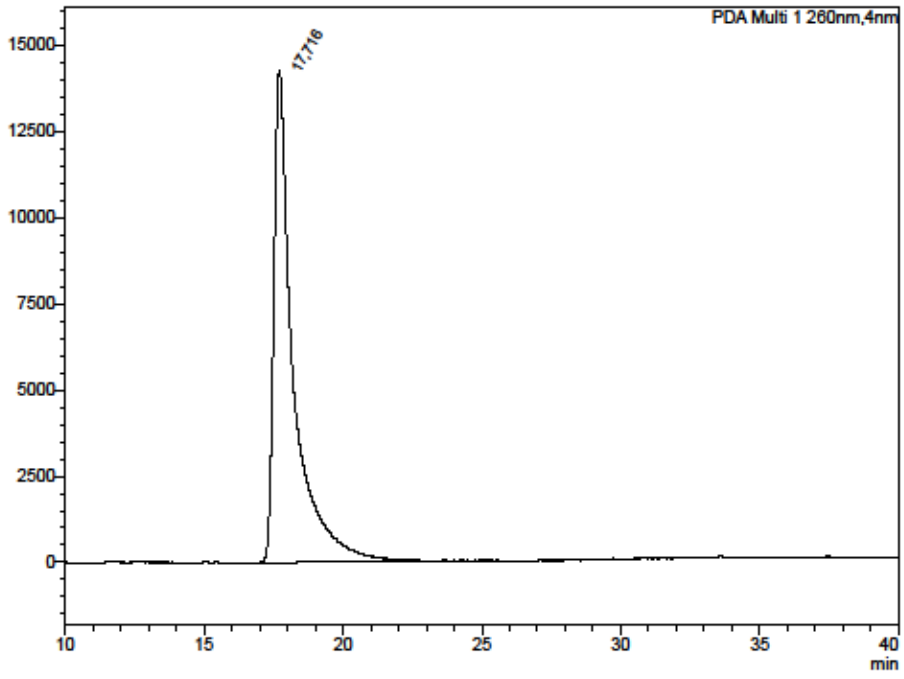

<PDA Chromatogram>

Peak Table

PDA Ch1 260nm

Peak#	Ret. Time	Area	Height	Area%	Capacity Factor(k')	Resolution(USP)	Lambda max
1	17,716	697738	14299	100,000	-	-	205/282/655/569/397
Total		697738	14299	100,000			

Figure VII-65 : Isolated (1'$_a$R,2'$_a$S)-8 chiral HPLC; e.r. >99 : 1

3. Rotational barrier of (a*R*,a*S*,*S*)-3fM

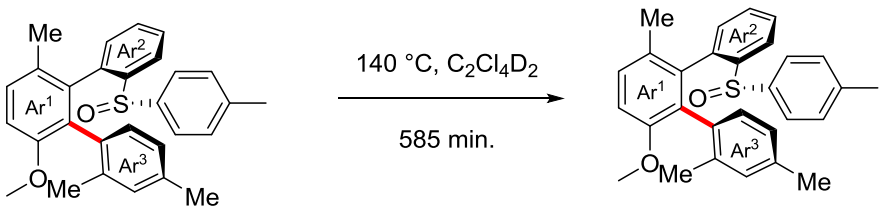

(a*R*,a*S*,*S*)-3fM
d.r >98:2

(a*R*,a*S*,*S*)-3fM
d.r. = 52:48

temp(min)	0	30	45	60	75	90	105	135	195	315	435	555	585
[A]	99	90	87	84	81	78	76	71	65	57	54	52	52
[B]	1	10	13	16	19	22	24	29	35	43	46	48	48
ln((Atx-Aeq/At0-Ae	0	-0.21256144	-0.29479954	-0.3844117	-0.48285177	-0.59205106	-0.672093771	-0.905708623	-1.285198244	-2.240709689	-3.157000421		

Figure VII-66 : evolution of the d.r. of 3fM at 140°C in $C_2Cl_4D_2$

reversible fisrt order								
kf+kb min-1	kf+kb s-1		Keq=					
0.00730	0.00012167		0.92					
			kf=	kb=		deltaG kf(J)	deltaG kf(kcal)	deltaG kb(J)	deltaG kb(kcal)
			0.0000584	6.32667E-05		1.3580E+05	3.25E+01	1.3552E+05	3.24E+01

Figure VII-67 : calculation of the rate of epimerization and the rotational barrier

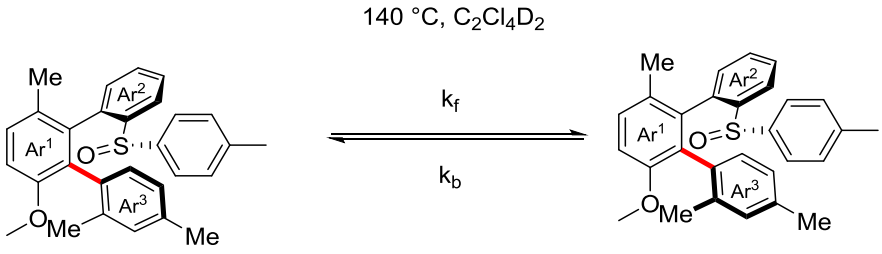

A = (a*R*,a*S*,*S*)-3fM

B = (a*R*,a*R*,*S*)-3fM

For Reversible first order kinetics, the rate law is ; $v = \frac{d[A]}{dt} = k_f[A] - k_b[B]$

And since $K_{eq} = \frac{k_f}{k_b} = \frac{[B]_{eq}}{[A]_{eq}} = \frac{[A]_0 - [A]_{eq}}{[A]_{eq}}$ and $K_{eq} = \frac{48}{52}$; it can be used to eliminate [B]

integration of the rate law gives $\ln(\frac{[A]-[A]_{eq}}{[A]_0-[A]_{eq}}) = -(k_f + k_b)t$

by plotting $\ln(\frac{[A]-[A]_{eq}}{[A]_0-[A]_{eq}})$ against t, a linear equation is obtained, with the slope = $(k_f + k_b)$.

Thus we have 2 equations with 3 unknowns;

Finally, insertion of (k_f) and (k_b) into the Eyring equation $\Delta G^{\ddagger} = RT \times \ln(\frac{k_B \cdot h}{k \cdot T})$ gives $\Delta G^{\ddagger}{}_{k_f}$ and $\Delta G^{\ddagger}{}_{k_b}$,

accordingly $\Delta G^{\ddagger}{}_{k_f} = 32.5\ kcal/mol$ and $\Delta G^{\ddagger}{}_{k_b} = 32.4\ kcal/mol$

4. Experiments on the arylation with simple control of axial chirality

a) Chiral HPLC optimization

The influence of various Pd sources, bases, silver salts and ligands on conversion, d.r. and e.r. was examined using the following procedure:

a. A Mixture of the substrate **1a**, and the 4 diastereomers of the product **3aA** (total concentration 0.1 mg/mL in 80 : 20 *n*-Hex/*i*-PrOH solution) was injected on a chiral HPLC column, to determine the retention time of each compound. *(conditions A: column AD-H; 1 mL/min; 20µL injected; 95 : 5 n-Hex/i-PrOH condiions B: column AD-H; 0.5 mL/min; 20µL injected; 95 : 5 n-Hex/i-PrOH)*
b. Reactions were conducted on 0.02 mmol scale in Wheaton 2 mL V-Vials under air, using stock solutions of the 1) substrate **1a** + *p*-iodoanisole + TFA and 2) $Pd(OAc)_2$ + Ligand, both in HFIP.
c. The required volume was transferred into the reaction vials containing all the insoluble reagents, and the vial were heated at 80 °C for 8 hours.
d. A qualitive screening by TLC against the product as reference was conducted after 8 hours at 80 °C, and the positive (i.e. reactions giving more than a trace of the expected product) reactions were then diluted with Et_2O, filtered on a silica gel plug, the volatiles were removed under reduced pressure and the crude mixture was dried under vacuum for at least 2 hours.
e. The crude mixture was diluted to reach a concentration of around 0.1 mg/mL in 80 : 20 *n*-Hex/*i*-PrOH solution, and was then injected on a chiral HPLC column, using the same conditions as in step a.
f. The results are summarized in the following table:

						en. Pair mino		en. Pair majo				
					Substrate	aR,R	aR,S	aS,R	aR,S			
Pd (10mol%)	L (20 mol%	base (2 eq.)	add 40 mol%	ret. time	50.82	56.49	58.43	127.93	180.2	conv.	d.r dia majo	e.r.dia majo
Pd(OAc)2	IPrHCl	Ag2CO3	TFA	254-A1	0.648	0.048	1.516	1.323	96.466	99%	98%	99%
Pd(OAc)2	IMeHCl	Ag2CO3	TFA	254-C1	0.073	0.818	2.389	1.117	95.602	100%	98%	99%

						en. Pair mino		en. Pair majo				
					Substrate	aR,R	aR,S	aS,R	aR,S			
Pd (10mol%)	L (20 mol%	base (2 eq.)	add 40 mol%	ret. time	25.96	30.75	31.82	67.63	94.15	conv.	d.r dia majo	e.r.dia majo
Pd(OAc)2	IMeHCl	K2CO3	TFA	254-C2	62.076	1.093	1.821	1.456	33.553	38%	95%	96%
Pd(OAc)2	IPrHCl	Ag2O	TFA	256-A1	71.659	0.595	0.025	0.059	27.663	28%	100%	100%
Pd(OAc)2	IMeHCl	Ag2O	TFA	256-A2	98.178	0.467	0.08	0.008	1.267	2%	94%	99%
Pd(OAc)2	IPrHCl	Ag2CO3	TFA	257-a1	0.456	0.152	1.558	0.206	94.135	100%	98%	100%
Pd(OAc)2	IMeHCl	Ag2CO3	TFA	257-a2	0.269	0.262	1.193	0.232	98.043	100%	99%	100%
Pd(OAc)2	IPrHCl	K2CO3	AgTFA	259-a2	87.182	0.125	0.388	0.694	11.612	13%	97%	94%
Pd(OAc)2	IPrHCl	NaHCO3	AgTFA	259-c	90.553	0.062	0.264	2.443	6.978	10%	96%	74%
[Pd(IMe)Cl]2 *	IPrHCl	Ag2CO3	TFA	261-1	31.767	0.45	0.677	0	67.106	68%	99%	100%
[Pd(IMe)Cl]2 *	IPrHCl	Ag2CO3	PivOH	261-2	77.573	0.541	0.36	0.171	21.355	22%	98%	99%
[Pd(IMe)Cl]2 *	IPrHCl	Ag2CO3	/	261-3	95.3	0.612	0.103	0.036	3.95	5%	97%	99%

Figure VII-68 : optimization of 1a arylation on product 3aA; * *: 5 mol%***

g. Conclusions :

-Nature of a ligand, ie. IPrHCl vs. IMeHCl has no effect on the conversion, d.r. or e.r. (entries 254-A1 vs. 254-C1 and 257-a1 vs. 257 a2), IPrHCl was chosen to conduct the scope for two reasons: readily commercial availability, and easier to crystallize.

-A strong, silver base (either Ag_2CO_3, or Ag_2O) is necessary to achieve e.r. >98 : 2 (entries 254-C2, 259-a2, 259-c show erosion of e.r.)

(1) Experiments with well-defined Pd-NHC pre-catalyst :

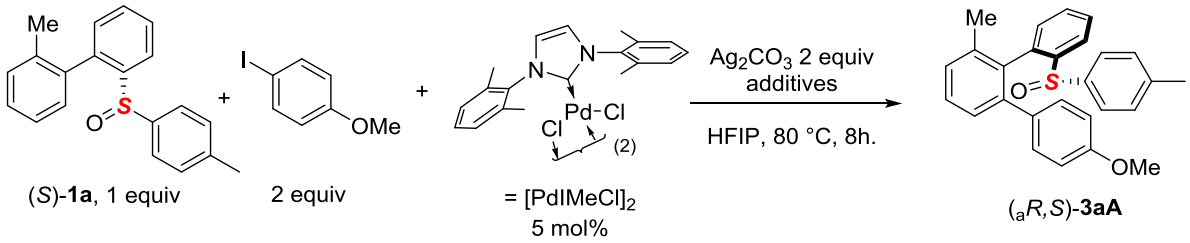

FigureVII-69 : experiments with well-defined Pd-NHC pre-catalysts

entry	additive 1	additive 2	Conversion[a]
1	IMeHCl 10 mol%	TFA 40 mol%	79%
2	IMeHCl 10 mol%	PivOH 40 mol%	33%
3	IMeHCl 10 mol%	-	23%
4	TFA 40 mol %	-	7%

Yield determined by integration of the ^1H NMR of the crude reaction mixture

(2) Reversibility of arylation in non-anhydrous conditions

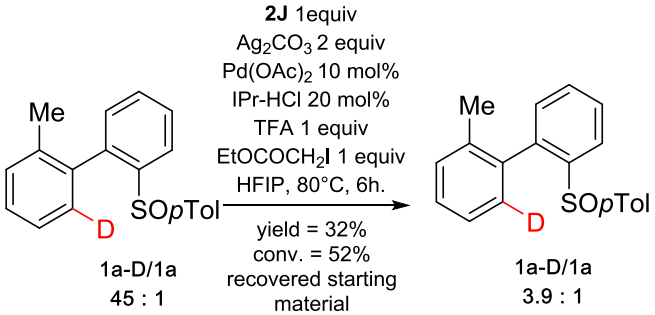

FigureVII-70 : reversibility of arylation of 1a in non-anhydrous conditions

The same procedure was followed or substrate **1f/1f-D**

(3) Role of ethyl iodoacetate in the direct arylation

After the reaction optimization, using **1**a as the substrate and **2A** (*p*-iodoanisole) as the coupling partner, and when switching to less electron-rich iodoarenes (**2B, 2C, 2D)** low yields were observed (c.a. 33%) even after extended reaction times. Our initial hypothesis was that an impurity present in commercial **2A** was catalyzing the reaction. Thus commercial **2A** was then purified by flash chromatography and also synthesize from *p*-iodophenol : however both reactions, using purified and freshly prepared **2A**, went to completion, ruling out the initial hypothesis. Then, we turned our attention to the quality of silver carbonate: a fresh batch was exposed for 48 hours to 1) light 2) air 3) light and air; no effect on the reaction yield was observed.

Finally, the possibility that, when using less electron-rich iodoarenes, the reaction was slower resulting in a faster deactivation of Pd^{II} to Pd^{0} through aggregation/cluster formation and finally Pd black precipitation was considered. Accordingly, a range of organic additives were tested as oxidant to avoid the deactivation of the catalyst and it was found that the most effective was ethyl iodoacetate.

To support this hypothesis the following control experiment was conducted: from a Pd^{0} pre-catalyst, and otherwise under the standard reaction conditions, addition to one reaction of ethyl iodoacetate allowed product formation, whereas the "oxidant-free" reaction did not yield anything more than a trace of the product.

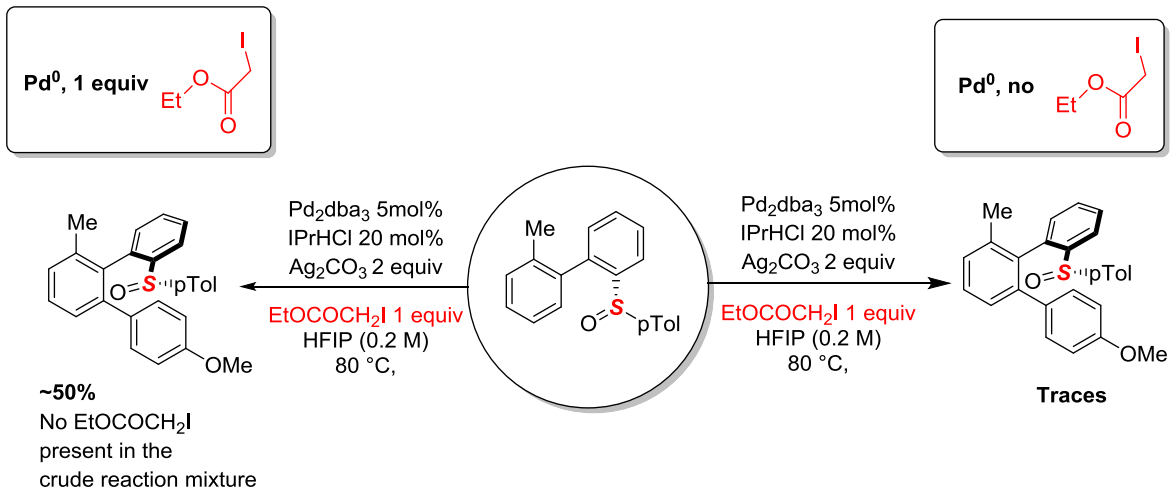

FigureVII-71 : experiments on the role of ethyl iodoacetate

5. Experiments on the arylation with double control of axial chirality

a) Mechanistic experiments

It should be noted that the ^{1}H NMR spectra of the substrate **1e** consist of a 1 : 1 mixture of two atropisomers (quick equilibrium at 25 °C) : therefore, in the following experiments, the ($C^{6'}$) -H integration was counted for half of the total **1e** integration (when present as a mixture of **1e** /**1e-d$^{6'}$)**

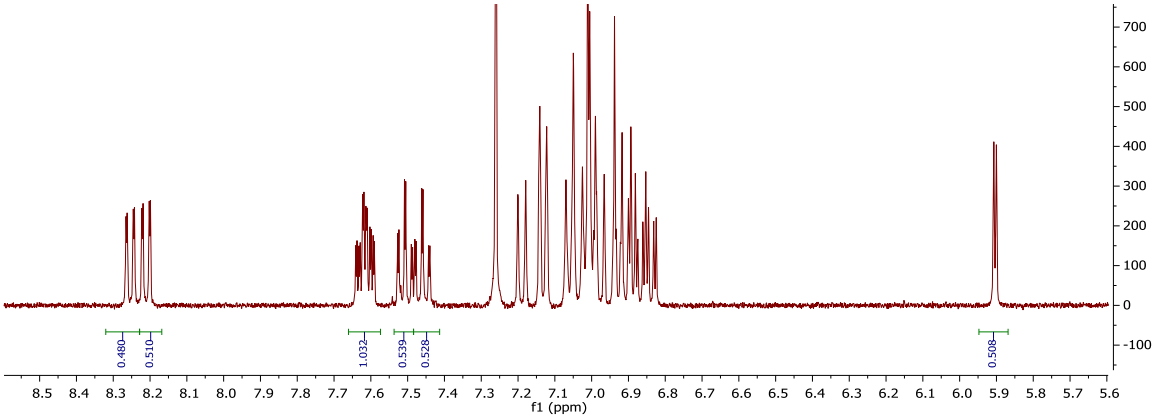

Figure VII-72 : identification of 1a characteristic signals

(1) Reversibility of arylation in anhydrous conditions

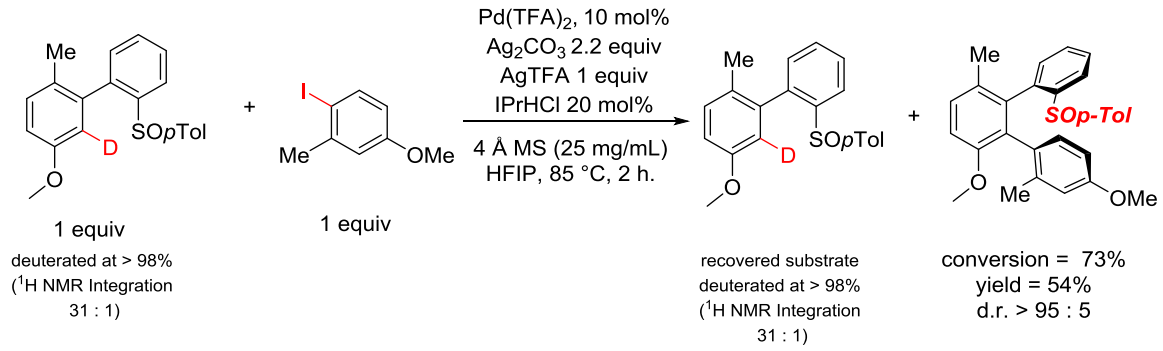

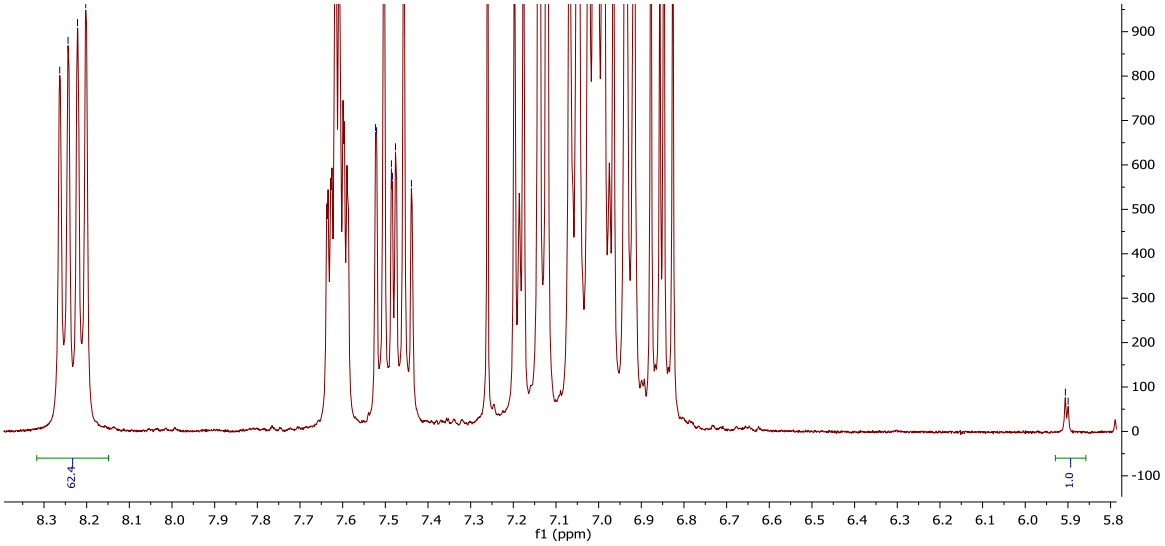

After the reaction (crude mixture after silica gel plug filtration)

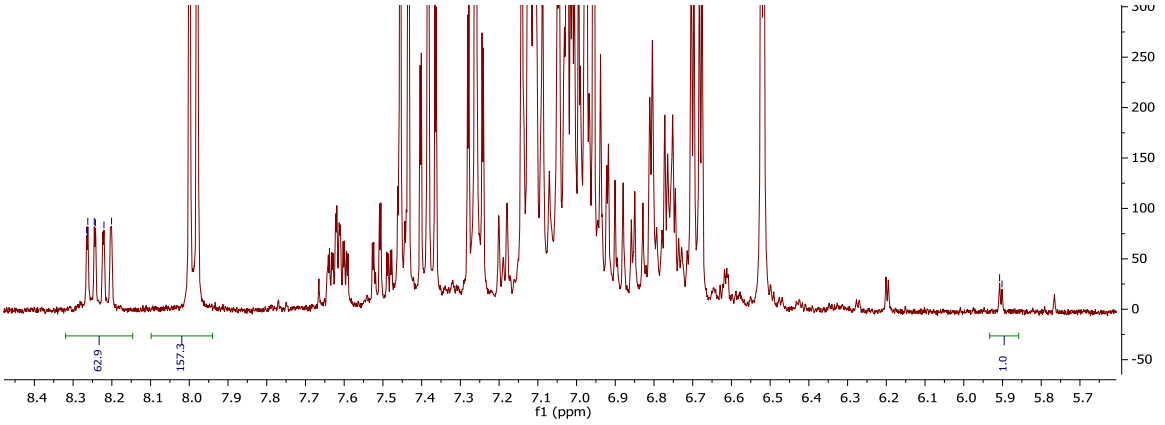

Figure VII-73 : revrsibility of 1f arylation in anhydrous conditions

the same procedure was followed for **1a**

(2) Kinetic Isotope Effect (KIE)

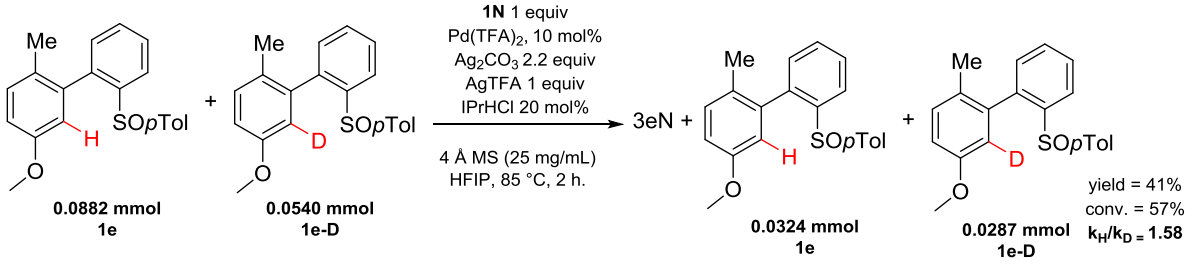

FigureVII-74 : KIE of arylation of 1e into 3eN

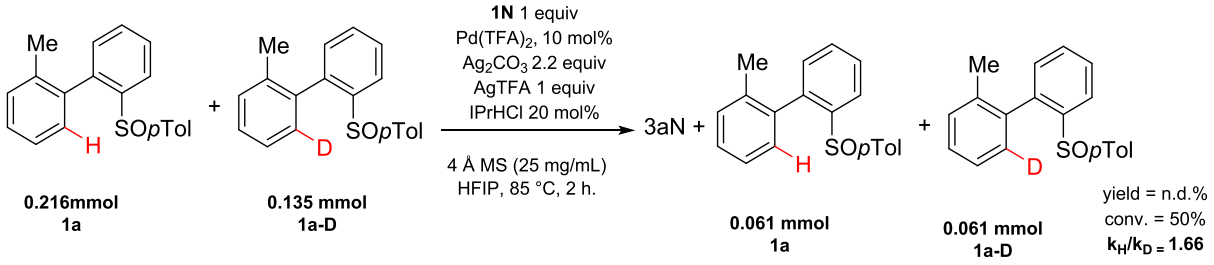

Figure VII-75 : KIE of arylation of 1a into 3aN

(3) Atropisomery of **7** = [IMe(**1a**)PdCl]

Isolation of this putative intermediate in the catalytic cycle allowed us to explore :

- When does the axial chirality of tha Ar^1-Ar^2 axis is set
- The role of silver salts on the oxidative addition/reductive elimination part of the catalytic cycle

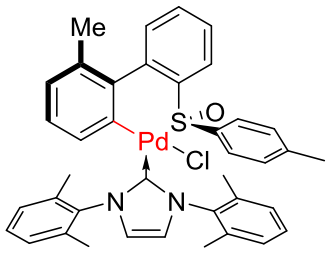

[(IMe)(($_a$*R*,*S*)-(**1a**))Cl]Pd

X-Ray analysis showed that the title compound is enantiomerically pure. Furthermore, as the ^{1}H spectra of the mono-crystal and the solid isolated after chromatography are identical, and because no diastereoenrichment occurred during the purification by silica gel column, it can be reasonable assumed that the palladacycle is formed in atropoisomerically pure form, with ($_a$*R*) configuration. However, as the enantiopure crystals were afforded in 44% yield, it cannot be ex-

cluded that in solution both atropisomers of the palladacycle are present. To exclude this possibility, a low temperature ^{1}H NMR spectra of the palladacycle was taken at -70 °C : if two atropisomers are indeed in fast equilibrium at room temperature, at low temperature the rotation around the Ar^{1}-Ar^{2} axis should be slower leading to a modification of the ^{1}H NMR spectra (presence of a set of two signals, one for each atropisomer or broadening of the existing signals). However, none of these effects was observed. Consequently, it can be assumed that [(IMe)((a*R*,*S*)-(1a))Cl]Pd is configurationally stable and exists only in one axially chiral configuration. Accordingly, as the starting material **1a** is not atropisomerically stable at 25 °C, the formation of this palladacycle increases the rotational barrier about the chiral axis.

Furthermore, we attempted to atropisomerize the chiral axis by heating [(IMe)((a*R*,*S*)-(1a))Cl]Pd in $C_2D_2Cl_4$ up to 85 °C, but decomposition happened before isomerization could be detected by ^{1}H NMR.

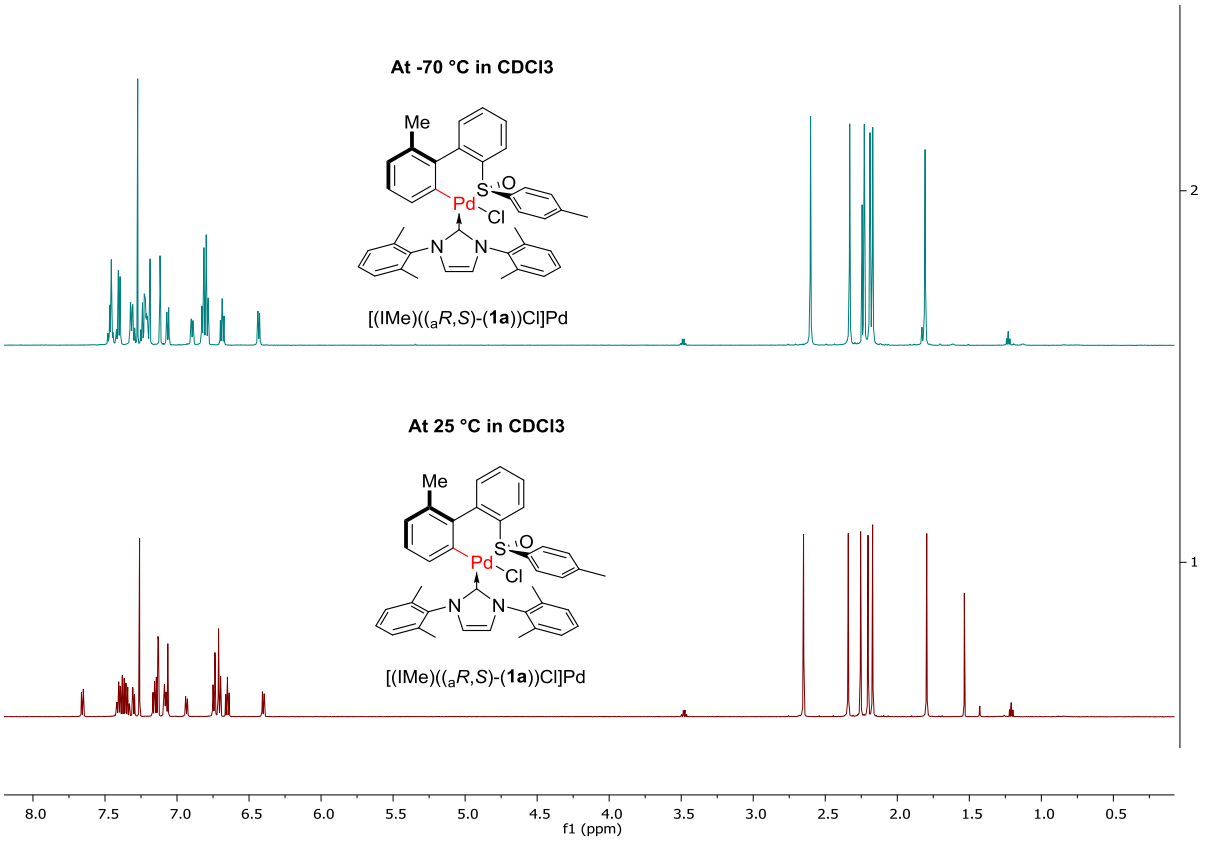

(4) Stoichiometric reactions from **7** = [IMe(**1a**)PdCl]

Under air, sealed and oven-dried tubes were loaded with the title compound (1 equiv, c.a. 0.015 mmol scale), *p*-iodoanisole (2 equiv), and some additives; then HFIP (c.a. 500 µL, 0.033 M) was added. The reaction mixture was stirred at room temperature for 5 min, and the light yellow clear solution was heated at 85 °C for 1 hour. The reactions were diluted with Et_2O and filtrated over a small silica gel plug. The volatiles were removed under reduced pressure and a ^1H NMR spectra was recorded, using CH_2Br_2 as an internal standard.

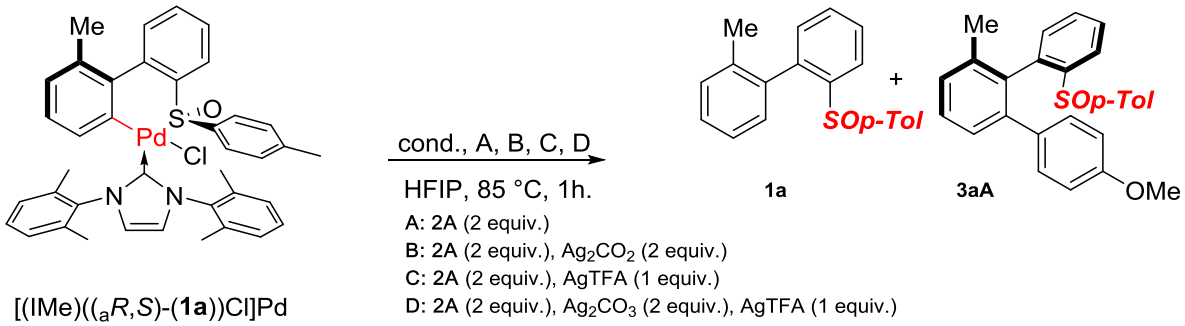

[(IMe)((aR,S)-(**1a**))Cl]Pd

cond.	A	B	C	D
conv.	>95%	>95%	>95%	>95%
1a	23	17	72	/
3aA	13	32	24	95%
d.r. 3aA	>95 : 5	n.d.	>95 : 5	>95 : 5
8.46	/	0.34	0.01	0.02
8.35	0.93	/	/	/
7.95	/	0.37	0.05	0.04
7.84	0.89	/	/	/

unkown by-products : δ (ppm) ratio /3aA

Figure VII-76 : stoichiometric experiments on the pallacacycle 7

(5) Attempt to form the palladacyle from substrate 1f

We did not succeed in forming or isolating the palladacycle 12-1f either by applying the standard protocol at 25 °C for 16 hours or at 85 °C for 16 hours (step 1).

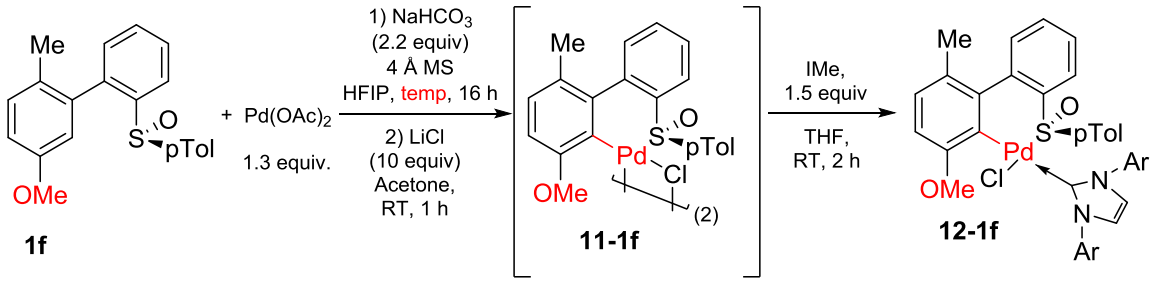

figureVII-77: attempt of isolation of 1f palladacycle in standard conditions

Furthermore, submission of **1f** to the standard reaction condition described in **GP2**, albeit without any aryl iodide, followed by ligand exchange towards the more stable chloride-bridge palladacyle **11-1f**, did not yield any isolable palladated product.

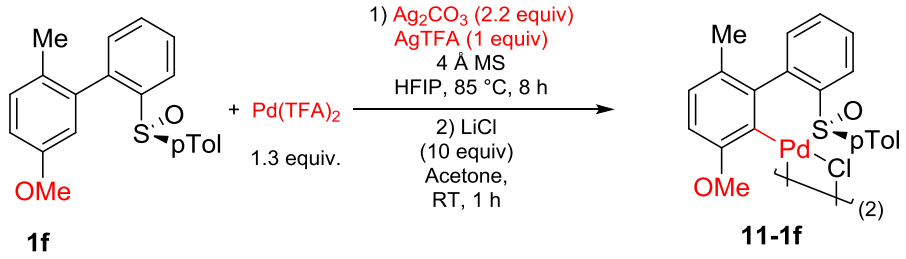

Figure VII-78 : attempt of isolation of 1f palladacycle in reaction conditions

b) Optimization experiments

(1) On the amount of molecular sieves

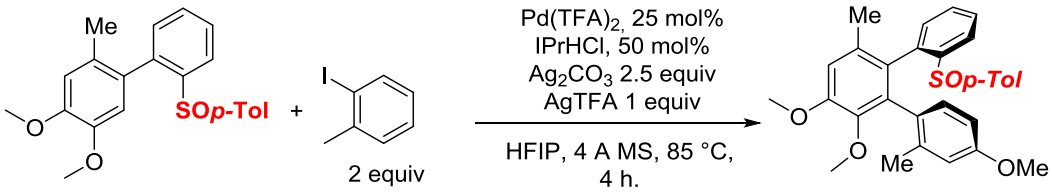

entry	powdered 4 Å MS (mg/mL)	Substrate[a]	Product[a]
a	0	6.83	1
b	25	0.71	1
c	75	2.36	1

a : ^{1}H NMR relative integration on the crude reaction mixture

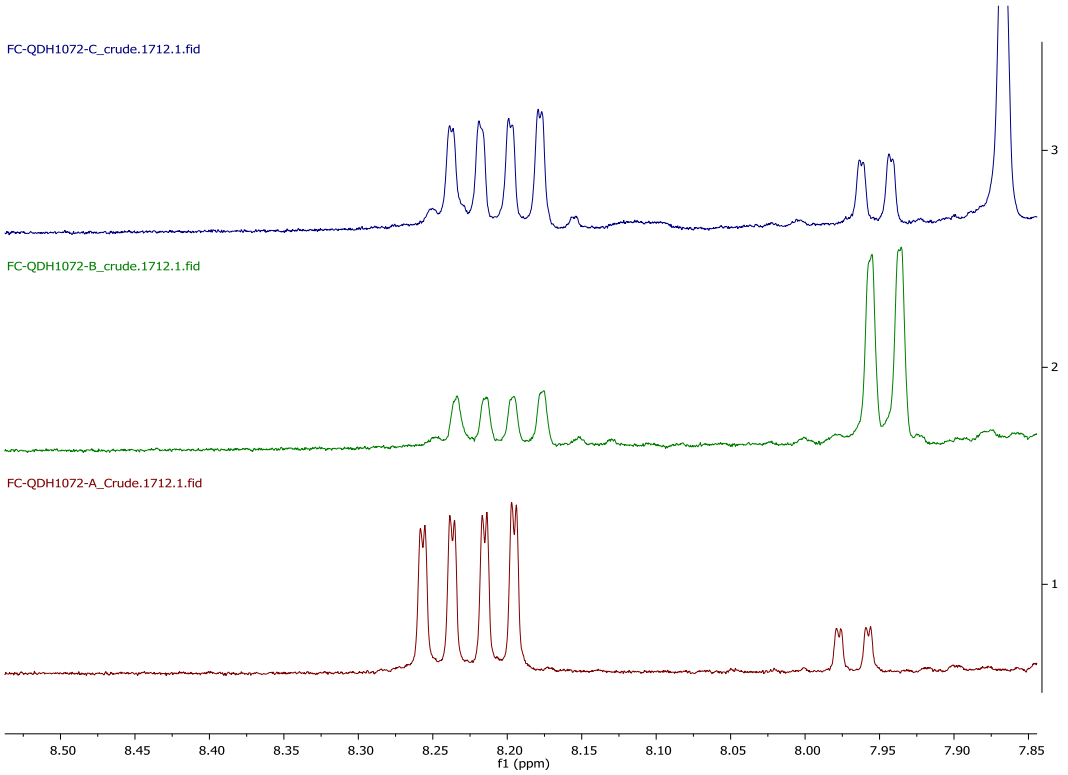

Figure VII-79 : optimization of the amount of MS o product 3eN

Furthermore, and as a representative example, the effect of MS on the yield and conversion of product **3fO** is given bellow:

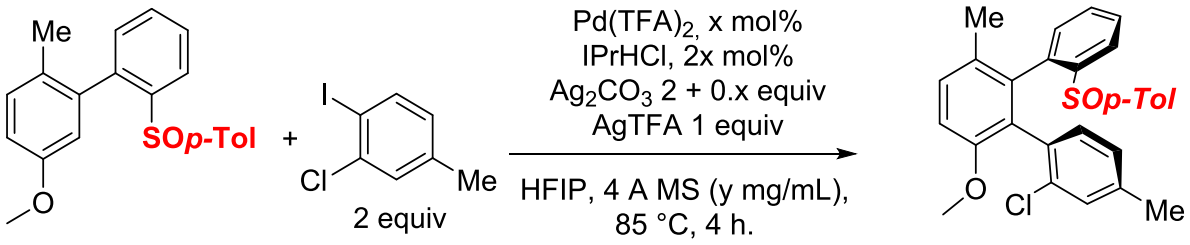

entry	X =	Y =	conversion[a]	Yield[a]
1	20	75	>95%	39%
2	10	75	low	<5%
3	10	25	70%	40%
4	20	25	>95%	70%

a : ^{1}H NMR with CH_2Br_2 as internal standard

Figure VII-80 : optimization of the amount of MS on product 3fO

(2) Control experiments

In order to probe the reaction variables and to gain some better understanding of the reaction, control experiments were carried out on a 0.06 to 0.12 mmol scale using the set of standard conditions described hereafter : the amount of $Pd(TFA)_2$ add to be lowered to 15 mol% in order to be able to prepare stock solutions in HFIP. The crude mixture were worked-up as described in **GP2** and analyzed by ^1H NMR.

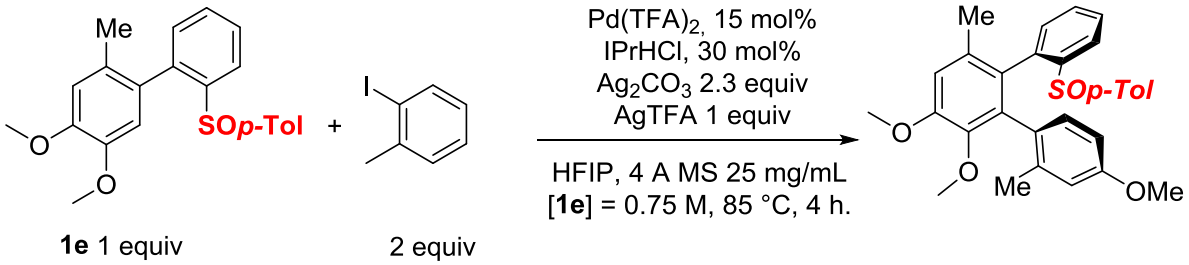

1e 1 equiv 2 equiv

crude analyzed by proton NMR using CH_2Br_2 as internal standard							
entry	***Deviation from standard conditions***		*Substrate*[a]	*Product*[a]	*Dia A*[b]	*Dia2 B*[b]	*Dia C+D*[b]
1	**No deviation**		47	33	28.1	1.6	1
2	EtOAcBr 2eq	AgTFA 3.5 eq	42	13	62.4	3.6	1
3	0.2M		53	22	32.1	2.8	1
4	Ag_2CO_3 3.3 eq		33	13	25.4	1	0
5	Ag_2CO_3 1.3 eq		36	9	31.5	5.6	1
6	Ag_2CO_3 0 eq		>95	0			
7	IPrHCl 10%		17	18	22.4	1.8	1
8	IPrHCl 0%		41	19	12.8	2.2	1
9	IPrHCl 0%		24	22	8.8	1.3	1
10	IPrHCl 0%	16 hours	5	10	n.d. (by-products)		
11	IPrAgCl		92	traces			
12	4AMS 250mg/mL	16 hours	8	5	n.d. (by-products)		
13	Pd(OAC)2 15%		13	4	100	1	1

Figure VII-81 : control experiments on product 3eN ; ***Eq. = equivalent; a: given as percentage; b : given as ratio of A : B : C+D***

From these experiments, one can make the following observations:

- With the reduced amount of MS (25 mg/mL), addition of $EtOCOCH_2Br$ and a large amount of AgTFA are detrimental (entry 2), as well as a more concentrated reaction mixture (entry 3)
- Ag_2CO_3 is absolutely necessary for the reaction (entry 6)
- IPrHCl, on the other hand, is not necessary in order to form some product, but its presence permits : 1) a better d.r. (entries 8 and 9); 2) limits the amount of decomposition (entry 10, after extended reaction time)

- Use of a carbene transfer reagent IPrAgCl leads to almost full inhibition of the reaction (entry 11).
- A very large amount of MS for an extended time allows to achieve a very good conversion, but not to the desired product: mostly decomposition (entry 12).
- Finally, $Pd(OAc)_2$ is inefficient in these conditions.

(3) Qualitative solvent screening:

1 : 1 mixtures of HFIP with several other solvent were tested : A reference reaction in pure HFIP was run using the same stock solutions of reagents than for the reaction using a co-solvent. The reactions were analyzed first by TLC and LC-MS against the reference reaction in pure HFIP, but no positive hits (i.e. reactions with results comparable to the reference reaction) were found.

co-solvent added as 1 : 1 HFIP mixture	Results : hit or no hit
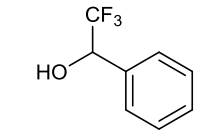	no reaction - Pd Black
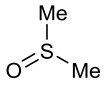	less 5% yield
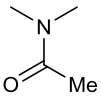	less 5% yield
	less 5% yield
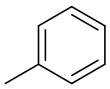	less 5% yield
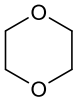	less 5% yield
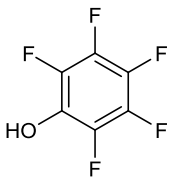	less 5% yield

Figure VII-82 : qualitative solvent screening

E. References

[351] M. Livendahl, A. M. Echavarren, *Isr. J. Chem.* **2010**, *50*, 630–651.
[352] L.-C. Campeau, M. Parisien, A. Jean, K. Fagnou, *J. Am. Chem. Soc.* **2006**, *128*, 581–590.
[353] D. García-Cuadrado, P. de Mendoza, A. A. C. Braga, F. Maseras, A. M. Echavarren, *J. Am. Chem. Soc.* **2007**, *129*, 6880–6886.
[354] D. García-Cuadrado, A. A. C. Braga, F. Maseras, A. M. Echavarren, *J. Am. Chem. Soc.* **2006**, *128*, 1066–1067.
[355] M. Lafrance, C. N. Rowley, T. K. Woo, K. Fagnou, *J. Am. Chem. Soc.* **2006**, *128*, 8754–8756.
[356] M. Lafrance, K. Fagnou, *J. Am. Chem. Soc.* **2006**, *128*, 16496–16497.
[357] D. L. Davies, S. M. A. Donald, O. Al-Duaij, S. A. Macgregor, M. Pölleth, *J. Am. Chem. Soc.* **2006**, *128*, 4210–4211.
[358] L. Ackermann, *Chem. Rev.* **2011**, *111*, 1315–1345.
[359] S. J. Tremont, H. U. Rahman, *J. Am. Chem. Soc.* **1984**, *106*, 5759–5760.
[360] O. Daugulis, V. G. Zaitsev, *Angew. Chem. Int. Ed.* **2005**, *44*, 4046–4048.
[361] A. Lazareva, O. Daugulis, *Org. Lett.* **2006**, *8*, 5211–5213.
[362] O. Daugulis, H.-Q. Do, D. Shabashov, *Acc. Chem. Res.* **2009**, *42*, 1074–1086.
[363] D. Shabashov, O. Daugulis, *Org. Lett.* **2006**, *8*, 4947–4949.
[364] H. A. Chiong, Q.-N. Pham, O. Daugulis, *J. Am. Chem. Soc.* **2007**, *129*, 9879–9884.
[365] V. G. Zaitsev, D. Shabashov, O. Daugulis, *J. Am. Chem. Soc.* **2005**, *127*, 13154–13155.
[366] D. Shabashov, O. Daugulis, *Org. Lett.* **2005**, *7*, 3657–3659.
[367] V. S. Thirunavukkarasu, K. Parthasarathy, C.-H. Cheng, *Angew. Chem. Int. Ed.* **2008**, *47*, 9462–9465.
[368] X.-H. Liu, H. Park, J.-H. Hu, Y. Hu, Q.-L. Zhang, B.-L. Wang, B. Sun, K.-S. Yeung, F.-L. Zhang, J.-Q. Yu, *J. Am. Chem. Soc.* **2017**, *139*, 888–896.
[369] T. Satoh, Y. Kawamura, M. Miura, M. Nomura, *Angew. Chem. Int. Ed. Engl.* **1997**, *36*, 1740–1742.
[370] A. Ros, B. Estepa, P. Ramírez-López, E. Álvarez, R. Fernández, J. M. Lassaletta, *J. Am. Chem. Soc.* **2013**, *135*, 15730–15733.
[371] T. Shibata, T. Fujimoto, K. Yokota, K. Takagi, *J. Am. Chem. Soc.* **2004**, *126*, 8382–8383.
[372] T. Shibata, K. Tsuchikama, *Chem. Commun.* **2005**, *0*, 6017–6019.
[373] K. Tanaka, T. Suda, K. Noguchi, M. Hirano, *J. Org. Chem.* **2007**, *72*, 2243–2246.
[374] T. Shibata, K. Tsuchikama, M. Otsuka, *Tetrahedron Asymmetry* **2006**, *17*, 614–619.
[375] D. Lotter, M. Neuburger, M. Rickhaus, D. Häussinger, C. Sparr, *Angew. Chem. Int. Ed.* **2016**, *55*, 2920–2923.
[376] K. Yamaguchi, J. Yamaguchi, A. Studer, K. Itami, *Chem. Sci.* **2012**, *3*, 2165.
[377] J. Oppenheimer, R. P. Hsung, R. Figueroa, W. L. Johnson, *Org. Lett.* **2007**, *9*, 3969–3972.
[378] T. Suda, K. Noguchi, M. Hirano, K. Tanaka, *Chem. – Eur. J.* **2008**, *14*, 6593–6596.

[379] S. Ye, W. Yang, T. Coon, D. Fanning, T. Neubert, D. Stamos, J.-Q. Yu, *Chem. – Eur. J.* **2016**, *22*, 4748–4752.
[380] A. S. McCall, H. Wang, J. M. Desper, S. Kraft, *J. Am. Chem. Soc.* **2011**, *133*, 1832–1848.
[381] P. L. Arnold, M. S. Sanford, S. M. Pearson, *J. Am. Chem. Soc.* **2009**, *131*, 13912–13913.
[382] D. Munz, T. Strassner, *Angew. Chem. Int. Ed.* **2014**, *53*, 2485–2488.
[383] P. W. Dyer, P. J. Dyson, S. L. James, C. M. Martin, P. Suman, *Organometallics* **1998**, *17*, 4344–4346.
[384] L. Hintermann, *Beilstein J. Org. Chem.* **2007**, *3*, 22.

General Experimental part

VIII. General Experimental part

A. General consideration

Unless otherwise noted, all reagents were purchased from commercial suppliers (Sigma-Aldrich, Acros, Alfa Aesar, Fluorochem, TCI) and were used without further purification.

Anhydrous solvents term denotes solvents dried over molecular Sieves (to the fresh commercial solvent bottle were added 3 or 4 angstrom MS in beads form, followed by static drying for at least 48 hours before use), kept under Argon and handle using the standard Schlenk techniques:

- Tetrahydrofuran (THF) was dried using 10% (m/v) 3 or 4 Å MS
- Diethylether was dried using 10% (m/v) 3 or 4 Å MS
- Dichloromethane and Toluene were purchased from Aldrich (Sure/Seal packaging, kept over 3 Å molecular sieves).
- HFIP was purchased from Fluorochem and dried sequentially 2 times over 3 Å MS (each time 20% (m/v), static drying for 72 hours). Molecular sieves were activated by heating at ~300 °C under vacuum overnight.

Organolithium reagents were titrated using the no-D NMR procedure[385].

Flash chromatography refers to column chromatography using silica gel (Merck 60, 40-63 µm size), driven by pressurized air and according to the guidelines of Still[386].

Thin layer chromatography (TLC): was carried out using Merck Kieselgel 60 F_{254} silica gel plates.

NMR : recorded on Brücker Avance 500, 400 or 300, the FID was treated with MestRec Nova, TopSpin. The chemical shift (δ) is given relative to the residual signal of the solvent ($CHCl_3$: δ (^1H) = 7.26 ppm; δ (^{13}C) = 77.16 ppm. CD_3CN: δ (^1H) = 1.94 ppm; δ (^{13}C) = 1.32 ppm), or relative to an external standard ($CFCl_3$: δ (^{19}F) = 0 ppm; H_3PO_4 (85%) = 0 ppm). Broad = Br, singulet = s, doublet = d, triplet = t, quadruplet = q, multiplet = m.

Specific description of signals: 7.06-7.03 (***AA'***BB', 2H) refers to an AA'BB' spin system using Pople notation[387], where the AA' multiplet part covers from 7.06 to 7.03 ppm and integrates for 2 protons.

Mixture of atropisomer on the NMR time scale: compounds that are not considered atropisomeric, in the sense that each atropisomer can be isolated, might exhibit atropisomeric feature on the NMR time scale. Indeed, if two atropodiastereoisomers are possible by symmetry consideration, each can give well-defined and resolved spectra. This is dependent on the rate of interconversion between the two atropodiastereoisomers, the chemical shift difference between the signals, and the temperature.

Quantitative NMR : CH_2Br_2 was used as an internal standard; stock solutions of 50 µL of CH_2Br_2 in $CDCl_3$ were prepared in a 5 mL volumetric flask. Known amounts of the resulting solution were added to a $CDCl_3$ solution of all the crude reaction mixture (or product) to be analyzed and ^1H NMR was spectra were recorded.

HRMS measurements were performed by Service de Spectrométrie de Masse de L'institut de Chimie at the University of Strasbourg.

Elemental Analysis measurements were performed by the Analytical, Physical Measurements and Optical Spectroscopy Service of the University of Strasbourg.

X-Ray analysis and structure determination were performed at the Service of radiocrystallography of the University of Strasbourg, and the structures were resolved by Dr. Lydia BRELOT and Corinne BAILLY.

B. Biaryls synthesis

Retrosynthetic scheme :

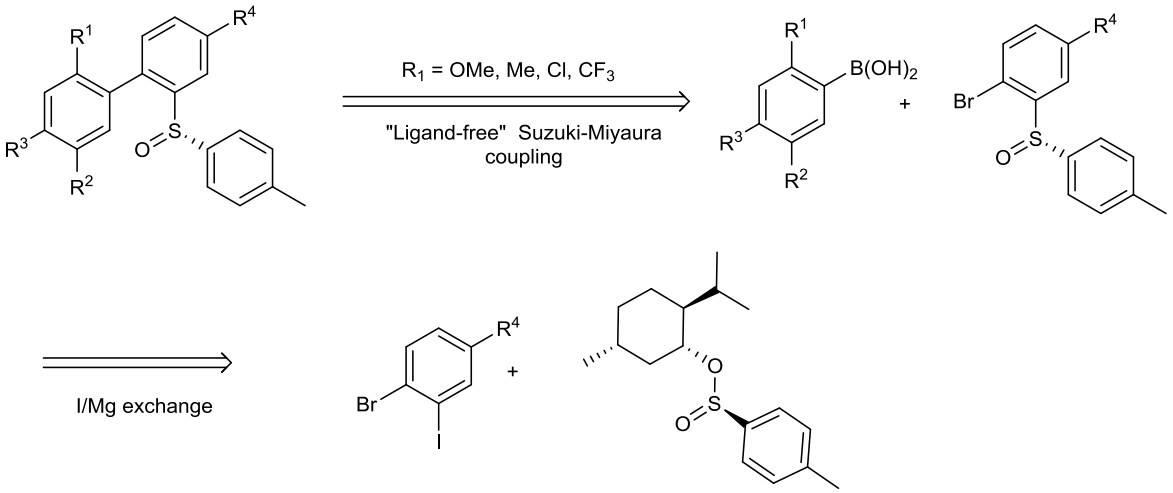

Figure VIII-1 : retrosynthetic scheme

1. Biaryl precursors

(-)-Menthyl-(*S*)-*p*-toluenesulfinate[388] :

^{1}H-NMR (400 MHz, $CDCl_3$) : δ = 7.60 (d, *J* = 8.0 Hz, 2 H), 7.32 (d, *J* = 8.0 Hz, 2 H), 4.12 (td, *J* = 10.7, 4.5 Hz, 1 H), 2.41 (s, 3 H), 2.33–2.23 (m, 1 H), 2.19–2.07 (m, 1 H), 1.74–1.62 (m, 2 H), 1.56–1.46 (m, 1 H), 1.40–1.30 (m, 1 H), 1.29–1.14 (m, 1 H), 1.12–0.98 (m, 1 H), 0.96 (d, *J* = 6.5 Hz, 3 H), 0.91-0.89 (m, 1H), 0.86 (d, *J* = 7.1 Hz, 3 H), 0.72 (d, *J* = 6.9 Hz, 3 H) ppm.
^{13}C-NMR (101 MHz, $CDCl_3$): δ = 143.2, 142.3, 129.5 (2 $C_{p\text{Tol}}$), 124.9 (2 $C_{p\text{Tol}}$), 80.0, 47.8, 42.9, 34.0, 31.7, 25.2, 23.1, 22.0, 21.4, 20.8, 15.4 ppm.
R_f (EtOAc/*c*-Hex 1:3) = 0.55.
IR (ATR): $\tilde{\nu}$ /cm^{-1} = 2948 (m), 2920 (m), 2865 (w), 1595 (w), 1492 (w), 1455 (m), 1388 (w), 1131 (s), 1079 (m), 951 (s), 915 (s), 852 (s), 820 (s), 777 (s), 756 (s).
$[\alpha]_D^{20}$ = –201 (c = 1, acetone).

a) General procedure for enantiopure bromosulfoxides precursors:

the bromoiodobenzene (1 equiv) was dissolved in anhydrous THF (1M) and cooled down to 0 °C. A solution of *i*-PrMgCl (2M in THF) was added dropwise and the resulting mixture stirred for 1 hour. It was then cannulated on a solution of (-)-(1*R*,2*S*,5*R*)-menthyl (*S*)-*p*-toluenesulfinate (1 equiv, 0.25M in anhydrous THF) at -40 °C. The reaction was then allowed to come back to 0°C over 2-3 hours when it was diluted with Et_2O and quenched by a sat.sol. of NH_4Cl. The phases were separated, the aqueous phase extracted once with Et_2O and the combined organic phases dried over Na_2SO_4. The solvent was removed under reduced pressure and the crude product was purified by crystallization as stated below.

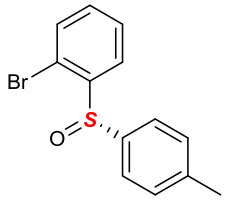

(*S*)-1-bromo-2-(*p*-tolylsulfinyl)benzene
Chemical Formula: $C_{13}H_{11}BrOS$
Molecular Weight: 295,1940

(*S*)-1-bromo-2-(*p*-tolylsulfinyl)benzene : Large scale : prepared from 2-bromoiodobenzene (1 eq., 20 g, 9.08 mL, 70.7 mmol) in THF (40 mL) and (-)-menthyl (*S*)-*p*-toluenesulfinate (1 eq., 20.8 g, 70.7 mmol) in THF (200 mL). The crude oily product was quickly dissolved in 100 mL of Et_2O and allowed to crystallize at 4-6 °C for several hours. The crystals were collected and washed with n-pentane. The mother liquor was concentrated and again dissolved Et_2O to afford a second batch of equal purity (^{1}H NMR), yielding a total of (*S*)-1-bromo-4-methyl-2-(*p*-tolylsulfinyl)benzene as colorless crystals (18.06 g, 61.2 mmol, 87%).
^{1}H-NMR (400 MHz, $CDCl_3$) : δ = 8.06 (dd, *J* = 7.8, 1.6 Hz, 1 H), 7.63 (d, *J* = 8.2 Hz, 2 H), 7.56 (ddd, *J* = 7.8, 7.4, 1.0 Hz, 1 H), 7.51 (dd, *J* = 8.0, 1.0 Hz, 1 H), 7.32 (ddd, *J* = 8.0, 7.4, 1.6 Hz, 1 H), 7.24 (d, *J* = 8.2 Hz, 2 H), 2.36 (s, 3 H) ppm.
^{13}C-NMR (101 MHz, $CDCl_3$) : δ = 145.1, 142.1, 141.3, 133.1, 132.2, 130.0 (2 $C_{p\text{Tol}}$), 128.5, 126.4 (2 $C_{p\text{Tol}}$), 126.3, 120.0, 21.5 ppm.
R_f (EtOAc/*c*-Hex 1:2) = 0.42.
$[\alpha]_D^{20}$ = –159 (c = 1, $CHCl_3$).
Chiral HPLC e.r. > 99 % [OD-H column, *n*-Hex/*i*-PrOH 80:20, 0.5 mL/min, (*R*) r_t = 13.49 min, (*S*) r_t = 16.01 min].

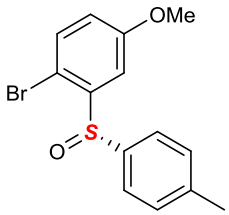

(*S*)-1-bromo-4-methoxy-2-(*p*-tolylsulfinyl)benzene
Chemical Formula: $C_{14}H_{13}BrO_2S$
Molecular Weight: 325,2200

(*S*)-1-bromo-4-methoxy-2-(*p*-tolylsulfinyl)benzene: Prepared from 1-bromo-2-iodo-4-methoxybenzene (1 eq., 1 g, 3.37 mmol) and (-)-menthyl (*S*)-*p*-toluenesulfinate (0.999 eq., 0.991 g, 3.37 mmol). The crude product was obtained as a greenish oil that was quickly dissolved in Et_2O (~10 mL for 1 g of expected product) and allowed to crystallized at 4-6 °C overnight. The crystals were filtrated and washed with *n*-pentane affording (S)-1-bromo-4-methoxy-2-(p-tolylsulfinyl)benzene (633 mg, 1.95 mmol, 61%) as light orange crystals.

^{1}**H-NMR** ($CDCl_3$, 400 MHz) : δ = 7.66 – 7.59 (***AA'***BB', 2H), 7.61 (d, J = 3.1 Hz, 1H), 7.37 (d, J = 8.7 Hz, 1H), 7.25 (AA'***BB***', 2H), 6.86 (dd, J = 8.7, 3.1 Hz, 1H), 3.88 (s, 3H), 2.36 (s, 3H) ppm.

^{13}C-NMR (101 MHz, $CDCl_3$) : δ = 160.04, 145.64, 142.11, 141.08, 133.83, 129.88 (2C), 126.41 (2C), 119.25, 110.22, 109.69, 55.85, 21.42 ppm.

$[\alpha]_D^{20}$ = +9.6° (c = 0.54, $CHCl_3$).

EA : cald for $C_{14}H_{13}BrOS$ C = 51.70 H = 4.03; found C = 51.68, H = 4.12.

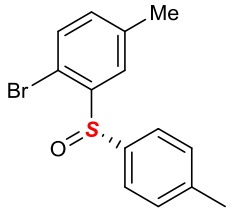

(*S*)-1-bromo-4-methyl-2-(*p*-tolylsulfinyl)benzene
Chemical Formula: $C_{14}H_{13}BrOS$
Molecular Weight: 309,2210

(*S*)-1-bromo-4-methyl-2-(*p*-tolylsulfinyl)benzene : Prepared from 1-bromo-2-iodo-4-methylbenzene (1 eq., 1 g, 3.37 mmol) and (-)-menthyl (*S*)-p-toluenesulfinate (0.999 eq., 0.991 g, 3.37 mmol). The crude product was obtained as a greenish oil that was quickly dissolved in Et_2O (~10 mL for 1 g of expected product) and allowed to crystallized first at 4-6 °C, then at -18 °C overnight. The crystals were filtrated and washed with n-pentane affording (*S*)-1-bromo-4-methyl-2-(p-tolylsulfinyl)benzene (732 mg, 2.37 mmol, 70%) as colorless crystals.

^{1}**H-NMR** ($CDCl_3$, 400 MHz) : δ = 7.84 (d, J = 1.7 Hz, 1H), 7.62 (d, J = 8.2 Hz, 1H), 7.37 (d, J = 8.0 Hz, 1H), 7.23 (d, J = 8.0 Hz, 1H), 7.11 (dd, J = 8.1, 1.6 Hz, 1H), 2.40 (s, 2H), 2.35 (s, 2H) ppm

^{13}C NMR (101 MHz, $CDCl_3$) : δ = 144.27, 141.93, 141.29, 138.92, 133.02, 132.76, 129.84 (2C), 126.41, 126.25 (2C), 116.37, 21.39, 21.05 ppm.
EA : cald for $C_{14}H_{13}BrOS$ C = 54.38 H = 4.24; found C = 54.55, H = 4.34.
$[\alpha]_D^{20}$ = -50.4° (c = 0.36, $CHCl_3$).

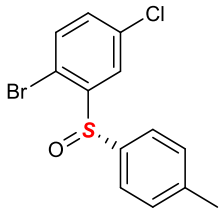

(*S*)-1-bromo-4-chloro-2-(*p*-tolylsulfinyl)benzene
Chemical Formula: $C_{13}H_{10}BrClOS$
Molecular Weight: 329,6360

(*S*)-1-bromo-4-chloro-2-(*p*-tolylsulfinyl)benzene :Prepared from 1-bromo-4-chloro-2-iodobenzene (1 eq., 2 g, 6.3 mmol) and (-)-menthyl (*S*)-p-toluenesulfinate (0.948 eq., 1.76 g, 5.98 mmol). The crude product solidified rapidly and was recrystallized by layering a concentrated DCM solution with n-Pen and letting the mixture equilibrate at 4-6°C. The white crystals were collected and washed with *n*-Pen, affording (*S*)-1-bromo-4-chloro-2-(p-tolylsulfinyl)benzene (1.75 g, 5.31 mmol, 89%).
^{1}H-NMR ($CDCl_3$, 400 MHz) : δ = 8.04 (d, J = 2.5 Hz, 1H), 7.64 (d, J = 8.2 Hz, 2H), 7.43 (d, J = 8.4 Hz, 1H), 7.32 – 7.21 (m, 3H), 2.37 (s, 3H ppm).
^{13}C NMR (101 MHz, $CDCl_3$) : δ = 146.81, 142.44, 140.41, 135.20, 134.10, 132.15, 129.95 (2C), 126.29 (2C), 126.05, 117.37, 21.38 ppm.
EA : cald for $C_{13}H_{10}BrClOS$ C = 47.37 H = 3.06; found C = 47.39, H = 3.12.
$[\alpha]_D^{20}$ = +33.3° (c = 0.87, $CHCl_3$).

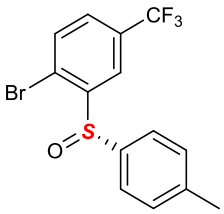

(*S*)-1-bromo-2-(*p*-tolylsulfinyl)-4-(trifluoromethyl)benzene
Chemical Formula: $C_{14}H_{10}BrF_3OS$
Molecular Weight: 363,1922

(S)-1-bromo-2-(p-tolylsulfinyl)-4-(trifluoromethyl)benzene : Prepared from 1-bromo-2-iodo-4-(trifluoromethyl)benzene (1 eq., 3.6 g, 10.3 mmol) and of (-)-menthyl (S)-p-toluenesulfinate (1 eq., 3.02 g, 10.3 mmol). The crude solid product was dissolved in the minimum of Et_2O and layered with n-Pen and the mixture was put at 4-6 °C. The colorless crystals were collected and washed with n-Pen, affording (S)-1-bromo-2-(p-tolylsulfinyl)-4-(trifluoromethyl)benzene (3.09 g, 8.5 mmol, 83%).
^{1}H-NMR ($CDCl_3$, 400 MHz) : δ = 8.37 (d, J = 2.0 Hz, 1H), 7.67 – 7.61 (m, 3H), 7.56 (dd, J = 8.2, 1.8 Hz, 2H), 7.27 (d, d, J = 6.8 Hz, 1H), 2.38 (s, 3H).

^{13}C-NMR ($CDCl_3$, 101 MHz): δ = 146.81, 142.73, 140.25, 133.75, 131.30 (q, J = 33.8 Hz), 130.10 (2C), 128.66 (q, J = 3.5 Hz), 126.54 (2C), 123.65 (q, J = 1.4 Hz), 123.32 (q, J = 3.8 Hz), 123.29 (q, J = 272.9 Hz), 21.47.
EA : cald for $C_{14}H_{10}BrF_3OS$ C = 46.30 H = 2.78; found C = 46.36, H = 2.82.
^{19}F-NMR ($CDCl_3$, 125.6 MHz): δ = -62.71ppm.
$[\alpha]_D^{20}$ = -69.2 ° (c = 0.6, $CHCl_3$).

b) Other enantiopure sulfoxides precursors

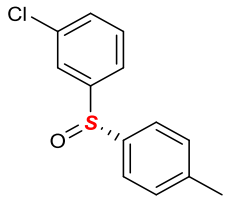

(*S*)-1-chloro-3-(*p*-tolylsulfinyl)benzene
Chemical Formula: $C_{13}H_{11}ClOS$
Molecular Weight: 250,7400

(*S*)-1-Chloro-3-(*p*-tolylsulfinyl)benzene (*anhydrous conditions*): A three necked flask, loaded with Mg (1 equiv, 0.34 g, 14 mmol) was flame-dried under vacuum. After cooling down to room temperature, ether (1.75 mL) was added to the magnesium. Then, a solution of 3-bromochlorobenzene (1 equiv, 2.68 g, 1.64 mL, 14 mmol) in ether (14 mL) was added dropwise to the magnesium suspension, first slowly to initiate the reaction, then more rapidly. Reflux was maintained for 1.5 h. after addition. After cooling down to room temperature, this solution was cannulated to a solution of (-)-menthyl-(*S*)-p-toluenesulfinate (1 equiv, 4.12 g, 14 mmol) in a mixture of toluene (45 mL) and ether (25 mL) at –30 °C and stirred for 30 min. The cooling bath was removed and the mixture was allowed back to –5 °C, when it was quenched with a sat. sol. of NH_4Cl. The reaction mixture was diluted with EtOAc and the phases were separated : the aqueous phase was extracted with EtOAc and the combined organic phases were washed with a sat. sol. of NH_4Cl, dried over Na_2SO_4 and the solvent was removed under reduced pressure. The crude oily mixture was then charged in a sublimator and placed in an oil bath at 60 °C to remove the (-)-menthol. Subsequent flash chromatography (EtOAc/*c*-Hex 1:3) yielded (*S*)-1-chloro-3-(*p*-tolylsulfinyl)benzene (2.71 g, 10.8 mmol, 77%) as white solid.
^{1}H-NMR (400 MHz, $CDCl_3$) : δ = 7.63–7.62 (m, 1 H), 7.55–7.52 (m, 2 H), 7.51–7.46 (m, 1 H), 7.39–7.37 (m, 2 H), 7.28 (d, *J* = 7.0 Hz, 2 H), 2.38 (s, 3 H) ppm.
^{13}C-NMR (101 MHz, $CDCl_3$): δ = 148.0, 142.2, 141.0, 135.5, 131.0, 130.5, 130.2 (2 C_{pTol}), 125.0 (2 C_{pTol}), 124.5, 122.6, 21.5 ppm.
R_f (EtOAc/*c*-Hex 1 : 3) = 0.4.
IR (ATR): $\tilde{\nu}$ /cm^{-1} = 3057 (w), 2920 (w), 1571 (m), 1491 (m), 1460 (m), 1408 (m) 1087 (m), 1044 (s), 1014 (m), 812 (s), 789 (s), 675 (s), 552 (s).
$[\alpha]_D^{22}$ = +66.25 (c = 1.1, $CHCl_3$).

e.r.: ≥ 95:5 [^{1}H NMR in presence of 3 equiv (w/w) of Pirkle's alcohol].

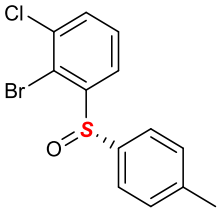

(*S*)-2-bromo-1-chloro-3-(*p*-tolylsulfinyl)benzene
Chemical Formula: $C_{13}H_{10}BrClOS$
Molecular Weight: 329,6360

(*S*)-2-Bromo-1-chloro-3-(*p*-tolylsulfinyl)benzene (*anhydrous conditions*). To a solution of diisopropylamine (1.3 equiv, 0.525 g, 0.733 mL, 5.19 mmol) in THF (10 mL) at –78 °C was added a 1.5 M solution of *n*-BuLi (1.18 equiv, 3.15 mL, 4.73 mmol). The mixture was stirred at –78 °C for 45 min. The LDA solution was added to a solution of (*S*)-1-chloro-3-(*p*-tolylsulfinyl)benzene (1 equiv, 1 g, 3.99 mmol) in THF (30 mL) at –78 °C. Upon addition, the color changed to a clear yellow-brown. The reaction mixture was stirred for 45 min. at –78 °C and then neat 1,2-dibromotetrafluoroethane (1.3 equiv, 1.35 g, 0.62 mL, 5.2 mmol) was quickly added, which caused instant discoloration. The mixture was stirred at –78°C for 30 min, then the dewar was removed and the reaction mixture was allowed to warm up in air to 0 °C. The reaction was quenched with a sat. sol. of NH_4Cl, the phases were separated and the aqueous layer was extracted with Et_2O. The combined organic layers were washed with brine, dried over Na_2SO_4 and concentrated under reduced pressure to afford the crude product. Flash chromatography (EtOAc/c-Hex 1:4) afforded (*S*)-2-bromo-1-chloro-3-(*p*-tolylsulfinyl)benzene (1.24 g, 3.76 mmol, 94 %) as off-white powder.

^{1}H-NMR (400 MHz, $CDCl_3$) : δ = 8.00 (dd, *J* = 7.2, 2.2 Hz, 1 H), 7.64 (d, *J* = 8.2 Hz, 2 H), 7.58–7.51 (m, 2 H), 7.25 (d, *J* = 8.2 Hz, 2 H), 2.37 (s, 3 H) ppm.

^{13}C-NMR (101 MHz, $CDCl_3$): δ = 147.9, 142.5, 140.8, 135.7, 132.3, 130.0, 129.1, 126.7, 124.3, 119.9, 21.5 ppm.

R_f (EtOAc/*c*-Hex 1:2) = 0.52.

Mp. = 113–118.7 °C.

IR (ATR): $\tilde{\nu}$ /cm^{-1} = 3060 (w), 2917 (w), 1593 (w), 1562 (w), 1490 (w), 1433 (w), 1403 (m), 1300 (w), 1188 (w), 1123 (m), 1078 (m), 1050 (s), 1012 (m), 806 (m), 786 (s), 704 (s), 619 (m), 554 (s).

$[\alpha]_D^{21}$= –275 (c = 1, $CHCl_3$).

Chiral HPLC e.r. ≥ 98% (OD-H column, *n*-Hex/*i*-PrOH 80:20, 0.5 mL/min, (*R*) r_t = 15.23 min, (*S*) r_t = 18.15 min).

EA = *calcd.* for $C_{13}H_{10}BrClOS$ 47.37 (C), 3.06 (H), *found* 47.42 (C), 3.07 (H).

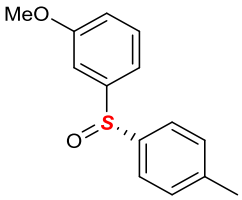

(*S*)-1-methoxy-3-(*p*-tolylsulfinyl)benzene
Chemical Formula: $C_{14}H_{14}O_2S$
Molecular Weight: 246,3240

(*S*)-1-Methoxy-3-(*p*-tolylsulfinyl)benzene (*anhydrous conditions*). A three necked flask, loaded with Mg (1.1 equiv, 0.535 g, 22 mmol), was dried overnight in an oven at 110 °C. After cooling down to room temperature in a dessicator, THF (2 mL) was added to the magnesium, followed by neat 1,2-dibromoethane (0.087 equiv, 0.33 g, 0.15 mL, 1.74 mmol). Then, a solution of 3-bromoanisole (1 equiv, 3.74 g, 2.54 mL, 20 mmol) in THF (12 mL) was added dropwise to the magnesium suspension. After 2 h. at reflux following the addition, the Grignard solution was cooled down to room temperature, and the solution was titrated following Paquette's procedure[389]. The Grignard solution was then cannulated to a solution of (-)-menthyl-(*S*)-*p*-toluenesulfinate (0.9 equiv, 5.3 g, 18 mmol) in a mixture of toluene (35 mL) and THF (15 mL) at -30 °C and stirred for 30 min. It was then slowly (~45 min.) allowed back to -10 °C and stirred for 1 h. The reaction was quenched at –10 °C with a sat. sol. of NH_4Cl and diluted with EtOAc. The phases were separated and the aqueous phase was extracted with EtOAc. The combined organic phases were washed with a sat. sol. of NH_4Cl, dried over Na_2SO_4 and the solvent was removed under reduced pressure. Flash chromatography on silica gel (EtOAc/*c*-Hex 1:4) yielded (*S*)-1-methoxy-3-(*p*-tolylsulfinyl)benzene (3.78 g, 15.3 mmol, 85 %) as colorless crystals.
^{1}H-NMR (400 MHz, $CDCl_3$): δ = 7.53 (d, *J* = 8.2 Hz, 2 H), 7.34 (t, *J* = 7.9 Hz, 1 H), 7.26 (d, *J* = 8.2 Hz, 2 H), 7.23 (t, *J* = 2 Hz, 1 H), 7.14 (d, *J* = 7.7 Hz, 1 H), 6.94 (dd, *J* = 8.2, 2.6 Hz, 1H), 3.82 (s, 3 H), 2.37 (s, 3 H) ppm.
^{13}C-NMR (101 MHz, $CDCl_3$): δ = 160.3, 147.1, 142.5, 141.6, 130.1, 130.0 (2 $C_{p\text{Tol}}$), 124.9 (2 $C_{p\text{Tol}}$), 117.1, 116.8, 108.9, 55.5, 21.4 ppm.
R_f (EtOAc/*c*-Hex 1:3) = 0.33.
$[\alpha]_D^{21}$ = +78 (c = 1.2, $CHCl_3$).
Chiral HPLC e.r. > 99 % [OD-H column, *n*-Hex/*i*-PrOH 95:5, 0.5 mL/min, (*R*) r_t = 40.45 min, (*S*) r_t = 45.11 min].

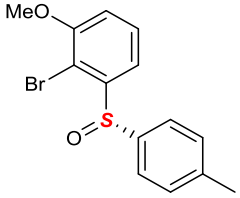

(*S*)-2-bromo-1-methoxy-3-(*p*-tolylsulfinyl)benzene
Chemical Formula: $C_{14}H_{13}BrO_2S$
Molecular Weight: 325,2200

(*S*)-2-Bromo-1-methoxy-3-(*p*-tolylsulfinyl)benzene (*anhydrous conditions*): To a solution of diisopropylamine (1.2 equiv, 246 mg, 0.344 mL, 2.44 mmol) in THF (10

mL) at –78 °C was added a 1.6 M solution of *n*-BuLi (1.1 equiv, 1.4 mL, 2.23 mmol). The mixture was stirred at –78 °C for 45 min. The LDA solution was added to a solution of (*S*)-1-methoxy-3-(*p*-tolylsulfinyl)benzene (1 equiv, 500 mg, 2.03 mmol) in THF (10 mL) at –78 °C. During the addition the color changed to a strong yellow. The reaction mixture was then stirred for 30 min. at –78°C and then neat 1,2-dibromotetrafluoroethane (1.2 equiv, 632 mg, 0.29 mL, 2.44 mmol) was quickly added, which caused instant discoloration. The mixture was stirred at -78°C for 30 min, and the reaction mixture was allowed to warm up in air to room temperature. The mixture was quenched by water and the aqueous layer was extracted with Et_2O. The combined organic layers were washed with brine, dried over Na_2SO_4, filtered and concentrated under reduced pressure to afford the crude product. Flash chromatography (EtOAc/*c*-Hex 1 : 3 then EtOAc/*c*-Hex 1:2) yielded (*S*)-2-bromo-1-methoxy-3-(*p*-tolylsulfinyl)benzene (445.7 mg, 1.37 mmol, 68%) as white crystal.

^{1}H-NMR (400 MHz, $CDCl_3$) : δ = 7.68 (d, *J* = 7.8 Hz, 1 H), 7.64 (d, *J* = 8.1 Hz, 2 H), 7.52 (t, *J* = 8.0 Hz, 1 H), 7.22 (d, *J* = 8.1 Hz, 2 H), 6.98 (d, *J* = 8.2 Hz, 1 H), 3.89 (s, 3 H), 2.35 (s, 3 H) ppm.

^{13}C-NMR (101 MHz, $CDCl_3$) : δ = 156.0, 146.7, 142.0, 141.4, 129.9 (2 $C_{p\text{Tol}}$), 129.2, 126.5 (2 $C_{p\text{Tol}}$), 117.7, 113.8, 109.3, 56.6, 21.5 ppm.

R_f (EtOAc/*c*-Hex 1:2) = 0.35.

Mp. = 108.9–110 °C.

IR (ATR): $\tilde{\nu}$ /cm^{-1} = 3050 (w), 3011 (w), 2945 (w), 2912 (w) 1578 (m), 1462 (s), 1426 (m), 1417 (m), 1296 (s), 1272 (s), 1172 (m), 1155 (m), 1082 (s), 1054 (s), 1040 (s), 1020 (s), 810 (s), 772 (s), 707 (s), 509 (s).

$[\alpha]_D^{25}$ = –216 (c = 1, $CHCl_3$).

Chiral HPLC e.r. > 99% (OD-H column, *n*-Hex/*i*-PrOH 80:20, 0.5 mL/min, (*R*) r_t = 19.73 min, (*S*) r_t = 24.04 min).

EA = *calcd.* for $C_{14}H_{13}BrO_2S$ 51.70 (C), 4.03 (H), *found* 51.74 (C), 4.09 (H).

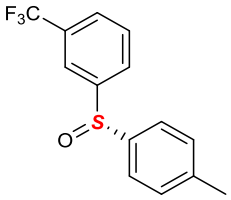

(*S*)-1-(*p*-tolylsulfinyl)-3-(trifluoromethyl)benzene
Chemical Formula: $C_{14}H_{11}F_3OS$
Molecular Weight: 284,2962

(S)-1-(p-Tolylsulfinyl)-3-(trifluoromethyl)benzene (*anhydrous conditions*): A three necked flask, loaded with Mg (1.1 equiv, 0.59 g, 24.4 mmol) was flame-dried under vacuum. After cooling down to room temperature, Et_2O (4.0 mL) was added to the magnesium. Then, a solution of 1-bromo-3-(trifluoromethyl)benzene (1 equiv, 5.0 g, 3.11 mL, 22.2 mmol) in Et_2O (30 mL) was added dropwise to the magnesium suspension, first slowly to initiate the reaction, then more rapidly. Reflux was maintained for 1 h after addition. After cooling down to room temperature, this solution was cannulated to a solution of (-)-menthyl-(*S*)-*p*-toluenesulfinate (1.4 equiv, 9.16 g, 31.1 mmol) in a mixture of toluene (52 mL) and Et_2O (20 mL) at –30 °C and stirred for 3 h

at –30 °C. The cooling bath was removed and the mixture was allowed back to –10 °C, when it was quenched with a sat. sol. of NH_4Cl. It was then diluted with EtOAc and the phases were separated: the aqueous phase was extracted with EtOAc and the combined organic phases were washed with a sat. sol. of NH_4Cl, dried over Na_2SO_4 and the solvent was removed under reduced pressure. The crude oily mixture was purified by flash chromatography (EtOAc/*c*-Hex 1:9) yielded (*S*)-1-(*p*-tolylsulfinyl)-3-(trifluoromethyl)benzene (5.56 g, 19.5 mmol, 88%) as white solid.

^{1}H-NMR (400 MHz, $CDCl_3$) : δ = 7.93 (s, 1H), 7.78 (d, *J* = 7.8 Hz, 1H), 7.68 (d, *J* = 7.8 Hz, 1H), 7.59 (d, *J* = 7.8 Hz, 1H), 7.55 (d, *J* = 8.2 Hz, 2H), 7.29 (d, *J* = 8.0 Hz, 2H), 2.38 (s, 3H) ppm.

^{13}C-NMR (101 MHz, $CDCl_3$): δ = 148.0, 142.9, 142.3, 132.3 (q, J_{CF} = 33.5 Hz), 130.8 ($2C_{pTol}$), 130.3, 128.2, 127.9 (q, J_{CF} = 3.5 Hz), 125.4 ($2C_{pTol}$), 123.8 (q, J_{CF} = 276 Hz), 121.8 (q, J_{CF} = 3.8 Hz), 21.2 ppm.

^{19}F-NMR ($CDCl_3$, 377 MHz): –63.4 ppm,

R_f (EtOAc/*c*-Hex 1:2.33) = 0.48.

$[\alpha]_D^{22}$= +58.6 (c = 1.05, $CHCl_3$).

Chiral HPLC e.r. ≥ 98% [OD-H column, *n*-Hex/*i*-PrOH 90:10, 0.5 mL/min, (*S*) r_t = 14.85 min, (*R*) r_t = 16.35 min].

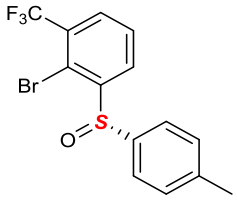

(*S*)-2-bromo-1-(*p*-tolylsulfinyl)-3-(trifluoromethyl)benzene
Chemical Formula: $C_{14}H_{10}BrF_3OS$
Molecular Weight: 363,1922

(S)-2-Bromo-1-(*p*-tolylsulfinyl)-3-(trifluoromethyl)benzene (*anhydrous conditions*): To a solution of diisopropylamine (1.2 equiv, 854.2 mg, 1.19 mL, 8.44 mmol) in THF (8.5 mL) at –78 °C was added a 1.6 M solution of *n*-BuLi (1.2 equiv, 5.28 mL, 8.44 mmol). The mixture was stirred at –78 °C for 30 min. The LDA solution was added to a solution of (*S)*-1-(*p*-tolylsulfinyl)-3-(trifluoromethyl)benzene (1 equiv, 2.0 g, 7.03 mmol) in THF (14 mL) at –78 °C. During the addition the color changed to a strong yellow. The reaction mixture was then stirred for 30 min. at –78°C and then neat 1,2-dibromotetrafluoroethane (1.2 equiv, 2.19 g, 1.0 mL, 8.44 mmol) was quickly added, which caused instant discoloration. The mixture was stirred at –78°C for 30 min, and the reaction mixture was allowed to warm up in air to room temperature. The mixture was quenched by water and the aqueous layer was extracted with Et_2O. The combined organic layers were washed with brine, dried over Na_2SO_4, filtered and concentrated under reduced pressure to afford the crude product. Flash chromatography (DCM/*c*-Hex 1:1 then DCM/*c*-Hex 1:0.2) yielded (*S*)-2-bromo-1-(*p*-tolylsulfinyl)-3-(trifluoromethyl)benzene (1.98 g, 5.45 mmol, 77 %) as white solid.

^{1}H-NMR (400 MHz, $CDCl_3$): δ = 8.28 (d, *J* = 7.8 Hz, 1H), 7.79 (d, *J* = 7.6 Hz, 1H), 7.69 (t, *J* = 7.8 Hz, 1H), 7.63 (d, *J* = 8.0 Hz, 2H), 7.26 (d, *J* = 7.8 Hz, 2H), 2.37 (s, 3H) ppm.

^{13}C-NMR (101 MHz, $CDCl_3$): δ = 149.1, 143.2, 141.1, 131.7 (q, J_{CF} = 31.7 Hz), 130.6 (2C$_{pTol}$), 130.5 (q, J_{CF} = 5.3 Hz), 130.0, 128.9, 127.0 (2C$_{pTol}$), 122.9 (q, J_{CF} = 277.0 Hz), 118.5 (q, J_{CF} = 1.7 Hz), 21.3 ppm.
^{19}F-NMR ($CDCl_3$, 377 MHz): –62. ppm.
R_f (EtOAc/*c*-Hex 1:2.33) = 0.47.
$[\alpha]_D^{25}$ = –136 ° (c = 1.05, $CHCl_3$).
Chiral HPLC e.r. > 95% (OD-H column, *n*-Hex/*i*-PrOH 80:20, 0.5 mL/min, (*R*) r_t = 14.73 min, (*S*) r_t = 17.77 min).

c) Preparation of Boronic acids:

The bromoarene (1 equiv) was dissolved in anhydrous THF (0.25M) and the resulting solution was cooled down to – 78 °C, when *t*-BuLi (2 equiv) was added dropwise and the resulting solution was stirred for 15 min. Then, under vigorous stirring, neat $B(OMe)_3$ was quickly added in one portion causing instant discoloration of the reaction mixture. After 15 min., the cooling bath was removed and the mixture allowed to come back to room temperature, when it was quenched by a 1M HCl solution, stirred for 1 more hour and finally diluted with Et_2O. The phases were separated and the aqueous phase extracted twice with a THF/Et_2O (1 : 1, v/v) solution. The combined organic phases were dried over Na_2SO_4 and the solvent removed under reduced pressure. The crude product thus obtained was purified as stated below.

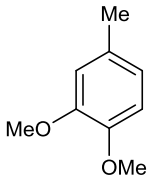

1,2-dimethoxy-4-methylbenzene
Chemical Formula: $C_9H_{12}O_2$
Molecular Weight: 152,1930

4-methylcatechol (1 eq., 10 g, 80.6 mmol) and triethylbenzyl ammonium chloride (5 %, 0.917 g, 4.03 mmol) were dissolved in DCM (350 mL) along with dimethylsulfate (2.5 eq., 25.4 g, 19.1 mL, 201 mmol). Then NaOH (19 M, 5 eq., 21.2 mL) was added dropwise (exotherm). After 2 hours of vigorous stirring at room temperature, water was then added (150 mL), and the mixture was stirred for 1 more hour. Then an ammonium hydroxide solution (20 mL) was added to quench the excess dimethyl sulfate, and the mixture was stirred for 1 more hour. The phases were then separated and the organic phase was washed with a 1M NaOH solution (1M), a sat. Sol. Of $NaHCO_3$, and finally with a 1M HCl solution (2 times). The crude product, 3,4-dimethoxytoluene (11.033 g, 72.5 mmol, 90 %) was isolated as an orange oil and is pure enough to be utilized in the next step *(the cude proton NMR is given in the SI)*. ^{1}**H-NMR** ($CDCl_3$, 400 MHz) : δ = 6.77 (d, J = 8.6 Hz, 1H), 6.78 – 6.67 (m, 2H), 3.87 (s, 3H), 3.85 (s, 3H), 2.31 (s, 3H) ppm. Spectral data matched the literature.

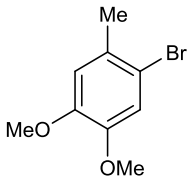

1-bromo-4,5-dimethoxy-2-methylbenzene
Chemical Formula: $C_9H_{11}BrO_2$
Molecular Weight: 231,0890

The title compound was prepared following litterature procedure from 4,5-dimethoxy-2-methylbenzene (1 eq., 2.73 g, 17.9 mmol), using DMSO (1.14 eq., 1.6 g, 1.45 mL, 20.4 mmol) and HBr (1.11 eq., 3.35 g, 2.25 mL, 19.9 mmol) in EtOAc (72.5 mL) at 60 °C for 16 hours, yielding 1-bromo-4,5-dimethoxy-2-methylbenzene (4.1 g, 17.7 mmol, 99%). The crude product was pure enough to be used directly in the next step (*the crude ^{1}H NMR is given in the SI)*.
^{1}**H-NMR** ($CDCl_3$, 400 MHz) : δ = 6.99 (s, 1H), 6.72 (s, 1H), 3.83 (s, 4H), 3.83 (s, 3H), 2.31 (s, 3H) ppm.
Spectral data matched the literature.

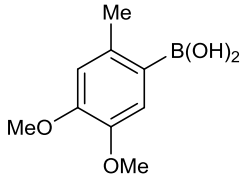

(4,5-dimethoxy-2-methylphenyl)boronic acid
Chemical Formula: $C_9H_{13}BO_4$
Molecular Weight: 196,0090

From 1-bromo-4,5-dimethoxy-2-methylbenzene (1 eq., 4.1 g, 17.7 mmol), application of the general procedure, followed by purifcation as stated hereafter : the off-white solid was dissolved in the minimum of warm THF and precipitated by the addition of pentane, followed by 2 hours at 4-6 °C. The resulting solid was then collected by filtration, and transfered in a round-bottom flask. A mixture of water and acetone (1 : 1; v/v) was added (~15 mL for 1 g of crude product), and the clear solution was heated at 80 °C on a rotary evaporator bath to remove the acetone under reduced pressure. The water solution might become cloudy at the end of the acetone evaporation. The resulting solution was then put at 4-6 °C overnight, yielding white crystals. A second batch can be obtained from the concentrated mother liquor: yielding a total of (4,5-dimethoxy-2-methylphenyl)boronic acid (2.28 g, 11.6 mmol, 66 %).
^{1}**H-NMR** (DMSO-d6, 400 MHz) : δ = 7.78 (brd, 2H), 7.06 (s, 1H), 6.71 (s, 1H), 3.73 (s, 3H), 3.71 (s, 3H), 2.36 (s, 3H) ppm.
Spectral data matched the literature.

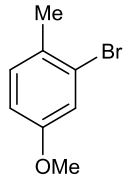

2-bromo-4-methoxy-1-methylbenzene
Chemical Formula: C_8H_9BrO
Molecular Weight: 201,0630

3-bromo-4-methylphenol (1 eq., 5 g, 26.7 mmol) was dissolved in DCM (200 mL) along with triethylbenzylammonium chloride (5 %, 0.304 g, 1.34 mmol) and dimethyl sulfate (1.2 eq., 4.05 g, 3.04 mL, 32.1 mmol). Then, under vigorous stirring, NaOH

(19 M, 2.5 eq.,3.5 mL) was added dopwise at room temperature. The reaction mixture became orange and turbid, then after 2 hours it regained its original greenish color. Water was then added (100 mL), and the mixture was stirred for 1 more hour. Then an ammonium hydroxide solution (10 mL) was added to quench the excess dimethyl sulfate, and the mixture was stirred for 1 more hour. The phases were then separated and the organic phase was washed with a 1M NaOH solution (1M), a sat. sol. of $NaHCO_3$, and with a 1M HCl solution (2 times). The product 2-bromo-4-methoxy-1-methylbenzene (5.02 g, 25 mmol, 93 %), isolated as an orange oil, is pure enough to be used in the next step (the crude ^1H NMR is given in the SI). **^{1}H-NMR** ($CDCl_3$, 400 MHz) : δ = 7.12 (d, *J* = 8.4 Hz, 1H), 7.10 (d, *J* = 2.6 Hz, 1H), 6.77 (dd, *J* = 8.4, 2.7 Hz, 1H), 3.77 (s, 3H), 2.33 (s, 3H) ppm.

Spectral data matched the literature.

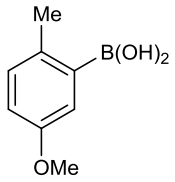

(5-methoxy-2-methylphenyl)boronic acid
Chemical Formula: $C_8H_{11}BO_3$
Molecular Weight: 165,9830

Mg turnings (3 eq., 3.97 g, 163 mmol) were loaded in a two-necked flask, followed by THF (10 mL) at room temperature. The magnesium was activated by dibromoethane (0.0531 eq., 0.543 g, 0.25 mL, 2.89 mmol), and then under stirring a solution of 2-bromo-4-methoxy-1-methylbenzene (1 eq., 11 g, 54.5 mmol) in THF (40 mL) was added dropwise at a rate sufficient to obtain a refluxing solution. After the addition, the light grey solution was stirred for a further 1 h. at 50 °C. Then, after cooling to room temperature, the reaction mixture was diluted with THF (50 mL), and cooled down to 0 °C. Then, under vigourous stirring, neat $B(OMe)_3$ (3.5 eq., 19.8 g, 21.6 mL, 190 mmol) was quickly added in one protion, which caused a white precipitate to appear. After 15 min. of stirring at 0 °C, the cooling bath was removed and the reaction mixture was stirred for 1 h. at room temperature. The reaction was then quenched by a 1M HCl solution, and stirred for 1h., diluted with Et_2O, and the phases were separated. The aqueous phase was extracted with an Et_2O/THF mixture (1:1, v/v), and the combined organic phases were dried over Na_2SO_4. The volatile were removed under reduced pressure (some MeCN can be added) and the crude off-white solid thus obtained was triturated with *n*-pentane with under sonication. The crude product is then recrystallized from MeCN (reflux to room temperature to 4-6 °C : it is difficult to obtain good crystals, a second recrystallization is sometimes needed). The titled compound (5-methoxy-2-methylphenyl)boronic acid (7.33 g, 44.2 mmol, 81%) was obtained as a white solid. The title compound as a low solubility in most water-free organic solvents except for THF.

^{1}H NMR ($NCCD_3$, 400 MHz) : δ = 7.07 (d, J = 8.3 Hz, 1H), 7.04 (d, J = 2.8 Hz, 1H),

6.82 (dd, J = 8.3, 2.9 Hz, 1H), 6.14 (s, 2H), 4.87 (s, 2H signal corresponding to the hydrated boronic acid, due the water-contaminated $NCCD_3$), 3.75 (s, 3H), 2.36 (s, 3H) ppm.
Spectral data matched the literature.

d) General procedure for di-ortho-subsituted biphenyls :

The bromophenylsulfoxide (1 equiv.), the boronic acid (1.25 equiv.), Na_2CO_3 (3.3 equiv.), *n*-Bu_4NBr (1 equiv.) and palladium diacetate (5 mol%) where all loaded in a microwave vial. A minimum amount of EtOH was then added in order obtain a somewhat homogenous paste. The vial was then filled with water ([substrate] = from 0.1 M to 0.25 M depending on the scale of the reaction and the size of the vial available), and after having been sealed the heterogenous mixture was stirred for 5 min. in order to dissolve the water-soluble reagents and to make sure that the stirring was efficient. Then the reaction was heated either at to 150 °C for 5 to 10 min in a microwave oven, or at 100 °C in a oil bath for 2 to 3 hours. After having cooled down to room temperature, the reaction was diluted with Et_2O and stirred for 10-15 min. (in order to dissolve the organic material that separated as a black oil. However a black precipitate will remain after this operation). It was then transferred to a separating funnel; diluted with more Et_2O and a 1M NaOH solution, and the phases were separated. The organic phase was dried over Na_2SO_4 and the solvent removed under reduced pressure. The crude product was then purified by flash chromatography.

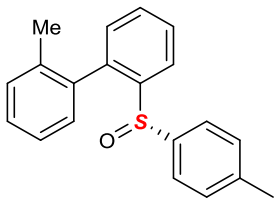

(*S*)-2-methyl-2'-(*p*-tolylsulfinyl)-1,1'-biphenyl
Chemical Formula: $C_{20}H_{18}OS$
Molecular Weight: 306,4230

(*S*)-2-methyl-2'-(*p*-tolylsulfinyl)-1,1'-biphenylThe general procedure was followed at 150 °C for 5 min., using: (*S*)-1-bromo-2-(p-tolylsulfinyl)benzene (1 eq., 450 mg, 1.52 mmol), in water (5 mL). Yielding (*S*)-2-methyl-2'-(p-tolylsulfinyl)-1,1'-biphenyl (455 mg, 1.48 mmol, 97 %) as a colorless oil that solidified upon days. ^{1}**H-NMR** (400 MHz, $CDCl_3$): δ = (*mixture of two atropodiastereomers 1:1.15*) 8.26 (dd, *J* = 7.9, 1.2 Hz, 1 H *major dia*), 8.18 (dd, *J* = 7.9, 1.3 Hz, 1 H *minor dia*), 7.64–7.58 (m, 1 H *major dia*, 1 H *minor dia*), 7.52–7.44 (m, 1 H *major dia*, 1 H *minor dia*), 7.36–7.27 (m, 3 H *major dia*, 2 H *minor dia),* 7.14-6.94 (m, 4 H *major dia*, 6 H *minor dia*), 6.87 (d, *J* = 8.2 Hz, 2 H *major dia*), 6.50 (d, *J* = 7.4 Hz, 1 H *minor dia),* 2.31 (s, 3 H *minor dia*), 2.29 (s, 3 H *major dia*), 2.25 (s, 3 H *minor dia*), 1.32 (s, 3 H, *minor dia*) ppm.
R_f (EtOAc/*c*-Hex 1:3) = 0.35.

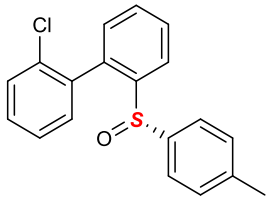

(*S*)-2-chloro-2'-(*p*-tolylsulfinyl)-1,1'-biphenyl
Chemical Formula: $C_{19}H_{15}ClOS$
Molecular Weight: 326,8380

(*S*)-2-chloro-2'-(*p*-tolylsulfinyl)-1,1'-biphenyl: The general procedure was followed at 150 °C for 7 min., using (*S*)-1-bromo-2-(*p*-tolylsulfinyl)benzene (1 eq., 600 mg, 2.03 mmol) in water (6 mL). Yielding (*S*)-2-chloro-2'-(p-tolylsulfinyl)-1,1'-biphenyl as a greenish oil (505 mg, 1.55 mmol, 76 %). **^{1}H-NMR** (400 MHz, $CDCl_3$): δ = (*mixture of two atropodiastereomers 1:1.2*) 8.23 (dd, *J* = 8.0, 1.2 Hz, 1 H *minor dia*), 8.10 (dd, *J* = 7.8, 1.2 Hz, 1 H *major dia*), 7.66–7.58 (m, 1 H *major dia*, 1 H *minor dia),* 7.53–7.47 (m, 2 H *major,* 2 H *minor dia*), 7.40–7.31 (m, 2 H *major dia*, 2 H *minor dia*), 7.27–7.24 (m 1 H *major*), 7.16–7.12 (m, 1 H *major* / 1 H *minor dia*), 7.08–7.01 (m, 4 H *major dia*, 4 H *minor dia*), 6.67 (dd, *J* = 7.6, 1.6 Hz, 1 H *minor dia*), 2.31 (s, 3 H *major dia*), 2.30 (s, 3 H *minor dia*). **^{13}C-NMR** (101 MHz, $CDCl_3$): δ = (mixture of two atropodiastereomers) 144.7, 144.1, 142.2, 141.7, 141.6, 140.7, 137.6, 137.1, 136.8, 136.2, 134.0, 133.5, 132.1, 132.0, 131.2, 130.9, 130.2, 130.2, 129.9, 129.9, 129.8, 129.7, 129.6, 129.3, 129.2, 126.7, 126.7, 125.9, 125.9, 124.5, 123.6, 21.5, 21.5 ppm. **R_f** (EtOAc/*c*-Hex 1:1) = 0.60.

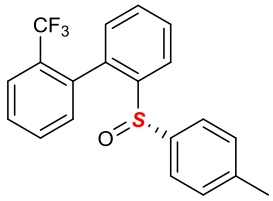

(*S*)-2-(*p*-tolylsulfinyl)-2'-(trifluoromethyl)-1,1'-biphenyl
Chemical Formula: $C_{20}H_{15}F_3OS$
Molecular Weight: 360,3942

(*S*)-2-(*p*-tolylsulfinyl)-2'-(trifluoromethyl)-1,1'-biphenyl: The general procedure was followed at 150 °C for 7 min using (*S*)-1-bromo-2-(*p*-tolylsulfinyl)benzene (1 eq., 600 mg, 2.03 mmol), in water (5 mL). Yielding (S)-2-(p-tolylsulfinyl)-2'-(trifluoromethyl)-1,1'-biphenyl (505 mg, 1.4 mmol, 69%) as colorless oil. **^{1}H-NMR** (400 MHz, $CDCl_3$): δ = (*mixture of two atropodiastereomers 1:1.6*) 8.22 (dd, *J* = 7.9, 1.2 Hz, 1 H *minor dia*), 8.00 (dd, *J* = 7.9, 1.2 Hz, 1 H *major dia*), 7.78 (d, *J* = 7.9 Hz, 1 H *minor dia*), 7.69–7.45 (m, 4 H *major dia,* 7 H *minor dia*), 7.31 (t, *J* = 7.5 Hz, 1 H *minor dia*), 7.27–7.25 (m, 1 H *major dia*), 7.18 (d, *J* = 7.3 Hz, 1 H *minor dia*), 7.15–7.10 (m, 2 H *major dia*), 7.07 (d, *J* = 8 Hz, 2 H *major dia*), 6.99 (d, *J* = 8 Hz, 2 H *major dia*), 6.54 (d, *J* = 7.6 Hz, 1 H *minor dia*), 2.34 (s, 3 H *minor dia*), 2.31 (s, 3 H *major dia*). **^{13}C-NMR** (101 MHz, $CDCl_3$): δ = (*mixture of two atropodiastereomers 1:1.6*) 143.9 (m), 143.6 (m), 142.1, 141.9, 141.6, 139.6, 138.1, 137.0, 135.9 (q, J_{CF} = 2.0 Hz),

135.8 (q, $J_{C\text{-}F}$ = 1.9 Hz), 133.6, 132.8, 132.7, 131.4 (q, J_{CF} = 1 Hz), 130.8 (q, J_{CF} = 1.0 Hz), 130.8 (q, J_{CF} = 1.3 Hz), 130.4 (q, J_{CF} = 2.2 Hz), 130.4 (q, J_{CF} = 1.1 Hz), 130.3, 130.1, 129.8, 129.6, 129.4, 129.3, 128.7, 128.6, 126.7 (q, J_{CF} = 5.1 Hz), 126.6, 126.2 (q, J_{CF} = 5.1 Hz), 125.8 (m), 124.8, 123.8, 123.7 (q, J_{CF} = 273.9 Hz), 123.5 (q, J_{CF} = 273.8 Hz), 21.4, 21.3 ppm. ^{19}**F-NMR** (377 MHz, $CDCl_3$) : δ = (*mixture of two atropdiastereomers 1 : 1.6*) –57.71 (*major dia*), –56.70 (*minor dia*) ppm. **R$_f$** (EtOAc/*c*-Hex 1:2) = 0.36.

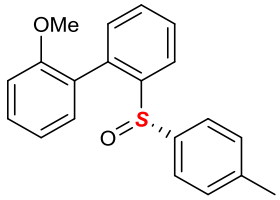

(*S*)-2-methoxy-2'-(*p*-tolylsulfinyl)-1,1'-biphenyl
Chemical Formula: $C_{20}H_{18}O_2S$
Molecular Weight: 322,4220

(*S*)-2-methoxy-2'-(*p*-tolylsulfinyl)-1,1'-biphenyl: The general procedure was followed at 150 °C for 5 min using (*S*)-1-bromo-2-(*p*-tolylsulfinyl)benzene (1 eq., 83 mg, 0.281 mmol) in water (3 mL). Yielding (*S*)-2-methoxy-2'-(p-tolylsulfinyl)-1,1'-biphenyl (85 mg, 0.264 mmol, 94 %) as a white powder. ^{1}**H-NMR** (400 MHz, C_6D_6, 70 °C): δ = 8.32 (d, *J* = 8.1 Hz, 1 H), 7.16 (d, *J* = 8 Hz, 2 H), 7.19–7.01 (m, 4 H), 6.93 (brd, 1 H), 6.77 (td, *J* = 7.5, 0.8 Hz, 1H), 6.71 (d, *J* = 8 Hz, 2 H), 6.57 (d, *J* = 8.3 Hz, 1 H), 3.13 (s, 3 H), 1.90 (s, 3H) ppm. **R$_f$** (EtOAc/*c*-Hex 1:1) = 0.44.

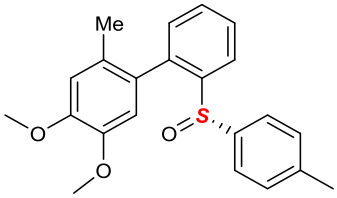

(*S*)-4,5-dimethoxy-2-methyl-2'-(*p*-tolylsulfinyl)-1,1'-biphenyl
Chemical Formula: $C_{22}H_{22}O_3S$
Molecular Weight: 366,4750

(*S*)-4,5-dimethoxy-2-methyl-2'-(*p*-tolylsulfinyl)-1,1'-biphenyl: The general procedure was followed at 150 °C for 10 min., using (*S*)-1-bromo-2-(*p*-tolylsulfinyl)benzene (1 eq., 200 mg, 0.678 mmol) in water (3.5 mL). Yielding (*S*)-4,5-dimethoxy-2-methyl-2'-(p-tolylsulfinyl)-1,1'-biphenyl (204 mg, 0.557 mmol, 82.2 %) as a colorless oil that solidified upon days. Mixture of two atropisomer (1 : 1.3) on the NMR time scale. ^{1}**H-NMR** ($CDCl_3$, 400 MHz) : δ = 8.26 – 8.19 (m, 1H major; 1H minor), 7.63 (td, J = 7.7, 1.4 Hz, 1H major), 7.60 (td, J = 7.7, 1.4 Hz, 1H minor), 7.50 (td, J = 7.5, 1.4 Hz, 1H major), 7.45 (td, J = 7.5, 1.4 Hz, 1H minor), 7.13 (dd, J = 7.5, 1.2 Hz, 1H minor), 7.12 (dd, J = 7.5, 1.1 Hz, 1H major), 7.09 – 7.04 (m, 2H major), 7.05 – 7.00 (m, 2H minor), 7.00 – 6.97 (m, 2H major), 6.97 – 6.92 (m, 2H minor), 6.86 (s, 1H minor), 6.78

(s, 1H major), 6.58 (s, 1H minor), 5.78 (s, 1H major), 3.95 (s, 3H major), 3.92 (s, 3H minor), 3.90 (s, 3H minor), 3.45 (s, 3H major), 2.30 (s, 3H minor), 2.29 (s, 3H major), 2.17 (s, 3H major), 1.29 (s, 3H minor) ppm. **^{13}C-NMR** ($CDCl_3$, 101 MHz): δ = 148.70, 148.50, 146.43, 146.35, 143.94, 143.91, 141.84, 141.44, 141.42, 140.91, 139.21, 139.14, 130.93, 130.59, 130.17, 129.84, 129.25, 129.18, 128.85, 128.81, 128.50, 128.16, 128.07, 127.84, 127.83, 55.95, 55.85, 55.78, 55.09, 21.22, 21.16, 19.37, 18.63 ppm. **HRMS (ESI):** *calc. for $C_{22}H_{23}O_3S^+$ 367.1290* ; found 367.1300

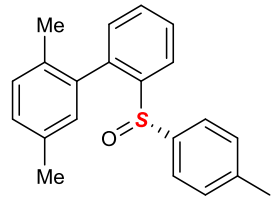

(*S*)-2,5-dimethyl-2'-(*p*-tolylsulfinyl)-1,1'-biphenyl
Chemical Formula: $C_{21}H_{20}OS$
Molecular Weight: 320,4500

(*S*)-2,5-dimethyl-2'-(*p*-tolylsulfinyl)-1,1'-biphenyl: The general procedure was followed at 150 °C for 10 min. using (*S*)-1-bromo-2-(*p*-tolylsulfinyl)benzene (1 eq., 509 mg, 1.73 mmol) in water (10 mL) Yielding (*S*)-2,5-dimethyl-2'-(p-tolylsulfinyl)-1,1'-biphenyl (500 mg, 1.56 mmol, 90%) as a white powder. Mixture of two atropisomer (1 : 1) on the NMR time scale.

^{1}H-NMR ($CDCl_3$, 400 MHz) : δ = 8.24 (dd, J = 7.9, 1.2 Hz, 1H), 8.21 (dd, J = 7.9, 1.3 Hz, 1H), 7.66 – 7.56 (m, 2H), 7.49 (td, J = 7.5, 1.4 Hz, 1H), 7.45 (td, J = 7.4, 1.3 Hz, 1H), 7.21 – 7.15 (m, 2H), 7.14 – 7.10 (m, 3H), 7.08 (d, J = 7.8 Hz, 1H), 7.07 – 7.03 (m, 2H), 7.03 – 6.99 (m, 2H), 6.99 – 6.94 (m, 3H), 6.92 – 6.86 (m, 2H), 6.14 (s, 1H), 2.39 (s, 3H), 2.32 (s, 3H), 2.29 (s, 3H), 2.18 (s, 3H), 2.11 (s, 3H), 1.29 (s, 3H) ppm. **^{13}C-NMR** ($CDCl_3$, 101 MHz): δ = 143.66, 143.57, 141.70, 141.31, 141.27, 140.87, 139.57, 139.41, 136.86, 136.35, 134.79, 134.68, 133.32, 132.44, 130.84, 130.68, 130.56, 130.41, 130.07, 129.73, 129.71, 129.71, 129.17 (2C), 129.08 (2C), 129.00, 128.75, 128.11, 128.00, 126.12 (2C), 126.01 (2C), 123.32, 123.14, 21.18 (2C), 20.73, 20.52, 19.35, 18.63 ppm. **HRMS (ESI):** *calc. for $C_{21}H_{21}OS^+$ 321.1308* ; found 321.1311

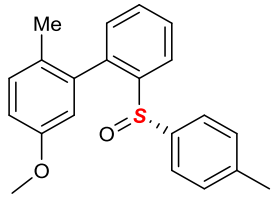

(*S*)-5-methoxy-2-methyl-2'-(*p*-tolylsulfinyl)-1,1'-biphenyl
Chemical Formula: $C_{21}H_{20}O_2S$
Molecular Weight: 336,4490

(*S*)-5-methoxy-2-methyl-2'-(*p*-tolylsulfinyl)-1,1'-biphenyl:The general procedure was followed at 100 °C for 2 h., using (*S*)-1-bromo-2-(*p*-tolylsulfinyl)benzene (1 eq., 3.87 g, 13.1 mmol) and $Pd(OAc)_2$ (2.5 mol%, 0.0735 g, 0.327 mmol) in EtOH (8 mL) and water (75 mL). The crude product was purified quickly by carefull filtration on silica gel, followed by recrystallization from a 95:5 heptane/toluene mixture (reflux to room temperature then to 4-6°C). The solution is seeded while hot and left undisturbed, yielding (*S*)-5-methoxy-2-methyl-2'-(*p*-tolylsulfinyl)-1,1'-biphenyl (3.8 g, 11.3 mmol, 86%) as white crystals. The seed crystals are obtained by carefull recrystallization of the pure product after column chromatography from a 95:5 heptane/toluene mixture (reflux to room temperature then to 4-6°C). Mixture of two atropisomer (1 : 1) on the NMR time scale.

^{1}**H-NMR** ($CDCl_3$, 400 MHz) : 8.25 (dd, J = 7.9, 1.2 Hz, 1H), 8.21 (dd, J = 7.9, 1.3 Hz, 1H), 7.62 (td, J = 7.7, 1.4 Hz, 1H), 7.61 (td, J = 7.7, 1.3 Hz, 1H), 7.51 (td, J = 7.4, 1.3 Hz, 1H), 7.46 (td, J = 7.5, 1.3 Hz, 1H), 7.19 (d, J = 8.4 Hz, 1H), 7.15 – 7.11 (m, 2H), 7.08 – 7.04 (***A₁A₁'***B_1B_1', 2H), 7.05 – 6.96 (m, 5H), 6.95 – 6.91 (A_1A_1'***B₁B₁'***, 2H), 6.91 – 6.81 (m, 3H), 5.90 (d, J = 2.8 Hz, 1H), 3.84 (s, 3H), 3.52 (s, 3H), 2.31 (s, 3H), 2.29 (s, 3H), 2.16 (s, 3H), 1.26 (s, 3H) ppm.
^{13}**C-NMR** ($CDCl_3$, 101 MHz): δ = 157.24, 157.22, 143.73, 143.68, 141.85, 141.55, 141.47, 140.96, 139.53, 139.32, 138.02, 137.41, 131.22, 130.96, 130.75, 130.49, 129.89, 129.78, 129.35 (2C), 129.32 (2C), 128.55, 128.42, 128.30, 127.74, 126.23 (2C), 126.20 (2C), 123.52, 123.46, 114.90, 114.79, 114.72, 114.60, 55.42, 54.81, 21.32, 21.29, 18.99, 18.25 ppm.
HRMS (ESI): *calc. for $C_{21}H_{21}O_2S^+$ 337.1257* ; found 337.1251

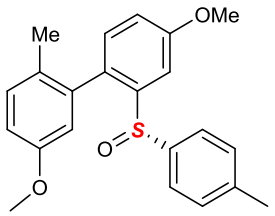

(*S*)-4,5'-dimethoxy-2'-methyl-2-(*p*-tolylsulfinyl)-1,1'-biphenyl
Chemical Formula: $C_{22}H_{22}O_3S$
Molecular Weight: 366,4750

(*S*)-4,5'-dimethoxy-2'-methyl-2-(*p*-tolylsulfinyl)-1,1'-biphenyl: The general procedure was followed at 100 °C for 3 hours, from (*S*)-1-bromo-4-methoxy-2-(*p*-tolylsulfinyl)benzene (1 eq., 200 mg, 0.615 mmol) in water (6 mL) yielding (S)-5'-methoxy-2',4-dimethyl-2-(p-tolylsulfinyl)-1,1'-biphenyl (194 mg, 0.529 mmol, 86%) as a colorless oil.
Mixture of two atropisomer (1 : 1) on the NMR time scale.
^{1}H-NMR ($CDCl_3$, 400 MHz) : δ = 7.81 (d, J = 2.6 Hz, 1H), 7.76 (d, J = 2.1 Hz, 1H), 7.17 (d, J = 8.4 Hz, 1H), 7.08 – 6.95 (m, 10H), 6.96 – 6.89 (m, 3H), 6.89 – 6.79 (m, 3H), 5.86 (d, J = 2.7 Hz, 1H), 3.96 (s, 3H), 3.95 (s, 3H), 3.83 (s, 3H), 3.51 (s, 3H), 2.30 (s, 3H), 2.29 (s, 3H), 2.15 (s, 3H), 1.23 (s, 3H) ppm.

^{13}C-NMR ($CDCl_3$, 101 MHz): δ = 159.86, 159.78, 157.22, 157.21, 144.77, 144.60, 141.65, 141.62, 141.57, 140.70, 137.76, 137.17, 131.74, 131.62, 131.32, 131.15, 131.04, 130.86, 129.34 (2C), 129.31 (2C), 129.01, 128.20, 126.27 (2C), 126.19 (2C), 117.37, 116.65, 115.38, 115.12, 114.55, 114.44, 107.50, 107.36, 55.69 (2C), 55.40, 54.78, 21.32, 21.30, 19.01, 18.26 ppm.
HRMS (ESI): *calc. for $C_{22}H_{22}LiO_3S^+$ 373.1445*; found 373.1457

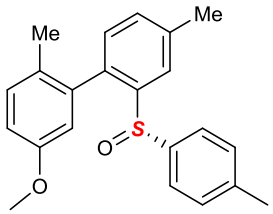

(*S*)-5'-methoxy-2',4-dimethyl-2-(*p*-tolylsulfinyl)-1,1'-biphenyl
Chemical Formula: $C_{22}H_{22}O_2S$
Molecular Weight: 350,4760

(*S*)-5'-methoxy-2',4-dimethyl-2-(*p*-tolylsulfinyl)-1,1'-biphenyl: The general procedure was followed at 100 °C for 3 hours, from (*S*)-1-bromo-4-methyl-2-(p-tolylsulfinyl)benzene (1 eq., 710 mg, 2.3 mmol) in water (11.5 mL) yielding (S)-5'-methoxy-2',4-dimethyl-2-(p-tolylsulfinyl)-1,1'-biphenyl (556 mg, 1.59 mmol, 69%) as a white solid (purified by recrystallization in a 95:5 mixture of heptane/toluene : 80°C to 4-6 °C).
Mixture of two atropisomer (1 : 1.05) on the NMR time scale.
^{1}H-NMR ($CDCl_3$, 400 MHz) : δ = 8.05 (t, J = 0.7 Hz, 1H), 8.00 (d, 1H), 7.30 (dd, J = 7.5, 1.0 Hz, 1H), 7.25 (dd, J = 6.1, 1.3 Hz, 1H), 7.17 (d, J = 8.5 Hz, 1H), 7.06 (d, J = 8.2 Hz, 2H), 7.04 – 6.98 (m, 6H), 6.96 (d, J = 8.3 Hz, 1H), 6.93 (d, J = 8.2 Hz, 2H), 6.88 (d, J = 2.6 Hz, 1H), 6.85 (dd, J = 8.3, 2.8 Hz, 1H), 6.82 (dd, J = 8.7, 2.7 Hz, 1H), 5.90 (d, J = 2.7 Hz, 1H), 3.84 (s, 3H), 3.52 (s, 3H), 2.51 (s, 3H), 2.51 (s, 3H), 2.31 (s, 3H), 2.29 (s, 3H), 2.15 (s, 3H), 1.26 (s, 3H) ppm.
^{13}C-NMR ($CDCl_3$, 101 MHz): δ = 157.08 (2C), 143.09, 143.01, 141.78, 141.34, 141.26, 140.90, 138.44, 138.34, 137.93, 137.31, 136.51, 136.23, 131.42, 131.04, 130.75, 130.57, 130.31, 129.60, 129.21 (2C), 129.18 (2C), 128.57, 127.73, 126.05 (2C), 126.02 (2C), 123.53, 115.04, 114.79, 114.40, 114.30, 55.24, 54.65, 21.23, 21.19 (2C), 21.16, 18.89, 18.17 ppm.
HRMS (ESI): *calc. for $C_{22}H_{23}O_2S^+$ 351.1413*; found 351.1413

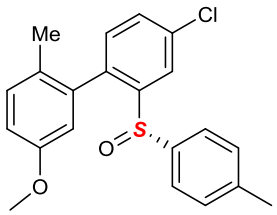

(*S*)-4-chloro-5'-methoxy-2'-methyl-2-(*p*-tolylsulfinyl)-1,1'-biphenyl
Chemical Formula: $C_{21}H_{19}ClO_2S$
Molecular Weight: 370,8910

(*S*)-4-chloro-5'-methoxy-2'-methyl-2-(*p*-tolylsulfinyl)-1,1'-biphenyl: The general procedure was followed at 100 °C for 3 hours, from (*S*)-1-bromo-4-chloro-2-(p-tolylsulfinyl)benzene (1 eq., 1.25 g, 3.79 mmol) in water (19 mL), yielding (*S*)-4-chloro-5'-methoxy-2'-methyl-2-(p-tolylsulfinyl)-1,1'-biphenyl (1.25 g, 3.37 mmol, 89%) as a colorless oil.
Mixture of two atropisomer (1 : 1) on the NMR time scale.
^{1}H-NMR ($CDCl_3$, 400 MHz) : δ = 8.25 (d, J = 2.2 Hz, 1H), 8.20 (d, J = 2.2 Hz, 1H), 7.46 (dd, J = 8.0, 2.2 Hz, 1H), 7.42 (dd, J = 8.0, 2.2 Hz, 1H), 7.19 (d, J = 8.5 Hz, 1H), 7.07 (d, J = 7.9 Hz, 3H), 7.06 (d, J = 8.0 Hz, 1H), 7.02 (d, J = 8.0 Hz, 2H), 6.97 (d, J = 8.1 Hz, 3H), 6.90 (d, J = 8.1 Hz, 2H), 6.88 – 6.82 (m, 3H), 5.82 (d, J = 2.8 Hz, 1H), 3.84 (s, 3H), 3.52 (s, 3H), 2.32 (s, 3H), 2.30 (s, 3H), 2.15 (s, 3H), 1.21 (s, 3H) ppm.
^{13}C-NMR ($CDCl_3$, 101 MHz): δ = 157.22, 157.19, 145.67, 145.61, 141.88, 141.81, 140.94, 140.04, 137.59, 137.36, 136.69, 136.13, 134.78, 134.66, 131.77, 131.27, 131.10, 130.98, 130.79, 129.93, 129.33 (2C), 129.31 (2C), 128.38, 127.40, 126.11 (2C), 126.07 (2C), 123.43, 123.34, 114.85, 114.76, 114.73, 114.50, 55.27, 54.67, 21.21, 21.19, 18.80, 18.02. ppm.
HRMS (ESI): *calc. for $C_{21}H_{20}ClO_2S^+$ 371.0867*; found 371.0876

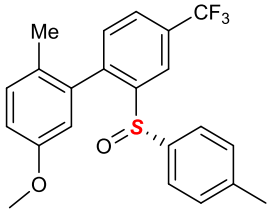

(*S*)-5'-methoxy-2'-methyl-2-(*p*-tolylsulfinyl)-4-(trifluoromethyl)-1,1'-biphenyl
Chemical Formula: $C_{22}H_{19}F_3O_2S$
Molecular Weight: 404,4472

(*S*)-5'-methoxy-2'-methyl-2-(*p*-tolylsulfinyl)-4-(trifluoromethyl)-1,1'-biphenyl: The general procedure was followed at 100 °C for 3 hours, from (*S*)-1-bromo-2-(p-tolylsulfinyl)-4-(trifluoromethyl)benzene (1 eq., 1278 mg, 3.52 mmol) in water (17.5 mL) (*S*)-5'-methoxy-2'-methyl-2-(p-tolylsulfinyl)-4-(trifluoromethyl)-1,1'-biphenyl (1.24 g, 3.07 mmol, 87%).

^{1}H-NMR ($CDCl_3$, 400 MHz) : δ = 8.55 (d, J = 1.4 Hz, 1H), 8.51 (d, J = 1.6 Hz, 1H), 7.75 (dd, J = 7.8, 1.1 Hz, 1H), 7.70 (dd, J = 7.7, 1.5 Hz, 1H), 7.25 (dd, J = 8.2, 1.6 Hz, 2H), 7.18 (d, J = 8.5 Hz, 1H), 7.04 (d, J = 8.0 Hz, 2H), 7.00 (d, J = 8.0 Hz, 2H), 6.97 (d, J = 8.5 Hz, 1H), 6.95 – 6.88 (m, 3H), 6.88 – 6.84 (m, 3H), 6.83 (d, J = 2.7 Hz, 1H), 5.76 (d, J = 2.7 Hz, 1H), 3.81 (s, 3H), 3.47 (s, 3H), 2.28 (s, 3H), 2.27 (s, 3H),

2.12 (s, 3H), 1.18 (s, 3H) ppm. **^{13}C-NMR** ($CDCl_3$, 101 MHz): δ = 157.22, 157.13, 145.15, 145.08, 142.81 (q, J = 1 Hz), 142.61 (q, J = 1.1 Hz), 141.99, 141.92, 140.44, 139.57, 136.28, 135.73, 131.30, 130.98, 130.94, 130.55 (q, J = 33.3 Hz), 130.42 (d, J = 33.2 Hz), 130.31, 129.21 (2C), 129.20 (2C), 127.96, 127.30 (q, J = 3.6 Hz), 126.74, 126.35 (q, J = 3.5 Hz), 126.05 (2C), 125.99 (2C), 123.46 (q, J = 272.8 Hz), 123.45 (q, J = 272.8 Hz), 120.43 (q, J = 3.7 Hz), 120.24 (q, J = 3.9 Hz), 114.94, 114.69, 114.50, 113.92, 54.96, 54.34, 20.88, 20.86, 18.43, 17.67 ppm. **^{19}F-NMR** ($CDCl_3$, 125.6 MHz): δ = -62.49, -62.50 ppm. **HRMS (ESI):** *calc. for $C_{21}H_{19}F_3NaO_2S^+$ 472.0950*; found 472.0956

e) Preparation of other di-ortho substituted biphenyls

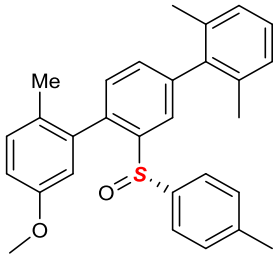

(*S*)-5-methoxy-2,2'',6''-trimethyl-2'-(*p*-tolylsulfinyl)-1,1':4',1''-terphenyl
Chemical Formula: $C_{29}H_{28}O_2S$
Molecular Weight: 440,6010

(*S*)-5-methoxy-2,2'',6''-trimethyl-2'-(*p*-tolylsulfinyl)-1,1':4',1''-terphenyl: (*S*)-4-chloro-5'-methoxy-2'-methyl-2-(p-tolylsulfinyl)-1,1'-biphenyl (1 eq., 300 mg, 0.809 mmol) was loaded in a schlenk along with 2,6-dimethylphenylboronic acid (3 eq., 364 mg, 2.43 mmol), K_3PO_4 (4 eq., 687 mg, 3.24 mmol), SPhos (10.4 %, 34.5 mg, 0.084 mmol) and $Pd_2(dba)_3$ (2.63 %, 19.5 mg, 0.0213 mmol). 4 vacuum-argon cycles were performed and toluene (9 mL) was added. The reaction was stirred at 100 °C for 8 h., when LC-MS showed complete conversion. The reaction was filtered on a silica gel pad (washed with Et_2O) and the solvent was removed under reduced pressure. Subsequent flash chromatography afforded (*S*)-5-methoxy-2,2'',6''-trimethyl-2'-(*p*-tolylsulfinyl)-1,1':4',1''-terphenyl (295 mg, 0.67 mmol, 83%) as a white powder. Mixture of two atropisomer (1 : 1.05) on the NMR time scale. **^{1}H-NMR** ($CDCl_3$, 400 MHz) : δ = 8.06 (d, *J* = 1.6 Hz, 1H), 8.02 (d, *J* = 1.6 Hz, 1H), 7.31 (dd, *J* = 7.6, 1.7 Hz, 1H), 7.26 (dd, *J* = 7.6, 1.6 Hz, 1H), 7.23 (s, 1H), 7.22 – 7.17 (m, 4H), 7.14 (d, *J* = 7.3 Hz, 4H), 7.08 (d, *J* = 8.0 Hz, 2H), 7.05 – 6.97 (m, 6H), 6.93 (d, *J* = 8.2 Hz, 2H), 6.90 (dd, *J* = 8.3, 2.8 Hz, 1H), 6.86 (dd, *J* = 8.4, 2.7 Hz, 1H), 5.99 (d, *J* = 2.7 Hz, 1H), 3.88 (s, 3H), 3.56 (s, 3H), 2.32 (s, 3H), 2.30 (s, 3H), 2.22 (s, 3H), 2.13 (s, 3H), 2.10 (s, 3H), 2.08 (s, 3H), 2.05 (s, 3H), 1.31 (s, 3H) ppm. **^{13}C-NMR** ($CDCl_3$, 101 MHz): δ = 157.20, 143.74, 141.96, 141.46, 141.42, 141.40, 141.33, 141.03, 140.42, 140.34, 137.82, 137.69, 137.53, 137.23, 135.85, 135.81, 135.62, 135.57, 131.47, 131.15, 130.91, 130.58, 130.55, 129.85, 129.28 (2C), 129.27 (2C), 128.57, 127.76, 127.38 (2C), 127.36, 127.35, 127.23 (2C), 126.11 (2C),

126.00 (2C), 124.03, 123.99, 114.93, 114.77, 114.67, 114.64, 55.35, 54.78, 21.23, 21.21, 20.88, 20.87, 20.76, 20.74, 18.94, 18.22 ppm.

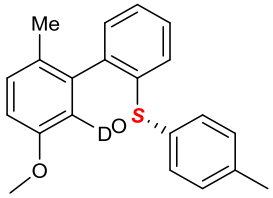

(*S*)-5-methoxy-2-methyl-2'-(*p*-tolylsulfinyl)-1,1'-biphenyl-6-*d*
Chemical Formula: $C_{21}H_{19}DO_2S$
Molecular Weight: 337,4551

(*S*)-5-methoxy-2-methyl-2'-(*p*-tolylsulfinyl)-1,1'-biphenyl-6-d : (*S*)-5-methoxy-2-methyl-2'-(p-tolylsulfinyl)-1,1'-biphenyl (1 eq., 125 mg, 0.372 mmol), $Pd(OAc)_2$ (15 mol%, 12.5 mg, 0.0557 mmol) and 4 Å powered molecular sieves (415 mg) were loaded in a sealed vial and flushed with argon. Then AcOD (5 mL) was added under argon and the resulting heterogenous mixture was stirred at 85°C for 18 hours. It was then diluted with DCM, filtrated on a celite pad and the solvent was removed under reduced pressure. Subsequent flash chromatography yielded (*S*)-5-methoxy-2-methyl-2'-(p-tolylsulfinyl)-1,1'-biphenyl-6-*d* (124 mg, 0.368 mmol, 99 %), proton MR showed more than 95% deuterium incorporation. Mixture of two atropisomer (1 : 1) on the NMR time scale. ^{1}**H-NMR** ($CDCl_3$, 400 MHz) : δ = 8.25 (d, J = 7.8 Hz, 1H), 8.21 (d, J = 7.7 Hz, 1H), 7.67 – 7.56 (m, 2H), 7.50 (td, J = 7.4, 0.9 Hz, 1H), 7.46 (t, J = 7.4 Hz, 1H), 7.19 (d, J = 8.4 Hz, 1H), 7.13 (d, j = 7.5 Hz, 2H), 7.09 – 7.04 (***A₁A₁'***B_1B_1', 2H), 7.03 – 6.95 (m, 5H), 6.95 – 6.90 (A_1A_1'***B₁B₁'***, 2H), 6.86 (d, J = 12.1 Hz, 1H), 6.84 (d, J = 12.1 Hz, 1H), 3.84 (s, 3H), 3.52 (s, 3H), 2.30 (s, 3H), 2.29 (s, 3H), 2.15 (s, 3H), 1.26 (s, 3H) ppm.

General Procedure 1 (GP1)*: (Dioxane was degased by 3 freeze-pump-thaw cycles)* In a flame-dried Schlenk tube were added the bromoarylsulfoxide (1 equiv), $Pd(OAc)_2$ (10 mol%) and diphenylphosphine ferrocenium (dppf) (0.3 equiv), followed by degassed dioxane ([substrate] = 0.25 M). The mixture was stirred for 30 min. Meanwhile, a solution of the adequate boronic acid (2.2 equiv) and CsF (4 equiv) in degassed dioxane ([boronic acid] = 0.25 M) was prepared and stirred for 30 min., when the pre-catalyst solution was cannulated to the boronic acid solution. The reaction mixture was stirred at reflux and followed by TLC. The mixture was allowed to cooled down to room temperature and worked-up with EtOAc and water. The crude product then was purified by flash column chromatography on silica gel.

General Procedure 2 (GP2): A microwave vial was successively charged with bromoarylsulfoxide (1.0 equiv), boronic acid (1.1–1.5 equiv), $Pd(PPh_3)_4$ (3-5 mol%), K_2CO_3 (4.0 equiv). Dioxane ([substrate] = 0.085 M) and H_2O ([substrate] = 0.33 M)

were added. The reaction mixture was heated in microwave at 110 °C (low absorption level) until an analysis of an aliquot by TLC indicated complete conversion of the biaryl substrates (2–3 h). The reaction was quenched with saturated NH_4Cl solution. Aqueous phase was extracted with ethyl acetate, the combined organic phase was washed with brine, dried over Na_2SO_4, filtrated and concentrated under vacuum to furnish the crude biaryl substrates 1a–1n. Purification by flash column chromatography on silica gel using afforded the analytically pure biaryl compounds.

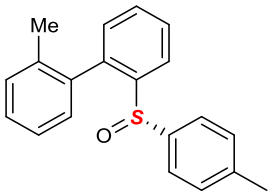

(*S*)-2-methyl-2'-(*p*-tolylsulfinyl)-1,1'-biphenyl
Chemical Formula: $C_{20}H_{18}OS$
Molecular Weight: 306,4230

(*S*)-2-Methyl-2'-(*p*-tolylsulfinyl)-1,1'-biphenyl : Prepared from (*S*)-1-bromo-2-(*p*-tolylsulfinyl)benzene (1 equiv, 1 g, 3.4 mmol) according to GP1, using $Pd(OAc)_2$ (10 mol%, 77 mg, 0.343 mmol), 2-tolylboronic acid (2.4 equiv, 1.09 g, 8.02 mmol), CsF (4 equiv, 2.03 g, 13.4 mmol), and dppf (0.31 equiv, 0.58 g, 1.03 mmol), in dioxane (44 mL). The reaction mixture was stirred at reflux overnight and the crude product was purified by flash chromatography on silica gel (EtOAc/*c*-Hex 1:3) to afford (*S*)-2-methyl-2'-(*p*-tolylsulfinyl)-1,1'-biphenyl (698 mg, 2.28 mmol, 67%) as white powder.

^{1}H-NMR (400 MHz, $CDCl_3$): δ = (*mixture of two atropodiastereomers 1:1.15*) 8.26 (dd, *J* = 7.9, 1.2 Hz, 1 H *major dia*), 8.18 (dd, *J* = 7.9, 1.3 Hz, 1 H *minor dia*), 7.64–7.58 (m, 1 H *major dia*, 1 H *minor dia*), 7.52–7.44 (m, 1 H *major dia*, 1 H *minor dia*), 7.36–7.27 (m, 3 H *major dia*, 2 H *minor dia),* 7.14-6.94 (m, 4 H *major dia*, 6 H *minor dia*), 6.87 (d, *J* = 8.2 Hz, 2 H *major dia*), 6.50 (d, *J* = 7.4 Hz, 1 H *minor dia),* 2.31 (s, 3 H *minor dia*), 2.29 (s, 3 H *major dia*), 2.25 (s, 3 H *minor dia*), 1.32 (s, 3 H, *minor dia*) ppm.
R_f (EtOAc/*c*-Hex 1:3) = 0.35.

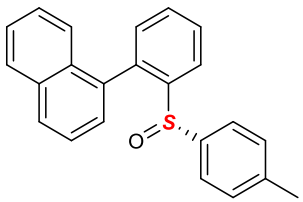

(*S*)-1-(2-(*p*-tolylsulfinyl)phenyl)naphthalene
Chemical Formula: $C_{23}H_{18}OS$
Molecular Weight: 342,4560

(*S*)-1-[2-(*p*-Tolylsulfinyl)phenyl]naphthalene : Prepared from (*S*)-1-bromo-2-(*p*-tolylsulfinyl)benzene (1 equiv, 0.985 g, 3.34 mmol), according to GP1, using 1-naphthaleneboronic acid (2.24 equiv, 1.29 g, 7.5 mmol), $Pd(OAc)_2$ (10.6 mol%, 80 mg, 0.356 mmol), dppf (0.32 equiv, 0.595 g, 1.07 mmol) and CsF (4.31 equiv, 2.23 g, 14.7 mmol) in dioxane (44 mL). Flash chromatography on silica gel (EtOAc/*c*-Hex

1:3) yielded (*S*)-1-[2-(*p*-tolylsulfinyl)phenyl]naphthalene (994 mg, 2.9 mmol, 87%) as yellow powder.

^{1}H-NMR (400 MHz, $CDCl_3$) : δ = (*mixture of two atropodiastereomers 1:1.6*) 8.30–8.28 (m, 1 H *major* / 1 H *minor dia*), 7.93–7.89 (m, 1 H *major* / 2 H *minor dia*), 7.79 (d, *J* = 8.2 Hz, 1 H *major dia*), 7.69 (t, *J* = 7.7 Hz, 1 H *major* / 1 H *minor dia*), 7.65–7.43 (m, 3 H *major* / 4 H *minor diar*), 7.34 (t, *J* = 7.4 Hz, 1 H *major* / 1 H *minor dia*), 7.30-7.24 (m, 1 H *major* / 1 H *minor dia*), 7.05 (d, *J* = 8.2 Hz, 2 H *minor dia*), 7.00–6.96 (m, 1 H *major dia*), 6.95 (d, *J* = 8.2 Hz, 2 H *minor dia*), 6.79–6.76 (m, 1 H *major* / 1 H *minor dia*), 6.62 (d, *J* = 8.2 Hz, 2 H *major dia*), 6.57 (d, *J* = 8.2 Hz, 2 H *major dia*), 2.30 (s, 3 H *minor dia*), 2.03 (s, 3 H *major dia*).
^{13}C-NMR (101 MHz, $CDCl_3$, *major and minor diastereomers reported together*): 145.3, 145.1, 142.4, 141.5, 141.2, 140.7, 138.5, 138.4, 135.6, 135.0, 133.7, 133.4, 132.0, 131.6, 131.6, 131.2, 131.1, 131.0, 130.1, 129.9, 129.6, 129.3, 129.1, 129.1, 128.9, 128.8, 128.8, 128.4, 128.3, 128.0, 127.9, 127.0, 126.4, 125.9, 125.9, 125.8, 125.6, 125.3, 125.1, 125.0, 125.0, 124.8, 124.3, 123.9, 21.5, 21.2 ppm.

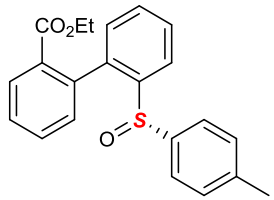

ethyl (*S*)-2'-(*p*-tolylsulfinyl)-[1,1'-biphenyl]-2-carboxylate
Chemical Formula: $C_{22}H_{20}O_3S$
Molecular Weight: 364,4590

(*S*)-Ethyl-2'-(*p*-tolylsulfinyl)-[1,1'-biphenyl]-2-carboxylate : Prepared from (*S*)-1-bromo-2-(*p*-tolylsulfinyl)benzene (1 equiv, 442 mg, 1.5 mmol), according to GP2, using [2-(ethoxycarbonyl)phenyl]boronic acid (1.4 equiv, 407 mg, 2.1 mmol), $Pd(PPh_3)_4$ (3.4 mol%, 59 mg, 0.051 mmol), K_2CO_3 (4.07 equiv, 843 mg, 6.1 mmol) in mixture of dioxane (12 mL) and water (3 mL). Flash chromatography (EtOAc/cyclohexane 1:2), yielded (*S*)-ethyl-2'-(*p*-tolylsulfinyl)-[1,1'-biphenyl]-2-carboxylate (278 mg, 0.76 mmol, 51%) as greenish oil.

^{1}H-NMR (400 MHz, $CDCl_3$): δ = *(mixture of two atropodiastereomer 1:1)* 8.16 (dd, *J* = 7.9, 1.2 Hz, 1 H), 8.12 (dd, *J* = 7.9, 1.2 Hz, 1 H), 8.05 (dd, *J* = 8, 1.1 Hz, 1 H), 7.93 (dd, *J* = 8.0, 1.1 Hz, 1 H), 7.64–7.39 (m, 8 H), 7.30 (dt, *J* = 7.3, 1.4 Hz, 1 H), 7.15 (dd, *J* = 7.5, 1.1 Hz, 1 H), 7.11 (dd, *J* = 7.5, 1.1 Hz, 1 H), 7.08-7.03 (m, 4 H), 7.02–6.93 (m, 4 H), 6.58 (dd, *J* = 7.6, 1.1 Hz, 1 H), 4.18–4.13 (ABX_3, *J* = 10.9, 7.2 Hz, 2 H), 3.81–3.62 (ABX_3, *J* = 10.9, 7.2 Hz, 2 H), 2.29 (s, 6 H), 1.03 (ABX_3, *J* = 7.2 Hz, 3 H), 0.76 (ABX_3, *J* = 7.2 Hz, 3 H) ppm.
^{13}C-NMR (101 MHz, $CDCl_3$): δ = 166.5, 166.1, 143.6, 142.8, 141.7, 141.5, 141.3, 140.7, 140.7, 140.0, 138.7, 138.5, 131.9, 131.9, 131.8, 131.7, 130.9, 130.7, 130.5, 130.4, 130.2, 130.2, 129.8, 129.5, 129.4, 129.3, 128.5, 128.4, 128.3, 128.3, 126.1, 125.9, 124.3, 123.0, 61.2, 60.4, 21.4, 21.4, 13.7, 13.5 ppm.
R_f (EtOAc/*c*-Hex 1:1) = 0.36.

IR (ATR): $\tilde{\nu}$ /cm^{-1} = 3052 (w), 2980 (w), 2923 (w), 1709 (s), 1597 (w), 1462 (m), 1442 (m), 1286 (s), 1254 (s), 1132 (m), 1083 (s), 1049 (s), 1048 (s), 1038 (s), 1015 (m), 1003 (m), 809 (m), 756 (s), 708 (m). **HRMS** (*ESI*) = 387.103 [M+Na$^+$]*, calcd.* for $C_{22}H_{20}O_3SNa^+$ = 387.103.

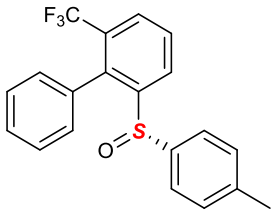

(*S*)-2-(*p*-tolylsulfinyl)-6-(trifluoromethyl)-1,1'-biphenyl
Chemical Formula: $C_{20}H_{15}F_3OS$
Molecular Weight: 360,3942

(*S*)-2-(*p*-Tolylsulfinyl)-6-(trifluoromethyl)-1,1'-biphenyl: Prepared from (*S*)-2-bromo-1-(*p*-tolylsulfinyl)-3-(trifluoromethyl)benzene (1 equiv, 500 mg, 1.38 mmol)), according to GP2, using phenylboronic acid (1.1 equiv, 185 mg, 1.51 mmol), $Pd(PPh_3)_4$ (5 mol%, 79.5 mg, 0.069 mmol), K_2CO_3 (4.0 equiv, 761.1 mg, 5.51 mmol) in mixture of dioxane (11 mL) and water (3 mL). Flash chromatography on silica gel (EtOAc/cyclohexane 1:4), yielded (*S*)-2-(*p*-tolylsulfinyl)-6-(trifluoromethyl)-1,1'-biphenyl (485 mg, 1.35 mmol, 98%) as light yellow solid.

^{1}H-NMR (400 MHz, $CDCl_3$) : δ = 8.44 (d, *J* = 7.8 Hz, 1H), 7.86 (d, *J* = 7.4 Hz, 1H), 7.75 (t, *J* = 7.9 Hz, 1H), 7.52–7.44 (m, 1H), 7.40 (2 overlapping d, *J* = 7.4 Hz, 2H), 7.15 (t, *J* = 7.6 Hz, 1H), 7.07 (d, *J* = 8.0 Hz, 2H), 6.94 (d, *J* = 8.2 Hz, 2H), 6.52 (d, *J* = 7.7 Hz, 1H), 2.32 (s, 3H) ppm. **^{13}C-NMR** ($CDCl_3$, 101 MHz): δ = 147.5, 142,6, 141.4, 139.5 (q, J_{CF} = 1.5 Hz), 133.7, 131,0 (q, J_{CF} = 1.4 Hz), 130.3 (q, J_{CF} = 30.1 Hz), 130.2 (1 C + 2 C_{pTol}), 129.2, 129.1, 128.7 (q, J_{CF} = 5.1 Hz), 128.4, 128.2, 127.9, 126.9 (2 C_{pTol}), 123.8 (q, J_{CF} = 277.3 Hz), 21.2 ppm. **^{19}F-NMR** ($CDCl_3$, 377 MHz): –57.7 ppm. **R_f** (EtOAc:*c*-hex 1:3) = 0.36. **IR** (ATR): $\tilde{\nu}$ /cm^{-1} = 3060 (w), 2918 (w), 1595 (w), 1432 (m), 1311 (s), 1137 (s), 1084 (s), 1069 (s), 1044 (s), 811 (s), 772 (s), 750 (s), 698 (s), 512 (s).

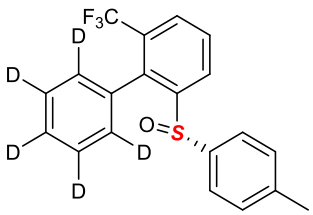

(*S*)-2-(*p*-tolylsulfinyl)-6-(trifluoromethyl)-1,1'-biphenyl-2',3',4',5',6'-d_5
Chemical Formula: $C_{20}H_{10}D_5F_3OS$
Molecular Weight: 365,4247

(*S*)-2-(*p*-Tolylsulfinyl)-6-(trifluoromethyl)-1,1'-biphenyl-2',3',4',5',6'-d5 [(*S*)-1h]: Prepared from (*S*)-2-bromo-1-(*p*-tolylsulfinyl)-3-(trifluoromethyl)benzene (1 equiv, 500 mg, 1.38 mmol), according to GP2, using d_5-phenylboronic acid (1.1 equiv, 192.3 mg, 1.51 mmol), $Pd(PPh_3)_4$ (5 mol%, 79.5 mg, 0.069 mmol), K_2CO_3 (4.0 equiv, 761.1 mg, 5.51 mmol) in mixture of dioxane (11 mL) and water (3 mL). Flash chromatography on silica gel (EtOAc/cyclohexane 1 : 4), yielded (*S*)-2-(*p*-tolylsulfinyl)-6-(trifluoromethyl)-1,1'-biphenyl-2',3',4',5',6'-d5 (455 mg, 1.25 mmol, 90%) as light yellow solid.

^{1}H-NMR (400 MHz, $CDCl_3$): δ = 8.44 (d, *J* = 7.9 Hz, 1H), 7.86 (d, *J* = 7.8 Hz, 1H), 7.75 (t, *J* = 7.9 Hz, 1H), 7.07 (d, *J* = 8.0 Hz, 2H), 6.94 (d, *J* = 8.1 Hz, 2H), 2.32 (s, 3H).
^{13}C-NMR ($CDCl_3$, 101 MHz): δ = 147.5, 142.6, 141.5, 139.5 (q, J_{CF} = 1.4 Hz), 133.5, 130.3 (q, J_{CF} = 30.4 Hz), 130.1 (2 C_{pTol}), 129.2, 128.7 (q, J_{CF} = 5.2 Hz), 127.9, 126.8 (2 C_{pTol}), 123.8 (q, J_{CF} = 277 Hz), 21.2.
^{19}F-NMR ($CDCl_3$, 377 MHz): –57.8 ppm.
R_f ((EtOAc:*c*-hex 1:3) = 0.34.
IR (ATR): $\tilde{\nu}$ /cm^{-1} = 3078 (w), 2921 (w), 1595 (w), 1438 (w), 1373 (w), 1306 (s), 1182 (m), 1163 (m), 1136 (s), 1067 (s), 1042 (s), 809 (s), 751 (s), 695 (m), 623 (m), 505 (s).

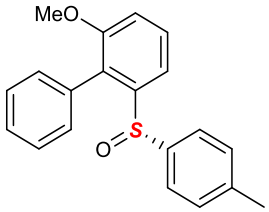

(*S*)-2-methoxy-6-(*p*-tolylsulfinyl)-1,1'-biphenyl
Chemical Formula: $C_{20}H_{18}O_2S$
Molecular Weight: 322,4220

(*S*)-2-Methoxy-6-(*p*-tolylsulfinyl)-1,1'-biphenyl : Prepared from (*S*)-2-bromo-1-methoxy-3-(*p*-tolylsulfinyl)benzene (1 equiv, 345 mg, 1.01 mmol), according to GP2, using phenylboronic acid (1.1 equiv, 141 mg, 1.16 mmol), $Pd(PPh_3)_4$ (5 mol%, 61.2 mg, 0.053 mmol), K_2CO_3 (3.8 equiv, 554 mg, 4.01 mmol) in mixture of dioxane (8 mL) and water (3 mL). Flash chromatography on silica gel (EtOAc/cyclohexane 1:3), yielded (*S*)-2-methoxy-6-(*p*-tolylsulfinyl)-1,1'-biphenyl (323 mg, 1 mmol, 95%) as a white powder.

^{1}H-NMR (400 MHz, $CDCl_3$): δ = 7.80 (d, *J* = 7.8 Hz, 1H), 7.55 (t, *J* = 8.1 Hz, 1 H), 7.45 (brd, 2 H), 7.37 (t, *J* = 7.3 Hz, 1 H), 7.24 (brd, 1 H), 7.05 (d, *J* = 7.9 Hz, 1 H), 7.03 (d, *J* = 8.2 Hz, 2 H), 6.96 (d, *J* = 8.2 Hz, 2 H), 6.73 (brd, 1 H), 3.7 (s, 3 H), 2.29 (s, 3 H).
R_f (Et_2O/*n*-Pentane 1:1) = 0.42.

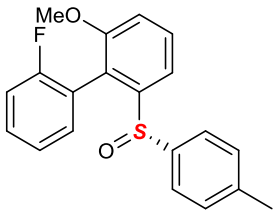

2'-fluoro-2-methoxy-6-((*S*)-*p*-tolylsulfinyl)-1,1'-biphenyl
Chemical Formula: $C_{20}H_{17}FO_2S$
Molecular Weight: 340,4124

(*S*)-2'-Fluoro-2-methoxy-6-(*p*-tolylsulfinyl)-1,1'-biphenyl: Prepared from (*S*)-2-bromo-1-methoxy-3-(*p*-tolylsulfinyl)benzene (1.00 equiv, 488 mg, 1.5 mmol) according to GP 2 for 2 h by using (2-fluorophenyl)boronic-acid (1.30 equiv, 273 mg, 1.95 mmol), $Pd(PPh_3)_4$ (5 mol%, 87 mg, 0.075 mmol), K_2CO_3 (4.0 equiv, 829 mg, 6.0 mmol), dioxane (13 mL) and water (3.5 mL). Purification by flash column chromatography on silica gel using mixture of cyclohexane and ethyl acetate (1/1, v/v) afforded the title compound [(*S*)-1j, 488 mg, 1.43 mmol, 96%, *dr* = 62:38] as a yellow solid.

^{1}H-NMR ($CDCl_3$, 400 MHz): [(Minor isomer integrate for 1.0, major isomer integrate for 1.63; expected ^{1}H integration of major and minor isomer is 45 (17+17*1.6 = 45)] δ = (*mixture of two atropodiastereomers 1:1.6*) 7.82 (d, *J* = 7.9 Hz, 1H), 7.74 (d, *J* = 7.9 Hz, 1.6H), 7.64–7.55 (m, 2.7H), 7.45–7.34 (m, 4.4H), 7.26–7.20 (m, 2.8H), 7.12–6.97 (m, 13.9H), 7.92 (t, *J* = 8.7 Hz, 1.6H), 7.66 (t, *J* = 7.0 Hz, 1H), 3.75 (s, 4.8H), 3.72 (s, 3H), 2.31 (s, 7.9H) ppm.
^{13}C-NMR ($CDCl_3$, 101 MHz): δ = (*mixture of two atropodiastereomers 1:1.63*) 160.5 (d, *J* = 248.2 Hz), 159.4 (d, *J* = 247.7 Hz), 157.3, 157.1, 146.4, 146.1, 142.2, 141.7, 141.3, 133.4 (d, *J* = 2.9 Hz), 132.2 (d, *J* = 2.9 Hz), 130.5, 130.4, 130.4, 130.4, 130.3, 130.2, 129.7 (2 $C_{p\text{Tol}}$), 129.6, 126.0, 125.9 (2 $C_{p\text{Tol}}$), 124.1 (d, *J* = 3.5 Hz), 123.7 (d, *J* = 3.5 Hz), 123.1, 121.5 (d, *J* = 16.9 Hz), 121.0 (d, *J* = 16.1 Hz), 116.3, 116.1 (d, *J* = 22.3 Hz), 115.9, 115.5 (d, *J* = 22.3 Hz), 113.5, 113.1, 56.3, 56.2, 31.1, 21.5 ppm.
^{19}F-NMR ($CDCl_3$, 377 MHz): –112.3, –112.8 ppm.
R_f (EtOAc:*c*-hex = 1:1): 0.44.
IR (ATR): $\tilde{\nu}$ /cm^{-1} = 3058 (w), 2940 (w), 2838 (w), 1586 (s), 1497 (m), 1463 (m), 1432 (m), 1261 (s), 1210 (m), 1154 (m), 1081 (m), 1030 (s), 822 (m), 789 (m), 759 (s), 503 (s).
HRMS: 363.0810 $[M+Na]^+$, *calcd*. for $C_{20}H_{17}FNaO_2S$ = 363.0825.

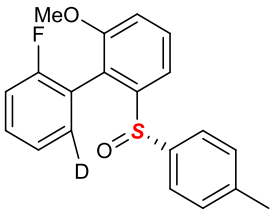

2'-fluoro-2-methoxy-6-((*S*)-*p*-tolylsulfinyl)-1,1'-biphenyl-6'-*d*
Chemical Formula: $C_{20}H_{16}DFO_2S$
Molecular Weight: 341,4185

(*S*)-2'-Fluoro-2'-deautero-2-methoxy-6-(*p*-tolylsulfinyl)-1,1'-biphenyl [(*S*)-6'-D-1j]: Prepared from (*S*)-2'-fluoro-2-methoxy-6-(*p*-tolylsulfinyl)-1,1'-biphenyl, a sealed tube, under argon, was charged with (*S*)-2'-fluoro-2-methoxy-6-(*p*-tolylsulfinyl)-1,1'-biphenyl (1.0 equiv, 187 mg, 0.55 mmol), $Pd(OAc)_2$ (10 mol%, 12.4 mg, 0.055 mmol). CD_3COOD (2.0 mL) was added. The reaction mixture was stirred at 60 °C for 48 h. The mixture was quenched with saturated NH_4Cl solution. Aqueous phase was extracted with ethyl acetate, the combined organic phase was washed with brine, dried over Na_2SO_4, filtrated and concentrated under vacuum to furnish the crude product. Purification by flash column chromatography on silica gel using mixtures of cyclohexane and ethyl acetate (1/1, v/v) afforded the analytically pure product [(*S*)-6'-D-1j, 156.9 mg, 0.46 mmol, 84%, *dr* = 65:35] as a yellow colored solid.

^{1}H-NMR ($CDCl_3$, 400 MHz): [(Minor isomer integrate for 1.0, major isomer integrate for 1.85; expected ^{1}H integration of major and minor isomer is 45 (16+16*1.85 = 45.6)] δ = (*mixture of two atropodiastereomers 1:1.89*) 7.82 (dd, *J* = 8.2, 1.0 Hz, 1H), 7.74 (dd, *J* = 7.9, 1.0 Hz, 1.89H), 7.64–7.56 (m, 3H), 7.44–7.34 (m, 3.13H), 7.30–7.25 (m, 1H), 7.20 (td, *J* = 8.9, 1.0 Hz, 1H), 7.09–7.03 (m, 10.3H), 7.02–6.97 (m, 5.3H), 7.91 (td, *J* = 9.0, 1.2 Hz, 1.88H), 3.74 (s, 5.7H), 3.72 (s, 3H), 2.30 (s, 8.7H) ppm.
^{13}C-NMR ($CDCl_3$, 101 MHz): δ = (*mixture of two atropodiastereomers 1:1.85*) 160.0 (d, *J* = 248.2 Hz), 159.4 (d, *J* = 247.7 Hz), 157.3, 157.1, 146.3, 145.9, 142.1, 141.7, 141.2, 132.2, 131.9, 130.5 (d, *J* = 8.4 Hz), 130.4, 130.3 (d, *J* = 5.9 Hz), 129.7 (2 $C_{p\text{Tol}}$), 129.7, 126.0, 125.9 (2 $C_{p\text{Tol}}$), 124.0 (d, *J* = 3.5 Hz), 123.6 (d, *J* = 3.6 Hz), 123.0, 122.1, 121.4 (d, *J* = 17.1 Hz), 120.9 (d, *J* = 16.3 Hz), 116.3, 116.0 (d, *J* = 21.8 Hz), 115.9, 115.5 (d, *J* = 22.4 Hz), 113.5, 113.1, 56.3, 56.2, 29.8, 21.5 ppm.
^{19}F-NMR ($CDCl_3$, 377 MHz): –112.3, –112.8 ppm.
R_f (EtOAc: *c*-hex = 1:1): 0.44.
IR (ATR): $\tilde{\nu}$ /cm^{-1} = 3056 (w), 2923 (w), 2838 (w), 1586 (s), 1463 (w), 1485 (m), 1446 (s), 1431 (s), 1263 (s), 1242 (s), 1154 (m), 1177 (m), 1031 (s), 801 (s), 788 (s), 729 (s), 622 (m), 501 (s).
HRMS: 364.0881 $[M+Na]^+$, *calcd*. for $C_{20}H_{16}DFNaO_2S$ = 364.0888.

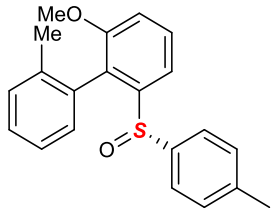

2-methoxy-2'-methyl-6-((*S*)-*p*-tolylsulfinyl)-1,1'-biphenyl
Chemical Formula: $C_{21}H_{20}O_2S$
Molecular Weight: 336,4490

(***S*)-2-Methoxy-2'-methyl-6-(*p*-tolylsulfinyl)-1,1'-**biphenyl: Prepared from (*S*)-2-bromo-1-methoxy-3-(*p*-tolylsulfinyl)benzene (1.0 equiv, 325 mg, 1.0 mmol) according to GP2, for 3 h by using $Pd(PPh_3)_4$ (5 mol%, 58 mg, 0.05 mmol), K_2CO_3 (4.0 equiv, 553 mg, 4.0 mmol), *o*-tolylboronic acid (1.5 equiv, 204 mg, 1.5 mmol), dioxane (12

mL) and water (3 mL). Purification by flash column chromatography on silica gel using mixture of cyclohexane and ethyl acetate (1/1, v/v) afforded the title compound [(*S*)-1k, 302.5 mg, 0.90 mmol, 90%, *dr* = 67:33] as a white solid.

^{1}H-NMR ($CDCl_3$, 400 MHz): [(Minor isomer integrate for 1.0, major isomer integrate for 2.0; expected ^{1}H integration of major and minor isomer is 60 (3*20 = 60)] δ = (*mixture of two atropodiastereomers 1:2*) 7.88 (d, *J* = 7.9 Hz, 2H), 7.79 (d, *J* = 7.9 Hz, 1H), 7.65–7.51 (m, 3H), 7.36–7.29 (m, 8H), 7.12–6.96 (m, 14H), 6.85 (d, *J* = 8.1 Hz, 4H), 6.44 (s, 1H), 3.71 (s, 9H), 2.32 (s, 3H), 2.29 (s, 6H), 2.18 (s, 3H), 1.22 (s, 6H) ppm.
^{13}C-NMR ($CDCl_3$, 101 MHz): δ = (*mixture of two atropodiastereomers 1:2*) 156.8, 156.8, 145.5, 142.0, 141.8, 141.7, 141.0, 138.7, 136.8, 133.1, 132.8, 131.5, 130.6, 130.3, 130.2 129.9, 129.7, 129.6, 129.5, 129.5, 128.7, 128.4, 128.1, 126.6, 126.4, 125.8, 125.4, 125.1, 116.0, 115.5, 113.4, 112.7, 56.2, 56.0, 21.6, 21.5, 20.2, 18.8 ppm.
R_f (EtOAc: *c*-hex = 1:1): 0.42.
IR (ATR): $\tilde{\nu}$ /cm^{-1} = 3056 (w), 3016 (w), 2834 (w), 1594 (m), 1462 (m), 1428 (m), 1263 (s), 1173 (s), 1083 (m), 1033 (s), 765 (s), 739 (s), 590 (m), 509 (s).
HRMS: 359.1074 $[M+Na]^+$, *calcd*. for $C_{21}H_{20}NaO_2S$ = 359.1076.

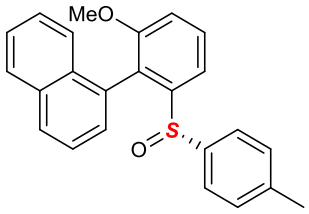

1-(2-methoxy-6-((*S*)-*p*-tolylsulfinyl)phenyl)naphthalene
Chemical Formula: $C_{24}H_{20}O_2S$
Molecular Weight: 372,4820

(*S*)-1-[2-Methoxy-6-(*p*-tolylsulfinyl)phenyl]naphthalene: Prepared from (*S*)-2-bromo-1-methoxy-3-(*p*-tolylsulfinyl)benzene (1.0 equiv, 390 mg, 1.2 mmol) according to GP2 for 2.5 h by using naphthalen-1-ylboronic-acid (1.5 equiv, 309 mg, 1.8 mmol), $Pd(PPh_3)_4$ (5 mol%, 69.6 mg, 0.06 mmol), K_2CO_3 (663 mg, 4.8 mmol, 4.0 equiv), dioxane (13 mL) and water (3.5 mL). Purification by flash column chromatography on silica gel using mixture of cyclohexane and ethyl acetate (1/1, v/v) afforded the title compound [(*S*)-1l, 434 mg, 1.17 mmol, 97%, *dr* = 63:37] as a colorless solid.

^{1}H-NMR ($CDCl_3$, 400 MHz): [(Minor isomer integrate for 1.0, major isomer integrate for 1.7; expected ^{1}H integration of major and minor isomer is 54 (20+20*1.7 = 54)] δ = (*mixture of two atropodiastereomers 1:1.7*) 7.91 (t, *J* = 7.6 Hz, 6.4H), 7.75 (d, *J* = 8.2 Hz, 1.7H), 7.72–7.64 (m, 2.5H), 7.59 (t, *J* = 7.5 Hz, 1.7H), 7.55–7.48 (m, 3.8H), 7.47–7.40 (m, 1H), 7.37–7.27 (m, 2.9H), 7.17–7.02 (m, 6.9H), 6.92 (td, *J* = 7.6, 1.1 Hz, 1.8H), 6.72 (dd, *J* = 7.0, 1.0 Hz, 1H), 6.60 (d, *J* = 8.4 Hz, 1.7H), 6.54 (brs, 6.4H), 3.64 (s, 3H), 3.62 (s, 5.2H), 2.32 (s, 3H), 2.03 (s, 5.2H) ppm.
^{13}C-NMR ($CDCl_3$, 101 MHz): δ = (*mixture of two atropodiastereomers 1:1.7*) 157.6, 157.5, 146.8, 146.6, 142.5, 141.6, 141.3, 140.6, 133.6, 133.4, 132.1, 131.6, 131.0,

130.1, 129.9, 129.7, 129.6, 129.1 (2C), 129.1, 128.8, 128.4, 128.1, 127.9, 127.1, 127.0, 126.9, 126.3, 126.2, 126.0 (2C), 125.6, 125.5, 125.5, 125.4, 124.8, 116.2, 116.1, 113.5, 112.8, 56.2, 56.2, 21.6, 21.2 ppm.
R_f (EtOAc: *c*-hex = 1:1): 0.38.
IR (ATR): $\tilde{\nu}$ /cm^{-1} = 3050 (w), 2933 (w), 2835 (w), 1769 (s), 1458 (m), 1430 (m), 1258 (s), 1153 (m), 1083 (m), 1031 (s), 1028 (s), 801 (s), 777 (s), 745 (m), 508 (m).
HRMS: 395.1068 [M+Na]$^+$, *calcd*. for $C_{24}H_{20}NaO_2S$ = 395.1076.

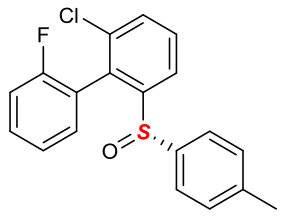

2-chloro-2'-fluoro-6-((*S*)-*p*-tolylsulfinyl)-1,1'-biphenyl
Chemical Formula: $C_{19}H_{14}ClFOS$
Molecular Weight: 344,8284

(*S*)-2-Chloro-2'-fluoro-6-(-*p*-tolylsulfinyl)-1,1'-biphenyl: Prepared from (*S*)-2-bromo-1-chloro-3-(*p*-tolylsulfinyl)benzene (1 equiv, 503 mg, 1.53 mmol), according to GP2 for 2 h by using 2-fluorophenylboronic acid (1.47 equiv, 321 mg, 2.25 mmol), K_2CO_3 (3.8 equiv, 802 mg, 5.8 mmol) and $Pd(PPh_3)_4$ (4.24 mol%, 75 mg, 0.065 mmol) in a mixture of dioxane (12 mL) and water (3 mL). Flash chromatography on silica gel (Et_2O/*n*-Pentane 3:2) yielded (*S*)-2-chloro-2'-fluoro-6-(-*p*-tolylsulfinyl)-1,1'-biphenyl (497 mg, 1.44 mmol, 94 %) as yellow sticky solid.

^{1}**H-NMR** (400 MHz, $CDCl_3$): δ = *(mixture of two atropodiastereomer 1:1.5)* 8.17 (dd, *J* = 5.6, 3.5 Hz, 1 H *minor dia*), 8.10 (dd, *J* = 5.9, 3.2 Hz, 1 H *major dia*), 7.61–7.57 (m, 2 H *major dia*, 2 H *minor dia*), 7.47-7.41 (m, 1 H *major dia*, 1 H *minor dia*), 7.38–7.35 (m, 1 H *major dia*), 7.31–7.21 (m, 1 H *major dia*, 1 H *minor dia*), 7.08–6.90 (m, 4 H *major dia*, 5 H *minor dia*), 6.92 (t, *J* = 8.8 Hz, 1 H *major dia*) 6.57 (t, *J* = 6.7 Hz, 1 H *minor dia*), 2.32 (s, 3 H *major dia*, 3 H *minor dia*).
^{13}**C-NMR** (101 MHz, $CDCl_3$): δ = 159.9 (d, J_{CF} = 248.9 Hz) 159.0 (d, J_{CF} = 248.7 Hz), 147.2, 147.0, 142.1, 142.1, 141.4, 140.5, 135.2 (d, J_{CF} = 0.9 Hz), 134.8 (d, J_{CF} = 0.6 Hz), 132.8 (d, J_{CF} = 2.8 Hz), 132.6, 131.8, 131.8, 131.4, 131.4, 131.4, 131.2 (d, J_{CF} = 8.3 Hz), 131.1 (d, J_{CF} = 8.1 Hz), 130.2, 130.2, 129.8, 129.7, 126.2, 126.1 (d, J_{CF} = 0.7 Hz), 124.3 (d, J_{CF} = 3.7 Hz), 123.9 (d, J_{CF} = 3.9 Hz), 122.9, 122.3, 122.3 (d, J_{CF} = 16.5 Hz), 121.8 (d, J_{CF} = 16.1 Hz), 116.1 (d, J_{CF} = 21.6 Hz), 115.7 (d, J_{CF} = 21.6 Hz), 21.5, 21.5 ppm.
^{19}**F-NMR** (377 MHz, $CDCl_3$): δ = –112.3 (*minor dia)*, –112.3 (*major dia*) ppm.
R_f (EtOAc/*c*-Hex 1:2) = 0.46.
IR (ATR): $\tilde{\nu}$ /cm^{-1} = 3063 (w), 2921 (w), 4194 (m), 1451 (m), 1432 (m), 1252 (m), 1211 (m), 1093 (s), 1044 (s), 809 (m), 754 (s), 503 (s).
HRMS (*ESI*) = 367.0296 [M+Na$^+$]*, calcd.* for $C_{19}H_{14}ClFOSNa^+$ = 367.0330.

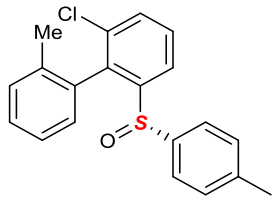

2-chloro-2'-methyl-6-((*S*)-*p*-tolylsulfinyl)-1,1'-biphenyl
Chemical Formula: $C_{20}H_{17}ClOS$
Molecular Weight: 340,8650

(*S*)-2-Chloro-2'-methyl-6-(*p*-tolylsulfinyl)-1,1'-biphenyl: Prepared from (*S*)-2-bromo-1-chloro-3-(*p*-tolylsulfinyl)benzene (1.0 equiv, 330 mg, 1.0 mmol) according to GP2 for 2.5 h by using $Pd(PPh_3)_4$ (5 mol%, 58 mg, 0.05 mmol), K_2CO_3 (4.0 equiv, 553 mg, 4.0 mmol), *o*-tolylboronic-acid (1.3 equiv, 177 mg, 1.3 mmol), dioxane (12 mL) and water (3 mL). Purification by flash column chromatography on silica gel using mixture of ether and *n*-pentane (4/6, v/v) afforded the title compound 1n, (300 mg, 88%, *dr* = 52:48) as a thick liquid.

^{1}H-NMR ($CDCl_3$, 400 MHz): [(Minor isomer integrate for 1.0, major isomer integrated for 1.1; expected ^{1}H integration of major and minor isomer is 36 (17+17*1.1 = 36)] δ = (*mixture of two atropodiastereomers 1:1.1*) 8.22 (dd, *J* = 7.5, 1.3 Hz, 1.1 H), 8.16 (dd, *J* = 6.7, 2.2 Hz, 1H), 7.70–7.50 (m, 4.6H), 7.44–7.18 (m, 4.5H), 7.25–7.20 (m, 1H), 7.17–6.96 (m, 9H), 6.87 (d, *J* = 8.1 Hz, 2.3H), 6.35 (d, *J* = 8.1 Hz, 1H), 2.34 (s, 3.2H), 2.31 (s, 3.3H,), 2.17 (s, 3.2H), 1.19 (s, 3.3H) ppm. **^{13}C-NMR** ($CDCl_3$, 101 MHz): δ = (*mixture of two atropodiastereomers 1:1.1*) 146.4, 146.4, 142.3, 142.2, 141.4, 140.3, 138.3, 137.8, 137.8, 136.4, 134.8, 134.5, 134.0, 133.6, 131.9, 131.2, 131.0, 130.4, 130.2, 129.9, 129.7 (2 $C_{p\text{Tol}}$) , 129.7, 129.6 (2 $C_{p\text{Tol}}$), 129.5, 129.3, 129.0, 126.9 (2 $C_{p\text{Tol}}$), 126.6 (2 $C_{p\text{Tol}}$), 126.1, 125.7, 122.6, 122.2, 21.6, 21.6, 20.0, 18.5 ppm
R_f (ether: *n*-pentane = 4:6): 0.31.
IR (ATR): $\tilde{\nu}$ /cm^{-1} = 3053 (w), 2921 (w), 2863 (w), 1595 (w), 1492 (m), 1425 (s), 1090 (s), 1044 (s), 809 (s), 790 (s), 755 (s), 742 (s), 639 (m).
HRMS: 363.0551 $[M+Na]^+$, *calcd*. for $C_{20}H_{17}NaClOS$ = 363.0581.

C. References

..
[385] T. R. Hoye, B. M. Eklov, M. Voloshin, *Org. Lett.* **2004**, *6*, 2567–2570.
[386] W. C. Still, M. Kahn, A. Mitra, *J. Org. Chem.* **1978**, *43*, 2923–2925.
[387] H. J. Bernstein, J. A. Pople, W. G. Schneider, *Can. J. Chem.* **1957**, *35*, 67–83.
[388] K. K. Andersen, *Tetrahedron Lett.* **1962**, *3*, 93–95.
[389] H.-S. Lin, L. A. Paquette, *Synth. Commun.* **1994**, *24*, 2503–2506.

Conclusion

IX. Conclusion

A. Conclusion et perspectives

L'exploration de la nouvelle stratégie de fonctionnalisation diatroposélective présentée dans cette thèse a conduit au développement de plusieurs nouvelles réactions atroposélectives.

Une réaction de Fujiwara-Moritani a été réalisé : l'utilisation d'HFIP comme solvant permet une aamélioration spectaculaire de la réactivité aussi bien que de la stéréosélectivité (conditions A contre conditions B, produits **1C** à **4C**, Figure IX-1) et ainsi un panel varié de biaryles tri-substitués a pu être obtenu avec des rendements et atroposélectivités excellents, et ceci à 25 °C. La principale limitation se trouvant lorsque l'encombrement stérique devient trop important (**7C** et **8C**), et ainsi seul les biaryles tetra-substitués par des groupes relativement petits (**5C, 6C**) ont fait preuve d'une bonne atropoinduction.

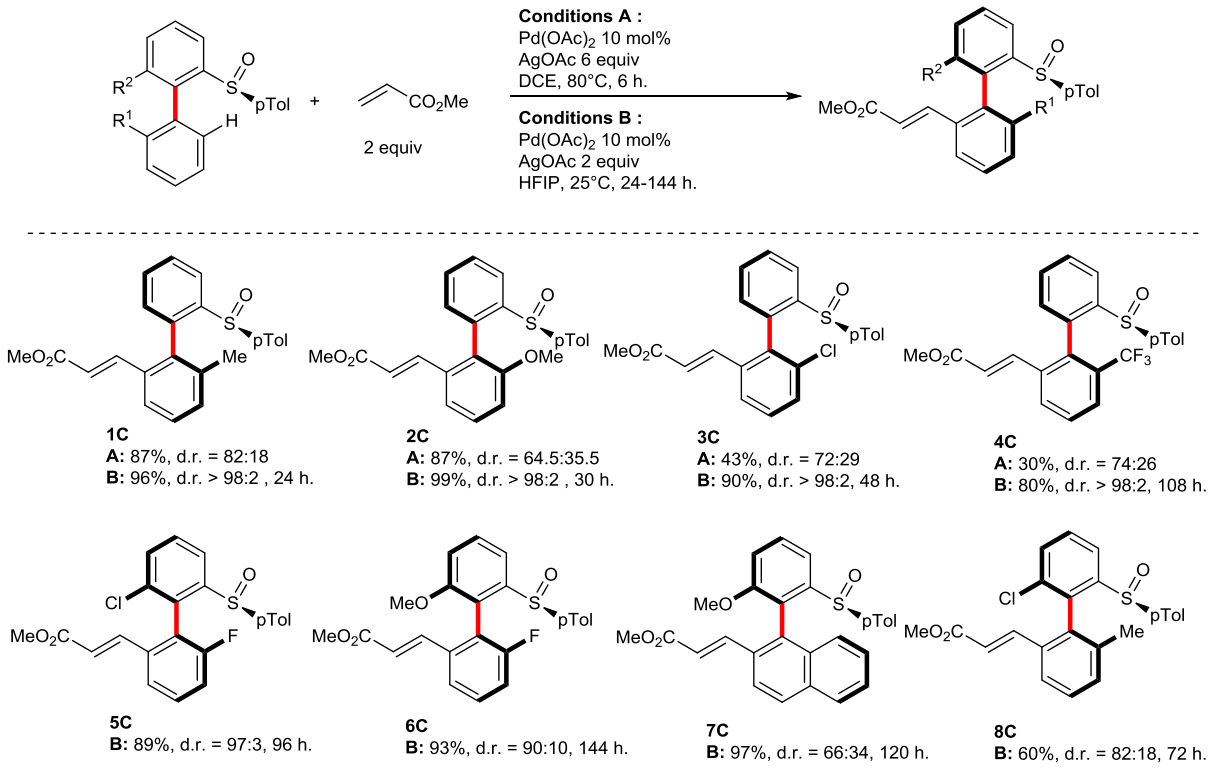

Figure IX-1 : portée de la réaction de Fujiwara-Moritani avec des acrylates

Remarquons aussi la possibilité de coupler des styrènes, cependant dans des conditions plus dures (80°C) et avec des rendements moins élevés, mais toujours d'excellentes atroposélectivités (Figure IX-2).

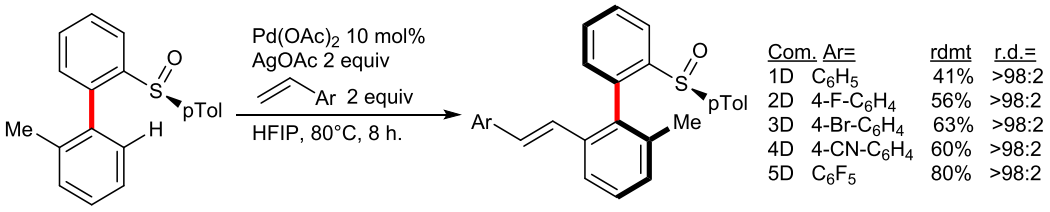

Figure IX-2 : portée de la réaction de Fujiwara-Moritani avec des styrènes

Une réaction d'acétoxylation (Figure IX-3) qui montrera une portée assez large vers des biaryles tri-substitués portant des groupements électro-donneurs (**1A, 2A, 7A**), électro-attracteurs (**3A, 4A, 6A**) et/ou coordinants (**5A**) aux positions critiques *ortho* ou *ortho'*, en gardant des rendements bons à excellents et des diastéréosélectivités très bonnes à excellentes (figure 3). De plus il a été possible d'accéder à des biaryles tetra-substitués avec de bons rendements et rapports diastéréomériques (r.d.) lorsque l'encombrement est relativement faible (8A, 9A), la limitation étant le passage d'un mécanisme de DCD à un dédoublement cinétique (DC) lorsque l'encombrement augmente (**10A à 11A**), avec cependant un DC très efficace car les produits aussi bien que les substrats ont pu être isolés avec un r.d. > 98:2 (**11A**).

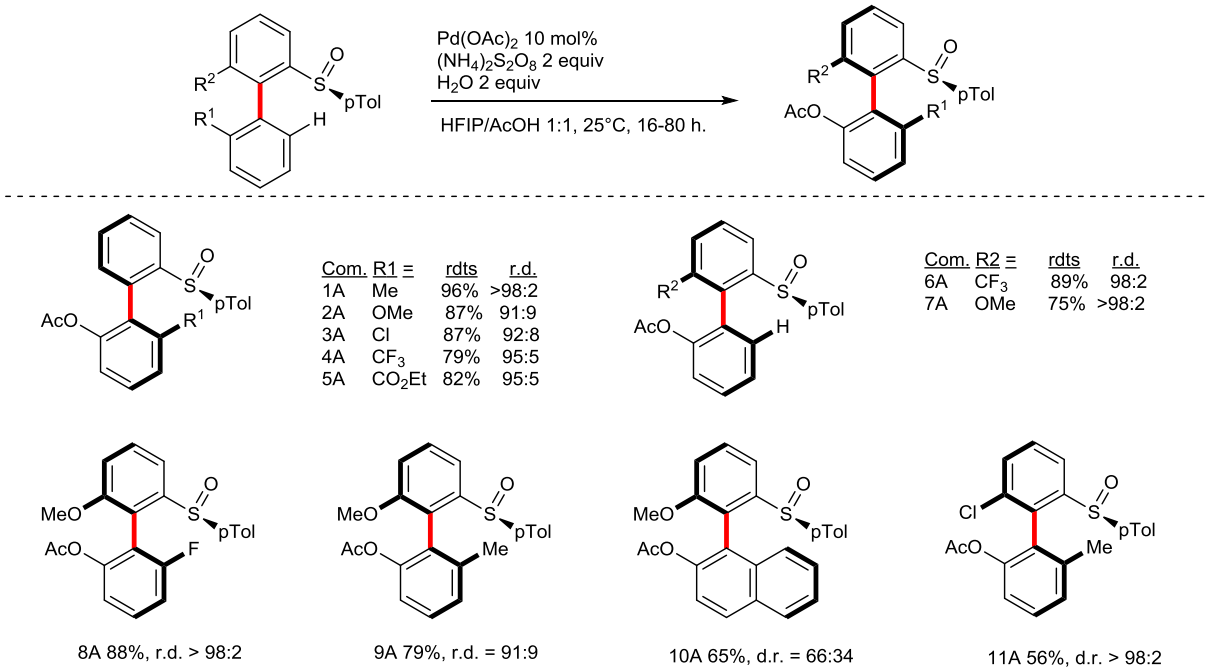

Figure IX-3 : portée de la réaction d'acétoxylation

Puis, un simple changement d'oxydant a permis de mettre en place une nouvelle fonctionnalisation : en effet le remplacement du persulfate par la *N*-iodosuccinimide (NIS) a ouvert la voie vers des biaryles atropopurs halogénés comportant ainsi une deuxième position pouvant être fonctionnalisée (Figure IX-4). Cette réaction d'iodation présente les mêmes carac-

téristiques générales que la précédente réaction d'acétoxylation, avec cependant la possibilité de diminuer la charge catalytique de $Pd(OAc)_2$ à 5 mol% en gardant des rendements excellents, avec cependant des temps de réactions plus longs.

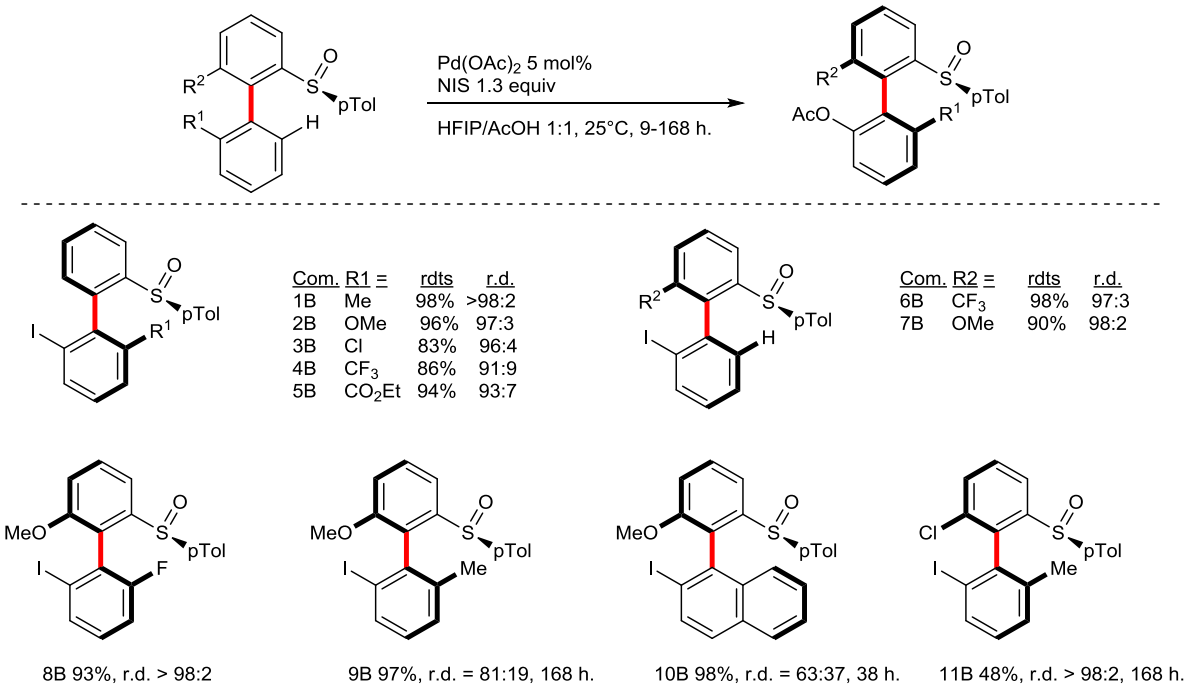

Figure IX-4 : portée de la réaction d'iodation

Notons qu'afin de comprendre l'origine de l'effet spectaculaire d'HFIP sur la sélectivité et la réactivité, des études mécanistiques ont été réalisées en collaboration avec le Dr. Jean-Pierre Djukic: la rupture de la liaison C-H a ainsi été identifiée comme étape limitante du cycle catalytique et une liaison hydrogène relativement forte entre l'oxygène du sulfoxyde et l'HFIP a été mise en évidence. Cette liaison hydrogène est présumée modifier les propriétés stériques et électroniques du groupement directeur et ainsi faciliter l'étape de cyclométallation.

Puis le potentiel de cette méthodologie à réaliser des synthèses plus économes en moyens et en étapes a été démontré à travers la synthèse formelle asymétrique atroposélective d'un composé naturel biologiquement actif, la (-)-steganone (Figure IX-5). Ainsi l'intermédiaire clé **4G** a été obtenu avec un rendement global sur 10 étapes linéaires de 41% et un rapport énantiomérique >99 :1.

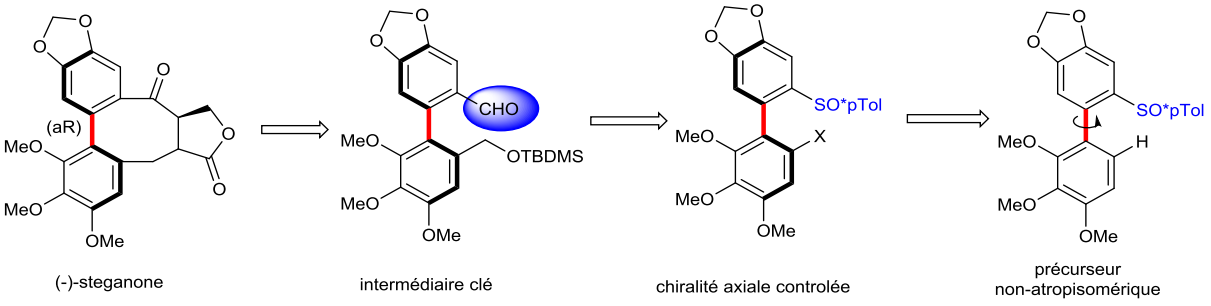

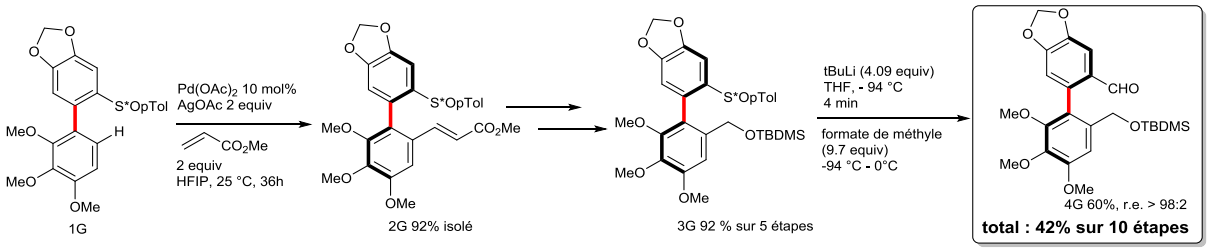

Figure IX-5 : synthèse formelle de la (-)-steganone

Enfin une réaction d'arylation directe a été mise au point sur les mêmes substrats, permettant de former des *ortho*-terphényles comportant un axe de chiralité avec une excellente atroposélectivité et de bons rendements (

Figure IX-6) : ici la température de réaction plus élevée compromet l'atropostabilité des produits les moins encombrés (**7E**), et on remarquera une réactivité plus importante des partenaires de couplage riche en électrons (**1E**, **2E** contre **5E** et **6E**).

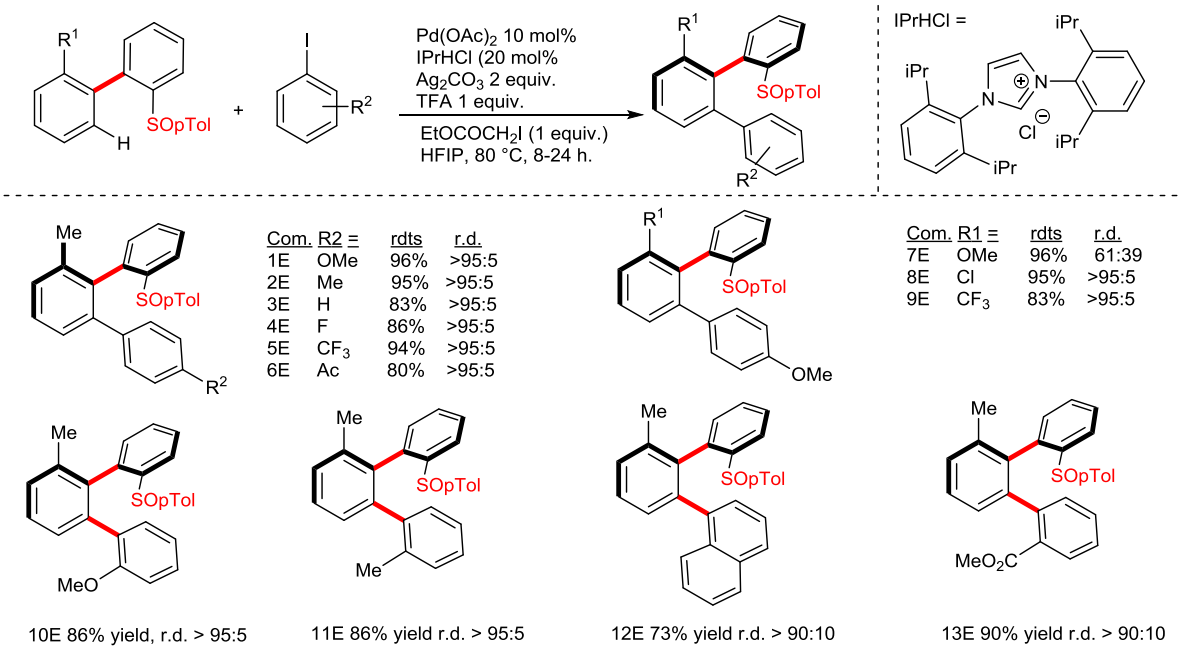

Figure IX-6 : portée de la réaction d'arylation

Le succès de cette première transformation nous a ensuite amené à explorer un nouveau concept : en effet l'augmentation de l'encombrement stérique autour du partenaire de couplage devrait nous permettre d'obtenir des *ortho*-terphényles comportant deux axes de chiralités, réalisant ainsi le premier exemple d'arylation directe hautement atroposélective. De plus les produits obtenus, *ortho*-terphényles doublement atropisomériques, ont peu de précédent dans la littérature et étaient jusque-là limité à des exemples symétriques issus de cycloadditions. Ainsi, un remaniement des conditions réactionnelles a permis la réalisation de ce couplage extrêmement encombré avec d'excellentes atroposélectivités, mais des rendements plus limités nous imposant d'augmenter la charge catalytique lorsque l'encombrement du substrat augmente et/ou la réactivité du partenaire de couplage est moindre (Figure IX-7). Cette réaction est alors le premier exemple d'arylation directe hau-

tement atroposélective. De plus cette méthode donne accès à un panel de produits modulables (**8F, 9F**) dans des positions stratégiques, et plus encore lorsqu'on prend en compte les possibilités de post-modification offerte par le sulfoxyde.

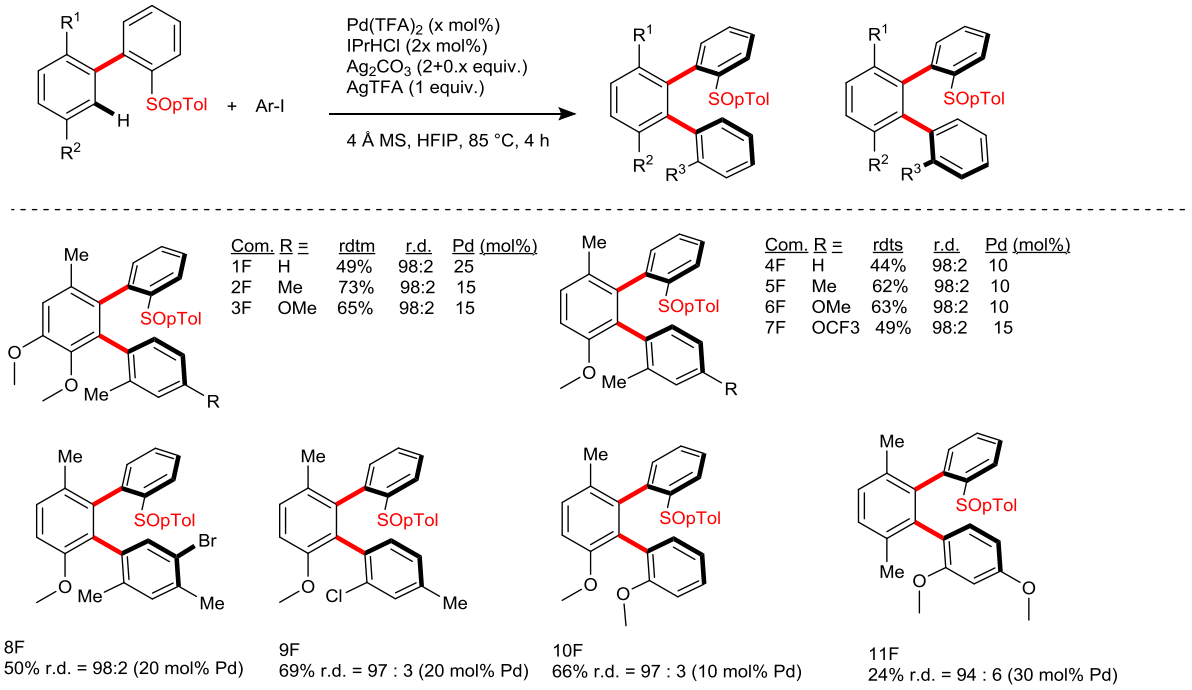

Figure IX-7 : portée de la réaction d'arylation avec double contrôle de chiralité axiale

Ainsi, la démonstration de la capacité de la stratégie d'activation et de fonctionnalisation de liaisons C-H à produire des squelettes inédits a été réalisée. Ces produits originaux ont été utilisés pour explorer un nouvel espace chimique de ligands inédits, en développant le concept de *pseudo*-chiralité planaire : ainsi la bis-phosphine **13b** a pu être obtenue avec un bon rendement à partir du bromosulfoxyde **8F** (Figure IX-8a). Les premières évaluations sur l'hydrogénation énantiosélective du (Z)-2-acetamidophenyl acrylate (Figure IX-8b) ont montré un fort potentiel de stéréoinduction.

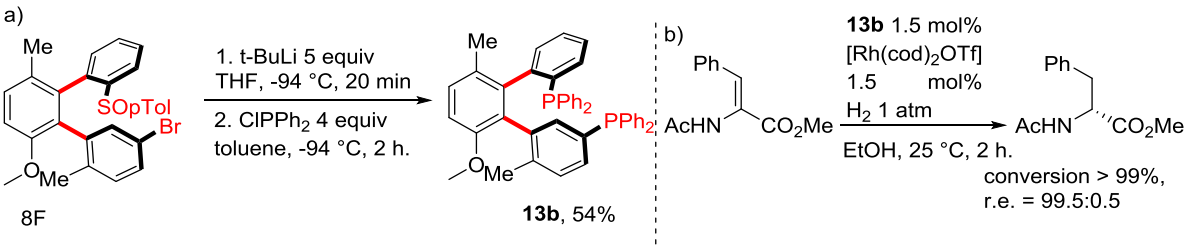

Figure IX-8 : synthèse de ligands originaux et test catalytique

En perspective, l'exploration de nouveaux types de ligands à partir de notre squelette à pseudo-chiralté planaire devrait permettre des multiples applications aussi bien en métallocatalyse qu'en organocatalyse (Figure IX-9).

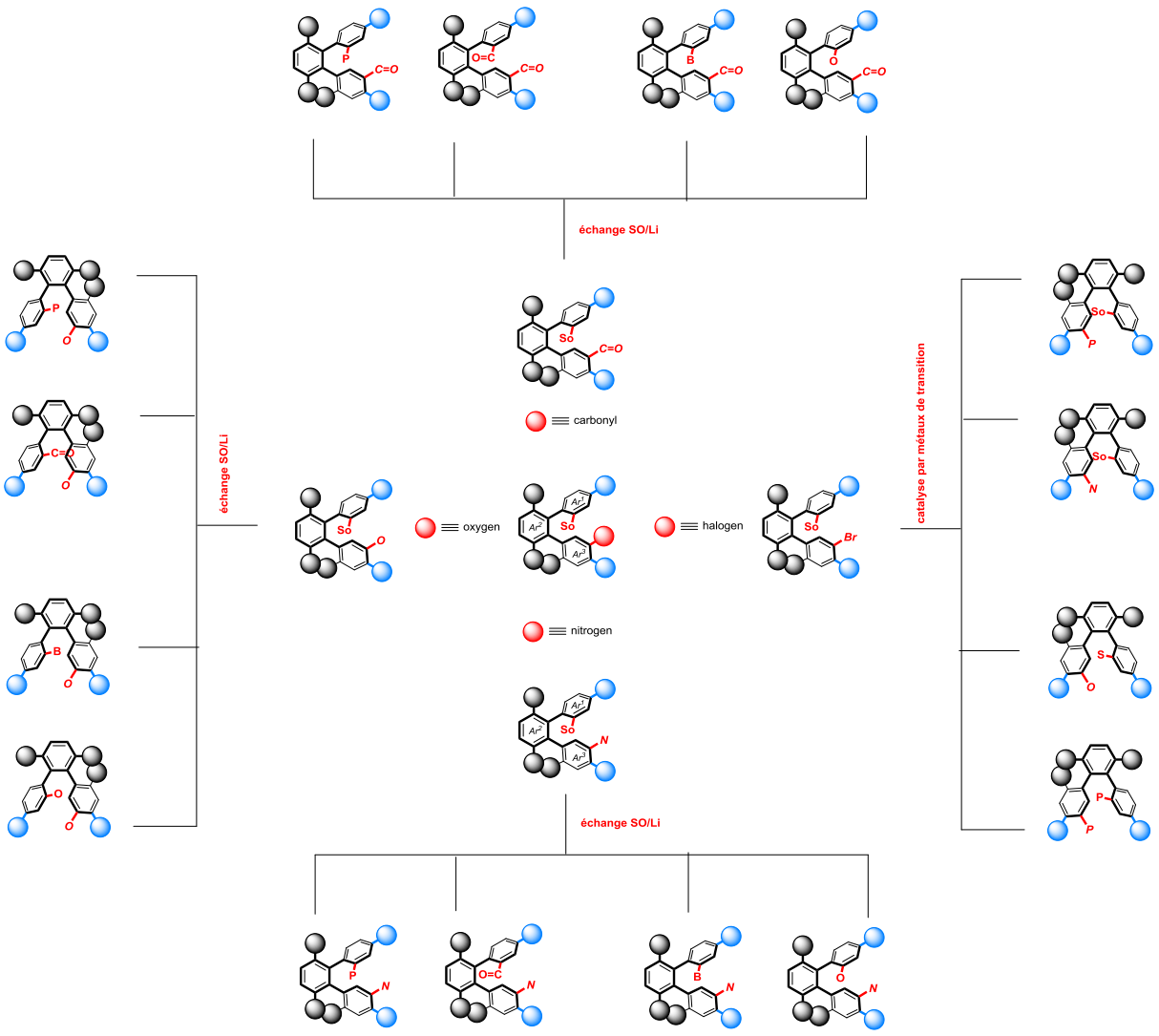

Figure IX-9 : possibilités de fonctionnalisations

B. Contribution scientifiques

LISTE DES PRESENTATIONS

Poster : Q.Dherbassy, C.K. Hazra, J. Wencel-Delord, F. Colobert ; « Sulfoxide as handful tool for stereoselective C-H activation », JCO 8 septembre 2016, école polytechnique Palaiseau, France

---

LISTE DES PUBLICATIONS

Synthesis of Axially Chiral Biaryls through Sulfoxide-Directed Asymmetric Mild C-H Activation and Dynamic Kinetic Resolution, C. K. Hazra, Q. Dherbassy, J. Wencel-Delord, F. Colobert, *Angew. Chem. Int. Ed.* **2014**, *53*, 13871–13875. doi: 10.1002/anie.201407865

Enantiopure Sulfoxides: Efficient Chiral Directing Group for Stereoselective C–H Bond Activation: Towards the Control of Axial Chirality, Q. Dherbassy, G. Schwertz, C. K. Hazra, T. Wesch, J. Wencel-Delord, F. Colobert, *Phosphorus Sulfur Silicon Relat. Elem.* **2015**, *190*, 1339–1351. doi : 10.1080/10426507.2015.1024791

1,1,1,3,3,3-Hexafluoroisopropanol as a Remarkable Medium for Atroposelective Sulfoxide-Directed Fujiwara–Moritani Reaction with Acrylates and Styrenes. Q. Dherbassy, G. Schwertz, M. Chessé, C. K. Hazra, J. Wencel-Delord, F. Colobert, *Chem. – Eur. J.* **2016**, *22*, 1735–1743. doi : 10.1002/chem.201503650

Asymmetric C–H activation as a modern strategy towards expedient synthesis of steganone. Q. Dherbassy, J. Wencel-Delord, F. Colobert, *Tetrahedron* **2016**, *72*, 5238–5245. doi : 10.1016/j.tet.2016.03.060

The publication on the arylation has ben submitted to JACS

A patent on enantiopur ligands has been submitted

The publication on mechanistic studies and DFT calculations is in preparation

Université de Strasbourg

EDSC École Doctorale des Sciences Chimiques

Quentin DHERBASSY

« Contrôle de la chiralité axiale par activation de liaisons C-H: Accès à des molécules naturelles et ligands inédits »

Résumé. La chiralité axiale est une propriété importante de composés biologiquements actifs, de matériaux avancés et plus particulièrement de ligands utilisés en catalyse asymétrique. En effet de nombreuses structures biaryliques atropisomériques ont montré un excellent pouvoir d'induction asymétrique. Ainsi le contrôle de l'atropisomérie et le développement de nouvelles méthodes synthétiques permettant la synthèse de composés à chiralité axiale optiquement purs attire l'attention de la communauté scientifique. Au cours de ce travail une nouvelle stratégie vers l'obtention de biaryles à chiralité axiale atropenrichis a été explorée. L'utilisation de sulfoxydes énantiopurs, jouant à la fois le rôle de groupe directeur et d'auxiliaire de chiralité, dans une stratégie de fonctionnalisation de liaisons C-H par catalyse homogène au palladium, a permis l'obtention efficace de nombreux composés biaryliques hautement atropenrichis . Les méthodologies développées ont ensuite été appliquées à la synthèse formelle d'un composé naturel bioactif à chiralité axiale, la (-)-steganone, ainsi qu'à la synthèse de ligands doublement atropisomériques inédits. Ces derniers ont montrés un excellent pouvoir d'induction asymétrique en catalyse pour l'hydrogénation asymétrique, ouvrant les portes vers l'élargissement dans d'autres domaines.

Mots-clefs : chiralité axiale, atropisomérie, atropisomères, biaryles, sulfoxydes, activation C-H, palladium, steganone, ligands, hydrogenation asymétrique.

Abstract. Axial chirality is an important property of biologically active compounds, advanced materials and more importantly of ligands used in asymmetric catalysis. Indeed, numerous atropisomeric biaryls have demonstrated an excellent asymmetric induction capacity. Thus, the control of atropisomery and the development of original synthetic methodologies allowing the synthesis and the obtention of optically pure axially chiral compounds is an important goal for the scientific community. In this work, a new strategy for the synthesis of atropenriched axially chiral biaryls was explored. The use of enantiopur sulfoxides playing the role of both, a directing group and a chirality auxiliary, in a palladium catalyzed C-H functionalization, allowed the efficient construction of numerous highly atropenriched biaryl compounds. The developed methodologies were furthermore applied to the formal synthesis of an axially chiral and bioactive compound, (-)-steganone, as well as the synthesis of doubly atropisomeric unprecedented ligands. These ligands displayed an excellent potential for asymmetric induction in homogenous asymmetric hydrogenation, thereby opening the way towards new applications.

Key words: axial chirality, atropisomery, atropisomeric, biaryls, sulfoxides, C-H activation, palladium, steganone, ligands, asymmetric hydrogenation.